MICROWAVE, PHOTO AND SONO ACTIVATED ADVANCED OXIDATION PROCESSES AND THEIR VARIATIONS FOR THE DECONTAMINATION OF WATER FROM TOXIC CHEMICAL POLLUTANTS

Thesis submitted to
Cochin University of Science and Technology
in partial fulfillment of the requirements
for the award of the degree of
Doctor of Philosophy
in
Environmental Technology
Under the faculty of Environmental Studies

By

Vidya Lekshmi K. P.
(Reg. No. 4410)

SCHOOL OF ENVIRONMENTAL STUDIES
COCHIN UNIVERSITY OF SCIENCE AND TECHNOLOGY
KOCHI - 682 022

August **2018**

Microwave, Photo and Sono Activated Advanced Oxidation Processes and Their Variations for the Decontamination of Water from Toxic Chemical Pollutants

Ph.D. Thesis under the Faculty of Environmental Studies

Author

Vidya Lekshmi K. P.
Research Scholar
School of Environmental Studies
Cochin University of Science and Technology
Kochi – 682 022
Kerala, India

Supervising Guide

Dr. Suguna Yesodharan
Professor (Emeritus)
School of Environmental Studies,
Cochin University of Science and Technology
Kochi – 682 022
Kerala, India

School of Environmental Studies
Cochin University of Science and Technology
Kochi, Kerala, India   682 022

August 2018

SCHOOL OF ENVIRONMENTAL STUDIES
COCHIN UNIVERSITY OF SCIENCE AND TECHNOLOGY
KOCHI - 682 022

Dr. Suguna Yesodharan
Professor (Emeritus)

Certificate

This is to certify that this thesis entitled **"Microwave, Photo and Sono Activated Advanced Oxidation Processes and Their Variations for the Decontamination of Water from Toxic Chemical Pollutants"** is an authentic record of the research work carried out by **Smt. Vidya Lekshmi K. P.**, Full-Time Research Scholar (Reg. No. 4410) under my guidance at the School of Environmental Studies, Cochin University of Science and Technology in partial fulfillment of the requirements for the award of the degree of Doctor of Philosophy in Environmental Technology and no part of this work has previously formed the basis for the award of any other degree, diploma, associateship, fellowship or any other similar title or recognition. All the relevant corrections and modifications suggested by the audience during the pre-synopsis seminar and recommended by the Doctoral committee have been incorporated in the thesis.

Kochi - 22   **Dr. Suguna Yesodharan**
August 2018   (Supervising Guide)

Declaration

I do hereby declare that the work presented in the thesis entitled **"Microwave, Photo and Sono Activated Advanced Oxidation Processes and Their Variations for the Decontamination of Water from Toxic Chemical Pollutants"** is based on the authentic record of the original work done by me, for my Doctoral Degree under the guidance of **Dr. Suguna Yesodharan**, Professor (Emeritus), School of Environmental Studies, Cochin University of Science and Technology in partial fulfillment of the requirements for the award of the degree of Doctor of Philosophy in Environmental Technology and no part of this work has previously formed the basis for the award of any other degree, diploma, associateship, fellowship or any other similar title or recognition.

Kochi – 22   **Vidya Lekshmi K. P.**
August 2018

I would like to express my sincere and heartfelt gratitude to all the research scholars of our laboratory, Mr. Shibin, Mr. Hariprasad, Mr. Rajeev, Ms. Veena, Ms. Gayathri, Ms. Sindhu, Ms. Phonsy, Ms. Deepthi, Dr. Anju and Dr. Jyothi and all other research scholars in SES for their timely advice, help and affection, which made my stay in the laboratory a pleasant one.

I would like to extend my sincere gratitude to CSIR for awarding me the Research Fellowship and to the CUSAT for providing me the facility to conduct my research work.

It's impossible to literally express my gratitude to my mother (Anitha), father (Parameswaran), mother in-law (Ponnamma), brothers (Vinod and Vijay), sisters-in-law (Sindhu, Suja and Parvathy), my husband (Binu) and our kids Abhinav and Niharika for their patience and understanding as well as the affection, support and hope they provided.

Above all, this piece of work is accomplished with the blessings and powers that work within me and also the people behind my life. I bow before GOD for all with a sense of humility and gratitude..........

Vidya Lekshmi K. P.

||||| Preface |||||

Advanced Oxidation Processes (AOPs) often termed as the "treatment methods of 21st century" have been investigated extensively in recent years as potential environment – friendly and economical procedures for the decontamination of water from chemical and bacterial pollutants. In the current study, five such AOPs i.e. Microwave (MW) catalysis, Sono (US) catalysis, Photo (UV) catalysis, Microwave-photocatalysis (in sequence) and Sonophotocatalysis (concurrent) are investigated in detail and their relative efficiencies are evaluated and compared.

MnO_2, MnO_2-TiO_2 and Co_3O_4 which are among the least explored catalysts in AOPs, are used in the study. Indigo Carmine (IC) which is a toxic recalcitrant dye with extensive application in textile and medical diagnostic sectors and is a contaminant often found in the effluent water from such activities is used as the test pollutant. The catalysts are characterised by SEM, TEM, FTIR, UV-DRS, XRD, Particle size, Pore size analysis etc. The reaction products and intermediates were analysed and quantified by UV-Visible spectroscopy, Gas Chromatography, Photoluminescence, LC-MS as well as other instrumental and wet analytical techniques.

Various reaction parameters relevant for the degradation and mineralisation of IC are identified and optimised under respective AOPs. The degradation follows variable kinetics and Langmuir-Hinshelwood mechanism. The study provided many interesting and unexpected findings. MnO_2 and MnO_2-TiO_2 are much more efficient than many other previously tested oxides as catalysts in MW-, Sono- and Photo- based AOPs. Irrespective of the similarity of MnO_2, Co_3O_4 and TiO_2 in terms of physicochemical characteristics, the effect of various parameters and

reaction components on AOPs mediated by them is different. For example H_2O_2 is an inhibitor of the degradation of IC in presence of MnO_2, under sono-, photo- and MW- catalysis, while it is an enhancer in presence of Co_3O_4. The combination of the oxidants H_2O_2 and potassium persulphate ($K_2S_2O_8$) enhances the degradation of IC in presence of Co_3O_4 synergistically, while the combination effect is less than additive in presence of MnO_2 or MnO_2-TiO_2. Similarly various salts/anions which are likely to be present in water influence the AOP degradation of organics inconsistently. The effect of same salt can vary from 'inhibition' to 'no effect' and even 'enhancement' depending on the catalyst and reaction conditions.

Another highlight of the study is the identification of (MnO_2-TiO_2) combination catalyst as highly efficient in the hybrid AOP, i.e, sonophotocatalysis which can successfully exploit the MW activity of the former and the photoactivity of the latter. The combination MnO_2-TiO_2 (18:1) is demonstrated as one of the most efficient catalyst systems for the complete mineralisation of IC under sonophotocatalysis. A surprising observation made in the study is that the degradation of IC will proceed unhindered even in deoxygenated systems making use of the lattice and strongly bound surface O_2 from MnO_2 and Co_3O_4. This conclusion was made with the help of suitably designed simple experiments and supported by EDX data. The potential of the most efficient AOP identified during the study i.e. 'MnO_2-TiO_2 sonophotocatalysis', for the mineralisation of a wide spectrum of pollutants in water including recalcitrant dyes, petrochemicals, pharmaceuticals and pesticides is proven conclusively in Chapter 7 of the thesis. Chapter 8 summarises the findings of the study and highlights the conclusions.

The thesis is presented in 8 Chapters and three annexures as follows:

Chapter 1. Introduction: Background literature

Chapter 2. Objectives of the study, Materials used and Plan of the thesis

Chapter 3. Microwave induced MnO_2, MnO_2-TiO_2 and Co_3O_4 mediated degradation of Indigo Carmine in water

Chapter 4. Photocatalysis mediated by MnO_2, MnO_2-TiO_2 and Co_3O_4 for the degradation of Indigo Carmine in water

Chapter 5. Sonocatalysis mediated by MnO_2, MnO_2-TiO_2 and Co_3O_4 for the degradation of Indigo Carmine in water

Chapter 6. Sonophotocatalysis mediated by MnO_2 and MnO_2-TiO_2 for the degradation of Indigo Carmine in water

Chapters 7. Sonophotocatalysis mediated by MnO_2-TiO_2 as a versatile AOP for the mineralisation of different category of pollutants

Chapters 8. Summary and Conclusions

Annexures:

Annexure I   List of abbreviations used in the thesis

Annexure II List of publications in peer-reviewed journals/presented in conferences

Annexure III Reprints of papers published in peer reviewed journals.

‖‖ Contents ‖‖

Chapter **3**

Microwave induced MnO$_2$, MnO$_2$-TiO$_2$ and Co$_3$O$_4$ mediated degradation of Indigo Carmine in water .... 95 - 239

Chapter 4

Photocatalysis mediated by MnO₂, MnO₂-TiO₂ and Co₃O₄ for the degradation of Indigo Carmine in water

Chapter **5**

Sonocatalysis mediated by MnO$_2$, MnO$_2$-TiO$_2$ and Co$_3$O$_4$ for the degradation of Indigo Carmine in water **351- 450**

List of Tables

|||| List of Figures ||||

.....ಶುಭ.....

Chapter **1**

Introduction: Background Literature

1.1 General

Water is one of our important natural resources. It is the driving force for life on our planet. Water also plays a key role in the origin of culture and arts. Contamination of water, among other consequences, can cause a wide variety of diseases. Millions of people die every year from water-borne diseases. According to the census reports of 2011, the population of India is 1.3 billion and is rising. This rapid increase in population and increasing demand for water result in the shortage of water which is already scarce. One of the root causes of India's water crisis is poor water quality resulting from insufficient and delayed investment in urban water-treatment facilities. In addition to that, relevant effluent standards are also not met by the industries and other establishments, in many instances. According to World Health Organization 97 million Indians lack access to safe water today. The World Bank estimates that 21 % of communicable diseases in India are linked to unsafe water and lack of good hygiene practices. Indiscriminate discharge of untreated waste water into rivers and lakes pollute water bodies. The wastewater may be of domestic, commercial or industrial origin. Persistent organic pollutants (POPs) such as heavy metals, radio isotopes, hydrocarbons, poly chlorinated biphenyls (PCBs) and pesticides should not

Microwave, Photo and Sono Activated Advanced Oxidation Processes and their Variations for the Decontamination of Water from Toxic Chemical Pollutants

1

be present in discharges because the biological accumulation of these compounds in the food chain can cause adverse effects. Untreated wastewater often contains pathogenic organisms, large amount of organic matter and nutrients. It is very important to remove the pollutants and pathogens from wastewater to satisfy the needs for irrigation, industrial and domestic use. Wastewater treatment processes are gaining more importance because of the increasing demand for water and stricter discharge regulations. In this context, identification of appropriate water treatment technology capable of meeting environmental quality objectives before discharge into fresh waters is of primary importance. Selection of suitable treatment process depends on the type of pollutant and its concentration [1-4].

The unit operations (physical, chemical and biological processes) in a typical wastewater treatment plant are commonly referred to as preliminary, primary, secondary and tertiary treatments.

1.   Preliminary treatment

It consists of physical unit operations such as screening for the removal of debris, grit removal for the elimination of coarse suspended matter and flotation for the removal of oil and grease. It also includes flow equalization, septage handling and odour control methods.

2.   Primary treatment

This is an extension of the preliminary treatment and involves screening and sedimentation processes. Aim of this treatment is to produce a liquid effluent suitable for biological treatment and separate solids as sludge. Pre -aeration with addition of suitable chemicals can be used to enhance the efficiency of primary treatment.

3.   Secondary treatment

This is used for the removal of soluble and colloidal organics and suspended solids that escaped from the primary treatment. It can be done by means of biological processes that include activated sludge process, lagoon systems, fixed bed reactors and sedimentation.

4.   Tertiary treatment

It is used to remove nitrogen, phosphorus, heavy metals, bacteria, viruses etc. The processes commonly used are flocculation, sedimentation and coagulation followed by filtration and adsorption by means of activated carbon.

Conventional waste water treatment processes can be summarised as in Fig.1.1.
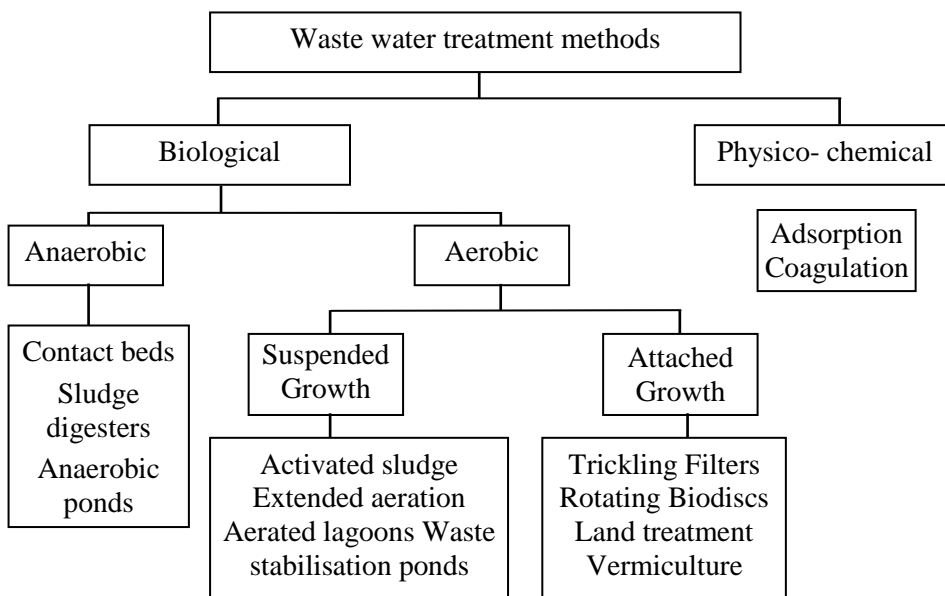
Fig. 1.1: Schematic diagram of conventional wastewater treatment methods.

The conventional treatment methods such as adsorption, precipitation, flocculation etc., are not effective to treat highly contaminated water. They merely transform the pollutants from one phase to another. In the case of industrial wastewater, biological treatment does not work in many cases because of the presence of biologically recalcitrant toxic pollutants. Many of these methods are non-destructive and rather ineffective at low contaminant levels. In such case more technologically advanced systems are needed to remove the pollutant molecules. In this respect, Advanced Oxidation Processes (AOPs), which are often referred to as the 'treatment methods of 21st century', have attracted a lot of attention in recent years as potential technologies for effective treatment of water containing trace contaminants.

1.2 Advanced Oxidation Processes (AOPs)

Advanced Oxidation Processes (AOPs) are different types of chemical treatment procedures that generate highly reactive free radicals insitu and convert toxic organic pollutants including pesticides, pharmaceuticals, dyes, poly aromatic compounds etc into biodegradable intermediates or completely mineralised products such as carbon dioxide and water [5-21]

Oxidation refers to the transfer of electrons from an electron donor (reductant) to an electron acceptor (oxidant). These electron transfers result in the chemical transformation of both the oxidant and the reductant as well as the formation of unpaired electrons resulting in species known as radicals which are unstable and hence highly reactive. These radicals undergo interactions among themselves as well as with

other reactants (both organic and inorganic) until thermodynamically stable oxidation products are formed. The ability of an oxidant to initiate chemical reactions is measured in terms of its oxidation potential. The oxidation potentials of some of the common oxidising agents are given in Table1.1

Table 1.1: Oxidation potential of common oxidizing agents.

Sl. No.	Oxidation species	Oxidation potential, eV
1	Fluorine	3.06
2	Hydroxyl radical	2.80
3	Sulphate radical	2.60
4	Atomic oxygen	2.42
5	Nascent oxygen	2.42
6	Ozone	2.07
7	Persulphate	2.01
8	Hydrogen peroxide	1.77
9	Perhydroxyl radical	1.70
10	Permanganate	1.68
11	Hypobromous acid	1.59
12	Hypochlorous Acid	1.49
13	Hypochlorite	1.49
14	Hypoiodous acid	1.45
15	Chlorine	1.36
16	Chlorine dioxide	1.27
17	Oxygen(molecular)	1.23
18	Bromine	1.09
19	Iodine	0.54

AOP involves the formation of highly reactive $^\bullet$OH radicals (oxidation potential 2.8 eV) which are the second strongest oxidants after fluorine. These radicals are responsible for the degradation of toxic pollutants leading to completely mineralised products such as H_2O, CO_2 and inorganic salts in many cases. Formation of $^\bullet$OH radical is accelerated by energy sources such as Ultraviolet light, Ultrasound, H_2O_2, Microwave radiation, Sunlight etc. Presence of oxidants such as H_2O_2, O_3 etc. can accelerate the formation of free radicals in both homogeneous and heterogeneous conditions. These radicals are highly reactive, non-selective and are electrophilic in nature. They react with the pollutant to form lower molecular weight intermediates and may even lead to complete mineralisation products in the end. The $\cdot$OH radicals attack the pollutant by radical addition (Eqn.1), hydrogen transfer (Eqn.2) or electron transfer (Eqn.3).

$$R + HO^\bullet \longrightarrow ROH \dots\dots\dots\dots\dots\dots\dots\dots\dots\dots(1)$$
$$R + HO^\bullet \longrightarrow R^\bullet + H_2O \dots\dots\dots\dots\dots\dots\dots\dots(2)$$
$$R + HO^\bullet \longrightarrow R^+ + OH^- \dots\dots\dots\dots\dots\dots\dots\dots(3)$$
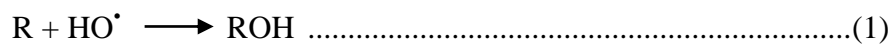
Where R is a typical organic chemical.

The efficiency of degradation depends on the concentration of pollutant, concentration of catalyst, pH, temperature, presence of ions in the solution etc.

Some of the typical AOPs in which $^\bullet$OH radicals play the decisive role are presented in Fig.1.2.
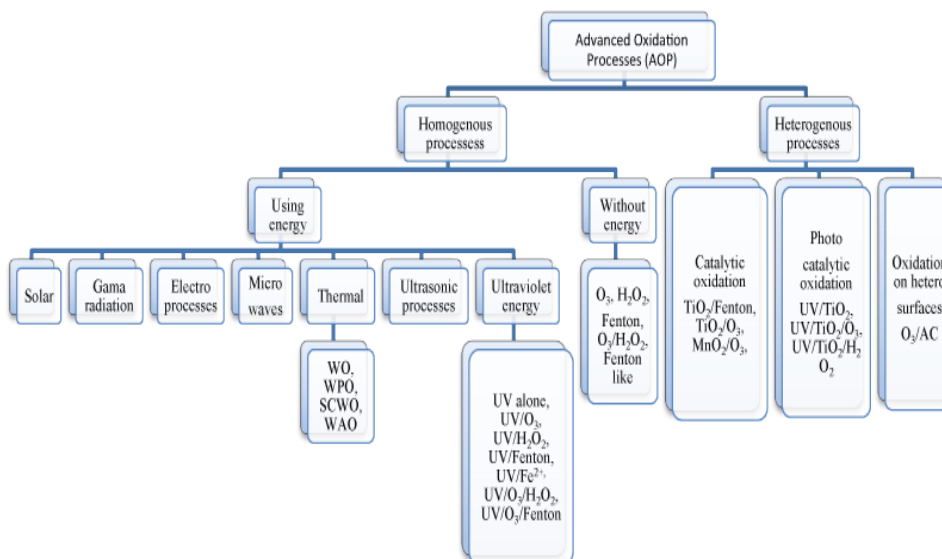
Fig.1.2. Classification of Advanced Oxidation Processes (AOPs)

1.2.1 Advantages and disadvantages of AOPs

1.2.1.1 Advantages

- Rapid reaction rates.
- Potential to reduce toxicity of organic compounds.
- Mineralization of organics, i.e. conversion to salt and CO_2.
- Do not create sludge as in the case of physical chemical processes or biological processes.
- Adaptable in flexible scales

1.2.1.2 Disadvantages

- High operation costs.
- Formation of oxidation intermediates which are potentially toxic.
- Specially skilled personnel are required for the design and often also for operation
- Still an emerging technology (more research is required)

1.2.2 Different types of AOPs

AOPs find application in many areas such as air, soil and water decontamination. They are often used as pre-treatment technique combined with biologic treatment. They can also be used as quaternary treatments for the removal of micro-pollutants from the effluents of municipal wastewater treatment plants and for the disinfection of water. The selection of AOP depends upon the type and concentration of pollutants in wastewater. In some cases combination of AOPs (sequential or simultaneous) is found to be more active than the individual ones. Synergic effect is also reported in many cases, ie the rate of degradation is enhanced many fold (more than the sum of individual AOPs) when different AOPs are combined. Thus combination of AOPs can be an efficient method for pollutant removal at reduced cost of operation.

Of the many AOPs, those based on light (photo), sound (sono) and microwave (MW) as the energy sources, with and without catalyst/additives are being investigated widely for the decontamination of water containing toxic pollutants. Their combinations sometimes provide synergic results. In the present study, MW-catalysis, photocatalysis and sonocatalysis are investigated in depth for their efficacy in degrading and mineralising the dye pollutant Indigo Carmine in water. Hence relevant literature on these processes are reviewed here.

1.2.2.1 Photocatalysis

Braslavsky et al. [22] defined Photocatalysis as a "change in the rate of a chemical reaction or its initiation under the action of UV, visible or infrared radiation in the presence of a substance, ie the photocatalyst that

absorbs light quanta and is involved in the chemical transformation of the reaction partners".

Semiconductors are often used in photocatalysis, because of their ability to generate charge carriers, when activated with appropriate energy. The behaviour of semiconductor as photocatalyst can be explained on the basis of band gap theory. According to the theory the highest occupied energy level is called valence band(VB) and lowest unoccupied energy level is called conduction band (CB). The difference between these two is called band gap. In semiconductors the gap is so small that thermal or other excitations can bridge the gap. A small amount of doping with the right kind of material can also increase the conductivity of semiconductors.

The relative band gap in the case of insulators, semiconductors and conductors is shown in Fig.1.3.
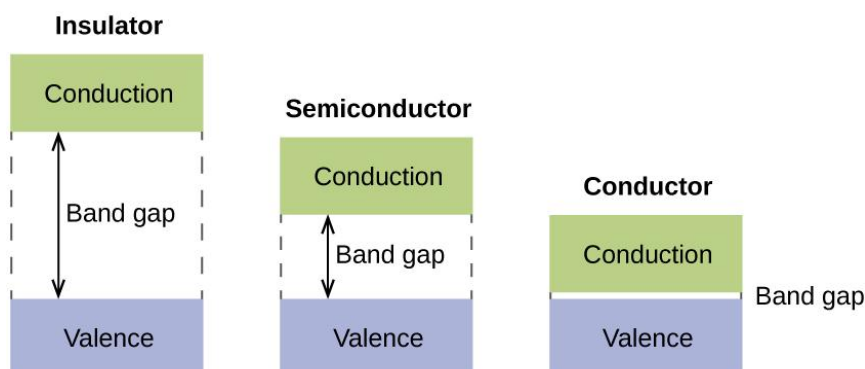
Fig. 1.3: Relative band gaps energy bands of insulators, semiconductors and conductors

Semiconductors are categorised into two types, ie intrinsic and extrinsic semiconductors. Intrinsic semiconductors are also called un-doped semiconductors and posses equal number of excited electrons and

holes. Here electrical conductivity can be due to crystallographic defects. In extrinsic semiconductor the band structure is modified by adding impurities, either by adding acceptor atoms or by adding donor atoms. When it is doped with acceptor atoms (eg: boron) there is deficiency of electrons or higher density of holes and is called p-type semiconductor. Here majority carriers are holes. But when it is doped with donor atoms (eg: arsenic) there is higher electron density and lower hole density and is called n-type semiconductor. Here electrons are majority carriers.

The classification of semiconductors is presented in Fig.1.4.
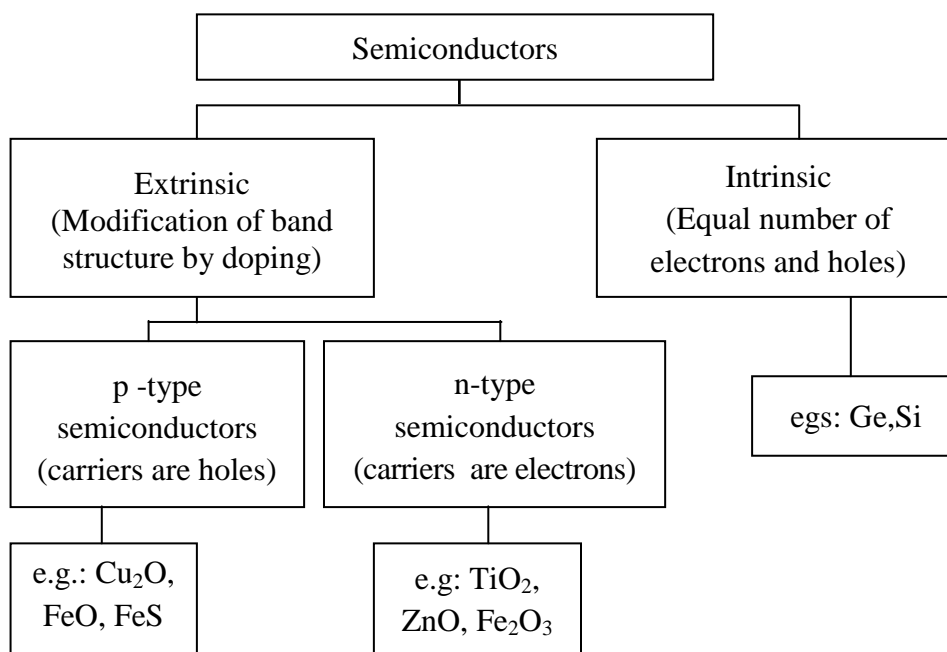
Fig.1.4: Classification of semiconductors.

Most common photocatalysts are transition metal oxides and semico nductors. All the semiconductors are not suitable for photocatalytic applications. They must have the following characteristics for photocatalysis.

    i.   Appropriate band gap (range1.7-3.2eV)

    ii.   Efficient light absorption.

    iii.   High carrier mobility.

    iv.   Non-toxic.

    v.   Chemically stable.

The photocatalytic activity depends on the ability of the catalyst to create electron– hole pairs (Eqn.4). When a semiconductor absorbs photon of energy equal to or higher than the band gap energy an electron is promoted from the valence band to the conduction band which creates a hole in the valence band. These charge carriers ultimately form reactive oxygen species (ROS) and subsequently a series of oxidation–reduction reactions occur at the photoactivated surface [23]

General mechanism of photocatalysis mediated by semiconductors can be schematically presented as in Fig.1.5. TiO_2 is chosen as an example here.
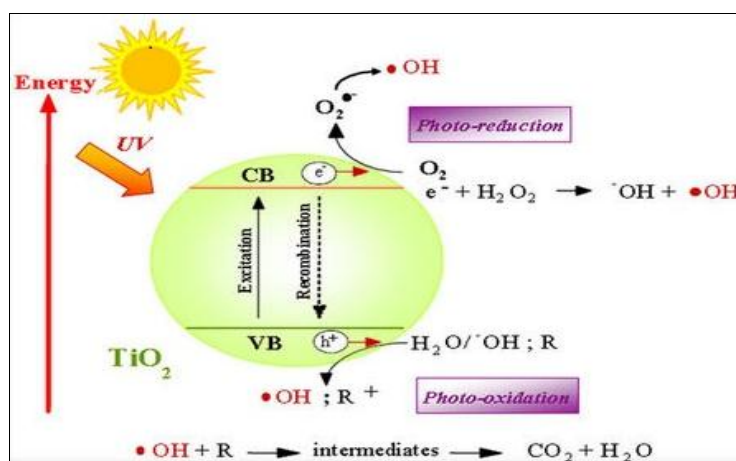
Fig. 1.5: Diagram illustrating the general mechanism of semiconductor photocatalysis.

ZnO and TiO_2 are two of the most commonly used photocatalysts.

The general mechanism can be better illustrated (with TiO_2 semiconductor as an example) as follows:

$$TiO_2 + hv \rightarrow TiO_2\,(e^- + h^+) \quad \text{......(4)}$$

Two major oxidation reactions can take place at the valence band of TiO_2.

(i) Adsorbed organic pollutants (RH) can be directly oxidized by the hole TiO_2 (h^+) producing cationic radicals $RH^{\bullet+}$ (Eqn. 5).

(ii) The hole can react with an adsorbed water molecule or OH^- anions to form powerful $^{\bullet}OH$ radicals (Eqns. 6 and 7) that can subsequently initiate the degradation of organic compounds.

$$TiO_2\,(h^+) + RH_{ads} \rightarrow TiO_2 + RH^{\bullet+}_{ads} \leftrightarrow TiO_2 + R^{\bullet}_{ads} + H^+ \quad \text{......(5)}$$
$$h^+ + H_2O \rightarrow HO^{\bullet} + H^+ \quad \text{......(6)}$$
$$h^+ + HO^- \rightarrow HO^{\bullet} \quad \text{......(7)}$$
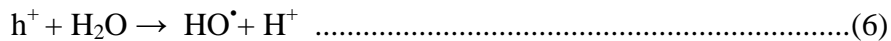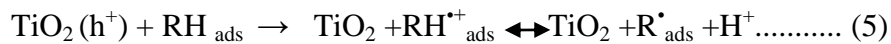
When molecular oxygen is, adsorbed onto the surface of TiO_2 it can scavenge an electron to form the superoxide radical anion, $O_2^{\bullet-}$ (Eqn.8) which can further give rise to •OH through a series of reactions (Eqns.9-11).

$$TiO_2\,(e^-) + O_2 \rightarrow TiO_2 + O_2^{\bullet-} \quad \text{......(8)}$$
$$O_2^{\bullet-}{}_{(ads)} + H^+ \leftrightarrow HO_2^{\bullet}{}_{,(ads)} \quad \text{......(9)}$$
$$2HO_2^{\bullet}{}_{(ads)} \leftrightarrow H_2O_2{}_{(ads)} + O_{2,(ads)} \quad \text{......(10)}$$
$$TiO_2\,(e-) + H_2O_2{}_{,(ads)} \rightarrow TiO_2 + {}^{\bullet}OH_{(ads)} + {}^-OH_{(ads)} \quad \text{......(11)}$$
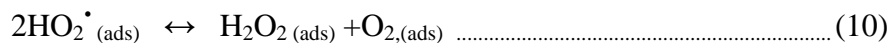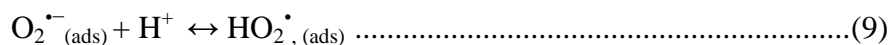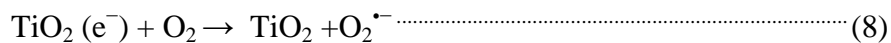
Among the various semiconductor oxides Degussa P25 (TiO_2) is the most studied one because of its non-toxicity, hydrophilicity, low cost and

resistance to photocorrosion. But it has some limitations, such as poor light absorption in the visible region and agglomeration of catalyst particles. Several binary oxides with TiO_2 as one component have been tested as photocatalytic materials. The other component includes ZnO, WO_3, Fe_2O_3, Nb_2O_5, V_2O_5, ZrO_2, CeO_2, CuO, MnO_2, Co_3O_4, NiO etc. Based on the synthetic procedures applied for the preparation, some of these have shown higher photocatalytic acitivity than TiO_2, for the degradation of pollutants.

Thermodynamically, valence band holes can oxidize adsorbed compounds if the redox potential of the VB is more positive than that of the adsorbates. Similarly, CB electrons can reduce adsorbed species if they have a more negative redox potential than the adsorbates. The band edge positions of several semiconductors in contact with aqueous media at pH=1 are given in Fig.1.6.
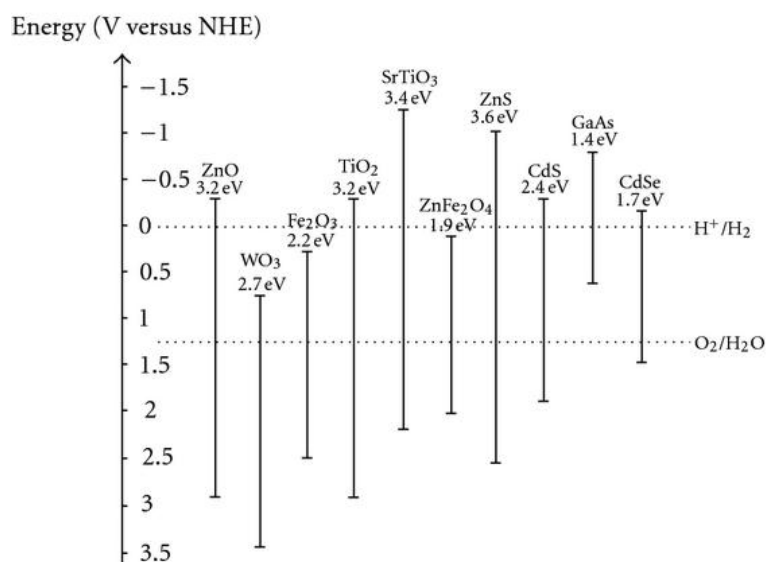
Fig. 1.6: Band edge positions of various semiconductor oxides at pH=1.

Usually the band edge positions of these oxides change with change in pH of the system and the efficiency of the photocatalyst depends on many factors, especially the intrinsic and extrinsic factors of the semiconductor. Intrinsic factors include crystallographic phase, crystallite size, presence of dopants and different surface sites, where as the pH of the system, concentration of the pollutant, light intensity, catalyst dosage etc contribute to the extrinsic factors.

1.2.2.1.1 Typical Photocatalytic degradation studies

Photocatalysis is highly effective for the degradation of organic pollutants such as petrochemicals, dyes, pesticides, pharmaceuticals etc. One major advantage of this process is the potential to use natural sunlight as the energy source. With the help of a highly active catalyst, this technology could be applied not only for water treatment, but for hydrogen production, self-cleaning coatings, and many other uses. Most of the reviews are focused on the photocatalytic activity of ZnO and TiO_2 towards waste water treatment (24).

In heterogeneous catalysis, the catalysts are in suspension and the recovery of the catalyst particles for reuse is difficult. This leads to increase in process costs. An alternative is to prepare a photocatalyst using catalyst support without affecting its photocatalytic activity. It provides very high surface area to volume ratio with low mass transfer limitations. Few studies have demonstrated the efficiency of photocatalysts using continuous flow reactors with fixed-bed photocatalysts [25]. Similarly, several studies have been focused on the synthesis and modification of nanostructured TiO_2 by making composite photocatalysts

with ceramics like SiO_2, ZrO_2, Al_2O_3 as well as semiconductor coated polymers in order to eliminate the above disadvantages.

Photocatalysis is being widely used in the decolourisation of industrial wastewaters especially those containing dye effluents. The textile industries consume huge amounts of water. Decolourisation of textile wastewater is equally or more important than the removal of colourless compounds [26, 27] because the treated water can be used in other industries or in agriculture that requires only lower quality of water. Decolourisation is important because of aesthetic and environmental concerns.

Hussen et al. [28] investigated the photocatalytic decolourization of two field samples from dye industrial effluents and also one simulated sample under high pressure mercury lamp using titanium dioxide (anatase and rutile) and zinc oxide as catalysts. The effects of various operational parameters such as catalyst mass, type of catalyst, type of reactor, type of dye, dye concentration, and temperature were investigated. The effect of type of catalyst (rutile, anatase, and zinc oxide) on the decolourization of real textile industrial wastewater showed that the activity of the catalysts follows the sequence

$$ZnO > TiO_2 \text{ (Anatase)} > TiO_2 \text{ (Rutile)}.$$

Complete decolourization of textile industrial wastewater could be obtained, in less than one hour of irradiation at 320 K, when 3.5 g L^{-1} ZnO was used and in less than 1.5 hours, when 1.75 g L^{-1} of anatase was used at the same temperature. The results indicate clearly that titanium

dioxide and zinc oxide could be used successfully in photocatalytic treatment of textile industrial wastewater.

Pekakis et al. [29] investigated the photocatalytic degradation of actual textile dye house water in presence of TiO_2. The UV-A induced degradation was capable of removing the dye stuff, as well as reducing COD after 4 hours of treatment.

The photocatalytic degradation efficiency of pure and Ag deposited TiO_2 was investigated by taking Methylene Blue (MB) as a model compound [30]. The effects of various operational parameters such as catalyst dosage, pH, concentration of the dye etc., were also investigated. As catalyst dosage increases degradation of dye also increases and reaches a maximum at 0.2 g/L. Beyond this dosage the degradation decreases. The degradation increases as the pH increases and the maximum is observed at pH 11. Time is also a factor and maximum degradation efficiency is observed in 80 min. From ANOVA results it is observed that the degradation time is the most influencing factor followed by pH and catalyst amount. The degradation in presence of Ag- TiO_2 was 94.21% while that in presence of un-deposited TiO_2 was only 63%.

The photocatalytic decolourization and mineralization of C. I. Basic Blue 41 (BB41) was studied using TiO_2 nanoparticles [31]. The reaction follows pseudo first order kinetics and Langmuir-Hinshelwood (L-H) mechanism. The % removal of the dye increases with increase in catalyst loading and reaches an optimum. Any further increase in catalyst loading will have no effect on photocatalytic activity.

The photo catalytic degradation of methylene blue in presence of photocatalyst & UV light were carried out in the batch photo reactor [32]. Titanium dioxide (TiO_2) and zinc oxide (ZnO) were used as the photo catalysts. The decolourisation efficiency increases with increase in pH exhibiting a maximum rate of degradation at pH 2. The addition of H_2O_2 in presence of UV, increases the decolourisation efficiency by the formation of hydroxyl radicals by the dissociation of H_2O_2. However at high concentration, H_2O_2 itself acts as scavenger of ˙OH radicals. Therefore, an optimum concentration of H_2O_2 should be used to achieve the best degradation. The maximum degradation efficiency of dye was achieved with the combination of $UV+H_2O_2+ZnO$. The complete decolourisation occurred in $\leq$ 90 min. The reaction follows first order kinetics.

Photocatalytic oxidation of phenol red was studied using nanocrystalline TiO_2 particle [33]. The study was aimed at elucidating the impacts of several processing parameters, such as initial concentration of the dye, photocatalyst dosage, initial pH, UV light intensity, initial H_2O_2 concentration, photocatalyst particle size and irradiation time on the photodegradation of phenol red employing synthesized slurry of nanoTiO$_2$ particles. The prepared nanoTiO$_2$ powder was found to have a large surface area and mesoporosity which enhances the speed of photocatalytic reaction. pH plays an important role in the degradation of phenol red and the optimum is at pH of 4.5. The impact of light intensity on the degradation was also studied. At low light intensity, reactions involving electron–hole formation are predominant, and electron–hole recombination is negligible. However, at increased light intensity, e^-/h^+

pair separation competes with recombination, thereby diminishing the reaction rate. Maximum quantum yields are obtained at lower light intensities. Electron acceptors such as H_2O_2 and O_2 in the reaction system inhibit the e^-/h^+ recombination. The degradation is 60 % in presence of O_2+TiO_2 where as it is 95% in presence of $O_2+H_2O_2+TiO_2$. The photocatalytic oxidation follows a L–H model which demonstrates the pseudo first order kinetics with respect to the initial concentration of the dye within the experimental concentration range. The effect of temperature from 293 to 318 K showed that the apparent rate constants follow the Arrhenius relation. The activation energy of the degradation of phenol red was found to be 38 kJ mol^{-1}.

Photodegradation of Acid Orange 67 in presence of TiO_2 was investigated in presence of visible light and UV light [34]. Complete degradation of dye requires more time under solar irradiation than under UV. The energy of UV irradiation is larger compared to the band gap energy of catalysts. Hence the problem of electron–hole recombination is largely avoided with UV source. Sunlight possesses only 5% UV component which is the quantum of energy for photo catalytic excitation and ultimate degradation of textile dyes. In the presence of visible light the degradation increases with an increase in pH up to 8.5 beyond which the degradation decreases. This is due to the presence of more OH$^-$ ions which make the surface of semiconductor negatively charged and will repel the approach of anionic dye molecules towards the surface. Same trend is observed in case of UV also. The reaction follows pseudo first order kinetics.

A comprehensive review on fundamental principles and application of heterogeneous photocatalytic degradation of dyes in solution summarising the effect of various reaction parameters and presence of additives on the TiO_2-photocatalysed degradation of dyes has been done by Rauf and Ashraf [35]. The degradation pathways, intermediates formed during the degradation etc are also discussed. pH has a strong influence on the degradation. Titania has a Point of Zero Charge (PZC) of 6.3 and hence its surface becomes positively charged in acidic medium and negatively charged in the alkaline medium. Titania have higher oxidising activity at lower pH. However excess H^+ decreases the rate of degradation. Acid Yellow17 has shown high degradation at pH 3 whereas Amido Black10 B has maximum degradation at pH 9. The presence of anions present in the dye solution also affect the degradation. The presence of CO_3^{2-} and HCO_3^- decreases the dye degradation because they scavenge $\cdot OH$ radicals. Similarly decrease in degradation in presence of Cl^- is due to its hole and $\cdot OH$ radical scavenging effect. SO_4^{2-} ions also inhibit the degradation because they react with $\cdot OH$ radicals and form relatively less reactive $SO_4^{\cdot -}$. $S_2O_8^{2-}$ also decreases the degradation because it produces sulphate ions in solution. BrO_3^- reacts in solution to form bromide ions which react with $\cdot OH$. This also leads to a decrease in the degradation of the dye. Increase in temperature increases the recombination of charge carriers and enhances the desorption process. This leads to a decrease in the photocatalytic activity. The use of TiO_2 in the photodegradation of monoazo and diazo dyes has been investigated. Diazo dyes are less degradable than monoazo dyes. Some of the intermediates identified were aromatic amines, phenolic compounds and

several organic acids. The degradation of triazine containing azo dyes, Procion Red MX-5B and Reactive Brilliant Red K-2G, was studied in order to identify the effect of substituent on the photocatalytic degradation. The decolourization and desulfuration occurred in the first step of photooxidation. The substituent attached to naphthalene moety of dye is hydroxylated more easily than those linked to triazine group. Cyanuric acid was the final product for both azo dyes. Several cationic and anionic dyes have been subjected to photodegradation in presence of TiO_2 and it was found that cationic dyes degrade faster than the anionic dyes. Doping with transition metals such as Pt, Li^+, Zn^{2+}, Cd^{2+}, Ag^+, Co^{3+}, Cr^{3+}, Fe^{3+}, Al^{3+} enhances the photocatalytic degradation by scavenging the electrons or modifying the surface properties of materials.

Wastewater containing pharmaceuticals, pesticides and petrochemicals can be treated by TiO_2-based photocatalysis. Elmolla et al. [36] investigated the degradation of antibiotic aqueous solutions containing ampicillin, amoxicillin and cloxacillin by different advanced oxidation processes such as Fenton, photo-Fenton, TiO_2- Photocatalysis and UV-ZnO process. The effect of various reaction parameters on the degradation was studied. It was found that homogeneous advanced oxidation processes (Fenton and photo-Fenton) are more effective for the degradation and mineralisation of antibiotics than heterogeneous processes (TiO_2 Photocatalysis and UV-ZnO process). The best operating conditions for the treatment of aqueous solution containing 104,105 and 103 mg/L amoxicillin, ampicillin, cloxacillin were : Fenton process- $UV/H_2O_2/Fe^{2+}$ molar ratio 1:3:0.30 and pH 3; Photo Fenton - $UV/H_2O_2/Fe^{2+}$ molar ratio 1:1.5:0.075 and pH 3; $UV/TiO_2/H_2O_2$ − TiO_2 1g/L, pH ≈ 5 and H_2O_2 100 g/L;

UV/ZnO process- ZnO 0.5 g/L and pH 11. All processes are able to improve biodegradability except UV/ZnO process. Photo Fenton showed the highest pseudo first order rate constant which is 1.4, 28 and 25 times higher than that of Fenton, $UV/TiO_2/H_2O_2$ and UV/ZnO processes respectively. It may due to the photochemical regeneration of Fe^{2+} ions by the photoreduction of Fe^{3+} and the increased hydroxyl radical production rate. Thus Photo-Fenton was found to be the most efficient method compared to others for the degradation of antibiotics.

Stapleton et al. [37] investigated the photolytic/TiO_2-photocatalytic degradation and mineralisation of 2-chloropyridine (2-CPY), 2-fluoropyridine (2-FPY) and 2-hydroxypyridine (2-HPY) (extensively used for the production of pesticides, medicinal drugs, industrial solvents, dyes, rubber chemicals etc.) by means of ultraviolet irradiation at 254 nm under a range of conditions. The effects of the radical scavenger tert-butanol, pH, different ions etc. were assessed. The photolytic 2-CPY removal rate was found to be unaffected by pH. Photocatalytic removal is faster at higher (controlled) pH values. Tert-butanol has only a marginal effect on the photocatalytic removal of 2-CPY indicating that the reaction rate is not exclusively due to hydroxyl radicals. The reaction in this case proceeds largely by charge transfer when 2-CPY is adsorbed on the TiO_2 surface and to a very limited extent by hydroxyl radical attack in the bulk of the liquid. This supports the view that higher 2-CPY removal rate under controlled pH is predominantly due to the greater substrate adsorption on the photocatalyst. The photocatalytic degradation of 2-hydroxypyridine (2-HPY), a major photolytic product of all 2-Halo Pyridines (2-HalPys) is studied under a range of conditions. The degradation is faster at lower

pH. Presence of chloride anions, which act as radical scavengers, had a detrimental effect on the degradation rate. Their scavenging effect was more significant at low pH. On the other hand, F^- and SO_4^{2-} anions accelerated the degradation. 2-hydroxypyridine and 2-chloro-3-pyridinol are the first major intermediates produced from 2-CPY, by photolysis and photocatalysis respectively. Hydroxyacetaldehyde, 2-pyridinecarboxylic acid and N-formyl-3-carbamoylpropenal were identified as later products formed from purely photocatalytic destruction of 2-CPY. Complete TOC removal was achieved in all cases. Photocatalytic TOC removal was faster than the photolytic process under identical conditions.

The photocatalytic degradation of Naproxen (NPX) and Diclofenac (DCF) was studied using Nano- TiO_2/diatomite (NTD) as the catalyst [38]. A photocatalytic reactor made of stainless steel with an effective volume of 7 L was used. The suspended NTD concentration at the operating conditions was 0.5 g/L. Three low pressure UV lamps (16 W, Philips, Holland) with wavelength of 254 nm were introduced vertically in the middle of the reactor. The suspension was maintained homogeneous by magnetic stirring. Provision for coarse bubble aeration was given at the bottom of the reactor to supply continued aeration and effective turbulent flow. A constant temperature of 27 °C was maintained in the reactor using a jacket through which water was circulated. Under the condition of a higher UV irradiation intensity and a lower initial concentration, NPX and DCF can be degraded completely at a flux of 3.0 L/h in 360 min and 30min, respectively. UV irradiation intensity plays more significant role in the degradation of DCF, compared with that of NPX. The nature of by

products showed that demethylation and decarboxylation are the principal initial processes in the degradation of NPX.

Akach et al. [39] investigated the solar photocatalytic degradation of Diclofenac in wastewater using activated carbon-TiO_2-silica xerogel (CTS) composite catalyst. The experiments were carried out in three phase fluidised bed reactors (FBPR), made of borosilicate glass which has a high transmittance of the solar UV. The distributor plate of the FBPR was made of sintered glass (pore size $10 - 16$ μm). Air was bubbled through the FBPR to induce fluidization of the composite catalyst. Adsorption and degradation studies were carried out. Effect of composite mass, superficial air velocity and initial concentration of DCF was studied in detail. Adsorption as well as degradation increase with increase in composite mass and reach an optimum at 1.5 g/L beyond which it is stabilised. This may be due to the shielding of some catalyst particles by others from sunlight. Adsorption and degradation of DCF increased with increasing superficial air velocity up to an optimum of 0.007 m/s beyond which no further increase was observed. Settling of catalyst particles on the wall and distributor of the reactor is a major problem. Only those CTS particles at the very top of the distributor were exposed to sunlight and could therefore photo degrade the DCF molecules. At the optimum superficial air velocity of 0.007 m/s, settling of the CTS on the reactor walls and distributor reduced markedly. Further increase in superficial air velocity, did not increase the adsorption or photo degradation. This was due to the fact that the maximum surface area of the catalyst is achieved at an air velocity of 0.007 m/s.

Czech et.al [40] studied the photocatalytic degradation of diclofenac, metoprolol, estrone and chloramphenicol using different commercially available TiO_2 samples. Photocatalytic degradation was conducted in a tube reactor with a UV source having a light intensity of 2 mW/cm^2. In the case of DCF almost 65% degradation is obtained within first 20-40 minutes. Anatase has high photocatalytic efficiency for the degradation of estrone, diclofenac and chloramphenicol. The efficiency decreases in presence of rutile TiO_2. But in the case of metoprolol, the presence of rutile enhances the degradation efficiency. Degradation of all the pollutants studied here follows pseudo-first order kinetics. The highest initial reaction rate was obtained for metoprolol removal.

Photodegradation of Diquat and Paraquat [41] pesticides in aqueous solution was investigated using TiO_2 as the catalyst. The effects of pH and types of catalyst on the degradation were studied. Both commercial and laboratory synthesized (sol gel method) TiO_2 are used as catalysts. The radiation source used was 125W mercury vapour lamp. Degradation is enhanced in the case of diquat and paraquat under highly alkaline conditions. Decrease in degradation was observed under high by acidic conditions, especially in the case of diquat. The catalytic activity of TiO_2 Degussa P25 is more compared to home-prepared pure anatase crystals. The efficiency of the catalyst depends on its grain size, the higher the grain size, the lower the active surface area and hence the less the activity. Degradation products were identified by ESI mass spectra. Complete degradation of paraquat is accomplished within 12 hr of irradiation. However diquat requires much more time for complete degradation. Hence diquat is more persistent than paraquat.

Cruz et al. [42] studied the photoactivity of TiO_2 and Graphene – TiO_2 (G-TiO_2) on the degradation of selected pesticides diuron, alachlor, isoproturon and atrazine in different water matrices (ultrapure and natural water). Ten daylight fluorescent lamps were used to obtain a spectral distribution close to the solar spectrum. The solution containing a mixture of these pollutants was taken and the adsorption as well as degradation was studied in two water matrices. In presence of ultrapure water, almost all pesticides were oxidized after 300min of irradiation. But in presence of natural water, the degradation decreases. In presence of bare TiO_2, TOC conversion was 12% and 7% in ultrapure and natural water respectively but in the case of G-TiO_2, it was 42% and 38% respectively. But in case of bare TiO_2-natural water matrix, some of the naturally occurring ions present in water, act as holes or hydroxyl radical scavengers and produce less active oxidants, resulting in decreased degradation efficiency. In the case of G-TiO_2, good interfacial coupling between graphene and TiO_2 promotes charge migration between the phases, lower the pH $_{zpc}$ and quench photoluminescence under visible and Near Infra Red (NIR) laser excitation. Thus photogenerated electrons in TiO_2 are transferred to Graphene thereby inhibiting charge recombination. These advantages of G-TiO_2 over TiO_2, contribute to the enhanced photocatalytic acivity.

Saien et al. [43] reported the degradation of the fungicide carbendazim in aqueous solutions using UV/TiO_2 process. The effect of operation parameters such as catalyst concentration, pH and temperature were investigated. The results showed that degradation of this fungicide proceeds under UV- irradiation as well as UV/TiO_2, photocatalysis and the latter is more efficient than the former. Degradation of more than 90% was

Microwave, Photo and Sono Activated Advanced Oxidation Processes and their Variations for the Decontamination of Water from Toxic Chemical Pollutants

25

achieved under optimal operational conditions of 70 mg L−1 of catalyst, natural pH of 6.73 and ambient temperature of 25 °C after 75 min irradiation. The reaction kinetics follows L-H mechanism.

Lhomme et al. [44] reported the degradation of pesticide cyproconazole by photocatalysis using TiO_2 coated on non-woven paper. Only 20% of the pollutant is degraded after 95h of UV irradiation in the absence of any catalyst. But in the presence of TiO_2, complete degradation was obtained within 12h of irradiation. Degradation kinetics was explained using L-H mechanism. Intermediates and final products were identified by LC-MS analysis. The use of TiO_2 coated on non-woven paper was found to be highly efficient for degrading and mineralising cyproconazole.

Phenol(PH) and Cumene Hydroperoxide (CHP) are hardly degraded by photolysis but almost completely degraded by photocatalysis in 4 h. Acetophenone (ACP) can be degraded by both photolysis and photocatalysis, but the latter is much more effective. The photocatalytic degradation rates is in descending order are ACP > CHP > PH [45]

Nano sized photocatalysts are found to be more active than those of the normal size because of its Quantum size effect and Higher Specific Surface Area. They have been widely used in the treatment of waste water. Hoffmann et al. [46] reported that selectively doped quantum- (Q-) sized particles have a much greater photoreactivity for oxidation and reduction than their undoped counterparts, in terms of quantum efficiency.

Meng and Juan [47] reported that nano zinc oxide is an excellent photocatalyst for the treatment of wastewater, contaminated with

pharmaceuticals, printing and dyeing wastes, papermaking industry pollutants etc. It can also absorb a wider spectrum of light. Its catalytic activity is influenced by the dosage of the catalyst, the original concentration of reactants, time and intensity of illumination, pH value, atmosphere (oxygen), etc.

Anatase TiO_2 is widely used for the degradation of a variety of pollutants. However it is thermodynamically meta stable and changes to rutile with severe sintering or growth of TiO_2 crystallites. Moreover, there are chances for the recombination of holes and electrons in larger crystalline materials. This phase transformation can be minimized by doping a metal or metal oxide into titania which enhances the photocatalytic activity. Reddy et al. [48] reported the preparation of titania–silica, titania–alumina, and titania–zirconia mixed oxides (1:1 molar ratio) by a microwave-induced solution combustion synthesis technique. The prepared materials were characterized by different techniques. All prepared samples possess large surface area in decreasing order TiO_2–SiO_2 > TiO_2–Al_2O_3 > TiO_2–ZrO_2. TGA analysis showed there was no phase transformation during the preparation of these materials. In photocatalysis the rate of degradation is directly proportional to the adsorption capacity of the catalyst. The adsorption of phenol in dark was found to be 68, 55, and 63% on samples of TiO_2–SiO_2, TiO_2–Al_2O_3, TiO_2–ZrO_2 respectively. Among the three materials, TiO_2–SiO_2 showed highest activity for phenol degradation (more than 95% of phenol was degraded within 3hrs of irradiation time) due to its higher surface area as well as higher adsorption.

Carbon and its different forms such as graphene and carbon nano tubes were incorporated in to TiO_2 and the ability of the material to enhance its photocatalytic activity is tested. Alosfur et al. [49] used a modified microwave technique to rapidly synthesise a TiO_2/ MWCNT (microwave carbon nano tube) nanocatalyst with a large surface area and the photocatalytic activity of the hybrid nanocatalyst was evaluated through a comparison of the degradation of methylene blue dye under irradiation with ultraviolet and visible light. The results showed that the TiO_2/MWCNT hybrid nanocatalyst degraded 34.9% of the methylene blue (MB) under irradiation with ultraviolet light, whereas 96.3% of the MB was degraded under irradiation with visible light in 120 minutes.

Zhang et al. [50] fabricated Core/shell nanofibers of TiO_2@carbon embedded by Ag nanoparticles (TiO_2@C/Ag NFs) by combining the electrospinning technique, the hydrothermal method and an in situ reduction approach. Photocatalytic activity of catalyst was evaluated by the degradation of methylene blue dye under visible light irradiation. Studies revealed that the TiO_2@C/Ag NFs exhibited enhanced photocatalytic efficiency for the photodegradation of Rhodamine B (RB) and Methyl Orange (MO) compared to pure TiO_2 nanofibers. The catalyst could be recycled without reduction in the photocatalytic activity.

Tang et al. [51] reported a novel photocatalyst i.e. Bi_2WO_6/Ag_2S hetero structures prepared by 3-mercaptopropionic acid (MPA)-assisted route at room temperature. The new material exhibited enhanced photocatalytic activity for the degradation of Rhodamine B (Rh B) under visible-light irradiation. This may be due to the synergistic effects of the

effective electron-hole separation combined with expansion of the light-absorption range. The pH of the solution plays a vital role in the photocatalytic activity of Bi_2WO_6/Ag_2S hetero structures. At low pH value, the photosensitization process is suppressed, while it is favoured at higher pH.

Savoskin et al. [52] reported a new method for producing TiO_2-exfoliated graphite amorphous carbon composites which was highly efficient for the photocatalytic degradation of phenol.

ZnO is another important semiconductor with significant photocatalytic activity and finds application in many areas such as biosensors, light emitting diodes, gas sensing and solar photovoltaics. ZnO is a photoactive semiconductor oxide, and hence it can be self activated by taking energy from incident photons. It can adsorb O_2 and the organic pollutant molecule simultaneously. It is an efficient photocatalyst for water detoxification, organic pollutant decomposition, photolysis etc. Hydrogen peroxide is an important product in all these cases, which is also a powerful oxidiser. [53-54]

Shibin et al. [55] investigated the solar photocatalytic removal of trace amounts of Alfa-Methyl styrene (AMS), Diquat and Indigo Carmine (IC) from water using ZnO catalyst. The effect of various reaction parameters such as catalyst loading, concentration, pH etc on the degradation was studied. The rate of degradation increases with increase in catalyst loading and reaches an optimum. Thereafter the rate stabilises in the case of AMS and Diquat but it decreases in the case of IC. The degradation follows pseudo first order kinetics at lower concentration

Microwave, Photo and Sono Activated Advanced Oxidation Processes and their Variations for the Decontamination of Water from Toxic Chemical Pollutants

29

which becomes zero order at higher concentration. The role of pH on the degradation of pollutants was investigated. In the case of diquat only acidic range was studied because the molecule undergoes self hydrolysis in the alkaline pH. Maximum degradation is obtained at pH 5. In the case of IC and AMS, maximum degradation is obtained at pH 4-5. Concentration of H_2O_2 formed during the degradation process undergoes an oscillatory pattern due to concurrent decomposition. The study reveals the role of ZnO as an efficient solar photocatalyst for the degradation of multiple pollutants.

Phonsy et al. [56] studied the photocatalytic degradation of polyethylene plastic waste. In the normal course, polyethylene takes 1000 years for degradation in the natural environment. The effect of ZnO and TiO_2 mediated photocatalysis on the degradation of plastics was profound. It was found that TiO_2 is 20% more efficient than ZnO. The authors reported ~ 12% degradation of polyethylene plastic in presence of TiO_2/PS (persulfate) under UV photolysis in ~ 400 hr time. Degradation is pH dependent with more degradation in the acidic range. However considerable degradation occurs in the neutral pH also. Oxidizers such as H_2O_2 and peroxydisulfate (PDS) enhance the degradation. PDS is three times more efficient than H_2O_2. A mechanism based on the observations is also proposed.

The light source used in photocatalysis plays an important role in the degradation of pollutants. At high intensity the e^- –h^+ formation is predominant and e^- –h^+ recombination is insignificant. But when the intensity is low separation of e^- –h^+ pair competes with recombination

resulting in a decrease in the formation of reactive free radicals. Consequently, the % degradation of the pollutant also decreased. In the case of TiO_2 and ZnO the absorption in the visible region is low. So in order to improve the absorption of visible light, the structure has to be modified especially the band gap energy. A number of reviews have been published in this field, highlighting the importance of modification of the semiconductors to enhance the photocatalytic efficiency and visible light activity [57-60].

Wantala et al. [61] reported that Mn doped TiO_2 prepared by impregnation method is an efficient photocatalyst for the degradation of Reactive Red-3 dye in aqueous solution. The effect of various reaction parameters such as catalyst loading, pH, concentration of the substrate etc on the degradation was studied. When Mn^{2+} is incorporated in TiO_2 the anatase phase is not affected. But rutile phase increases with increasing Mn^{2+} content. The band gap energy of Mn doped on TiO_2 did not show red shift though it exhibited higher absorbance than neat TiO_2 in visible region.

Mittal et al. [62] investigated the photocatalytic degradation of Rose Bengal (RB) using MnO_2 as the catalyst. The effect of various reaction parameters, on the degradation was studied. pH of the medium and intensity of light influence the degradation significantly.

Hankare et al. [63] also studied the photocatalytic degradation of Rose Bengal in visible light using Cr substituted $MnFe_2O_4$ ferrospinel as the catalyst. The degradation was studied over different compositions of $MnFe_{2-x}Cr_xO_4$ ($0 \leq x \leq 2.0$) catalyst. The efficiency of the catalyst was

$MnFe_2O_4 < MnFe_{1.5}Cr_{0.5}O_4 < MnFe_{1.0}Cr_{1.0}O_4 < MnFe_{0.5}Cr_{1.5}O_4 < MnCr_2O_4$. The rate of degradation decreased with increase in concentration of the dye which may be due to the poor penetration of light through the medium and consequent decrease in the energy available for the activation of the catalyst. The rate of degradation increases with increase in pH up to 7 and then decreases. The amount of catalyst also plays an important role in the rate of degradation upto optimum then decreases. The activity of recycled catalyst decreases for each cycle, which is attributed to the fouling of the catalyst and loss of catalyst particles during separation.

Mogal et al. [64] reported that doping of TiO_2 with various metals like Ag, Ni, Co, Au, Cu, V, Ru, Fe, La, Pt, Cr, Ce, etc. influences the band gap, surface area, particle size and thermal property. The photocatalytic activity towards degradation of pollutants is also enhanced by this modification. The modified catalyst absorbs light in visible region. (i.e. at wavelength >400 nm). Different synthesis routes for doping and its effect on the structural, and photocatalytic properties of titanium dioxide have been reviewed.

Schneider and co-workers [65] prepared various visible light responsive photocatalyts applying transition metal implantation. Implantation of metal such as V, Cr, Mn, Fe and Ni resulted in a large shift in the absorption band of TiO_2 catalyst towards the visible light region. Among the various ions tested, Cr and V were especially effective to induce a red shift of absorption band of TiO_2.

One of the consistent conclusions from all these studies is that the effect of pH on the photodegradation is a complex process. This is

explained based on the 3 possible mechanisms of dye degradation. (1) ·OH attack (2) direct oxidation by holes (3) direct reduction by e⁻ in the conduction band [66-67]. pH also influences the surface properties of the catalyst. There is no consistent or universally applicable mechanism for the pH effect on the photocatalytic degradation of dyes. Different authors report different results which are explained based on the interplay of a number of factors such as physicochemical characteristics of the catalyst, substrates and the additives. A number of operating parameters such as catalyst loading [68], concentration of the pollutant [69], temperature of the system [70] nature of the catalyst [71] etc influence the photocatalytic degradation of pollutants.

1.2.2.2 Sonocatalysis for the decontamination of water

Ultra Sound (US) in the frequency range 20-1000 KHz (above the hearing capacity of human beings) is being investigated, of late, as an energy source in the field of environmental remediation, to remove persistent organic chemicals in wastewater. US and US based catalytic processes are effective tools for degrading a variety of pollutants including dyes. US waves consist of compression and rarefaction cycles [72]. During compression cycle a positive pressure is created on liquid which pushes the molecules together. In rarefaction cycle a negative pressure is created which pull the molecules apart. So when the distance between molecules exceeds the specific molecular distance required to hold the liquid together (for water molecules the critical molecular distance R is 10^{-8} m) cavities/voids can be generated [73]. Application of US mainly depends upon the formation, growth and collapse of

Microwave, Photo and Sono Activated Advanced Oxidation Processes and their Variations for the Decontamination of Water from Toxic Chemical Pollutants

33

microbubbles from acoustic wave. Schematic presentation of the formation, growth and collapse of cavitation bubbles is shown in Fig.1.7.
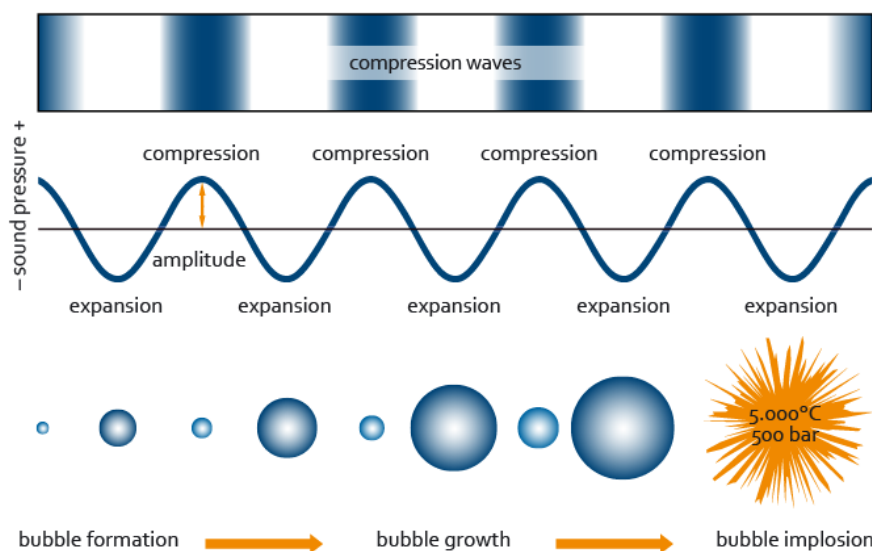
Fig. 1.7: Schematic presentation of the formation, growth and collapse of cavitation bubbles.

There are 3 main theories about cavitation- i.e. hot spot theory, electrical theory and plasma theory. The most recognised theory is the hot spot theory. Collapse of the cavitational bubbles creates localised hot spots in an irradiated liquid. As a result of this, very high temperatures of 2000-5000 K and pressures up to 1800 atm are created inside the collapsing cavity. Under this extreme condition, O_2 molecules and water molecules are cleaved to produce free radicals. These free radicals are highly active and lead to the degradation of pollutants.

In the case of homogenous liquids irradiated with US the reactions occur in three different regions as shown in   Fig.1.8.
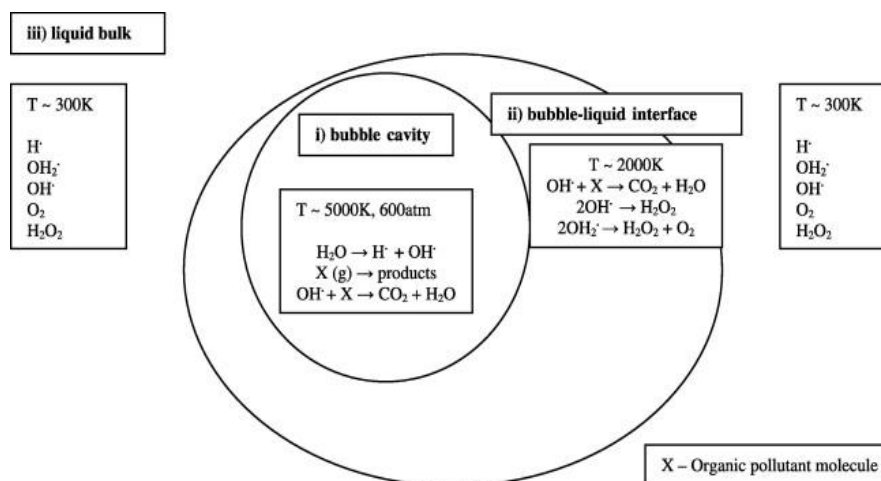
Fig. 1.8: Schematic presentation of three different zones of US.

i)   Cavity interior of the bubble

Very high temperature and pressure are created in the interior of the bubble (600atm pressure and 5000 °C temperature).

$^{\bullet}$OH Radicals are formed mainly by the pyrolysis of water and to a smaller extent by sonolysis.

$$H_2O \quad >>> \quad H^{\bullet} + {}^{\bullet}OH \quad \dots\dots\dots\dots\dots\dots\dots\dots\dots\dots\dots\dots\dots\dots\dots\dots\dots(12)$$

Most of the volatile and hydrophobic species are degraded through pyrolytic reaction.

ii)   Liquid –Gas interface

Region between bubbles and bulk solution. Very high concentration of $^{\bullet}$OH radicals is achieved here which was estimated to be as high as 4μM. Here also temperature increases up to 2000K. Oxidation of organic pollutants (particularly hydrophobic and non – volatile ones) takes place

mainly in this phase. Heterogeneous catalytic reactions are occurring in this region.

iii) Bulk solution media

Here small amount of $^{\cdot}$OH radicals diffuse from bulk- liquid interface to the bulk solution (approx. 10% of the generated $^{\cdot}$OH radicals). Diffusion of $^{\cdot}$OH radical depends on the frequency and power, reactor geometry, presence of oxidants etc. Here also hydrophobic and non-volatile compounds are degraded but to a smaller extent compared to liquid-gas interface.

Many factors affect cavitation and sonochemical degradation including applied frequency, input power, height of the liquid column, volume of the reactor, pH, concentration of the pollutant, presence of oxidants and presence of anions [74-78]

Sonochemical degradation proceeds not only by the interaction of $^{\cdot}$OH radical but also by direct pyrolytic reactions in the hot spot of the collapsing bubbles and at the interface region. Cavitation involves physical effects such as micro jets, acoustic streams, shock waves, intense micro and macro mixing in the solution etc. which can accelerate the degradation of molecules in many cases.

Ultrasonic irradiation alone is unable to provide high degradation efficiency in the case of recalcitrant organic pollutants. US degradation results in the rapid destruction of dye chromophoric group but mineralization of the intermediates thus formed takes place at a slow rate and requires more time. In such cases suitable catalysts such as

semiconductor metal oxides can be used to facilitate the process. The catalyst particles provide additional nuclei for bubble formation and enhance the mass transfer between solution and semiconductor surface. Further the surface area of the catalyst increases due to deaggregation of particles. In the case of heterogeneous catalyst sonoluminesence and hot spot phenomena are also possible. Sonoluminescence (light emitted by cavitational bubbles) created by cavitational collapse involves an intense UV radiation (<375nm) which excites catalyst resulting in the formation of photogenerated e^-- hole pairs. Holes react either with H_2O molecules to produce ·OH radicals or directly react with pollutant and degrade it.

The effective utilization of the ultrasound and its combination with other AOPs could achieve improved degradation of a wide spectrum of environmental pollutants and even mineralisation thereby avoiding the generation of secondary pollutants generation. Several studies have been reported on the sonolytic and sonocatalytic degradation of organic pollutants. Some important results relevant in the present context are discussed below.

1.2.2.2.1 Some typical sonocatalytic degradation studies

Sonocatalytic degradation of organic dyes in presence of TiO_2 and the influence of Al_2O_3, Y_2O_3 and Fe_2O_3 on catalytic activity of TiO_2 were investigated. The products were identified by UV-Vis spectra. The rate of degradation increase in the order $TiO_2 < Fe_2O_3/TiO_2 < Y_2O_3/TiO_2 < Al_2O_3/TiO_2$ [79]

High power ultrasonication (600 W) in the presence of porous manganese dioxide doped titanium dioxide catalysts was tested for the degradation of Methylene blue. TiO_2 alone performed better compared to porous manganese oxide doped titania catalysts in the sonocatalytic degradation of the dye. This is attributed to the fine particle size and ordered surface morphology of TiO_2. Porous manganese oxide increases the particle size, and inhibits the formation of reactive radicals which results in a lower dye degradation rate, compared with that of bulk TiO_2[80].

Destaillats et al. [81] studied the sonochemical oxidation of azobenzene or methyl orange at 500 kHz and found that the extent of mineralization measured as total organic carbon (TOC) increased to more than 80% after 150 min in the presence of O_3 as compared to 20% for US alone and 30% for O_3 alone. It was also shown that nitrobenzene (NB) and benzoquinone (BQ), two rather persistent byproducts of sonolysis, were rapidly and completely mineralized by the combined oxidation treatment. Similarly with Methyl Orange (MO), it was shown that ozonation or sonication led to about 50% TOC reductions, but their combination achieved a faster and more complete mineralization.

Sonocatalytic degradation of parathion was investigated [82] using nano rutile titanium dioxide (TiO_2) powder. The degradation of parathion surpassed 90% within 120 min of ultrasonic irradiation under optimum conditions. Eventually the parathion in aqueous solution is completely degraded and is transformed into simple inorganic ions such as NO_3^-, PO_4^{3-}, SO_4^{2-}, etc. The sonocatalytic activity of recycled TiO_2 catalysts was

also studied and was found to decline gradually with the number of recycles. The degradation was found to follow pseudo first-order kinetics.

Similar to photocatalysis, sonocatalysis also has been investigated in recent years for the removal of pharmaceutical pollutants. The degradation of the drug diclofenac [83] in water was investigated at ultrasound frequencies of 24 kHz, 216 kHz, 617 kHz, and 850 kHz in the presence of various catalysts (TiO_2, SiO_2, SnO_2, and titanosilicate). The degradation at 617 kHz followed first-order kinetics. Catalysts, especially TiO_2, increased the rate of degradation. The relative concentration of diclofenac in water decreased from 100% to 16% in the presence of titanium dioxide (P25) in 30 min irradiation. Intermediates identified by HPLC and GC-MS methods include chlorinated anilines, phenols and carboxylic acid derivatives. About 35% of organic chlorine was transformed into inorganic chloride.

Hoseini et al. [84] studied sonocatalytic degradation of tetracycline (TC) antibiotic using TiO_2 nano-particles as catalyst. The effect of pH, initial TC concentrations, reaction times, and H_2O_2 concentrations were evaluated. In presence of TiO_2, degradation was very high compared to the effect of US alone. Addition of H_2O_2 enhances the degradation. Increase of pH and concentration of pollutant decrease the degradation efficiency.

Investigations on the sonochemical degradation of n-butyric acid using 200-kHz ultrasound [85], showed that the degradation was higher in acidic solutions below pH 4. The pKa value of n-butyric acid (C_3H_7COOH)

Microwave, Photo and Sono Activated Advanced Oxidation Processes and their Variations for the Decontamination of Water from Toxic Chemical Pollutants

39

is 4.63 at 25°C. As a result, the major chemical structure is C_3H_7COOH at pH less than 4 and $C_3H_7COO^-$ at pH greater than 5. Therefore, the more highly hydrophobic compound C_3H_7COOH degraded faster than $C_3H_7COO^-$.

Khataee et al. [86] studied the sonocatalytic degradation of Reactive Orange 29(RO 29) using Er- doped ZnO catalyst. The effect of various reaction parameters such as catalyst loading, concentration of dye, ultrasound power etc. on the degradation of dye was studied. The decolourisation efficiency increases from 68% to 88% by increasing the iridium content from 2 to 4%. The % degradation decreases with increasing initial concentration of dye. For 5 and 20mg/L of dye, the degradation was 91% and 56% respectively. The strong adsorption of the dye at high concentration prevents catalyst particles from absorbing heat and energy generated by ultrasound. As a result of this the generation of hydroxyl radicals also is less, which results in decreased degradation of dye molecules. When the ultrasonic power increases from 150 to 400 W degradation increases from 88 to 93%. At high power the turbulence of the solution as well as the mass transfer rate increases and the number of reactive radicals increases. Moreover ultrasound always cleans the surface of catalyst, and helps to increase the available active surface sites. The effect of radical scavengers such as chloride, sulphate, carbonate and t-butanol was also studied. The addition of radical scavengers decreases the degradation significantly. The order of inhibition is chloride > t- butanol > carbonate > sulphate. The degradation is enhanced by the addition of oxidants persulphate and peroxide. The intermediates formed in the

treatment process were studied by GC-MS analysis. The Er-doped ZnO possess high reusable sonocatalytic activity for the degradation of pollutants.

Pang et al. [87] reviewed the fundamental aspects of ultrasound irradiation, its basic principles, the effect of catalyst and additives on the sonocatalytic degradation of organic pollutants. In this review they discussed various methods to modify TiO_2, in order to enhance the degradation rate of organic pollutants. Most often transition metals and noble gases are used as dopants. Another catalyst used is CuO. CuO-ZnO supported alumina enhances the oxidation of sodium dodecyl benzene sulphonate. The degradation of 2,4-dinitrophenol increases from 14% to 96% in presence of $CuO/H_2O_2/air$. Sonolysis of acetic acid is enhanced by the addition of zeolite and SiO_2. The role of ·OH on the mechanism of sonolysis is verified by using radical scavenger CCl_4. Addition of salts such as NaCl, $CaCl_2$, $NaHCO_3$ and KI increases the degradation of organic pollutants. However the addition of Na_2SO_4 and Na_2CO_3 inhibit the sonochemical degradation of methylene blue. The addition of H_2O_2 enhances the sonochemical degradation of organic pollutants. Under ultrasonic cavitation H_2O_2 readily decomposes to ·OH radical because the dissociation energy for O-O bond is less than O-H bond in water. In presence of 0.05M H_2O_2 the degradation of poly phenolic compound is 94% at pH 11.4. Combination of US and fenton reagent (Fe^{2+}/H_2O_2) enhances the production of ·OH radicals thereby enhancing the degradation of organic pollutants. US/ozone combination enhances the mass transfer of ozone from the gas phase to the bulk solution to react

with the substrate. The mechanism of sonocatalytic degradation follows Langmuir- Hinshelwood mechanism.

Wang et al. [88] studied the sonocatalytic degradation of organic dye acid red B using CeO_2/TiO_2, SnO_2/TiO_2, ZrO_2/TiO_2 composites. The order of sonocatalytic activity is CeO_2/TiO_2 > SnO_2/TiO_2 >TiO_2 > ZrO_2/TiO_2 > SnO_2 > ZrO_2. In presence of US irradiation only (without catalyst), the degradation is 16%. The reaction follows pseudo first order kinetics. Degradation decreases with increase in the solution pH in the case of SnO_2/TiO_2, ZrO_2/TiO_2 and TiO_2 powder. But CeO_2/TiO_2 shows a different trend, ie degradation increases with increase in pH up to 7 then it decreases. The degradation of methylene blue, rhodamine B and acid red B is compared in presence of the above catalysts. The CeO_2/TiO_2 shows high degradation efficiency in the case of rhodamine B and acid red B. Anionic dyes are completely degraded in presence of CeO_2/TiO_2 but cationic dyes are degraded efficiently.

Lakshmi et al. [89] studied the degradation of 2-chloro 5-methyl phenol using TiO_2 and H_2O_2. The experiment was carried out under US and UV. Degradation efficiency is higher at low pH when contribution from pyrolysis is more and substrate molecules enter in to the cavitation bubbles. The degradation increases with increase in temperature. At high temperature number of cavitational bubbles increases, which ultimately results in the generation of more $^{\cdot}OH$ radicals. Maximum degradation is obtained in the case of $UV/H_2O_2/TiO_2$ compared to US/H_2O_2 and US/TiO_2. The rate of degradation decreases in presence of anions in the order Cl^- > SO_4^{2-} > HPO_4^{2-} > HCO_3^-. Degradation follows pseudo first

order kinetics. The maximum COD removal was observed in the case of UV/H_2O_2/TiO_2 (70%) compared to US/H_2O_2 (35%) and US/TiO_2 (52%) after 2h of US irradiation.

Behnajady et al. [90] investigated sonocatalytic degradation of Malachite Green (MG) from aqueous solution. The effect of different operational parameters such as MG concentration, power density, temperature, mechanical agitation and addition of ethanol (EtOH), 2-propanol (2-PrOH) and iso-butanol (iso- BuOH) on the degradation were investigated. Ultrasonic bath with frequency of 35 kHz was used. The degradation decreases with increasing initial concentration and increases with increasing temperature, power density and the use of mechanical agitation. The activation energy was 30.95 kJ/mol in the temperature range of 21–34°C, suggesting a diffusion-controlled reaction. The reaction follows pseudo first order kinetics. Alcohols such as EtOH, 2-PrOH and iso-BuOH act as hydroxyl radicals scavengers which is unfavourable for the degradation. The competitive reaction of ˙OH radicals with alcohols and MG is proved with N, N-dimethyl-p-nitroso-aniline (RNO) test. UV–vis spectral change of MG on sonication showed hypsochromic shift ie wavelength change from 617 to 609 nm predicting N-demethylation route for the degradation.

Xiong et al. [91] studied the pre treatment of heterocyclic pesticide wastewater using US/O_3 combined process. Effect of ultrasonic frequency, ultrasonic power, probe diameter, initial pH and O_3 dosage on the COD removal were studied.   In presence of US only, COD removal was 33.7% at 20 kHz and 5.8% at 60 kHz. In presence of O_3/ ultrasonic

Microwave, Photo and Sono Activated Advanced Oxidation Processes and their
Variations for the Decontamination of Water from Toxic Chemical Pollutants

43

process COD is reduced by 60%. COD removal increases with increase in solution pH and reaches a maximum at pH 8.9. With increase in pH more free radicals are formed in the reaction system which accelerates the reaction. But in highly alkaline condition the solubility of ozone decreases and causes a decrease in the mass transfer. Hence the reaction rate decreases. When the ultrasonic power increases from 100 to 300W the COD removal also increases and reaches an optimum at 300W. At very high power, extra energy is wasted in the form of heat and hence the increase in degradation is negligible above the optimum.

Zhao et al. [92] studied sonocatalytic degradation of Methyl Orange using MnO_2/CeO_2 as catalyst. 85% of dye could be removed in 10min, which is much higher than the degradation in presence of US alone (3.8%). The MnO_2/CeO_2 composite enhances the cavitation effect, by acting as cavitation nucleus. Methyl Orange molecules adsorbed on catalysts could enter cavitation bubbles and undergo strong activation. Very high concentration of H_2O_2 formed in the process also enhances cavitation effects.

Eren et al. [93] presented an extensive summary of the studies on ultrasonic dye degradation using homogeneous and heterogeneous solutions. Dye mineralisation is required more time in the case of US alone. Combination of US with other techniques such as biochemical, electrochemical, ozonation, photolysis, photocatalysis and Fenton processes aimed at enhancing the degradation as well as mineralisation of dye pollutants is also discussed. Studies were limited to the lab scale only due to constraints in facility and economy. However, the authors conclude

that when better ultrasonic transducer technology is used electrical energy is converted to acoustic energy more effectively and this helps in the mineralisation of the textile effluents.

Little et al. [94] investigated the sono-degradation of phenanthrene in an aqueous environment using UV/Vis photo-spectrometry. The effect of several parameters on the degradation of phenanthrene were studied (power ultrasound energy, temperature and light). In the initial stages the degradation is slow. At that stage most of the ultrasound radiation is used for the dispersion of phenanthrene molecules. The chemical effect of US is more effective, only thereafter. The first degradation product was anthracene, followed by naphthalene formed from the former by the elimination of butadiene. It was then again degraded to phenol. UV-Visible spectrophotometry confirmed 88% reduction in the phenanthrene concentration within 240 min of ultrasonic irradiation.

Anju et al. [95] investigated the sonocatalytic degradation of organic pollutants using ZnO, TiO_2 and ZnO-TiO_2. Phenol is taken as the model compound. The degradation of phenol is slow under ultrasound, but presence of catalyst enhances the degradation. Combination of ZnO-TiO_2 showed synergic effect towards degradation. The effect of various reaction parameters such as catalyst loading, concentration, pH, effect of oxidants, effect of anions etc on the degradation was also studied. The % degradation increases with increasing catalyst loading reaches an optimum and then decreases. It was found that ZnO is more efficient than TiO_2 for the degradation of phenol. The rate of degradation increases with

Microwave, Photo and Sono Activated Advanced Oxidation Processes and their Variations for the Decontamination of Water from Toxic Chemical Pollutants

45

increase in concentration of the pollutant and reaches an optimum and then decreases. The reaction follows first order kinetics. The degradation is higher in acidic medium than in the alkaline medium. H_2O_2 formed during the sonocatalytic degradation of phenol undergoes simultaneous decomposition resulting in periodic increase and decrease in its concentration. Possible mechanism for the sonocatalytic degradation of phenol is discussed.

Song et al. [96] studied the degradation of C.I. Acid Red 88 by using a combination of Fenton reagent and US irradiation. The experiment was carried out under different conditions such as US, US/H_2O_2, US/Fe^{2+}, Fenton and US/Fenton processes. The degradation in each case was 8.2, 27.3, 22.3, 38.9 and 94% respectively, in 135 min of irradiation. The best degradation was obtained under US/Fenton process and this may be due to the synergic effect between Fenton reaction and US based process. The degradation is favoured at acidic pH. Degradation increases with increasing Fe^{2+} and H_2O_2 dosage. The intermediates were identified by LC-MS analysis. The azo linkage of acid red 88 is broken and some carbonyl compounds are formed. But complete mineralization of dye cannot be achieved.

The selection of appropriate AOP for a particular purpose depends on the type and concentration of pollutants. In order to enhance the efficiency of degradation as well as to reduce operating cost and time, integration of different AOPs are often recommended in the case of dye pollutants, which are very toxic and resistant to biodegradation, and hence require more time for degradation. Sometimes AOPs produce undesirable

toxic byproducts or intermediates which are more toxic than the parent compound itself. So complete mineralization is essential in the case of such pollutants. Combination of different AOPs, whether they are applied in sequence or simultaneously is found to be highly effective in degrading and mineralizing the pollutant within a short period of time. One of the most efficient combination of AOPs reported so far is sonophotocatalysis which is a combination of sono and photocatalysis.

1.2.2.3 Sonophotocatalysis

The basic mechanism of sonophotocatalysis is the combination of the mechanism of individual process and involves the generation of free radicals and their attack on the pollutant. The photocatalyst provides the nucleation sites for the formation of micro bubbles under sonication while the band gap excitation by light leads to the initiation of various free radicals. The production of high temperature and pressure as a result of acoustic cavitation result in enhanced number of free radicals. US promotes de-agglomeration of catalyst particles thereby increasing the surface area and ultimately enhancing the formation of reactive free radicals and the degradation of pollutant. At the same time shock waves from sonication, decrease the number of molecules adsorbed on catalyst surface thereby enhancing the mass transfer of organic pollutants between the liquid phase and catalyst surface. Synergy has been reported in many cases ie rate of degradation is enhanced many fold compared to that of the individual methods or their sum.

The following equation is used to calculate synergy in sonophotocatalysis.

$$\text{Synergy effect\%} = \{[D_{SPC}-(D_{SC}+ D_{PC})]/(D_{SC}+ D_{PC})\}\times100 ....(13)$$

Where D_{SPC} = Decolourisation/degradation under sonophotocatalysis

D_{SC} = Decolourisation/degradation under sonocatalysis

D_{PC} = Decolourisation/degradation under photocatalysis

Gogate and Pandit [97] presented an excellent review on various types of sonophotocatalytic reactors for wastewater treatment. Sonophotocatalytic oxidation eliminates disadvantages of photocatalytic process such as fouling of catalyst and mass transfer resistance. US helps in the de-agglomeration of catalyst particles thereby increasing the surface area. So more pollutant molecules are adsorbed on the surface of catalyst which results in enhanced degradation rate. Simultaneous irradiation of US and UV is more important than sequential operation because continuous cleaning of catalyst plays an important role in the degradation of pollutants. Additional reagents such as H_2O_2, O_3, air, ferrous ions etc act as source or initiators of free radicals, resulting in an enhanced degradation. Reactor design is another important parameter affecting synergic effect of US and UV irradiations. Reactors offer flexibility in terms of operation for different pollutant loadings as well as contribute to economic savings. Sonophotocatalysis can be applied for the treatment of a variety of pollutants.

Kavitha et al. [98] studied sonophotocatalytic degradation of reactive red (RR) 120 dye under visible light using dye sensitized TiO_2.

The effect of initial substrate concentration, pH and catalyst loading on the sonolytic, photocatalytic and sonophotocatalytic degradation under visible light were studied. The increase in the amount of reactive radical species is responsible for the synergy. It is also proved that the reaction takes place via formation of singlet oxygen, superoxide and hydroxyl radicals.

Joseph et al. [99] gave a concise review on a variety of pollutants that are degraded under sonophotocatalysis.

Hua et al. [100] investigated the degradation of RhodamineB (RhB) dye by sonophotocatalysis using poly ethylene glycol (PEG) modified TiO_2 film as catalyst in a circular Photocatalytic-Ultrasonic system. The photocatalytic activity of PEG- TiO_2 is found to be better than pure TiO_2. Around 17.5% of RhB were degraded after 120 min by sonocatalysis (PEG 2000-TiO_2 film, US), while 71.1% degraded in photocatalysis (PEG2000- TiO_2 film, UV) and 97.2% Rh B molecule degraded in sonophotocatalysis (PEG2000-TiO_2 film, US + UV). When optimized PEG 2000-TiO_2 film was used, the synergy obtained was 0.6519 which indicates high efficiency of sonophotocatalysis for RhB degradation. The higher degradation is explained based on the smallest crystallite size, optimal particle size, higher specific surface area and the highest photocatalytic activity of the PEG 2000-TiO_2 film.

Ragaini et al. [101] investigated the degradation of 2-chlorophenol in water using 3 different techniques; photocatalysis, sonocatalysis and sonophotocatalysis with different types of TiO_2 as catalysts under different conditions. Among the catalysts, TiO_2 P25 was the most

effective one. The experiment was conducted in presence of different gases and it was observed that the gas mixtures Ar-O_2 favoured maximum reaction rate.

Mrowetz et al. [102] investigated the degradation of organic water pollutants by sonophotocatalysis in the presence of TiO_2. The effect of substrate concentration and catalyst loading was investigated in detail. The amount of H_2O_2 formed during the reaction was also monitored. Synergic effect observed was attributed to the deagglomeration of photocatalyst by US and also the mass transport acceleration of chemical species between the solution phase and the photocatalyst surface and vice versa. Moreover H_2O_2 formed by both photocatalysis and sonolysis increases the amount of reactive radical species inducing further oxidation of the pollutant and intermediates. This is also partially responsible for the observed synergy.

Selli et al. [103] investigated the sonocatalytic degradation of methyl tert-butyl ether (MTBE) in water using TiO_2 as catalyst. 90% of degradation was achieved by sonophotocatalysis. The concentration of the MTBF intermediate is lower under sonophotocatalysis than under photocatalysis.

Hayashi et al. [104] investigated the efficiency of sonophotocatalysis in weight and volume reduction of organic sludges and recovery of biomass resources. When sonophotocatalysis was used, 50% reduction was observed in the emission amount of sewage sludge. Sonophotocatalytic treatment also helps to enhance the recovery of methane and phosphorus.

The recovery of methane gas and dissolved phosphorus were 1.7 and 2.5 times more than that in the process without sonocatalytic treatment.

Selli et al. [105] studied efficiency of 1,4-dichlorobenzene degradation in water under photolysis, sonolysis, photocatalysis and sonophotocatalysis using TiO_2 as a catalyst. 20 kHz US frequency at different powers was used. Two lamps, both emitting in the 340–400 nm wavelength range with different energy, were employed as light irradiation sources. The highest degradation and mineralization rate was attained with the combined use of photocatalysis and sonolysis, i.e. under sonophotocatalytic conditions.

Theerthagiri et al. [106] investigated sonophotocatalytic degradation of organic pollutants using nano-sized materials such as TiO_2, ZnO, metal sulfides, and composite materials. The degradation efficiency is low when sonolysis or photocatalysis is used individually. But when sonophotocatalysis is used the degradation efficiency is enhanced.

Volkova1 et al. [107] studied sonophotocatalytic degradation of azo dye Direct Blue 71 (DB71) using titanium dioxide (TiO_2) as the catalyst. They proposed that the sonodegradation of azo dyes was a multistage process that involved: (1) direct attack of azo bonds and phenyl rings of dyes by the sonochemically formed reactive oxygen species; (2) activation of semiconductor particles by the light emitted during cavitation and the triggering of the photocatalytic pathways of dye degradation; and (3) increase in the adsorption capacity of the semiconductor particles due to the sonomechanically induced interparticle collisions.

Microwave, Photo and Sono Activated Advanced Oxidation Processes and their Variations for the Decontamination of Water from Toxic Chemical Pollutants

51

Selli [108] investigated synergistic effects of sonolysis combined with photocatalysis in the degradation of an azo dye Acid Orange 8. An ultrasound frequency of 20 kHz was employed. The degradation was evaluated under sonolysis, photocatalysis and sonophotocatalysis as a function of dye concentration, amount and type of photocatalyst (TiO_2 or ZnO) etc. The evolution of hydrogen peroxide was also monitored. Synergistic effect is observed which is due to the formation of additional OH radicals by photocatalysis from the extra hydrogen peroxide produced by US. When compared to TiO_2, the synergic effect is more in the case of ZnO, because of the high amount of H_2O_2 formation.

Mosleh et al. [109] studied sonophotocatalytic degradation of Trypan Blue (TB) and vesuvine (VS) dyes using Ag_3PO_4/Bi_2S_3-HKUST-1-MOF as a novel visible light active photocatalyst. The effect of operational parameters on the degradation was studied. Maximum sonophotodegradation was 98.44% and 99.36% for TB and VS, respectively. Synergistic index was 2.53 which indicated that the hybrid systems consisting of ultrasound irradiation and photocatalysis have much higher efficiency compared to the sum of the individual processes.

Jelic et al. [110] studied the degradation of the antiepileptic carbamazepine (CBZ) by sonolysis and heterogeneous photocatalysis under UV-A, simulated solar irradiation, and by the combined use of UV-A and ultrasound irradiation (i.e. sonophotocatalysis) in demineralized water, ground water and effluent wastewater. Under sonophotocatalysis degradation rate was much higher compared to the other techniques. Intermediates formed in the reaction were identified by HPLC-(+ESI)-QToF-MS.

Panda et al. [111] published a review based on recent advancements in sonophotocatalysis (SPC) and doped sonophotocatalysts for the treatment of hazardous organic water pollutants. The efficiency of SPC treatments is evaluated and the selection of optimum parameters has been discussed. Synergy has been reported in many cases. Influence of doped materials on the degradation has also been discussed.

Jyothi et al. [112] investigated the sono, photo and sonophotocatalytic degradation of Phenol using ZnO as the catalyst. The effect of various reaction parameters such as catalyst loading, concentration of the pollutant, pH etc on the degradation was studied. The reaction follows first order kinetics. Degradation is favoured in the acidic conditions (pH 4-6). Almost 90% degradation is obtained under sonophotocatalysis which is more than the sum of the degradation under sonocatalysis (13%) and photocatalysis (55%). The H_2O_2, formed in the reaction process cannot be quantitatively correlated with phenol degradation. Oscillation in the concentration of H_2O_2 is observed which is explained based on the concurrent formation decomposition of H_2O_2 during the reaction. The intensity of oscillation in the concentration of H_2O_2 which is measured in terms of the height of the crest and the depth of the trough in the oscillation curve is in the order sonocatalysis > photocatalysis > sonophotocatalysis. However, the order of phenol degradation is sonocatalysis < photocatalysis < sonophotocatalysis.

A brief summary of the recent developments in the field of sonophotocatalysis was provided above. Another AOP which has been

receiving the attention of researchers in recent years is Microwave (MW) based process, in particular combination processes.

1.2.2.4 Microwave catalysis

MW based catalytic and non-catalytic processes are under intensive investigation in recent years for wastewater treatment. Microwaves lie in the region of electromagnetic spectrum between radio waves and IR waves. They travel at the speed of light. The frequencies allowed for industrial, scientific and medical applications of microwave are 915 and 2450MHz. The frequency 2450MHz has a wavelength of 12.2cm and energy of 1.6×10^{-5}eV which has the appropriate penetration depth for use in the case of small molecules. MW alone, being a low energy radiation with $E = 1.6x10^{-5}$ eV may not be able to degrade many pollutants. However, in combination with light and catalyst MW has been found to be highly efficient for the degradation of many pollutants such as dyes, phenolic compounds, pesticides and sulphonated aromatic compounds. The electromagnetic spectrum is shown in Fig.1.9.
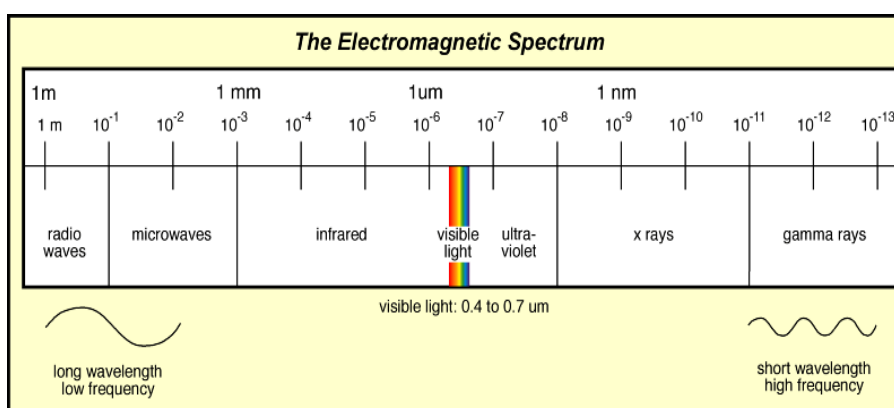
Fig. 1.9: Electromagnetic spectrum

There are two components of a microwave: an electric field and a magnetic field (see Fig1.10).
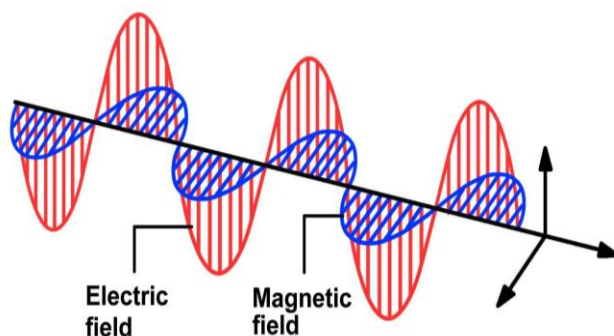
Fig. 1.10: Components of microwave- electric field and magnetic field The electric component of an electromagnetic field causes heating by two mechanisms:

1. Dipolar polarization mechanism

It is the interaction of the electric field component with the matrix. When sample is irradiated at MW frequencies, the dipoles in the sample attempt to re-align with the alternating electric field of MW. As a result energy is lost in the form of heat. The amount of heat generated is directly proportional to the ability of dipoles to align with the frequency of applied field.

2. Ionic conduction mechanism

Ions in a sample oscillate back and forth under the influence of the microwave field, collide with their neighboring molecules or atoms and cause agitation or motion, creating heat.

Each material responds differently to MW. Polarity is not the only factor that determines the absorption of MW energy though it is an

important one. All the material cannot absorb MW. The substances that absorb MW are termed as dielectrics. The ability of a material to convert electromagnetic energy into heat energy at a given frequency and temperature is called loss tangent and is expressed as tan δ

$$\tan\delta = \varepsilon' / \varepsilon'' \text{ ....(14)}$$

ε' is the relative permittivity - ability of a molecule to be polarised by an electric field (dielectric constant).

ε'' is the dielectric loss - ability of a medium to convert dielectric energy into heat.

So a medium with high tanδ is required for good absorption and heating.

Solvents used in MW are classified into low (tan δ < 0.1 eg: toluene, hexane), medium (tan $\delta \approx$ 0.1-0.5 eg: DMF, water) and high absorber of MW (tan δ > 0.5 eg: ethylene glycol, DMSO). Sometimes high absorbing solvents are used to increase the absorbing efficiency of low absorbers. Metal and metal oxides are heated efficiently under MW through coupling to the electric or magnetic field component of MW. MW radiation induces a flow of electrons on the surface of semiconductors and heat is generated through resistance to heating mechanisms. Besides the thermal effect there exists a non- thermal effect in MW ie rate acceleration that cannot be obtained by conventional heating. This may be due to the superheating of solvents, selective heating of MW absorbing catalyst or elimination of wall effects by inverted temperature gradients. The existence of this non-thermal effect is still a matter of debate.

Microwave radiation finds application in domestic, industrial and medical fields such as inorganic and organic synthesis, polymerization, plastic and rubber treating, wood drying, food sterilization, environmental remediation, pharmaceutical synthesis etc. The advantages of MW heating compared to conventional heating are:

i) Accelerates reaction rate.

ii) Provides better yields and uniform and selective heating.

iii) Greater reproducibility of reactions.

iv) Directly heat samples, ie temperature is raised uniformly throughout the medium. So energy consumption is less.

v) Cleaner and greener synthetic routes.

Nowadays microwave technology is widely used as a potential activation source in the field of environmental remediation. It is a remedial tool in the area of sludge processing, contaminated soil and waste water clean-up, and regeneration of activated carbon. Microwave heating removes moisture as well as volatile matter of sewage sludge. It also helps to reduce the volume. MW plays an important role in the decontamination of toxic metals from soil.

1.2.2.4.1 Application of MW in Advanced Oxidation Process for waste treatment

In the field of environmental remediation, microwave technology is widely investigated for the removal of toxic and recalcitrant pollutants from waste water.

Some of the important studies on the application of MW in this respect are summarised below.

Xu et al. [113] investigated the degradation of Methyl Orange in aqueous solution by Microwave Irradiation in the presence of Granular-Activated Carbon as catalyst. Synergic effect was observed when MW is combined with GAC. The catalyst is active even after six reaction cycles under MW irradiation.

Ferrihydrate nanoparticles [114] exhibit high adsorption capability towards methyl orange and this property is exploited favourably by MW irradiation. MW assisted Catalytic Wet Air Oxidation (CWAO) experiments were carried out in a domestic microwave oven operating at a frequency of 2450MHz with a power of 119W. The results are compared with the conventional CWAO method, by performing the experiments under similar conditions in a water bath. In the case of CWAO conducted at 95^0C for 1min, 33% of the dye is degraded. In presence of MW-CWAO, 90% degradation is obtained. In order to understand the role of adsorption on degradation, the sample is analysed using UV-Visible spectrophotometer after 5, 10 and 30 min of adsorption. Methyl Orange (MO) gives two characteristic absorption peaks at 460nm and 280nm corresponding to azo group and phenyl rings. After 30min of adsorption the peak at 480nm disappeared completely. But in the case of MW assisted catalytic wet air oxidation, the characteristic peaks at 480 and 280nm disappeared in 4min, and a new band corresponding to 248nm appeared. This may be due to the presence of an intermediate. The effect of pH on the degradation was also studied. Optimum efficiency was obtained under neutral conditions. The role of ˙OH radicals on the degradation was confirmed by the addition of the radical scavenger t-butanol to the reaction system. The degradation was inhibited by the

addition of t-butanol but the effect is more in the case of conventional CWAO than in MW, probably because simultaneous decomposition of MO and t-butanol occurs under MW. MW facilitates the generation of the active oxygen species from H_2O and O_2 dissolved in water and also the formation of hot spots on the surface of ferrihydrate.

Park et al. [115] investigated the degradation of Bromothymol Blue in aqueous solution by microwave/UV/TiO_2/ozone/ H_2O_2 hybrid process. A double-tube type microwave discharge electrodeless lamp (MDEL) that emits UV upon irradiation by microwave was developed because typical UV lamp contains metal electrodes which cannot be used in microwave. Degussa P-25 TiO_2 was used as the catalyst. Effect of catalyst dosage, microwave intensity, concentration of ozone and H_2O_2 etc. were studied. The degradation increases with increase in the catalyst dosage and microwave intensity. Addition of H_2O_2 increases the degradation to a maximum and then it decreases. Comparing the two oxidants, i.e. H_2O_2, and O_3 it is seen that the degradation rate is higher in the case of hydrogen peroxide added microwave-assisted UV-TiO_2 photo-catalysis.

Yin et al. [116] reported the microwave catalytic degradation of crystal violet using activated carbon (AC) as support material. The two catalysts used are CuO @AC and CuO-CeO_2@AC. The effects of catalyst loading, power, time, and initial concentration on degradation were studied. The degradation achieved is almost 99% in presence of 0.8% of CuO/AC compared to only 7% in the case of pure AC. AC is a material which can absorb MW radiations and create a lot of hot spots. CuO which uses energy from hot spots gets excited to produce e⁻-hole pairs. As a

result large number of ˙OH radicals are formed, which can enhance the degradation of pollutants. This is called "microwave photoelectric effect" i. e, MW can excite catalyst surface to produce ˙OH radical. Optimum degradation is obtained when 1% of CeO_2 is loaded on the surface of CuO-AC. In presence of MW only, negligible amount of degradation is obtained and in presence of AC-MW it was 80%. In the case of CuO@AC and CuO-CeO_2@AC, the degradation was 95 and 99.5% respectively within 5min of irradiation time, under 400 W microwave power.

Yin et al. [117] investigated the microwave catalytic degradation of 4-nitrophenol using Mn_2O_3/AC as the catalyst. Optimization of reaction parameters such as catalyst dosage, time, power, and initial concentration was studied. Higher degradation efficiency and TOC removal were obtained in the case of Mn_2O_3/AC compared to pure AC or MnO_2 individually. Proposed mechanism for the reaction involves the generation of OH radical by microwave photoelectric effect.

Chen et al. [118] studied microwave catalytic degradation of organic pollutants using carbon nanotubes of different diameters (10-20nm, 20-40nm and 40-60nm). The degradation of a large number of organic pollutants in their presence was studied. Carbon nano tubes of 10-20nm exhibit higher catalytic activity under MW compared to others.

Liu et al. [119] reported microwave assisted catalytic degradation of Methylene Blue by porous ferrate nanocomposites i.e. $MnFe_2O_4$ and $CoFe_2O_4$. The reaction follows pseudo second order kinetics. The degradation rate increases with increasing power, catalyst dosage and pH. Degradation is very high in presence of ferrate nanocomposites.

Zhang and Shan [120] studied the degradation of Congo Red by activated carbon under microwave radiation. Influence of time, concentration of the dye, catalyst dosage, pH, activity of recycled catalyst etc. were studied. 97.88% degradation was obtained by using an amount of 3.6g\L carbon in 2.5 min.

Zhang et al. [121] investigated the degradation of acid orange 7 under microwave discharge lamp (MWL) and oxidiser H_2O_2. Reaction follows pseudo first order kinetics. Results showed that MWL/H_2O_2 process was 32% more effective than H_2O_2/TEL (Traditional Electrode Lamp). In the case of MWL alone less than 2% of TOC was removed. But MWL/H_2O_2 removes more than 30% of TOC, in the same duration of irradiation.

Gayathri et al. [122] investigated the microwave catalytic degradation of Rhodamine B (RhB) in water using ZnO as the catalyst. Degradation in MW is faster compared to conventional heating which indicates that MW heating is not simply thermal, and non thermal effect also exists. The effect of operating parameters such as catalyst loading, concentration, pH etc. on the degradation was studied in detail. The % degradation increases with increase in catalyst loading and reaches an optimum at 0.1g/L. The reaction follows pseudo first order kinetics. The degradation is quite high at pH < 4 and > 9 and remains more or less steady in the pH range 5-9. The effect of addition of the oxidant H_2O_2 to the reaction system is also studied. The rate increases first and then stabilises. Further addition of higher concentration of H_2O_2 at this stabilisation stage increases the rate again. The enhancing effect of H_2O_2

is reconfirmed by the addition of H_2O_2 to a reaction system that is already in progress. The increased degradation can be attributed to an increased formation of reactive free radicals and their interaction with the dye.

Zhang et al. [123] investigated the photolytic degradation of Acid Orange 7 (AO7) under microwave irradiation using microwave electrodeless lamp (MWL). Effect of pH and inorganic ions on the degradation was also studied. Simultaneous application of UV−Vis/microwave irradiation is very effective for decolourization and mineralization. Complete degradation is obtained in 50 min and mineralization in 150 min. The mechanism was studied by means of radical scavengers. Large amounts of H_2O_2 and O_3 generated in AO7 solution, under MW irradiation help to produce higher number of ˙OH radicals which in turn enhance the degradation.

Hu et al. [124] reported the removal of atrazine insecticide under microwave irradiation using Cu and Fe exchanged dealuminated Y zeolites. The exchange of transition metals like Cu and Fe into zeolites micropores enhances the sorption capacity and selectivity towards atrazine and the microwave degradation rate. Presence of anions, cations and humic acid has little effect on the sorption of atrazine. But dissolved organic carbon, in natural and ground water samples affects sorption. This method is highly useful for the destruction of atrazine from contaminated water.

Wang et al. [125] studied the mechanism of methylene blue degradation under MW using manganese oxide as the catalyst. Akhtenskite and birnessite had no dipolemoment in crystal structure even

though high percentage degradation was observed. This was attributed to larger spin dipole moment of central manganese ion in octahedral structure. Methylene blue removal efficiency was 40% in the case of akhtenskite and 98% in the case of birnessite after 30min MW irradiation. In the absence of microwave irradiation it was 9.8 and 10.9% respectively. There was no degradation in the absence of manganese oxide. The high % removal of birnessite is attributed to the larger spin magnetic moment, which absorbs more microwaves. Manganese oxides are absorbers of MW, and create hot spots at a temperature of 1378 K, on the catalyst surface which is responsible for high % degradation. Moreover dissolved Mn(11) oxidised by O_2 at high temperature results in cyclic oxidation reduction process. The initial proportion of Mn(1V), Mn(111), Mn(11) ions on the surface of birnessite increases after microwave irradiation. After the oxidation reaction with methylene blue, it declines again. The proportion again increased after a second microwave irradiation. So microwave irradiation provides high temperature for the cyclic redox reaction process until methylene blue was completely removed.

Lai et al. [126] investigated the microwave enhanced catalytic degradation of phenol using nickel oxide as the catalyst. Catalyst was suspended in the solution. Air is bubbled continuously through the solution. Phenol is degraded completely into harmless products within 8 minutes of microwave irradiation, at neutral pH. Degradation of phenol depends mainly on the oxidation state of nickel and the surface area of NiO catalyst.

Microwave catalytic degradation of Malachite Green was examined using magnetic copper ferrites as catalyst [127]. Scavengers of free radicals are used to identify the degradation mechanism. Formation of ·OH radicals is confirmed using photoluminescence spectra. The participation of reactive $O_2^{·-}$ radicals and holes on the degradation was investigated by adding the scavengers, benzoquinone and potassium iodide respectively. In the presence of benzoquinone the degradation efficiency decreased from 58 to 41%. Benzoquinone traps superoxide radicals by electron transfer mechanism. So the radical available for the degradation of Malachite Green decreases. In the presence of I^-, which is generally a hole scavenger the degradation efficiency decreased from 58 to 35%. Hence the holes play an important role in the degradation of malachite green.

Ravera et al. [128] studied the oxidative degradation of 1, 5-naphthalenedisulfonic acid (NDS) in aqueous solution by microwave irradiation in the presence of H_2O_2. The effect of H_2O_2 concentration, pH, microwave power and irradiation time on the oxidative degradation was also studied. Degradation follows first order kinetics. 70% of NDS is removed in 20 minutes of irradiation. Acidic conditions favour the degradation.

Degradation of pesticide-containing wastewater using Fenton Reagent is enhanced by Microwave Electrodeless Ultraviolet/Fenton method [129]. Pesticides used in the study are dimethoate, triazophos, and malathion. This system (MWEUV/Fenton) was effective for COD removal also. The reaction follows pseudo first order kinetics.

Some of the important applications of the AOPs; sonocatalysis, photocatalysis, sonophotocatalysis and MW catalysis for the decontamination of water from trace pollutants are discussed here with special focus on the removal of chemical pollutants. Inspired by these findings, these four AOPs are investigated in detail in the present study for the removal of the dye pollutant Indigo Carmine from water. IC is a hazardous pollutant in the effluent water from many dye related industries and it is also an acknowledged carcinogen. Very few investigations have been reported on the application of AOPs for the removal of IC from water. In addition to identifying the optimum parameters for the decolourisation of the dye and its mineralisation, the influence of naturally occurring salt contaminants and various oxidants on the efficiency of respective AOPs also is investigated in detail. The fate of MnO_2 during the process and its recycling efficiency are also evaluated experimentally.

.....ಲ೦ಢ.....

Microwave, Photo and Sono Activated Advanced Oxidation Processes and their Variations for the Decontamination of Water from Toxic Chemical Pollutants

65

Objectives of the Study, Materials Used and Plan of the Thesis

2.1 Objectives

As mentioned in Chapter1, semiconductor mediated microwave catalysis, sonocatalysis, photocatalysis and sonophotocatalysis are promising AOPs for the degradation/mineralisation of a variety of pollutant molecules in water. The possibility of using these techniques individually and in combination for the removal of trace toxic pollutants from water will be a major step towards the decontamination of water, especially industrial wastewater laden with toxic organic chemical pollutants. Hence the current study is focussed on this aspect. Accordingly, the main objectives of the investigation are:

- Assessment of the feasibility of using AOPs based on MW, UV light, Ultrasound and their combinations for the decontamination of water from toxic chemical pollutants.

- Evaluation of the potential of relatively less investigated catalytic materials such as MnO_2, Co_3O_4 and their combinations with TiO_2 as AOP catalysts for the mineralization of selected dye polutants.

Microwave, Photo and Sono Activated Advanced Oxidation Processes and their Variations for the Decontamination of Water from Toxic Chemical Pollutants

67

- Identification of the most efficient AOP and optimization of relevant parameters for the mineralization of the test pollutant and

- Preliminary investgations on the application of the selected AOP for the mineralization of multiple pollutants of varying physicochemical and structural characteristics such as dyes, petrochemicals, pesticides and pharmaceuticals.

Indigo Carmine, a widely used dye in textile and medical diagnostic sector is chosen as the model pollutant. MnO_2, MnO_2-TiO_2 and Co_3O_4 are selected as the catalysts. Since the study was mostly focused on the removal of pollutants from wastewater under natural pH (around neutral range), the corrosion of MnO_2 under extreme acidic condition and photo corrosion are not expected to be of much concern.

Specific activities undertaken to achieve the above objectives include:

- Comparison of the efficiency of AOPs, i.e., microwave, sono, photo and sonophoto catalysis for the removal of trace organic pollutants in water.

- Characterization of the commercially available semiconductor oxide catalysts, MnO_2, TiO_2 and Co_3O_4.

- Laboratory testing of the above catalysts for the possible removal of selected dye pollutant IC under different conditions using microwave, sono, photo and sonophoto catalysis.

- Optimization of various reaction parameters such as catalyst dosage, particle size, pH, pollutant concentration, presence of O_2, reaction volume, temperature etc., for the degradation of IC under each of the above AOPs.

- Investigations on the role of commonly available oxidants on the degradation efficiency.

- Study of the influence of naturally occurring contaminants/salts on the efficiency of the process.

- Identification of reaction intermediates and elucidation of a suitable mechanism for the degradation of IC under various AOP conditions.

- Comparison of the efficiency of MnO_2, MnO_2-TiO_2 and Co_3O_4 towards mineralization of IC.

- Preliminary investigations on the suitability of the short-listed 'catalyst-activation source combination' for the mineralization of IC.

2.2 Materials used

2.2.1 Manganese Oxide (MnO_2)

Manganese (IV) oxide is the inorganic compound with the formula MnO_2. This blackish or brown solid occurs naturally as the mineral pyrolusite, which is the main ore of manganese. The principal use for MnO_2 is for dry-cell batteries, such as the alkaline battery and the zinc-carbon battery. MnO_2 is also used as an inorganic pigment in ceramics and as a precursor to other manganese compounds, such

as KMnO$_4$. It is also used as an oxidant in organic synthesis. The structure of MnO$_2$ is given in Fig. 2.1[130].
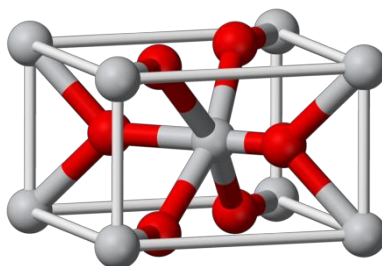
Fig. 2.1: Structure of MnO$_2$

MnO$_2$ exists in several polymorphs, it crystallizes in the rutile crystal structure (β MnO$_2$) with an octahedral metal center and three co-ordinate oxide. It is non-stochiometric and deficient in oxygen. Naturally occurring manganese dioxide contains impurities. So manganese dioxide is prepared from natural one by mixing with N$_2$O$_4$ and H$_2$O to form manganese (II) nitrate solution. Evaporation of the water, leaves the crystalline nitrate salt. At temperatures of 400 °C, the salt decomposes, releasing N$_2$O$_4$ and leaving a residue of purified manganese dioxide.

$$MnO_2 + N_2O_4 \rightleftharpoons Mn (NO_3)_2 \text{...(15)}$$

The deficient oxygen sites get filled in the process. MnO$_2$ catalyses several reactions that form O$_2$. Manganese dioxide also catalyses the decomposition of hydrogen peroxide to oxygen and water:

$$2 H_2O_2 \rightarrow 2 H_2O + O_2 \text{ ....(16)}$$

Various physico chemical properties of MnO_2 are summarised in Table 2.1.

Table 2.1: Physico chemical properties of MnO_2

Chemical formula	MnO_2
Molar Mass	86.9368 g/mol
Appearance	Brown-black solid
Density (gm/cm^3)	5.026
Melting Point (°C)	535 °C (995 °F; 808 K) (decomposes)
Boiling point	900 °C (1,650 °F; 1,170 K) (decomposes)
Solubility in water	Insoluble
Odour	odourless

2.2.2 Cobalt oxide

Cobalt (II, III) oxide is an inorganic compound with the formula Co_3O_4. It is a black antiferromagnetic solid. Mixed valancies such as Co^{2+} and Co^{3+}, are present in Co_3O_4. Its formula is written as $Co^{II}Co^{III}_2O_4$ / $CoO \cdot Co_2O_3$. Co_3O_4 adopts the normal spinel structure, with Co^{2+} ions in tetrahedral interstices and Co^{3+} ions in the octahedral interstices of the cubic close-packed lattice of oxide anions. The structure of Co_3O_4 is given in Fig.2.2 [131].

Fig. 2.2: structure of Co_3O_4

Microwave, Photo and Sono Activated Advanced Oxidation Processes and their Variations for the Decontamination of Water from Toxic Chemical Pollutants

71
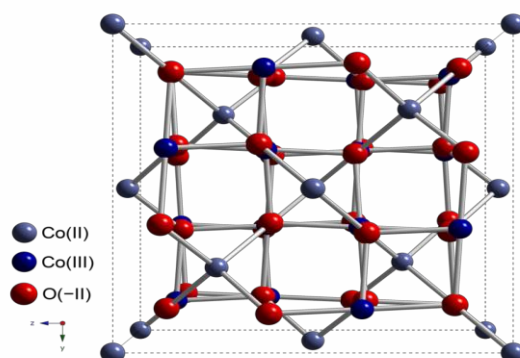
Physico chemical properties of Co_3O_4 are given in Table 2.2.

Table 2.2: Physico chemical properties of Co_3O_4

Chemical formula	Co_3O_4
Molar Mass	240.80 g/mol
Appearance	black solid
Density (gm/cm^3)	6.44
Sensitivity	air & moisture sensitive
Melting Point (°C)	895 °C
Boiling point	900 °C (1,650 °F; 1,170 K) (decomposes)
Solubility	Insoluble
Odour	odourless
Crystallography	Cubic

Co_3O_4 is a magnetic p-type semiconductor with wide application in solid state sensors, electro chromic devices, heterogeneous catalysis etc. Cobalt catalysts also lead to a greener society by lowering the activation energy (e.g. pressure, temperature) needed for industrial processes, such as the creation of recyclable plastics. Less energy therefore needs to be used to obtain the same yield, which in turn means less carbon emissions. Cobalt catalysts are widely used for the removal of sulphur moieties from natural gas and refined petroleum products, synthesis of polyester precursors and for the production of aldehydes from alkenes in the OXO reaction.

Co_3O_4 can be prepared in different nanostructures such as nanotubes, nanorods, nanofibres, hollow nanostructures etc. and offers the potential for wide variety of applications.

2.2.3 Titanium dioxide (TiO$_2$)

TiO$_2$ is the most investigated photocatalyst for the removal of organic pollutants from water. It is white in colour, inexpensive, chemically stable and harmless, and has no absorption in the visible region. In photocatalysis, the activity of TiO$_2$ in suspension depends on the physical properties of the catalyst (e.g. crystal structure, surface area, surface hydroxyls, particle size) and operating condition (e.g light intensity, oxygen, initial concentration of substrste, amount of TiO$_2$ and pH value).

Titanium dioxide can crystallize in three structures, i.e. rutile (tetragonal), anatase (tetragonal) and brookite (orthorhombic). Among these, rutile is thermodynamically the most stable, whereas anatase and brookite are metastable and transform to rutile on heating. In spite of the similarity between anatase and brookite, the latter occurs rarely compared to the anatase form and exhibits no significant photocatalytic activity under daylight irradiation. Rutile and anatase have more industrial applications. Rutile has the smallest band gap, i.e 3.0 eV (corresponding to a cut-off wavelength 413 nm), while anatase has a slightly higher band gap of 3.2 eV (cut of wavelength 388 nm). Both band gaps are close to the limiting wavelength between UV-A light (320–400 nm) and visible light (400–700 nm). Particle size experiments suggested that, in TiO$_2$, crystals are less than a few tens of nanometers in diameter. Anatase is more stable than rutile due to surface energy effects. Only anatase and rutile forms find application in most cases. Fig. 2.3 shows the bulk structures of rutile and anatase TiO$_2$. Anatase has been found, to be photocatalytically more active than rutile in most of the cases.

Microwave, Photo and Sono Activated Advanced Oxidation Processes and their Variations for the Decontamination of Water from Toxic Chemical Pollutants

73
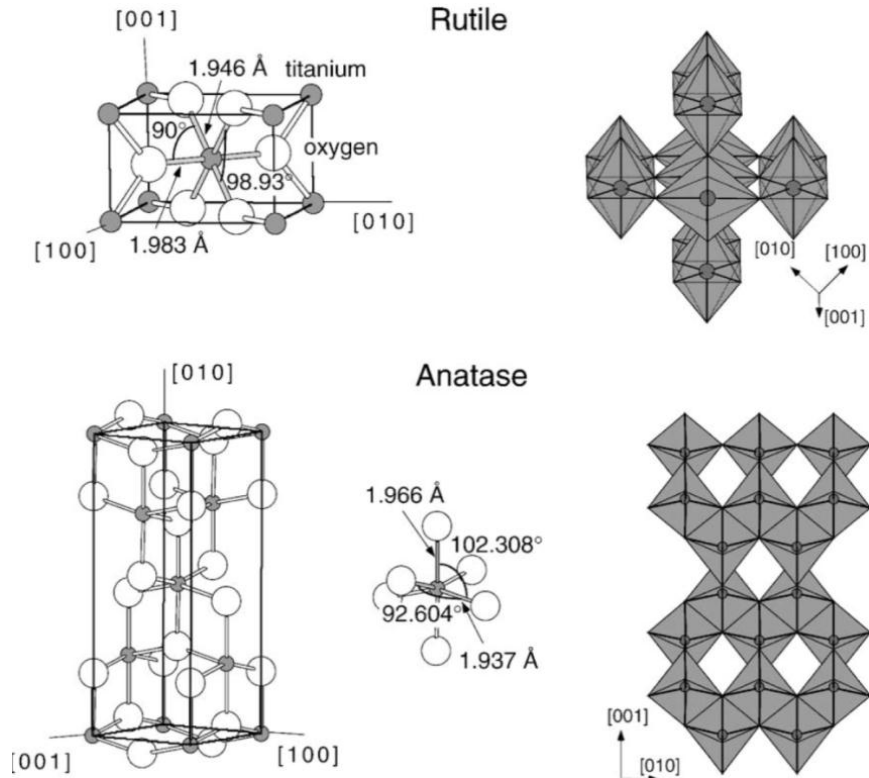
Fig. 2.3: Bulk structure of Rutile and Anatase TiO_2

Fig.2.4. shows the unit cell structure of the rutile and anatase crystal where the grey spheres are oxygen atoms and black spheres are Ti.
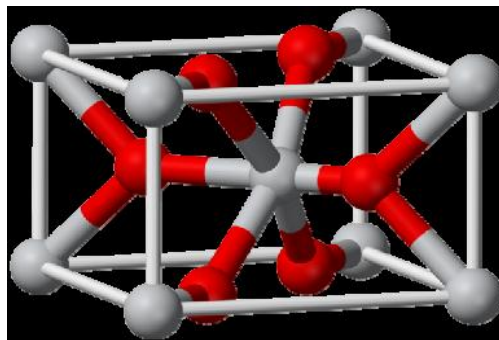
Fig. 2.4: Unit cell of rutile TiO_2

The structure of rutile and anatase can be described in terms of chain of TiO_6 octahedra. The crystal structures of the two differ by the distortion of each octahedron and by the assembly pattern of the octahedral chain. Each Ti^{4+} ion is surrounded by an octahedron of six O^{2-} ions. The octahedron in rutile is not regular, showing a slight orthorhombic distortion. The octahedron in anatase is significantly distorted so that its symmetry is lower than orthorhombic. In rutile structure each octahedron is in contact with 10 neighbour octahedron each (two sharing edge oxygen pairs and eight sharing corner oxygen atoms) while in the anatase structure, each octahedron is in contact with eight neighbours (four sharing an edge and four sharing a corner). Of the two crystalline phases, anatase is believed to possess better photocatalytic and photoelectrochemical conversion performances probably because of its open structure compared to rutile [132-134].

2.2.4 Indigo Carmine

Indigo Carmine (3,3'-dioxo-2,2'-bisindolylidene-5,5'-disulphonic acid disodium salt) is an important industrial dye used for dying of clothes and also for medical diagnostic purposes. It is administered intravascularly in a variety of treatments such as; to locate ureteral orifices, to endoscopically examine gastric cancer and to adjust the position of a catheter in the chemotherapy of hepatic and oral maxillofacial tumours. It can also help to target biopsies even better since the homogeneously stained or unstained areas can be correlated with intraepithelial neoplasia. It is also a pH indicator. The chemical structure of IC is as in Fig. 2.5 [135].

Microwave, Photo and Sono Activated Advanced Oxidation Processes and their
Variations for the Decontamination of Water from Toxic Chemical Pollutants

75
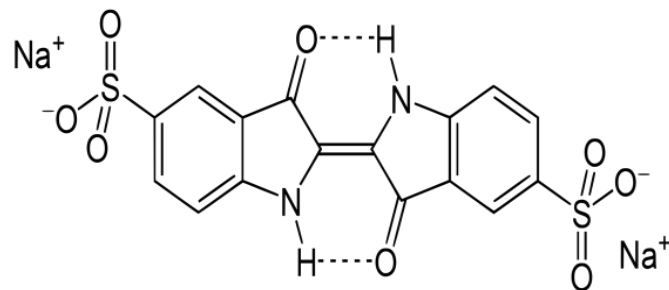
Fig. 2.5: Structure of Indigo Carmine

The dye is highly toxic, carcinogenic and has the potential to cause permanent injury to eyes. It can also lead to reproductive and developmental disorders as well as neuron and acute toxicity. Other health effects include possible tumors at the site of application, cardiovascular and respiratory effects and gastrointestinal irritation. Relevant physicochemical characteristics of IC are given in Table 2.3.

Table 2.3: Physico chemical properties of Indigo Carmine

Chemical formula	$C_{16}H_8N_2Na_2O_8S_2$
Molar Mass	466.36 g/mol
Appearance	purple solid
Melting Point (°C)	>300 °C (572 °F)
Solubility	10 g/L (25 °C (77 °F))
Toxicity data: LD_{50}	2000 mg/kg

2.2.5 Hydrogen peroxide (H_2O_2)

H_2O_2 is a colourless liquid with viscosity slightly greater than that of water. It is used as an oxidizer, bleaching agent and disinfectant. Structure of H_2O_2 is shown in Fig.2.6.
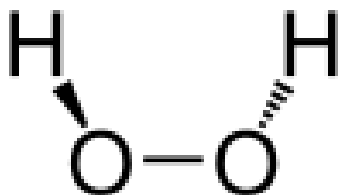
Fig. 2.6: Structure of H_2O_2

Aqueous solution of H_2O_2 differs in its properties from pure H_2O_2 due to the presence of hydrogen bonding. It is thermodynamically unstable and decomposes into water and oxygen as in equation (16).

Major properties of H_2O_2 are summarized in Table 2.4.

Table 2.4: Physical properties of H_2O_2

Molecular formula	H_2O_2
Molecular mass	34.0147 g/mol
Density	1.1 g/cm^3
Melting point	-0.43^{0}C
Boiling point	150.2^{0}C
Solubility in water	Miscible
Acidity (pKa)	11.75
Viscosity	1.245 cP
Dipole moment	2.26 D

2.2.6 RhodamineB

Rhodamine B is a commonly used xanthene dye containing 4 N-ethyl groups on either side of the xanthene ring. It is used in textile industry, biological stains and dye laser materials. It can cause harmful effects such as allergic dermatitis, skin irritation, mutations and cancer. It is highly soluble in water and its use in food and cosmetic application is

prohibited due to potential toxic and carcinogenic effects. Acute exposure causes eye irritation, coughing, difficulty in breathing, nausea and headache. The chemical structure of RhB is given in Fig.2.7. Physico chemical properties are given in Table 2.5.
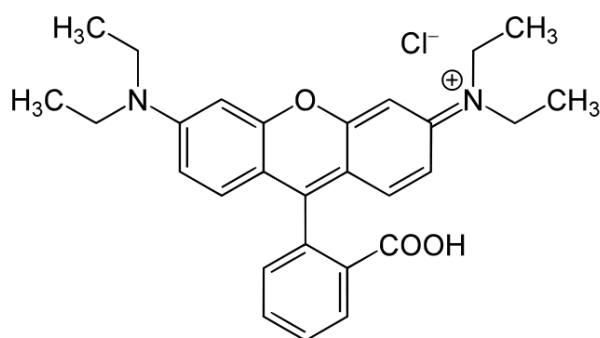
Fig. 2.7: Structure of RhB

Table 2.5: Physico-chemical properties of RhB

IUPAC name	[9-(2-carboxyphenyl)-6-diethylamino-3-xanthenylidene]-diethylammonium chloride
Molecular formula	$C_{28}H_{31}ClN_2O_3$
Molar mass	479.02
Appearance	red to violet powder
Melting point	210 to 211 °C (410 to 412 °F; 483 to 484 K)
Solubility in water	~15 g/L (20 °C
UV- Vis (λ_{max})	554nm

LD_{50} of Rh B is 887 mg/kg [137].

2.2.7 Acetophenone (ACP)

Acetophenone is a colourless to yellow-tinted liquid with a sweet strong odour resembling the odour of oranges. It is the simplest aromatic ketone. Acetophenone comes mainly as a byproduct of the phenol-acetone synthesis in the cumene oxidation process to cumene hydroperoxide. It is

used as a solvent for synthesis of pharmaceuticals, chemicals, dyestuffs and corrosion inhibitors; as flavouring ingredient in fruit flavours; as catalyst for the polymerization of olefins; added as fragrance ingredient in soaps, detergents, creams, lotions, perfumes etc. Structure of ACP is given in Fig.2.8. Physico chemical properties are given in Table2.6.
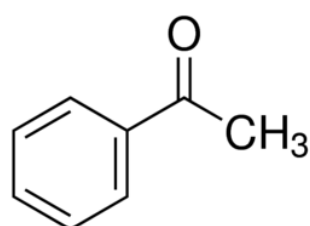
Fig. 2.8: Structure of ACP

Table 2.6: Characteristics of ACP

Chemical Name:	Acetophenone
Molecular formula	C_8H_8O
Molecular weight	120.16 g/mole
Melting point	19.7^0C
Boiling point	201.7^0C
Specific gravity	$1.0296 @ 20^0C$
Density	1.028 g/cm^3
Vapour pressure	0.33 mm Hg @ 20°C
Solubility in water	5.5 g/L @ 25°C
Viscosity	1.62 cP @25°C

The LD_{50} is 815 mg/kg [138]. Acute exposure of humans to acetophenone vapour may produce skin irritation and transient corneal injury. Oral exposure has been observed to cause hypnotic or sedative effects, haematological effects, and a weakened pulse in humans, gastrointestinal irritation with nausea, vomiting and diarrhoea, central

Microwave, Photo and Sono Activated Advanced Oxidation Processes and their Variations for the Decontamination of Water from Toxic Chemical Pollutants

79

nervous system depression, characterized by excitement followed by headache, dizziness, drowsiness, and nausea. Advanced stages may cause collapse, unconsciousness, coma and possible death due to respiratory failure.

2.2.8 Phenol

Phenol, is an aromatic organic compound with molecular formula C_6H_5OH. It is also known as carbolic acid. Structure of phenol is shown in Fig.2.9.
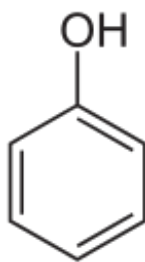
Fig. 2.9: Structure of Phenol

It is one of the most common pollutants found in effluents from industries such as petrochemicals, pharmaceuticals, pesticides, paints, dyes, organic chemicals, etc. Presence of minute quantity of phenol in water results in a high level of toxicity. It is listed as a priority pollutant in the list of 129 toxic pollutants by the US Environmental Protection Agency (EPA). According to Environment Protection Rules of Central Pollution Control Board, India (1992), the discharge limit of phenols in land water is less than 1 ppm.

Table 2.7: Properties of phenol

Molecular formula	C_6H_5OH
Molar mass	94.11 g/mol
Appearance	Transparent crystalline solid
Stability	Stable, Flammable
Odour	Sweet and tarry
Density	1.07 g/cm^3
Melting point	40.5^{o}C
Boiling point	181.7^{o}C
Solubility in water	8.3 g/ 100 mL
UV- Vis (λ_{max})	270.75 nm
Dipole moment	1.224 D
Acidity (pK$_a$)	9.95 (in water)

LD$_{50}$ of phenol is 300 mg/kg [139].

Major use of phenol includes its conversion to plastics and related materials. It also has medicinal value as antiseptic. Inhalation of phenol and dermal exposure results in high irritation to the skin, eyes and mucous membranes. Acute toxicity in humans includes symptoms such as irregular breathing, muscle weakness and tremors, loss of coordination, convulsions, coma and respiratory arrest at lethal doses.

2.2.9 Paracetamol

Paracetamol, also known as acetaminophen or APAP, is a medicine used to treat pain and fever. It is classified as a mild analgesic. The structure of paracetamol is shown in Fig.2.10.
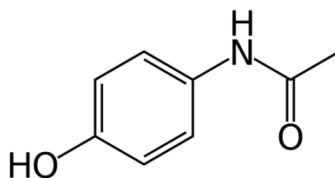
Fig. 2.10: Structure of Paracetamol

Microwave, Photo and Sono Activated Advanced Oxidation Processes and their Variations for the Decontamination of Water from Toxic Chemical Pollutants

81

Table 2.8: Physical properties of paracetamol

Molecular formula	$C_8H_9NO_2$
Molar mass	151.163 g/mol
Density	1.263 g/cm^3
Melting point	169 °C (336 °F)
Boiling point	420 °C (788 °F)
Solubility in water	12.78 g/kg (20 °C) ~14 mg/mL (20 °C)
UV- Vis (λ_{max})	243nm

Acute overdoses of paracetamol can cause potentially fatal liver damage. Gastrointestinal complications such as stomach bleeding are also reported when high doses are taken chronically. Kidney damage is seen in rare cases, most commonly in overdose. It can also cause severe skin reactions like Stevens–Johnson syndrome and toxic epidermal necrolysis. It is the most common cause of acute liver failure in both the United States and the United Kingdom. Hence accumulation of paracetamol in water bodies, soil, and other components of environment can ultimately reached humans and other living beings which will be extremely harmful to the biodiversity.

The LD_{50} of paracetamol is 2000 mg/kg [140].

2.2.10 Diclofenac

Diclofenac is a nonsteroidal anti-inflammatory drug (NSAID) taken or applied to reduce inflammation and as an analgesic for reducing pain in certain conditions. It is a benzene-acetic acid derivative. The chemical name of diclofenac is 2-[(2,6-dichlorophenyl)amino] benzeneacetic acid, monosodium salt. The structural formula is given in Fig.2.11.
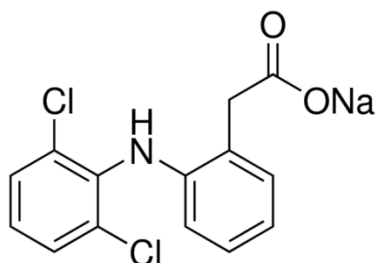
Fig. 2.11: Structure of Diclofenac sodium

Diclofenac consumption has been associated with significantly increased vascular and coronary risk including myocardial infarction and stroke, which can be fatal. Gastrointestinal complaints including bleeding, ulceration, and perforation of the stomach or intestines, liver damage, embryo-fetal toxicity etc. are also reported. Psychological side effects include depression, anxiety, irritability, nightmares, and psychotic reactions.

Table 2.9: Physico-chemical properties of diclofenac.

Chemical formula	$C_{14}H_{11}Cl_2NO_2$
Appearance	White/off white
Molar mass	296.15
Melting point	$283\text{-}285^0C$
Solubility in water	2.37mg/L
UV- Vis (λ_{max})	340 nm

The LD_{50} of diclofenac is 2000 mg/kg [141].

2.2.11 Diquat

Diquat is a herbicide that is commercially available in different trade names such as, Aquacide, Dextrone, Reglone, Reglox, Weedtrine-D, Aquakill, Vegetrole, Deiquat, Reglon, Tag etc. It is also used as a plant growth regulator. The structure of diquat is given in figure.2.12.
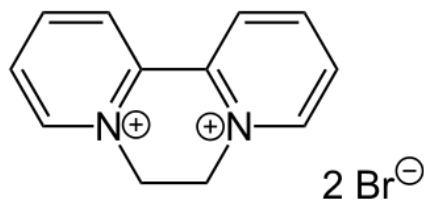
Fig. 2.12: Structure of Diquat

Diquat is a quick acting non- selective herbicide and can affect the non-target plants also. It is known as a desiccant because diquat dries out quickly the entire plant or leaf where it is applied. Diquat is a moderately toxic chemical and can cause kidney failure and liver damage. Also it is acutely toxic if absorbed through the skin. It will not get degraded by microbes and binds with the organic matter and sediments and remains without significant degradation for years. It is known to be toxic to fish. The pesticidal activity of diquat is by interfering with the photosynthesis, thereby leading to the destruction of cell membrane. The physico-chemical properties of diquat are given in Table 2.10.

Table 2.10: Physico-chemical properties of diquat.

IUPAC name	6,7-Dihydrodipyrido[1,2-a:2',1'-c] pyrazinediium dibromide
Chemical formula	$C_{12}H_{12}Br_2N_2$
Appearance	Yellow crystals
Molar mass	344.05 g/mol
Density	$1.22 - 1.27$ g/cm^3
Melting point	335 °C (635 °F; 608 K)
Solubility in water	70g/100mL
UV- Vis (λ_{max})	310 nm

The LD_{50} of diquat is 120 mg/kg [142].

2.2.12 Carbendazim

Carbendazim is a systemic benzimadazole fungicide that has extensive application. It is used to control diseases in cereals, fruits, vegetables and ornamental plants. It is also used for seed pre-planting treatment and postharvest food storage. The fungicidal action of carbendazim involves the inhibition of the development of the fungi by interfering with spindle formation at mitosis (Mitosis is a process where a single cell divides into two identical daughter cells). The structure of carbendazim is shown in Fig.2.13. The physico-chemical properties of carbendazim are shown in Table 2.11.
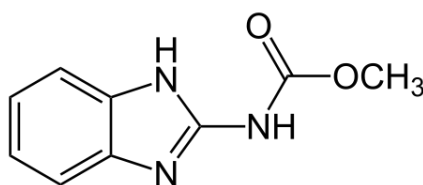
Fig. 2.13: Structure of Carbendazim

Table 2.11: Physico-chemical properties of carbendazim.

IUPAC name	Methyl *1H*-benzimidazol-2-ylcarbamate
Chemical formula	$C_9H_9N_3O_2$
Appearance	Light Grey Powder
Molar mass	191.187g/mol
Density	1.45 g/cm^3
Melting point	302 to 307 °C (576 to 585 °F; 575 to 580 K)
Solubility in water	8mg/L
Acidity (pK$_a$)	4.48
UV- Vis (λ_{max})	284 nm

The LD 50 of carbendazim is 10,000 mg/kg [142].

Carbendazim is identified as an endocrine disruptor. It also affects the number of chromosomes in human even at low exposures by

Microwave, Photo and Sono Activated Advanced Oxidation Processes and their Variations for the Decontamination of Water from Toxic Chemical Pollutants

85

inhibition of polymerization of tubulin, the protein that is essential for segregation of chromosome during cell division. Carbendazim gets strongly adsorbed to sediments thereby affecting the aquatic organisms. It is toxic to earthworm and non-target plants.

2.3 Experimental set up

The experimental set up and the procedures are described in respective Chapters, for ease of reference and convenience.

2.4 Analytical procedures

The analytical procedures adopted in this study include chromatography, spectroscopy, microscopy as well as conventional wet methods. Details are provided in respective Chapters.

2.4.1 Analysis of H_2O_2

H_2O_2 was analysed by standard iodometry. The oxidation of iodide ions by H_2O_2 was carried out in 1N sulphuric acid in presence of a few drops of saturated ammonium molybdate solution, which acts as a catalyst. The reaction was allowed to go to completion (5 minutes) in the dark. The liberated iodine was then titrated against a standard solution of sodium thiosulphate, (usually of $5 \times 10^{-3}N$) prepared freshly from 10^{-1} N stock solution. Freshly prepared starch was used as the indicator.

2.4.2 Chemical Oxygen Demand (COD)

COD of the samples were determined using open reflux method [143]. 50 ml of the sample was pipetted into a refluxing flask. Few glass beads were introduced to facilitate smooth reflux. $HgSO_4$ (1 g) was added to the sample. Added 5 ml of sulphuric acid reagent (5.5g Ag_2SO_4 + 543

ml Conc. H$_2$SO$_4$) slowly with mixing to dissolve HgSO$_4$. The sample was cooled while mixing to avoid the possible loss of volatile material. 25 ml of 0.05N K$_2$Cr$_2$O$_7$ solution was also added and mixed well. Remaining (70 ml) sulphuric acid reagent was added through the open end of the condenser. The whole mixture was refluxed for 2 hours and cooled thereafter to room temperature. The mixture was diluted to 150 ml and the excess K$_2$Cr$_2$O$_7$ was titrated against 0.05N ferrous ammonium sulphate (FAS) solution. The end point was sharp change of colour from blue-green to reddish brown. A blank was also carried out under identical conditions using the reagents and distilled water in place of the sample.

COD is calculated from the following equation:

$$\text{COD as mg O}_2/\text{L} = \frac{(A-B) \times M \times 8000}{\text{mL Sample}} \quad \dots\dots\dots\dots\dots\dots\dots\dots\dots\dots\dots(17)$$

A   = ml FAS used for blank

B   = ml FAS used for sample

M   = molarity of FAS

8000 = milliequivalent weight of oxygen $\times$ 1000 ml/L

2.4.3 Adsorption

Adsorption of various molecules on respective catalysts was measured as follows.

A fixed amount (0.1 g) of the catalyst was added to 100 ml of IC solution in a 250 ml flask and the pH was adjusted if required. The suspension was agitated continuously at constant temperature of 29 $\pm$ 1°C for sufficient time to achieve equilibrium. This was then centrifuged at 3000 rpm for 10 min. After centrifugation the concentration of IC in the

supernatant was determined colourimetrically. The adsorbate uptake was calculated from the relation

$$q_e = (C_0 - C_e)\,V\,/\,W \dots\dots\dots\dots\dots\dots\dots\dots\dots\dots\dots\dots\dots\dots(18)$$

where C_0 is the initial adsorbate concentration (mg/L), Ce is the equilibrium adsorbate concentration in solution (mg/L), V is the volume of the solution in litre, W is the mass of the adsorbent in gram and qe is the amount adsorbed in mg per gram of the adsorbent.

2.4.4 Detection of hydroxyl radicals

The formation of hydroxyl radicals in the presence of catalyst during irradiation (MW/UV/US) is tested by the photoluminescence (PL) technique using terephthalic acid (TPA) as the probe molecule.

The hydroxyl radicals formed insitu in the system react with TPA and form 2-hydroxy terephthalic acid (HTPA), which is a fluorescent molecule. The intensity of PL is proportional to the formation of $^\bullet$OH radicals in the system. In this method, the catalyst (0.1 g) is suspended in a mixed aqueous solution of TPA ($2\text{x}10^{-4}$ M) and NaOH ($2\text{x}10^{-3}$ M) and irradiated by MW. The PL spectrum of the product HTPA is recorded in the range of 400 to 450 nm after 5 and 10 minutes of irradiation. The excitation wavelength was 315 nm. The PL intensity at 425 nm corresponds to the concentration of HTPA and hence of the $^\bullet$OH radicals formed in the system. Shimadzu model RF-5301PC fluorescence spectrophotometer is used for recording the spectrum.

2.4.5. Any specific method used for any specific parameter in a Chapter is explained in respective Chapters.

2.5 Plan of the thesis

The current thesis is divided into eight Chapters. Each Chapter has its own specific objectives, experimental procedures, results, discussion and conclusions.

Chapter 1 entitled '**Introduction: Background literature'** gives an overview of the recent relevant literature and discussion on various types of AOPs with special focus on the application of microwave catalysis, sonocatalysis, photocatalysis and sonophotocatalysis in pollution control and water treatment.

Chapter 2 entitled '**Objectives of the study, Materials used and Plan of the thesis**' describes the main objectives of the study, specific activities undertaken to accomplish the objectives and characteristics of the main materials used in the study. The Chapter also provides the general layout of the thesis.

Chapter 3 entitled '**Microwave induced MnO_2, MnO_2-TiO_2 and Co_3O_4 mediated degradation of Indigo Carmine in water**' deals with studies on the microwave catalytic degradation of IC in presence of MnO_2, MnO_2/TiO_2 and Co_3O_4 catalysts under different conditions. Detailed experimental procedures followed, reaction details, analytical procedures, etc., are also provided. The effect of various reaction parameters on the degradation of IC is discussed. The effect of oxidants and anions on the degradation of IC is investigated in detail and the results are discussed. The role of dissolved O_2 and comparative efficiency of fresh and recycled MnO_2 for the microwave catalytic degradation of IC are investigated and the results are explained. The intermediates formed during the MW/MnO_2 degradation

Microwave, Photo and Sono Activated Advanced Oxidation Processes and their Variations for the Decontamination of Water from Toxic Chemical Pollutants

89

of IC are identified and a possible mechanism for the degradation is also suggested. The comparative efficiency of MnO_2, MnO_2/TiO_2 and Co_3O_4 for the mineralization of IC under MW irradiation is also verified experimentally and the observations are eventually reviewed and discussed.

Parts of major findings reported in this Chapter were published in peer-reviewed journals/presented as original research papers in Conferences as follows:

Paper 1. 'MnO_2 catalysed microwave mediated removal of trace amount of indigo Carmine dye from water', IOSR, J. Appl. Chem.1 (2014) 29-40.

Paper 2. 'Microwave assisted catalytic degradation of traces of Rhodamine B in water in presence of H_2O_2', IOSR, J. Appl. Chem.1, (2014) 1-11

Paper 3. 'Co_3O_4 mediated microwave catalysis: A new innovative Advanced Oxidation Process (AOP) for the removal of dye pollutants from water', IOSR, J. Appl. Chem.3 (2016) 25-46.

Paper 4. 'Microwave assisted Advanced oxidation Process for the degradation of indigo Carmine in water using MnO_2', Presented at the 3rd International Conference on Advanced Oxidation Process, Munnar, India (2014), Proc. of the conf. pp. 90.

Paper 5. 'Novel unusual application for microwave radiation: removal of last traces of toxic chemical pollutants from industrial wastewater'. Presented as a competition paper at the 28th Kerala Science Congress held at Calicut, India (2016), Proc. of the conf. pp. 739-742.

Chapter 4 entitled '**Photocatalysis mediated by MnO$_2$, MnO$_2$-TiO$_2$ and Co$_3$O$_4$ for the degradation of Indigo Carmine in water'** deals with the detailed investigations on the photocatalytic degradation of IC in water. The effect of various reaction parameters, anions, oxidants etc., on the degradation is investigated and the results are discussed in this Chapter. Some of the major reaction intermediates formed during the degradation are identified by LC-MS. The comparative efficiency of MnO$_2$, MnO$_2$/TiO$_2$ and Co$_3$O$_4$ for the photo mineralisation of IC is also discussed.

Parts of major findings reported in this Chapter were published as original research paper in peer reviewed international journal as follows:

Paper 1. 'MnO$_2$ and MnO$_2$ mediated persulphate enhanced photocatalysis for the removal of Indigo Carmine dye pollutant from water' European Chem. Bull. 6, (2017) 177-191.

Chapter 5 entitled "**Sonocatalysis mediated by MnO$_2$, MnO$_2$-TiO$_2$ and Co$_3$O$_4$ for the degradation of Indigo Carmine in water"** presents the results of the study on the sonocatalytic degradation of IC and the effect of various reaction parameters influencing the degradation efficiency. The role of dissolved oxygen and the reusability of catalysts on the degradation are also tested and the results are evaluated. Various reaction intermediates were identified and a possible mechanism for the degradation is proposed. The Chapter presents sonocatalysis as a highly efficient AOP for the degradation/decolourisation of IC in water.

Some of the findings reported in this Chapter were published as original research paper as follows:

Microwave, Photo and Sono Activated Advanced Oxidation Processes and their Variations for the Decontamination of Water from Toxic Chemical Pollutants

91

Paper 1. ʻApplication of ultrasound under different conditions for the purification of water contaminated with chemical and bacterial pollutantsʼ Gurukulam International Journal of Innovations in Science and Engineering, 1, (2016) 35-52.

Chapter 6 entitled **ʻSonophotocatalysis mediated by MnO_2 and MnO_2/TiO_2 for the degradation of Indigo Carmine in waterʼ** deals with study on the sonophotocatalytic degradation of IC and the effect of various reaction parameters influencing the degradation efficiency. Comparison of the degradation and mineralisation of IC under sono, photo and sonophotocatalytic conditions is also made in this Chapter. The viability of the hybrid process (sonophotocatalysis) as a highly efficient AOP for the decontamination of water from chemical pollutants is demonstrated.

Chapter 7 entitled **ʻSonophotocatalysis mediated by MnO_2/TiO_2 as a versatile AOP for the mineralisation of different category of pollutantsʼ** presents the results on the application of the best identified AOP system in the study, i.e ʻsonophotocatalysis mediated by $MnO_2\text{-}TiO_2$ʼ for the degradation and mineralization of wide spectrum of chemical pollutants, including dyes, petrochemicals, pharmaceuticals and pesticides. The Chapter conclusively demonstrates that sonophotocatalysis mediated by $MnO_2\text{-}TiO_2$ [$MnO_2\text{-}TiO_2/(US+UV)$] is a highly efficient, viable and environment- friendly process for the purification of water from IC and possibly from other chemical contaminants.

Chapter 8 entitled '**Summary and Conclusions**' summarizes the findings of the study and highlights the conclusions.

Annexure I   Lists the abbreviations used in the thesis. Expansions of respective abbreviation are shown in the text also in the first place where they appear in the thesis.

Annexure II   Provides the list of original research papers, based on the results of this study published in peer reviewed journals and/or presented in conferences.

Annexure III Compiles the reprints of the papers already published.

…..∞∞…..

Chapter **3**

Microwave induced MnO$_2$, MnO$_2$-TiO$_2$ and Co$_3$O$_4$ mediated degradation of Indigo Carmine in water

3.1   Introduction

Microwave (MW) induced advanced oxidation process (AOP) is emerging as a promising technology in the field of environmental remediation. Due to its capability for molecular level heating, increased selectivity of reaction, lower activation energy and ease of control, MW as well as its combination with other energy sources has been increasingly investigated as a possible tool for wastewater treatment. The ability of molecules to absorb, transmit and utilize MW energy for the creation of highly reactive species, which in turn can interact with the target organic molecules is being exploited for selective molecular synthesis. The same principle can be applied for breaking down toxic complex organic molecules. In this context, the possibility of application of MW   based   processes   for

the decontamination of water from chemical pollutants has attracted the attention of environmental technologists around the world [144].

Most of the organic compounds do not absorb electromagnetic energy in the S-band (4-8 GHz) of the MW which is a major limitation for its application in AOPs. This needs to be overcome if MW - based reactions are to be used as AOPs. One possible option is the identification of appropriate materials that can absorb considerable amount of MW and then transfer the energy to the reactants. Water can absorb MW strongly which makes aqueous pollutants amenable to catalytic degradation by MW. In addition to the widely recognized thermal role, MW could also induce the phenomenon known as 'athermal', 'nonthermal' or 'specific effect' of electromagnetic radiation as discussed in Section 1.2.2.4 of Chapter1. The level of coupling with the electric field of MW radiation which determines the efficiency of the process relies on the dielectric constant of the material. The dielectric constant determines the ability of the material to be polarized by an electric field [145, 146].

In the current study, the application of three different materials, i. e, MnO_2, MnO_2 -TiO_2 and Co_3O_4 as MW catalysts for the decontamination of water from the pollution caused by one of the widely used special application dyes, i.e. Indigo Carmine (IC) is examined in order to identify an appropriate MW active catalyst. Indigo Carmine (3, 3'-dioxo-1, 3,1',3'-tetrahydro-[2,2']-bi-indolylidene-5,5'-disulphonic acid disodium salt) is an important industrial dye used for dyeing of clothes and also for medical diagnostic purposes. Detailed chemistry, toxicology etc. of IC is discussed in Chapter 2, Section 2.2.4. In the current chapter the results of our investigations on the

application of MW catalysis using the above three catalysts i.e. MnO_2, MnO_2-TiO_2 and Co_3O_4 individually for the removal of IC in small concentrations from water are presented and discussed. The efficacy of the MW- based technique is evaluated by examining the degradation of IC under various reaction conditions and the optimum parameters are identified.

3.2 Experimental details

3.2.1 Materials used

The catalysts used in the study i.e. MnO_2, Co_3O_4 and TiO_2 were supplied by Merck India Limited. The particles of all three materials were approximately spherical and nonporous with over 99% purity. The surface area of MnO_2 as determined by the BET method is $31 m^2/g$. The surface area of Co_3O_4 and TiO_2 were 14.18 m^2/g and 11 m^2/g respectively. The pore volume of MnO_2 was approximately 0.05 cm^3/g and the average pore width was 74.2 Å. The pore volume of Co_3O_4 and TiO_2 were 0.08 cm^3/g and 0.04 cm^3/g respectively and the average pore width was 253.46 Å and 168.18 Å respectively. Indigo Carmine (AnalaR Grade 99.5% purity) from Sisco Research Laboratories Pvt. Ltd (India) was used as such without further purification. Doubly distilled water was used in all the experiments. All other chemicals were of AnalaR Grade or equivalent, unless indicated otherwise.

3.2.2 Experimental set up

A microwave oven (Whirpool Model GT288/BL) of 2450 MHz frequency and variable power upto 500W was used in the experiments. Major parts of a typical MW oven are shown in Fig.3.1. A front view of the MW oven with the reactors stacked on the turn table is shown in Fig. 3.2 A and B.

Microwave, Photo and Sono Activated Advanced Oxidation Processes and their Variations for the Decontamination of Water from Toxic Chemical Pollutants

97
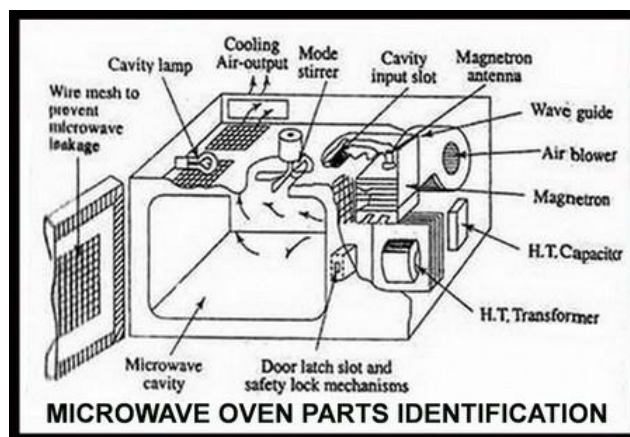
Fig. 3.1: Schematic diagram of MW oven used for the study

Fig. 3.2: Microwave reactor assembly: A) MW oven, B) Reaction samples inside the oven

The door was kept open for recording the photograph. The door will be closed when experiments are performed. Experiments are initiated by supplying the desired power to the system. The reaction temperature was not allowed to go above $35^0C\pm2^0$ and is controlled by regulating coolant water flow in the jacket/switching off the MW oven periodically as the case may be. Samples were drawn at specific intervals, centrifuged in the case of experiments with heterogeneous catalysts to remove the suspended materials and analysed for IC using Spectrophotometry.

The reactor was placed in the microwave oven on the turn table as is done normally for heating food items. Upto ten reactors could be placed in the oven at a time. The experiments were performed using aqueous solutions of IC of desired concentration. Pyrex glass reactor (cylindrical vessel of 250 mL capacity) is used for the experiments. Comparison of the data using this pyrex vessel and simple laboratory beakers showed that the results were identical within the limits of experimental error (±3%). Hence most of the experiments were performed using the beakers, unless mentioned otherwise. The temperature of the reaction medium was noted using a digital pyrometer. In the case of experiments with added catalysts, specified quantity of the catalyst was suspended in the solution. Periodic mechanical mixing ensured that the suspension was maintained uniformly.

As and when required, an in-house designed jacketed reactor with provision for circulating water, bubbling of gases, thermometer pocket and sampling point was also used (Fig.3.3). In this case an opening of appropriate size was made at the top cover of MW oven, and the reactor was inserted through the same.

Fig. 3.3: Inhouse designed MW/photocatalytic reactor

Conventional Heating (CH) experiments were conducted in a water bath instead of the microwave oven under otherwise identical conditions. The removal efficiency (%) was calculated by applying the following equation.

$$\% \text{ Removal efficiency} = [(C_0 - C_t)/C_0] \times 100 \dots\dots\dots\dots\dots\dots\dots\dots (19)$$

Where C_0 is the initial IC concentration and C_t is the concentration retained in solution at any point of time t.

Whenever required, the concentration of the other product of reaction, i. e. H_2O_2 is determined by standard iodometry.

3.2.3 Analytical procedures

3.2.3.1 Indigo Carmine (IC)

The concentration of IC was determined by spectrophotometry. Periodically samples were drawn, centrifuged/micro-filtered using 0.45 μm membrane filter and analysed for IC using UV-Vis Spectrophotometry at 608 nm. A similar reaction system kept in the dark under exactly identical conditions but without MW irradiation was used as the reference. The major intermediates of IC degradation before ultimate mineralization were verified by Liquid Chromatography/Mass Spectroscopy (LC-MS).

3.2.3.2 H_2O_2

H_2O_2 was analysed by standard iodometry as explained in Section 2.4.1.

3.2.3.3 Chemical Oxygen Demand (COD)

COD of the samples were determined using open reflux method [143] as explained in Section 2.4.2, Chapter 2.

3.2.3.4 Total Organic Carbon (TOC)

Total Organic Carbon in the reaction solution was measured at different intervals, as needed, using TOC analyser model Elementar analysensysteme GmbH by standard procedure.

3.2.3.5 Adsorption

Adsorption of various molecules on the respective catalysts was measured as explained in Section 2.4.3, Chapter 2.

3.2.3.6 Detection of hydroxyl radicals

The formation of hydroxyl radicals in the presence of catalyst during MW irradiation is tested by the photoluminescence (PL) technique using terephthalic acid (TPA) as the probe molecule as explained in Section 2.4.4, Chapter 2.

3.3   Results and Discussion

3.3.1 Preliminary results

Preliminary investigations on the use of microwave irradiation for the removal of trace amounts of IC from water were made using various oxides as catalysts. Of these, MnO_2 was found to be the most efficient. The results are shown in Fig.3.4.

Microwave, Photo and Sono Activated Advanced Oxidation Processes and their Variations for the Decontamination of Water from Toxic Chemical Pollutants

101
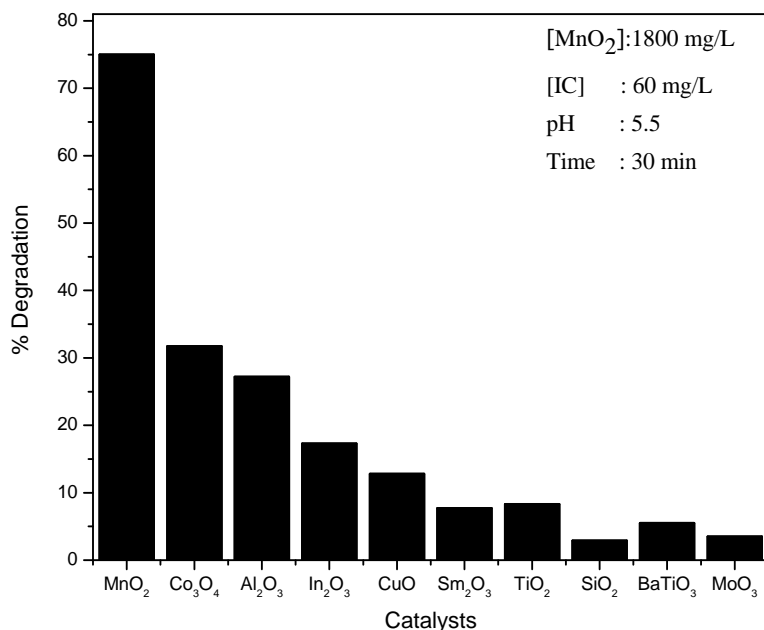
Fig. 3.4: MW assisted degradation of IC in presence of various catalysts

MnO_2 is at least 8 times more MW active than TiO_2 which is one of the most active photocatalysts. The second best catalyst in this respect is Co_3O_4 whose efficiency is ~ 40% of that of MnO_2. Hence these two catalysts are investigated in detail for their efficiency for the MW degradation of the IC.

3.3.2 Catalyst characterization

The catalyst MnO_2 used in the study is characterized by surface area, particle size analysis, adsorption, X-Ray Diffraction (XRD), Scanning Electron Microscopy (SEM) and Transmission Electron Microscopy (TEM). The surface area, determined by the Brunauer Emmett and Teller (BET) method is 36 m^2/g. The characterization results are shown in Fig. 3.5 to Fig.3.9.
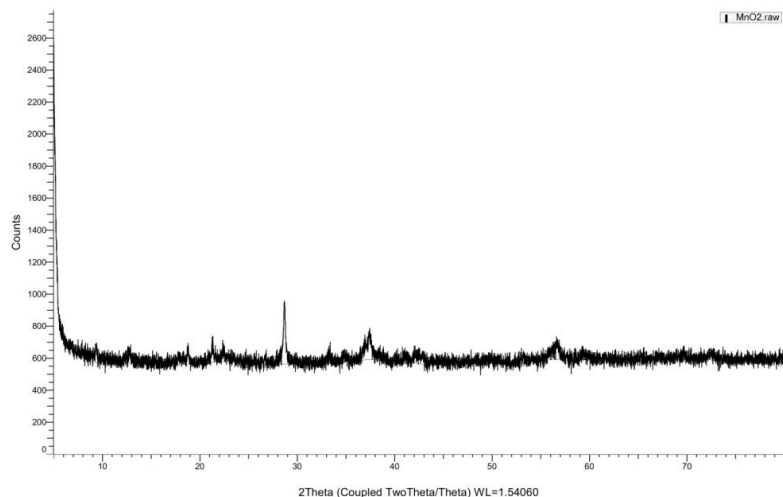
Fig. 3.5: XRD of MnO$_2$

The XRD results show that the MnO$_2$ is amorphous in nature with weak diffraction pattern (Fig. 3.5).

The morphology and particle size analysis were done using SEM (Fig. 3.6). Particles were approximately rod-shaped with an average particle size of 220nm. The characteristics of the particles are appropriate for efficient AOP properties such as adsorption and diffusion. The morphology and particle size are further confirmed by TEM analysis (Fig.3.7) which shows platelet and rod-like structure.
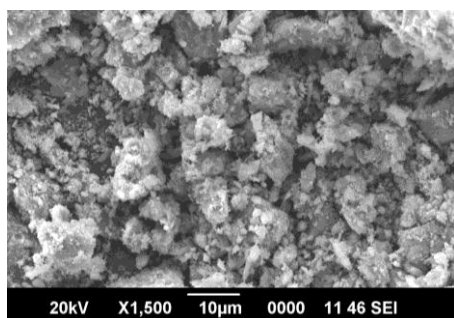
Fig. 3.6: SEM of MnO$_2$

Fig. 3.7: TEM of MnO$_2$

Microwave, Photo and Sono Activated Advanced Oxidation Processes and their Variations for the Decontamination of Water from Toxic Chemical Pollutants

103
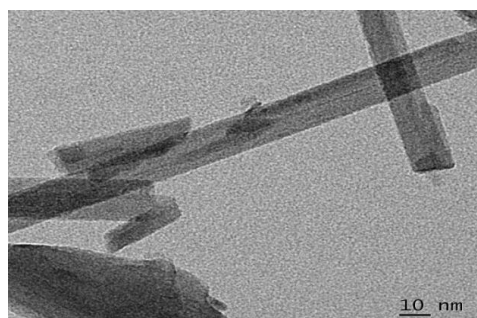
Diffuse Reflectance spectrum (DRS) (Fig.3.8) shows a sharp reflectance band between 200 and 300 nm indicating that the material absorbs in the UV range. The optical absorption intensity of MnO_2 steadily increases from 300 to 800 nm with no clear band edge. This indicates that MnO_2 is not a typical semiconductor like TiO_2 or ZnO. The brown colour of MnO_2 also indicates favourable absorption of visible light [147].

These characteristics indicate the possibility of using MnO_2 as a photocatalyst and this aspect is investigated in detail, as reported in Chapter 4.
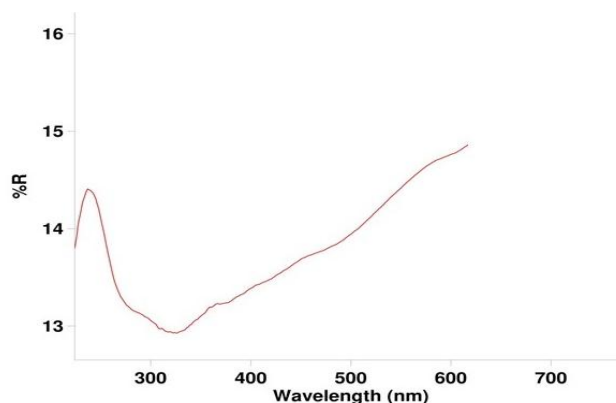
Fig. 3.8: UV- DRS of MnO_2
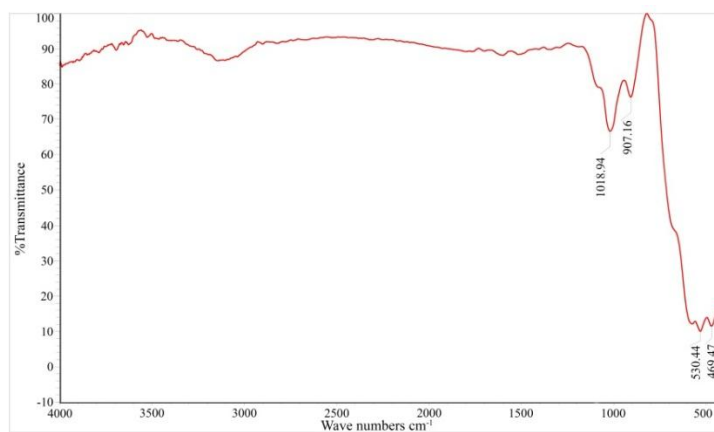
Fig. 3.9: FT-IR Spectrum of MnO_2

The FTIR pattern (Fig.3.9) shows very week absorption intensity of ·OH (3100-3600 cm^{-1}) or H$_2$O (1600 and 3600 cm^{-1}). The general spectral pattern shows that MnO$_2$ is pure with no contamination from any of the precursors as it happens in many cases.

3.3.3 Degradation studies

Since MW irradiation leads to a rise in temperature of the reaction system, the degradation of IC needs to be compared with the results under identical conditions using conventional heating (CH) to attain the same temperature. The degradation is also measured at normal room temperature (RT) under identical conditions. Comparative degradation/removal of IC under MW (35^{0}C), CH (35^{0}C) and RT (29^{0}C) is shown in Fig.3.10.
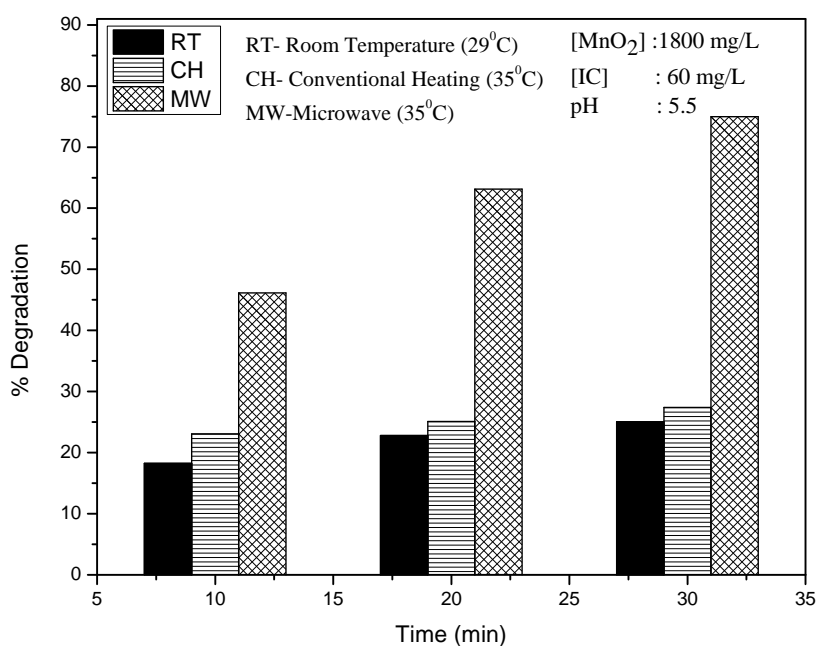
Fig. 3.10: Comparative degradation of IC in presence of MnO$_2$ under various conditions

Microwave, Photo and Sono Activated Advanced Oxidation Processes and their Variations for the Decontamination of Water from Toxic Chemical Pollutants

105

MW/MnO$_2$ is~3 times more efficient (75% degradation in 30 minutes) than CH/MnO$_2$ and RT/MnO$_2$ the latter two having comparable efficiency (25% in 30 minutes). This clearly demonstrates that the role of MW irradiation in the degradation of IC in presence of MnO$_2$ is not simply thermal. The decrease in concentration of IC under CH/MnO$_2$ and RT/MnO$_2$ is probably due to adsorption. MnO$_2$ is a good adsorbent of IC with an optimum adsorption of ~ 6 mg/g as determined experimentally (Fig.3.11). The effect of varying concentration of IC on its adsorption on MnO$_2$ is verified by keeping MnO$_2$ dosage constant at 1800 mg/L. The results are presented in Fig.3.11. It is evident that for a fixed amount of catalyst, there is an optimum adsorption of IC irrespective of the concentration of the dye.
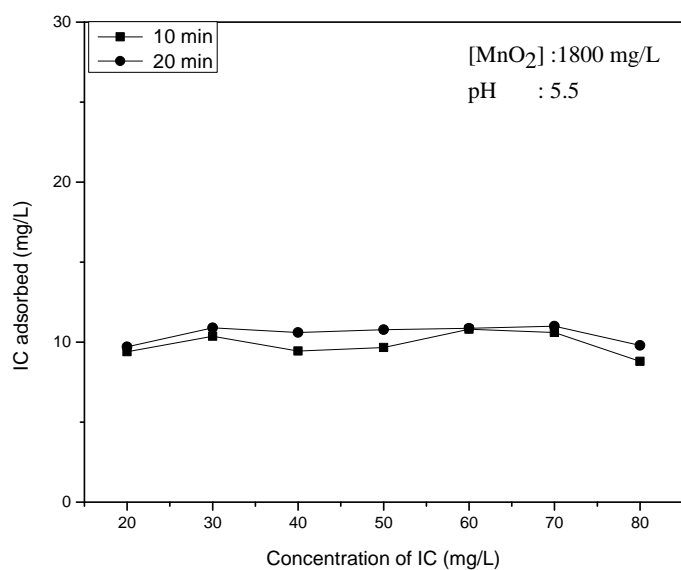
Fig. 3.11: Effect of concentration of IC on its adsorption on MnO$_2$

The effect of various reaction parameters on the MW degradation of IC is investigated in detail and the results are presented below.

3.3.3.1 Effect of MnO₂ dosage

The effect of MnO_2 dosage on the MW degradation of IC is presented in Fig.3.12. The data is collected after two time periods of MW irradiation i. e, 10 and 20 min. The concentration of IC is kept constant at 20 mg/L.
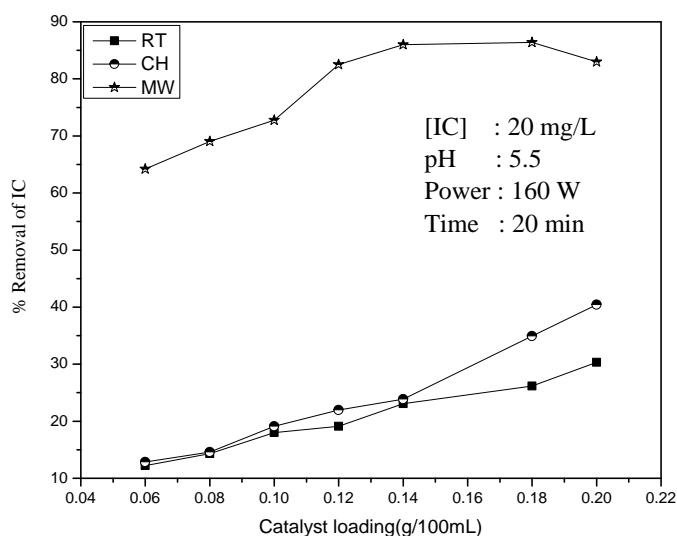
Fig. 3.12: Effect of catalyst dosage on the degradation of IC under MW, CH and RT conditions

IC degradation increases with increase in loading both under CH and MW conditions. The degradation under MW irradiation increases with increase in dosage upto 0.14g/100mL and stabilises thereafter. At this stage the degradation of IC is almost complete (~ 90%) and hence any further increase in degradation will be slow. In the case of CH the degradation continues to rise gradually even at the dosage of 0.2 g/100mL studied here. This is primarily because the decrease in the concentration of IC under CH at 35^0C is mainly due to adsorption and partially due to mild degradation. Naturally, as the catalyst dosage increases, the adsorption

Microwave, Photo and Sono Activated Advanced Oxidation Processes and their Variations for the Decontamination of Water from Toxic Chemical Pollutants

107

and degradation also increase. The slow decrease in the concentration of IC even at the room temperature (RT) of 29^0C is also due to the adsorption of the dye on the catalyst. The results reconfirm that the MW effect is significantly more than simple thermal effect at all dosages of the catalyst.

At higher loadings there will be more number of active surface sites and hence better adsorption of the dye leading to more effective MW activity and degradation. However, beyond the optimum, aggregation of particles may cause decrease in the number of available active surface sites and reduced adsorption. Under MW, the adsorbed molecules get degraded fast and mostly desorbed from the surface where fresh molecules can get adsorbed. However, as the reaction advances the surface will gradually get covered by the relatively more stable intermediates and the optimum is reached. Since most of the IC molecules are degraded at this stage the rate of degradation also slows down leading to stabilisation. In the case of RT, the initially adsorbed dye molecules stay on the surface longer and saturate the active sites. In this case there is no degradation or desorption and the decrease in concentration of IC is due to simple adsorption only. Another reason for the optimum dosage is that the particles cannot be effectively suspended beyond a particular loading in a particular reactor which leads to suboptimal penetration of radiation. Yet another reason is the deactivation of the activated catalyst particles by interaction with the ground state particles at higher catalyst dosages.

$$MO* + MO \longrightarrow MO^{\#} + MO \quad ....(20)$$

(MO represents MnO_2, MO* and $MO^{\#}$ are its activated and deactivated forms respectively).

The optimum catalyst loading will also depend on the size, shape and geometry of the reactor. Hence, for each reactor the optimization has to be made separately.

Since the optimum loading of MnO_2 under MW is 1.4 - 1.8 g/L, all further experiments were carried out with 1.8 g/L dosage. The higher value is chosen to take advantage of possible positive interaction of various reaction components/parameters with MnO_2.

3.3.3.2 Effect of concentration of IC

Percentage degradation of IC at different concentrations at different reaction times (5-20 min) under MW/MnO_2 is presented in Fig.3.13. The % degradation decreases with increase in concentration at all reaction times.

The effect of initial concentration of IC on its rate of degradation is shown in Fig.3.14.
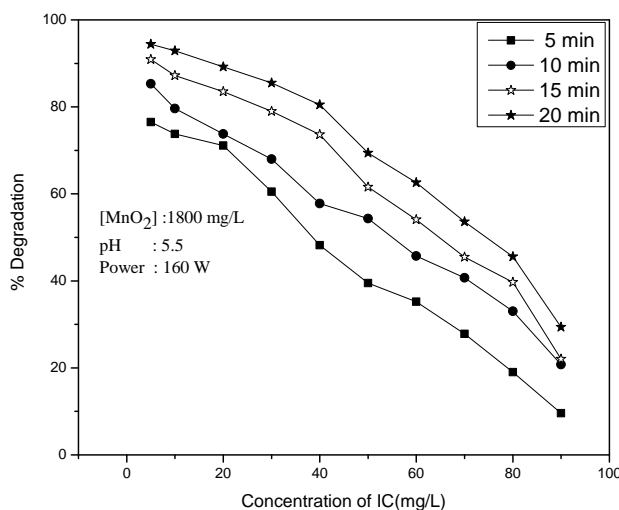
Fig. 3.13: Effect of concentration on the MW/MnO_2 degradation of IC
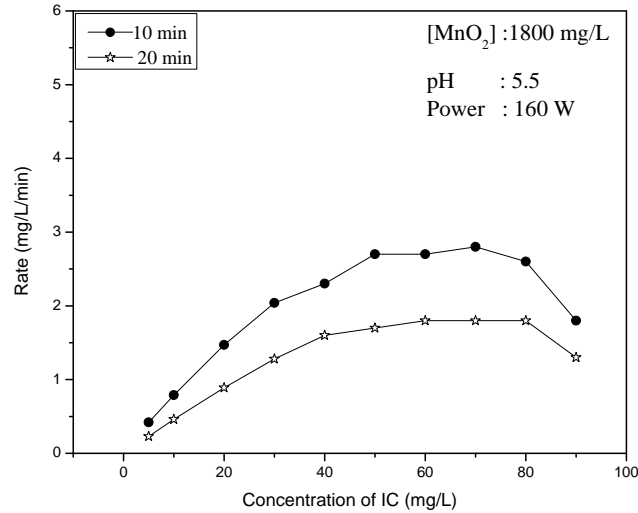
Fig. 3.14: Rate of MW/MnO$_2$ degradation of IC at various concentrations
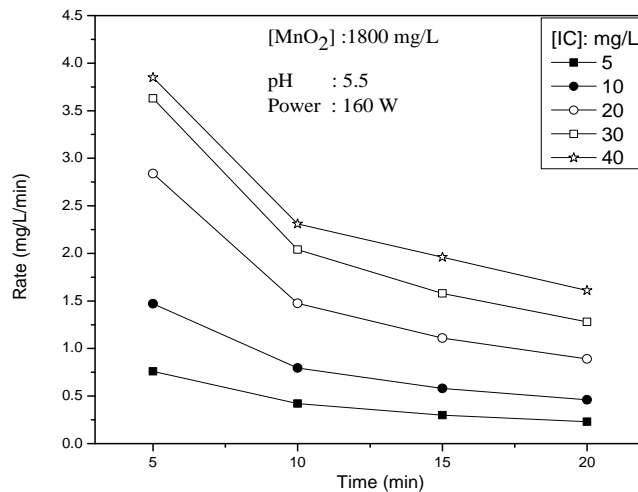
Fig. 3.15: Rate of degradation of IC at various time intervals

The rate increases gradually with increase in concentration. Eventually, the rate is stabilised in the range 50-80mg/L. The rate of degradation is evaluated at different times of reaction for different concentrations of substrate and the results are shown in Fig.3.15. The rate slows down with time. In the early stages of the reaction the entire

catalyst surface as well as the MW irradiation are available exclusively for the substrate and the rate of degradation is high. Once the reaction progresses more and more slow degrading intermediates get accumulated in the system which compete with the substrate for the ROS, catalyst surface and the MW radiation. The concentration of the substrate also becomes less and less reducing its competitive power. These factors lead to a decrease in rate of degradation with time. Once the concentration of the substrate is enough to occupy all the active sites on the catalyst and to interact with the optimum available ROS and/or other reactive free radicals, any further increase cannot result in increased reaction and the IC removal becomes independent of concentration. It is also possible that at higher substrate concentration, some of the reaction intermediates may get adsorbed onto the surface or remain in the bulk for relatively longer period resulting in less frequent interaction between fresh IC molecules and the ROS. Complete domination of the catalyst surface by the reactant/ intermediates/products can also result in suppression of the generation of surface-initiated reactive free radicals. However, at any point of time, there will be an optimum for the number of substrate molecules that can interact with the reactive free radicals generated by the surface. This optimum will depend on a number of parameters such as initial concentration of the substrate, frequency and power of MW, mass and type of catalyst, type and geometry of reactor etc. Consequently, the measurements and calculations apply only to the specific reaction conditions and cannot be generalized.

The rate vs concentration plot in Fig.3.14 shows that the reaction becomes independent of the concentration of the dye above 40-50 mg/L

Microwave, Photo and Sono Activated Advanced Oxidation Processes and their Variations for the Decontamination of Water from Toxic Chemical Pollutants

111

i.e., the kinetics is zero order. The rate even decreases at still higher concentration indicating negative order. Variable kinetics which is concentration-dependent and pseudo first order kinetics have been reported in the case of many AOP based degradation reactions [46,95,112]. This is rationalized in terms of the modified Langmuir- Hinshelwood model. Accordingly the degradation, can be represented as

$$r_0 = -dC/dt = k_r K C_0 / (1 + K C_0) \quad \dotfill (21)$$

where r_0 - rate of disappearance (mg L^{-1} min^{-1}) of the reactant.

C_0 - initial concentration (mg L^{-1}) of reactant.

K - equilibrium adsorption coefficient of the reactant

k_r - optimum reaction rate constant.

Equation (21) can be rewritten as

$$1/r_0 = 1/k_r + 1/k_r K * 1/C_0 \quad \dotfill (22)$$

Plot of $1/r_0$ against $1/C_0$ give straight line as shown in Fig. 3.16.
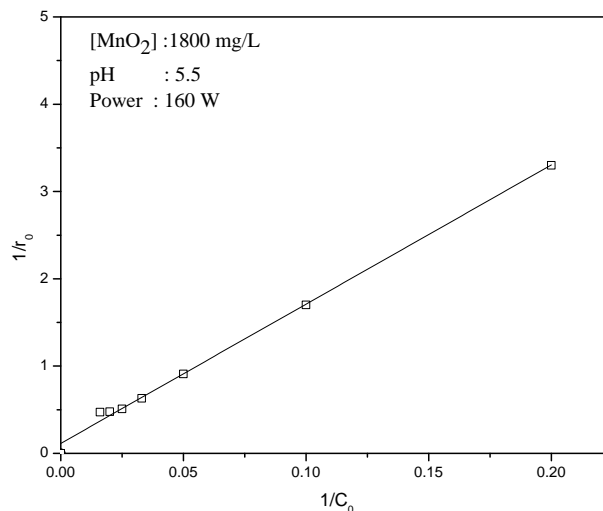
Fig. 3.16: Reciprocal plot of $1/r_0$ vs $1/C_0$ for various concentrations of IC

Based on equation (22), plot of $1/r_0$ vs $1/C_0$ must yield a straight line, if the reaction follows first order kinetics. Fig.3.16 shows that this condition is satisfied in the concentration range, 5-40 mg/L thereby confirming first order kinetics and L-H mechanism for the degradation.

Another mode of verifying the pseudo first order kinetics is based on the logarithmic plots as follows.

Integrating equation (21)

$$\ln (C_0/C)+K(C_0-C) = k_r Kt. \dotfill (23)$$

When C_0 is small the equation becomes

$$\ln (C_0/C) = -\ln(C/C_0) = k_r Kt = k_{app}t \dotfill (24)$$

where k_{app} is the pseudo first order rate constant.

Plot of $\ln (C_0/C)$ vs time in the concentration range 10-40 mg/L is linear indicating pseudo first order kinetics (Fig.3.17).
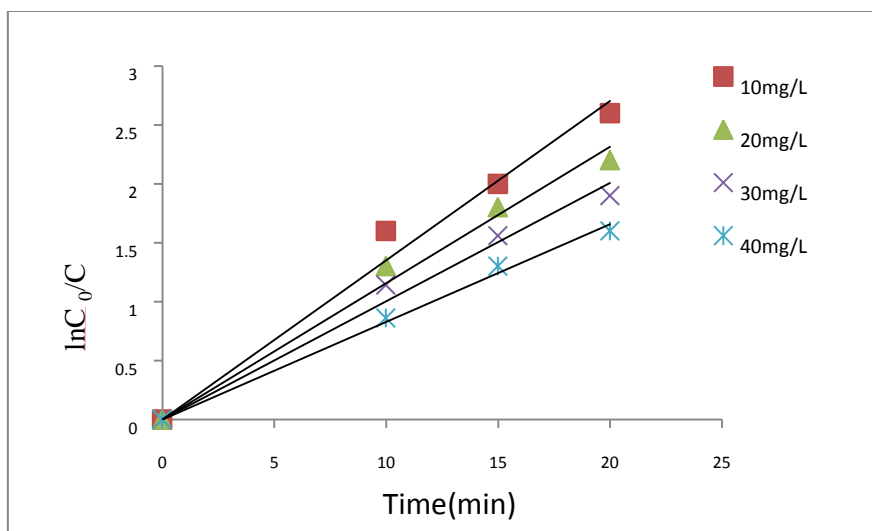
Fig. 3.17: Logarithmic plot for the MW/MnO₂ degradation of IC.

Microwave, Photo and Sono Activated Advanced Oxidation Processes and their Variations for the Decontamination of Water from Toxic Chemical Pollutants

113

The pseudo first order rate constants calculated from the plot are given in Table 3.1.

Table 3.1: Pseudo first order rate constants for the MW/MnO$_2$ degradation of IC

Experiment	[MnO$_2$] g/L	[IC] mg/L	k$_{app}$(min^{-1})
1	1.8	10	0.135
2	1.8	20	0.119
3	1.8	30	0.097
4	1.8	40	0.081

The value of k$_{app}$ decreases as the concentration of IC is increased. For a particular catalyst dosage, the number of active surface sites and the reactive species generated will be constant. The number of substrate molecules increases as its concentration increases. However, effective interaction between the substrate and the reactive oxygen species will be finite because the number of ROS is the limiting factor at higher concentration of the substrate. In other words, the relative percentage fraction of substrate interacting with the ROS will be less at higher concentration and this leads to the lowering of the rate constant with increase in concentration.

3.3.3.3 Effect of MW power

The effect of MW power on the degradation of IC is examined in the range 90-500 W and the results are plotted in Fig. 3.18.
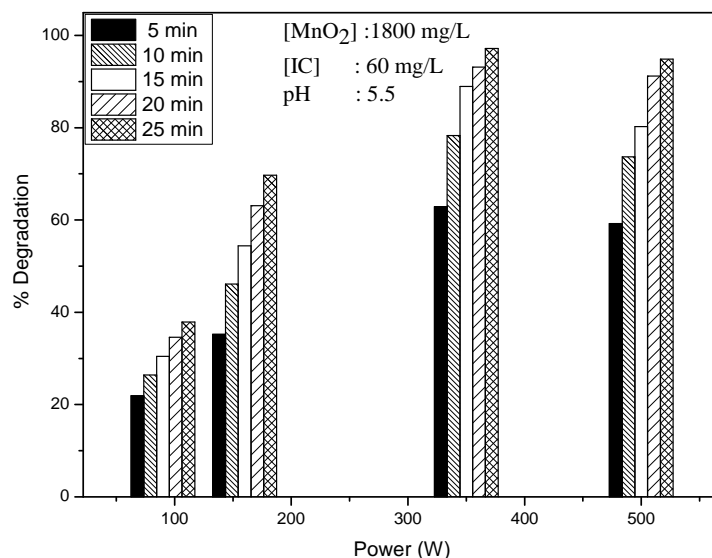
Fig. 3.18: Effect of power on the MW/MnO₂ degradation of IC

Increasing the MW power from 90 to 350 W, keeping all other parameters constant, enhanced the degradation from ~ 20 % to ~ 63% in 5 minutes. The degradation remained more or less same at >350W indicating an optimum power for the degradation of IC under the reaction conditions. However maintenance of precise reaction parameters under the over-volatilizing high power environment was difficult and hence all further studies were carried out at 160W. The increase in MW power is known to increase the temperature and hence the degradation at higher power can be partially attributed to this. The lack of correlation between power and degradation at higher input power can also be attributed to the difference in the effect of temperature on various intermediates formed during the degradation of the pollutant [148].

At higher MW power, relatively more stable intermediates from IC degradation such as oxalic acid, acetic acid, nitrobenzene, malic acid etc. may be getting accumulated faster in the system [149, 150]. The effect of MW may be relatively more on them than on the IC. Hence the effect of increasing the power beyond the optimum may not be reflecting in the degradation. Detailed investigation on this is beyond the scope of the current study and is hence not done here.

3.3.3.4 Effect of Temperature

The effect of temperature on the degradation is verified from experiments under controlled temperature conditions in presence of MW. The results are given in Fig. 3.19.
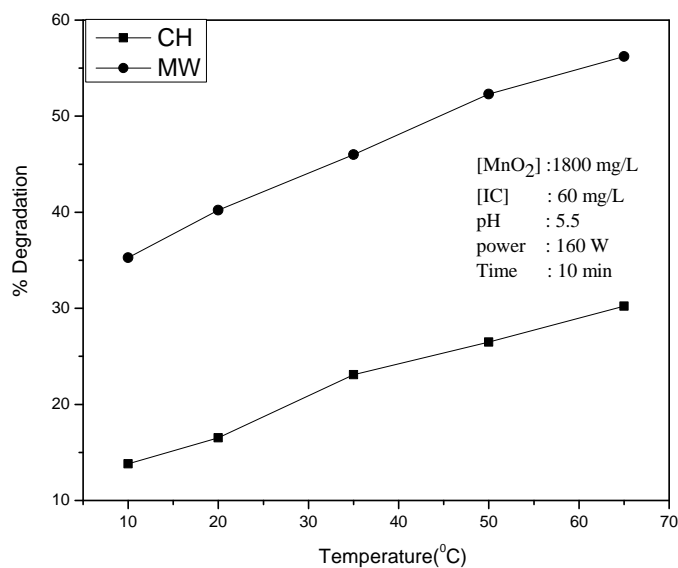
Fig. 3.19: Effect of temperature on the MW/MnO$_2$ degradation of IC

As the figure shows, even at a low temperature of 20^{0}C, the degradation in presence of MW irradiation is 40% in 10 minutes. In the

case of CH, it is only 17.5%, which can be attributed to adsorption. The degradation/disappearance of IC increases with increase in temperature in presence of MW. Rate of degradation also increases with increase in temperature (Fig.3.20). However, just as in the case of optimum MW power as seen in Fig.3.18, there is an optimum temperature in presence of MW (50^0C) beyond which the degradation increases very slowly or becomes even stable. In the case of CH the degradation increases slowly with temperature and is more or less stabilized in the range $> 50^0$C. Hence it may be concluded that the effect of temperature on the degradation of IC in presence of MW is moderate and the optimum temperature is $\sim 50^0$C at least in the range of $10\text{-}65^0$C studied here.
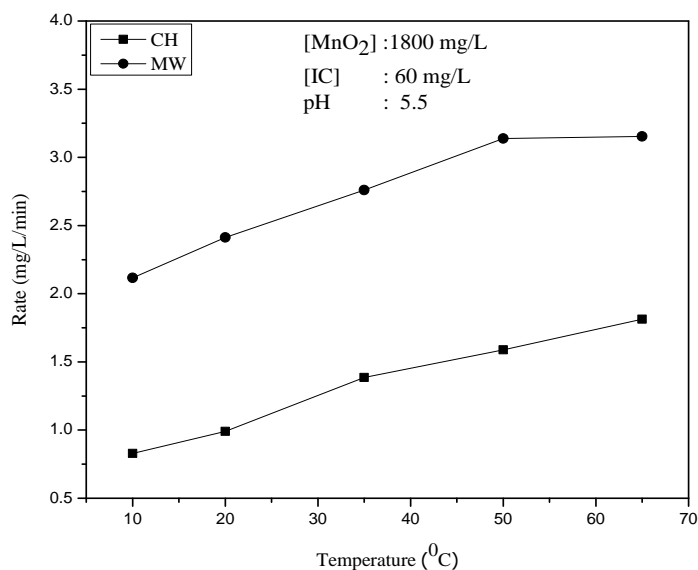
Fig. 3.20: Effect of temperature on the rate of degradation of IC in presence of conventional heating (CH) and MW radiation

Microwave, Photo and Sono Activated Advanced Oxidation Processes and their Variations for the Decontamination of Water from Toxic Chemical Pollutants

117

The apparent activation energy, Ea of the degradation of IC under MW and CH in presence of MnO_2 is calculated from the Arrhenius equation, assuming pseudo first order kinetics as follows.

$$lnk = (-Ea/RT) + lnA \quad ....(25)$$

where k- Rate constant

T- Temperature of the reaction in Kelvin

A- Arrhenius factor

R- Universal gas constant (8.314×10^{-3} kJ/mol)

Ea is calculated from the Arrhenius plot of lnk vs 1/T

Fig.3.21 shows the Arrhenius plot for the degradation under conventional heating. The Ea calculated here is 11.62 kJ/mol. Under identical conditions, the Arrhenius plot for the degradation under MW is presented in Fig.3.22. The Ea calculated in this case is 7.7 kJ/mol. The apparent activation energy for the degradation under CH condition is higher compared to the MW condition. The lower activation energy in the case of MW radiation implies that the non-thermal effect of MW facilitates reduction in the activation energy and this is responsible for the enhanced degradation compared to CH. The relative enhancement in the degradation under MW over CH is less at higher temperatures. For eg. the enhancement at 20^0C is~135% while it is ~ 80% at 60^0C. Hence at higher temperatures, CH will be providing more energy for the degradation so much so that a stage may be reached at very high temperature, when the non -thermal component can be offset by the heat provided by CH.
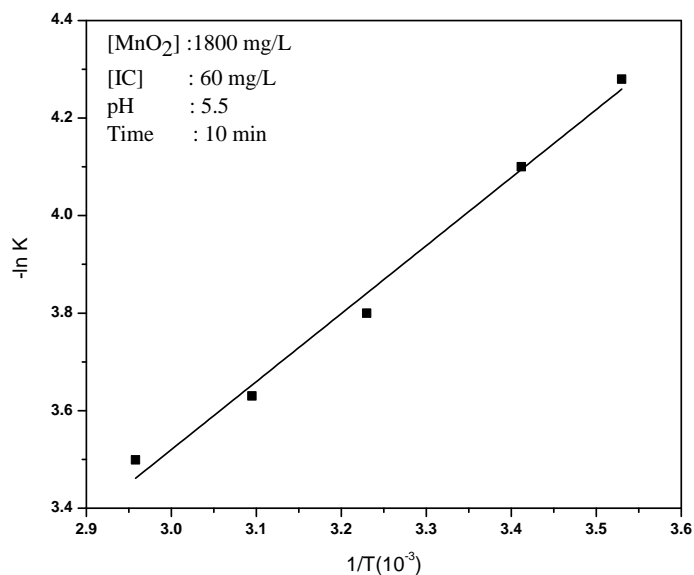
Fig. 3.21: Arrhenius plot for the degradation of IC under MnO₂/CH condition
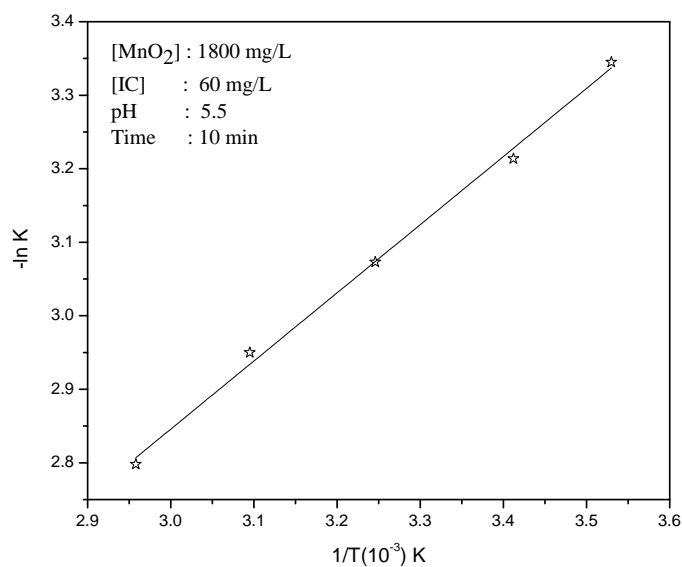
Fig. 3.22: Arrhenius plot for the degradation of IC under MW/MnO₂ condition

Microwave, Photo and Sono Activated Advanced Oxidation Processes and their Variations for the Decontamination of Water from Toxic Chemical Pollutants

119

3.3.3.5 Effect of pH

The effect of pH on the degradation of IC under MW/MnO$_2$, CH/MnO$_2$ and RT/MnO$_2$ conditions is shown in Fig. 3.23. The effect at different times in the case of MW/MnO$_2$ is shown in Fig.3.24.
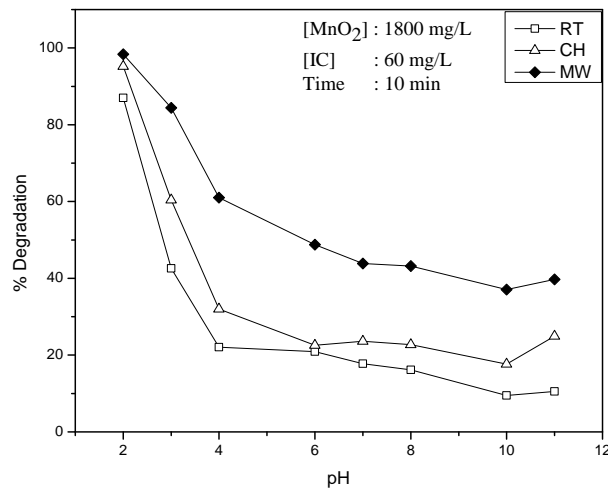
Fig. 3.23: Effect of pH on the degradation of IC under various conditions
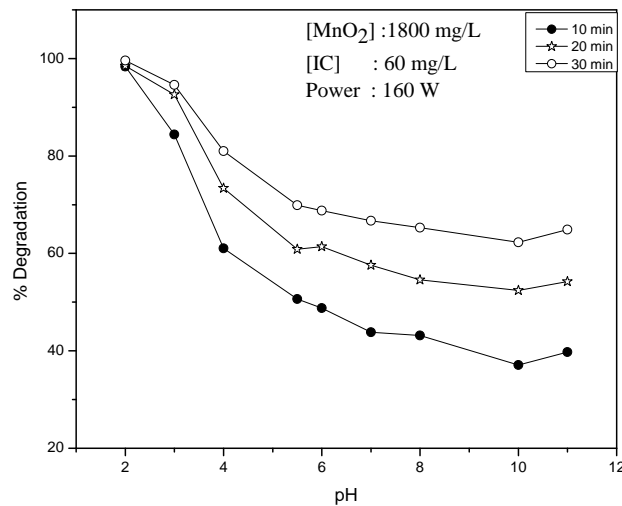
Fig. 3.24: Effect of pH on the MW/MnO$_2$ degradation of IC at different reaction times.

At all pH, the degradation follows the order $MW/MnO_2 > CH/MnO_2$ $> RT/MnO_2$. The degradation remains more or less steady at their respective values under all three conditions in the pH range 6-10. The degradation is significantly high at pH 2-3 and is almost complete ($\approx$100%) at pH 2. Variation in pH has no effect on the dye as such in the range 2-11 thereby indicating that the higher degradation at pH < 4 takes place only in the presence of MnO_2. High degradation under extreme pH of 2 even under RT further shows that it is due to MnO_2 induced degradation only with little contribution from MW or CH. However, MW and CH play an accelerating role once the reaction is initiated. The dramatic increase in the degradation of IC at around pH 2-3 has been reported during the photocatalytic oxidation of the dye on Mn supported TiO_2 [151]. The drastic shift in degradation occurring below pH 4 can be explained partially based on the point of zero charge (PZC) of ~ 4.7 of MnO_2 [152]. Below this pH value the surface is positively charged and hence its oxidizing ability will be sharply enhanced. IC is a dianionic dye in aqueous solution and it can keep the configuration in the pH range 3-11 [151].

At low pH < 4.7 electrostatic interaction between the positively charged catalyst surface and the dianions can lead to strong interaction and subsequent reaction. Heterogeneous catalytic degradation in presence of MnO_2 is known to be initiated with the formation of precursor complex between the target contaminants and surface bound Mn [153]. Electrons are transferred from the organic compound to the surface bound Mn (IV) on the MnO_2 surface. This results in the oxidative degradation of the pollutant and the Mn (II) is reductively dissolved from MnO_2 into bulk solution. Thus MnO_2 can also play the role of an oxidant. Dissolved O_2 in solution

Microwave, Photo and Sono Activated Advanced Oxidation Processes and their Variations for the Decontamination of Water from Toxic Chemical Pollutants

121

can oxidize the Mn (II) to Mn (IV) oxide again. In this respect MnO_2 plays the role of a catalyst and dissolved O_2 acts as the oxidant. It is the solution pH beyond the PZC that promotes the re-adsorption of free Mn(II) ions in solution back onto MnO_2 surface which is responsible for the catalytic oxidation. At the natural pH of 5.6 of the reaction system, CH/MnO_2 is ~ 20% more efficient than RT/MnO_2 while MW/MnO_2 is ~ 2.5 times more active than RT/MnO_2. The alleviation of pH dependence of MnO_2 assisted degradation of methylene blue by MW [151] is not seen in the present context. The slow but steady degradation of IC in the pH range 6-10, which is above the PZC of MnO_2 is surprising. At this pH, the surface is negatively charged and the anionic dye may be getting repelled from the surface. It may be inferred that at higher pH, when there are more OH^- ions present in the system, formation of more reactive $^{\cdot}OH$ radicals is possible and these radicals can interact with the IC in the bulk and cause higher degradation.

However, PZC of the catalyst and its consequence on the adsorption of IC may not be the only factor that determines the pH effect. The PZC itself is a complex parameter which depends on the characteristics of the system as a whole. The complexity and unpredictability of the pH effect has been reported in many AOP based catalytic processes earlier also [154].

3.3.3.6 Corrosion of MnO_2

The possibility of corrosion of MnO_2 under extreme acidic and alkaline conditions as responsible for the pH effect on the degradation of IC is tested by measuring the loss in weight of MnO_2 at different pH. The loss in weight, if any, of MnO_2 after exposure to the IC solution at different pH is used as the indicator of corrosion. IC solution (100mL,

60 mg/L) was taken in different 250 mL beakers and the pH was adjusted as required. MnO$_2$ (0.18 g/100mL) was precisely weighed and added to each of these beakers and mixed well. The suspensions were kept agitated for a specific period (120 min). Thereafter the suspension in each beaker was centrifuged and the clear supernatant solution was transferred to dry previously weighed 250 mL beakers. The IC solution in each beaker was evaporated, at 50^{0}C. Once the evaporation is complete, weight of the dry beaker was determined. It was then dried again and weighed. The process was continued until the weight becomes constant. The % corrosion of MnO$_2$ was calculated from the weight difference as given below:

$$\% \text{ Corrosion} = (W_f - W_0) \times 100/m \quad \dots\dots\dots\dots\dots\dots\dots(26)$$

Where W_f - is the final constant weight of the beaker

W_0- is the initial weight of the dry beaker

m- is the mass of MnO$_2$ taken initially

The results are plotted in Fig.3.25.
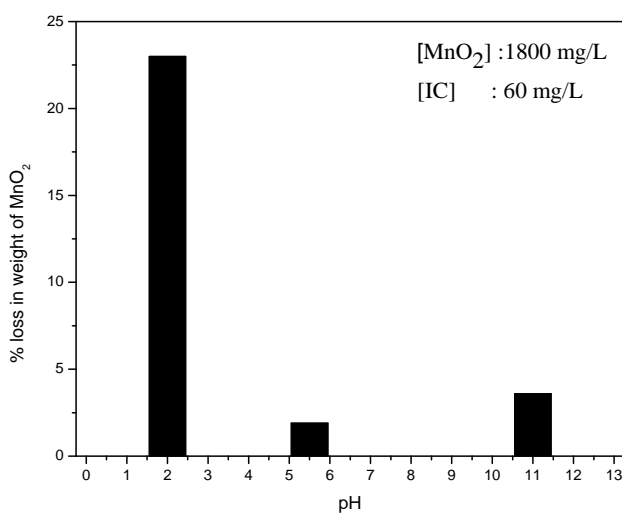
Fig. 3.25: Corrosion of MnO$_2$ at different pH

Microwave, Photo and Sono Activated Advanced Oxidation Processes and their Variations for the Decontamination of Water from Toxic Chemical Pollutants

123

The corrosion is ~ 23% at pH 2, 1.9 % at pH 5.5 and ~ 3.6% at pH 11 after 120 minutes at room temperature (29^0C). Since all experiments are carried out at the optimized pH of 5.5, corrosion can be considered negligible under the conditions of the study. Since the corrosion is high under extreme acidic pH of 2 it may be inferred that the degradation of IC should have been even higher had there been no loss of MnO_2. In any case, the process at extreme acidic condition of pH~2 may not be viable for implementation, environmentally and economically and hence all investigations were made at the natural pH~5.6 of the reaction system.

3.3.3.7 Effect of reaction volume

Effect of volume of the reaction medium on the efficiency of degradation of IC is verified by conducting the reactions with different volumes in the same reactor. The volume ranges from 100 to 800 mL. The results are shown in Fig. 3.26.
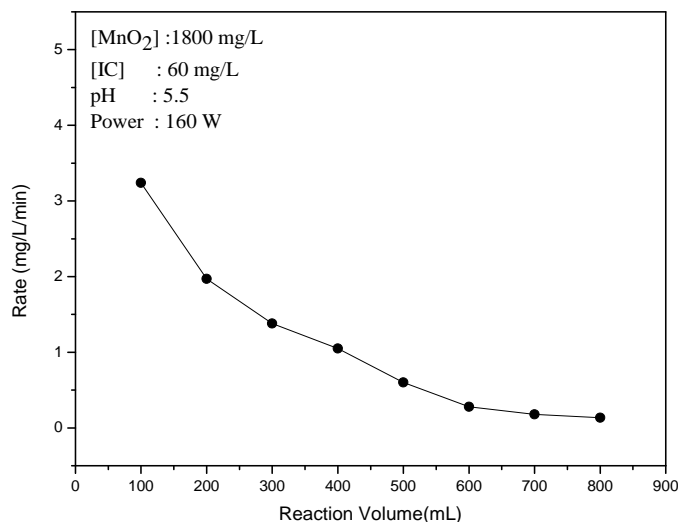
Fig. 3.26: Effect of reaction volume (at constant weight of catalyst) on the MW/MnO_2 degradation of IC

It is seen that the rate decreases with increase in reaction volume and eventually the degradation is almost completely inhibited when the suspension is too dilute at 600-800 mL. It can be attributed to the relatively slower penetration of MW radiation through the reaction medium with increase in volume. The relatively decreasing availability of the catalyst particles with respect to IC is another possible reason for the poor degradation at higher volume. This is further verified by increasing the dosage of catalyst proportionally with volume and the results are shown in Fig. 3.27.
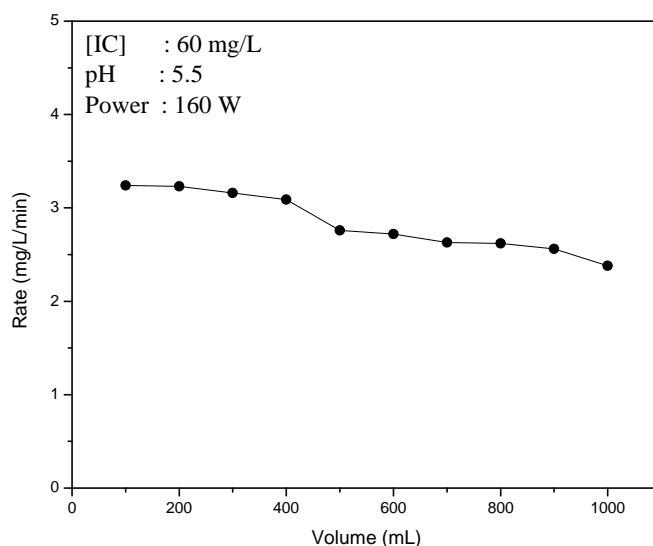
Fig. 3.27: Effect of reaction volume (at constant volume/catalyst weight ratio) on the MW/MnO$_2$ degradation of IC

In this case the rate of degradation is sustained upto 400 mg/L (MnO$_2$ dosage 7.2 g/L) thereby confirming the importance of relative concentration of catalyst and the substrate. Beyond 400 mL, the rate of degradation decreases slowly thereby indicating that the penetration of

MW becomes weaker with increase in volume and simple increase in catalyst dosage is not enough to compensate for this.

3.3.3.8 Formation of H_2O_2

Since the measurement of H_2O_2 is difficult when the coloured dye is still present in the system (due to analytical constraints), the concentration of H_2O_2 is determined immediately on decolourisation (time '0' in Fig.3.28). Thereafter, the MW irradiation is continued for some more time and the H_2O_2 is measured periodically. The results are shown in Fig.3.28.
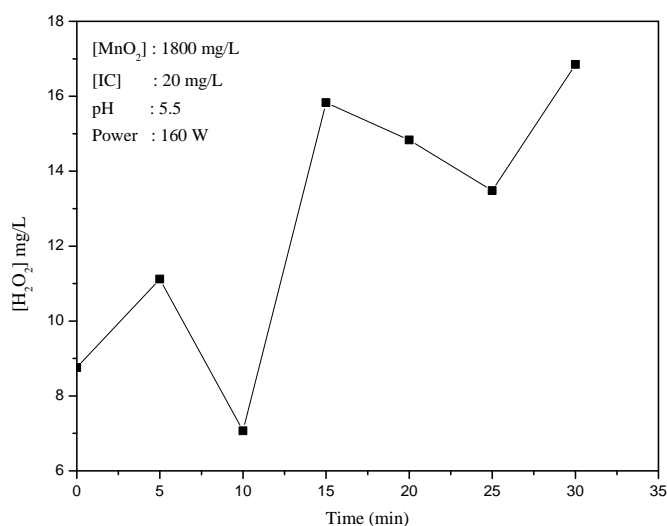
Fig. 3.28: Oscillation in the concentration of insitu formed H_2O_2 with time

The concentration of H_2O_2 increases initially then decreases with time and increases again in a wave-like fashion resulting in periodic crests and troughs i.e. oscillation. The oscillation in the concentration shows that H_2O_2 is generated and decomposed/consumed simultaneously depending on the reaction conditions, in particular its concentration. The oscillation may

also be due to adsorption and desorption of MnO_2 occurring intermittently since MnO_2 is known to be a good adsorbent of a variety of molecules. This aspect is verified by a series of experiments as follows.

3.3.3.9 H_2O_2 adsorption/decomposition

The decrease in concentration of H_2O_2, which can be attributed to its adsorption/decomposition is tested experimentally at various concentrations of MnO_2 and the results are plotted in Fig. 3.29.
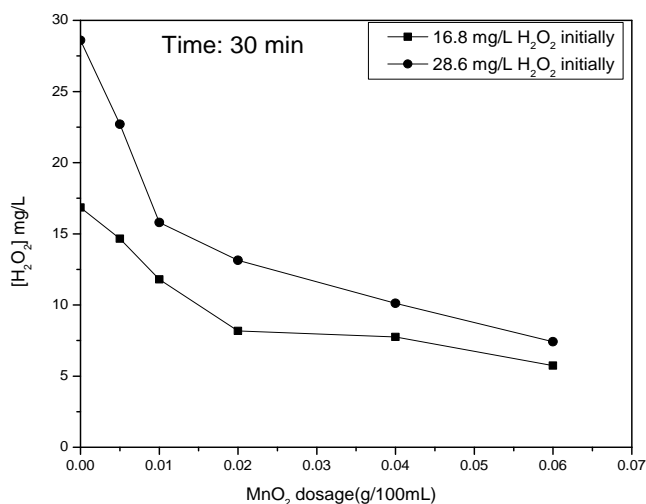
Fig. 3.29: Effect of MnO_2 dosage on the adsorption/decomposition of H_2O_2

The disappearance of H_2O_2 increases steeply with increase in MnO_2 dosage initially. After reaching an optimum dosage, the concentration of H_2O_2 is stabilised. The uptake/adsorption/decomposition increases also with increase in concentration of H_2O_2 as seen from the data for (16.8 mg/L and 28.6 mg/L) of initial concentrations. The decrease in the concentration of H_2O_2 is ~ 60% and ~ 75% for initial concentration of 16.8 and 28.6 mg/L respectively. This indicates that the adsorption of H_2O_2 by

MnO_2 can be at least one of the reasons for its decrease in concentration. The stabilisation in the concentration of H_2O_2 irrespective of the dosage of MnO_2 shows that there is some kind of equilibrium between adsorption and desorption after the optimum adsorption is reached. When the surface is saturated, no further decrease in the concentration of H_2O_2 can be noticed. This also indicates that, the surface has a role in the decrease in the concentration of H_2O_2, which can be adsorption/decomposition or both.

In order to find out whether H_2O_2 is adsorbed or decomposed another experiment is conducted as follows:

Higher concentration of H_2O_2 is taken and its decrease in concentration in presence of MnO_2 is measured with 1800 mg/L of the catalyst. 100 mg/L each of H_2O_2 is added in sequence and the results are plotted in Fig.3.30.
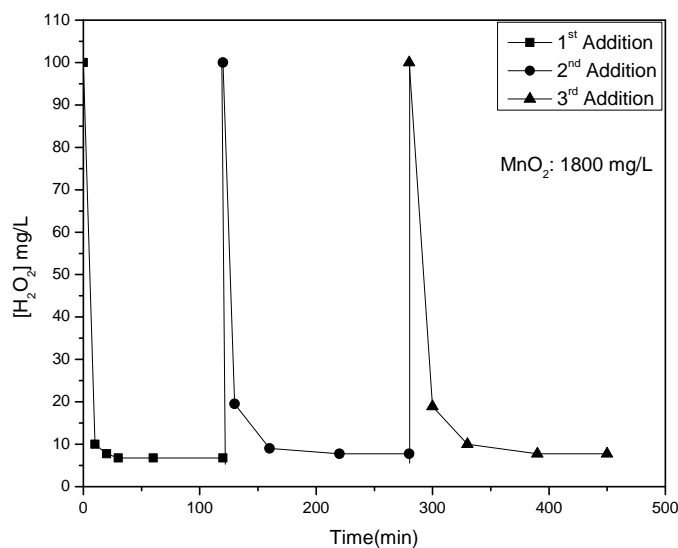
Fig. 3.30: Disappearance of sequentially added H_2O_2 in presence of MnO_2

Sequential addition of H$_2$O$_2$ to the system shows that even up to 3 additions (300 mg/L) of H$_2$O$_2$ can be readily adsorbed/decomposed by 1800 mg/L of MnO$_2$. In this case the decrease in concentration of H$_2$O$_2$ is quite fast probably because the relative concentration of the catalyst is very high. Hence the same experiment was conducted at a lower dosage of MnO$_2$ (200 mg/L). The results are plotted in Fig.3.31.
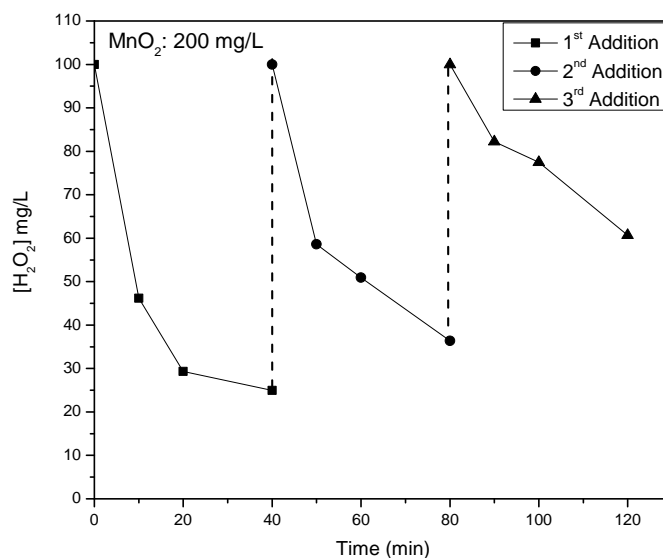
Fig. 3.31: Disappearance of sequentially added H$_2$O$_2$ in presence of lower dosage of MnO$_2$

The data shows that the adsorption/decomposition of H$_2$O$_2$ is slower at lower concentration of MnO$_2$. Further, the H$_2$O$_2$ is not fully disappearing and the concentration stabilises at~30 mg/L initially. With subsequent addition of H$_2$O$_2$, the stabilisation happens at~40 mg/L and with the third addition the decrease in H$_2$O$_2$ concentration is still lower with a higher stabilised value of 60mg/L. From the data it may be inferred that the H$_2$O$_2$

Microwave, Photo and Sono Activated Advanced Oxidation Processes and their Variations for the Decontamination of Water from Toxic Chemical Pollutants

129

is getting adsorbed as well as decomposed in presence of MnO_2. Had it been only the decomposition the concentration could have reached zero or close to that. Hence the decrease in concentration of H_2O_2, at least in the initial stages when most of the surface sites are available can be due to adsorption. Even after stabilisation in the concentration of H_2O_2 subsequent addition results in a further decrease. This shows that decomposition also takes place in presence of MnO_2. At higher dosage of MnO_2, there will be more sites for adsorption and promotion of decomposition. Hence the disappearance is faster. At lower dosage of MnO_2, the rate at which the adsorbed H_2O_2 will decompose will be slower and hence the availability of free sites for fresh H_2O_2 will take longer time. Hence, adsorption/decomposition takes longer time and stabilisation occurs at higher concentration of H_2O_2 for every subsequent addition.

MW irradiation of H_2O_2/MnO_2 system accelerates the disappearance of H_2O_2. This is evident from the results presented in Fig.3.32 which shows faster and complete disappearance of H_2O_2 under MW irradiation in presence of MnO_2. In the absence of MW, the H_2O_2 disappears faster initially followed by stabilisation, which can be attributed to adsorption. From these observations it may be inferred that H_2O_2 gets adsorbed in presence of MnO_2. Decomposition of H_2O_2 also is possible and MW irradiation accelerates the decomposition.
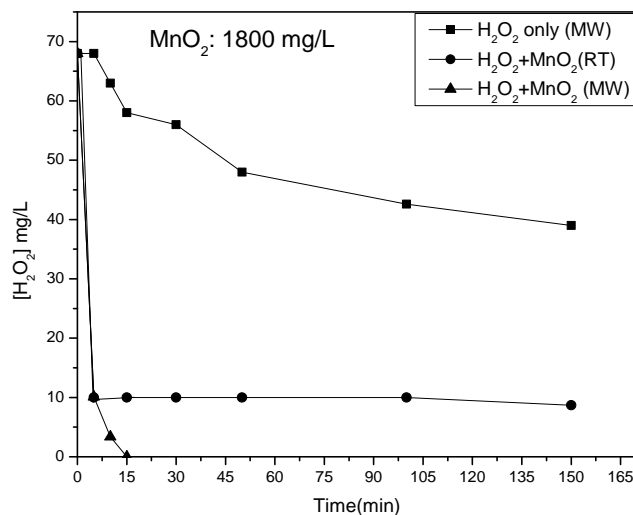
Fig. 3.32: Fate of H_2O_2 under different reaction conditions

3.3.3.10 Effect of Oxidants

Addition of oxidants such as H_2O_2 and persulphate is known to enhance the rate of degradation of many organic pollutants by AOP techniques. The mechanism of enhancement involves the generation of highly reactive ˙OH and other radicals capable of interacting with the pollutants and degrading them. Hence the effect of addition of H_2O_2 which can form ˙OH radicals under MW irradiation on the degradation of IC is examined.

Persulfate ($S_2O_8^{2-}$) is one of the strongest oxidants known in aqueous solutions and has higher potential ($E^0 = 2.01eV$) than H_2O_2 ($E^0 = 1.76eV$). Advantages of persulfate include convenience of storage and transport, high stability, high aqueous solubility and relatively low cost. These features make it a promising choice for clean- up applications. Reactions of persulfate with organic pollutants in water, however, are

Microwave, Photo and Sono Activated Advanced Oxidation Processes and their Variations for the Decontamination of Water from Toxic Chemical Pollutants

▌131

generally slow at ambient temperature, and activation of persulfate is necessary to accelerate the process. Oxidants such as H_2O_2 and $S_2O_8^{2-}$ have been receiving increasing attention in recent years as accelerators of AOTs. Hence the effect of addition of these two oxidants on the MW degradation of IC is investigated in detail.

3.3.3.10.1 Effect of added H_2O_2

In many AOPs the reaction is accelerated by H_2O_2 primarily through the production of extra $\cdot OH$ radicals. Hence the effect of addition of H_2O_2 on the degradation of IC under MnO_2/MW is examined. It is observed that the degradation is inhibited by H_2O_2 (Fig.3.33). The inhibition increases with increase in concentration of H_2O_2 and eventually stabilises in the range 50-60 mg/L.
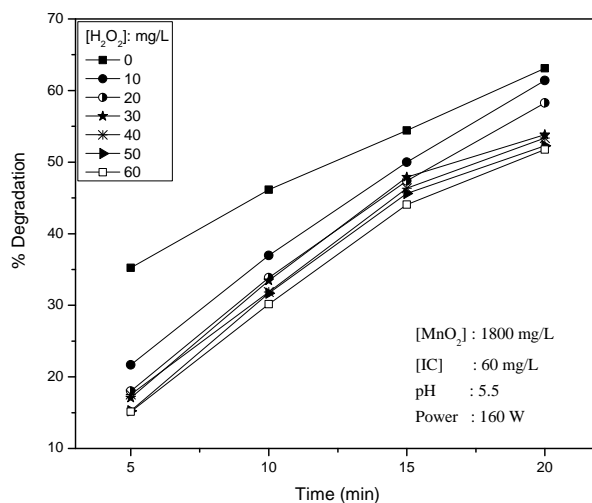
Fig. 3.33: Effect of added H_2O_2 on the MW/MnO_2 degradation of IC

Beyond a particular concentration of H_2O_2 (50mg/L), further increase does not lead to increase in the inhibition. However there are instances in

which H_2O_2 shifts its role from inhibitor at lower concentration to enhancer at higher concentration [56]. This possibility is tested by studying the effect of H_2O_2 at higher concentrations (100-400 mg/L) on the degradation of IC. The results presented in Fig.3.34 show that above a particular concentration i.e 50 mg/L in this case, H_2O_2 which is an inhibitor at lower concentration neither inhibits nor enhances the degradation of IC.
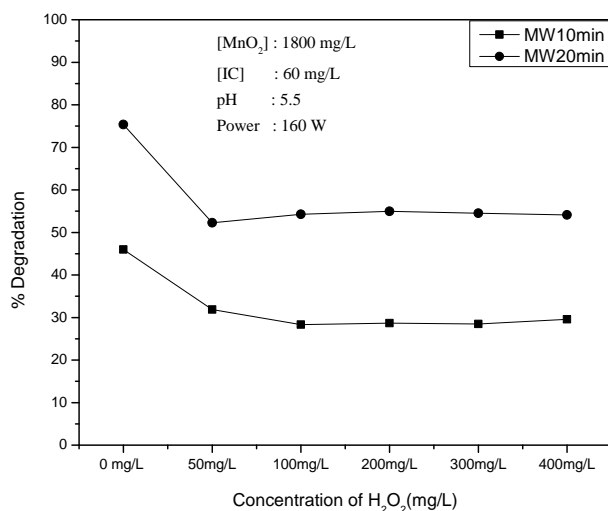
Fig. 3.34: Effect of higher concentrations of H_2O_2 on the MW/MnO₂ degradation of IC

H_2O_2 is known to absorb MW energy and undergo decomposition to H_2O and O_2 as in eqn.27

$$\overset{MW}{2H_2O_2 \rightarrow 2H_2O + O_2} \quad\text{...(27)}$$
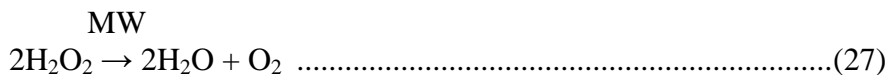
This naturally limits the MW energy available for catalyst activation and formation of ROS such as ·OH. This leads to decrease in the degradation of IC.

In addition to reaction (27) decomposition of H_2O_2 can also lead to the formation of $^\cdot OH$ radicals as in eqn.28.

$$H_2O_2 \xrightarrow{MW} 2 \, ^\cdot OH \qquad \text{...(28)}$$
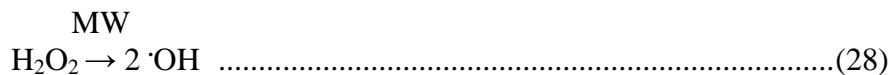
These $^\cdot OH$ radicals, as well as the $^\cdot OH$ radicals formed under MW catalysis will interact with H_2O_2 as in eqn.29.

$$H_2O_2 + \, ^\cdot OH \rightarrow HO_2^\cdot + H_2O \text{...(29)}$$

$$HO_2^\cdot + HO_2^\cdot \rightarrow H_2O_2 + O_2 \text{...(30)}$$

However, the $HO_2^\cdot$ thus formed is less reactive compared to $^\cdot OH$ radicals resulting in decreased degradation of the substrate. Thus it may be seen that H_2O_2 serves simultaneously as a producer and a scavenger of $^\cdot OH$ radicals. Part of the $^\cdot OH$ radicals formed from the decomposition of H_2O_2 will be used for the degradation of IC and the other part will be interacting with H_2O_2 itself and degrading it. Thus the net concentration of $^\cdot OH$ radicals available for degrading the dye is reduced resulting in decreased degradation. This concurrent formation and decomposition of H_2O_2 as well as various other complex free radical interactions together with the partial absorption of MW by H_2O_2 result in decreased degradation of IC at lower concentration of H_2O_2. Beyond the critical concentration of H_2O_2 formation and consumption of $^\cdot OH$ are balanced, resulting in stable degradation.

The inhibition of the degradation of IC by H_2O_2 is further confirmed by the addition of H_2O_2 in between to a reaction in progress at different time intervals (20, 35 min). The results are shown in Fig.3.35.
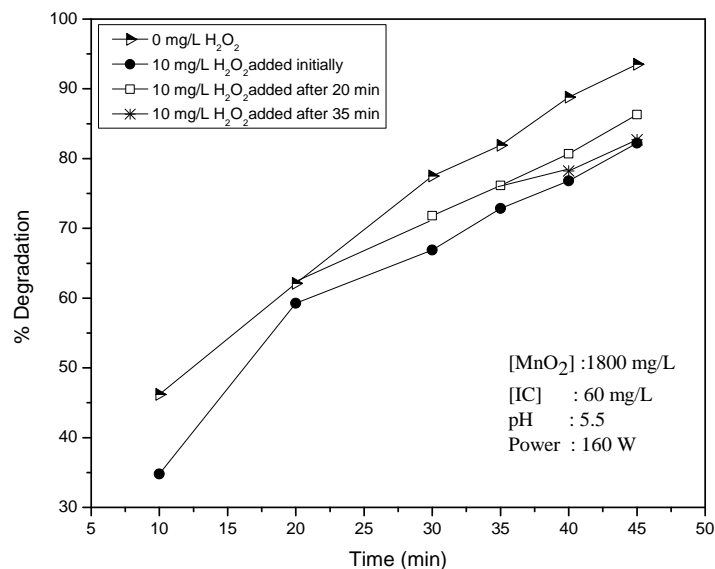
Fig. 3.35: Effect of initial and in-between addition of H_2O_2 on the MW/MnO₂ degradation of IC.

The addition of H_2O_2 after 20 min decreases the degradation of IC. Further addition after 35 min brings down the rate again thereby reconfirming the inhibiting role of H_2O_2 at lower concentration in the degradation of IC.

Another possible reason for the decrease in degradation of IC in presence of H_2O_2 can be the adsorption of the latter on the catalyst thereby preventing the molecules of IC from interacting with the surface. The effect of the presence of H_2O_2 on the adsorption of IC at various concentrations on MnO₂ is measured and the results are shown in Fig. 3.36. Irrespective of the concentration of IC, H_2O_2 inhibits the adsorption moderately. However the adsorption of IC does not increase with increase in its concentration indicating that competitively H_2O_2 can get better adsorbed. Even at H_2O_2/IC ratio of 1:8 the adsorption of IC is inhibited. Hence it is possible that in presence of added or in situ formed H_2O_2, some of the sites on

MnO_2 may be utilized for adsorption and/or decomposition of H_2O_2 and this may be one of the reasons for the initial inhibition by H_2O_2.

If the competition from H_2O_2 as above, is indeed the reason for the inhibition in the adsorption of IC, its adsorption at constant concentration (of IC) must decrease with increase in concentration of H_2O_2. This is experimentally tested by varying H_2O_2 concentration from 0-60 mg/L, keeping concentration of IC constant at 60 mg/L. Results are presented in Fig.3.37. The adsorption decreases with increase in concentration of H_2O_2 up to 30 mg/L and stabilises thereafter. This clearly shows that H_2O_2 and IC compete effectively for adsorption on MnO_2. However, there is a limit to the number of sites that can be occupied by H_2O_2 at any point of time on a given amount of MnO_2. This partially explains the stabilization of 'H_2O_2 effect' on the adsorption as well as degradation of IC.
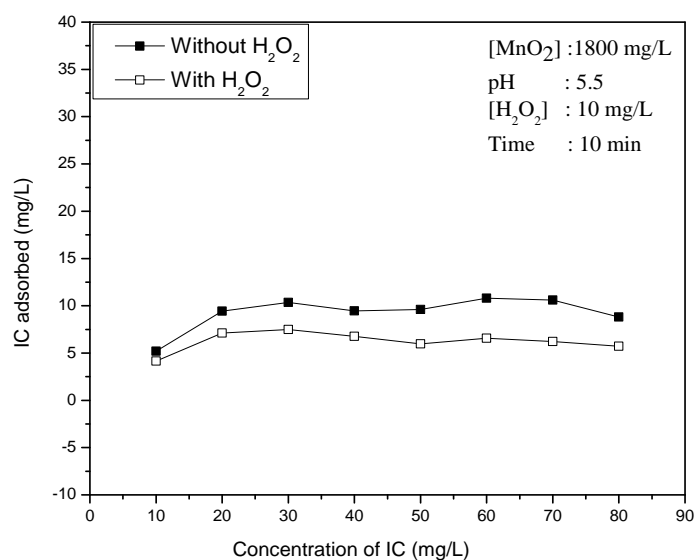
Fig. 3.36: Effect of concentration of IC on its adsorption on MnO_2 in presence of H_2O_2
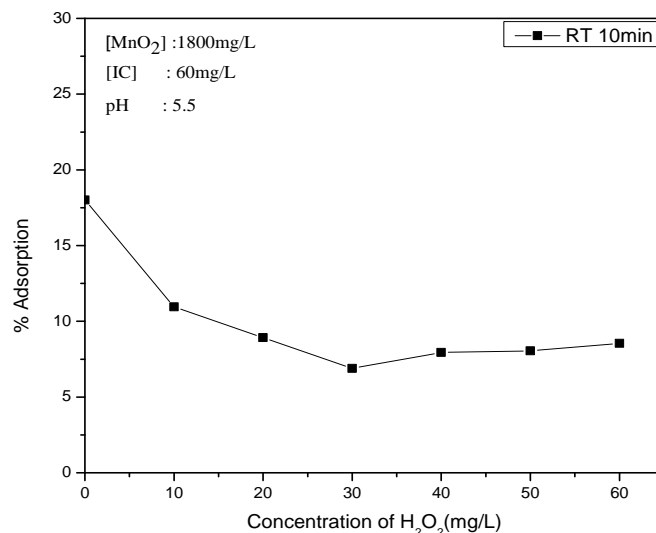
Fig. 3.37: Effect of concentration of H_2O_2 at various
concentrations on the adsorption of IC on MnO_2

The competition between IC and H_2O_2 for adsorption sites on MnO_2 is further checked by measuring the adsorption of H_2O_2 on fresh and IC- preadsorbed MnO_2. The experiment is done as follows. 180 mg of MnO_2 is added to 100mL of IC solution (60 mg/L). The suspension was allowed to stay long enough (4 days) to ensure complete decolourisation and hence 100% adsorption. The catalyst is separated, washed with water and dried under normal atmospheric conditions. This catalyst with pre-adsorbed IC is used as the adsorbent for H_2O_2. The result obtained is shown in Fig.3.38 which clearly illustrates that the adsorption of H_2O_2 is much less on IC- preadsorbed MnO_2.

All these results reconfirm that there is competition between H_2O_2 and IC for the adsorption sites on MnO_2 and also that MnO_2 is a very efficient medium for adsorption and/or decomposition of H_2O_2.

Microwave, Photo and Sono Activated Advanced Oxidation Processes and their Variations for the Decontamination of Water from Toxic Chemical Pollutants

137
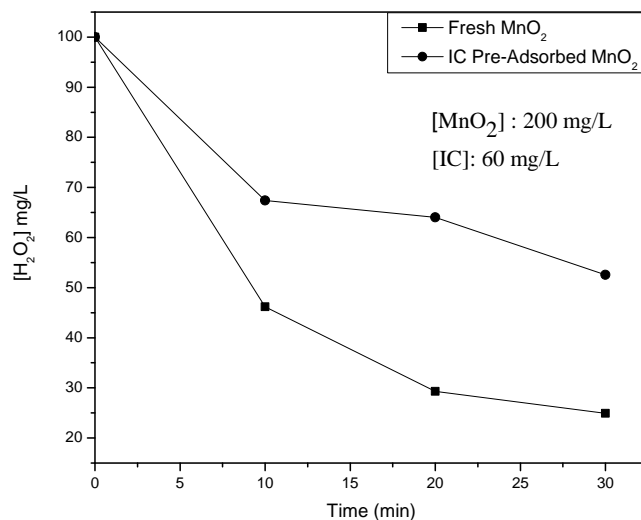
Fig. 3.38: Adsorption/decomposition of H_2O_2 on lower concentration of MnO_2 and IC-Pre adsorbed MnO_2

Even after the stabilisation of adsorption of IC (and presumably saturation of the surface) few sites may still be available and these are the sites where H_2O_2 will get adsorbed. The presence of few vacant sites on IC-preadsorbed MnO_2 is further verified by exposure of IC-preadsorbed MnO_2 to fresh IC solution again twice (Fig.3.39). Small amounts of the dye is adsorbed in this case also. However, this amount of dye is relatively less compared to the amount of H_2O_2 that could get adsorbed on IC preadsorbed catalyst (Ref. Fig.3.38). Hence it is possible that H_2O_2 can even displace/react with some of the preadsorbed IC. It is also possible that there may be different types of sites on MnO_2 where IC or H_2O_2 can get preferentially adsorbed. Further investigations on adsorption characteristics and related aspects is beyond the scope of the current study.
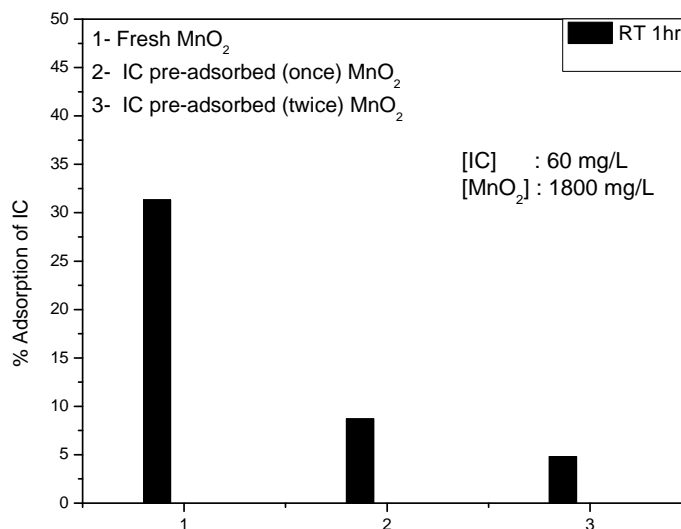
Fig. 3.39: Adsorbtion of IC on fresh MnO$_2$ and IC- preadsorbed MnO$_2$.

3.3.3.10.2 Effect of persulphate

Another powerful oxidant in AOP is peroxy disulphate, also known as persulphate (PS).

In addition to the high solubility and stability at ambient temperature, a major advantage of PS is that the SO$_4^{2-}$ ions, which are the major products of PS reduction are relatively harmless and considered to be environment-friendly. Hence the effect of application of PS as an oxidant is investigated in detail.

PS as such does not cause any degradation of IC. The decrease in concentration under CH and RT conditions in presence of MnO$_2$ and PS is primarily due to adsorption. The comparative effect of PS on the degradation of IC under identical RT, CH and MW conditions is given in Fig.3.40. The MW initiated, MnO$_2$ catalysed degradation is enhanced

Microwave, Photo and Sono Activated Advanced Oxidation Processes and their Variations for the Decontamination of Water from Toxic Chemical Pollutants

139

significantly in presence of PS. This implies that MnO_2 assists the formation of more reactive oxidising species from PS under MW.
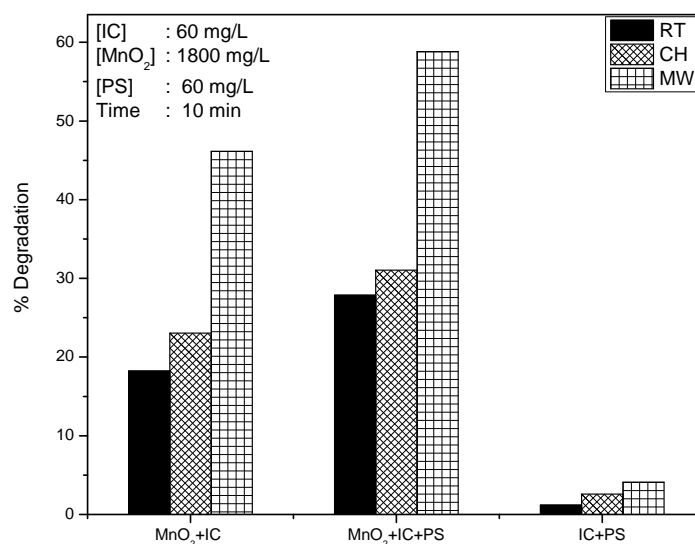
Fig. 3.40: Comparative degradation of IC in presence of PS under various reaction conditions.

The effect of PS at different concentrations (0-60mg/L) on the MW/MnO_2 degradation of IC is studied and the results are shown in Fig.3.41. The enhancing effect of PS is concentration-dependent with an optimum of 50 mg/L.

The enhancing effect is also confirmed by the in-between addition of PS to a reaction that is in progress (Fig.3.42). The degradation is enhanced from the point of each addition of PS.
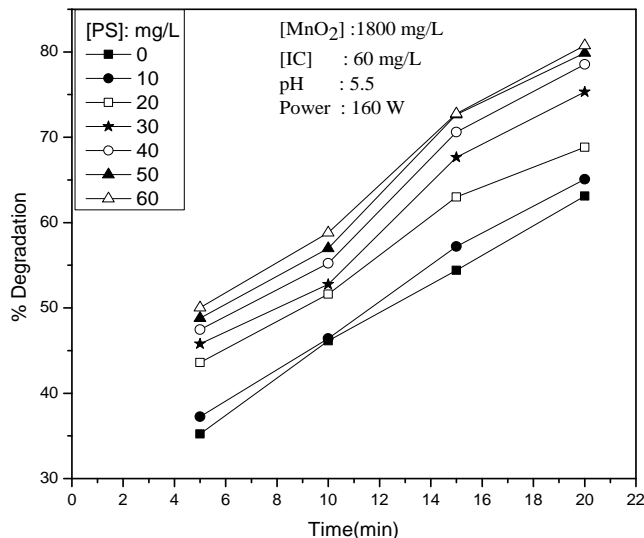
Fig. 3.41: Effect added $K_2S_2O_8$ on the MW/MnO$_2$ degradation of IC.
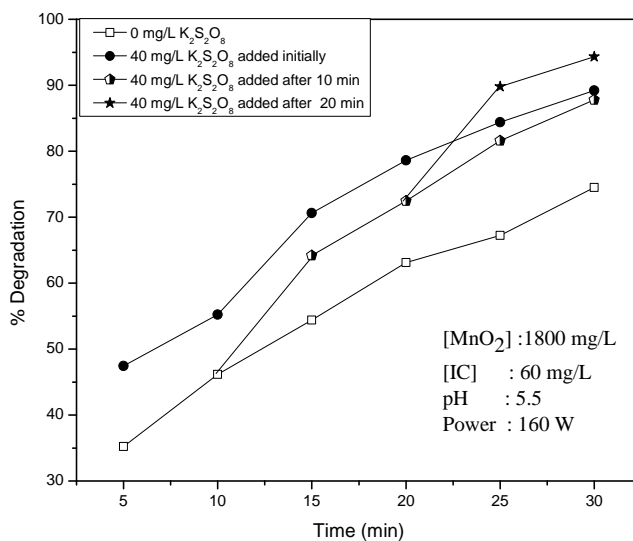
Fig. 3.42: Effect of initial and in-between addition of $K_2S_2O_8$ on the MW/MnO$_2$ degradation of IC.

The results show that excess PS has no negative effect on the degradation of IC. Hence any unused oxidant can be used for fresh input

Microwave, Photo and Sono Activated Advanced Oxidation Processes and their Variations for the Decontamination of Water from Toxic Chemical Pollutants

141

of IC pollutant which is important for the commercial application of the process. This is verified by conducting the experiments at still higher concentrations of PS as shown in Fig.3.43. In this case also excess of PS in the system does not inhibit the degradation.
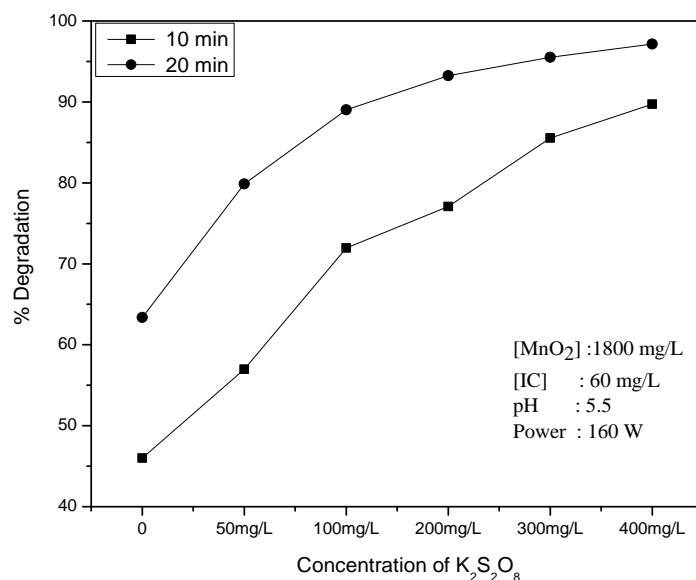
Fig. 3.43: Effect of higher concentrations of $K_2S_2O_8$ on the MW/MnO_2 degradation of IC

In order to verify the utility of unused PS remaining in the system for further oxidation, more IC is added when the initial dye is completely decolourised. The decolourisation/degradation of the newly added dye under MW irradiation is followed (Fig.3.44). The rate of decolourisation is sustained even with the repeated addition of the dye thereby confirming that presence of excess PS can be beneficially used for the decontamination of water in an environment- friendly manner. In presence of initially added PS (200 mg/L), four cycles of decolourisation (of 60 mg/L of IC each) can be

consecutively completed without any decrease in efficiency. Thereafter, 120 mg/L of IC is added in the 5th cycle. In this case the rate of decolourisation is slower. At this stage of low degradation rate more PS is introduced into the system and the decolourisation is accelerated. This reconfirms the enhancing effect of PS on the degradation of IC in presence of MW/MnO$_2$ and its potential for commercial application.
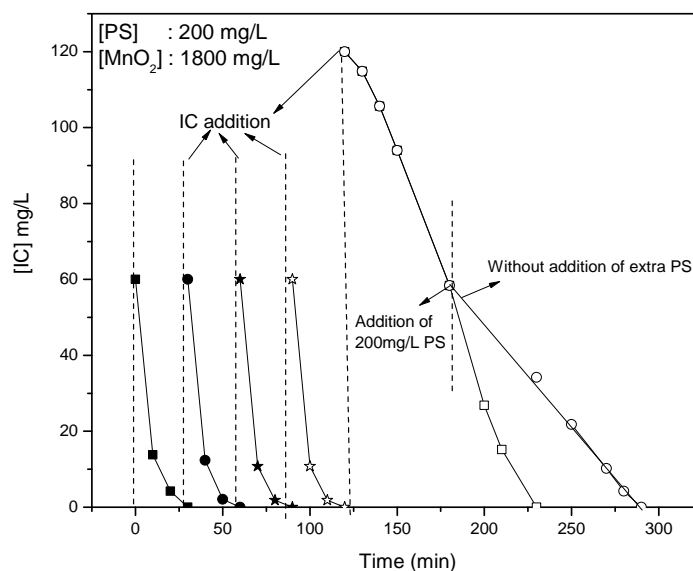
Fig. 3.44: Degradation of repeatedly added IC in presence of residual PS in the system

PS is known to generate highly reactive SO$_4^{-}$ radicals under AOP conditions such as photo, sono, and MW irradiation. The PS/MW degradation of organics may be taking place by the interaction of the substrate with insitu formed SO$_4^{-}$. With increase in concentration of PS, more reactive SO$_4^{-}$ radicals are formed under MW irradiation and a series of chain reactions follow ultimately resulting in the degradation of IC (Eqns. 31-43).

Microwave, Photo and Sono Activated Advanced Oxidation Processes and their Variations for the Decontamination of Water from Toxic Chemical Pollutants

143

Various steps involved in the PS enhanced degradation are [155]:

$$S_2O_8^{2-} \xrightarrow{\text{MW}} 2SO_4^{\cdot-} \quad \text{.. (31)}$$

$$S_2O_8^{2-} + R \rightarrow 2SO_4^{\cdot-} + R^{\cdot} \quad \text{... (32)}$$

R: organic pollutant

$$SO_4^{\cdot-} + H_2O \rightarrow SO_4^{2-} + H^+ + {}^{\cdot}OH \quad \text{..................................(33)}$$

$$SO_4^{\cdot-} + R \rightarrow R^{\cdot} + \text{products} \quad \text{.......................................(34)}$$

$${}^{\cdot}OH + R \rightarrow \text{Intermediates} \rightarrow \text{products} \quad \text{...............................(35)}$$

$$SO_4^{\cdot-} + R^{\cdot} \rightarrow \text{Chain termination} \quad \text{................................(36)}$$

$$SO_4^{\cdot-} + {}^{\cdot}OH \rightarrow \text{Chain termination} \quad \text{...............................(37)}$$

$$R^{\cdot} + {}^{\cdot}OH \rightarrow \text{Chain termination} \quad \text{...............................(38)}$$

$$2SO_4^{-} \rightarrow S_2O_8^{2-} \text{ Chain termination} \quad \text{...................................(39)}$$

$$2\,{}^{\cdot}OH \rightarrow H_2O_2 \text{ Chain termination} \quad \text{....................................(40)}$$

$$2R^{\cdot} + \rightarrow \text{Chain termination} \quad \text{...(41)}$$
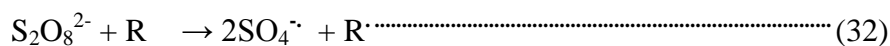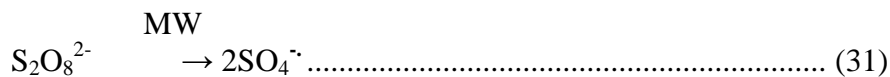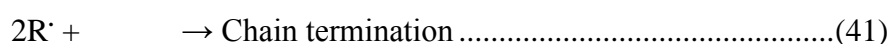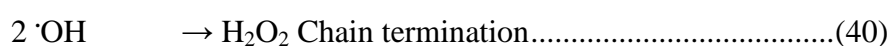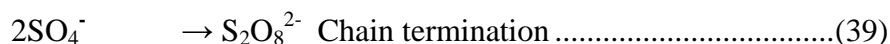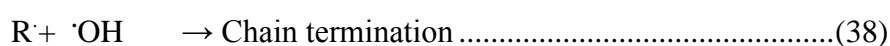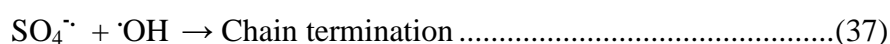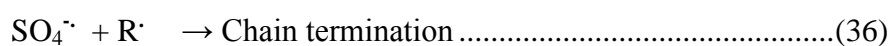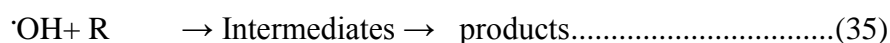
In addition to $SO_4^{\cdot-}$ various ROS such as H_2O_2, $HO_2^{\cdot}$, ${}^{\cdot}OH$ etc. formed during the irradiation can interact with IC on the surface as well as in the bulk leading to its degradation into various intermediates and eventual mineralization.

$$IC + ROS\,(ads) \rightarrow \text{Intermediates} \rightarrow \text{Mineralization} \quad \text{.................(42)}$$

$$IC + ROS\,(bulk)) \rightarrow \text{Intermediates} \rightarrow \text{Mineralization} \quad \text{..............(43)}$$
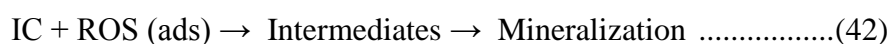
However the formation of ${}^{\cdot}OH$ radicals by this route is less dominant and the degradation is mostly taking place by the interaction with the $SO_4^{\cdot-}$ radicals. At higher concentrations of PS, $SO_4^{\cdot-}$ can interact with the former and transform the same to less reactive $S_2O_8^{-}$ as follows:

$$SO_4^{\cdot-} + S_2O_8^{2-} \rightarrow SO_4^{2-} + S_2O_8^{\cdot-} \quad \text{..(44)}$$
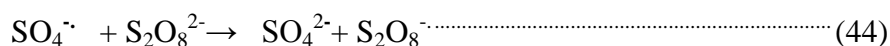
Hence the rate of degradation slows down at higher concentration of PS and with reaction time (Fig. 3.43). However at very high concentration of PS, the rate of formation of the highly reactive SO$_4^{\cdot-}$ radicals also will be more and hence the enhancement continues until, the degradation is complete.

Combination of the two oxidants H$_2$O$_2$ and PS resulted only in the average of the negative effect of H$_2$O$_2$ and the positive effect of PS for the degradation of IC under MW/MnO$_2$ (See Fig. 3.45).
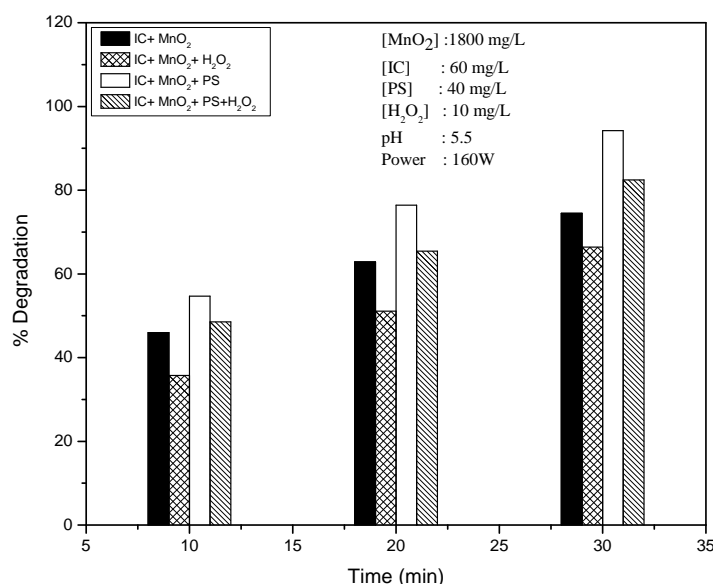
Fig. 3.45: Effect of combination of K$_2$S$_2$O$_8$ and H$_2$O$_2$ on the MW/MnO$_2$ degradation of IC.

3.3.3.11 Effect of anions

Many of the anionic contaminants which are naturally present in water inhibit the efficiency of AOPs for the degradation of organic water pollutants [156]. Instances of anions functioning as enhancers of the

degradation of pollutants also have been reported [78]. In this context, the effect of some of the commonly occurring anions in water, i.e. SO_4^{2-}, Cl^-, PO_4^{3-}, CO_3^{2-}, HCO_3^- and NO_3^- on the efficiency of MW/MnO_2 degradation of IC is tested at various concentrations and reaction times. The results showed that almost all the anions inhibit the degradation of IC except Cl^- and CH_3COO^-. The most powerful inhibitors are PO_4^{3-}, CO_3^{2-}, and $HCO_{3.}^-$

However, the anion effect has been proven to be dependent not only on concentration but also on the reaction time. This is verified by studying the effect of the above anions on the degradation of IC at different concentrations and reaction times. The effect of concentration of anions on the degradation is presented in Fig. 3.46A.
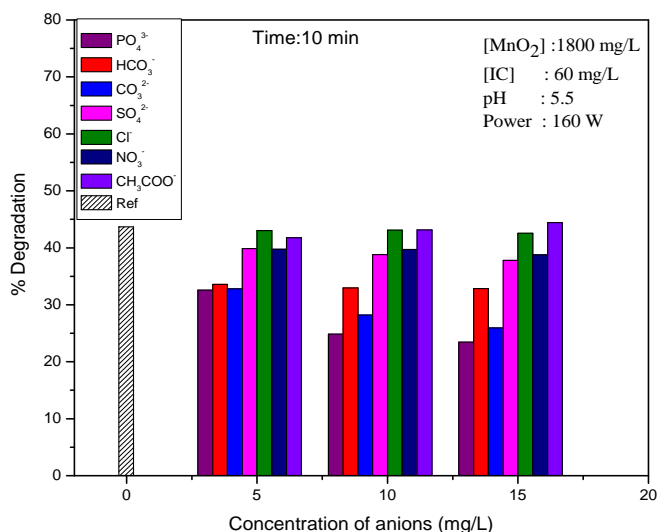
Fig. 3.46A: Effect of concentration of anions on the MW/MnO_2 degradation of IC.

The results show that the anion effect follows more or less same trend at all concentrations. The effect of anions at different concentration is summarised in Table 3.2.

Table 3.2: Effect of concentration of anions on the MW/MnO$_2$ catalytic degradation of IC

[MnO$_2$]: 1800 mg/L, [IC]: 60 mg/L, Time: 10 min

Concentration of Anion(mg/L)	Inhibition	No Effect
5	$PO_4^{3-} \approx CO_3^{2-} \approx HCO_3^- > SO_4^{2-} \approx NO_3^-$	CH_3COO^-, Cl^-
10	$PO_4^{3-} > CO_3^{2-} > HCO_3^- > SO_4^{2} > NO_3^-$	CH_3COO^-, Cl^-
15	$PO_4^{3-} > CO_3^{2-} > HCO_3^- > SO_4^{2-} > NO_3^-$	CH_3COO^-, Cl^-

The effect of reaction time on the degradation is presented in Fig. 3.46B and findings are summarised in the Table 3.3.
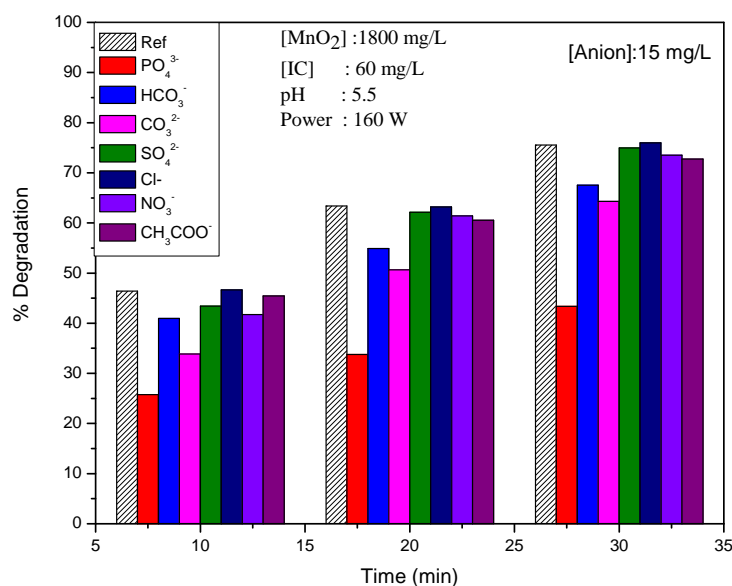
Fig. 3.46 B: Effect of reaction time on the 'anion effect on the MW/MnO$_2$ degradation of IC'

Table 3.3: Effect of reaction time on the 'anion effect'.

[MnO$_2$]: 1800 mg/L, [IC]: 60 mg/L, [Anion]:15 mg/L

Time	Inhibition	No Effect
10min	$PO_4^{3-} > CO_3^{2-} > HCO_3^- > NO_3^- \approx SO_4^{2-}$	CH_3COO^-, Cl^-
20min	$PO_4^{3-} > CO_3^{2-} > HCO_3^-$	CH_3COO^-, NO_3^-, Cl^-, SO_4^{2-}
30min	$PO_4^{3-} > CO_3^{2-} > HCO_3^-$	CH_3COO^-, NO_3^-, Cl^-, SO_4^{2-}

The results show that reaction time has little effect on the nature of the influence of anions, thereby suggesting that the in situ formed reaction intermediates do not influence the anion effect.

Since the 'anion effect' on AOPs is complex and often inconsistent, the effect of each anion on the microwave catalytic degradation of IC is investigated in detail. The results are plotted in Fig. 3.47 to 3.53.

3.3.3.11.1 SO_4^{2-}
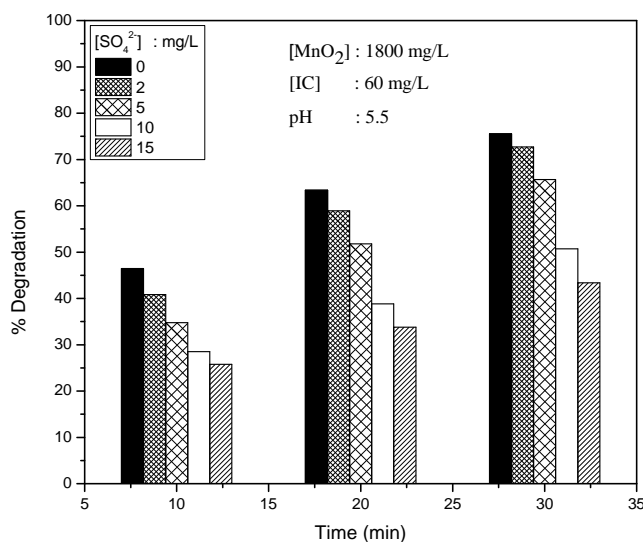
Fig. 3.47: Effect of SO_4^{2-} on the MW/MnO$_2$ degradation of IC

SO_4^{2-} is a clear inhibitor of the degradation at all concentration and reaction times. The inhibition increases with increase in concentration of SO_4^{2-}. The inhibiting trend also remains similar at all time periods.

3.3.3.11.2 PO_4^{3-}
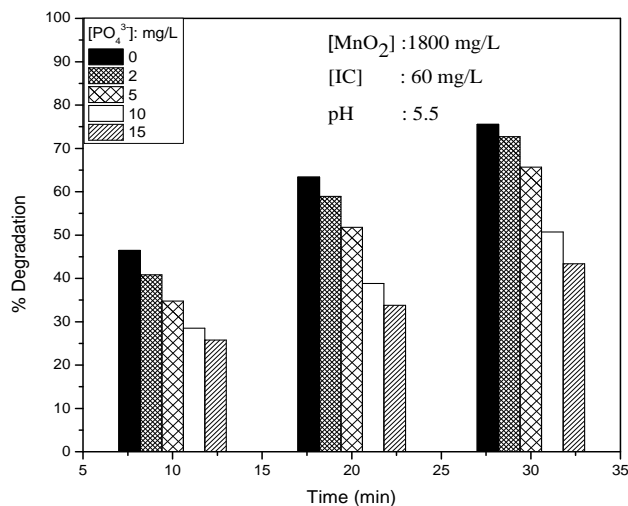
Fig. 3.48: Effect of PO_4^{3-} on the MW/MnO₂ degradation of IC

PO_4^{3-} is a strong inhibitor at all concentrations. The inhibition increases with increase in concentration. The inhibition trend is similar at all reaction periods.

3.3.3.11.3 Cl^-
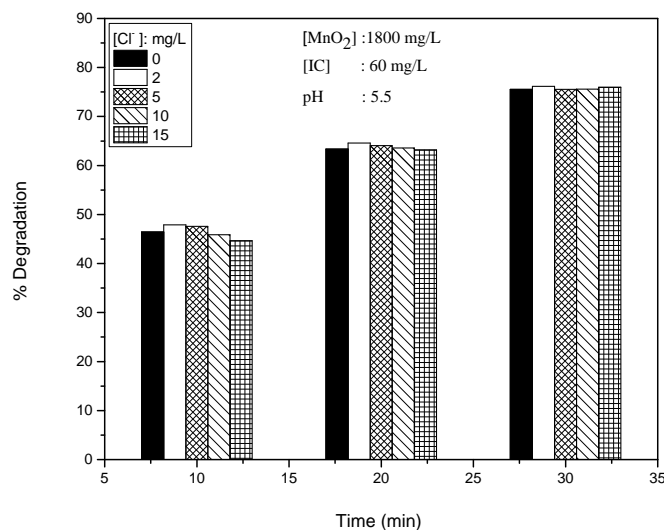
Fig. 3.49: Effect of Cl⁻ on the MW/MnO₂ degradation of IC

Cl⁻ has no effect on the degradation at least in the concentration range of 2-15 mg/L studied here. The trend is same irrespective of the concentration of the anion or the reaction time.

3.3.3.11.4 HCO_3^-
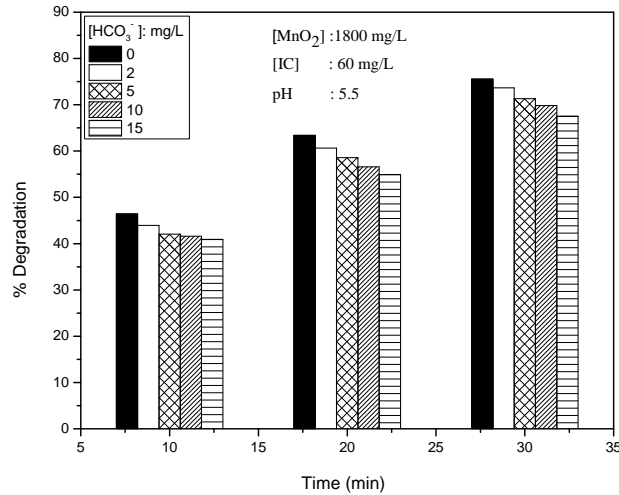
Fig. 3.50: Effect of HCO_3^- on the MW/MnO₂ degradation of IC

HCO_3^- remains a mild inhibitor of the degradation of IC. Increase in concentration of the anion has mild increasing effect on the inhibition

3.3.3.11.5 CO_3^{2-}
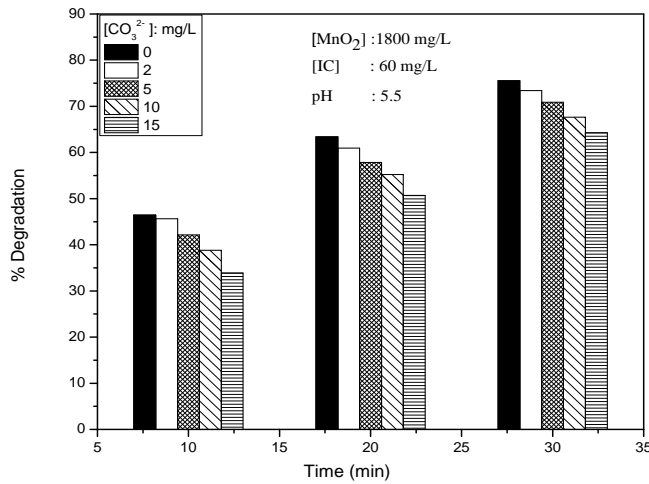
Fig. 3.51: Effect of CO_3^{2-} on the MW/MnO₂ degradation of IC

CO_3^{2-} is a moderate inhibitor of the degradation at all concentrations. The degradation increases slowly with increase in concentration of the anion. The inhibition trend remains the same at all reaction time periods.

3.3.3.11.6 CH_3COO^-
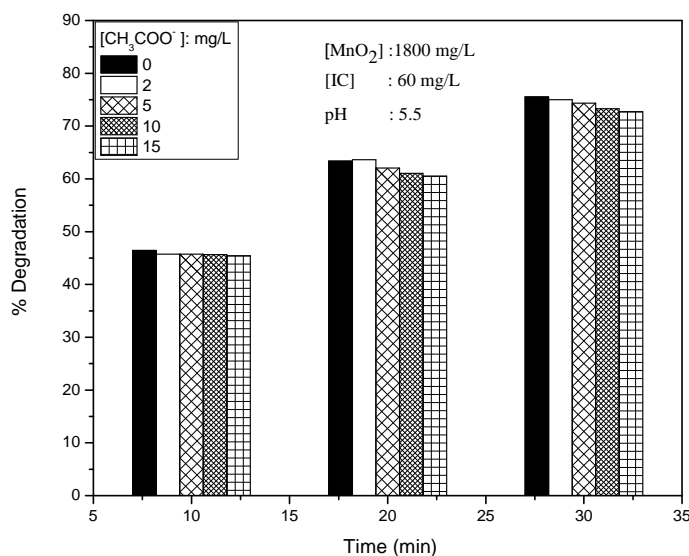
Fig. 3.52: Effect of CH_3COO^- on the MW/MnO$_2$ degradation of IC

Acetate ion has practically no effect on the degradation of IC. Change in concentration of the ion or extended reaction time does not make any change in the 'no effect'.

Microwave, Photo and Sono Activated Advanced Oxidation Processes and their Variations for the Decontamination of Water from Toxic Chemical Pollutants

151

3.3.3.11.7 NO_3^-
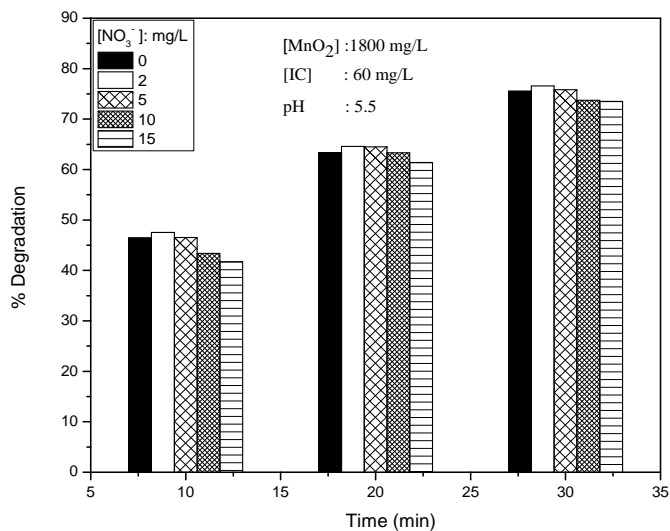
Fig. 3.53: Effect of NO_3^- on the MW/MnO$_2$ degradation
of IC

NO_3^- ion at higher concentration is a mild inhibitor of the degradation of IC, especially in the early stages of reaction. Towards later stages of reaction, when most of IC has already degraded, the anion effect becomes negligible at all concentrations. However, for all practical purposes, the effect of NO_3^- on the degradation can be treated as 'no effect'.

3.3.3.12 Probable causes for the anion effect

The inconsistent and unpredictable effect of anions on the AOP degradation of organics can be attributed to a number of factors, depending on the reaction conditions and characteristics of the components involved.

3.3.3.12.1 Adsorption of anion

One of the reasons for the inhibition by anions is their preferential adsorption on the catalyst surface, thereby inhibiting the adsorption of the substrate. This possibility is verified by measuring the adsorption of IC on MnO$_2$ in presence of various anions. The results are tabulated in Table 3.4.

Table 3.4: Effect of presence of anions on the adsorption of IC on MnO$_2$. [IC]: 60 mg/L, [MnO$_2$]: 0.18 g/100 ml, [Anion]: 10 mg/L Time: 5min

Anion	Adsorption of IC (%)
Nil	18.24
PO$_4^{3-}$	8.136
CO$_3^{2-}$	11.03
HCO$_3^-$	13.81
CH$_3$COO$^-$	16.78
SO$_4^{2-}$	17.33
Cl$^-$	19.05
NO$_3^-$	19.72

Adsorption is inhibited the most in the presence of PO$_4^{3-}$ followed by CO$_3^{2-}$ and HCO$_3^-$ while Cl$^-$, CH$_3$COO$^-$, SO$_4^{2-}$ and NO$_3^-$ do not influence the adsorption. The cation was kept the same in all cases, i.e, Na$^+$. The inhibition of the adsorption of IC by the anions is in the order

$$PO_4^{3-} > CO_3^{2-} > HCO_3^- > CH_3COO^- \sim SO_4^{2-} \sim NO_3^- \dots\dots\dots\dots\dots(45)$$

The results of the adsorption studies in presence of anions clearly show good correlation between the adsorption of the anions on MnO$_2$ and the inhibition caused by them, except in the case of CH$_3$COO$^-$. The effect of these anions on the degradation of IC is as follows.

$$PO_4^{3-}(\text{inhibition}) >> CO_3^- \text{ (inhibition)} \sim HCO_3^{2-} \text{ (inhibition)} >$$
$$SO_4^{2-} \text{ (inhibition)} \sim NO_3^- \text{ (mild inhibition)} > Cl^- \text{ (no effect)} \approx$$
$$CH_3COO^- \dots\dots\dots\dots\dots\dots\dots\dots\dots\dots\dots\dots\dots\dots\dots\dots\dots\dots\dots\dots\dots(46)$$

Microwave, Photo and Sono Activated Advanced Oxidation Processes and their Variations for the Decontamination of Water from Toxic Chemical Pollutants

153

The 'mild inhibition' by NO_3^- and the 'no effect' by CH_3COO^- can be treated interchangeably within the limits of experimental error. Hence it can be stated that the 'anion effect' can be correlated reasonably well with the effect of respective anions on the adsorption of the substrate IC.

Strong adsorption of PO_4^{3-} on MnO_2 is confirmed from the FTIR spectra of pure MnO_2, pure Na_3PO_4, and 'MnO_2 brought in contact with Na_3PO_4' (Fig.3.54). Characteristic bands of PO_4^{3-} are seen in the case of 'MnO_2 brought in contact with Na_3PO_4' showing the strong adsorption. This also supports the observations that the inhibition by anions can be attributed to their preferential adsorption on the catalyst.
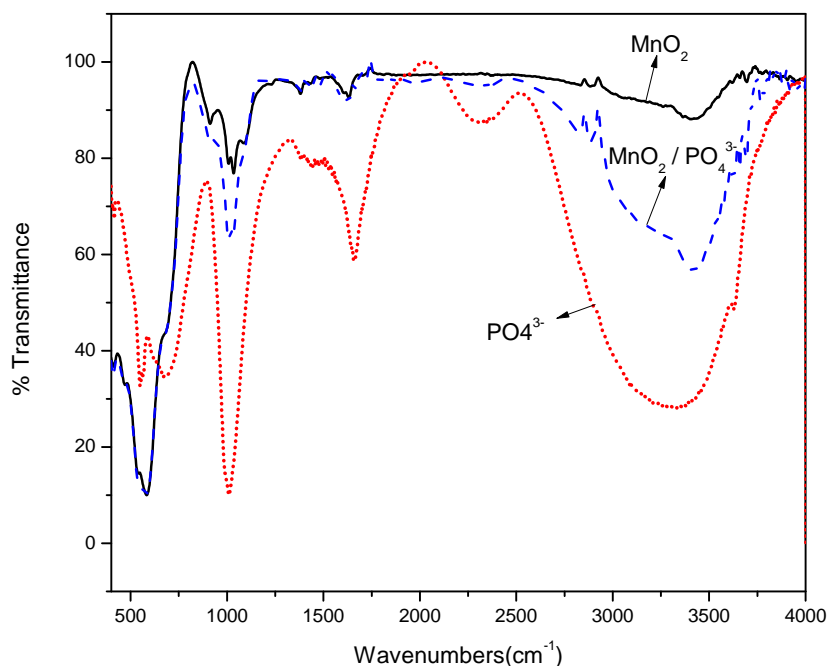
Fig. 3.54: FTIR spectrum showing adsorption of phosphate on MnO_2

MnO_2 is a very efficient adsorbent as well as oxidant and the IC gets moderately adsorbed and activated even in the presence of the anions. This results in reasonable degree of degradation even in the presence of strong inhibiting anions such as PO_4^{3-}.

3.3.3.12.2 Formation of radical anion

The anions are known to scavenge the ROS, especially $^\cdot OH$, which also could cause the inhibition of the degradation of IC. Such scavenging of the $^\cdot OH$ by anions would yield respective radical anion species as follows:

$$^\cdot OH + HCO_3^- \rightarrow H_2O + CO_3^{\cdot-} \quad\quad\quad (47)$$

$$^\cdot OH + CO_3^{2-} \rightarrow OH^- + CO_3^{\cdot-} \quad\quad\quad (48)$$

$$^\cdot OH + SO_4^{2-} \rightarrow OH^- + SO_4^{\cdot-} \quad\quad\quad (49)$$

$$^\cdot OH + NO_3^- \rightarrow OH^- + NO_3^\cdot \quad\quad\quad (50)$$

$$^\cdot OH + Cl^- \rightarrow OH^- + Cl^\cdot \quad\quad\quad (51)$$

$$Cl^\cdot + Cl^- \rightarrow Cl_2^{\cdot-} \quad\quad\quad (52)$$
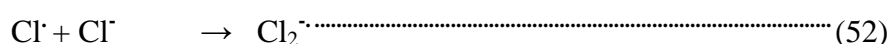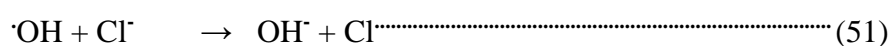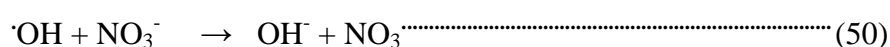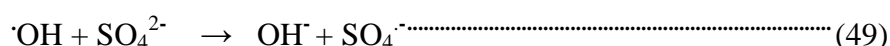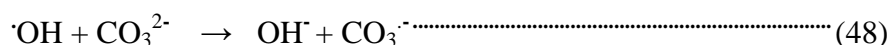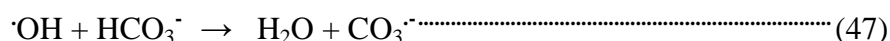
The scavenging rate constants of $^\cdot OH$ by some of the anions tested here are summarized in Table 3.5: [157, 158, 159].

Table 3.5: Scavenging rate constants of $^\cdot OH$ by various anions.

Anions	Scavenging rate constants ($mol^{-1}s^{-1}$)
NO_3^-	1.4×10^8
Cl^-	4.3×10^9
CO_3^{2-}	3.9×10^8
SO_4^{2-}	1×10^{10}
$H_2PO_4^-$	2×10^4
CH_3COO^-	7.0×10^7
HCO_3^-	8.5×10^6

Microwave, Photo and Sono Activated Advanced Oxidation Processes and their Variations for the Decontamination of Water from Toxic Chemical Pollutants

155

Immediate outcome of the scavenging of reactive $^{\bullet}$OH radicals by anions is the formation of respective radical anion. These radical anions are also reactive towards organic compounds although less efficiently than $^{\bullet}$OH [160].

However the inhibiting effect of anions is not quite significant in the current instance, probably because the contribution by the reactive radical anion species is more or less sufficient to compensate for the negative effect of trapping of the $^{\bullet}$OH radicals. The relatively mild inhibition of the degradation of IC or even 'no effect' by the anions, in spite of the competitive adsorption and scavenging of $^{\bullet}$OH radicals shows that the inhibition is compensated by other effects.

3.3.3.12.3 Layer formation

Another possible reason, often cited for the inhibition by anions, is the formation of an inorganic layer on the catalyst surface irrespective of adsorption. The efficiency of layer formation depends on the solubility of the salts [161].

Higher solubility of the salt decreases its layer formation. The solubility of the salts (in mg/g of water at 20^0C) tested here is in the order;

$$NaNO_3 \ (94.9) \ > \ CH_3COONa \ (54.6) \ > \ Na_2SO_4 \ (40.8) \ \geq$$
$$Na_2CO_3 \ (39.7) > NaCl \ (36.1) > Na_3PO_4 \ (16.3) > NaHCO_3 \ (11.1) \ ......(53)$$
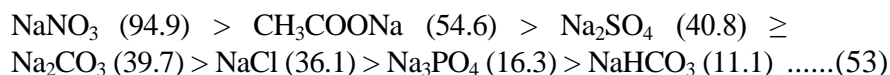
Correspondingly the layer formation, if any, will be in the order:

$$HCO_3^- > PO_4^{3-} > Cl^- > CO_3^{2-} \sim SO_4^{2-} > Ac^- > NO_3^- \ ....(54)$$
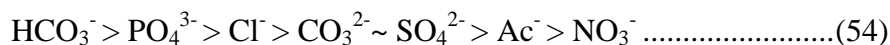
If layer formation is indeed at least one of the for the inhibition, the inhibition must be in the same order as in (eqn.54). The experimentally

observed inhibition in the current instance is shown in (46). Except in the case of chloride ion the observed inhibition is qualitatively consistent with the layer formation concept as above.

3.3.3.12.4 Reduction in diffusion coefficient

Another possible reason for the inhibition may be the reduction in the diffusion coefficient of the organic pollutants [162] by the anions. Consequently, they are less accessible to the ˙OH, resulting in inhibition of the degradation.

3.3.3.12.5 Effect of pH

The effect of anions on the pH of the reaction medium and consequent effect on the degradation of IC is examined by measuring the pH in presence of anions. The results are presented in Table.3.6.

Table 3.6: Effect of various anions on the pH of MnO_2/IC system
[IC]: 40 mg/L, [MnO_2]: 0.14 g/100 ml, [Anion]: 10 mg/L

Anion	pH
Nil	5.4
HCO_3^-	7.1
CO_3^{2-}	7.89
Cl^-	5.28
SO_4^{2-}	5.43
CH_3COO^-	5.7
NO_3^-	5.65
PO_4^{3-}	6.53

The pH is increased in presence of the anions PO_4^{3-}, CO_3^{2-} and HCO_3^-. In all other cases, the effect is practically negligible. The effect of pH on the degradation of IC (Section 3.3.3.5) shows that the degradation

is more in the acidic range and it decreases initially with increase in pH. The degradation remains steady in the pH range 5-10. In the present case, the pH in presence of all the anions remains in the range 5.2-7.9. Hence, effect of anions on the pH cannot be a reason for the 'anion effect' on the degradation.

3.3.3.12.6 Why Cl⁻ has no effect?

Cl⁻ ions are known to be powerful inhibitors of many AOP degradations. In the present study, Cl⁻ ions have practically no effect on the degradation of IC. This may be explained as follows:

The Cl⁻ anion can quench the ˙OH radicals as follows:

$$\text{˙OH} + \text{Cl}^- \quad \rightarrow \quad \text{Cl}^{\cdot} + \text{OH}^- \quad\quad\quad\quad\quad\quad (55)$$
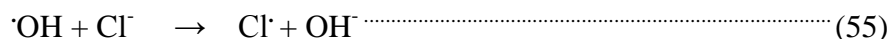
Accordingly Cl⁻ should have been a strong inhibitor. However in the current instance, Cl⁻ has practically 'no effect'.

The Cl˙ is also a good oxidizing agent capable of degrading many pollutants though relatively less efficiently compared to ˙OH due to lower oxidation potential [163]. Further as explained earlier, the radical anion of $Cl_2^{\cdot-}$ (eqn. 52) is also a good oxidant.

Hence the effect of Cl⁻ on the degradation of IC will be the net effect of the inhibiting and enhancing factors. The formation of radical anions which enhance the degradation has been explained earlier. It has also been reported that in presence of Cl⁻ ions in the pH range 2-6, the ˙OH radical concentration in the reaction system increases with increase in pH [164] with optimum at pH 6.

Thus the negative effect if any, by Cl^- ions caused by adsorption, surface layer formation or scavenging of $\cdot OH$ radicals is compensated by various other factors leading to 'no effect'.

The effect on the degradation of IC by all the anions cannot be quantitatively correlated in many instances by a simple thumb rule or interpretation. However, in the current instance, the contribution of various complimenting and opposing factors can explain the anion effect to some extent. Depending on the relative dominance of specific parameters the effect varies from 'strong inhibition' to 'no effect'. It will be more appropriate to consider individual anions, their characteristics and specific interactions to explain specific effects.

3.3.3.13 Effect of Oxygen

In many AOPs the dissolved oxygen plays an important role in the degradation of pollutants. Here also the role of dissolved O_2 on the degradation of IC is investigated by deaerating the system using N_2. The results show moderate enhancement in the degradation of IC, in the case of deaerated system (Fig.3.55A). This is contrary to the results in the case of most AOPs in which absence of dissolved O_2 leads to inhibition of the reaction. Hence the mechanism of microwave catalytic degradation may be different from that of other AOPs. It is possible that in the case of MnO_2, which is a strong oxidant and reservoir of O_2, lattice O_2 from MnO_2 and strongly bound surface O_2 which cannot be easily removed by N_2 flushing may be providing necessary oxygen for the formation of ROS. Eventually when the lattice oxygen concentration goes below a critical level, the degradation of IC also decreases. This is illustrated in subsequent sections.
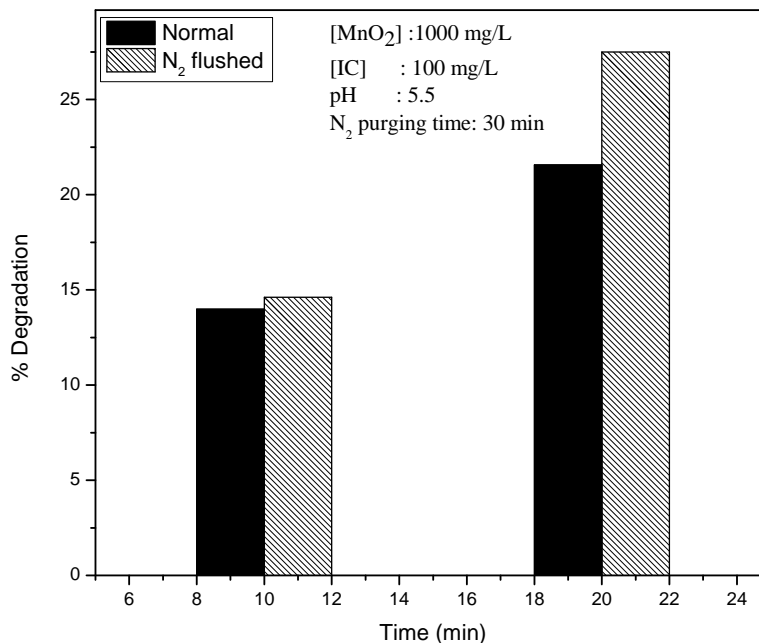
Fig. 3.55A: Effect of deaeration with N_2 on the MW/MnO_2 degradation of IC.

In order to verify the effect of N_2 on the MW/MnO_2 degradation of IC, experiments were done at 3 different lower MnO_2 dosages (50,100,200 mg/L) with and without N_2 flushing (Fig.3.55B). At very low concentration of MnO_2 (50mg/L) degradation of IC is strongly inhibited by N_2 flushing. This clearly shows that at very low dosage of MnO_2, the amount of lattice oxygen that can be utilised for the degradation of IC is very low and hence the deaeration by N_2 inhibits the degradation. However with increasing dosage of MnO_2 the inhibiting effect of deaeration is slowly decreasing thereby suggesting that the main source of O_2 for the reaction is surface – bound and/or lattice oxygen. Thus the strong inhibition in presence of 50mg/L of MnO_2 becomes 'no effect' in presence of 200mg/L (Fig.3.55B) and even enhancement with 1000mg/L of MnO_2 (Fig.3.55A). Amorphous

MnO$_2$ is known to release bulk oxygen more easily to the surface which makes it a better catalyst with respect to facile activation and regeneration. MnO$_2$ with multiple oxidation states together with its electron donor-acceptor properties is an excellent oxidation – reduction catalyst.
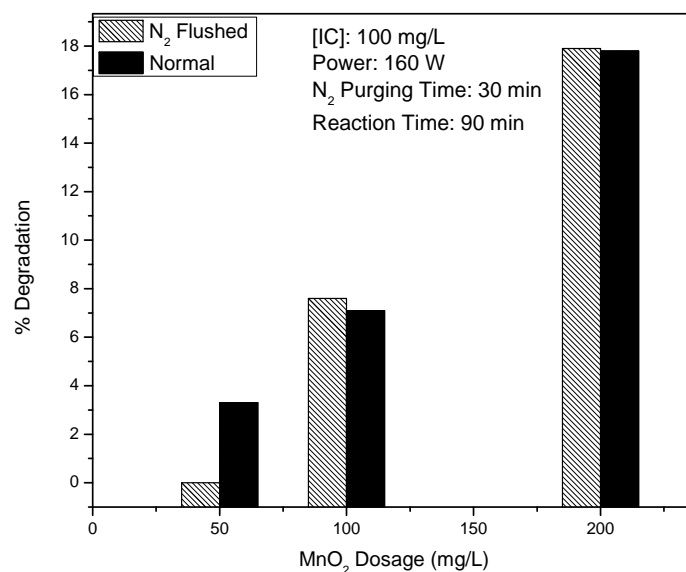
Fig. 3.55B: Effect of deaeration with N$_2$ on the MW/MnO$_2$ degradation of IC.

3.3.3.14 Recycling of MnO$_2$

Commercial application of any catalyst depends on its potential for reuse. Accordingly possible recycling of MnO$_2$ in the current process is examined by separating the catalyst from the system by filtration/ centrifugation followed by washing with water and drying at 35^{0}C until constant weight is obtained. The catalyst thus separated is reused for MW degradation of IC and the results are shown in Fig.3.56A.

Microwave, Photo and Sono Activated Advanced Oxidation Processes and their Variations for the Decontamination of Water from Toxic Chemical Pollutants

161
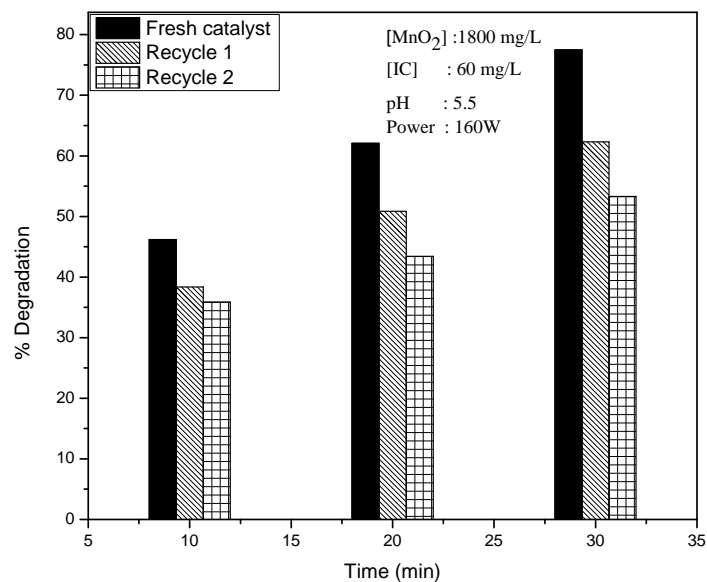
Fig.3.56A: Comparative efficiency of fresh and recycled MnO$_2$ for the microwave catalytic degradation of IC.

The degradation of IC (in 30 minutes) decreased from ~ 77 % in the presence of the fresh catalyst to ~ 62% in first recycling, and ~ 53 % in second recycling. This confirms major change in the catalyst including changes in the surface characteristics, loss of adsorption sites and loss of oxygen from the lattice, bulk and/or the surface of MnO$_2$. This loss is not fully compensated by contact with atmospheric oxygen or dissolved oxygen as is evident from the recycling results. Catalytic activity decreases slightly after first use and moderately in subsequent recycling. The decreasing activity may be due to the partial deactivation of the catalytic sites caused by multiple reasons such as surface reactions, presence of the remnants of strongly bound substrate/ intermediate species on the surface, which prevent the efficient absorption of MW by MnO$_2$ and subsequent generation of reactive free radicals, depletion of

adsorbed and/or lattice oxygen from MnO$_2$ etc. If the reasons for the decreasing activity of recycled catalyst are any or all of the above, increase in the initial concentration of the substrate will influence the parameters more drastically since more of surface sites and ROS will be required for effective degradation. In order to verify this, the recycling of MnO$_2$ is tested using higher concentration of IC and the results are plotted in Fig.3.56B. The results show that the efficiency of the fresh catalyst is substantially depleted in 40 minutes (34 to 12%) when the concentration of the substrate is higher. Hence the possible causes suggested above for the decreasing activity of the catalyst with every recycling are likely to be relevant in the case of MnO$_2$/MW degradation of IC.
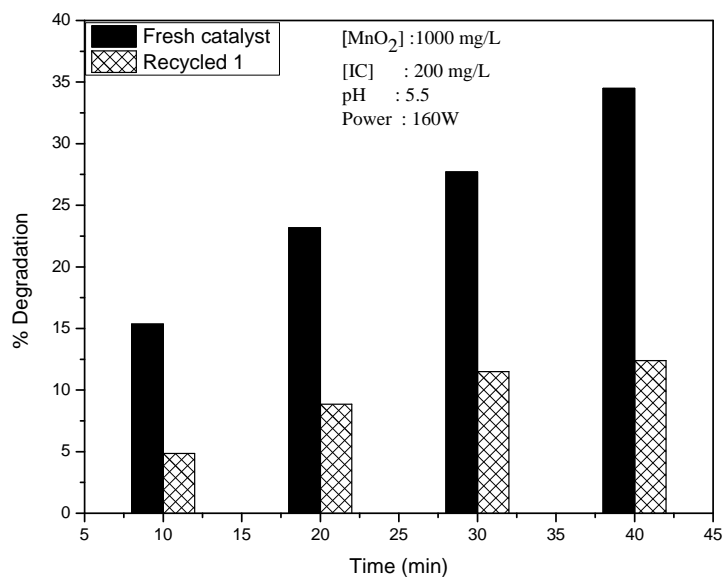
Fig. 3.56B: Comparative efficiency of fresh and recycled MnO$_2$ for the Microwave catalytic degradation of high concentration of IC.

The abstraction of oxygen from the lattice of MnO_2 for the degradation of IC is further verified by recording the EDX spectrum of MnO_2 before and after use (Fig.3.57A, 3.57B and 3.57C). The wt% as well as atomic % of oxygen before and after use (shown in Table 3.7) clearly illustrate that oxygen from the lattice of MnO_2 is used for the degradation of IC.
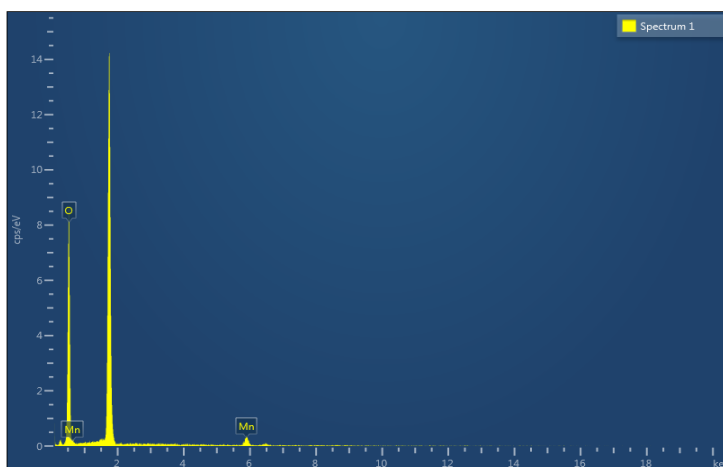
Fig. 3.57A: EDX spectrum of Fresh MnO_2
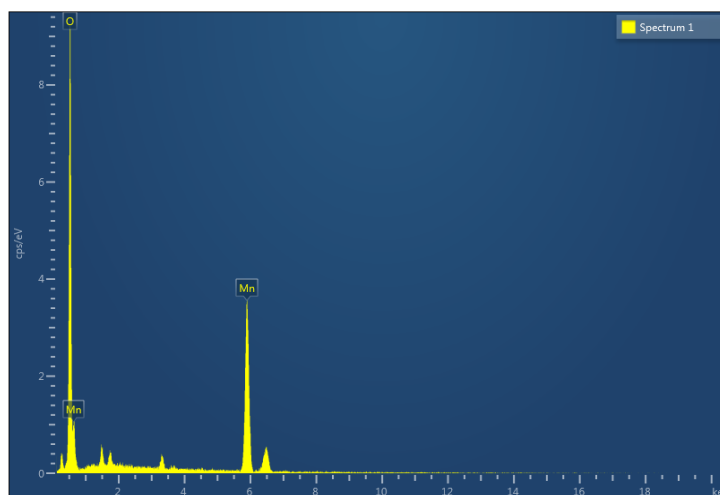
Fig. 3.57B: EDX spectrum of MnO_2 used for the degradation of IC
{[IC]:60mg/L, [MnO_2]:1800mg/L}
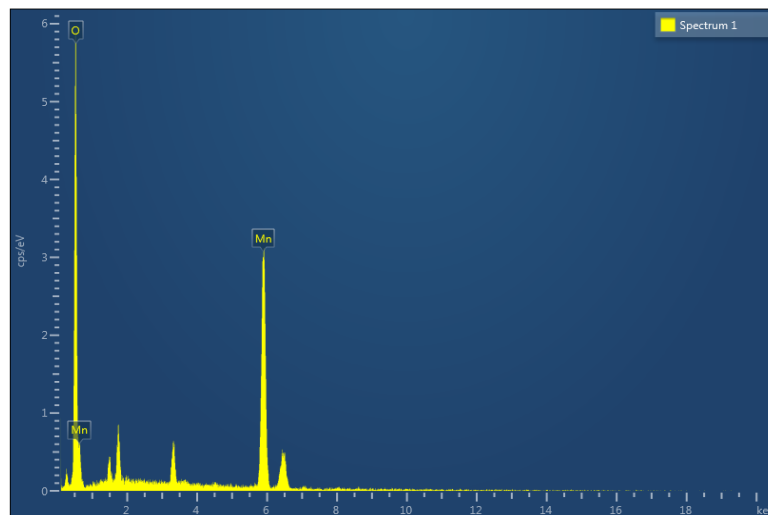
Fig. 3.57C: EDX spectrum of MnO$_2$ used for the degradation of higher concentration IC {[IC]:200mg/L, [MnO$_2$]:1000mg/L}

This further reiterates the observation that unlike in the case of many other oxides, the oxygen rich MnO$_2$ can be a good catalyst even after the system is flushed off dissolved O$_2$. The increase in depletion of lattice O$_2$ with increasing concentration of the substrate (IC) used in the reaction re-confirms the use of lattice O$_2$ for the degradation in deaerated system (Table 3.7). Comparative consumption of lattice oxygen, at two different concentrations of IC as measured by the EDX spectrum is given in Table 3.7.

Table 3.7: Comparative consumption of lattice O$_2$ at two different concentrations of IC under identical conditions of MnO$_2$/MW degradation.

[IC]	[MnO$_2$]	Wt% O		Wt% Mn		Atomic% O		Atomic% Mn	
		Before	After	Before	After	Before	After	Before	After
60 mg/L	1800 mg/L	85.8	44.54	14.2	55.41	95.4	73.42	4.6	26.58
200 g/L	1000 mg/L	85.8	37.2	14.2	62.8	95.4	67.04	4.6	32.96

Microwave, Photo and Sono Activated Advanced Oxidation Processes and their Variations for the Decontamination of Water from Toxic Chemical Pollutants

165

3.3.3.15 Chemical Oxygen Demand (COD)

The decolourisation of a dye does not always results in its complete mineralisation. It is also possible that the decolourisation may result in the formation of more stable toxic intermediates. Hence complete mineralisation is the real measure of water purification. In this context, the complete mineralisation of IC is verified by determining the chemical oxygen demand (COD) of the MW/MnO$_2$ treated IC solution at various intervals of irradiation. The COD gradually decreases from 60 to 40 mg/L in 2hr but does not decrease further even after MW irradiation for another 4hr (Fig.3.58).
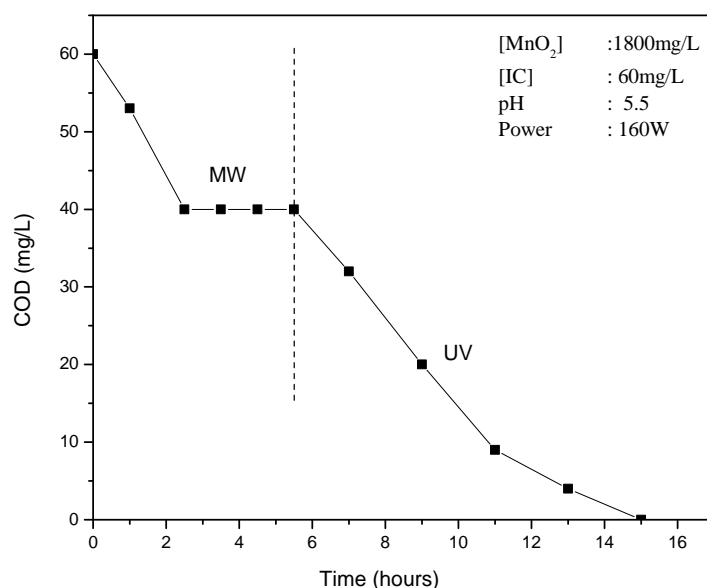
Fig. 3.58: COD of the MnO$_2$/IC reaction system under MW and UV irradiation at different time intervals
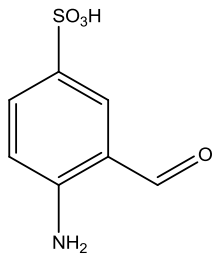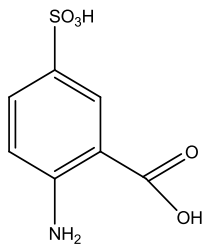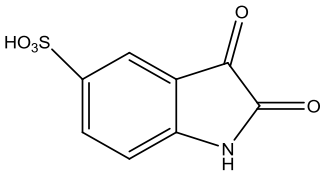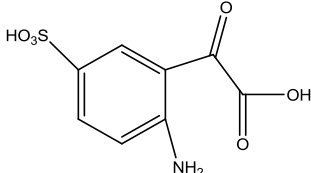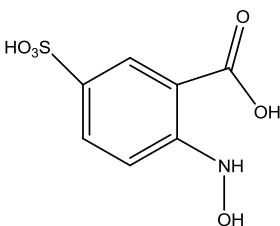
This shows that the degradation is proceeding through various intermediates which demand more severe conditions for mineralisation.

Some of the intermediates formed during the degradation of IC as reported in literature include organic acids such as oxalic acid (OA), malic acid (MA), acrylic acid (AcrA), acetic acid (Ac. A), tartaric acid (TA) etc. [149]. However, in the current study only oxalic acid and acetic acid are detected occasionally. Other intermediates could not be detected either because they are formed in very small amounts or the inadequacy of the analytical procedure followed by us. Once the COD is stabilised, further MW irradiation does not result in any decrease in COD indicating that MW radiation is not energetic enough to degrade/mineralise the intermediates. Hence at this stage another source of irradiation, i. e, UV light is tested. UV irradiation of the same reaction system decreases the COD and brought it down to nil in another 9hr. This indicates that integration of MW/MnO₂ and UV will be an effective AOT for the complete mineralisation of IC. This possibility is investigated in detail and the results are reported in the subsequent chapters.

3.3.3.16 Identification of reaction intermediates

In this context, the intermediates formed during the MW/MnO₂ degradation of IC are tested by LC/MS, analysis of reaction products at ~50% degradation of IC. Five intermediates were detected as in Table 3.8.

Microwave, Photo and Sono Activated Advanced Oxidation Processes and their Variations for the Decontamination of Water from Toxic Chemical Pollutants

167

Table 3.8: Major intermediates identified during the MW/MnO$_2$ degradation of IC

Sl No.	m/z	Proposed Structure
1	200	
2	216	
3	226	
4	245	
5	233	

However, they are not detected consistently. Hence these intermediates may be undergoing further degradation in parallel to form more stable organic acid intermediates as reported earlier [149]. They take longer time for degradation/mineralisation.

Independent studies on the photocatalytic degradation of oxalic acid in presence of MnO_2 shows that it can be mineralised efficiently in less than 1 hr. Other acids may be getting degraded slowly and hence the decrease in COD (See Fig.3.58) also is slow. The effect of organic acids likely to be accumulated in the system during the degradation of IC is tested individually under comparable reaction conditions. All of them mildly enhance the degradation of IC in the following order (Fig.3.59A).

$$OA > TA \approx AcrA > MA > Ac. A \ (10 \ min)$$
$$AcrA > TA \approx OA \approx Ac. A > MA \ (20 \ min)$$
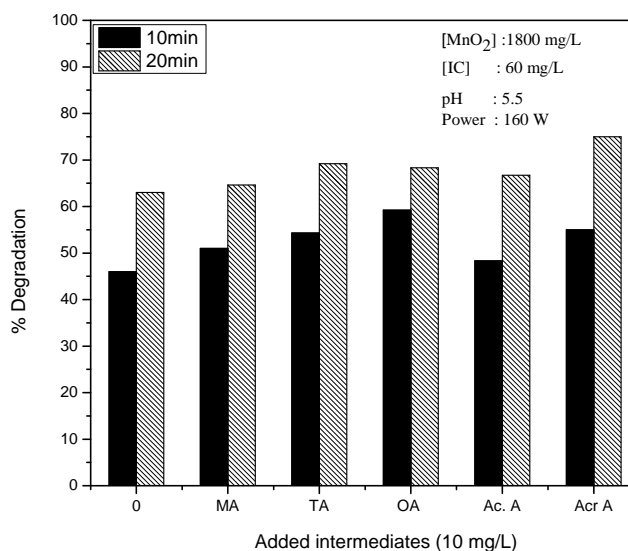
Fig. 3.59A: Effect of added organic acids on the MW/MnO₂ degradation of IC.

Microwave, Photo and Sono Activated Advanced Oxidation Processes and their
Variations for the Decontamination of Water from Toxic Chemical Pollutants

169

The addition of these acids do not degrade IC in the absence of either MnO_2 or MW. Minor variation in the relative effect of the organic acids on the degradation of IC with time (10 min/20 min) may be due to the competitive reaction of IC and the acids in presence of MW/MnO_2 and consequent inconsistency. In order to verify this, the effect of concentration of two typical intermediates, OA and MA on the degradation of IC is tested. The results are plotted in Fig.3.59B. The enhancement increases with increase in the acid concentration.
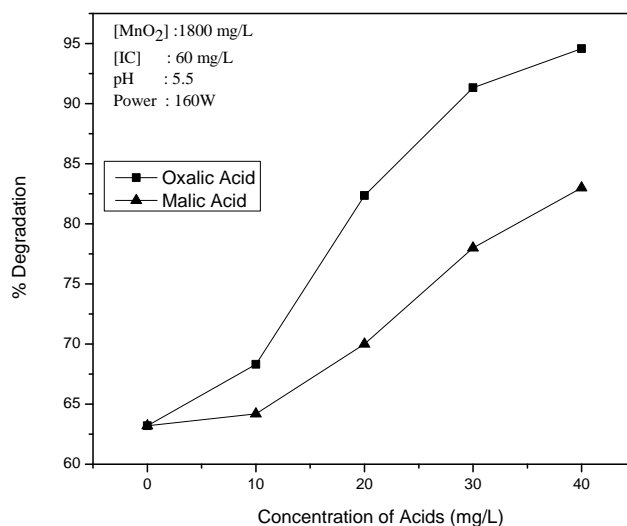
Fig. 3.59 B: Effect of concentration of OA and MA on the MW/MnO_2 degradation of IC after 20 minutes of irradiation

Hence the variation in the relative effect of the acids on the degradation of IC at different times is mainly due to the concurrent degradation of the components, i.e, the acid and IC and consequent variation in their relative concentration.

In order to verify whether the increase in degradation in presence of the organic acids is due to any variation in the pH, the pH is measured in presence of added oxalic acid. The pH is recorded before and after MW irradiation and the results are shown in Fig.3.60.
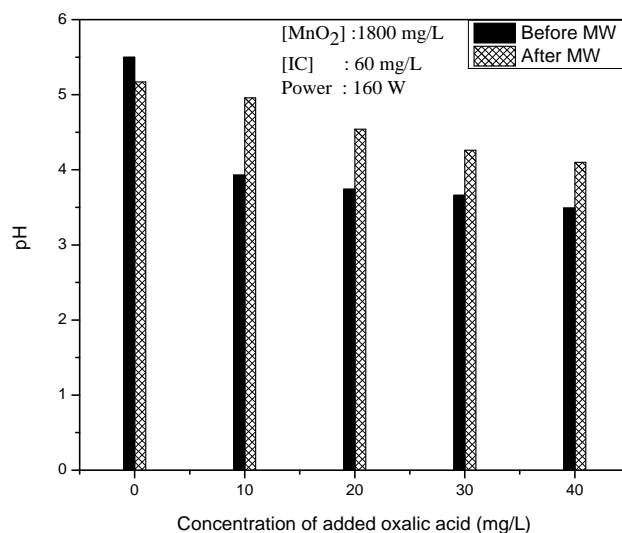
Fig. 3.60: Effect of oxalic acid in the pH of MnO_2/IC system before and after MW irradiation

As expected addition of oxalic acid decreases the pH of the system. Also, as the MW irradiation progresses, the pH increases indicating that the oxalic acid is getting degraded. It is possible that the enhancement by the organic acids as above is partially due to decrease in the pH of the medium, since extreme acidic conditions are known to increase the degradation of IC (Fig.3.24). As Fig.3.60 shows the pH decreases from 5.5 in the absence of oxalic acid to 3.5 in presence of OA at 40 mg/L. Since the degradation is more under acidic pH, part of the enhancement in presence of these acids can be attributed to the decrease in pH.

Microwave, Photo and Sono Activated Advanced Oxidation Processes and their Variations for the Decontamination of Water from Toxic Chemical Pollutants

171

In many instances presence of extra components compete with main substrate for adsorption on the surface sites, leading to decrease in the degradation (of the substrate). In this context, the effect of organic acids on the adsorption of IC on MnO_2 is tested. The results are presented in Fig.3.61 which show that the adsorption of IC is moderately enhanced in the presence of the added acid. This can be another reason for the enhancement in the degradation in presence of acids. The enhancement in adsorption of IC in presence of acids is consistent with the increase in degradation. For eg. the enhancement is negligible in presence of acetic acid, which does not increase the adsorption of IC either. This may be a rare instance of assisted adsorption where the constituents, mutually assist the adsorption, instead of competing for surface sites. The surface sites of MnO_2 may be getting protonated by the acids and the sites can then attract the molecules of the dianionic dye IC. Comparison of the adsorption and degradation data of IC in presence of the acids show good correlation, thereby confirming that acid assisted adsorption is a major factor contributing to the enhanced degradation of IC. The enhancement in degradation is not due to simple interaction of IC and oxalic acid as seen from the absence of any decrease in IC concentration by simple mixing of the two (without MnO_2) in the presence and absence of MW. The exploitation of this kind of enhanced adsorption possibility will be beneficial for the faster effective degradation of pollutants. However, further in depth study is needed on this.
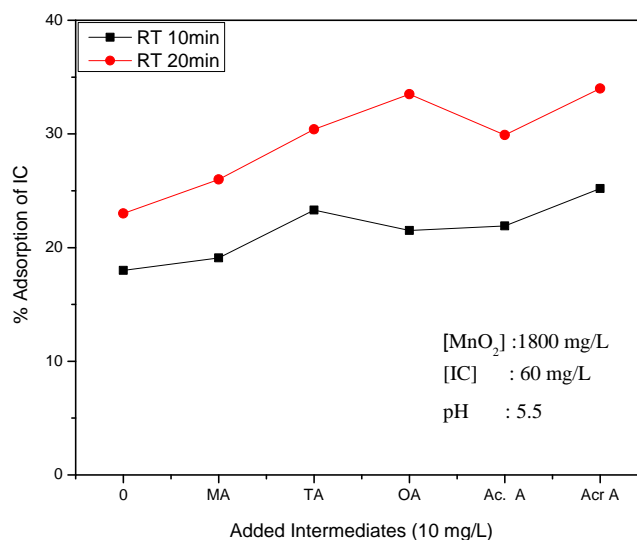
Fig. 3.61: Adsorption of IC in presence of Intermediates

Under standardized MW/MnO$_2$ conditions, the organic acids formed in the system are fairly stable preventing total mineralization (Fig.3.58). Since UV radiation of MnO$_2$/IC system is found to enhance the mineralisation of IC, the possibility of combining either MnO$_2$/MW with photolysis or even using a combination catalyst including an effective photocatalyst such as TiO$_2$ with MnO$_2$ for achieving faster mineralisation needs to be examined. In this context, the possible use of MnO$_2$-TiO$_2$ as a combination catalyst (at different ratios) under MW irradiation for the degradation of IC is tested and the results are presented in Fig.3.62.

Microwave, Photo and Sono Activated Advanced Oxidation Processes and their Variations for the Decontamination of Water from Toxic Chemical Pollutants

173
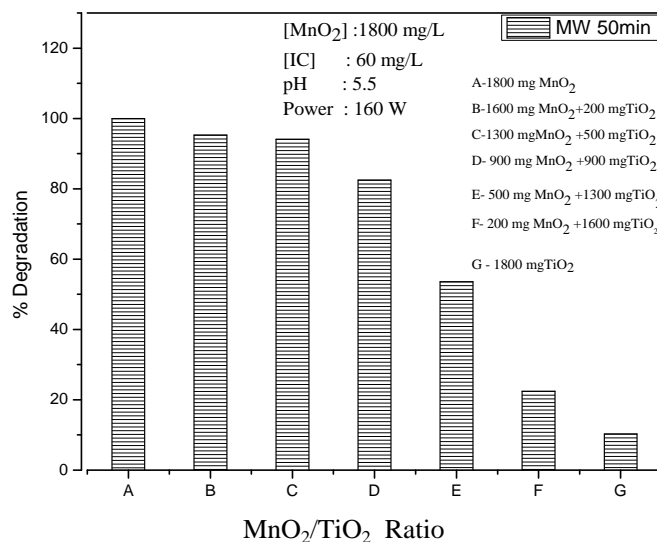
Fig. 3.62: Effect of TiO_2 on the MW activity of MnO_2 for
the degradation of IC.

The Figure shows that incorporation of TiO_2 in small dosages does
not affect the MW activity of MnO_2. Thus MnO_2-TiO_2 in the ratio 8:1 or
even 2.6:1 is having almost same MW activity as pure MnO_2. This opens up
the possibility of a combination catalyst of MnO_2 and TiO_2 at the appropriate
ratio, which can take advantage of the MW activity of the oxygen-rich
former and the photoactivity of the latter without either of them adversely
affecting the benefits of the other. The degradation of IC falls steeply when
the concentration of TiO_2 is increased by $> 50\%$ in the combination.

3.4 Investigations on the MW degradation of IC in presence of MnO_2-TiO_2

3.4.1. Preliminary experiments

TiO$_2$ at lower dosages does not inhibit the MW activity of MnO_2 for
the degradation of IC, as demonstrated in Fig.3.62. Hence the ratio of

MnO_2-TiO_2 is optimised and the results are presented in Fig.3.63. The inhibition of MnO_2 activity by TiO_2 begins at 0.02 g/ 100mL of the latter keeping the former constant at 0.18 g/100mL i.e MnO_2-TiO_2 = 9:1.
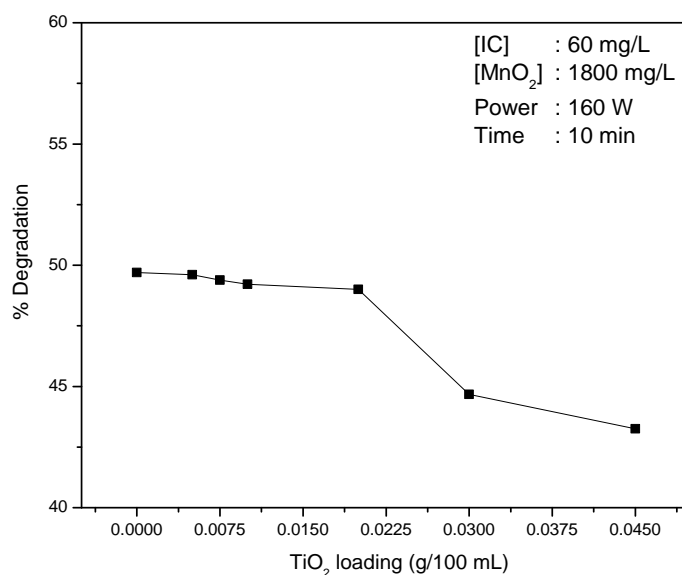
Fig. 3.63: Ratio optimisation of MnO_2-TiO_2 for MW/IC degradation

Since the presence of TiO_2 is proven to decrease the MW activity of MnO_2, the more consistent and safer ratio of 18:1 of (MnO_2-TiO_2) is selected for further studies, instead of the optimum of 9:1.

3.4.2. Effect of catalyst (MnO_2-TiO_2) dosage

The catalyst dosage {at the selected ratio of MnO_2-TiO_2 (0.18/ 0.01g/100mL)}for optimum degradation of IC is tested in the range 0.02g to 0.24g/ 100mL. The result is shown in Fig.3.64. The degradation increases with increase in catalyst loading.

Microwave, Photo and Sono Activated Advanced Oxidation Processes and their Variations for the Decontamination of Water from Toxic Chemical Pollutants

175
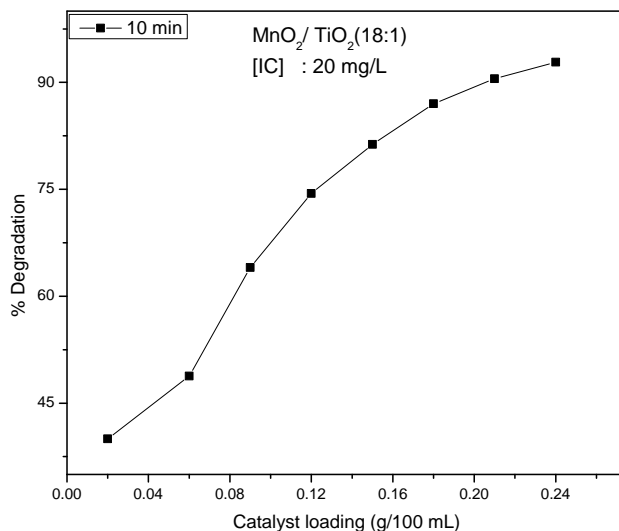
Fig. 3.64: Effect of MnO_2-TiO_2 dosage on the degradation of IC.

The increase in % degradation with increase in dosage shows slight decline from 0.18g/100 mL onwards. In the absence of any well-defined optimum for the catalyst dosage, 1800 mg/L of the combination catalyst is chosen for further studies.

3.4.3 Effect of concentration of IC

The effect of concentration of IC on its MW degradation in presence of MnO_2/TiO_2 is investigated and the results are shown in Fig.3.65. The % degradation of IC decreases with increasing concentration of IC. However the rate of degradation increases with increasing the concentration up to 40 mg/L, stabilises up to 60 mg/L and then decreases (Fig.3.66). The concentration effect is similar to that in the case of MnO_2 alone (Section 3.3.3.2). The 'concentration vs rate' plot shows that the kinetics is similar to that in the case of 'MnO_2 only' with the reaction following pseudo first order kinetics at lower concentration (0-40 mg/L)

followed by zero order in the concentration range (40-60 mg/L) and negative order at concentrations (> 60 mg/L).
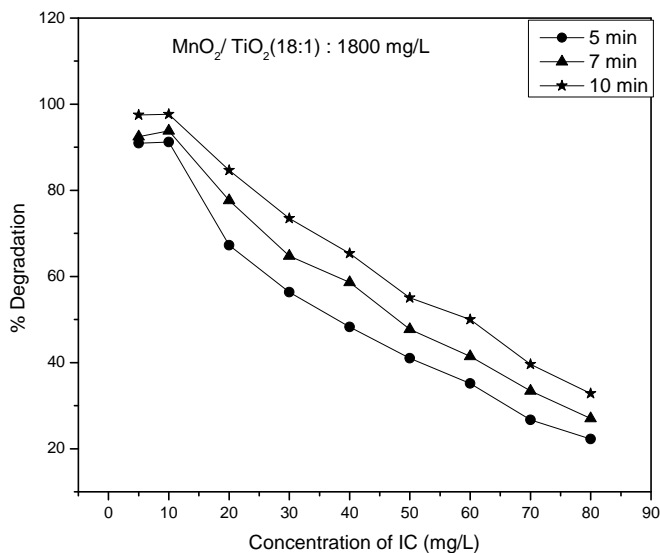
Fig. 3.65: Effect of concentration on the MW/MnO$_2$-TiO$_2$ degradation of IC
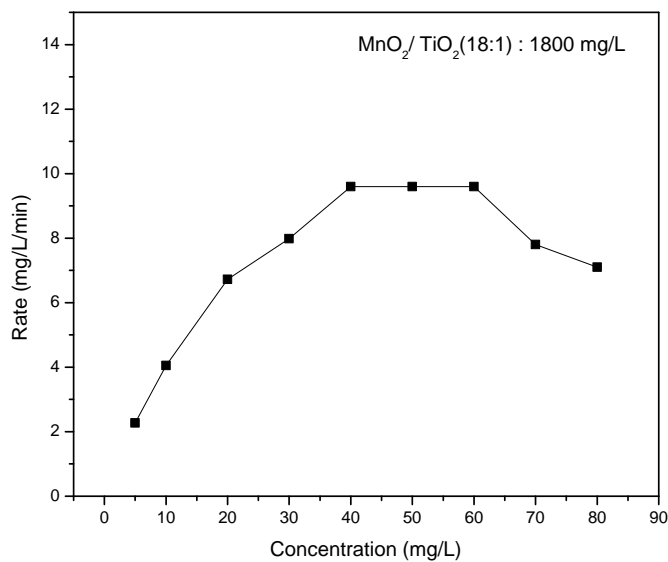
Fig. 3.66: Effect of concentration of IC on its rate of degradation in presence of MnO$_2$-TiO$_2$

Microwave, Photo and Sono Activated Advanced Oxidation Processes and their Variations for the Decontamination of Water from Toxic Chemical Pollutants

177

The pseudo first order kinetics in the concentration range 5 to 40mg/L of IC is further verified by the inverse plot ($1/r_0$ vs $1/C_0$) as in Fig.3.67. The straight line plots confirm the pseudo first order kinetics. Details are discussed in Section 3.3.3.2.
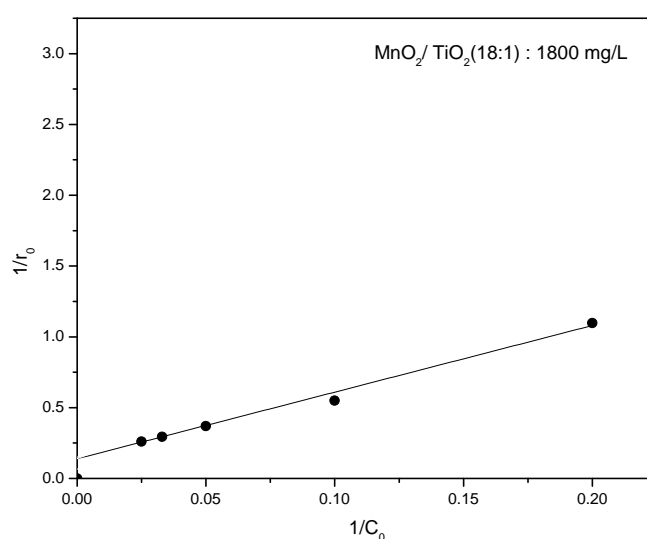
Fig. 3.67: Reciprocal plot of $1/r_0$ vs $1/C_0$ for various concentrations of IC

The plot of ln (C_0/C) vs time (Fig.3.68) in the concentration range 5-40 mg/L shows linear dependence indicating pseudo first order kinetics and L-H mechanism (Details are discussed in Section 3.3.3.2). Hence, it may be concluded that the kinetics of MW degradation of IC on MnO_2-TiO_2 is same as in the case of MnO_2.
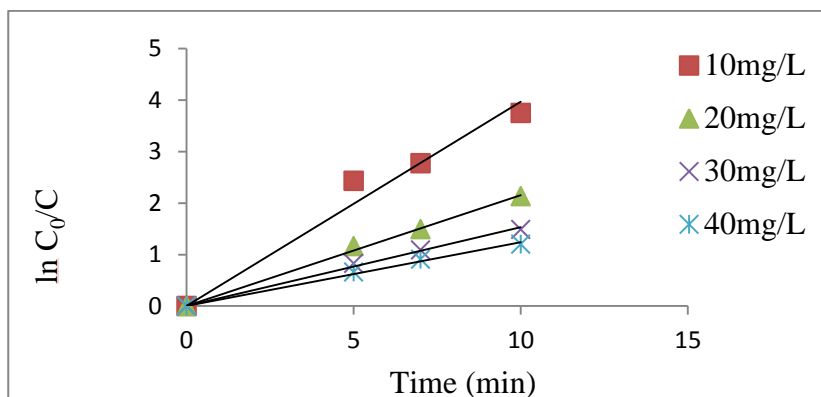
Fig. 3.68: Logarithmic plot for the MW/(MnO$_2$ - TiO$_2$) degradation of IC.

3.4.4 Effect of pH

The effect of pH on the degradation of IC is investigated in the range 2-11. The pH of the suspension was adjusted at respective values before irradiation and was not controlled thereafter. The results are shown in Fig.3.69.
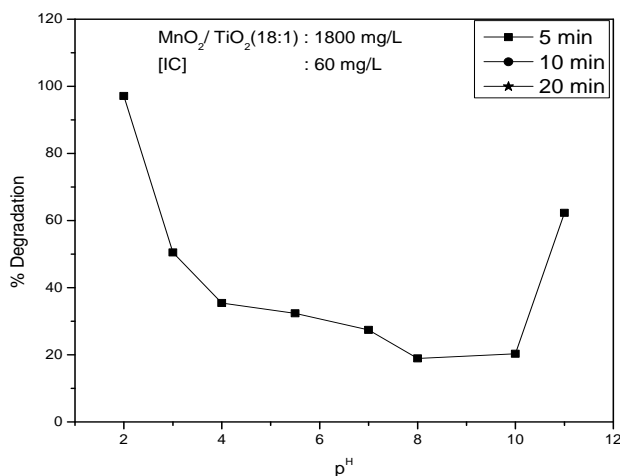
Fig. 3.69: Effect of pH on the MW/(MnO$_2$ - TiO$_2$) degradation of IC

Degradation is very high under extreme acidic pH of 2, which decreases steeply upto pH ~ 4 followed by fairly steady degradation upto

pH 7. Thereafter the degradation decreases mildly up to pH. Then there is a steep increase when pH is raised to 11. This is fairly similar to the effect of pH in presence of pure MnO_2 catalyst (Section 3.3.3.5). The enhanced degradation under extreme acidic pH can be partially explained based on the point of zero charge (PZC) (~ 4.7 of MnO_2 and ~ 6.3 for TiO_2) as explained in Section 3.3.3.5. Since the quantity of TiO_2 in the combination catalyst is very small (~5%) it may be presumed that the PZC will be same as that of pure MnO_2.

pH effect depends on many factors, i.e. chemistry of the substrate and the surface, extent and mode of adsorption, concentration and type of interactions of reactive free radicals such as $^{\cdot}OH$ etc. The adsorption of the substrates is more in the acidic range while the concentration of the $^{\cdot}OH$ radical is more in the alkaline region. Since the pH effect is similar to that in the case of 'MnO_2 only' catalyst, the mechanism of the effect also may be identical. Details are discussed under Section 3.3.3.5.

3.4.5 Effect of Oxidants

AS done in the case of MnO_2 catalyst, the effect of two common oxidants, i.e H_2O_2 and $K_2S_2O_8$ on the degradation of IC is investigated in presence of MnO_2-TiO_2 catalyst.

3.4.5.1 Effect of H_2O_2

The effect of externally added H_2O_2 at different concentrations on the microwave catalytic decolourisation of IC in presence of MnO_2-TiO_2 is tested. Addition of H_2O_2 at low concentration inhibits the degradation of IC. The inhibition increases with increase in concentration of H_2O_2 upto 20 mg/L and stabilises thereafter (See Fig. 3.70).
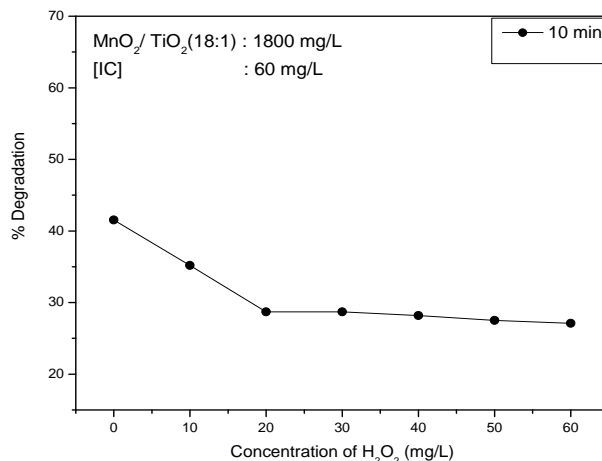
Fig. 3.70: Effect of H$_2$O$_2$ on the MW/(MnO$_2$ - TiO$_2$) degradation of IC

The inhibition by H$_2$O$_2$ is further confirmed by the addition of H$_2$O$_2$ in-between to a reaction in progress. Results are shown in Fig. 3.71. Every extra addition of H$_2$O$_2$ (10 min and 20 min) decreases the % degradation of IC.
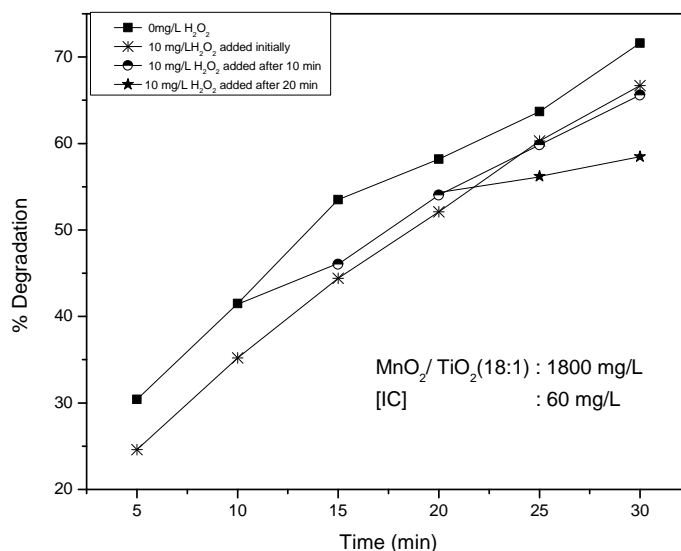
Fig. 3.71: Effect of initial & in between addition of H$_2$O$_2$ on the degradation of IC.

Microwave, Photo and Sono Activated Advanced Oxidation Processes and their Variations for the Decontamination of Water from Toxic Chemical Pollutants

181

The comparative effect of H_2O_2 on the degradation of IC in presence of MnO_2 and MnO_2-TiO_2, under otherwise identical conditions is shown in Fig.3.72. The figure shows that the effect follows similar trend in both cases. Hence it may be inferred that the addition of small amounts of TiO_2 to MnO_2 (MnO_2 - TiO_2) does not change the nature and quantum of the effect of H_2O_2 on the MW/MnO_2 degradation of IC. Detailed mechanism of the role of H_2O_2 is discussed in Section. 3.3.3.10.1.
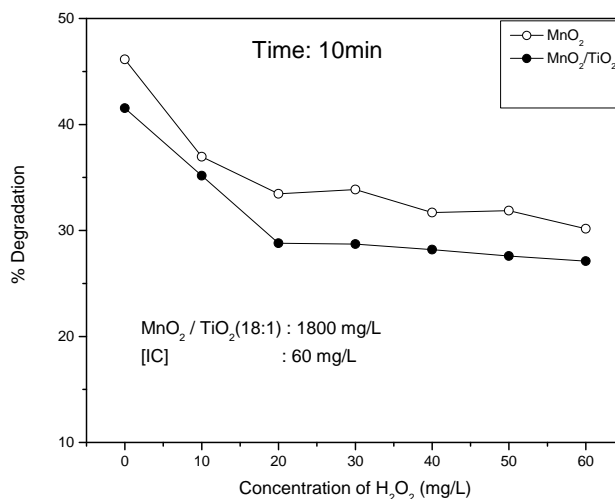
Fig. 3.72: Comparison of the effect of added H_2O_2 on the degradation of IC in presence of MnO_2 and MnO_2 - TiO_2

3.4.5.2 Effect of added PS

The effect of externally added PS on the degradation of IC in presence of MnO_2 -TiO_2 is studied and the results are shown in Fig 3.73. The % degradation increases with increase in concentration of PS initially. The increase is very slow at PS > 10 mg/L.
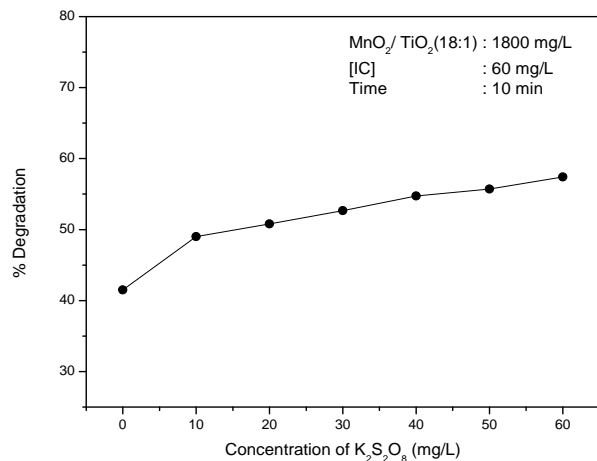
Fig. 3.73: Effect of added K$_2$S$_2$O$_8$ on the MW/(MnO$_2$ - TiO$_2$) degradation of IC

The enhancing effect is also confirmed by the in-between addition (Fig 3.74.) of PS to the degradation in progress after 10 and 20 minutes of MW irradiation. The results show clear enhancement in the degradation of IC on the addition of PS.
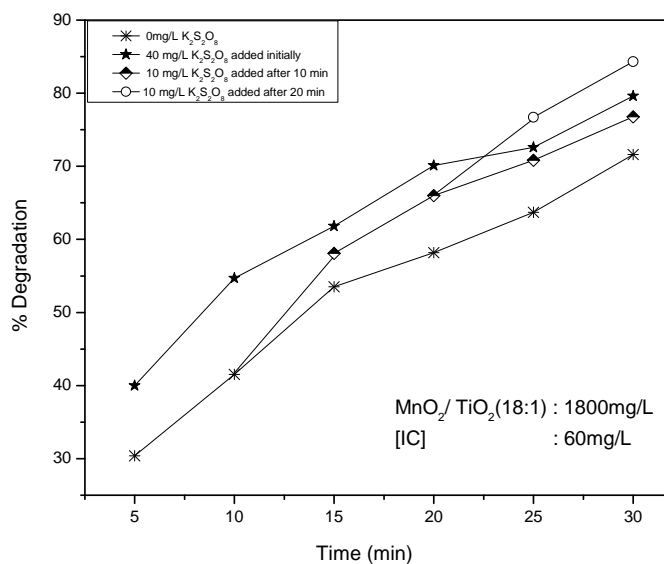
Fig. 3.74: Effect of initial & in between addition of K$_2$S$_2$O$_8$ on the MW/(MnO$_2$ - TiO$_2$) degradation of IC.

The effect of PS is similar in the case of MnO_2 as well as MnO_2 - TiO_2 catalysed degradation of IC. The degradation is enhanced in both cases and the degree of enhancement is more in the case of MnO_2 than MnO_2 - TiO_2 i. e. ~30% enhancement in presence of MnO_2 (Fig.3.40) while only ~15% enhancement in presence of MnO_2 - TiO_2 in 10 min with 40 mg/L of PS under otherwise identical condition. Details of PS effect, on the degradation and probable mechanism are discussed under Section 3.3.3.10.2.

Combination of these two oxidants, i.e. H_2O_2 and PS, widely used in many AOTs, resulted in the same percentage of degradation achieved in presence of PS (Fig.3.75) at later stages of reaction.
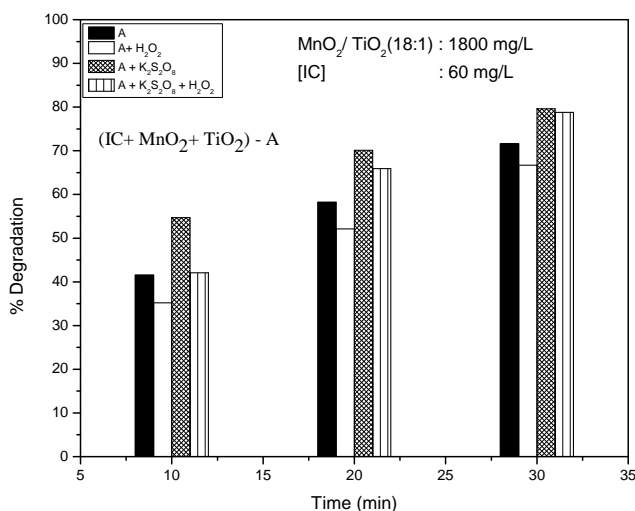
Fig.3.75: Combination of $K_2S_2O_8$ and H_2O_2 on the MW/(MnO_2 - TiO_2) degradation of IC

Hence it may be inferred that PS can partially compensate for the inhibition of the degradation by H_2O_2. However in the beginning, the effect on the degradation is the average of the inhibition by H_2O_2 and the enhancement by PS.

3.4.6 Effect of Anions

As done in the case of MnO_2 the effect of some of the anions which are likely to be present in water, i.e. SO_4^{2-}, Cl^-, PO_4^{3-}, CO_3^{2-}, F^-, CH_3COO^-, HCO_3^- and NO_3^- on the efficiency of MW/ MnO_2 -TiO_2 degradation of IC is tested at various concentrations and reaction times (Figs. 3.76A and 3.76B). The observations are summarised in Tables 3.10 and 3.11.
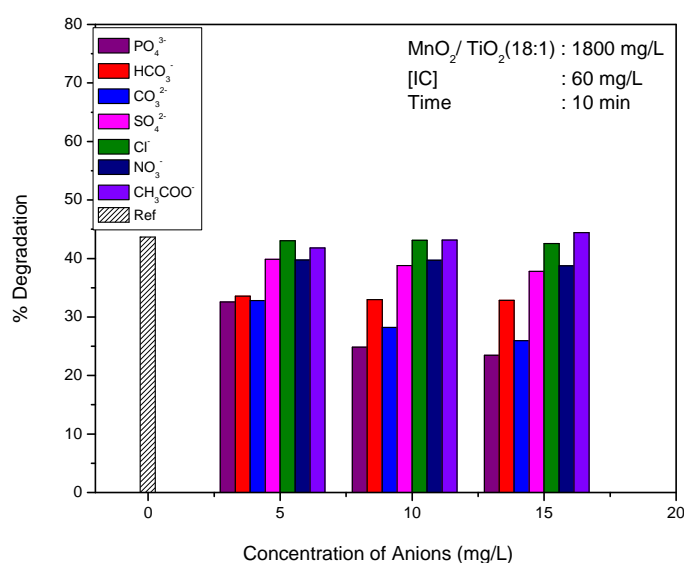
Fig. 3.76A: Effect of concentration of anions on the MW/(MnO_2 - TiO_2) degradation of IC.

PO_4^{3-}, CO_3^{2-}, HCO_3^- are strong inhibitors. SO_4^{2-} is a mild inhibitor. Other anions have no effect in the concentration range 5-15 mg/L. However, the trend varies slightly with concentration as summarised in Table 3.9.

Table 3.9: Effect of concentration of the anion on the MW/(MnO_2 - TiO_2) degradation of IC.

Concentration of Anion(mg/L)	Inhibition	No Effect
5mg/L	$PO_4^{3-} \approx CO_3^{2-} \approx HCO_3^- > SO_4^{2-} \approx NO_3^-$	CH_3COO^-, Cl^-
10mg/L	$PO_4^{3-} > CO_3^{2-} > HCO_3^- > SO_4^{2-} \approx NO_3^-$	CH_3COO^-, Cl^-
15mg/L	$PO_4^{3-} > CO_3^{2-} > HCO_3^- > SO_4^{2-} \approx NO_3^-$	CH_3COO^-, Cl^-

At low concentration of the anions, i.e. 5 mg/L, PO_4^{3-} , CO_3^{2-} and HCO_3^- have comparable inhibitive effect. However at higher concentration, the inhibition by PO_4^{3-} and CO_3^{2-} is more which is consistent with the observation reported in the case of many substrates in various AOPs.

Another parameter that can influence the effect of anions is the duration of the reaction. The relative concentration of the ion with respect to the substrate increases progressively with reaction time (because the substrate concentration decreases due to degradation) and this may be leading to enhanced inhibition. The effect is tested at three different reaction times, i.e., 10, 20 and 30 min and the results are plotted in Fig.3.76B.
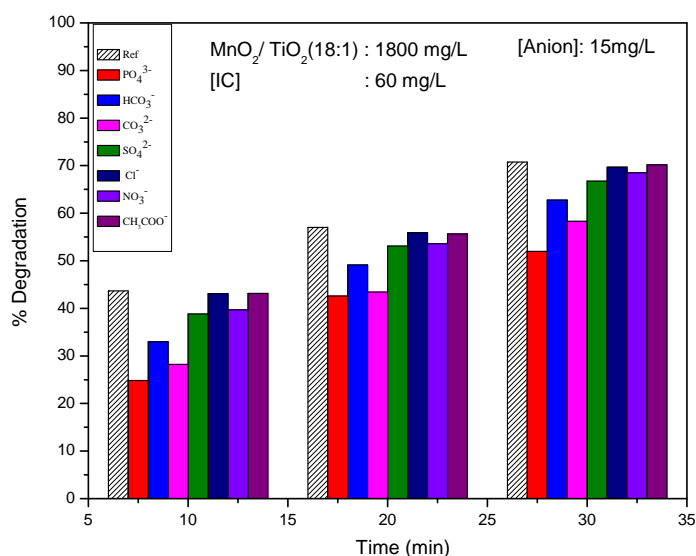
Fig.**3.76B**: Effect of reaction time on the 'anion effect on the MW/(MnO$_2$ - TiO$_2$) degradation of IC'

The trend remains the same at all reaction times. The relative effect of anions at different duration of reaction is summarised in Table 3.10.

Table 3.10: Effect of reaction time on the 'anion effect on the MW/(MnO$_2$ - TiO$_2$) degradation of IC'

Time	Inhibition	No Effect
10min	PO$_4^{3-}$ > CO$_3^{2-}$ > HCO$_3^-$ > SO$_4^{2-}$ ≈ NO$_3^-$	CH$_3$COO$^-$, Cl$^-$
20min	PO$_4^{3-}$ ≈ CO$_3^{2-}$ > HCO$_3^-$ > SO$_4^{2-}$ > NO$_3^-$	CH$_3$COO$^-$, Cl$^-$
30min	PO$_4^{3-}$ > CO$_3^{2-}$ > HCO$_3^-$ > SO$_4^{2-}$ ≈ NO$_3^-$	CH$_3$COO$^-$, Cl$^-$

The results show that the inhibition trend remains the same at all reaction times. The effect of CH$_3$COO$^-$ and Cl$^-$ at various reaction times between 'no effect' and 'mild inhibition'. It may be concluded that reaction time has no effect on the influence of anions, thereby suggesting that change in the concentration of the substrate or the in situ formed reaction intermediates do not influence the anion effect.

As done in the case of MnO$_2$, the effect of individual anions on the microwave catalytic degradation of IC in presence of MnO$_2$ -TiO$_2$ is investigated at different concentrations and reaction times and the results are plotted in Fig. 3.77 to 3.83.

3.4.6.1 PO$_4^{3-}$
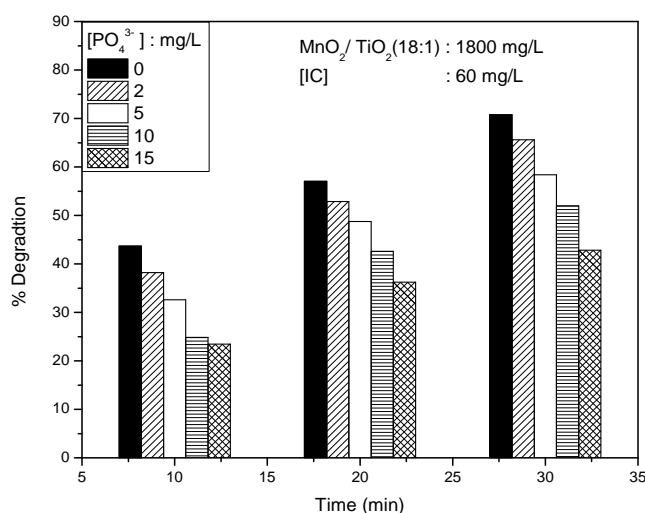
Fig. 3.77: Effect of PO$_4^{3-}$ on the MW/(MnO$_2$ - TiO$_2$) degradation of IC

Microwave, Photo and Sono Activated Advanced Oxidation Processes and their Variations for the Decontamination of Water from Toxic Chemical Pollutants

187

PO$_4^{3-}$ is a strong inhibitor, with the inhibition increasing with increase in concentration of the anions. The trend in concentration effect is maintained at all reaction time.

3.4.6.2 HCO$_3^-$
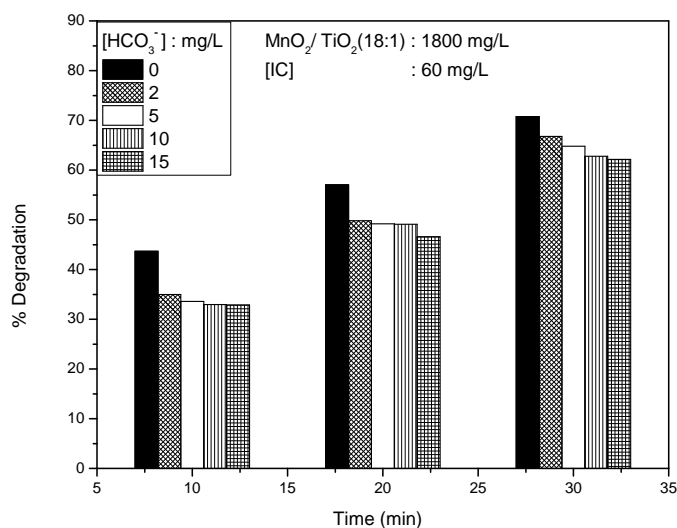
Fig. 3.78: Effect of HCO$_3^-$ on the MW/(MnO$_2$ - TiO$_2$) degradation of IC

HCO$_3^-$ remains as a strong inhibitor at all concentrations and reaction times tested here. However the extent of inhibition remains more or less the same at all its concentrations, at least in the range 5-15mg/L. The stabilisation in the inhibition irrespective of increasing concentration of anions can be due to the balancing of enhancing and inhibiting effect of the anion as explained in Section 3.3.3.12.

3.4.6.3 CO$_3^{2-}$
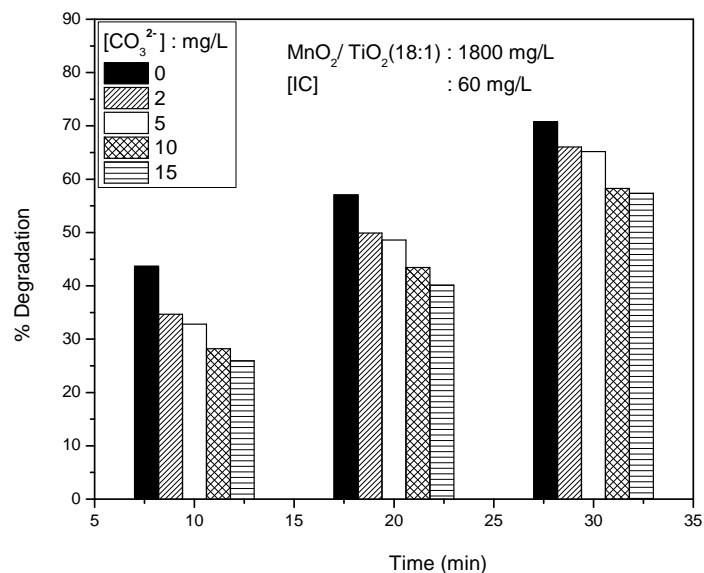
Fig. 3.79: Effect of CO$_3^{2-}$ on the MW/(MnO$_2$ - TiO$_2$) degradation of IC

CO$_3^{2-}$ also remains as an inhibitor at all concentrations. Inhibition increases with increase in concentration of CO$_3^{2-}$. However the intensity of inhibition decreases with reaction time. For e.g. in the case of 15mg/L of CO$_3^{2-}$, the inhibition after 10 minute of reaction is~45%. While it is~20% after 30 minutes. As the reaction advances more radical anions which enhance the degradation are also formed as explained in Section 3.3.3.12 and the competition between inhibiting and enhancing factors sets in. This results in decrease in the inhibition and the possible 'no effect' eventually.

Microwave, Photo and Sono Activated Advanced Oxidation Processes and their Variations for the Decontamination of Water from Toxic Chemical Pollutants

189

3.4.6.4 SO₄²⁻
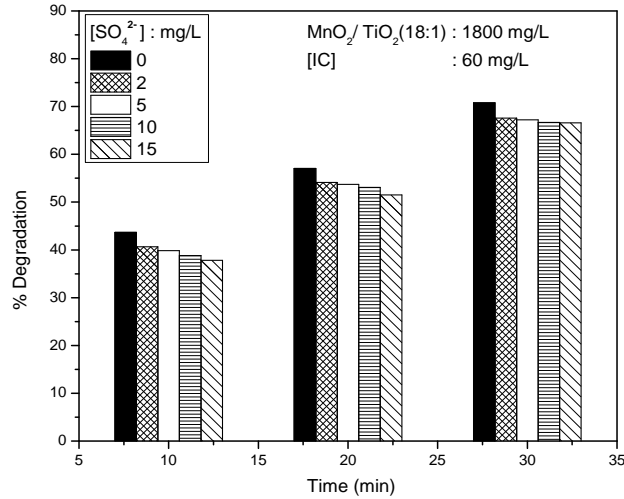
Fig. 3.80: Effect of SO$_4^{2-}$ on the MW/(MnO$_2$ - TiO$_2$) degradation of IC

SO$_4^{2-}$ remains as a mild inhibitor at all concentrations and reaction times. However, for all practical purposes, SO$_4^{2-}$ can be considered as having 'no effect'. This indicates the balancing of enhancing and inhibiting effects of SO$_4^{2-}$ ions, both of which are well documented in literature [165].

3.4.6.5 Cl⁻
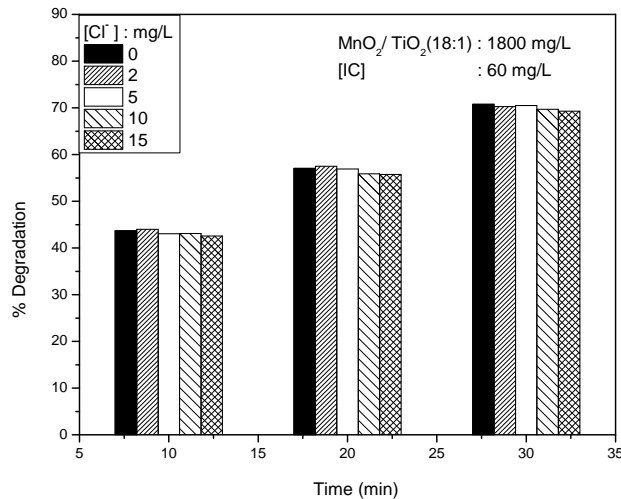
Fig. 3.81: Effect of Cl$^-$ on the degradation of IC

Chloride has no effect in the degradation at all concentrations and reaction times. Probable causes are discussed under Section 3.3.3.12

3.4.6.6 NO_3^-
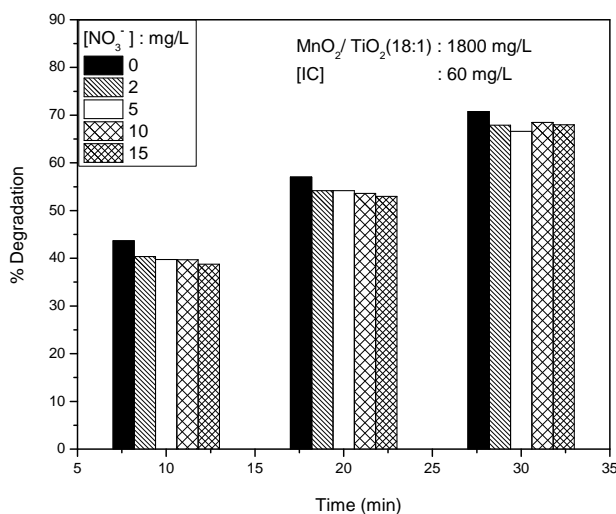
Fig. 3.82: Effect of NO_3^- on the MW/(MnO₂ - TiO₂) degradation of IC

NO_3^- can be considered as a mild inhibitor at all concentrations and reaction times. However, the inhibition is independent of the concentration of the anion and the inhibition is < 5 %. Hence it will be more appropriate to consider the effect as 'no effect'.

3.4.6.7 CH$_3$COO$^-$
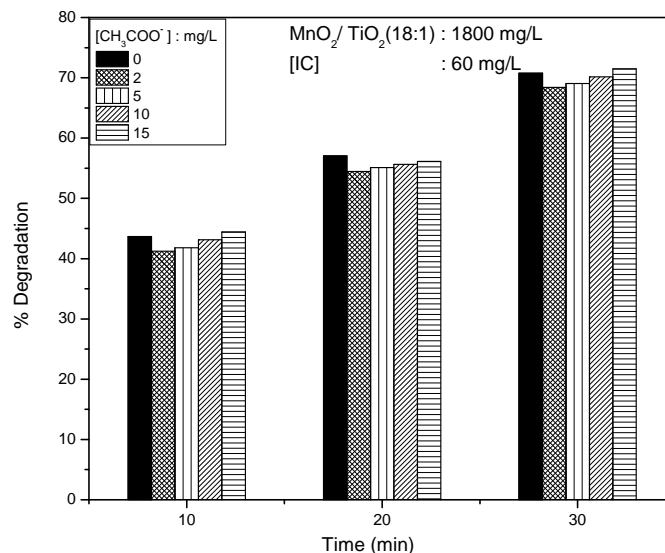
Fig. 3.83: Effect of CH$_3$COO$^-$ on the MW/(MnO$_2$ - TiO$_2$) degradation
of IC

Acetate has 'no effect' on the degradation at all concentrations and reaction times.

Probable causes for the anion effect under MnO$_2$ mediated MW catalysis are explained in Section 3.3.3.12. These include enhancing factors such as radical anion formation, enhanced diffusion of substrate etc. and inhibiting factors such as ˙OH radical scavenging, competitive adsorption, layer formation etc. The results show that the anion effect is comparable in the case of both MnO$_2$ and MnO$_2$ - TiO$_2$ mediated MW degradation of IC. Hence the mechanism of 'anion effect' also is expected to be similar. Hence details are not discussed here.

3.4.7 Mineralisation of IC in presence of MnO_2 - TiO_2 under MW irradiation

The objective of incorporating TiO_2 in MnO_2 (MnO_2 - TiO_2) was to explore the possibility of combining photocatalytic activity of TiO_2 and the MW activity of MnO_2, so that if necessary MW and UV can be combined for the efficient mineralisation of IC. In order to verify this, the degradation and mineralisation of IC in presence of MnO_2 - TiO_2 at two different ratios (18:1 and 9:1) was examined by MW, and UV irradiation in sequence (Fig.3.84). The reaction system is subjected to MW irradiation for 1hr so that the dye is completely decolourised. At this stage the COD is determined. The COD decreases only slightly under MW and in this respect MnO_2 - TiO_2 (9:1) is slightly less efficient than MnO_2. Comparison of the COD decrease in presence of MnO_2-TiO_2 in the ratios of 18:1 and 9:1(Fig.3.84) suggests that, under MW, the more the TiO_2, the less the COD reduction. This is further evident from the results presented in Fig.3.85. The results clearly demonstrate that with increase in the concentration of TiO_2 in MnO_2-TiO_2, the reduction in COD decreases. Eventually the COD stabilises in each case irrespective of MnO_2-TiO_2 ratio. The stabilised value of COD is higher at higher TiO_2 dosage, thereby reconfirming the role of TiO_2 in inhibiting the MW effect of MnO_2. The COD remains the same, even after 5 hrs of MW irradiation suggesting that MW is unable to mineralise the intermediates formed in the system.

Microwave, Photo and Sono Activated Advanced Oxidation Processes and their Variations for the Decontamination of Water from Toxic Chemical Pollutants

193
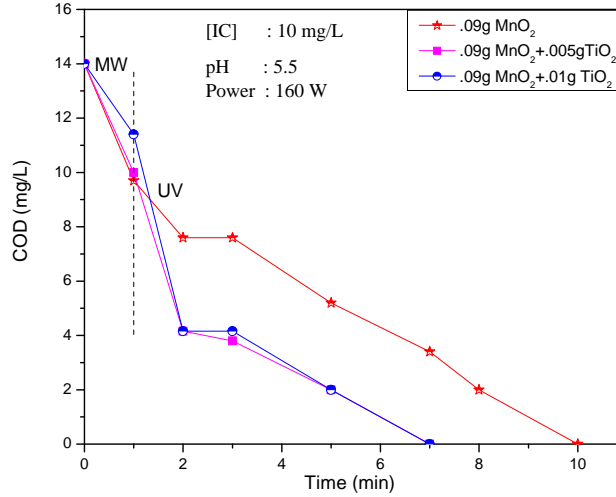
Fig. 3.84: COD of the IC solution under $MnO_2/TiO_2/MW$ and $MnO_2/TiO_2/UV$
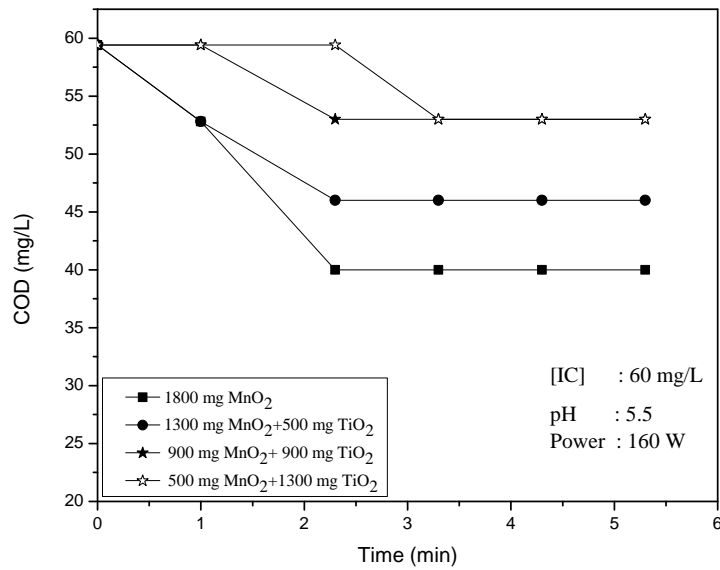
Fig. 3.85: Effect of TiO_2 in the MnO_2 - TiO_2 combination for the mineralisation (COD) removal of IC.

Under these circumstances the system containing MnO_2 and MnO_2 - TiO_2 was subjected to UV irradiation (Fig.3.84). It is observed that the

mineralisation is completed in 10hr time in the case of MnO$_2$ whereas it takes only 7hrs in the case of MnO$_2$-TiO$_2$. The results thus confirm that MnO$_2$-TiO$_2$ at the appropriate ratio is a viable catalyst system for the mineralisation of IC under MW/UV. The effect of UV irradiation (photocatalysis) on this catalyst system is investigated in detail and discussed in chapter 4 that follows.

The results show that TiO$_2$ at lower dosages (MnO$_2$/TiO$_2$: 18:1) does not affect the MW activity of MnO$_2$. Combination of MW with UV enhances the mineralisation of pollutant. The efficiency of the combination process is further enhanced by the combination catalyst MnO$_2$-TiO$_2$. Development of more efficient combination catalysts will be of particular importance in the simultaneous presence of MW and UV irradiation which is beyond the scope of the current study and is not attempted here.

3.5. Investigations on the MW catalytic degradation of IC in presence of Co$_3$O$_4$

3.5.1 Introduction

Previous section has demonstrated that MnO$_2$ which has a dielectric constant of ~10000 is excellent as a MW catalyst for the degradation of organic pollutants in water [166].

MnO$_2$ has very good coupling with MW radiation, excellent porosity, semiconductivity and mixed-valent properties which make it an efficient MW catalyst for the degradation of a variety of pollutants. Another semiconductor oxide shown to have comparable physical characteristics is Co$_3$O$_4$. Co$_3$O$_4$ is a magnetic p-type semiconductor with wide application in solid state sensors, electro chromic devices, heterogeneous catalysis etc.

Microwave, Photo and Sono Activated Advanced Oxidation Processes and their Variations for the Decontamination of Water from Toxic Chemical Pollutants

195

Co_3O_4 can be prepared in different nanostructures such as nanotubes, nanorods, nanofibres, hollow nanostructures etc. and offers the potential for a wide variety of applications. Considering these, the application of Co_3O_4 as MW catalyst for the degradation of one of the widely used special application dyes, i.e. Indigo Carmine (IC) is examined. This is only a preliminary investigation, as an extension of the study with MnO_2 as catalyst, in order to verify the effectiveness of Co_3O_4 as a MW catalyst and to identify relevant parameters. Extensive investigations on Co_3O_4 as an AOP catalyst is beyond the scope of the current project.

3.5.2 Results and Discussions

3.5.2.1 Catalyst characterization

The catalyst Co_3O_4 used in the study was characterized by surface area, particle size analysis, pore size distribution, adsorption, XRD, SEM and TEM. The surface area is 14 m^2/g. SEM image of Co_3O_4 is shown in Fig.3.86.
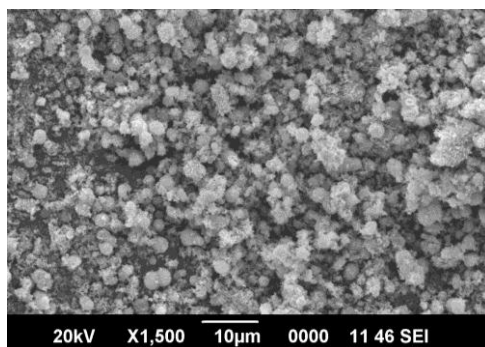
Fig. 3.86: SEM image of Co_3O_4

The image shows generally uniform shaped particles with porous structure and smooth surface with average particle size in the range of 200 nm.

TEM image of Co$_3$O$_4$ is shown in Fig.3.87.
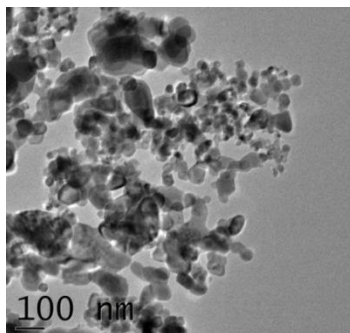
Fig. 3.87: TEM image of Co$_3$O$_4$

The image also confirms the generally uniform shape of particles. The particle size vary over a wide range though the average size is comparable to that obtained in the case of SEM analysis.

FTIR spectrum (Fig.3.88) reveals characteristic absorption peaks for metal-oxygen bonding.
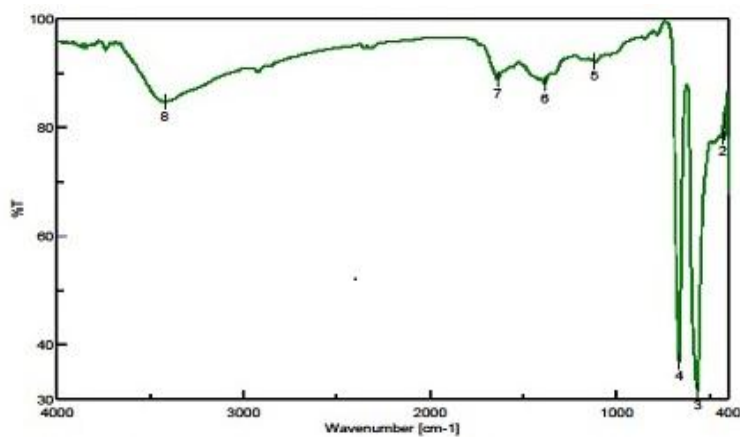
Fig. 3.88: FTIR Spectrum of Co$_3$O$_4$

The peaks around 664 and 564 cm^{-1} may be originating from two strong metal-oxygen stretching and bending vibrations respectively which is characteristic of spinel metal oxide [167].

The band at 564 cm^{-1} may be associated with the OB$_3$ vibration in the spinel lattice where B denotes Co^{3+} in an octahedral hole. The band at 664 cm^{-1} can be attributed to the ABO$_3$ vibration where A denotes the Co^{2+} in a tetrahedral hole. The stretching frequency at 3420cm^{-1} and a weak asymmetric band at 1630cm^{-1} can be attributed to the presence of OH group due to absorption of moisture. The data shows that the presence of small amounts of other oxides of Co in addition to Co$_3$O$_4$ cannot be ruled out.

The XRD pattern (Fig.3.89) showed typical diffraction peaks characteristic of Co$_3$O$_4$.
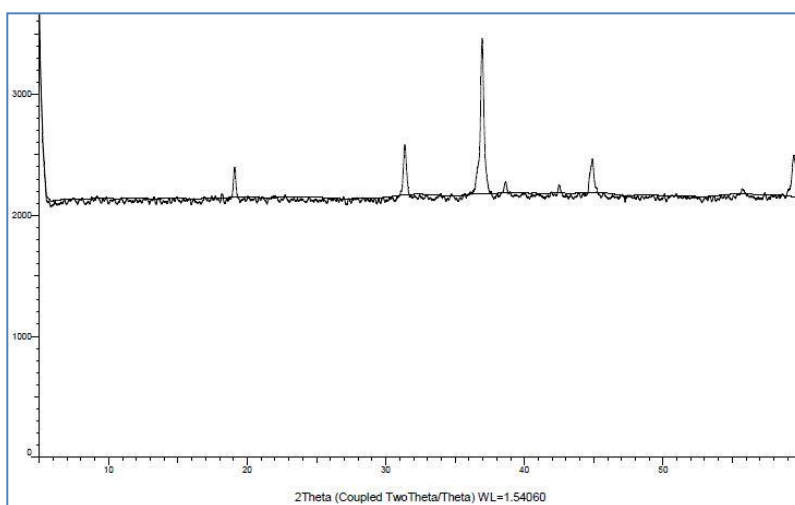
Fig. 3.89: XRD pattern of Co$_3$O$_4$

The position of the characteristic peaks at 2Theta (degree) of 59, 56, 45, 39, 37, 31 and 18 and their relative intensity are in good agreement with the literature data for Co$_3$O$_4$ [168] from which it is inferred that the material has good crystalline structure. All the diffraction peaks are

distinct and can be indexed to pure cubic phase of Co_3O_4. No peaks from other phases are detected indicating that the oxide has high purity.

The UV-DRS spectrum of Co_3O_4 is shown in Fig.3.90.
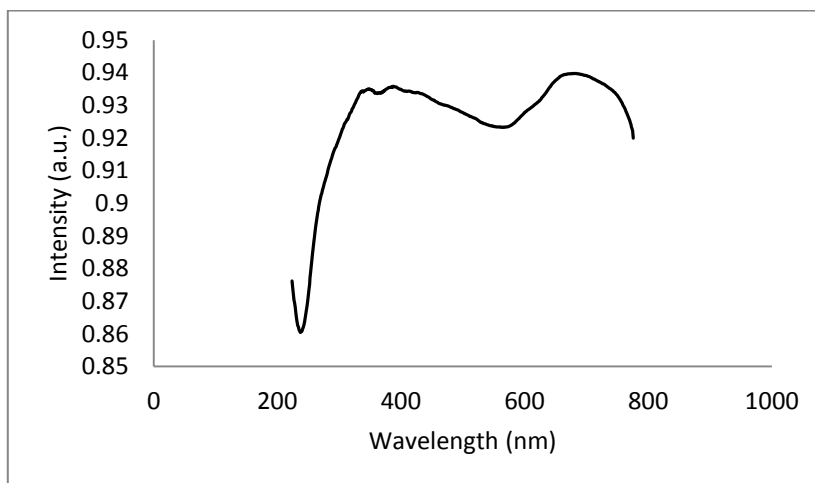
Fig. 3.90: UV-VIS-DRS of Co_3O_4

Maximum absorbance is in the ranges 250-400 nm and 550-700 nm. The maxima in the range match well with the spectra of Co_3O_4 reported in literature [169]. This is attributed to ligand to metal charge-transfer. The optical band gap energy of Co_3O_4 is~ 3.5eV which makes it a potential p-type semiconductor oxide photocatalyst in the UV range.

3.5.2.2 Preliminary MW Experiments

Preliminary experiments on the degradation of IC in presence of Co_3O_4 under MW irradiation showed that the dye is degrading at moderate rate in presence of the oxide (Fig.3.91).
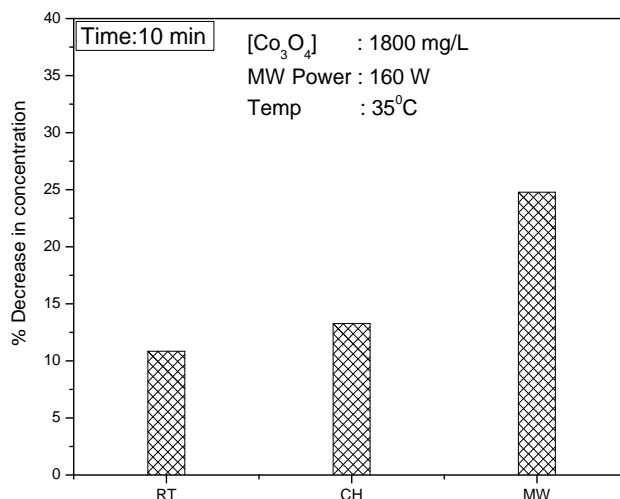
Fig. 3.91: Comparative degradation of IC in presence of Co$_3$O$_4$ under various conditions

Moderate decrease in concentration even at RT may be due to adsorption of the dye. Conventional heating (CH) results in small decrease in the concentration of IC over and above the adsorption under RT suggesting that there is no sufficient degradation under thermal catalysis at this temperature ~30^{0}C. Hence the degradation under MW cannot be due to the thermal effect. Hence detailed investigation is undertaken, beginning with optimisation of the dosage of the catalyst.

3.5.2.3 Effect of Co$_3$O$_4$ dosage

The catalyst dosage for optimum degradation of IC is experimentally checked in the range 0.06 to 0.20 g/100 mL and the results are shown in Fig.3.92.
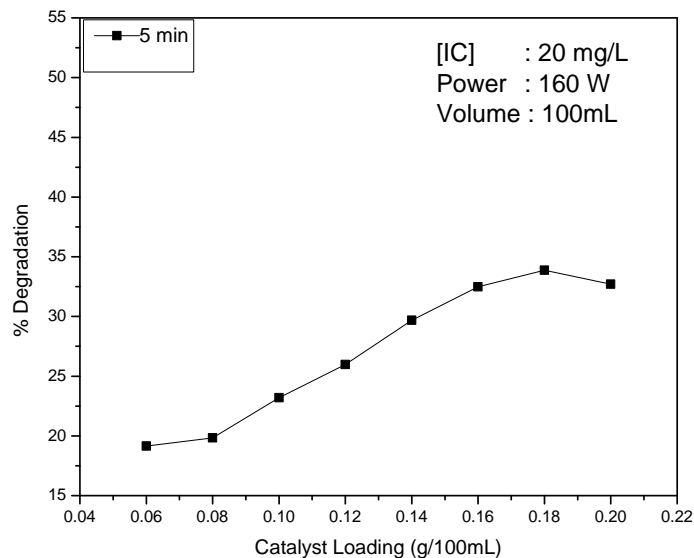
Fig. 3.92: Effect of Co_3O_4 dosage on the MW/Co_3O_4 degradation of IC.

The degradation increases steadily with increase in loading and reaches an optimum at 1.8 g/L. At higher loadings there will be more number of adsorption sites resulting in better adsorption of the dye. This will lead to more effective MW activation of the dye molecule leading to increased degradation. However, at very high loadings in the same reactor, the catalyst particles may get agglomerated causing relative decrease in the number of available active surface sites accessible per gram of the catalyst. The particles cannot be fully and effectively suspended beyond a particular loading in a particular reactor and this also leads to suboptimal penetration of radiation. Hence the degradation stabilises or even decreases at higher loadings. However, the optimum catalyst loading identified here is applicable under specific experimental conditions only as it will depend on the physicochemical characteristics

Microwave, Photo and Sono Activated Advanced Oxidation Processes and their Variations for the Decontamination of Water from Toxic Chemical Pollutants

201

of the reaction medium, as well as on the size, shape and geometry of the reactor assembly. Hence, for each reactor configuration, the optimization has to be made individually. Since the optimum loading of Co_3O_4 under MW is 1.8 g/L, all further experiments were carried out with this dosage, unless mentioned otherwise.

3.5.2.4 Effect of concentration of IC
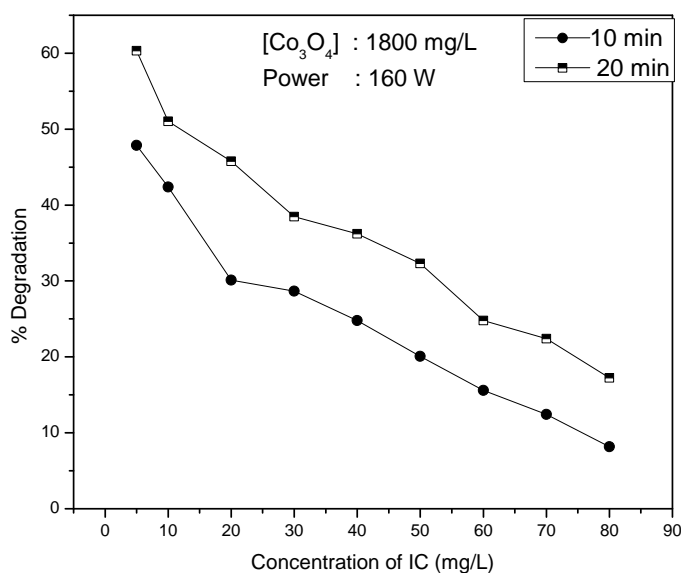
Fig.3.93: Effect of concentration on the MW/Co_3O_4 degradation of IC

As expected, from previous results, the percentage degradation decreases with increase in concentration (Fig.3.93). The rate of degradation increases with increase in concentration and reaches steady state in the range 40-60 mg/L studied here (Fig.3.94). Above this concentration, the rate decreases.
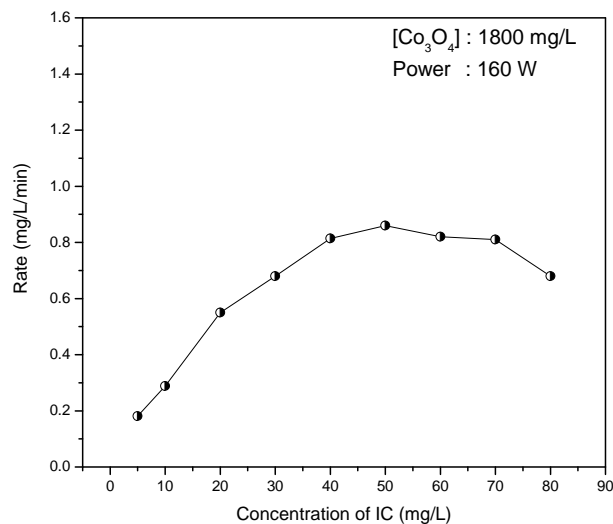
Fig. 3.94: Rate of MW/Co_3O_4 degradation of IC at various concentrations

This is similar to the effect of concentration of IC on its degradation in presence of MnO_2 as well as MnO_2 - TiO_2. The variation in the rate with concentration follows pseudo first order kinetics and L-H mechanism as is demonstrated by the 'inverse' plot ($1/r_0$ vs $1/C_0$) shown in Fig.3.95 and the logarithmic plot shown in Fig.3.96.
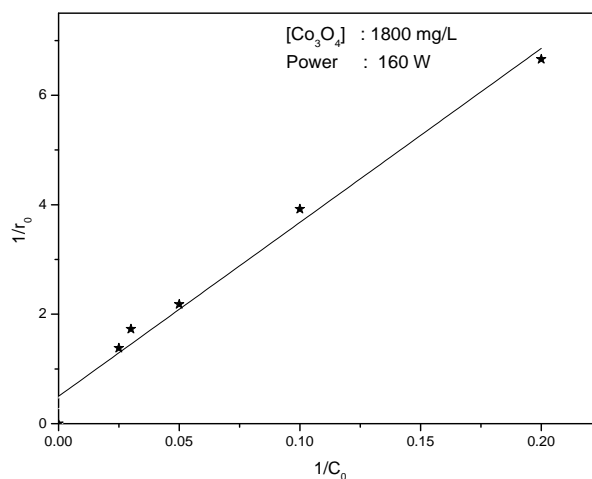
Fig. 3.95: Reciprocal plot of $1/r_0$ vs $1/C_0$ for various concentrations of IC
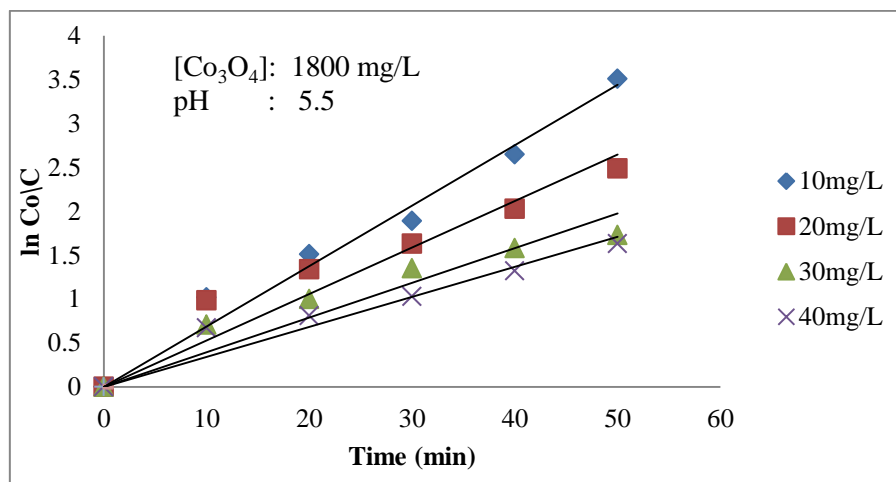
Fig. 3.96: Logarithmic plot for the MW/Co$_3$O$_4$ degradation of IC.

Similarity in the kinetics of degradation in the case of MnO$_2$ (as discussed earlier in Section 3.3.3.2) and Co$_3$O$_4$ catalyst suggests that the mechanism of degradation of IC is the same in both cases.

3.5.2.5. Effect of MW power

The MW degradation of IC in presence of MnO$_2$ as catalyst was found to increase with increase in the power of MW (see Section 3.3.3.3). The effect of variation in power on the degradation was tested in the case of Co$_3$O$_4$ catalyst also (Fig.3.97). When the power increased ~ 4 times from 90 W to 350 W, keeping all other parameters constant, the degradation in 10 minutes almost doubled from ~ 22% to ~ 40 %. The enhancement effected in 20 minutes by increase in power from 90 to 500 W was ~ 2.5 times, i.e. from ~ 30% to ~ 70 %. Hence increase in MW power can be beneficially used for enhancing the degradation. However, at higher MW power, the rate of heating is quite faster leading

to over-volatilizing of water during the reaction. This can affect the reproducibility and reliability of the data. In order to avoid this, all further experiments were carried out at 160 W and in most cases, for two durations of reaction i.e., 10 and 20 minutes. Under these conditions, the rate of degradation is proceeding at reasonable rates and can be followed more reliably and consistently.
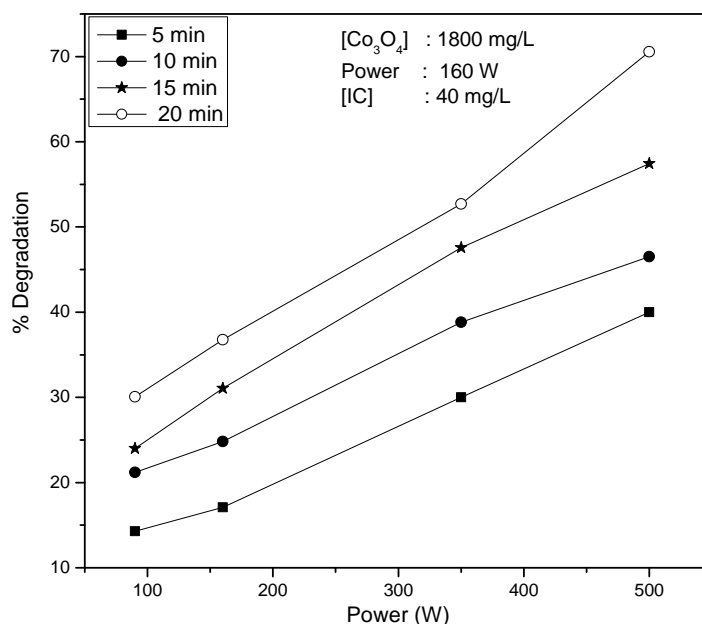
Fig. 3.97: Effect of power on the MW/Co_3O_4 degradation of IC.

3.5.2.6 Effect of pH

The effect of pH on the degradation of IC in presence of MW/Co_3O_4 and RT/Co_3O_4 is tested under identical conditions and the results are shown in Fig.3.98.

Microwave, Photo and Sono Activated Advanced Oxidation Processes and their Variations for the Decontamination of Water from Toxic Chemical Pollutants

205
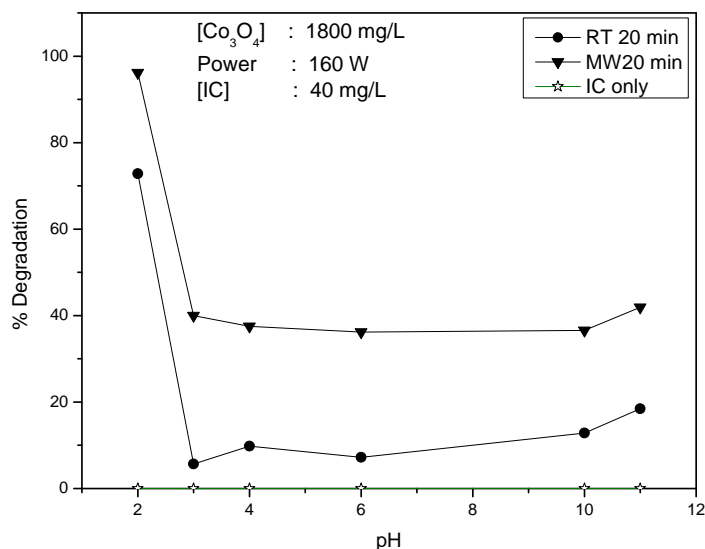
Fig. 3.98: Effect of pH on the MW/Co$_3$O$_4$ degradation of IC.

The degradation is maximum at pH 2. With increase in pH, the degradation decreases sharply and remains stable in the range pH 3-10, with slight increase above pH ~ 10. At all pH, the degradation is more under MW, compared to RT. The degradation remains more or less steady in the pH range 4-10 at the respective values in both cases. The drastic increase in degradation occurring below pH 3 cannot be explained based on the point of zero charge (PZC) of ~ 7.3 of Co$_3$O$_4$ as is done in the case of AOPs involving semiconductors. Below the PZC the surface is positively charged and hence its oxidizing ability can be sharply enhanced. IC is a dianionic dye in aqueous solution and it can keep the dianionic configuration in the pH range 3-11 [151]. This implies that there will be strong electrostatic interaction between the positive catalyst surface and the dianions at lower pH which can lead to better adsorption

and higher degradation. However, under MW irradiation, the typical zeta potential curve may not be precise as under normal photo or thermal activation processes and the zeta potential may remain positive over a wider range [170]. Hence a simple correlation between the PZC based surface charge on the catalyst and the surface-substrate interaction may not be quite relevant under MW irradiation. The distortion of pH effect on chemical reactions by MW and other AOP processes has been reported earlier too [95]. The extremely high degradation at pH~2 is mostly pH effect on the catalyst which facilitates the adsorption of IC at RT and the degradation under MW.

Heterogeneous degradation of many organics is known to be initiated with the formation of precursor complex between the substrates and surface bound metal atom [171], i.e. Co in this case. Electrons are transferred from the organic compound to the surface bound Co on the Co$_3$O$_4$. This results in the oxidative degradation of the pollutant and concurrent reduction of Co to low-valent state. Thus Co$_3$O$_4$ can also play the role of an oxidant. Dissolved O$_2$ in solution can oxidise the Co (II) to Co (IV) again. Normally at solution pH < PZC when the surface is positively charged, the re-adsorption of free Co(II) ions in solution back onto Co$_3$O$_4$ surface is less probable. This results in depletion of catalytically active surface sites and consequently decreased degradation. However, such a simple explanation is not applicable in this case, since the degradation is maximum at pH ~ 2. In the current instance, at the natural pH of 5.6 of the reaction system, Co$_3$O$_4$/MW is ~ 6-8 times more efficient than Co$_3$O$_4$/RT after 20 minutes of irradiation. Hence the role of MW as a powerful activation source for Co$_3$O$_4$ is evident at all pH.

In any case, like in the case of many heterogeneous AOPs, the effect of pH on the degradation of organics is complex and cannot be explained based on any single parameter or simple interaction.

3.5.2.7 Volume effect

The volume of the reaction medium influences the rate of degradation, as seen in the case of MnO_2 (see Section 3.3.3.7). Hence the effect of volume of the reaction medium on the efficiency of degradation of IC is verified in the case of Co_3O_4 catalyst also by conducting the reactions at different volumes ranging from 100 to 800 mL in a 1L reactor. The results are shown in Fig.3.99.
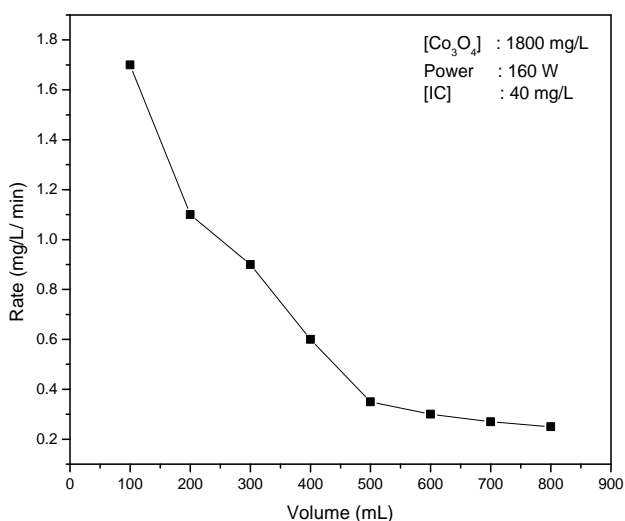
Fig. 3.99: Effect of volume (at constant catalyst weight) on the MW/Co_3O_4 degradation of IC

It is seen that the rate decreases with increase in reaction volume and eventually the degradation is almost completely inhibited. The decrease in degradation with increase in reaction volume can be attributed

to the decreasing penetration of MW radiation through the reaction medium. The relatively decreasing availability of the catalyst particles with respect to IC is another possible reason. This is further verified by increasing the relative dosage of catalyst with volume and the results are shown in Fig.3.100.
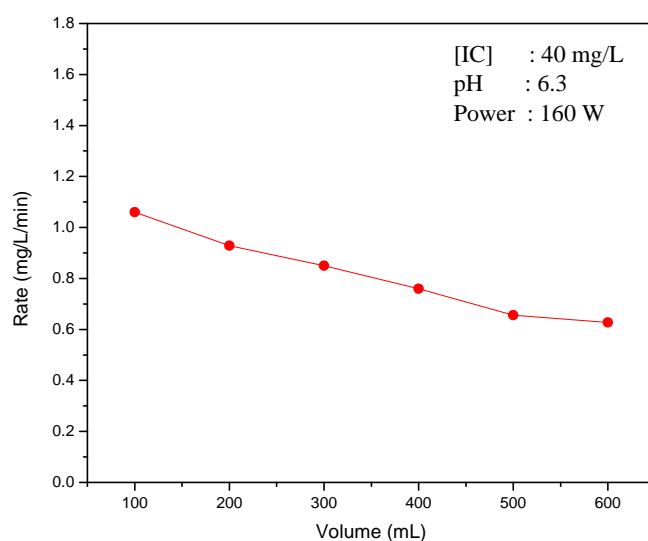
Fig. 3.100: Effect of reaction volume (catalyst weight corresponding to volume) on the MW/Co₃O₄ degradation of IC

In this case the rate of degradation is more or less sustained thereby confirming the importance of relative concentration of catalyst and the substrate for effective degradation. This is consistent with the results in the case of MnO$_2$ as explained in Section 3.3.3.7.

3.5.2.8 Temperature Effect

Temperature is one of the factors that contribute to the MW catalytic degradation of pollutants as seen from the results under CH and

MW. The comparative degradation of IC at various temperatures in presence of CH and MW irradiation under otherwise identical conditions is given in Fig.3.101.
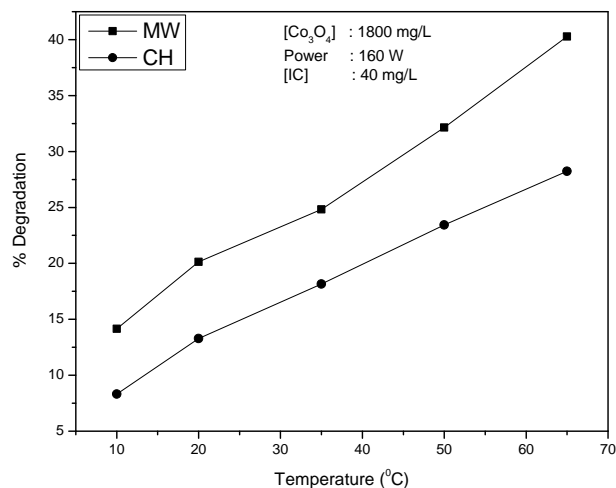
Fig. 3.101: Effect of temperature on the degradation of IC under CH and MW radiation in presence of Co_3O_4

The degradation increases with increase in temperature in both cases. At the temperature of 65^0C, the degradation is 40% in presence of MW, while it is only 28% in the case of CH. The mechanism by which MW accelerates the degradation of pollutants, other than the thermal effect is already explained in Section 3.3.3.4. The activation energy of the reaction is calculated under MW as well as CH conditions from the Arrhenius plot of lnk vs I/T as shown in Fig.3.102 and 3.103.
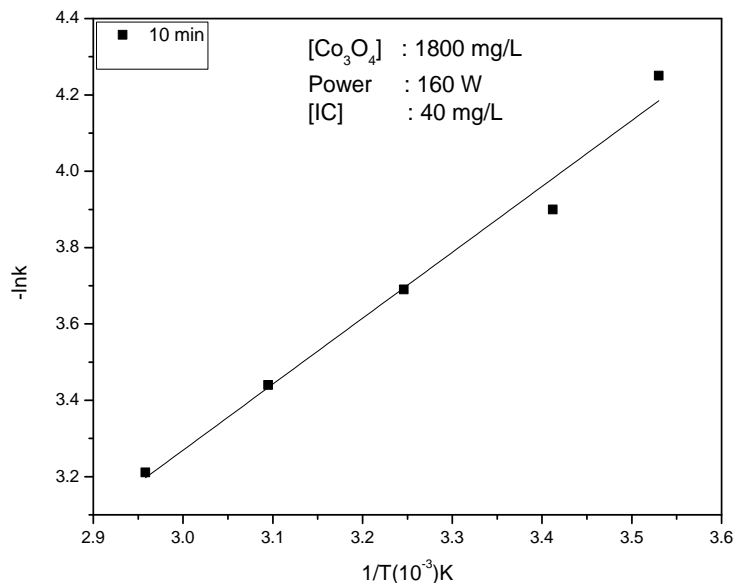
Fig. 3.102: Arrhenius plot for the degradation of IC under MW/Co₃O₄
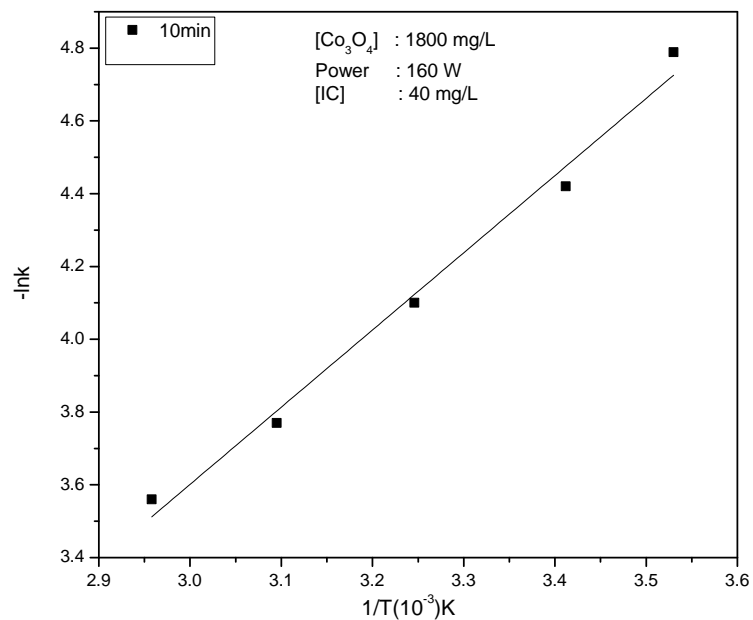
Fig. 3.103: Arrhenius plot for the degradation of IC under CH/Co₃O₄

Microwave, Photo and Sono Activated Advanced Oxidation Processes and their Variations for the Decontamination of Water from Toxic Chemical Pollutants

211

The apparent activation energy was calculated from the Arrhenius equation (eqn. 25) (Section 3.3.3.4).

The activation energy for the MW degradation is 14.4 KJ/mol, while under CH it is 17.6 KJ/mol. Hence it is clear that MW reduces the activation energy for the degradation as in the case of MnO_2. Hence the enhancement in the degradation under MW may be partially due to decrease in Ea. However, the decrease in Ea is not very significant thereby suggesting that the contribution on account of this may be only marginal (Details are given in Section 3.3.3.4).

3.5.2.9 Effect of Oxidants

3.5.2.9.1 Effect of added H_2O_2

The effect of added H_2O_2 on the MW degradation of IC in presence of Co_3O_4 is tested and the results are presented in Fig.3.104.

The effect of H_2O_2 on the rate of degradation is practically negligible at lower concentrations. As the concentration of H_2O_2 increases, in small dosages the degradation increases mildly and is stabilised. Various factors contributing to the often conflicting and inconsistent effect of H_2O_2 on MW degradation of organics are discussed in Section 3.3.3.10.1. H_2O_2 forms ·OH radicals under MW irradiation (eqn.28) which is expected to enhance the degradation. However in the presence of MW radiation, H_2O_2 also undergoes decomposition to H_2O and O_2 as in (eqn. 27) (Section 3.3.3.10.1). This naturally results in a decrease in the MW available for the catalyst and the substrate as well as reduction in the availability of reactive OH radicals which lead to the

decrease in the degradation of IC. The mutual destruction of H_2O_2 and $^{.}OH$ by interaction with each other result in the formation of less active $HO_2^{.}$ radicals (eqn. 29). The $HO_2^{.}$ radicals also participate in the degradation of IC, though less efficient compared to $^{.}OH$ radical. When these opposing factors balance, the effect of H_2O_2 on the degradation is stabilised. Depending on the domination of respective reactive free radicals and their interactions with the substrate/H_2O_2, the degradation is enhanced or inhibited.
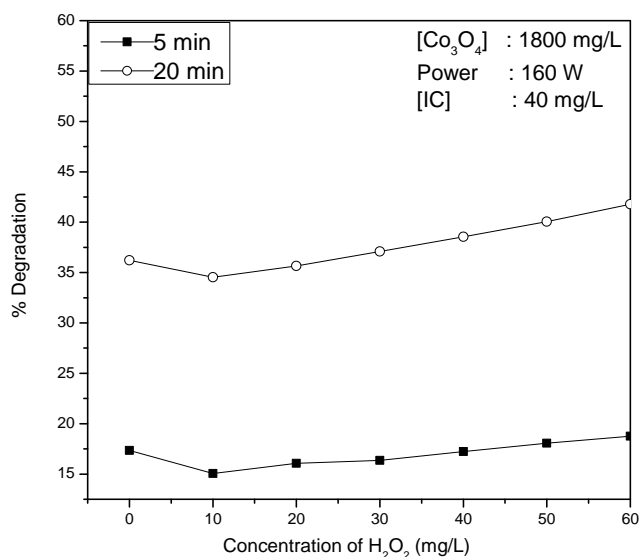
Fig. 3.104: Effect of added H_2O_2 on the MW/Co₃O₄ degradation of IC

The complex effect of H_2O_2 is further verified by its in-between addition to the MW/Co₃O₄/IC reaction in progress. The result is shown in Fig.3.105.

Microwave, Photo and Sono Activated Advanced Oxidation Processes and their Variations for the Decontamination of Water from Toxic Chemical Pollutants

213
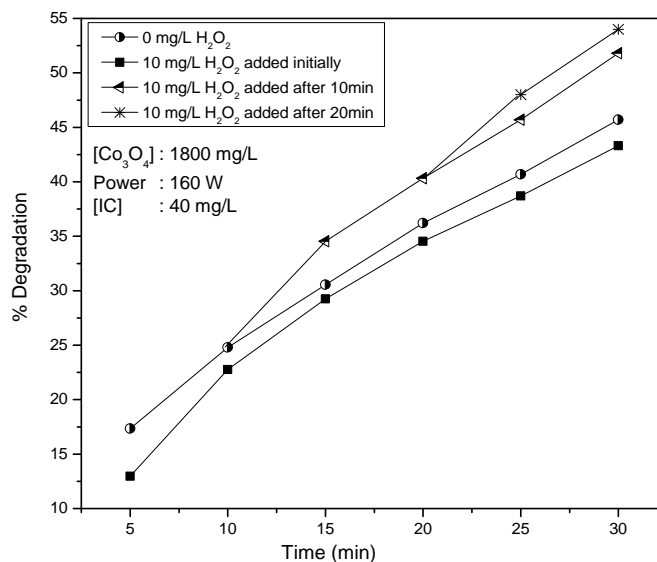
Fig. 3.105: Effect of initial and in-between addition of H$_2$O$_2$ on the MW/Co$_3$O$_4$ degradation of IC.

Initial addition of H$_2$O$_2$, at lower concentration of 10 mg/L inhibited the degradation mildly. However, when same amount of H$_2$O$_2$ is added after 10 min of MW irradiation when ~25% of IC has degraded, the degradation is enhanced mildly. Further addition of 10 mg/L of H$_2$O$_2$ after 20 minutes enhanced the degradation further. At relatively lower IC concentration, (at later stages of the reaction), the net amount of reactive oxygen species (H$_2$O$_2$, HO$_2$·, ·OH etc.) present in the system after the in-between addition of H$_2$O$_2$, is sufficient to compensate for the inhibiting interactions as discussed earlier in Section 3.3.3.10.1. At this stage even those interactions with very few molecules of IC will be sufficient to register an enhancement. Hence the degradation is enhanced slowly. Thus it is confirmed that the effect of H$_2$O$_2$ is concentration-dependent and once sufficient concentration of H$_2$O$_2$ is available to overcome the detrimental (to the degradation of IC) in situ processes by other reactive

radicals, the effect is enhancement. This is further evident from the enhancing effect at higher concentration of H$_2$O$_2$. The degradation of IC steadily increases with increase in the concentration of H$_2$O$_2$ (Fig.3.106) in the range 50 -300mg/L.
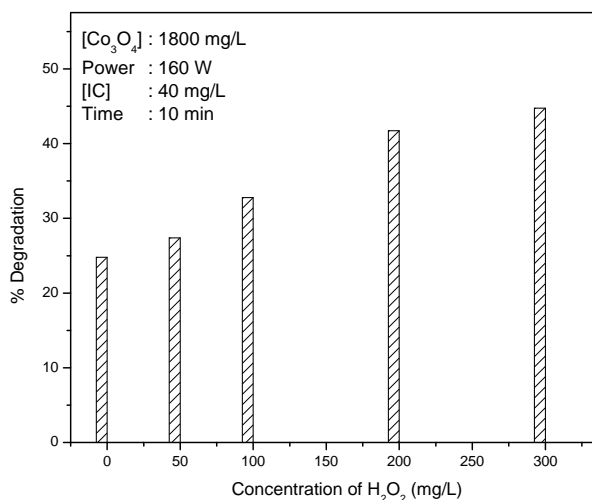
Fig. 3.106: Effect of added H$_2$O$_2$ at higher concentration on the MW/Co$_3$O$_4$ degradation of IC

At higher concentrations of H$_2$O$_2$ there will be higher rate of formation and hence sufficient population of ˙OH radicals which can compensate for the competitive mutual destruction of ˙OH and H$_2$O$_2$. This reconfirms that the net concentration of H$_2$O$_2$ in the system is critical in deciding its role as an inhibitor or enhancer in the MW degradation of IC in presence of Co$_3$O$_4$.

It is also known that H$_2$O$_2$ is formed in situ in the system though its concentration does not increase with time. H$_2$O$_2$ is known to undergo periodic increase and decrease i.e., oscillation in its concentration under sonolysis, photolysis and sonophotocatalysis [112]. Hence the net concentration of H$_2$O$_2$ in the system at any point of time during the reaction

may be varying and inconsistent. This will also make the effect of H_2O_2 on the degradation unpredictable especially at lower concentrations.

3.5.2.9.2 Effect of added persulphate

Another oxidant, i.e. persulphate $(S_2O_8^{2-})$ (PS) $(E^0 = 2.1\ V)$ is also investigated as a potential enhancer of the MW/Co_3O_4 degradation of IC. Specific advantages of PS as already discussed earlier, include high solubility and stability at ambient temperature. Further, the end-product of PS - promoted mineralisation is the SO_4^{2-} ions, which are relatively harmless. However PS as such does not cause any degradation of IC or other organic pollutants. It requires a powerful activation source such as light, sound or MW. Hence MW/PS is tested for the degradation/ mineralization of IC in presence of Co_3O_4. The effect of concentration of PS on the degradation is shown in Fig.3.107.
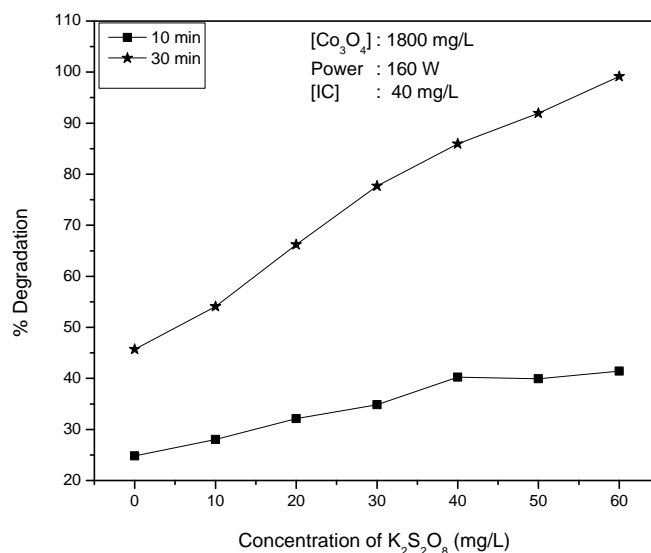
Fig. 3.107: Effect added $K_2S_2O_8$ on the MW/Co_3O_4 degradation of IC.

The degradation increases with increase in concentration of PS. The enhancing role is further verified by the in-between addition of PS to the reaction system in which the degradation of IC is in progress. The results are plotted in Fig.3.108.
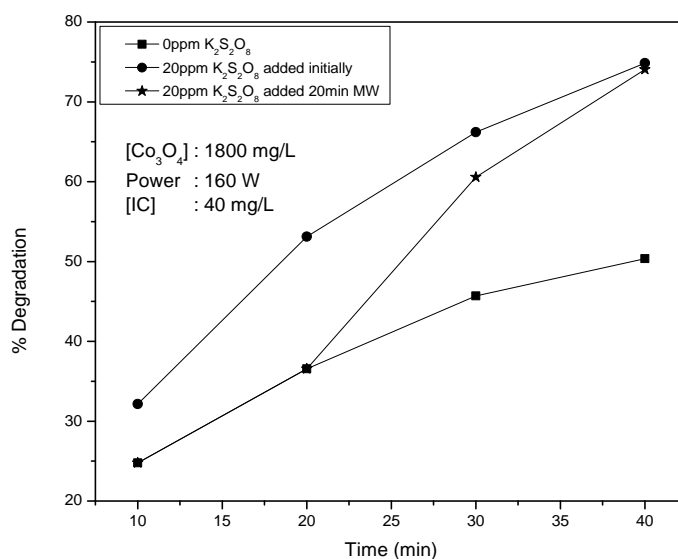
Fig. 3.108: Effect of initial and in-between addition of K$_2$S$_2$O$_8$ on the MW/Co$_3$O$_4$ degradation of IC.

Initial addition of PS enhances the degradation. In between addition of PS after 20 minutes enhances the degradation and eventually reaches the same level as in the case of initially added PS.

The mechanism of the enhancement of MW initiated degradation of IC by PS in presence of MnO$_2$ has been explained under Section 3.3.3.10.2. The same is applicable in the case of Co$_3$O$_4$ also as seen from the similarity in the results.

The comparative enhancing effect of H_2O_2 and PS is illustrated in Fig.3.109 by the in-between addition of the oxidants to the degradation reaction in progress.
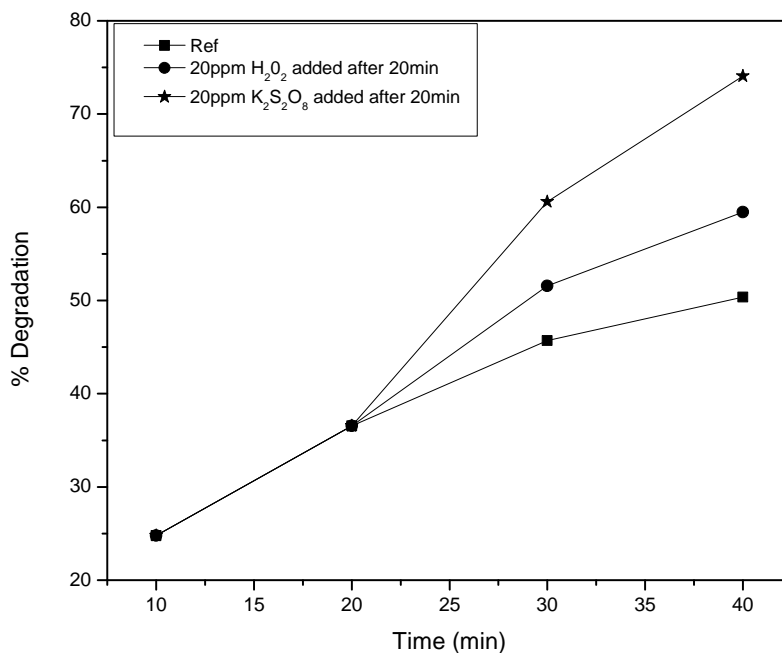
Fig. 3.109: Effect of initial and in-between addition of $K_2S_2O_8$ and H_2O_2 on the MW/Co$_3$O$_4$ degradation of IC.

Under normal MW/Co$_3$O$_4$ conditions, the degradation of IC in 40 minutes is ~50%. Addition of PS at the 20th minute, enhances the same to ~75%. Addition of H_2O_2 in place of PS in the above experiment increases the degradation to ~ 60% only.

The investigations have also revealed that excess addition of PS has no negative effect and hence any unused oxidant can be used for fresh input of IC pollutant. This is important from the economic angle (See Section 3.3.3.10.2 and Fig. 3.44). Combination of these two oxidants, i.e.

H$_2$O$_2$ and PS, widely used in many AOTs, gave only the same extent of degradation achieved in the case of PS with no additive or synergic effect (Fig.3.110).
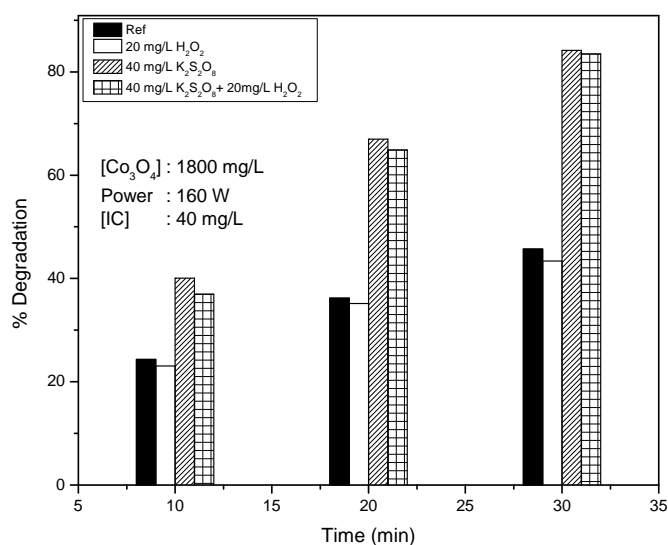
Fig. 3.110: Combination of K$_2$S$_2$O$_8$ and H$_2$O$_2$ on the MW/Co$_3$O$_4$ degradation of IC.

3.5.2.10 Effect of Anions / Salts

The water used in industries often contains a variety of salts/anions as contaminants. Since it is not economical to decontaminate the water, these salts will form an inherent part of the effluent as well. Hence any AOP aimed at mineralizing the toxic/hazardous pollutants in water must consider the effect of these salts on the efficiency of the respective processes. Accordingly, the effect of few commonly found anions in water, i.e. PO$_4^{3-}$, CO$_3^{2-}$, HCO$_3^-$, NO$_3^-$, SO$_4^{2-}$ and Cl$^-$ on the MW/Co$_3$O$_4$ degradation of IC is tested. Preliminary results with varying concentration of the anions at various reaction times are presented in Fig.3.111A and 3.111B.
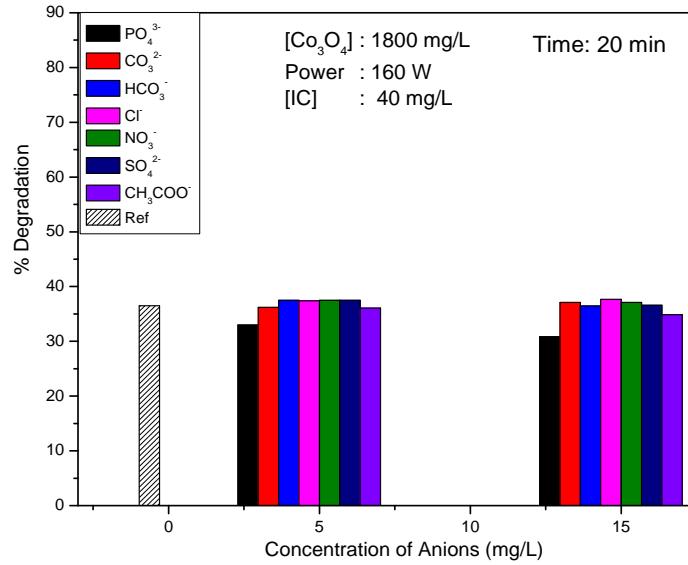
Fig. 3.111A: Effect of concentrations of anions on the MW/Co₃O₄ degradation of IC.
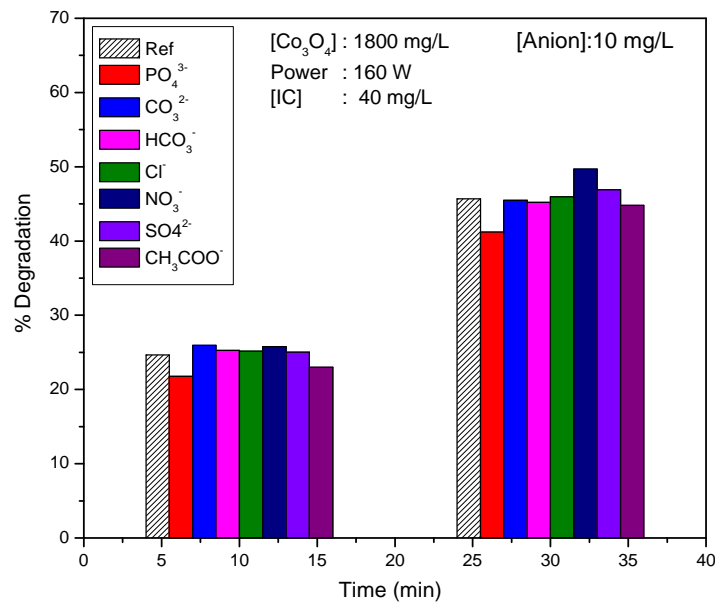
Fig. 3.111B: Effect of reaction time on the 'Anion effect on the MW/Co₃O₄ degradation of IC'

Except PO_4^{3-}, other anions have practically no effect on the degradation of IC at all concentrations or reaction times tested here. Even in the case of PO_4^{3-} also, the inhibition is much less compared to its inhibitive effect in many other AOPs.

Earlier studies from our laboratory have shown that the effect of salts/anions on the AOP degradation of many pollutants is dependent on the concentration of the respective anion and the reaction duration. Hence this possibility is tested in detail in this case also, even though preliminary investigations showed that the effect is only mild. The results are plotted in Figs.3.112 to 3.118.

3.5.2.10.1 PO_4^{3-}
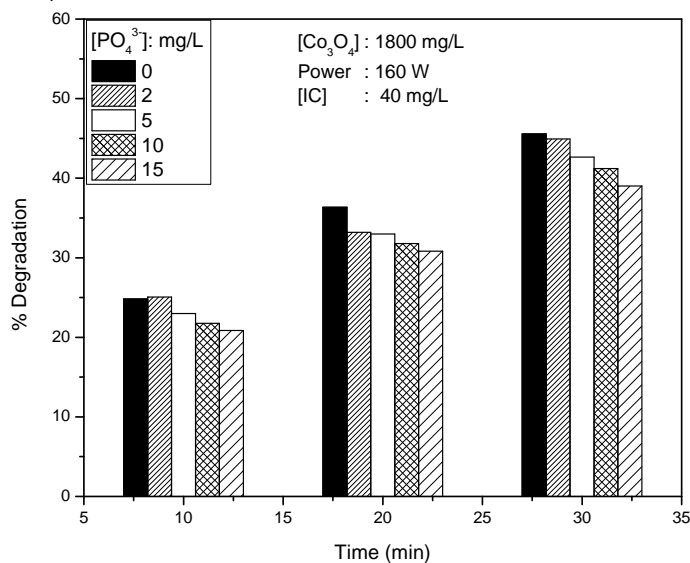
Fig. 3.112: Effect of PO_4^{3-} on the MW/Co₃O₄ degradation of IC

As expected, PO_4^{3-} remains as an inhibitor at all concentrations and all reaction times. The degree of inhibition increases with increase in concentration. The trend is maintained at different reaction times also.

3.5.2.10.2 CO$_3^{2-}$
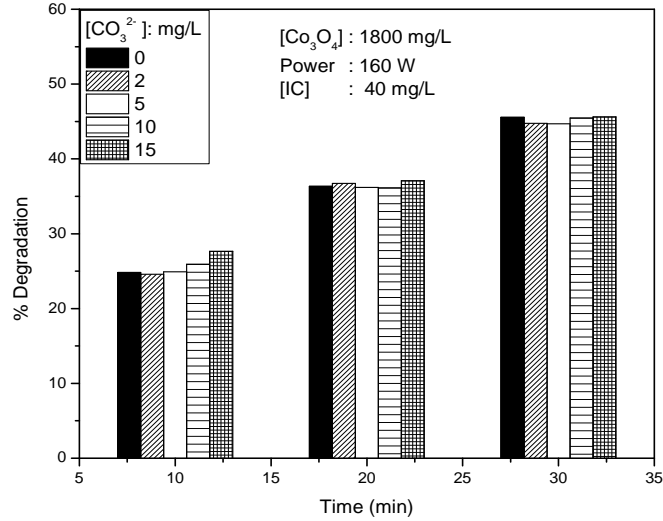
Fig. 3.113: Effect of CO$_3^{2-}$ on the MW/Co$_3$O$_4$ degradation of IC

The effect of carbonate is practically 'nil' within the limits of experimental error at all concentrations and reaction times tested here.

3.5.2.10.3 HCO$_3^-$
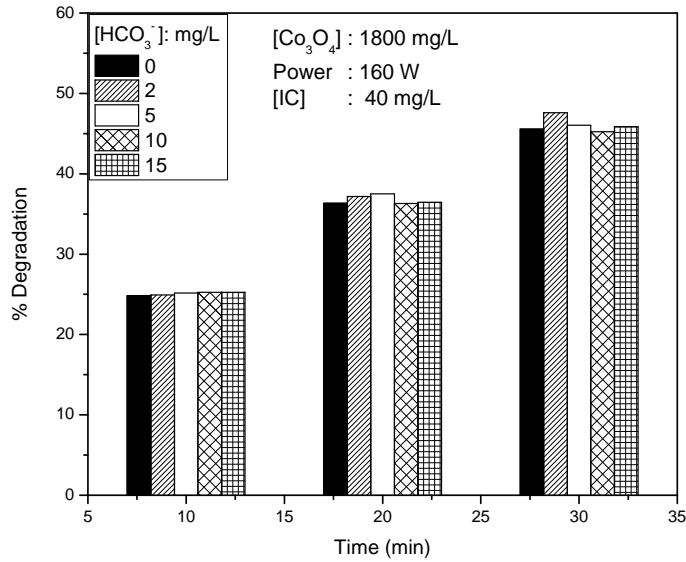
Fig. 3.114: Effect of HCO$_3^-$ on the MW/Co$_3$O$_4$ degradation of IC

The effect of HCO$_3^-$ on the degradation of IC is practically 'nil' at all concentrations and reaction times tested here.

3.5.2.10.4 Cl$^-$
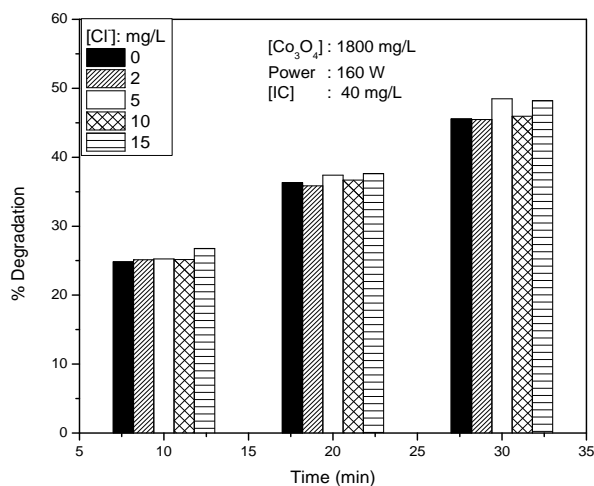
Fig. 3.115: Effect of Cl$^-$ on the MW/Co$_3$O$_4$ degradation of IC

The effect of Cl$^-$ is also practically 'nil' at all concentrations and reaction times tested here.

3.5.2.10.5 NO$_3^-$
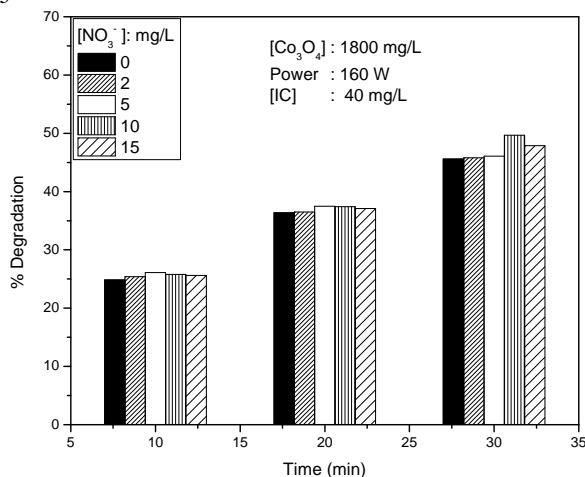
Fig.3.116: Effect of NO$_3^-$ on the MW/Co$_3$O$_4$ degradation of IC

Microwave, Photo and Sono Activated Advanced Oxidation Processes and their Variations for the Decontamination of Water from Toxic Chemical Pollutants

223

The effect of NO_3^- is practically nil at all concentrations and reaction times tested here.

3.5.2.10.6 SO_4^{2-}
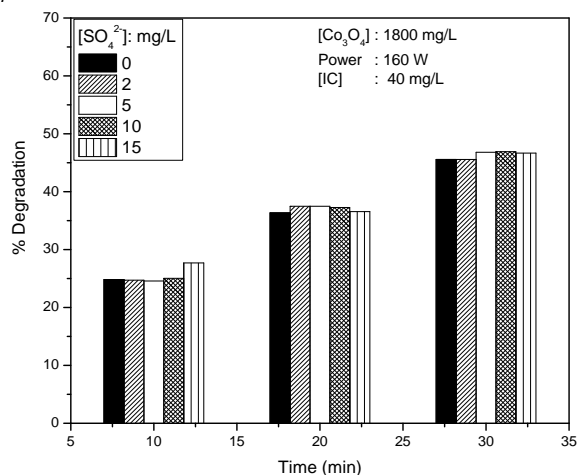
Fig. 3.117: Effect of SO_4^{2-} on the MW/Co$_3$O$_4$ degradation of IC

The effect of SO_4^{2-} is practically nil at all concentrations and reaction times tested here.

3.5.2.10.7 CH_3COO^-
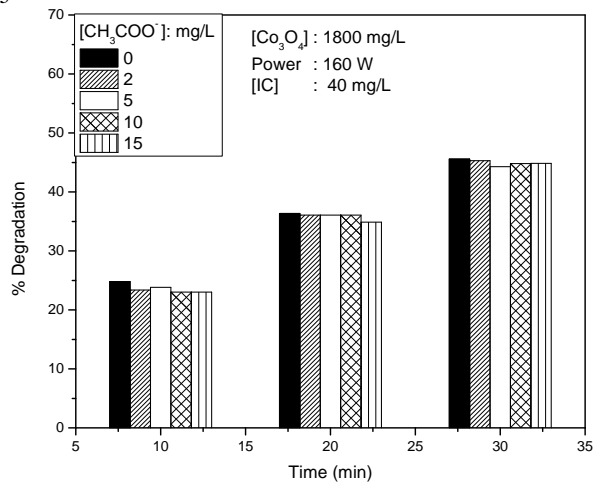
Fig. 3.118: Effect of CH$_3$COO$^-$ on the MW/Co$_3$O$_4$ degradation of IC

Acetate ion also have only negligible effect on the degradation of IC at all concentrations and reaction times tested here.

Since the effect of the anions on the degradation of IC under MW/Co_3O_4 is practically 'nil'. A study on the effect of these salts on the characteristics of the reaction system to search for reasons for the 'anion effect' (as done in the case of MnO_2 and MnO_2-TiO_2) is not relevant here.

3.5.2.11 Effect of Oxygen

It has been observed in the case of MnO_2 that deaerating the system with N_2, which removes the dissolved O_2 in the suspension and loosely bound O_2 on the surface does not inhibit the degradation much, especially at higher dosages of the catalyst.
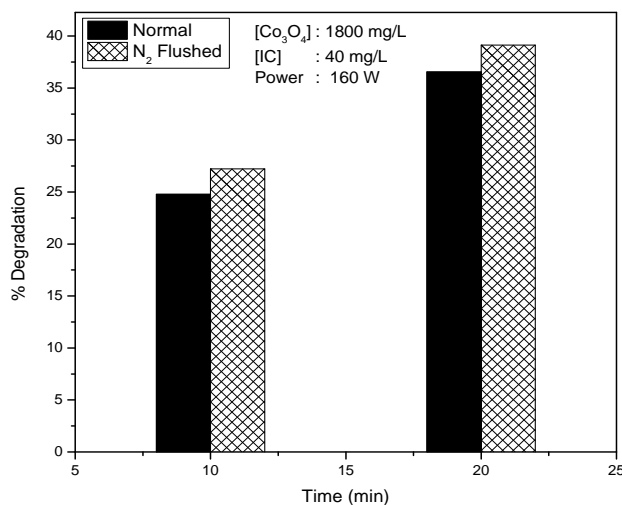
Fig. 3.119: Effect of deaeration with N_2 on the MW/Co_3O_4 degradation of IC

Similar experiments are conducted in presence of Co_3O_4 catalyst also by flushing the reaction system with N_2. Preliminary results plotted in Fig.3.119 shows that at higher dosage (1800 mg/L) of Co_3O_4, deaeration has very little effect on the degradation.

Microwave, Photo and Sono Activated Advanced Oxidation Processes and their Variations for the Decontamination of Water from Toxic Chemical Pollutants

225

This is contrary to the observation in the case of many AOPs in which dissolved O_2 is an essential component for trapping the electrons and the formation of various ROS. In the case of MnO_2 this is explained based on the participation of lattice oxygen as well as strongly bound surface oxygen in the process, which was confirmed by EDX data as well as from experiments.

If the requirement of O_2 for the degradation, in deaerated system is met with O_2 from the lattice of the catalyst, the availability of O_2 may not be adequate at lower dosage of the catalyst. If so, deaeration must lead to inhibition when Co_3O_4 loading is low. This is verified by testing the effect of N_2 bubbling of the reaction system on the degradation of IC at lower dosages of 50-200 mg/L of Co_3O_4. Results are shown in Fig.3.120.
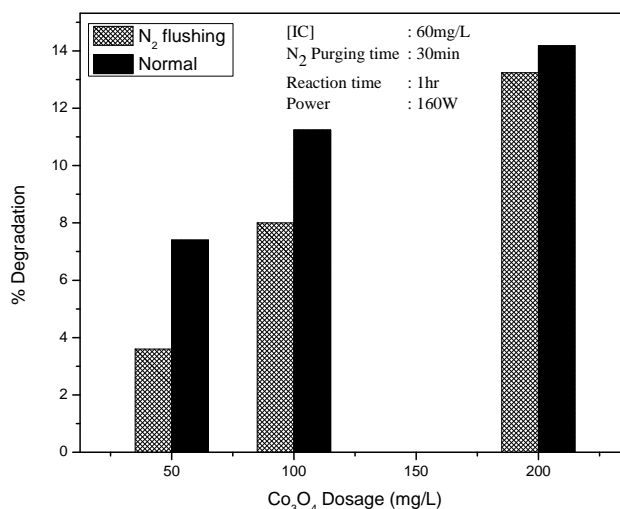
Fig.3.120: Effect of deaeration with N_2 on the MW/Co_3O_4 degradation of IC at lower dosages

The deaeration by N_2 inhibits the degradation of IC at 50 mg/L of Co_3O_4. With increase in dosage of Co_3O_4 to 100 mg/L the inhibition is reduced and at 200 mg/L of the catalyst deaeration has practically no effect.

This 'no effect' is maintained even at 1800 mg/L of Co_3O_4. From these results it may be confirmed that in the case of Co_3O_4 also lattice O_2 and/or strongly bound surface O_2 plays an important role in the degradation of IC under MW, especially in deaerated systems.

3.5.2.12. Recycling of Co_3O_4

If the microwave catalytic process is to be applied commercially, recycling of the used catalyst is important. The reusability of Co_3O_4 used in the current study is tested as follows: Co_3O_4 used for the MW degradation of IC is separated from the reaction system by simple centrifugation. It is then washed with distilled water, centrifuged again, air dried at room temperature ($\sim 30^0$C) and then reused as such for the microwave catalytic degradation of IC. The results are presented in figure 3.121.
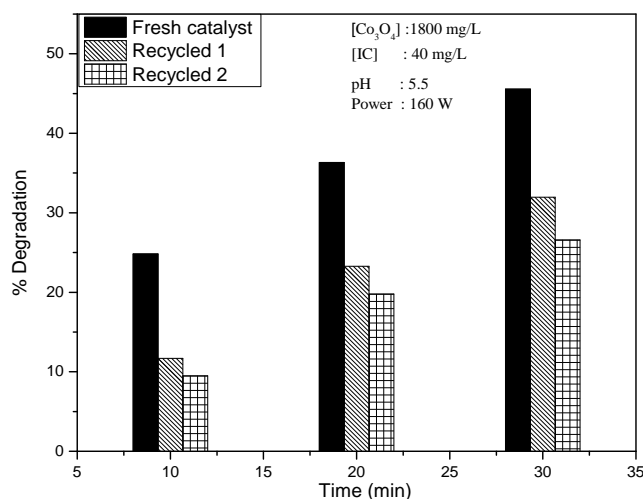
Fig. 3.121: Efficiency of recycled Co_3O_4 for the Microwave catalytic degradation of IC.

The catalytic activity decreases significantly after first use and thereafter moderately after second use. With increasing number of

Microwave, Photo and Sono Activated Advanced Oxidation Processes and their Variations for the Decontamination of Water from Toxic Chemical Pollutants

227

recycles at least some of the substrate and/or the intermediate molecules might be remaining strongly adsorbed or getting trapped in the cavities of Co_3O_4 resulting in subsequent lower adsorption and hence decreased catalytic degradation. Recycling will also use up more of the lattice O_2. If this is the case, increase in the initial concentration of the substrate which will require more surface sites and more ROS will lead to faster deactivation with each use. At higher concentration of substrate, the concentration of in situ formed intermediates also will be more and they can occupy more surface sites. Consequently, the efficiency of recycling is expected to be less. In order to verify this, the recycling of Co_3O_4 is tested using higher concentration of IC and the results are plotted in Fig.3.122.
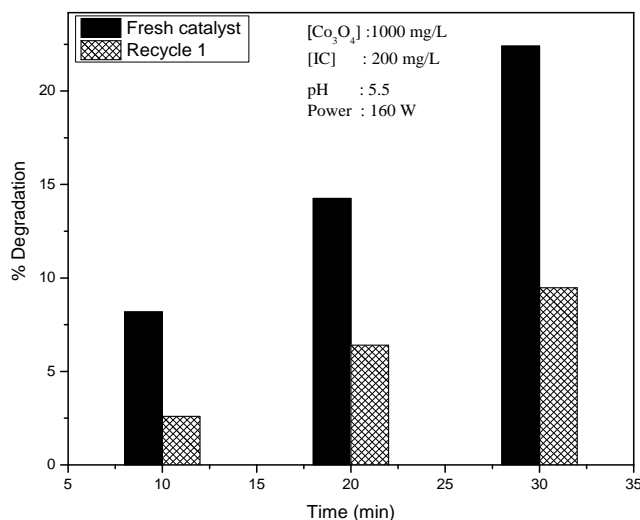
Fig.3.122: Efficiency of recycled Co_3O_4 for the Microwave catalytic degradation of higher concentration of IC.

The results show that the efficiency of the fresh catalyst is substantially depleted by ~ 60% (28 to 11% at 30 min) when the concentration of the substrate is higher (200 mg/L). The decrease in

efficiency of fresh catalyst when the concentration of IC is low i.e. 40 mg/L, is ~ 30% (45 to 32% in 30 min) (Fig.3.121). These experiments confirms that lattice O$_2$ from Co$_3$O$_4$ is taking part in the degradation of IC. The extraction of oxygen from the lattice of Co$_3$O$_4$ for the degradation of IC is further verified by recording the EDX spectrum of Co$_3$O$_4$ before and after use (Fig.3.123 and 3.124). The wt% as well as atomic% of oxygen before and after use clearly illustrate that oxygen from the lattice of Co$_3$O$_4$ is used for the degradation of IC (Table 3.11).
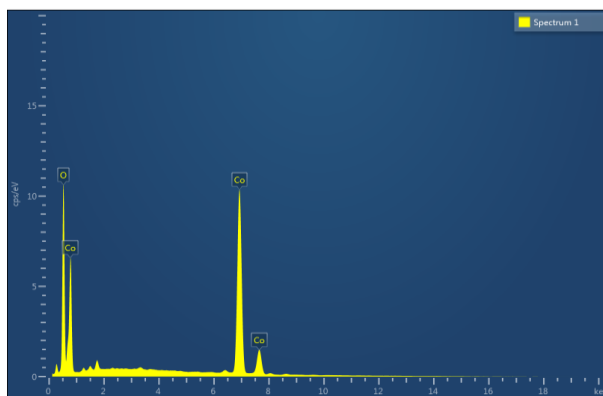
Fig.3.123: EDX spectrum of Fresh Co$_3$O$_4$
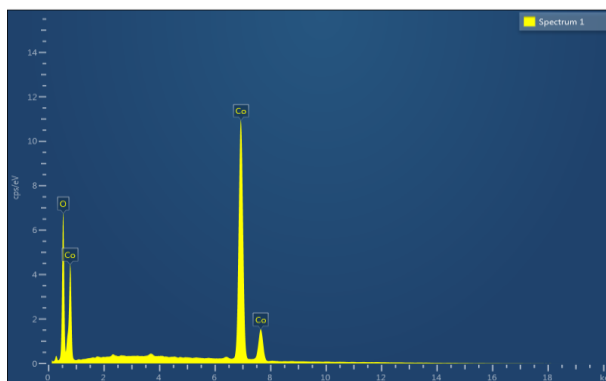
Fig. 3.124: EDX spectrum of Recycled Co$_3$O$_4$ ([IC]: 60mg/L [Co$_3$O$_4$]: 1800mg/L)

Microwave, Photo and Sono Activated Advanced Oxidation Processes and their Variations for the Decontamination of Water from Toxic Chemical Pollutants

229

Table 3.11: Comparative EDX data of Co_3O_4 before and after use

[IC]	[Co$_3$O$_4$]	Wt% O		Wt% Co		Atomic% O		Atomic% Co	
		Before	After	Before	After	Before	After	Before	After
200 mg/L	1000mg/L	23.44	16.32	76.56	83.68	53.01	41.81	46.99	58.19

3.5.2.13 Determination of COD

The efficiency of the MW/Co$_3$O$_4$ for the mineralisation of IC is tested by measuring the COD at different times of reaction (Fig.3.125). The COD is reduced on decolourisation. The decrease in COD continues with MW irradiation for some more time and is stabilises thereafter.
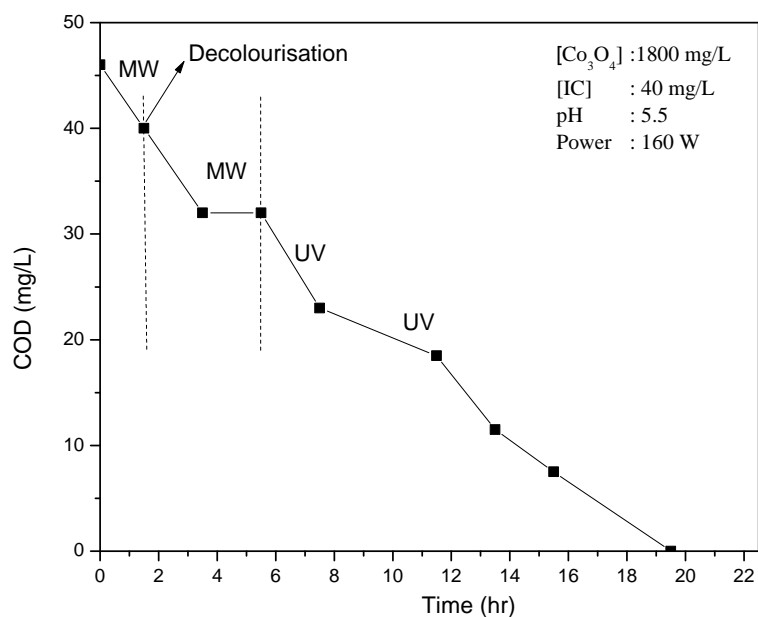
Fig. 3.125: COD of the reaction mixture at different time intervals during MW/Co$_3$O$_4$ degradation of IC

Some of the intermediates formed during the degradation/ decolourisation may be stable and hence their removal becomes difficult. In such cases the MW irradiation may not be fully effective to make the water reusable. The intermediates formed during decolourisation also have to be

degraded and eventually converted to harmless products such as CO_2, H_2O and salts.

Once the COD is stabilised (3-5hr) and further MW irradiation does not result in any decrease in COD the system is subjected to UV irradiation. This results in steep decrease in the COD thereby suggesting that the intermediates get degraded and mineralised faster under UV. Eventually the COD becomes 'zero' after ~ 20hrs (i.e 4hr MW followed by ~15hr UV). Hence MW/UV is an effective combination for the mineralisation of IC in presence of Co_3O_4 as catalyst.

3.6   General Mechanism of the MW catalytic process

The degradation of the organics under MW irradiation is often attributed to the volumetric heating of the substrate and the more effective mixing due to the micro stirring caused by the absorption of MW energy by the molecules. The high temperature generated instantly can also accelerate the formation of free radicals, which are known to enhance the degradation of organic pollutants under AOPs.

The mechanism of various processes investigated in this chapter is discussed in detail in the respective sections/subsections. The general mechanism of MW induced catalytic degradation of organics can be summarised as follows [166]:

In chemical reactions under thermal conditions, the reactants are activated by heat. Increase in temperature induces an increment of kinetic energy in molecules which results in increased molecular collision. Among these collisions only few have sufficient energy and the necessary

orientation to participate in effective reaction and formation of the product. Heating causes an isotropic excitation of the molecules which make the collisions inefficient. However, anisotropic excitation which modifies the energy distribution in molecules can enhance the rate of collision and hence the rate of reaction. At identical temperatures of reaction medium (i.e. same average value of energy distribution), distribution of kinetic energies of molecules can be different. Hence different reaction rates could be observed. Specific or non-thermal or 'athermal' effect is rationally based on this premise. Under MW irradiation, MnO_2 or Co_3O_4 which are strong MW absorbents can absorb and/or transfer MW energy. This results in the creation of large number of hotspots which can enhance the degradation of molecules [172]. The electrophilic oxygen ions (O_2^-, O^-, O^{2-} etc.) that are derived from the lattice oxygen of MnO_2 or Co_3O_4 are highly reactive and forms ROS such as $^{\cdot}OH$, $HO_2^{\cdot}$, H_2O_2 etc. as explained earlier [173, 174]. They interact with IC and degrade it in different stages with multiple intermediates. Eventually these intermediates also interact with powerful oxidants and get mineralised. The vacancy of oxygen in the lattice will be replenished by molecular oxygen from the solution.

The reaction may be summarised as follows.

$$MnO_2 + MW \rightarrow MnO_2 \ (O_2^-, O^-, O_2{-} \ etc.) \ ....(56)$$

$$O_2^- + H+ \ \rightarrow HO_2^{\cdot} ....(57)$$

$$O^- + H+ \ \rightarrow HO. \ ....(58)$$

$$2^{\cdot}OH \rightarrow H_2O_2 ....(59)$$

$$HO_2^{\cdot} + HO_2^{\cdot} \rightarrow H_2O_2 + O_2 ....(60)$$

$$^{\cdot}OH + H_2O_2 \rightarrow HO_2^{\cdot} + H_2O \ ....(61)$$
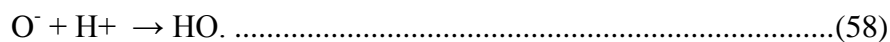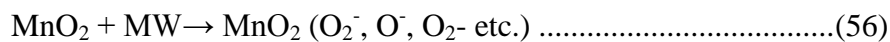
These and many other reactive ROS will interact with IC on the surface as well as in the bulk resulting in degradation and eventual mineralisation.

$$IC + ROS \rightarrow Intermediates \xrightarrow{ROS} CO_2 + H_2O \quad ....(62)$$
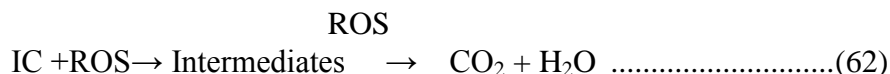
Multitude of other interactions taking place in presence of additives which influence the degradation and mineralisation are already discussed in respective sections.

The reaction is very slow in presence of 'MW only' without catalyst, probably because the energy of the MW radiation is quite low (10^{-3} eV) compared to the energy of the chemical bonds. Hence MW alone cannot successfully initiate a degradation reaction while the presence of a catalyst like MnO_2 or Co_3O_4 can initiate and accelerate the reaction. The degradation is more in the case of MW/MnO_2 compared to CH/MnO_2 suggesting that it is not only the thermal effect that is responsible for the degradation, though its contribution cannot be ruled out.

Various Reactive Oxygen Species (ROS) such as H_2O_2, $HO_2\cdot$, $\cdot OH$ etc formed from the lattice, surface and dissolved oxygen as explained earlier, can interact with IC leading to its degradation and eventual mineralization as in the case of many AOPs (eqn. 62).

Major intermediates formed during the degradation of IC are also identified as shown in Section 3.3.3.16.

Microwave, Photo and Sono Activated Advanced Oxidation Processes and their Variations for the Decontamination of Water from Toxic Chemical Pollutants

233

The formation of ˙OH radicals under MW irradiation is verified by PL spectrum measurements (Fig.3.126). The quantum of ˙OH radicals obtained is also less compared to other energy sources such as US and UV.
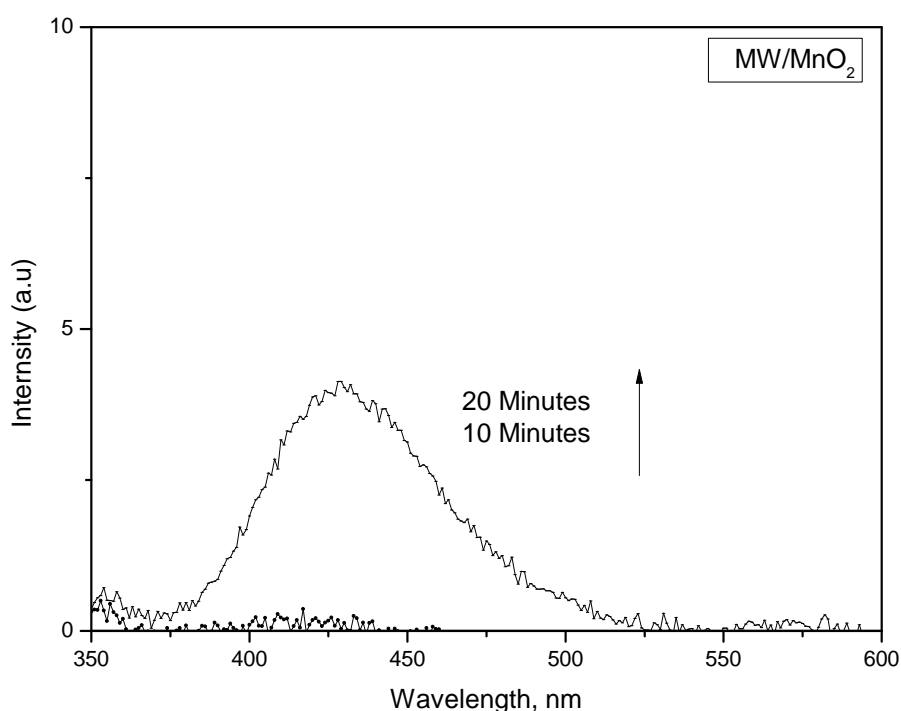
Fig.3.126: PL spectral changes during MW irradiation of MnO_2/Terephthalic acid/NaOH

Hence, the concentration of ˙OH radicals is not adequate to effect the mineralisation of the dye and its intermediates. The MW activation of the catalyst also may not be powerful enough to mediate reactions leading to mineralisation. Many earlier experiments have shown that the combination of UV with MW enhances ˙OH radical generation by over 2 fold. The mechanism of UV initiated photocatalytic degradation and

mineralisation of organics is discussed in Chapter 4. MW does not adversely affect the photoactivity of the oxide because in a heterogeneous suspension, the MW is primarily absorbed by the aqueous medium and the solid particles get only secondary effect. The medium can attenuate any direct effect of MW on the oxides. Hence combination of MW with UV irradiation will not have any adverse effect on the efficiency of either photocatalysis or MW catalysis as is demonstrated in the case of MnO$_2$-TiO$_2$ catalysed MW and MW-UV degradation of IC.

The MW radiation impacts the surface as well as the bulk of the oxide material in different ways. The most important cause for the change is the magnetic field. However, in heterogeneous systems as in current case, magnetic effects are not always observed and the catalytic degradation is mostly influenced by the MW thermal effect and a non-thermal effect. Many studies correlate the thermal effect of MW radiation to the dielectric constant of the suspended material in the system. The dielectric constant reflects the ability of a material to transform electromagnetic energy of MW in to heat. However there is no correlation between dielectric constant of MnO$_2$ or Co$_3$O$_4$ and their efficiency to degrade IC. Horikoshi EDX [175] demonstrated that the induction heating of the suspended materials by the magnetic field of MW irradiation is non-existent and any increase in temperature is due to the electric field. When the material couples strongly with MW radiation field, the rise in temperature will be faster leading to more efficient generation of ROS.

Microwave, Photo and Sono Activated Advanced Oxidation Processes and their Variations for the Decontamination of Water from Toxic Chemical Pollutants

235

3.7 Summary of the comparative efficiency of MnO₂, MnO₂ - TiO₂ and Co₃O₄ for the MW mineralisation of IC

Parameters	MnO$_2$	MnO$_2$-TiO$_2$(18:1)	Co$_3$O$_4$
Optimum Loading	1800 mg/L	1800 mg/L	1800 mg/L
Optimum Concentration of IC	60 mg/L	60 mg/L	40 mg/L
Kinetics	Variable kinetics. Pseudo first order at lower concentration (up to 40mg/L) and zero order at higher (>50 mg/L) concentration L-H Mechanism	Variable kinetics. Pseudo first order at lower concentration(up to 40mg/L) and zero order at higher (>50mg/L) concentration L-H Mechanism	Variable kinetics. Pseudo first order at lower concentration (<40 mg/L)and zero order at higher (>40 mg/L) concentration L-H Mechanism
pH effect	Maximum degradation at pH 2-3 followed by slight decrease with increase in pH. Thereafter stable in the range pH 5-10.	Maximum degradation at pH 2 followed by decr ease up to 4. Thereafter stable in the range 4-10. Slight increase in degradation at pH >10	Maximum degradation at pH 2 followed by steep fall upto pH 3. Thereafter stable in the range 3-11.
H$_2$O$_2$ effect	Inhibition, which increases with concentration upto 50 mg/L. Stable degradation of IC at higher concentration of H$_2$O$_2$.	Inhibition, which increases with increase in concentration upto 20mg/L. Stabilized degradation of IC at higher concentration of H$_2$O$_2$.	Mild inhibition at lower concentration of H$_2$O$_2$. Moderate enhancement at higher concentration of H$_2$O$_2$ which increases with increase in concentration
Persulphate effect(PS)	Enhancement, increases with increase in concentration of PS. Stable degradation of IC at higher concentration of PS	Mild enhancement, which increases slowly with increase in concentration of PS. Degradation stabilises eventually.	Enhancement, increases with increase in concentration of PS. Stabilizing degradation eventually.
Activation Energy	7.7 KJ/mol (MW) 11.6 KJ/mol (CH) Activation energy is lowered by MW irradiation	Not Done. (Since the results are similar in the case of MnO$_2$ and MnO$_2$/TiO$_2$ in most cases)	14.4 KJ/mol (MW) 17.6 KJ/mol (CH) Activation energy is lowered by MW irradiation

	MnO₂	MnO₂-TiO₂	Co₃O₄
Deaeration by N₂ bubbling	Effect dependent on MnO₂ dosage. No Effect on IC degradation at high dosages(1800 mg/L) of MnO₂ Inhibition of the degradation of IC at lower dosages of MnO₂ ($\sim<100$mg/L)	Not Done. (Since the results are similar in the case of MnO₂ and MnO₂-TiO₂ in most cases)	Effect is dependent on Co₃O₄ dosage. No Effect at high dosages (1800 mg/L) of Co₃O₄. Inhibition of the degradation of IC at lower dosages ($\sim<200$mg/L)
Recycling of catalyst	22% decrease in 1st recycling and 30% decrease in 2nd recycling	Not Done. (Since the results are similar in the case of MnO₂ and MnO₂-TiO₂ in most cases)	52% decrease in 1st recycling and 60% decrease in 2nd recycling
COD decrease	Initial decrease under MW. Stabilises later on. No further decrease under MW. Complete mieralisation under (MW+UV) Eventually COD = 0	Initial decrease under MW. Stabilises thereafter. No further decrease under MW. Complete mieralisation under (MW+UV) Eventually COD = 0	Initial slow decrease. Stabilises thereafter. Slow but complete mieralisation under (MW+UV) Eventually COD = 0
Effect of Anions* (2-15 mg/L)			
i)PO₄³⁻	Inhibition	Inhibition	Mild Inhibition
ii)HCO₃⁻	Mild inhibition	Mild inhibition	No effect
iii)CO₃²⁻	Inhibition	Inhibition	No effect
iv)Cl⁻	No effect	No effect	No effect
v)CH₃COO⁻	No effect	No effect	No effect
vi)SO₄²⁻	Initial 'Mild inhibition' becomes 'no effect' at later stages of reaction	Mild inhibition to no effect	No effect
NO₃⁻	Initial 'Mild inhibition' becomes 'no effect' at later stages of reaction	Mild inhibition to no effect	No effect

*'Mild inhibition' and 'mild enhancement' are considered as 'no effect' in this table.

Microwave, Photo and Sono Activated Advanced Oxidation Processes and their Variations for the Decontamination of Water from Toxic Chemical Pollutants

237

The lack of correlation between the dielectric constant of the catalysts (MnO_2, Co_3O_4) and their MW activity indicates that the non-thermal component of MW plays an important role in the degradation of organics which can be attributed primarily to the enhancement in the reaction dynamics by non-thermal or specific effect of MW. This cannot be obtained by conventional heating. The non- thermal effect might be due to 'hot spots' on the suspended particles. The presence of such hotspots is documented by Horikoshi et al. [176]. Another consequence of the 'specific effect' or 'non-thermal' effect of MW is decrease in the activation energy for the reaction. In the present study, this is clearly established in the case of both MnO_2 and Co_3O_4 catalysts. Other non-thermal effect include additional formation of charge carriers on the catalyst and formation of additional trap sites that can prolong the lifetime of charge carriers through diminished re-combination.

3.8 Conclusions

The results presented in this chapter illustrate that the MnO_2, MnO_2-TiO_2 and Co_3O_4 are efficient MW catalysts for the degradation/ decolourisation of the recalcitrant dye pollutant Indigo Carmine in water. The degradation proceeds through many intermediates some of which are identified by LC-MS. MW is unable to mineralise the intermediates efficiently. However combination of MW with UV irradiation in sequence can mineralise the intermediates faster thereby achieving COD of 'zero'. H_2O_2 inhibits the MW/MnO_2 degradation while PS enhances it. However in the case of Co_3O_4/MW degradation of IC, H_2O_2 also is a mild

enhancer. The degradation of IC follows variable kinetics in all cases ranging from pseudo first order at lower concentrations to zero order or even negative order at higher concentrations. The reaction is facile even in deoxygenated system thereby suggesting the possibility of participation of lattice O_2 or strongly bound surface oxygen from MnO_2/Co_3O_4 in the degradation. The possibility is conclusively established with the help of appropriately designed experiments and EDX data. The activity of both MnO_2 and Co_3O_4 diminishes progressively with every recycling. Various anions/salts likely to be present in water do not influence the degradation of the dye significantly at the concentration at which they are present in water. PO_4^{3-} is the only clear inhibitor at all concentration while the effect of CO_3^{2-} and HCO_3^{-} as inhibitors is concentration dependent. Organic acids such as oxalic acid and acetic acid are relatively more stable intermediates formed during the degradation of IC. Eventually they also get mineralised.

Possible mechanisms for the observations made during the study are proposed and discussed. The results demonstrate the potential of the combination catalyst MnO_2- TiO_2 in the hybrid process MW-UV (in sequence) for the total removal of the dye pollutant IC from water.

This is the first instance of the application of MnO_2, MnO_2-TiO_2 and Co_3O_4 mediated MW and its variations for the removal of the recalcitrant dye pollutant IC from water.

.....ഇരു.....

Microwave, Photo and Sono Activated Advanced Oxidation Processes and their Variations for the Decontamination of Water from Toxic Chemical Pollutants

239

Photocatalysis mediated by MnO₂, MnO₂-TiO₂ and Co₃O₄ for the degradation of Indigo Carmine in water

Photocatalysis mediated by MnO_2, MnO_2-TiO_2 and Co_3O_4 for the degradation of Indigo Carmine in water

</div>

4.1 Introduction

Semiconductor mediated heterogeneous photocatalysis is an efficient AOP for the degradation of various organic pollutants in water. In this context, one of the least investigated semiconductor oxides in AOPs, in particular photocatalysis, is MnO_2, in spite of its excellent semiconductivity, porosity and mixed-valent properties which make it a potential catalyst for many applications. Considering these, inspired by the excellent MW catalytic properties, as reported in Chapter 3, the application of MnO_2 as photocatalyst for the removal of recalcitrant toxic materials is examined. One of the widely used special application dyes, i.e. Indigo Carmine (IC) is used as the test pollutant.

Microwave, Photo and Sono Activated Advanced Oxidation Processes and their Variations for the Decontamination of Water from Toxic Chemical Pollutants

241

4.2 Experimental details

4.2.1 Materials used

The materials used, relevant details and their characteristics are the same as provided in Chapter 3 Section 3.2.1.

4.2.2 Analytical procedures

Sampling and analysis were performed as explained in Chapter 3 Section 3.2.3.

4.2.3 Photocatalytic experimental set up

The experiments were performed using aqueous solutions of IC of desired concentration. Simple glass beakers (250 mL) were used as reactors in routine experiments. Specified quantity of the catalyst was suspended in the solution taken in the beakers. The beakers were placed in a water bath through which water at the required temperature ($29 \pm 1^{\circ}$C), unless indicated otherwise, is circulated. The reaction suspension was continuously mixed using a magnetic stirrer. The suspension was illuminated with a 400W high-pressure mercury lamp mounted above the system (Fig.4.1a).
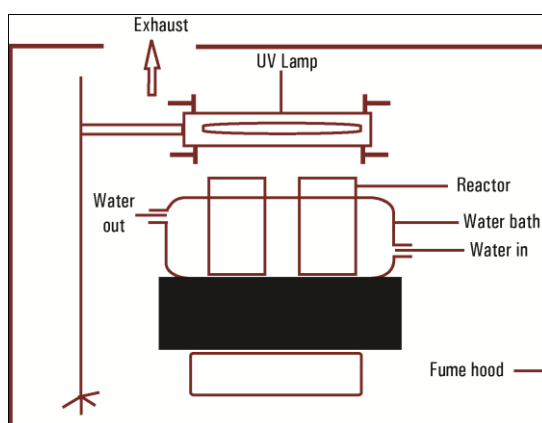
Fig.4.1a: Schematic diagram of the photocatalytic experimental set up

For specific experiments, specially designed jacketed reactor (Fig 4.1b) was used. This reactor has provision for circulation of water at the desired temperature in the jacket and to bubble gas through the suspension.
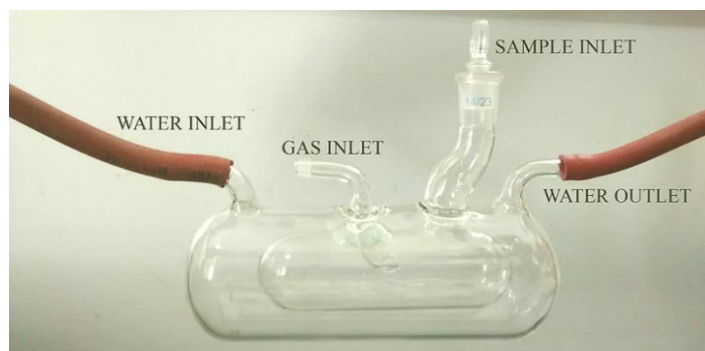
Fig. 4.1b: Special photoreactor used in the study

Samples were analysed at various intervals as explained under analytical procedure in Section 3.2.3.

4.3   Results and discussion

4.3.1 Preliminary results

Preliminary investigations on the photocatalytic degradation of IC showed that no significant degradation took place in the absence of catalyst and light suggesting that both catalyst and UV are essential to effect reasonable degradation. There is significant decrease in the concentration of the dye in presence of MnO_2 even without irradiation. However, the decrease in concentration remains fairly steady with time. This indicates that the disappearance of the dye is not due to degradation and may be due to adsorption on MnO_2. Once the surface is saturated under the experimental conditions, no further decrease is noticed. Moderate degradation of the dye takes place under UV irradiation, even in

the absence of the catalyst. This degradation increases with time of exposure to the radiation. When the MnO_2/dye suspension is exposed to UV irradiation, the concentration decreases rapidly resulting in decolourization. Preliminary results are presented in Fig. 4.2.
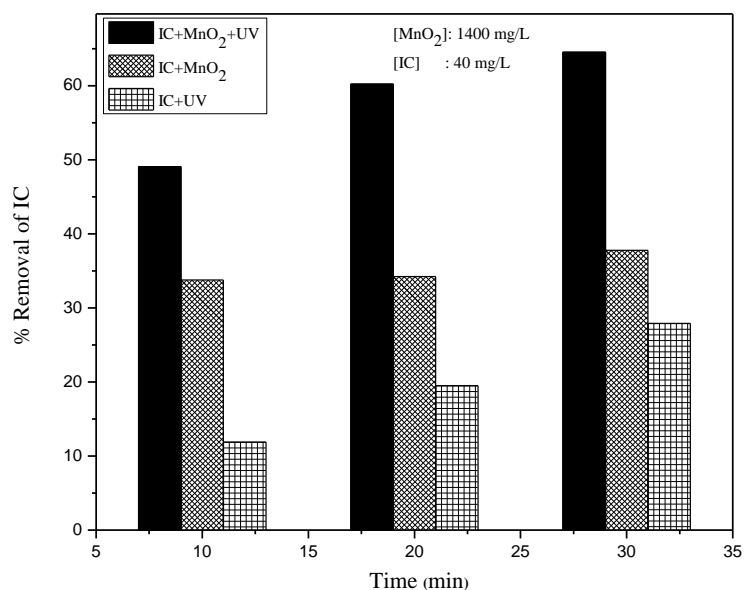
Fig. 4.2: Comparative 'decrease in concentration' of IC in presence of MnO_2 under various conditions

The decrease in concentration in presence of MnO_2 in the absence of UV irradiation is simple adsorption, i.e, transfer of the pollutant from one phase to another. Hence this cannot be used as an effective method for the removal of IC from water.

4.3.2 Effect of catalyst dosage

The catalyst dosage for optimum degradation of IC is experimentally verified in the range of 600 to 1800 mg/L and the results are shown in Fig.4.3.
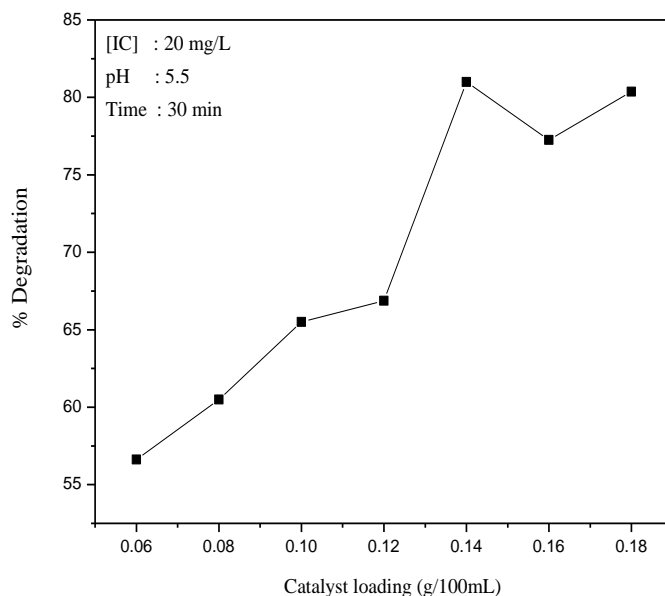
Fig.4.3: Effect of MnO_2 dosage on the photocatalytic degradation of IC.

The degradation increases with increase in catalyst loading and reaches an optimum at 0.14 g/100 mL (1400mg/L) under the reaction conditions. Possible reasons for the increase in degradation with increase in catalyst dosage under MW radiation are explained in Chapter 3. In the case of photocatalysis, the enhanced degradation at higher catalyst loadings can be attributed to the increased number of adsorption and interaction sites for the IC and/or the intermediates and more effective harvesting of light. This leads to the formation of higher number of reactive hydroxyl and other radicals and their interactions with the pollutant. Any further increase in catalyst concentration beyond the optimum will only result in scattering and reduced passage of light through the suspension medium. Another reason may be the aggregation of catalyst particles causing decrease in the number of available active surface sites. Beyond a particular loading of the catalyst, the particles

cannot be fully and effectively suspended in a particular reactor which also leads to suboptimal penetration of light and reduced adsorption of the substrate on the surface. At higher concentration of catalyst, the effective working volume of the suspension is relatively less and this will affect the efficiency of penetration of light through the dense medium. It is also possible that at higher loading, part of the originally activated MnO_2 is deactivated through collision with ground state catalyst according to the following equation [177].

$$MO^* + MO \longrightarrow MO^{\#} + MO \dots\dots\dots\dots\dots\dots\dots\dots\dots(63)$$

(MO represents MnO_2, MO* and $MO^{\#}$ are its activated and deactivated forms respectively).

In the case of MnO_2 which is a good adsorber/absorber and reservoir for O_2, increased dosage provides more photogenerated reactive oxygen species (ROS). From binding energy calculations Cao and Suib [147] suggested that MnO_2 is a mixed-valent system consisting of Mn^{4+} and Mn^{3+}. The multiple oxidation states enable them to function as good electron donors/acceptors and hence as oxidation-reduction catalysts [178]. This property also favours increased photocatalytic activity with increase in catalyst dosage. This naturally makes them amenable to facile regeneration after use by replenishing the depleted oxygen. Surface and lattice oxygen species in MnO_2 are known to take part in the catalytic oxidation process. Photolysis of MnO_2 is reported to result in five-fold increase in the surface oxygen, either by migration of oxygen to the surface or by migration of Mn to the bulk or both [147]. During the photocatalytic reaction, surface oxygen is consumed and bulk oxygen

moves to the surface. Hence, the more the catalyst dosage, the more the availability of reactive oxygen and consequently better the degradation. This can continue until other reaction parameters such as the size, shape and geometry of the reaction assembly are also appropriate to facilitate various processes involved in the degradation. Hence, for each reactor configuration the optimization of catalyst dosage has to be made separately. In the present case the optimum loading of MnO_2 is 0.14 g/100 mL. Hence all further studies were carried out with this loading.

4.3.3 Effect of concentration of IC

The percentage degradation decreases as the concentration of IC increases (Fig.4.4). In contrast, the rate of removal increases steadily with increase in the initial concentration of IC upto 40 mg/L and stabilizes thereafter (Fig.4.5).
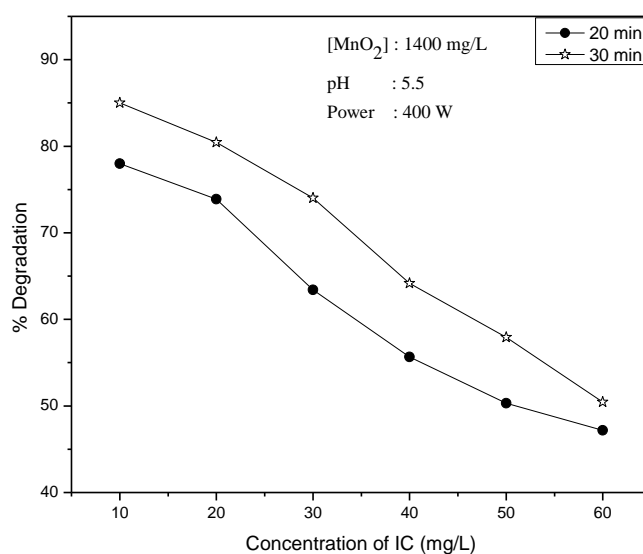
Fig. 4.4: Effect of concentration on the UV/MnO_2 degradation of IC

Microwave, Photo and Sono Activated Advanced Oxidation Processes and their Variations for the Decontamination of Water from Toxic Chemical Pollutants

247
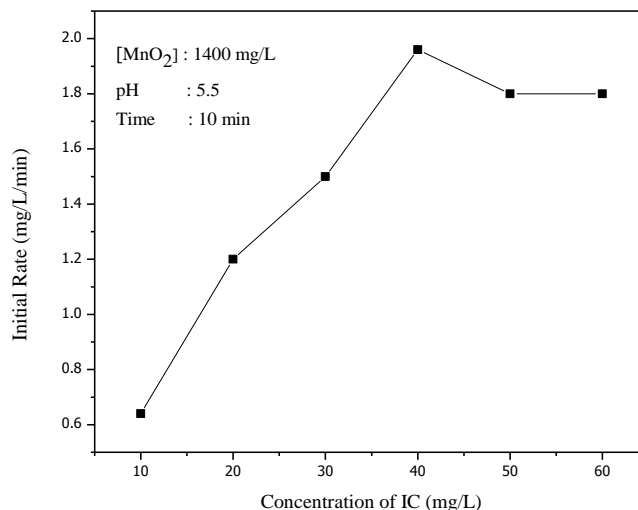
Fig. 4.5: Rate of UV/MnO$_2$ degradation of IC at various concentrations

The increase in rate of photocatalytic degradation with increase in concentration up to 40 mg/L may be due to increase in adsorption of IC on MnO$_2$ which will continue until the surface is fully covered and all the active sites are occupied. Further, at higher concentration, there will be more IC molecules available in the bulk as well as in the proximity of the surface which can also interact with the surface-generated active free radicals and ROS such as $^{\cdot}$OH and H$_2$O$_2$. At higher concentration beyond the optimum as above, at least a part of the irradiating UV light may be blocked and/or absorbed by IC and the intermediates formed from it thereby reducing the photons available for catalyst activation. Another reason may be that major portion of the reaction occurs in the region (reaction zone) close to the irradiated side where the irradiation intensity is much higher than the other side. The retardation in the penetration of light at longer distance from the light source and resultant decrease in its path length, also lead to decreased degradation [179]. As the initial

concentration of IC increases, the requirement of catalyst surface needed for maintaining corresponding rate of degradation also increases. Since illumination intensity and catalyst concentration are maintained constant, the relative number of ROS available for interacting with the IC is also presumably decreased leading to stabilized/ decreased rate of degradation. Thus it is clear that higher concentration of the dye affects the light absorption and the effectiveness of activation of the surface sites.

Once the concentration of the substrate is enough to interact with all the optimum available ROS and/or other reactive free radicals, any further increase cannot result in increased reaction and the IC removal becomes independent of concentration. It is also possible that at higher substrate concentration, some of the reaction intermediates formed at accelerated rate may get adsorbed onto the surface or remain in the bulk for relatively longer period resulting in less frequent interaction between fresh IC molecules and the ROS. Complete domination of the reaction system by the reactant/intermediates/products can also result in decrease in the quantum of light reaching the surface, resulting in suppression of the generation of surface-initiated reactive free radicals. However, at any point of time, there will be an optimum for the number of substrate molecules that can interact with the reactive free radicals generated by the surface. This optimum will depend on a number of parameters such as initial concentration of the substrate, intensity of illumination, wavelength of light, mass and type of photocatalyst, type and geometry of photoreactor etc. Consequently, any measurements and calculations made, apply only to the specific reaction conditions and cannot be generalized.

Microwave, Photo and Sono Activated Advanced Oxidation Processes and their
Variations for the Decontamination of Water from Toxic Chemical Pollutants

249

Since the degradation is accelerated by both catalyst and light, the negative effect of increasing concentration implies that at higher concentration, the dye is inhibiting the action of catalyst and/or light. At higher concentration there will be better adsorption of the dye on the surface of the catalyst. This will inhibit the direct absorption of light by the catalyst thereby affecting its ability to generate free radicals and reactive oxygen species. This results in deceleration of continued significant degradation, and consequently the adsorbed dye will not degrade easily and/or leave the surface sites. This prevents the adsorption of new molecules. Hence the degradation is inhibited at higher concentrations of the dye.

Evaluation of the kinetics of heterogeneous AOPs based on modified L-H mechanism is discussed in detail in Section 3.3.3.2 of Chapter 3. Photocatalytic processes generally follow pseudo first order kinetics which is dependent on the concentration range of the substrate. The order of the reaction decreases with increase in concentration and eventually reaches 'zero order' or even negative order. Such variation in kinetics is evident in this case also as seen from the 'rate vs concentration' plot in Fig.4.5. The rate becomes independent of the concentration above 40 mg/L.

The pseudo first order kinetics is verified by the inverse plot ($1/r_0$ vs $1/C_0$), as explained in Section 3.3.3.2 of Chapter 3. The plot in Fig.4.6 gives straight line thereby confirming the first order kinetics in the concentration range 10 to 40 mg/L. Further the logarithmic plot ln C_0/C vs t (Fig.4.7) also gives straight line in this concentration range. Thus it is confirmed that the photocatalytic degradation of IC in presence of MnO_2

catalyst follows pseudo first order kinetics at lower concentration range of the dye.
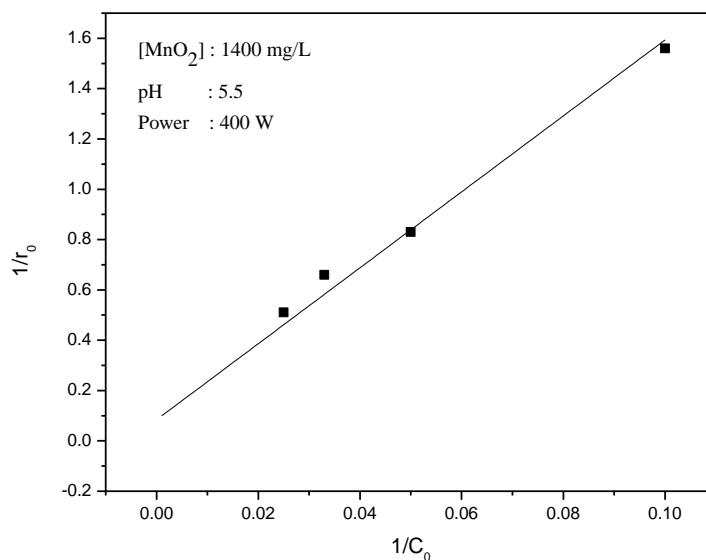
Fig. 4.6: Reciprocal plot of $1/r_0$ vs $1/C_0$ for various concentrations of IC.
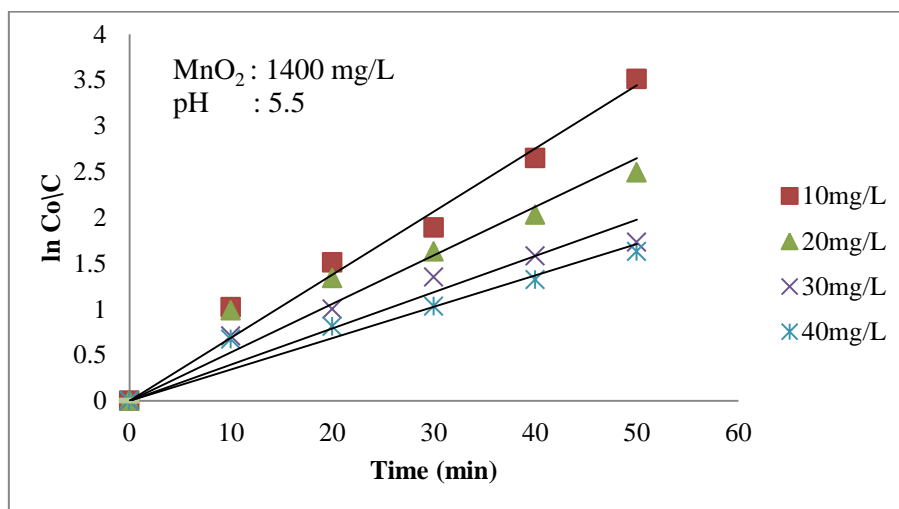
Fig. 4.7: Logarithmic plot for the UV/MnO₂ degradation of IC

Rationalization for this kinetics may be seen in the Langmuir-Hinshelwood model, modified to accommodate reactions occurring at solid-liquid interface [180, 181]. This model underlines the key role of the adsorption constant K on the kinetics, assuming that the adsorption-desorption kinetics is faster than the photochemical reaction. The rate of unimolecular surface reaction is proportional to the surface coverage, assuming that, compared to the products, the reactant is more strongly adsorbed on the semiconductor oxide catalyst particles [182].

The slope of each line in Fig.4.7 is the apparent rate constant of degradation k_{app} at the corresponding concentration of the dye. The results are tabulated in Table.4.1.

Table 4.1: Pseudo first order rate constants for the degradation of IC under MnO_2/UV.

Experiment	MnO_2 (g/L)	IC (mg/L)	$k_{app}(min^{-1})$
1	1.8	10	0.060
2	1.8	20	0.045
3	1.8	30	0.032
4	1.8	40	0.029

The value of k_{app} decreases as the concentration of IC is increased. This is similar to the observation made in the case of MW/MnO_2 degradation of IC (Section 3.3.3.2 of Chapter 3.). Hence the explanation for the variation in the rate constant based on the decrease in the relative fraction of interacting substrate holds good in this case as well.

Since MnO_2 is a very powerful adsorbent compared to common semiconductor oxides such as ZnO and TiO_2 (adsorption is ~ 11% and ~

8% in the case of ZnO and TiO$_2$ respectively while it is ~ 32% in the case of MnO$_2$, as determined experimentally), the kinetics of the degradation of IC on MnO$_2$ may not necessarily follow pseudo first order kinetics at all concentrations. In the case of highly adsorbing particles, there will be competition between the solvent and the solute molecules for adsorption sites and hence the interfacial adsorption-desorption equilibrium of the solute will be a better parameter to be considered, i.e.

$$\text{Solvent (ads.)} + \text{Solute (bulk)} \leftrightarrow \text{Solute (ads.)} + \text{Solvent (bulk)} \dots\dots (64)$$

In the case of very dilute aqueous solution of pollutants, with a strong adsorbent like MnO$_2$ there will be severe competition between the pollutant and water for adsorption sites and this can complicate the kinetics of adsorption of IC and its degradation. This implies that the basic assumptions implicit in the application of L-H mechanism and associated kinetic analysis may not be strictly applicable at all concentrations of IC with MnO$_2$ as the catalyst. These assumptions are [183]: i) The reaction of adsorbed species is the rate-determining step ii) Fractional surface coverage (θ_A) of the reactant species is the more appropriate concentration parameter to be applied in rate laws, iii) $\theta_A \rightarrow 1$ for saturation coverage corresponding to a monolayer of adsorbate on the surface and iv) Langmuir adsorption isotherm type equation represents the relationship between θ_A and the activity. Cunningham and Sayyed [183], also reported that the above assumptions may not always hold good in the case of aqueous solutions containing a photodegradable solute (in this case IC) at low concentrations. In view of these factors, the possibility of higher order kinetics under different set of reaction parameters for the same reaction, i.e, photodegradation of IC on MnO$_2$, cannot be ruled out.

4.3.4 Effect of pH

The effect of pH on the photodegradation of IC in presence of MnO_2 is investigated and the results are given in Fig. 4.8.
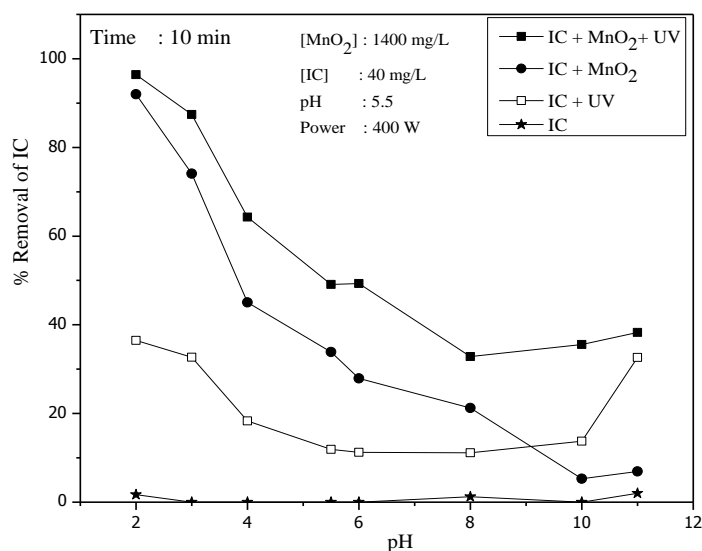
Fig. 4.8: Effect of pH on the removal of IC under various conditions

The maximum degradation (~97%) of IC in presence of MnO_2 occurs under extreme acidic conditions, which decreases steadily with increase in pH up to 10 and increases slightly thereafter. The very fast decolourization in presence of MnO_2 under acidic pH, in the absence of UV irradiation shows that the simple adsorption of IC on MnO_2 also is facilitated at acidic pH. Similar pH effect on the adsorption of IC on TiO_2 catalyst has been reported by Barka et al. [184]. This is attributed to the influence of pH on the surface state of the catalyst and ionization state of the dye. IC is a weak acid. It will be mostly in the basic anionic form or neutral electric form $\varphi\text{-}SO_3H$ with electrostatic attraction between the surface and the dye. Hence adsorption is strong in the acidic range. At pH

< PZC of MnO_2 (~ 4.7), the surface is positively charged and this will facilitate the adsorption and/or oxidation of the dye.

When the pH > PZC of MnO_2 the catalyst surface is negatively charged. Hence the adsorption is less due to the electrostatic repulsion between the negatively charged surface and φ-SO_3^-. Consequently the degradation also is less. The very fast decolourization and decrease in the concentration of IC in the pH range 2-3 can be primarily due to strong adsorption of IC on positively charged surface below the PZC of MnO_2 and consequent degradation facilitated by light.

The pH effect on the photocatalytic efficiency of a highly adsorbing and reactive oxide such as MnO_2 may not be often fully consistent quantitatively because it depends on the complex interplay of many factors, i.e. chemistry of the substrate and the surface, extent and mode of adsorption (of IC as well as the numerous intermediates), concentration and type of interactions of reactive free radicals such as ˙OH etc. However, the qualitative trend in pH effect will be consistent. The adsorption of the substrates is more in the acidic range while the concentration of the ˙OH radical is more in the alkaline region due to higher concentration of OH^- ions. Thus the effect of pH on these two factors, i.e. adsorption of substrate on the catalyst and concentration of reactive ˙OH radicals, which are important for the degradation of IC, is different and opposite. As a consequence, the combined net effect need not necessarily be exactly the same quantitatively at any pH at different times. Hence precise correlation of the effect of pH on the adsorption or degradation of IC with the PZC of MnO_2 is also not fully applicable. Lack

Microwave, Photo and Sono Activated Advanced Oxidation Processes and their Variations for the Decontamination of Water from Toxic Chemical Pollutants

255

of direct correlation between the PZC and the adsorption/degradation rate can also be due to the fact that the PZC itself depends on a number of factors including the size and nature of dispersion of the particles, chemistry of substrates and the intermediates and the type of catalyst itself.

4.3.5 Formation of H_2O_2

H_2O_2 is invariably formed in almost all AOPs as a by-product. In this case of photocatalytic degradation of IC, also, the formation of H_2O_2 is verified. Concentration of H_2O_2 increases and reaches an optimum and then it decreases (Fig.4.9). Since the measurement of H_2O_2 is difficult when the coloured dye is still present in the system (due to analytical constraints), the concentration of H_2O_2 is determined immediately on decolourisation. Thereafter, UV irradiation is still continued for some more time and the H_2O_2 is measured periodically. The results are shown in Fig.4.9.
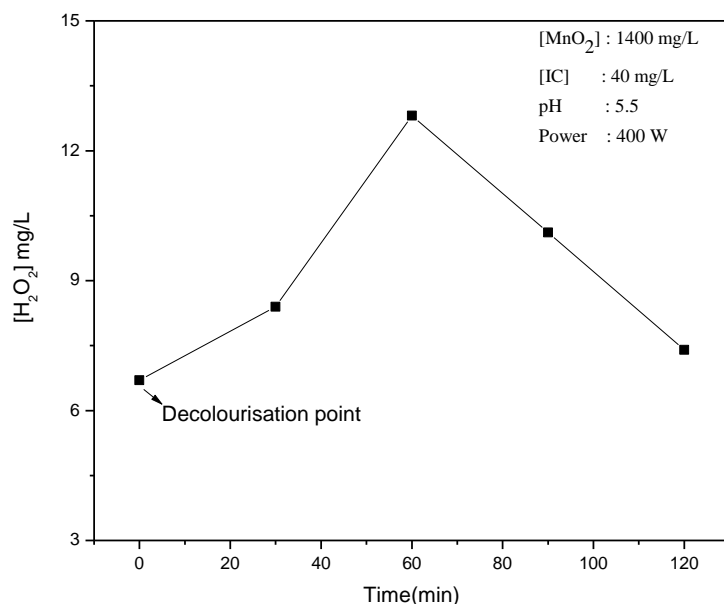
Fig. 4.9: Variation in the concentration of insitu formed H_2O_2 with time.

Since the degradation of the insitu formed colourless intermediates will be continuing under irradiation the concentration of H_2O_2 also would have increased or at least stabilised when the degradation of the organics is completed. However in this case, the concentration of H_2O_2 reaches a peak after 60 minutes and decreases thereafter. This is similar to the phenomenon of oscillation in the concentration of H_2O_2 observed under MnO_2/MW reported in Chapter 3 Section 3.3.3.8 as well as in many other AOPs [112].

As a result of concurrent formation and decomposition of H_2O_2, (which causes the oscillation) the net concentration of H_2O_2 remains relatively lower when compared to the degradation of the dye [112] Eventually the concentration of H_2O_2 may level off or decrease and may increase again (oscillation).

4.3.6 Effect of oxidants

4.3.6.1 Effect of added H_2O_2

H_2O_2, which is concurrently formed in many photocatalytic processes is a powerful oxidant and has been widely investigated for its potential to enhance the mineralization of organic water pollutants. H_2O_2 is well known as an oxidant in many AOPs, capable of enhancing the degradation of pollutants. It is also reported to be an inhibitor [156]. The dual function is attributed to the ability of H_2O_2 to be an electron donor as well as electron acceptor. In this context, the effect of externally added H_2O_2 at different concentrations on the photocatalytic decolourisation of IC is tested. The degradation of IC is inhibited at lower concentrations of H_2O_2 i.e <10 mg/L in the presence of the catalyst (Fig.4.10). Even in the

Microwave, Photo and Sono Activated Advanced Oxidation Processes and their Variations for the Decontamination of Water from Toxic Chemical Pollutants

257

absence of UV irradiation, the removal of IC by adsorption on MnO_2, is inhibited in presence of H_2O_2. This is explained as due to the competitive adsorption of H_2O_2 and IC on MnO_2 resulting in decreased adsorption of the latter. At higher concentration (> 20 mg/L), the 'inhibited' degradation is mildly enhanced and is then stabilised. In any case, the net effect of H_2O_2 on the degradation is 'mild inhibition'. However in the absence of MnO_2, the photo degradation of IC increases in presence of H_2O_2, but is stabilised at higher concentrations. The effect of reaction time on the degradation of IC in presence of H_2O_2 is studied and the results are presented in Fig.4.11. The degree of inhibition remains the same irrespective of the concentration of H_2O_2 at different reaction times, indicating that the decreasing concentration of IC with time does not influence the effect of H_2O_2.
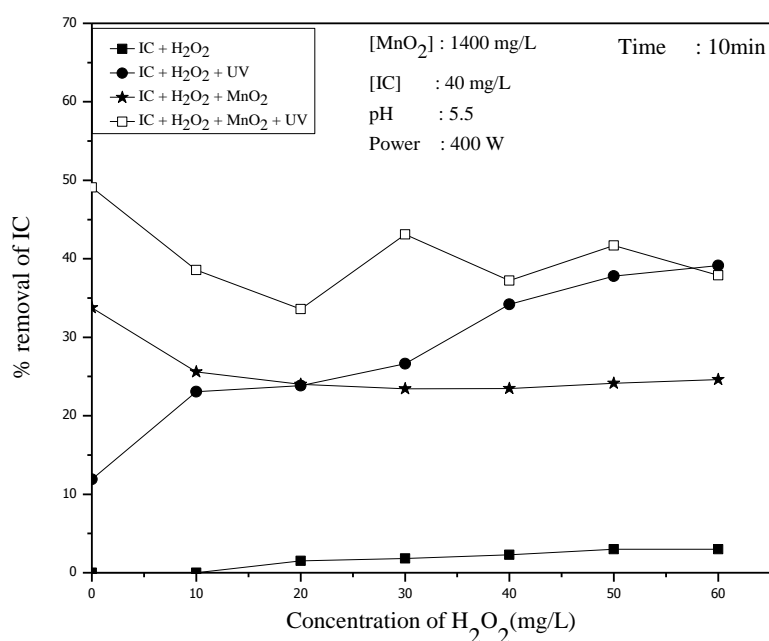
Fig. 4.10: Effect of H_2O_2 on the removal of IC under various reaction conditions
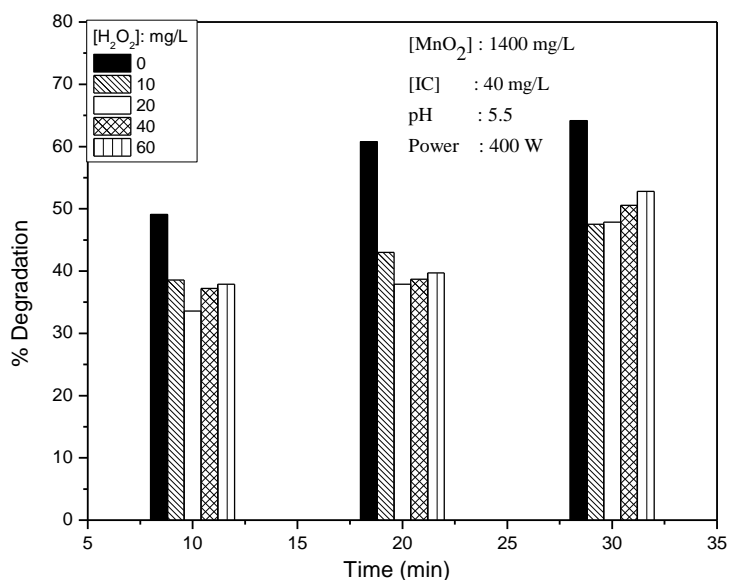
Fig. 4.11: Effect of added H_2O_2 on the degradation of IC at various reaction times

The effect of H_2O_2 on the MnO₂/UV degradation of IC is further verified by addition of H_2O_2 in-between to a reaction in progress. Results are shown in Fig 4.12. Every extra addition of H_2O_2 (20 min and 40 min) decreases the % degradation of IC. However, the inhibition is much less after the second addition (after 40 min) compared to that after the first addition (after 20min). The qualitative degradation profile of IC in the presence of 'in-between' added H_2O_2 becomes eventually comparable to that in which H_2O_2 is added initially.
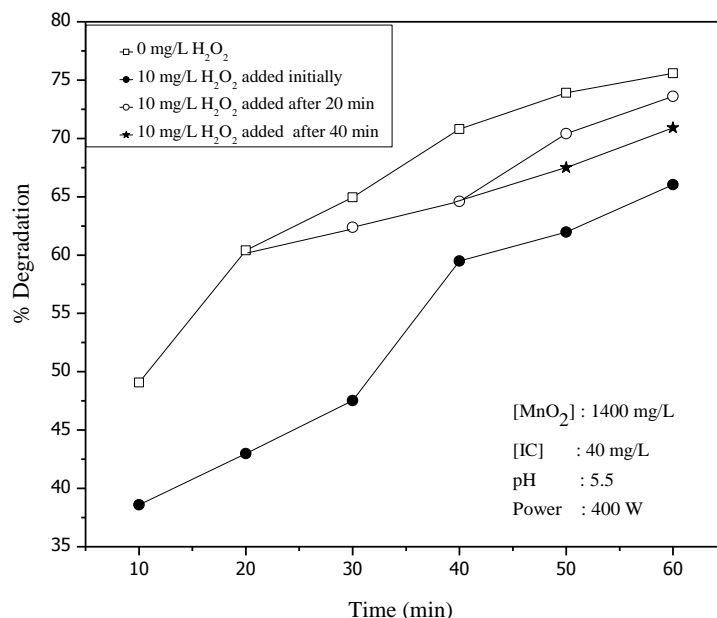
Fig. 4.12: Effect of initial and in-between addition of H_2O_2 on the UV/MnO$_2$ degradation of IC.

The concurrent formation and decomposition of H_2O_2 (resulting in the formation and consumption of $\cdot$OH) as well as various other complex free radical interactions result in decreased availability of ROS for interaction with IC. This leads to a decrease in degradation of IC. The decomposition of H_2O_2 results in the formation of reactive $\cdot$OH radicals. However, at higher concentration of H_2O_2 (added H_2O_2), the $\cdot$OH radicals interact more frequently with the former rather than with the substrate molecules.

Various reactions leading to the concurrent formation and decomposition of H_2O_2 can be summarised as follows.

$$MnO_2 \xrightarrow{h\nu} h^+ + e^- \quad ....(65)$$
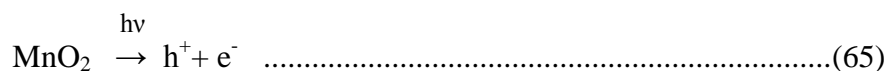
Formation of H_2O_2 from various ROS is shown below:

$$\text{}^{\bullet}OH + \text{}^{\bullet}OH \quad\quad\quad\rightarrow\quad H_2O_2 \quad\text{.. (66)}$$

$$O_2 + 2e_{cb}^{-} + 2H^{+} \quad\rightarrow\quad H_2O_2 \quad\text{.. (67)}$$

$$2H_2O + 2h_{vb}^{+} \quad\quad\rightarrow\quad H_2O_2 + 2H^{+} \quad\text{.. (68)}$$

$$O_2^{\bullet -} + H^{+} \quad\quad\quad\rightarrow\quad HO_2^{\bullet} \quad\text{... (69)}$$

$$HO_2^{\bullet} + HO_2^{\bullet} \quad\quad\rightarrow\quad H_2O_2 + O_2 \quad\text{... (70)}$$

$$O_2^{\bullet -} + HO_2^{\bullet} \quad\quad\rightarrow\quad O_2 + HO_2^{\bullet -} \quad\text{.. (71)}$$

$$HO_2^{\bullet -} + H^{+} \quad\quad\quad\rightarrow\quad H_2O_2 \quad\text{.. (72)}$$
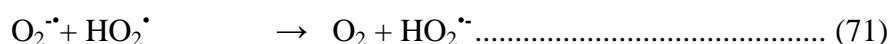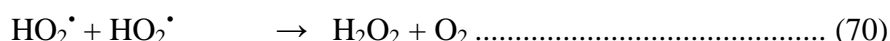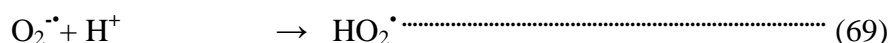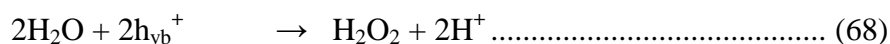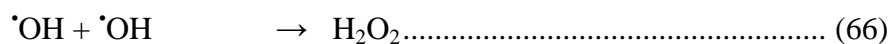
Various steps involved in the decomposition of H_2O_2 are:

$$H_2O_2 + UV \quad\quad\quad\rightarrow\quad 2\text{}^{\bullet}OH \quad\text{..(73)}$$

$$2h_{vb}^{+} + H_2O_2 \quad\quad\rightarrow\quad O_2 + 2H^{+} \quad\text{.. (74)}$$

$$2e_{cb}^{-} + 2H^{+} + H_2O_2 \rightarrow\quad 2H_2O \quad\text{.. (75)}$$

$$H_2O_2 + \text{}^{\bullet}OH \quad\quad\rightarrow\quad H_2O + HO_2^{\bullet} \quad\text{... (76)}$$

$$H_2O_2 + HO_2^{\bullet} \quad\quad\rightarrow\quad H_2O + \text{}^{\bullet}OH + O_2 \quad\text{.................................. (77)}$$

$$H_2O_2 + O_2^{\bullet -} \quad\quad\rightarrow\quad \text{}^{\bullet}OH + OH^{-} + O_2 \quad\text{.................................. (78)}$$
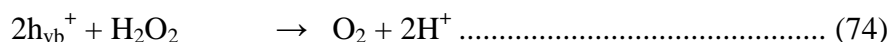
Thus, the same free radicals can contribute to the formation and decomposition of H_2O_2 depending on the conditions. At the same time, being a complex free radical system, other interactions leading to the formation and decomposition of H_2O_2 are also possible.

These interactions, together with the partial absorption of UV by H_2O_2 result in decreased degradation. When the formation as well as consumption rate of $^{\bullet}OH$ is balanced by the multitude of interactions, the degradation is stabilized or increases only very slowly. Hence the concentration of H_2O_2 in the system is critical in deciding its role as an enhancer/inhibitor/no effect.

The ROS ($^\bullet$OH, HO$_2^\bullet$, H$_2$O$_2$, etc.) will interact with IC on the surface of MnO$_2$ as well as in the bulk resulting in the degradation and mineralization of the latter as shown in reaction (79).

ROS ($^\bullet$OH, HO$_2^\bullet$etc) + IC $\rightarrow$ Intermediates + H$_2$O$_2$ $\rightarrow\rightarrow$ H$_2$O$_2$ + H$_2$O + CO$_2$ .....(79)
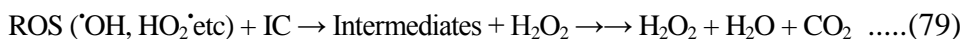
The formation of $^\bullet$OH radicals in MnO$_2$/UV system is confirmed by PL spectral studies. The increase in the fluorescence with time (Fig. 4.13) corresponds to the progressive formation of $^\bullet$OH radicals (as explained in Chapter 2 Section 2.4.4)
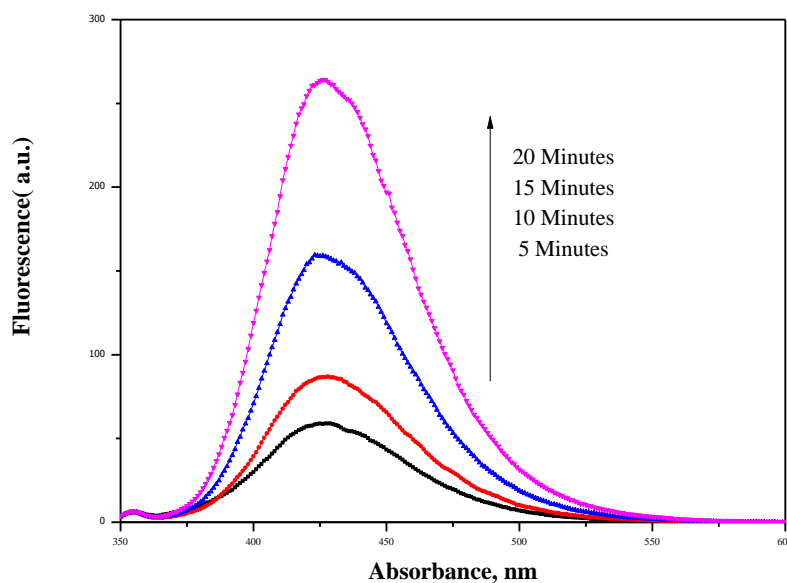
Fig. 4.13: PL spectral changes during UV irradiation of MnO$_2$/ Terephthalic acid/NaOH.

4.3.6.2 Effect of added K$_2$S$_2$O$_8$

Persulphates are powerful oxidants, especially under UV photolysis. The effect of K$_2$S$_2$O$_8$ on the photocatalytic degradation of IC is studied and the results are shown in Fig. 4.14.
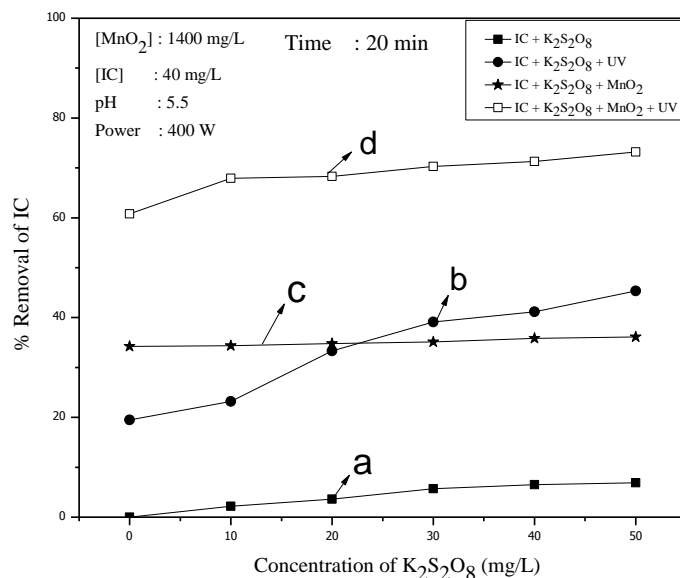
Fig. 4.14: Effect of $K_2S_2O_8$ on the removal of IC under different conditions
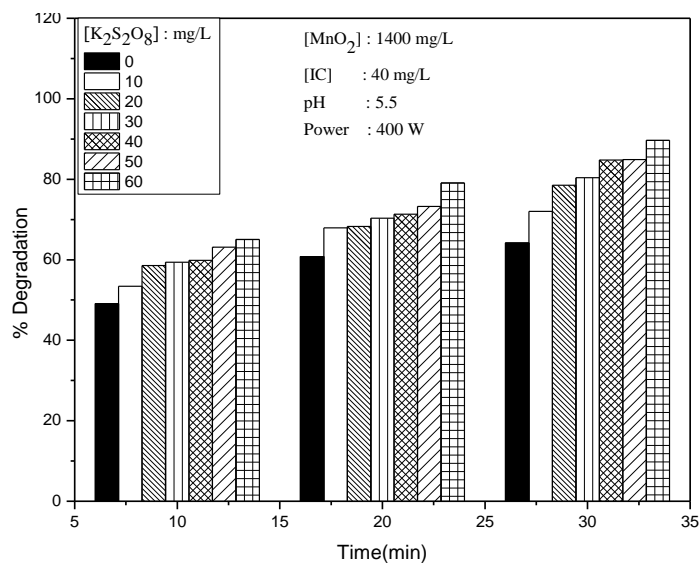
Fig. 4.15: Effect added $K_2S_2O_8$ on the UV/MnO$_2$ degradation of IC at different reaction times

PS as such causes very little change in the concentration of IC (Fig.4.14a). Irradiation by UV in presence of PS enhances the degradation

Microwave, Photo and Sono Activated Advanced Oxidation Processes and their Variations for the Decontamination of Water from Toxic Chemical Pollutants

263

of IC moderately which increases with increase in concentration of PS upto 40 mg/L and stabilizes thereafter (Fig.4.14b). The decolourization is ~35% in presence of MnO_2 with or without PS in the absence of UV irradiation (Fig.4.14c). This is due to the adsorption of IC on MnO_2 which is not affected by PS. The enhancing effect of externally added PS at different concentrations on the photocatalytic decolourisation of IC is not significant. The photodegradation of IC in presence of MnO_2 increases only mildly with increase in the concentration of PS and stabilises soon (Fig.4.14d). However there is no negative effect at higher concentration of PS. The mildly enhanced degradation in presence of PS is maintained at all concentrations (of PS) even after extended reaction times as seen in Fig.4.15. The enhancing effect is further verified by the in-between addition of PS at 20 and 40 minutes (Fig 4.16). The results show a slow enhancement in the degradation of IC with every addition of PS.
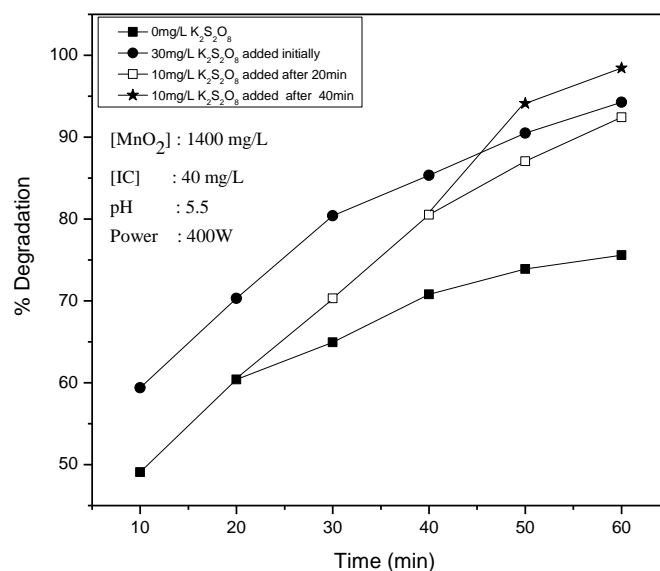
Fig. 4.16: Effect of initial and in-between addition of $K_2S_2O_8$ on the UV/MnO_2 degradation of IC.

Periodic addition of increments of PS is more economical compared to initial addition of higher quantities of the oxidant. Addition of 20 mg/L in 2 increments of 10 mg/L each (20min, 40min) resulted in~ 100% degradation in 60 minutes compared to the initial addition of 30mg/L which yielded only ~ 90%. PS initiated enhancement in the degradation of organics under AOPs takes place by the interaction of the insitu formed SO_4^{-} with the substrate.

The mechanism of enhancement of photocatalytic degradation of organics in presence of PS involves the insitu formation of reactive species such as $SO_4^{-\cdot}$, $OH^{\cdot}$ etc and their interaction with the substrate. As the concentration of PS is increased, more reactive SO_4^{-} radicals are formed under UV irradiation and a series of chain reactions follow as in equations 80-88 [185].

$$S_2O_8^{2-} \xrightarrow{h\nu} 2SO_4^{-\cdot} \quad\text{..} (80)$$

$$S_2O_8^{2-} + RH \xrightarrow{h\nu} SO_4^{-} + HSO_4^{-} + R^{\cdot} \quad\text{..........................} (81)$$

RH: organic pollutant

$$SO_4^{-} + H_2O \rightarrow SO_4^{2-} + H^+ + {}^{\cdot}OH \quad\text{............................} (82)$$

$$SO_4^{-\cdot} + RH \rightarrow R^{\cdot} + HSO_4^{-} \quad\text{.....................................} (83)$$

$${}^{\cdot}OH + RH \rightarrow R^{\cdot} + H_2O \quad\text{.......................................} (84)$$
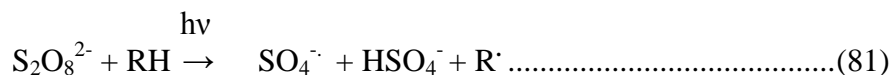
Further interaction will result in complete mineralisation of the dye.

It is also possible that some of the reactive free radicals get deactivated by interaction with themselves as follows.

Microwave, Photo and Sono Activated Advanced Oxidation Processes and their Variations for the Decontamination of Water from Toxic Chemical Pollutants

265

$$2SO_4^{\cdot-} \quad \rightarrow \quad S_2O_8^{2-} \text{ (Chain termination)} ....(85)$$

$$2\,^{\cdot}OH \quad \rightarrow \quad H_2O_2 \text{ (Chain termination)} ....(86)$$

$$2R^{\cdot} \quad \rightarrow \quad RR \text{ (Chain termination)} ....(87)$$
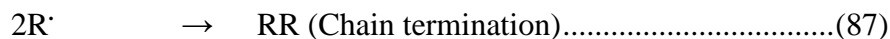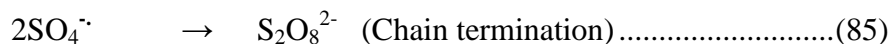
The interaction of insitu formed ROS such as H_2O_2, $HO_2^{\cdot}$, $^{\cdot}OH$ etc. and $SO_4^{\cdot-}$ with IC takes place on the surface of the catalyst as well as in bulk, leading to its degradation into various intermediates and eventual mineralization. However, the degradation is not increasing with increase in the concentration of PS, after the initial enhancement. The excess of $SO_4^{\cdot-}$ radicals formed in situ at higher concentration of PS may be getting deactivated as in reaction (85). The reactive $SO_4^{\cdot-}$ radicals can also interact with PS and form less reactive $S_2O_8^{\cdot-}$ radicals as follows:

$$SO_4^{\cdot-} + S_2O_8^{2-} \rightarrow \quad SO_4^{2-} + S_2O_8^{\cdot-} ....(88)$$
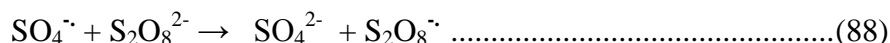
Thus the $SO_4^{\cdot-}$ radicals which are responsible for the enhancement of the degradation of IC in the presence of PS can get deactivated by unproductive interactions. This leads to stabilization in the rate of degradation at higher concentration of PS and with reaction time.

The results indicate that the enhancement of the degradation of IC in presence of PS is only moderate. Further, it is more effective to add PS to the system in small increments rather than the entire quantity in one lot.

Combination of the two oxidants, i.e. H_2O_2 and PS resulted only in the average of the negative effect of H_2O_2 and positive effect of PS in presence of UV irradiation (Fig.4.17).
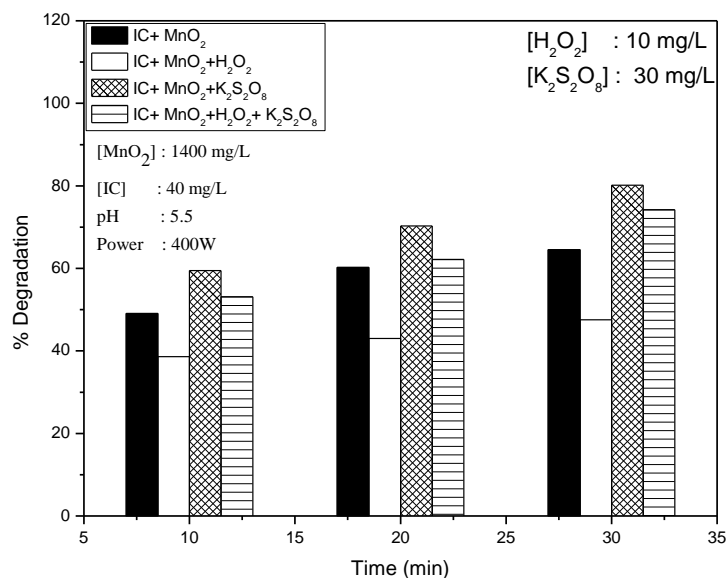
Fig. 4.17: Effect of combination of $K_2S_2O_8$ and H_2O_2 on the UV/MnO₂ degradation of IC

The results thus show that in presence of a highly efficient catalyst like MnO₂, the oxidants do not enhance the degradation significantly.

4.3.7 Effect of dissolved salts/anions

Many of the anionic contaminants which are naturally present in water inhibit the efficiency of AOPs for the degradation of organic water pollutants [154, 157, 160]. Instances of anions functioning as enhancers of the degradation of pollutants also have been reported [78].

In this context, the effect of some of the commonly occurring anions in water, i.e. SO_4^{2-}, Cl^-, PO_4^{3-}, CO_3^{2-}, HCO_3^- and NO_3^- on the efficiency of UV/MnO₂ degradation of IC is tested at various concentrations and reaction times. The results are plotted in Fig. 4.18A and Fig. 4.18B respectively. The results showed that the anion PO_4^{3-} at lower concentrations (5mg/L)

has only negligible effect on the degradation of IC, within the limits of experimental error. CH_3COO^-, CO_3^{2-}, HCO_3^-, Cl^- and NO_3^- inhibit the degradation mildly at all concentrations. PO_4^{3-} also becomes a powerful inhibitor at higher concentrations. SO_4^{2-} has practically 'no effect'.
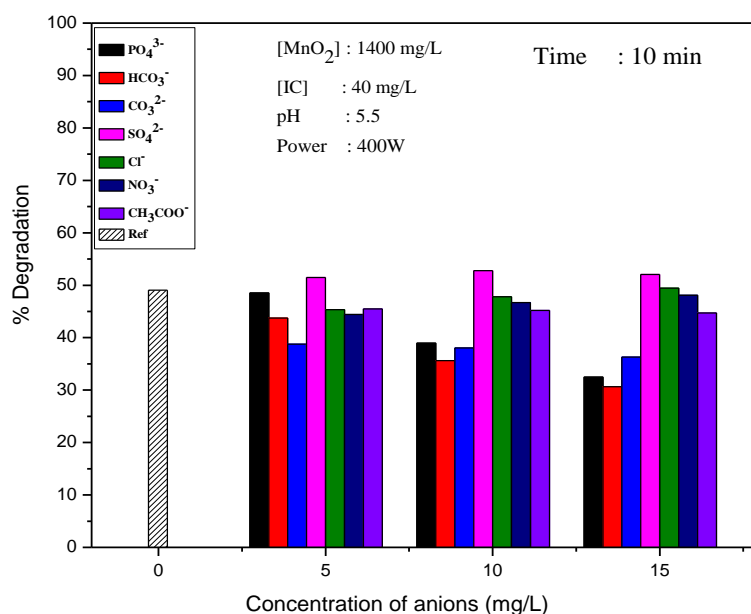
Fig. 4.18A: Effect of concentration of anions on the UV/MnO$_2$ degradation of IC.

The effect of different anions added at different concentrations on the degradation after 10 minutes of irradiation is summarised in Table 4.2.

Table 4.2: Effect of concentration of anions on the UV/MnO$_2$ degradation of IC (Time: 10 min)

Concentration of Anions(mg/L)	Inhibition	No Effect
5	$CO_3^{2-} > HCO_3^- > NO_3^- > Cl^- \approx CH_3COO^-$	PO_4^{3-}, SO_4^{2-}
10	$HCO_3^- \approx CO_3^{2-} \approx PO_4^{3-} > CH_3COO^- > Cl^- \approx NO_3^-$	SO_4^{2-}
15	$HCO_3^- \approx PO_4^{3-} > CO_3^{2-} > CH_3COO-$	Cl^-, NO_3^-, SO_4^{2-}

Other than concentration of the anions, the irradiation time also is known to influence the effect of anions on the degradation. The relative concentration of the ion with respect to the substrate (which is degrading) increases progressively with time leading to more inhibition. The effect is tested and the results are plotted in Fig.4.18B.
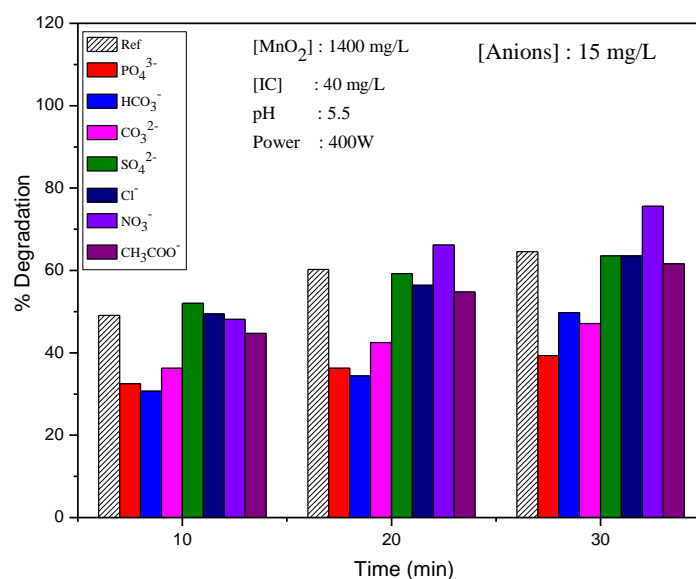
Fig. 4.18 B: Effect of reaction time on the 'anion effect on the UV/MnO$_2$ degradation of IC'.

Table 4.3: Effect of reaction time on the 'anion effect on the UV/MnO$_2$ degradation of IC'

Time	Inhibition	No Effect	Enhancement
10 min	HCO$_3^-$ ≈ PO$_4^{3-}$ > CO$_3^{2-}$ > CH$_3$COO-	NO$_3^-$, Cl$^-$, SO$_4^{2-}$	-
20 min	HCO$_3^-$ ≈ PO$_4^{3-}$ > CO$_3^{2-}$ > CH$_3$COO$^-$ > Cl$^-$	SO$_4^{2-}$	NO$_3^-$ (mild)
30 min	PO$_4^{3-}$ > CO$_3^{2-}$ ≈ HCO$_3^-$	SO$_4^{2-}$, Cl$^-$,CH$_3$COO$^-$	NO$_3^-$ (moderate)

The trend remains more or less the same irrespective of the reaction time. The 'moderate to significant enhancement' in the photocatalytic degradation of organics in the presence of semiconductor oxides such as

ZnO or TiO_2 is not observed here indicating that in presence of a strong adsorbent such as MnO_2, the anion can get adsorbed even at lower concentration and inhibit the degradation.

As done in the case of MW catalysts, the effect of individual anions over a wider concentration range on the photocatalytic degradation of IC is investigated in detail and the results are plotted in Figs. 4.19 to 4.25.

4.3.7.1 PO_4^{3-}
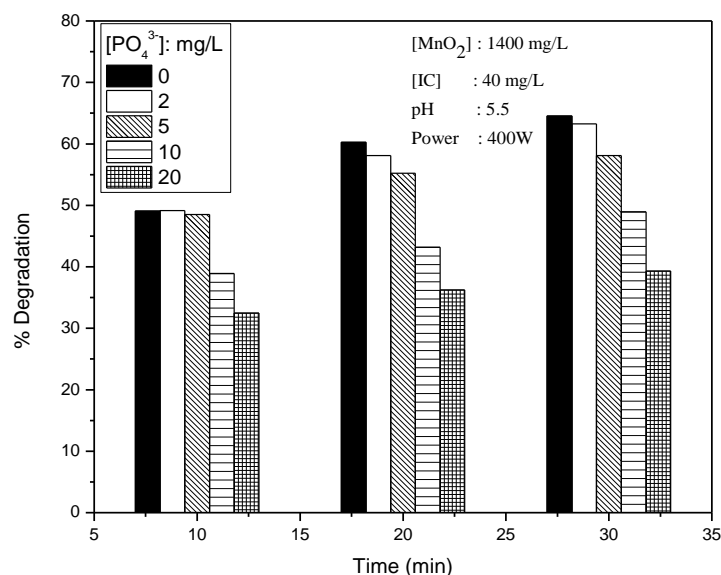
Fig. 4.19: Effect of PO_4^{3-} on the UV/MnO_2 degradation of IC

PO_4^{3-} (> 5 mg/L) is a strong inhibitor at all reaction times (Fig.4.19). At very low concentrations the effect is negligible in the beginning (see 10 minutes data). This may be because at this stage, the relative concentration of the anions with respect to IC is very small and the adsorption of the substrate is relatively much more.

4.3.7.2 HCO₃⁻
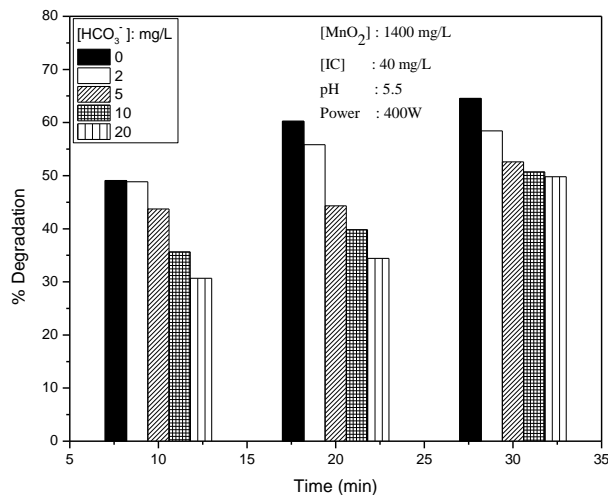
Fig.4.20: Effect of HCO_3^- on the UV/MnO₂ degradation of IC

HCO_3^- is also a strong inhibitor except at the lowest concentration of 2 mg/L (Fig.4.20).

4.3.7.3 CO₃²⁻
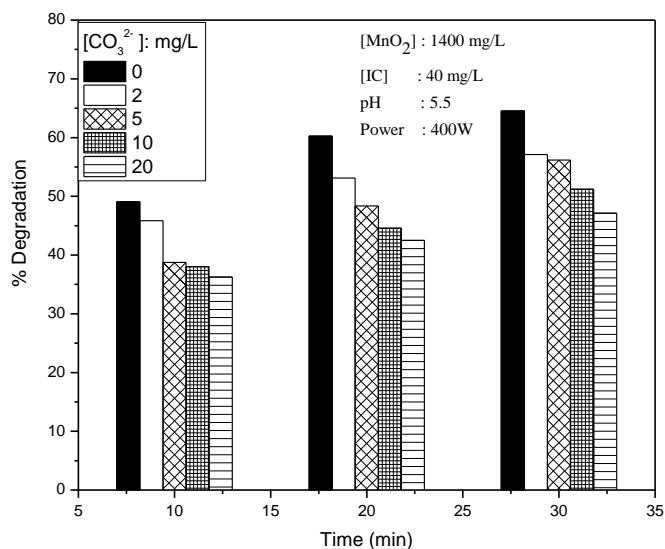
Fig. 4.21: Effect of CO_3^{2-} on the UV/MnO₂ degradation of IC

CO$_3^{2-}$ also as a strong inhibitor at all concentrations and reaction times (Fig.4.21).

4.3.7.4 SO$_4^{2-}$
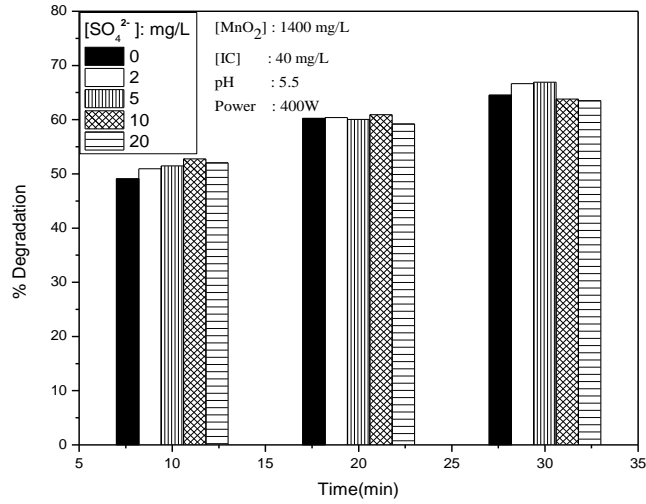
Fig. 4.22: Effect of SO$_4^{2-}$ on the UV/MnO$_2$ degradation of IC

SO$_4^{2-}$ has practically no effect at all reaction times and concentration (Fig.4.22).

4.3.7.5 Cl$^-$
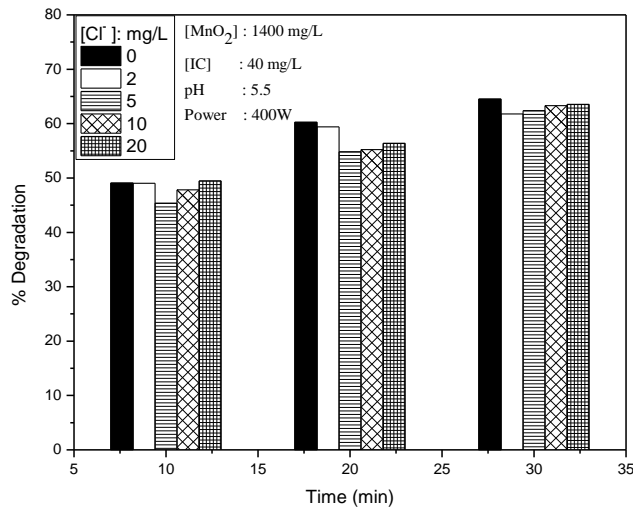
Fig. 4.23: Effect of Cl$^-$ on the UV/MnO$_2$ degradation of IC

Cl⁻ is a mild inhibitor at higher concentration and at later stages of reaction (Fig.4.23). However, the inhibition is so mild that it can be treated as 'no effect' within the limits of experimental error

4.3.7.6 NO₃⁻
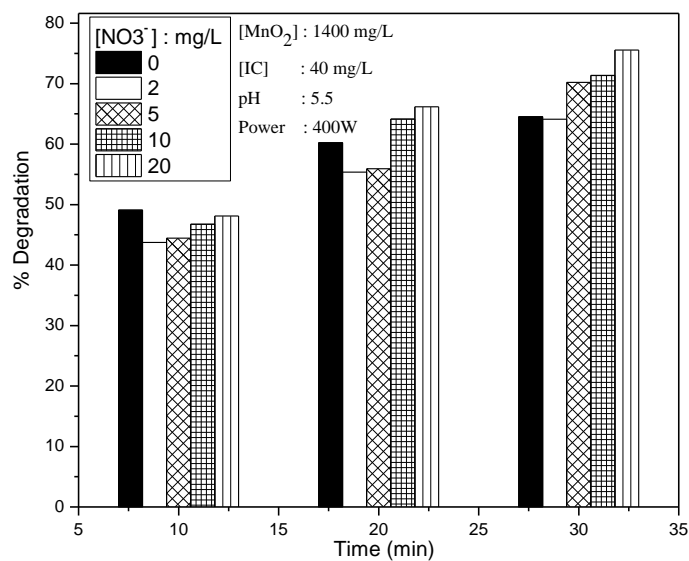
Fig.4.24: Effect of NO_3^- on the UV/MnO₂ degradation of IC

At low concentration, NO_3^- is a mild inhibitor but at later stages of the reaction and higher concentrations, it becomes a mild enhancer (Fig.4.24).

Microwave, Photo and Sono Activated Advanced Oxidation Processes and their Variations for the Decontamination of Water from Toxic Chemical Pollutants

273

4.3.7.7 CH₃COO⁻
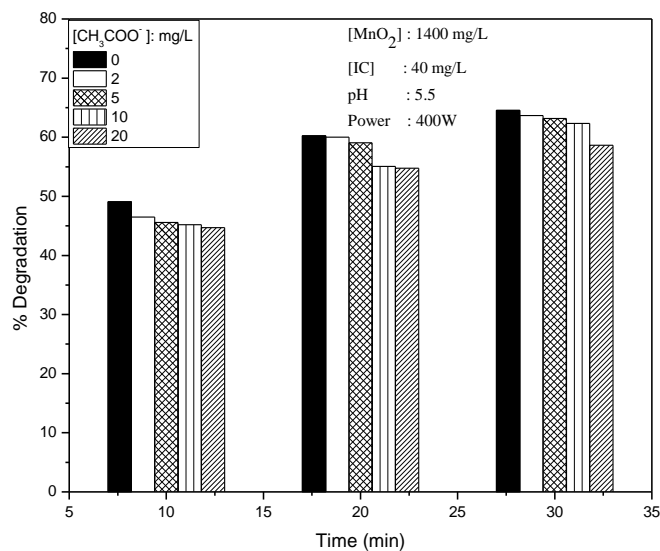
Fig.4.25: Effect of CH_3COO^- on the UV/MnO₂ degradation of IC

Acetate ion is also a mild inhibitor of the degradation of IC (Fig.4.25). However, within the limits of experimental error, this may be treated as 'no effect' also.

The inhibition of the photo catalytic degradation of organics by anions is often explained based on blocking of the active surface sites by preferential adsorption of the anions, surface layer formation and scavenging of reactive ˙OH radicals. Studies on the adsorption of IC in presence of anions show that PO_4^{3-} inhibits the adsorption the most. The results of the adsorption studies under parameters comparable to those of the degradation reaction are given in Table 4.4.

MnO$_2$ is a very efficient adsorbent as well as oxidant and the IC gets adsorbed and activated even in the presence of the anions thereby maintaining a reasonable degree of degradation.

Table 4.4: Adsorption of IC on MnO$_2$ in presence of anions
[IC]: 40 mg/L, [MnO$_2$]: 1400 mg/L, [Anion] : 10 mg/L, Time:30min

Anion	% Adsorption of IC
None	32.2
PO_4^{3-}	14.3
HCO_3^-	21.3
CO_3^{2-}	19.4
Cl^-	33.5
SO_4^{2-}	30.5
CH_3COO^-	29.5
NO_3^-	34.7

The comparative photo degradation of IC in presence of those anions clearly shows good correlation between the adsorption of the anion and the inhibition caused by it. Comparison of the adsorption data in Tables 3.4 (Chapter 3) and 4.4 show that irrespective of the quantity of MnO$_2$ or the concentration of IC, the trend in adsorption remains the same.

The cation was kept the same in all cases, i.e., Na$^+$. If competitive adsorption of the anions is the main cause of the inhibition of the degradation, it should have been in the order:

$$PO_4^{3-} > CO_3^{2-} > HCO_3^- > CH_3COO^-$$ ....(89)

SO_4^{2-}, Cl^- and NO_3^- should not inhibit the degradation of IC.

Microwave, Photo and Sono Activated Advanced Oxidation Processes and their Variations for the Decontamination of Water from Toxic Chemical Pollutants

275

The order of experimentally observed inhibition is (15mg/L anion) at 10min is

$$HCO_3^- > PO_4^{3-} \geq CO_3^{2-} \geq CH_3COO^- \geq NO_3^- \quad ....(90)$$

This sequence of inhibition is fairly consistent with the expected result based on adsorption (eqn.89). However, the inhibition by anions is not significant in the case of photocatalytic degradation of IC in presence of MnO_2 and hence any comparison based on adsorption alone may not be that appropriate.

Another reason for the inhibition by anions may be their scavenging of the ROS, especially highly reactive $^{\cdot}OH$ as discussed in detail under Section 3.3.3.12 of Chapter 3. The scavenging results in the formation of relatively less reactive 'radical anion'. Moderate degradation even in presence of the strongly adsorbing anions can also be due to the radical anions on the surface as well as in the bulk.

Yet another factor contributing to the inhibition in presence of salts is their effect on colloidal stability of the suspension. Consequently surface charges get neutralised which can increase the mass transfer limitation and reduce the interaction between the pollutants and catalysts. However, at lower concentration of the anions, in presence of a powerful adsorbent such as MnO_2, inhibition by this factor also will be negligible as observed here.

Another possible reason, often cited for the inhibition by anions, is the formation of an inorganic layer on the catalyst surface irrespective of adsorption. This has been discussed in detail in Chapter 3 Section 3.3.3.12.

However, inhibition in this case is not significant and hence layer formation may not be very relevant in the case of a highly active catalyst such as MnO_2.

As illustrated in Chapter 3 Section 3.3.3.12, in the case of MnO_2/IC systems, the variation in the pH caused by anions also cannot be correlated with their effect on the degradation. The effect of anions on the diffusion co-efficient of the organic pollutants as the cause for inhibition also may not be relevant in the absence of any significant inhibition. In the highly reactive photoactivated, free radical environment, that too in presence of a hyperactive catalyst such as MnO_2, multitude of interactions are possible. This makes any general interpretation on the anion effect difficult. In the case of SO_4^{2-} causes for the mild enhancement have to be analysed independently. Such exceptions are natural and reported in many instances in the case of anions which are known to participate in a number of complex interactions.

NO_3^- is a mild enhancer of the degradation of IC under MnO_2/UV. In the present case the adsorption of IC is not affected by NO_3^- ions (See table 4.4). This may be one of the reasons for its mild 'enhancement or 'no effect'. One factor leading to the enhancement in degradation by NO_3^- ions is the formation of $NO_3^{\cdot}$ radicals (as in reaction 91), which is also a powerful oxidant.

$$NO_3^- + {}^{\cdot}OH \rightarrow NO_3^{\cdot} + OH^- \quad \text{...(91)}$$

The efficiency of $NO_3^{\cdot}$ as an oxidant is less compared to ${}^{\cdot}OH$. However, in the case of ${}^{\cdot}OH$, the radical can get deactivated as

$$^{\cdot}OH + {}^{\cdot}OH \rightarrow H_2O_2 \quad \text{...(92)}$$

Thus, the options available for insitu formed ˙OH are:

1) Interaction with NO_3^- to form reactive $NO_3^˙$ Radicals

2) Deactivation by recombination forming H_2O_2

3) Interaction with the substrate IC and degradation.

Obviously, the most effective route for the efficient utilization of ˙OH is the interaction with the substrate. Similarly when route 1 as above is facile and faster than route (2) interaction with the resulting $NO_3^˙$ also accelerates the degradation. Thus the ˙OH which should have been deactivated and wasted by route (2) is more beneficially transformed in presence of NO_3^-. These positive interactions compete with the inhibiting factors as discussed above and depending on the relative dominance of either, the degradation is enhanced or inhibited. In the case of NO_3^- the enhancement suggests the slight dominance of the positive interactions.

The mild enhancement may also be linked to direct and indirect formation of ˙OH radicals as follows [186].

$$NO_3^- + h\nu \rightarrow NO_2^- + O \quad ....(93)$$

$$NO_3^- + H_2O + h\nu \rightarrow NO_2^- + OH^- + .OH \quad ....(94)$$

$$O + H_2O \rightarrow 2^˙OH \quad ....(95)$$

In short, the effect of anions on the photocatalytic degradation of pollutants in water, is the net effect of a number of competing and complimenting factors such as competitive adsorption, competition for the photons, inhibition of light penetration, surface layer formation, deposition of elementary metals, radical and hole scavenging, formation of new reactive radical species etc. Depending on the

domination or balancing of these factors the net anion effect can be enhancement, inhibition or stabilisation.

4.3.8 Effect of Oxygen

The role of dissolved O_2 on the photocatalytic degradation of IC is studied by deaerating the system using N_2 bubbling. The results show that (Fig.4.26) the effect of deaeration is not significant thereby suggesting that the main source of O_2 for the reaction is not the dissolved form. The required O_2 is provided primarily by the surface (strongly adsorbed) and the lattice of MnO_2 (as illustrated in Section 3.3.3.13) which cannot be easily removed by flushing with N_2.
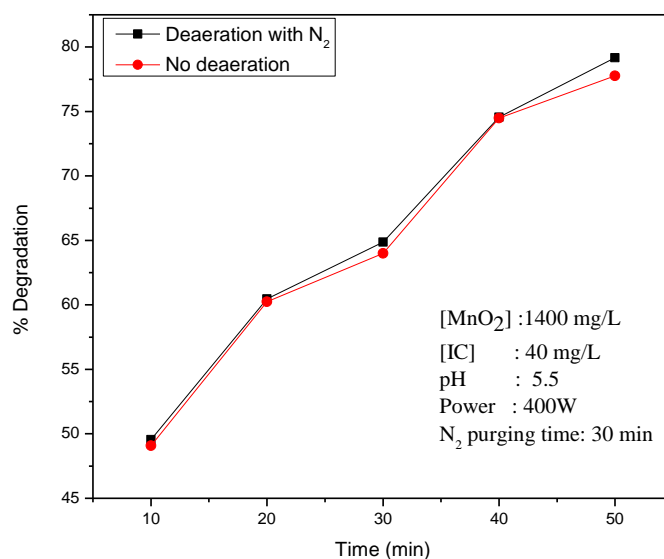
Fig. 4.26: Effect of deaeration of the system by N_2 on the UV/MnO_2 degradation of IC.

If the oxygen required for the generation of ROS is provided by the lattice as well as the surface, as explained earlier, the deaeration effect

Microwave, Photo and Sono Activated Advanced Oxidation Processes and their Variations for the Decontamination of Water from Toxic Chemical Pollutants

279

will be more evident at lower dosages of MnO_2 where the availability of oxygen will be limited. This is verified by conducting experiments at lower dosages of MnO_2 (50,100 and 200 mg/L in place of 1400 mg/L in normal experiments). The results are presented in Fig. 4.27.
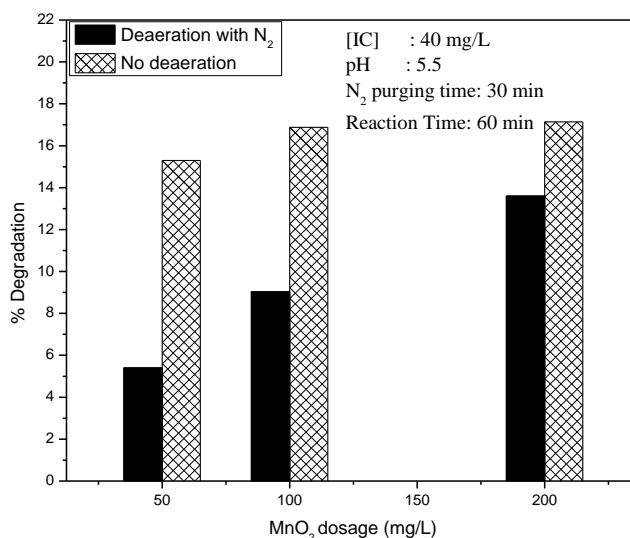
Fig. 4.27: Effect of deaeration with N_2 on the UV/MnO_2 degradation of IC

From the Fig.4.27, it is seen that the degradation is inhibited by deaeration at lower dosage of MnO_2 thereby confirming the role of dissolved and/or adsorbed O_2, in the process. This also confirms that the lack of inhibition by deaeration at higher dosages of MnO_2 is due to the availability of adequate O_2 supply from the lattice as well as from the surface. Fig. 4.27 also shows that the inhibition of the degradation on deaeration is progressively decreasing with increase in MnO_2 dosage, because of the increased availability of lattice and adsorbed O_2, which cannot be easily removed by flushing with N_2.

Amorphous MnO_2 is known to release bulk oxygen more easily to the surface which makes it a better catalyst with respect to activation and regeneration [147]. This has been explained in detail in Section 3.3.3.13 of Chapter 3. Relevant explanation applicable in the context of photocatalysis also is briefly as follows.

MnO_2 with multiple oxidation states together with its electron donor- acceptor properties is an excellent oxidation – reduction catalyst. Photolysis of MnO_2 increases the oxygen species on the surface either by oxygen migration to the surface or by Mn migration to the bulk or both. Surface oxygen is consumed faster upon irradiation and oxygen from the bulk moves to the surface. In the case of MnO_2, the loss of oxygen takes place at temperatures as low as 50°C. The photo-initiated oxygen release from MnO_2 may be due to movement of O^{2-} (bulk) to the surface consequent to the weakening of Mn-O bonds [187]

In the re-oxidation of oxides, atmospheric oxygen and/or dissolved O_2 is taken up by the surface of the partially reduced MnO_2 as follows

$$O_2 \ (g) + e^- \rightarrow (O_2^-) \dots\dots\dots\dots\dots\dots\dots\dots\dots\dots\dots \quad (96) \quad \text{g-gas phase}$$

$$(O_2^-) + e^- \rightarrow 2(O^-) \rightarrow O_2^- \ (s) + e^- \dots\dots\dots\dots\dots \quad (97) \quad \text{s-surface}$$

Most of the oxygen radicals are present in the bulk of the catalyst while some of them may remain on the surface for a short period. These highly active oxygen radicals can regenerate reduced manganese species. Under UV irradiation, the bonds in MnO_2 are weakened and O_2^- is released to the surface. Even though the lifetime of excited state oxygen

species is short, they possess adequately high energy and electro negativity to facilitate the reduction or hydrogen abstraction from the substrate. Possible reaction pathways are:

$$O_2^{-}(s) \xrightarrow[- e-]{h\nu} (O^{-}) \xrightarrow[- e-]{h\nu} O \text{ (surface)} \dots\dots\dots\dots\dots\dots\dots\dots\dots\dots\dots\dots(98)$$

$$O_2 + RH \text{ (i.e., IC)} \rightarrow HO_2^{\cdot} + R^{\cdot} \dots\dots\dots\dots\dots\dots\dots\dots\dots (99)$$

$$O_2 + R \rightarrow \text{Intermediates} \rightarrow \text{Mineralization} \rightarrow CO_2 + H_2O \dots\dots(100)$$

The $H^{\cdot}$ abstracted from R interacts with the hole and gets oxidized to form acid sites on the surface of MnO_2.

$$H^{\cdot} + h^{+} \rightarrow H^{+} \dots\dots\dots\dots\dots\dots\dots\dots\dots\dots\dots\dots\dots\dots\dots(101)$$

The regeneration of MnO_2 may be represented as:

$$-Mn(^{3+} \text{ or } ^{2+})- \xrightarrow[- e-]{h\nu} -Mn (^{4+} \text{ or } ^{3+})- \dots\dots\dots\dots\dots\dots\dots\dots\dots(102)$$

$$\{-Mn(^{4+} \text{ or } ^{3+})-\} + O_2^{-}(\text{from reaction 96}) \rightarrow MnO_2 \text{ (or } Mn_3O_4) \dots\dots(103)$$
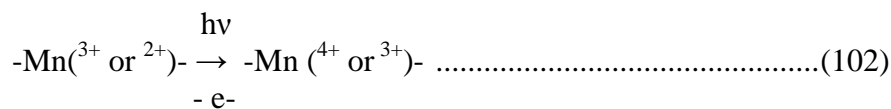
Unless the oxygen is replenished periodically, the activity of the catalyst will be lost faster. This is verified by recycling the catalyst immediately after use by simple filtration followed by quick drying at 120°C for 1 h.

4.3.9 Recycling of MnO$_2$
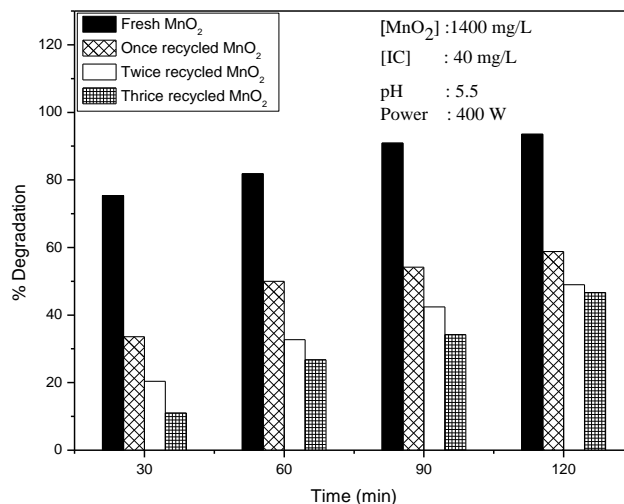
Fig. 4.28: Efficiency of recycled catalyst for the photocatalytic degradation of IC.

The degradation of IC (in 30 minutes) decreased from ~75 % in the presence of the fresh catalyst to ~33% in first recycling, ~20 % in second and ~11 % after 3rd recycling. This confirms the drastic change in the surface characteristics, loss of adsorption sites and loss of oxygen from the lattice, bulk and/or the surface of MnO$_2$. This loss is not fully compensated by contact with atmospheric oxygen. Catalytic activity decreases significantly after first use and moderately in subsequent recycling. The decreasing activity may be due to the partial deactivation of the catalytic site due to surface reactions, remnants of strongly bound substrate/ intermediate species on the surface, which prevent the efficient absorption of UV by MnO$_2$ and subsequent generation of reactive free radicals, depletion of adsorbed and lattice oxygen from MnO$_2$ etc.

The depletion of oxygen from the lattice of MnO$_2$ by the photodegradation of IC is proven from the EDX spectrum of MnO$_2$ before

and after use (Fig.4.29A and B and Table 4.5). The wt% as well as atomic % of oxygen is considerably depleted and correspondingly the wt% as well as atomic% of Mn is increasing in the catalyst after use.
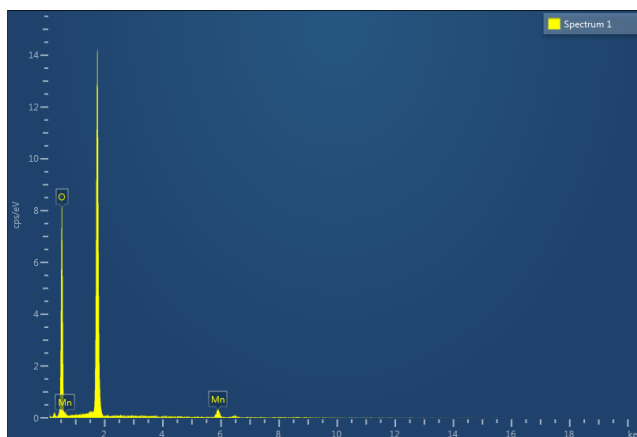
Fig.4.29A: EDX spectrum of Fresh MnO_2
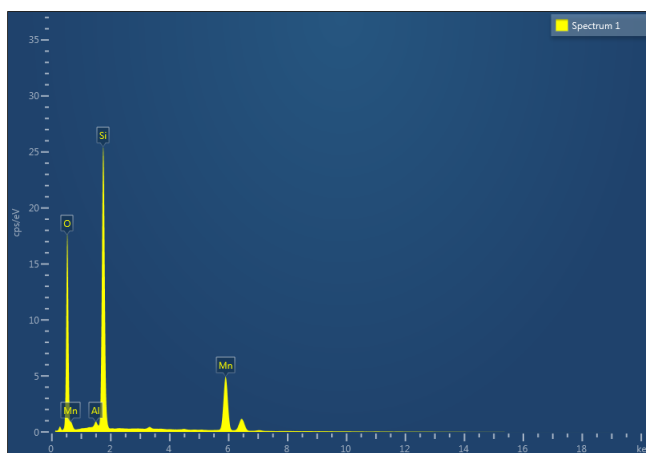
Fig. 4.29B: EDX spectrum of Recycled MnO_2 (200 mg/L IC, 1000 mg/L MnO_2)

Table 4.5: Relative ratio of Mn and 'O' in MnO_2 before and after use.

[IC]	[MnO₂]	Wt% O		Wt% Mn		Atomic% O		Atomic% Mn	
		Before	After	Before	After	Before	After	Before	After
200 mg/L	1000 mg/L	85.8	44.4	14.2	24.59	95.4	64.13	4.6	10.34

4.3.10 Chemical oxygen demand

Estimation of chemical oxygen demand (COD) of the optimized reaction system UV/MnO$_2$/IC at various intervals of irradiation shows that the degradation and decolourisation of IC do not lead to instant mineralization. However, once the solution is decolourized and the UV/MnO$_2$ irradiation is continued, mineralization becomes faster and the COD reaches a stable level. Beyond this, the COD does not decrease even after further UV radiation for another 2 hr indicating the presence of stable intermediates which cannot be mineralized under these conditions (Fig.4.30A). It takes another 4hr of UV irradiation for the complete mineralisation. The formation of transient intermediates which undergo further degradation to yield more stable organics such as acetic acid, tartaric acid, malic acid, oxalic acid, anthranilic acid etc. has been reported [149] in the AOP degradation of IC.
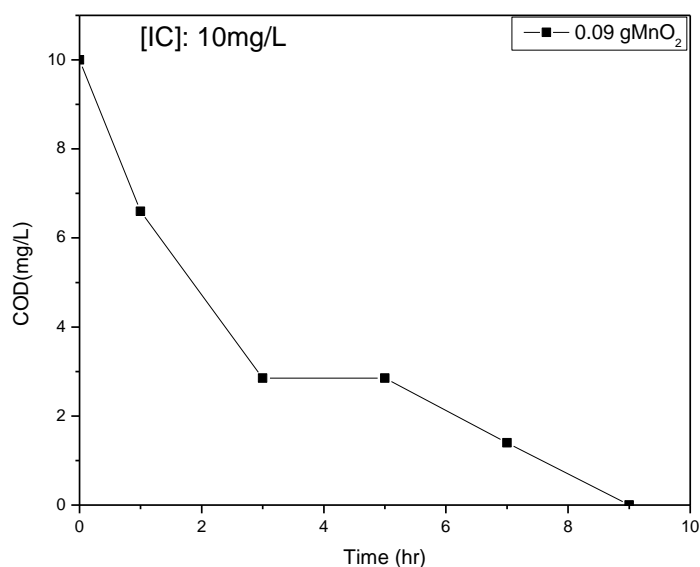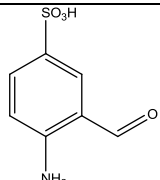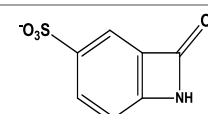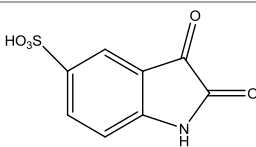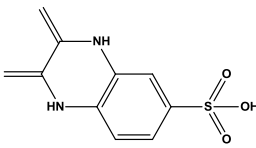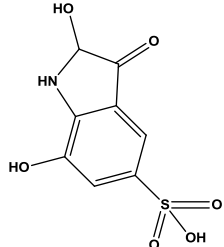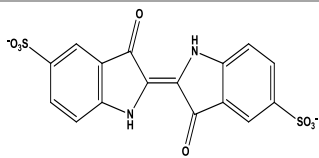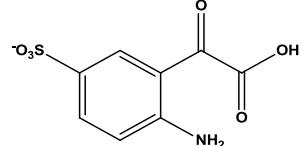
Fig. 4.30A: COD of the reaction system at different times of irradiation

Microwave, Photo and Sono Activated Advanced Oxidation Processes and their Variations for the Decontamination of Water from Toxic Chemical Pollutants

285

In the present case, various transient intermediates formed during the MnO$_2$/UV degradation are identified by LC-MS and are listed in Table.4.6.

Table 4.6: Intermediates identified during UV/MnO$_2$ degradation of IC

Sl No.	m/z	Proposed Structure
1	200	
2	198	
3	226	
4	244	
5	210	
6	161	
7	172	

The disappearance of COD completely shows that these intermediates as well as the more stable organic acids formed from them also get mineralised eventually.

In this context, the possibility of combining a more efficient photocatalyst TiO_2 with MnO_2 in order to enhance the mineralization capability of the catalyst is examined. The results are presented in Fig.4.30.B.
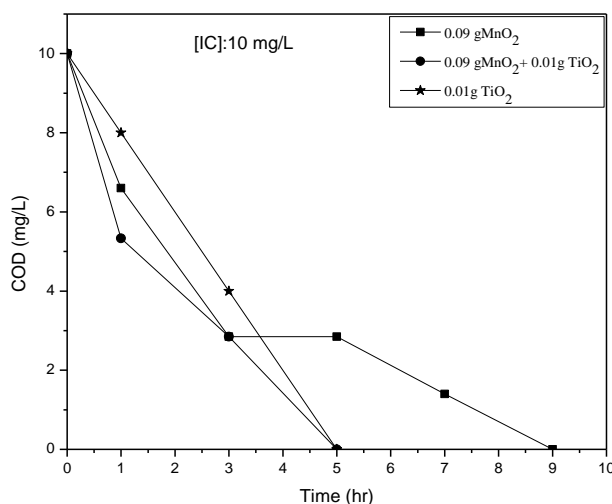
Fig. 4.30B: COD of the reaction system with MnO_2/TiO_2/(MnO_2-TiO_2) as catalyst at different times of irradiation

As Fig.4.30B shows the incorporation of ~10% of TiO_2 in MnO_2 enhances the COD removal significantly especially in the early stages of reaction. The result is comparable to that in the presence of TiO_2 only at later stages of reaction. MnO_2 takes 9 hrs while MnO_2-TiO_2 as well as TiO_2 takes 5 hrs for the complete mineralisation of IC. However in the early stages, MnO_2-TiO_2 is better for COD reduction than 'TiO_2 only'. Since the composition of the reaction system at different stages of irradiation is

different due to the presence of multiple intermediates which themselves are undergoing degradation it may be presumed that the characteristics of the organics also is relevant in determining COD removal efficiency of the catalysts. In view of these results it is important to have a detailed investigation on the MnO_2/TiO_2 combination including the optimisation of the ratio of the components for the photocatalytic mineralisation of IC

4.3.11 Photocatalytic degradation of IC using combination catalyst MnO_2-TiO_2

Optimisation of the ratio of components in a combination catalyst is important for its use as an efficient photocatalyst. The effect of MnO_2-TiO_2 at different ratios, on the photocatalytic degradation of IC is tested and the results are presented in Fig.4.31. As the figure shows incorporation of TiO_2 increases the photocatalytic activity of MnO_2 only mildly. Hence the role of TiO_2 may be primarily in the mineralisation of IC and the intermediates rather than simple decolourisation in the early stages.
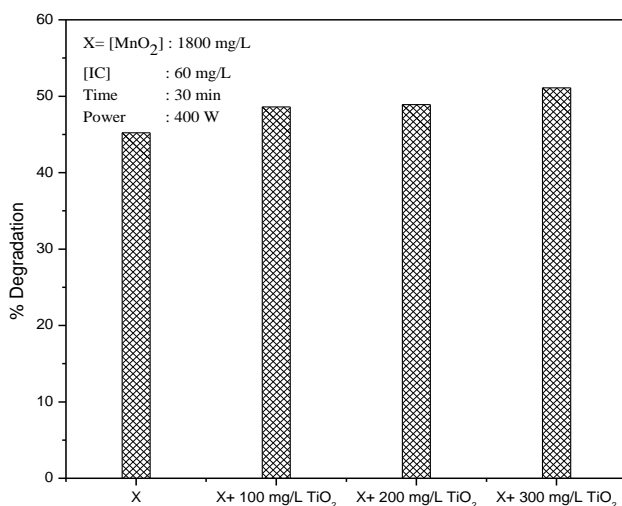
Fig.4.31: Optimisation of ratio of MnO_2-TiO_2 for the UV degradation of IC

The % degradation does not change much in the range 0.01- 0.03g of TiO_2 in 0.18g MnO_2/100mL. Since the presence of TiO_2 is known to increase the photoactivity of MnO_2, the more consistent and safer (with respect to the MW activity of MnO_2, which is inhibited at higher dosages of TiO_2), ratio of 0.01 / 0.18 (TiO_2 / MnO_2) g/100 mL is selected for further studies. The ratio is important in cases where MW and UV irradiation are to be combined to improve the mineralisation efficiency.

4.3.11.1 Effect of catalyst dosage

The catalyst dosage at the selected ratio of MnO_2-TiO_2 (0.18/0.01) for optimum degradation of IC is investigated in the range 0.06 g to 0.21 g/100 mL. The result is shown in Fig.4.32.
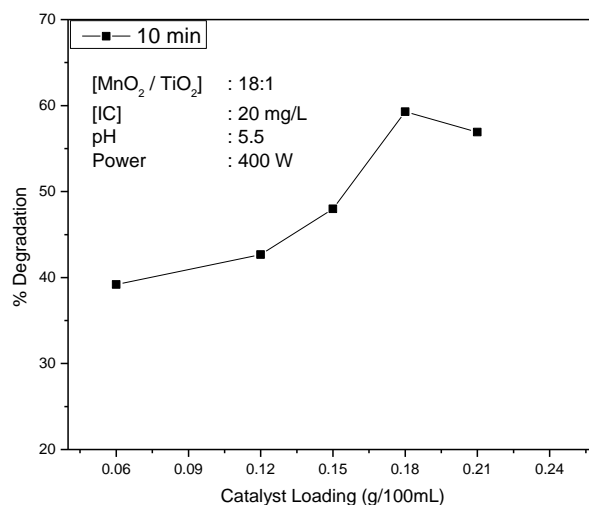
Fig. 4.32: Optimisation of catalyst loading for the UV/(MnO_2-TiO_2) degradation of IC.

The degradation increases with increase in catalyst loading with an optimum at 0.18 g/100mL. Hence 1800 mg/L of the combination catalyst is taken as the optimum loading for detailed investigation. Probable

causes for the increase in degradation of IC with increase in catalyst dosage and the eventual optimum are discussed in detail under Section. 4.3.2.

4.3.11.2 Effect of concentration of IC

The effect of concentration on the degradation of IC has been investigated and the results are shown in Fig.4.33. The % degradation of IC decreases with increase in its concentration. The rate of degradation as a function of concentration is computed and shown in Fig.4.34. The rate of degradation increases with increasing the concentration upto 60 mg/L, and then stabilises or even decreases. This indicates the variable kinetics in the degradation of IC under MnO_2-TiO_2/UV as in the case of MnO_2 /UV also.
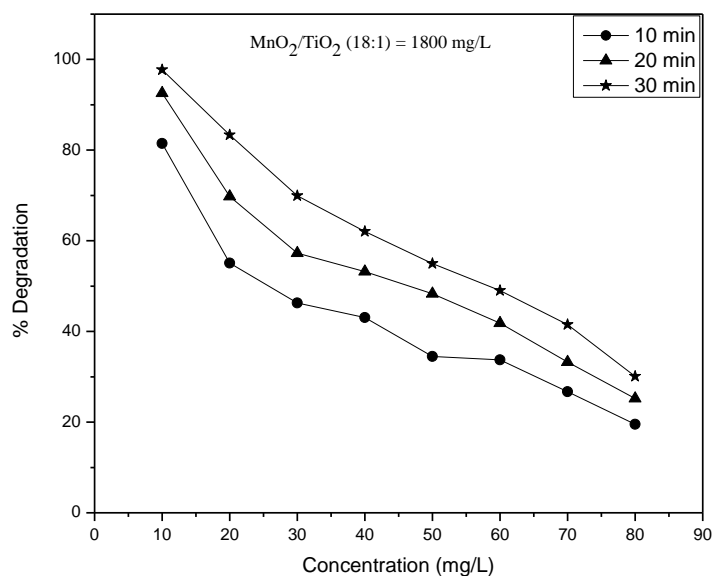
Fig. 4.33: Effect of concentration on the UV/(MnO_2-TiO_2) degradation of IC
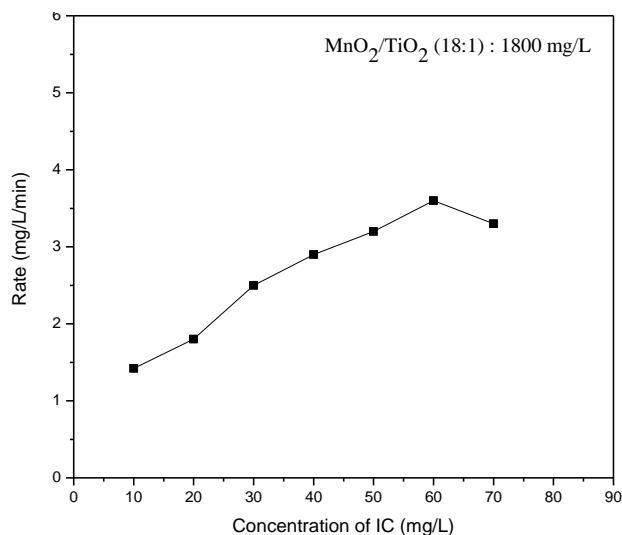
Fig. 4.34: Rate of UV/(MnO$_2$-TiO$_2$) degradation of
IC at various concentrations

The first order kinetics of degradation in the concentration range 10-60 mg/L of IC and the application of modified L-H mechanism, as in the case of MnO$_2$ catalyst is verified by the inverse rate plot (1/r$_0$ vs1/C$_0$) (Fig.4.35) and the logarithmic plot Fig.4.36.
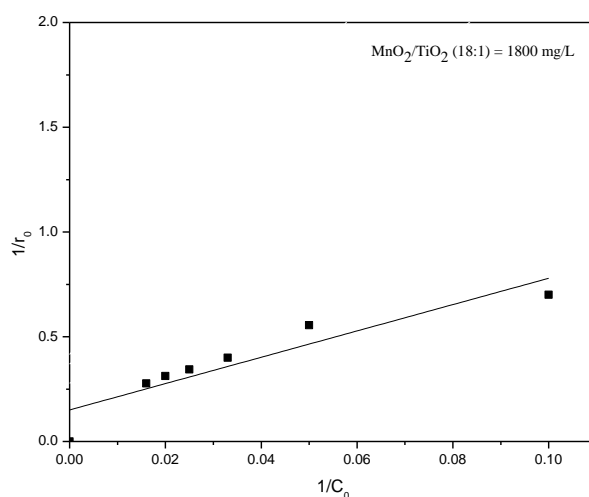
Fig. 4.35: Reciprocal plot of 1/r$_0$ vs 1/C$_0$ for various
concentrations of IC

*Microwave, Photo and Sono Activated Advanced Oxidation Processes and their
Variations for the Decontamination of Water from Toxic Chemical Pollutants*

291

The inverse plot yields a straight line. The plot of ln (C_0/C) vs Time (Fig.4.36) in the concentration range 10-50 mg/L also shows linear dependence indicating that the reaction follows first order kinetics. It can be explained based on the L-H mechanism as done in Section 3.3.3.2 Chapter 3.
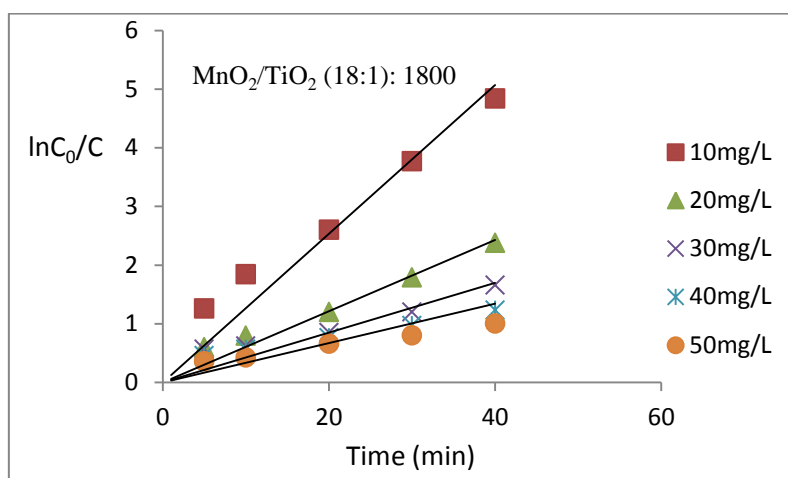
Fig.4.36: Logarithmic plot for UV/(MnO$_2$-TiO$_2$) degradation of IC

The rate constant at different concentrations are calculated from the logarithmic plot and are tabulated in Table 4.7. The rate constant decreases with increase in concentration as in the case of almost all photocatalytic processes following pseudo first order kinetics. Relevant causes for this are explained in Section 3.3.3.2, Chapter 3.

Table 4.7: Pseudo first order rate constants

Experiment	[MnO$_2$-TiO$_2$] g/L	[IC] mg/L	k_{app}(min^{-1})
1	1.8	10	0.110
2	1.8	20	0.055
3	1.8	30	0.035
4	1.8	40	0.026

4.3.11.3 Effect of pH

The effect of pH on the degradation of IC in presence of MnO_2-TiO_2 is investigated in the range 2-11. The results are shown in Fig.4.37.
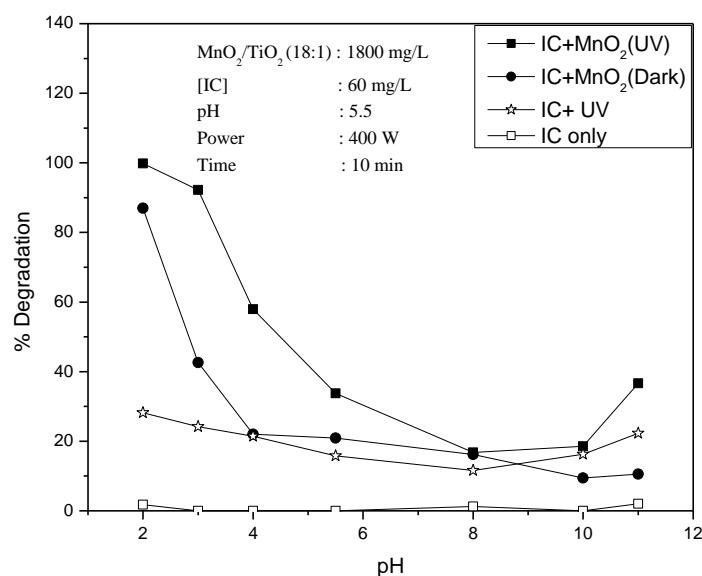
Fig. 4.37: Effect of pH on the UV/(MnO₂-TiO₂) degradation of IC

Degradation is high in the acidic range, then it decreases with increase in pH and stabilises from pH 4-8 followed by slight increase in the alkaline medium. High degradation under acidic pH is facilitated by the strong adsorption of IC on MnO_2 and subsequent reactions as explained in Section 4.3.4. Slight increase in degradation under alkaline pH is due to the formation of increased number of ˙OH radicals. The effect of pH is almost the same as in the case of MnO_2. This suggests that incorporation of small amounts of TiO_2 in MnO_2 does not influence the pH effect on the latter.

Microwave, Photo and Sono Activated Advanced Oxidation Processes and their Variations for the Decontamination of Water from Toxic Chemical Pollutants

293

4.3.11.4 Formation of H_2O_2

The formation of H_2O_2 and its influence on the photocatalytic degradation of IC in presence of MnO_2 is demonstrated in Section 4.3.5 and 4.3.6.1 of this Chapter.

In the present case, concentration of H_2O_2 formed in presence of MnO_2-TiO_2 catalyst is determined immediately on decolourisation. UV irradiation is continued for some more time after decolourisation and the H_2O_2 is measured periodically. The results are shown in Fig.4.38.
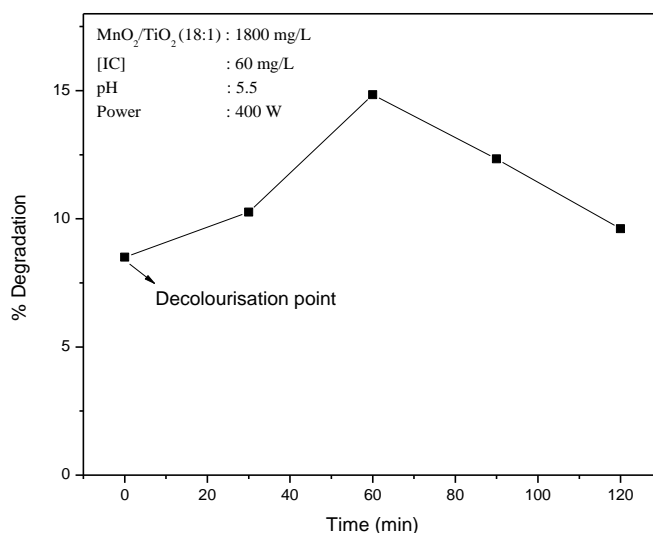
Fig. 4.38: Concentration of H_2O_2 formed during the UV/(MnO_2-TiO_2) degradation of IC

Concentration of H_2O_2 increases with increasing the irradiation time, reaches an optimum and then decreases. This variation in the concentration of H_2O_2 shows that it is decomposed/consumed/generated simultaneously depending on the reaction conditions, in particular its concentration. When the concentration reaches a particular maximum, the decomposition

dominates bringing its net concentration down. Similarly when the concentration reaches a critical minimum, the formation process gets precedence. This process happens many times again and again. The periodic change in the concentration of insitu formed H_2O_2 and the phenomenon of oscillation occurring under AOP processes has been well demonstrated in this study as well as earlier studies [112]. The mechanism and other relevant details in this respect are discussed under Section 4.3.6.1.

4.3.11.5 Effect of oxidants

4.3.11.5.1 Effect of H_2O_2

The effect of externally added H_2O_2 on the photocatalytic degradation of IC in presence of MnO_2-TiO_2 as catalyst is studied and the results are plotted in Fig.4.39.
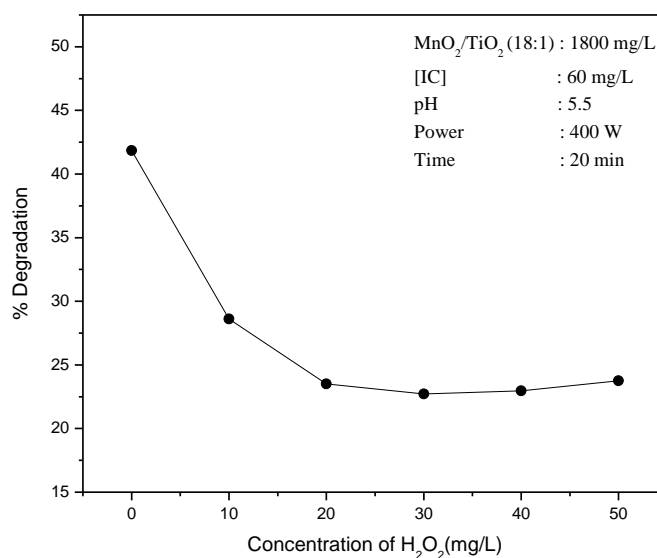
Fig. 4.39: Effect of added H_2O_2 on the UV/(MnO₂-TiO₂) degradation of IC

H$_2$O$_2$ inhibits the degradation of IC upto 20mg/L. Thereafter, the degradation stabilises suggesting that further addition of H$_2$O$_2$ does not result in enhanced inhibition. The inhibition is further confirmed by the addition of H$_2$O$_2$ in-between to a reaction that is in progress and the results are plotted in Fig.4.40.
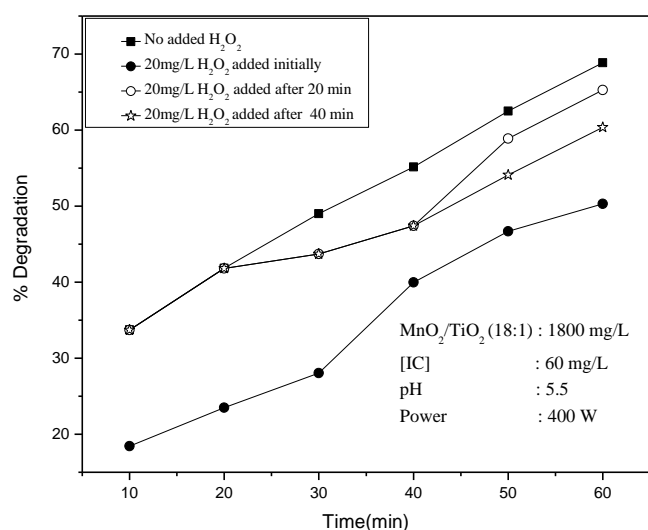
Fig. 4.40: Effect of initial and in-between addition of H$_2$O$_2$ on the UV/(MnO$_2$-TiO$_2$) degradation of IC.

The addition of H$_2$O$_2$ inhibits the degradation of IC whether it is added initially or in-between to a reaction system. H$_2$O$_2$ formed in situ in the reaction system will decompose in presence of MnO$_2$-TiO$_2$ and form H$_2$O and O$_2$. Further, the H$_2$O$_2$ competes with the substrate IC and reaction intermediates for the reactive ROS in the system thereby making them (ROS) less available for the degradation of IC. Adsorption of H$_2$O$_2$ on catalyst surface and consequent decomposition will prevent the IC from occupying at least some of the surface sites and interacting with the ROS. H$_2$O$_2$ also may slow down the penetration of UV light through the

suspension. The cumulative effect of all these parameters will lead to drastic inhibition in the degradation of IC. Beyond the optimum concentration of 20 mg/L, the degradation is stabilized. At this stage various interactions involving H_2O_2, the ROS, IC, in situ formation and decomposition of H_2O_2 etc. with enhancing and inhibiting effects on the degradation of IC will be balancing each other. The net concentration of .OH and other ROS available for IC will be stable from this stage onwards and hence degradation of IC is stabilized. Various reactions involved in the process are similar to those discussed in Section 4.3.6.1.

4.3.11.5.2 Effect of persulphate ($K_2S_2O_8$)

Potassium persulphate (PS) is a powerful oxidant of many AOPs. The effect of PS on the photocatalytic degradation of IC is studied using MnO_2-TiO_2 as catalyst and the results are plotted in Fig.4.41. The degradation of IC increases slowly with increase in concentration of PS.
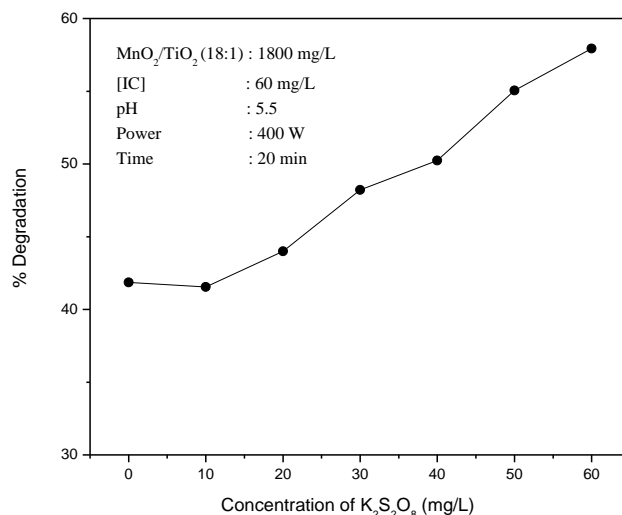
Fig. 4.41: Effect of $K_2S_2O_8$ on the UV/(MnO_2-TiO_2) photocatalytic degradation of IC

The enhancing effect of $K_2S_2O_8$ is further confirmed by the addition of PS to the MnO$_2$-TiO$_2$/UV/IC reaction that is in progress (Fig.4.42).
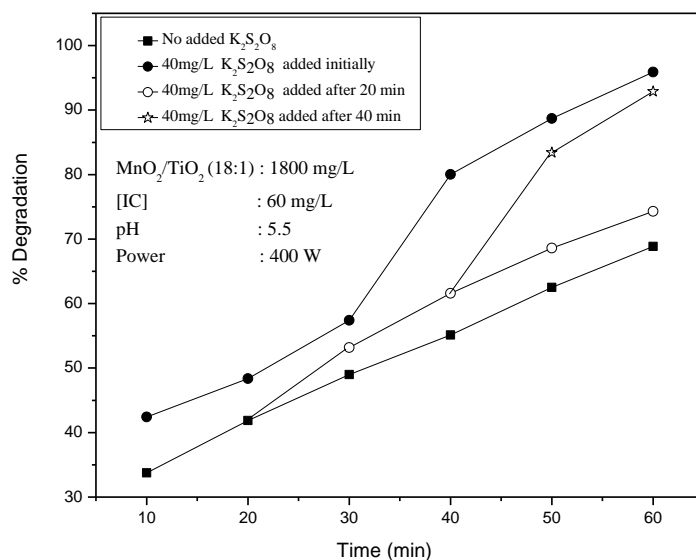
Fig.4.42: Effect of initial and in-between addition of $K_2S_2O_8$ on the UV/(MnO$_2$-TiO$_2$) degradation of IC

The degradation is enhanced from the point of addition of PS and goes on increasing with every increase in the concentration of PS. Probable mechanism of enhancement in presence of PS is explained in Section 4.3.6.2 and Section 3.3.3.10.2 of Chapter 3.

Combination of these two oxidants, i.e. H_2O_2 and PS, widely used in many AOTs, resulted only in slight enhancement in the degradation achieved in presence of PS and the combined effect is slightly more than the average of the positive effect of PS and the negative effect of H_2O_2 (Fig.4.43). Hence the combination oxidant (PS + H_2O_2) does not offer any significant advantage over PS for the degradation of IC.
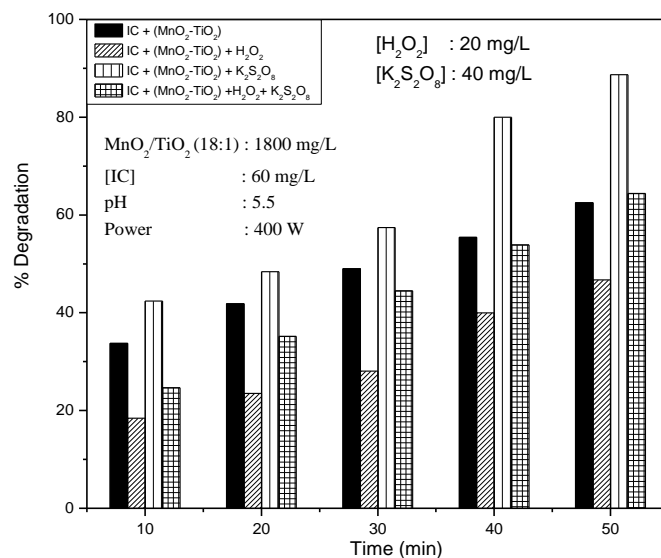
Fig. 4.43: Effect of combination of K$_2$S$_2$O$_8$ and H$_2$O$_2$ on the UV/(MnO$_2$-TiO$_2$) degradation of IC

4.3.11.6 Effect of Anions

The presence of dissolved salts (anions) in water has been shown to influence the degradation of many organic pollutants. The effect of some of the common anions usually present in water on the degradation of IC in presence of MnO$_2$ catalyst and UV light irradiation is already discussed in Section 4.3.7. The effect of these anions i.e. SO$_4^{2-}$, Cl$^-$, PO$_4^{3-}$, CO$_3^{2-}$, CH$_3$COO$^-$, HCO$_3^-$ and NO$_3^-$ on the efficiency of UV/(MnO$_2$-TiO$_2$) degradation of IC is tested at various concentrations and reaction times. The results are presented in Fig. 4.44A and Fig.4.44B.
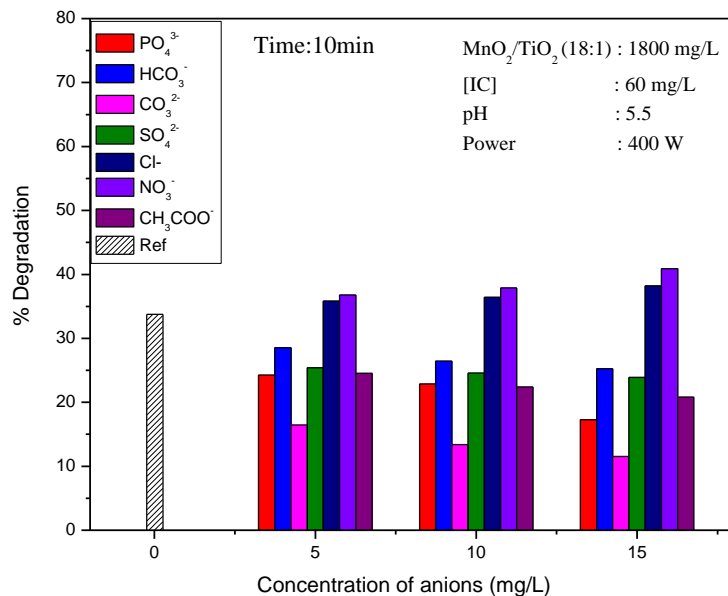
Fig. 4.44A: Effect of concentration of anions on the UV/(MnO$_2$-TiO$_2$) degradation of IC.

In the concentration range of 5-15 mg/L of the anions, the trend remains the same; i.e Cl$^-$ and NO$_3^-$ are mild enhancers while other anions are inhibitors. The effect is summarised in Table 4.8.

Table 4.8: Effect of concentration of anions on the UV/(MnO$_2$-TiO$_2$) degradation of IC

Concentration of Anions(mg/L)	Inhibition	Enhancement
5	$CO_3^{2-} > CH_3COO^- \approx PO_4^{3-} \approx SO_4^{2-} > HCO_3^-$	$NO_3^- \geq Cl^-$
10	$CO_3^{2-} > CH_3COO^- \approx PO_4^{3-} \approx SO_4^{2-} > HCO_3^-$	$NO_3^- \geq Cl^-$
15	$CO_3^{2-} > PO_4^{3-} > CH_3COO^- > SO_4^{2-} \approx HCO_3^-$	$NO_3^- \geq Cl^-$

The results show that the nature of the anion effect is independent of its concentration.

The effect of reaction time on the degradation is tested and the results are plotted in Fig.4.44B.
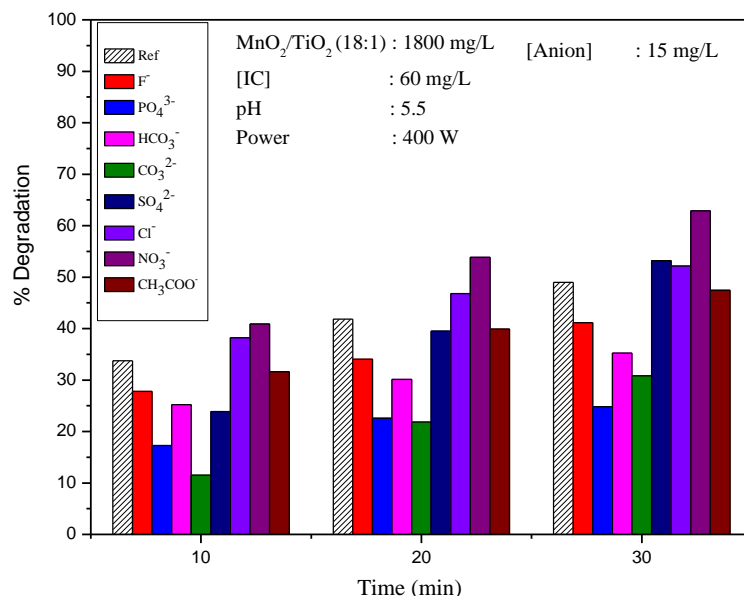
Fig. 4.44B: Effect of reaction time on the 'anion effect on
the UV/(MnO$_2$-TiO$_2$) degradation of IC'.

The effect of various anions follows the same trend at all reaction times (10-30min). The effect is summarised in Table 4.9.

Table 4.9: Effect of reaction time on the 'anion effect on the UV/(MnO$_2$-TiO$_2$) degradation of IC'.

Time(min)	Inhibition	Enhancement
10	$CO_3^{2-} > PO_4^{3-} > SO_4^{2-} \approx HCO_3^- > CH_3COO^-$	$NO_3^- > Cl^-$
20	$CO_3^{2-} \approx PO_4^{3-} > HCO_3^- > SO_4^{2-} \approx CH_3COO^-$	$NO_3^- > Cl^-$
30	$PO_4^{3-} > CO_3^{2-} > HCO_3^{--} > CH_3COO^-$	$NO_3^- > SO_4^{2-} \approx Cl^-$

The effect of added anions on the degradation of IC in presence of MnO$_2$-TiO$_2$ is somewhat different from that in presence of MnO$_2$ as demonstrated earlier in Section 4.3.7. In the case of MnO$_2$ mediated degradation, SO$_4^{2-}$ is a mild enhancer or has 'no effect'. In presence of MnO$_2$-TiO$_2$, SO$_4^{2-}$ is an inhibitor. However, towards later stages of the

*Microwave, Photo and Sono Activated Advanced Oxidation Processes and their
Variations for the Decontamination of Water from Toxic Chemical Pollutants*

301

reaction, SO_4^{2-} becomes a mild enhancer in this case also. In any case the 'anion effect' on the degradation of IC in presence of MnO_2 and MnO_2-TiO_2 can be considered fairly the same in general qualitatively.

The effect of individual anions on the photocatalytic degradation of IC is investigated in detail at more concentrations and the results are plotted in Figs. 4.45 to 4.51. The results show that the trend of anion effect remains the same; i.e, the inhibitor remains as the inhibitor at all concentrations and reaction times and the enhancer remains as enhancer throughout. The effect of SO_4^{2-}, which functions as an enhancer or an inhibitor in various AOPs depending on the reaction conditions retains the ambiguity in this instance also.

4.3.11.6.1 PO_4^{3-}
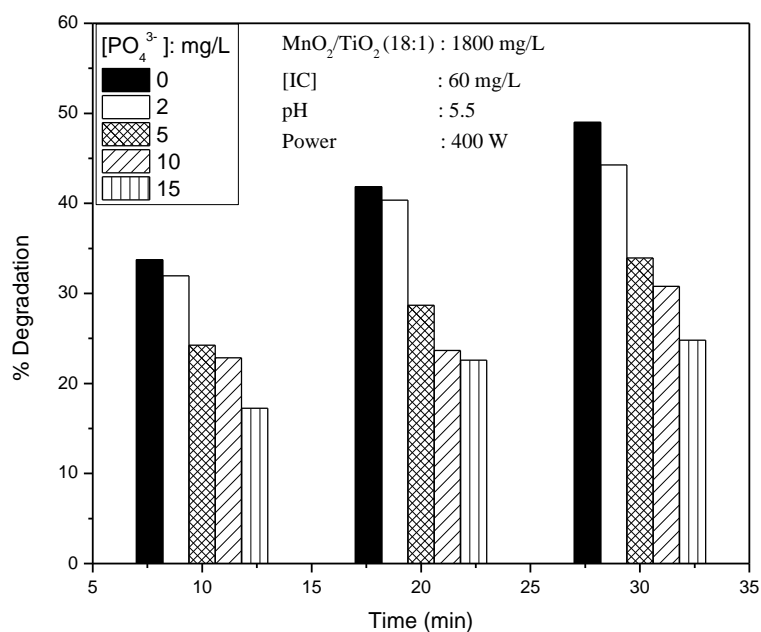
Fig. 4.45: Effect of PO_4^{3-} on the UV/(MnO_2-TiO_2) degradation of IC

PO$_4^{3-}$ remains as a strong inhibitor at all concentrations of the anion and all reaction times (Fig.4.45). The inhibition increases with increase in concentration.

4.3.11.6.2 CO$_3^{2-}$
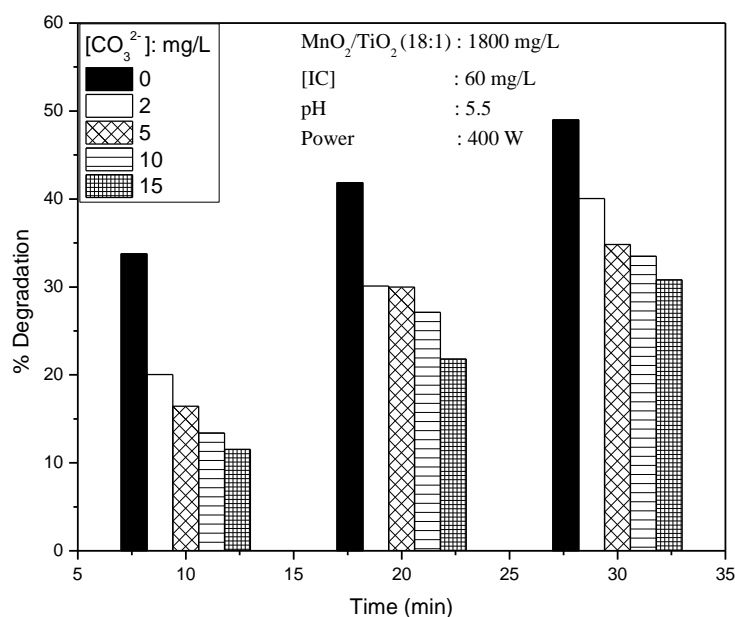
Fig. 4.46: Effect of CO$_3^{2-}$ on the UV/(MnO$_2$-TiO$_2$) degradation of IC

CO$_3^{2-}$ remains as a strong inhibitor at all concentrations of the anion and all reaction times (Fig.4.46). The inhibition increases with increase in concentration of the anion. However, the extent of inhibition decreases gradually with time (for 15 mg/L of anion, the inhibition is~70% in 10 minute while it is only 40% after 30min).

Microwave, Photo and Sono Activated Advanced Oxidation Processes and their Variations for the Decontamination of Water from Toxic Chemical Pollutants

303

4.3.11.6.3 SO_4^{2-}
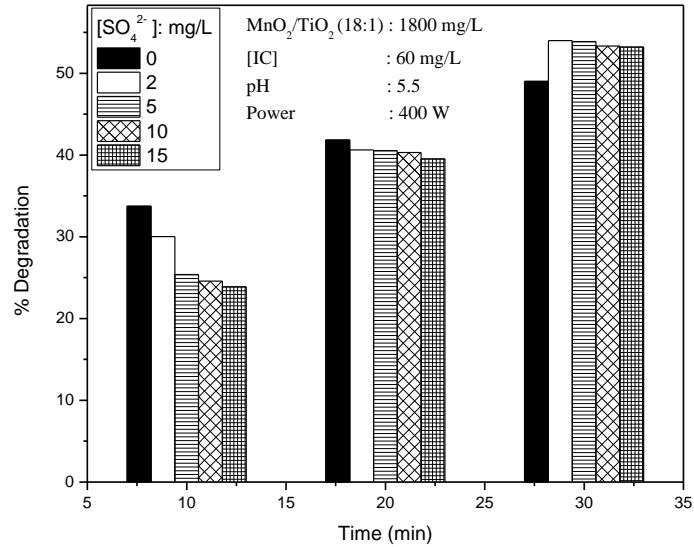
Fig. 4.47: Effect of SO_4^{2-} on the UV/(MnO$_2$-TiO$_2$) degradation of IC

In the initial stages of reaction, i.e, in 10 min, SO_4^{2-} is an inhibitor (Fig.4.47). However, the inhibition diminishes with time and it becomes practically 'nil' at~ 20min and mild enhancement in 30 minutes. The initial inhibition may be due to the adsorption of SO_4^{2-} on the catalytically active surface sites thereby preventing the photoactivation of the catalyst and inhibition of the adsorption of IC on the surface. However, with time more reactive $SO_4^{\cdot-}$, $\cdot OH$ etc are formed as follows:

In the case of SO_4^{2-} the limited number of anions that get adsorbed on the surface can interact with the photoproduced holes [188] to generate sulphate radical anions as follows:

$h^+ + SO_4^{2-} \rightarrow SO_4^{\cdot-}$ ....(104)
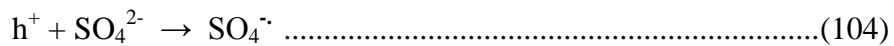
S is a strong oxidizing agent and hence the $SO_4^{\cdot-}$ radical can accelerate the degradation process according to reactions 31-41.

$$SO_4^{\cdot-} + H_2O \rightarrow SO_4^{2-} + {}^{\cdot}OH + H^+ \quad ....(105)$$

$$SO_4^{\cdot-} + \text{Pollutant} \rightarrow SO_4^{2-} + \text{Intermediate} \quad ....(106)$$

$$SO_4^{\cdot-} + \text{Intermediate} \rightarrow \cdots\cdots \rightarrow SO_4^{2-} + CO_2 + \text{Salts} \quad ....(107)$$
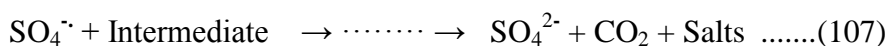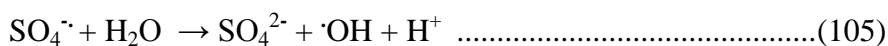
As seen in reaction 105, presence of $SO_4^{\cdot-}$ can lead to the formation of more reactive $^{\cdot}OH$ radicals. The $^{\cdot}OH$ radicals can accelerate the degradation of the dye. Hence, unlike in the case of other anions which scavenge the $^{\cdot}OH$, the SO_4^{2-} anions concurrently generates them. These are powerful oxidants and can accelerate the degradation of IC. This will also compensate for the decrease in degradation due to the loss of surface sites by SO_4^{2-} adsorption. The net effect is 'mild enhancement' towards later stages of reaction.

4.3.11.6.4 NO_3^-
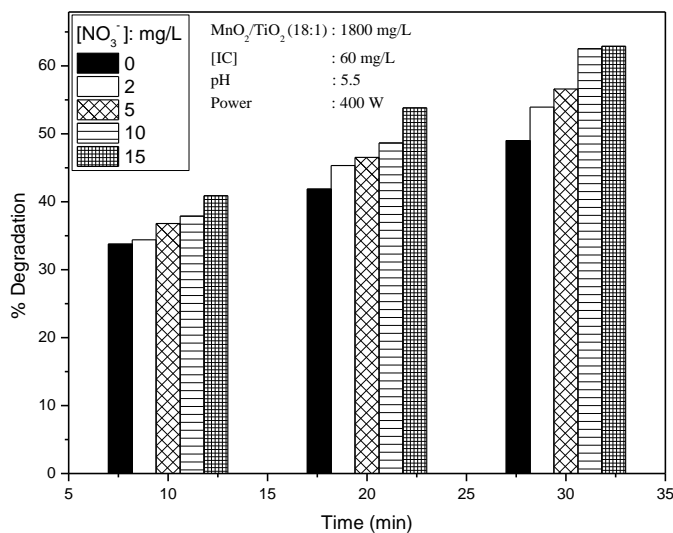
Fig. 4.48. Effect of NO_3^- on the UV/(MnO₂-TiO₂) degradation of IC

Microwave, Photo and Sono Activated Advanced Oxidation Processes and their Variations for the Decontamination of Water from Toxic Chemical Pollutants

305

As expected NO_3^- enhances the degradation at all concentrations and reaction times tested here (Fig.4.48). Probable causes for the enhancement by NO_3^- ions are discussed earlier (Section 4.3.7).

4.3.11.6.5 CH$_3$COO$^-$
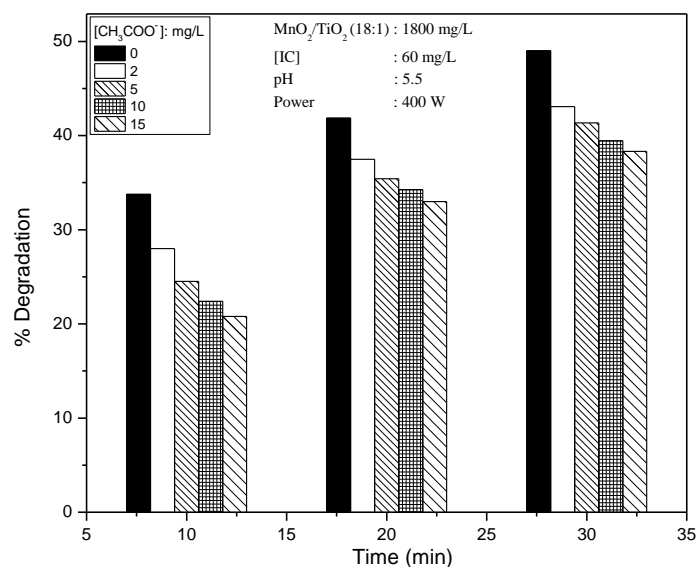
Fig. 4.49: Effect of CH_3COO^- on the UV/(MnO$_2$-TiO$_2$) degradation of IC

Acetate anion remains as an inhibitor throughout (Fig.4.49). The extent of inhibition diminishes with time. For eg. for 15 mg/L of the anions, the inhibition is~40% in the first 10 min. However, the inhibition becomes~20% by 30 min. The progressive formation of reactive radical anions which themselves are good oxidants and their more frequent interaction with the reduced amounts of IC gradually increases the rate of degradation. This results in a decrease in the degree of inhibition with time.

4.3.11.6.6 Cl$^-$
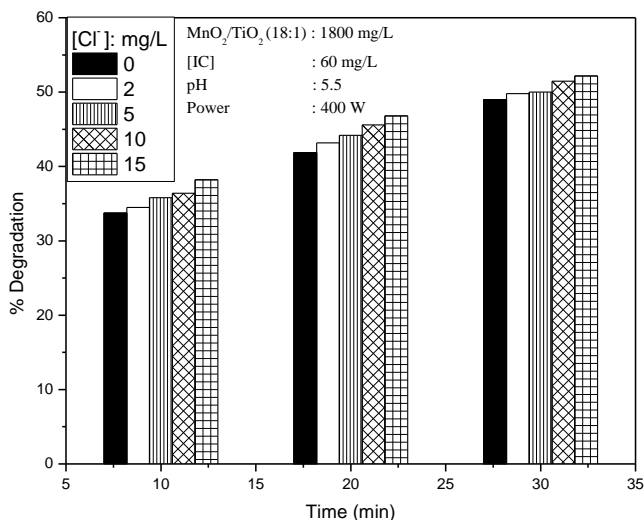
Fig. 4.50: Effect of Cl$^-$ on the UV/(MnO$_2$-TiO$_2$) degradation of IC

As in the case of MnO$_2$ catalyst, in the presence of the combination catalyst MnO$_2$-TiO$_2$ also, the degradation is mildly enhanced by Cl$^-$ (Fig.4.50). Probable causes are discussed in Section 3.3.3.12 of Chapter 3.

4.3.11.6.7 HCO$_3^-$
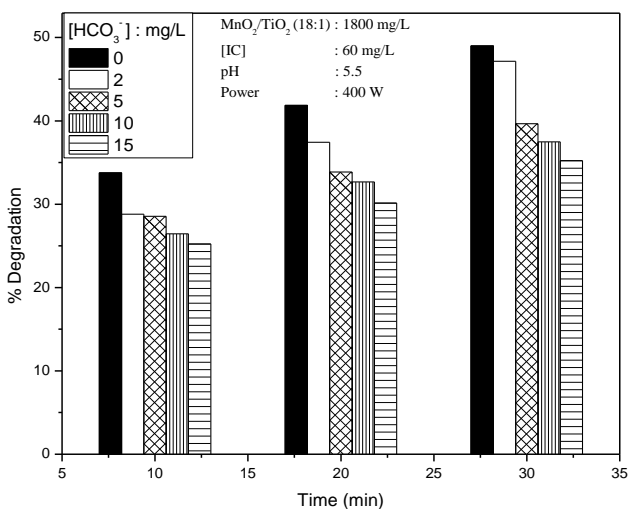
Fig. 4.51: Effect of HCO$_3^-$ on the UV/(MnO$_2$-TiO$_2$) degradation of IC

HCO_3^- continues to be a strong inhibitor at all concentrations and reaction times (Fig.4.51). The extent of inhibition remains almost the same throughout. Thus the inhibition which is ~ 27% in the beginning (15mg/L HCO_3^- 10min.) remains even after 30 min.

The effect of various anions on the MnO_2-TiO_2 catalysed photodegradation as above remains identical to the effect in presence of MnO_2 catalyst with only minor variations. Possible reasons for the effect including the inconsistent behaviour of certain anions at times are explained under Section 4.3.7. The explanations can be extrapolated in the case of MnO_2-TiO_2 also.

4.3.11.7 Effect of Oxygen

The role of dissolved O_2 in the solution and adsorbed as well as lattice O_2 in the catalyst on the photodegradation of IC is well illustrated in the case of MnO_2 in Section 3.3.3.13 of Chapter 3. The role of O_2, in particular the dissolved O_2 in the photocatalytic degradation of IC on MnO_2-TiO_2 also is verified by deaerating the system using N_2. The results show that deoxygenation has practically no effect on the degradation of IC (Fig.4.52). As discussed earlier, the effect of deaeration on MnO_2 catalysed degradation is different from that in presence of other semiconductor oxide catalysts, which require dissolved O_2 as an essential component. However in presence of MnO_2, lattice O_2 from it can take the place of dissolved O_2 and play an important role in the degradation of IC. The results indicate that this is possible in the case of MnO_2-TiO_2 also.
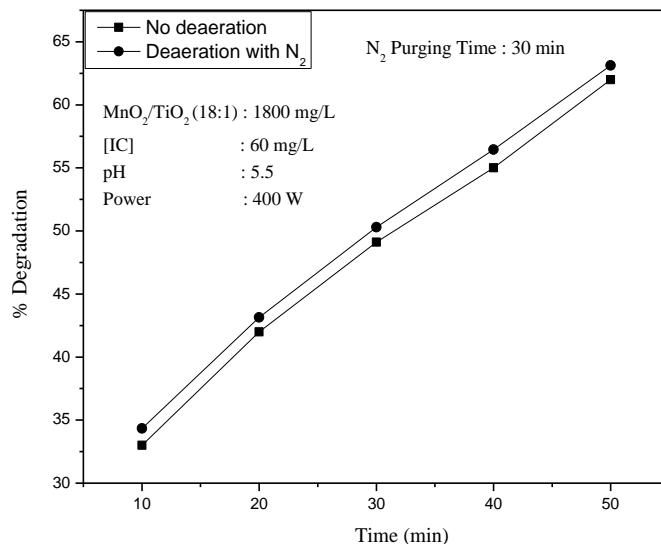
Fig. 4.52: Effect of deaeration with N_2 on the UV/(MnO₂-TiO₂) degradation of IC

It has been proven in the case of MnO_2 that at lower dosages of the catalyst, when the relative amounts of lattice oxygen and strongly adsorbed surface oxygen are less, removal of dissolved O_2 by deaeration with N_2 will inhibit the degradation of the substrate. The experiment is repeated with MnO_2-TiO_2 catalyst also at two different lower dosages of 50 and 100mg/L. The results are presented in Fig.4.53. The degradation is significantly inhibited in this case. This implies that at lower dosages of MnO_2-TiO_2, the lattice O_2 from the catalyst is not enough and dissolved O_2 is essential for the degradation of IC. However at higher concentrations (1800mg/L) the effect of deaeration is practically negligible because the requirement of O_2 can be satisfied by the lattice O_2 as well as strongly bound surface O_2 available in the O_2 - rich MnO_2. Further details are discussed in Section 4.3.8.

Microwave, Photo and Sono Activated Advanced Oxidation Processes and their Variations for the Decontamination of Water from Toxic Chemical Pollutants

309
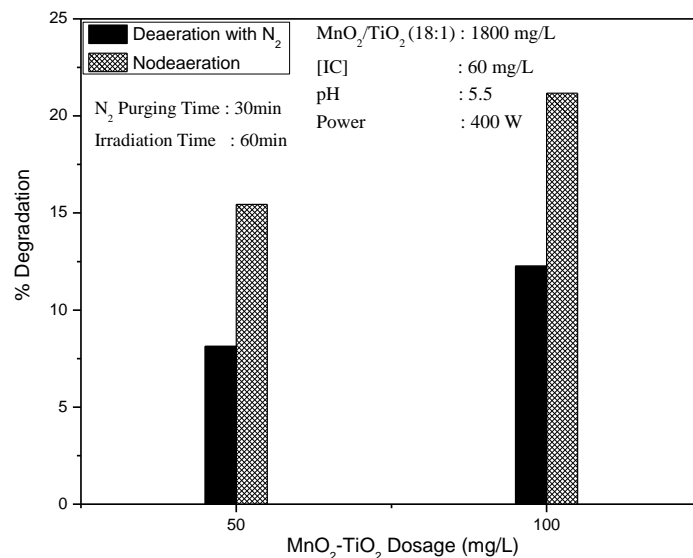
Fig. 4.53: Effect of deaeration with N_2 on the UV/(MnO_2-TiO_2) degradation of IC at lower dosages of the catalyst

4.3.11.8 Recycling of the Catalyst

Commercial application of any catalyst depends on its potential for reuse. Recycling of MnO_2-TiO_2 catalyst is studied by separating it from the reaction system (after complete decolourisation of IC), followed by washing and drying. This catalyst is then used for studying the % degradation of IC at various reaction times. The results are presented in Fig.4.54. The degradation of IC (in 30 minutes) decreased from ~ 49 % in the presence of the fresh catalyst to ~ 42% in first recycling, and ~37% in second recycling. Catalytic activity decreases slightly after first use and moderately in subsequent uses. The decreasing activity may be due to the partial deactivation of the catalytic sites due to surface deactivation, remnants of strongly bound substrate/ intermediate species on the surface, which prevent the efficient absorption of UV by MnO_2-TiO_2 and subsequent generation of reactive free radicals, depletion of adsorbed and

lattice oxygen from MnO_2 etc. The decrease in activity with recycling is less compared to that in the case of MnO_2, thereby suggesting that the presence of TiO_2 enhances the reusability of the catalyst (MnO_2).
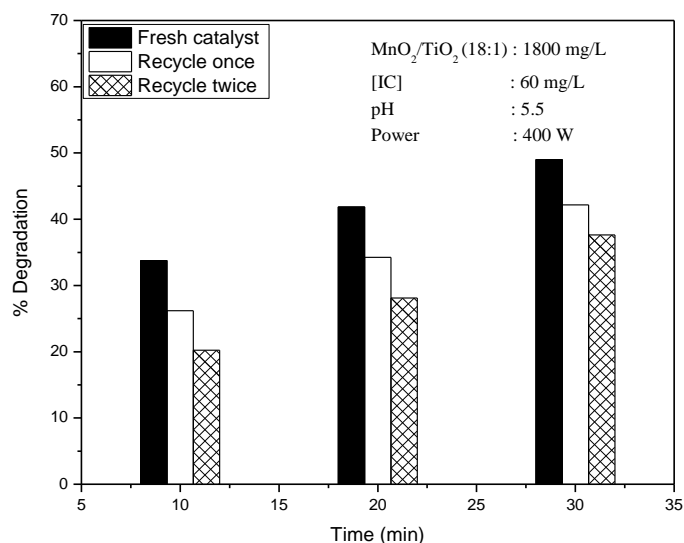
Fig. 4.54: Comparative efficiency of fresh and recycled catalyst for the UV/(MnO_2-TiO_2) degradation of IC

4.3.11.9 COD of the reaction system under UV/(MnO_2-TiO_2)

The ability of MnO_2/TiO_2 to completely mineralise IC under UV irradiation has been demonstrated in Section 4.3.10, Fig.4.30B. While MnO_2 takes ~ 9 hrs, MnO_2-TiO_2 takes only 5 hrs under respective optimised conditions to achieve complete mineralisation. The results also show that while TiO_2 alone is as efficient as MnO_2-TiO_2 for mineralisation, the latter is superior for the faster decolourisation of IC. Depending on the concentration of the dye in the effluent water, appropriate catalyst combination has to be identified and optimised. If faster decolourisation followed by slow mineralisation is the preferred option, MnO_2-TiO_2 will be more advisable.

Microwave, Photo and Sono Activated Advanced Oxidation Processes and their Variations for the Decontamination of Water from Toxic Chemical Pollutants

311

4.4 Photocatalytic degradation of IC using Co_3O_4

Previous Chapter has demonstrated that Co_3O_4 is an efficient MW catalyst for the degradation of trace amounts of IC in water. Co_3O_4 is a p-type semiconductor which has been successfully used in many heterogeneous catalytic processes. However, the potential of Co_3O_4 as a photocatalyst has not received much attention. In this context, investigations on the application of Co_3O_4 as a photocatalyst are undertaken here in view of the encouraging results obtained using Co_3O_4 under MW radiation (Section 3.3.1 of Chapter 3). Since MnO_2 and MnO_2-TiO_2 which are active under MW are also proven to be very efficient photocatalysts, a similar study is extended to Co_3O_4 also.

Preliminary studies on the photocatalytic degradation of IC in the presence and absence of ultraviolet light and catalyst Co_3O_4 revealed that both catalyst and light are essential for reasonable degradation (Fig.4.55).
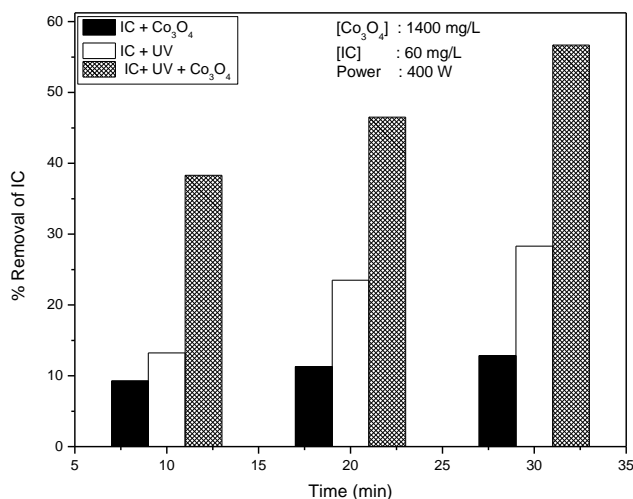
Fig. 4.55: Comparative 'decrease in concentration' of IC in presence of Co_3O_4 under various conditions

Moderate decrease in concentration of IC in presence of Co_3O_4, without UV is due to adsorption. In presence of Co_3O_4 and UV the degradation of IC is at least two times more than that in presence of UV only. Comparison of the results with MnO_2 or MnO_2-TiO_2 shows that Co_3O_4 also is an efficient photocatalyst. Hence all relevant parameters are optimised in this case also.

4.4.1 Effect of catalyst dosage

The catalyst dosage for optimum degradation of IC is experimentally verified in the range 100 to 1800 mg/L and the result is shown in Fig.4.56.
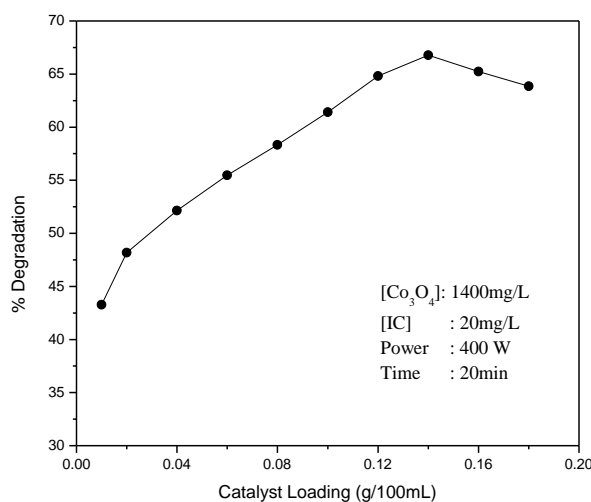
Fig. 4.56: Effect of catalyst loading on the UV/Co_3O_4 degradation of IC

The degradation of IC increases with increase in catalyst loading, reaches an optimum at 1400 mg/L and then stabilises or decreases slightly. As the loading increases, the availability of active surface sites for adsorption of the substrate also increases. Hence more molecules of IC

Microwave, Photo and Sono Activated Advanced Oxidation Processes and their Variations for the Decontamination of Water from Toxic Chemical Pollutants

313

will get adsorbed on the catalyst surface. Further, with increased number of particles getting exposed to UV irradiation, the generation of reactive free radicals also increases resulting in enhanced degradation of IC. But beyond the optimum dosage of catalyst, the degradation decreases because of the reduced passage of light through the medium. Aggregation of catalyst particles at higher loading also results in poor light activation of all particles. Other reasons for optimum in the catalyst dosage are discussed in earlier Chapters 3 and 4 Sections 3.3.3.1 and 4.3.2 respectively. The optimum catalyst loading under the current reaction conditions is 1400 mg/L. Hence all further studies are carried out with this dosage.

4.4.2 Effect of concentration of IC
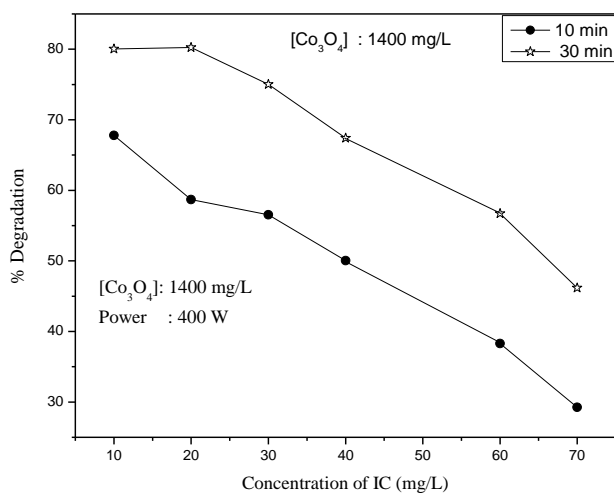
Fig. 4.57: Effect of concentration on the UV/Co_3O_4 degradation of IC

The percentage degradation of IC decreases with increase in its concentration (Fig.4.57). However the rate of degradation increases with increase in concentration up to 60 mg/L (Fig.4.58) and stabilises thereafter. The pseudo first order kinetics of the degradation and the

mechanism involving modified L-H model (as in the case of MnO_2 and MnO_2-TiO_2 mediated degradation and as explained in Sections 4.3.3 and 4.3.11.2 respectively) are verified by the plot ($1/r_0$ vs $1/C_0$) and the logarithmic plot Figs.4.59 and 4.60 respectively. The first order kinetics holds good up to 60 mg/L beyond which the reaction is almost zero order.
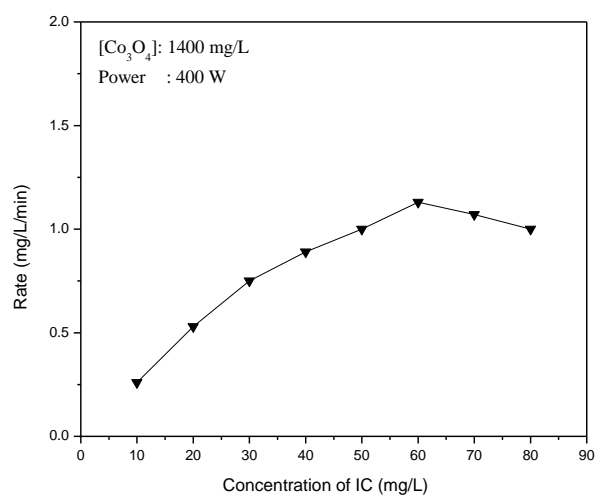
Fig. 4.58: Rate of UV/Co_3O_4 degradation of IC at various concentrations
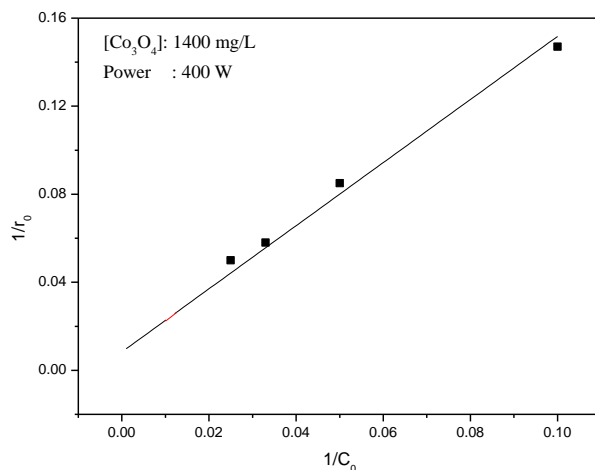
Fig. 4.59: Reciprocal plot of $1/r_0$ vs $1/C_0$ for the UV/Co_3O_4 degradation of IC
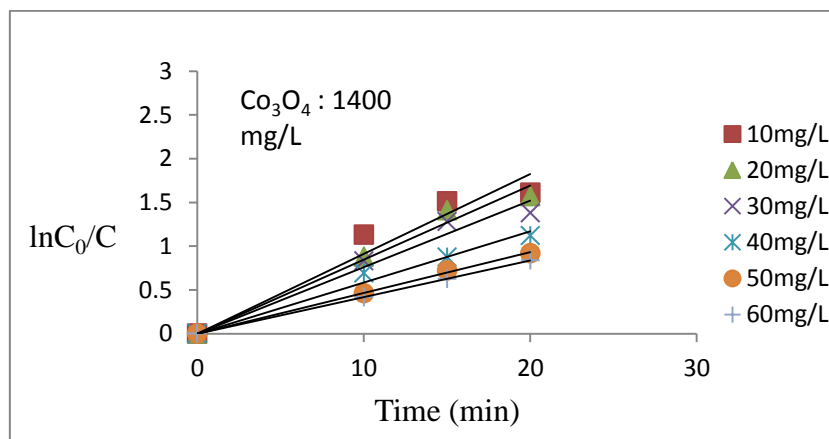
Fig. 4.60: Logarithmic plot for the UV/Co$_3$O$_4$ degradation of IC

Details on the variable kinetics, pseudo first order kinetics gradually changing to zero order, significance of variation in rate constants with concentration etc. are discussed in detail in Section 3.3.3.2 of Chapter 3.

4.4.3 Effect of pH

pH plays an important role in the photocatalytic degradation of pollutants in water as demonstrated in Sections 4.3.4 and 4.3.11.3 respectively. The effect of pH on the degradation of IC in presence of UV/Co$_3$O$_4$ is also investigated. The pH of the suspension was adjusted before irradiation and it was not controlled thereafter. The results are presented in Fig.4.61.
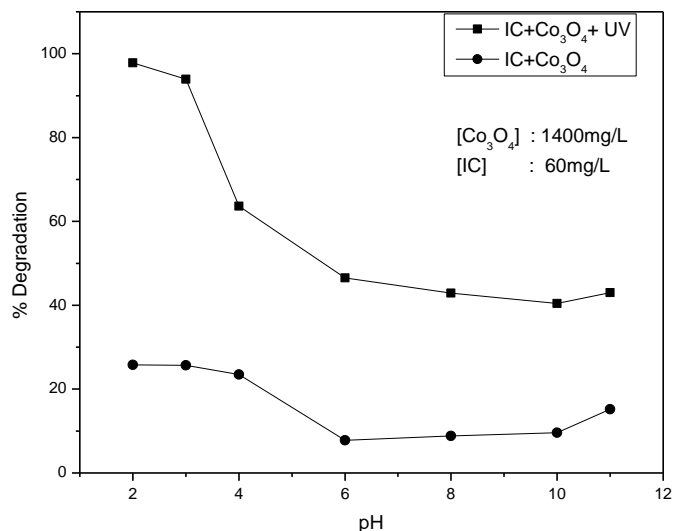
Fig. 4.61: Effect of pH on the photocatalytic degradation of IC

Degradation is more in the acidic region (pH 2-3). The degradation falls sharply from pH 3 to 6 and remains almost steady in the pH range 6-10. The dye removal in the range 2-4 is partially due to enhanced adsorption of IC on the catalyst as seen from the results even in the absence of UV radiation. The adsorption in 20 min in the absence of UV irradiation is ~ 25% while the UV/Co₃O₄ degradation under same conditions is ~100%. Hence, it may be concluded that the photocatalytic degradation of IC in presence of Co_3O_4 is facilitated by acidic pH aided by the strong adsorption and subsequent interactions with the ROS at the surface. This drastic increase in degradation occurring below pH 3 cannot be explained based on the point of zero charge (PZC) alone or any single parameter as already demonstrated in the case of MnO_2 (Section 4.3.4). The PZC of Co_3O_4 is ~7.3 below which the surface is positively charged. IC is a dianionic dye in aqueous solution and it can keep the dianionic

Microwave, Photo and Sono Activated Advanced Oxidation Processes and their Variations for the Decontamination of Water from Toxic Chemical Pollutants

317

configuration in the pH range 3-11. This implies that there will be strong electrostatic interaction between the positive catalyst surface and the dianions at pH < 7.3 which can lead to strong surface-substrate interaction and subsequent reaction. However the observed pH effect is not strictly according to this expected pattern since the high degradation is not sustained at all pH below 7.3. Hence, the pH effect cannot be attributed to any single specific parameter. This is consistent with the earlier observations reported in the case of MnO_2 and MnO_2-TiO_2 mediated degradation of IC (Sections 3.3.3.5 and 3.4.4 of Chapter 3 as well as Section 4.3.4 of this Chapter). The pH effect is the net result of the interplay of a number of surface and bulk processes which requires an in-depth study.

4.4.4 Formation of H_2O_2

Concentration of H_2O_2 formed during/after decolourisation of IC increases initially reaches an optimum then it decreases. The result is almost similar in the case of MnO_2-TiO_2 catalyst. The increase and decrease in the concentration of H_2O_2 during the degradation is due to the simultaneous formation and decomposition processes taking place during irradiation. Depending on the domination of either at any point of time, the concentration of H_2O_2 may be decreasing, increasing or even stabilising. Details of this phenomenon which at times leads to oscillation in the concentration of H_2O_2 are discussed in Section 4.3.5 as well as Chapter 3, Section 3.3.3.8.
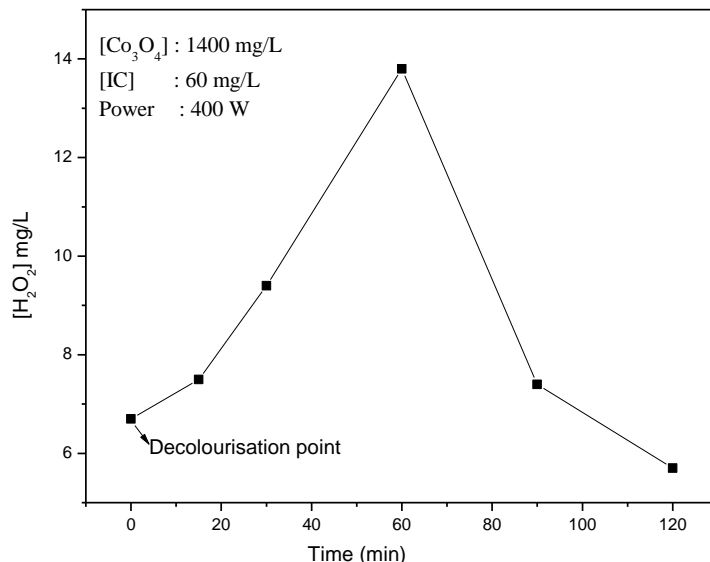
Fig. 4.62: Concentration of insitu formed H_2O_2 with time during UV/Co$_3$O$_4$ degradation of IC

4.4.5 Effect of Oxidants

4.4.5.1 Effect of added H_2O_2

The effect of H_2O_2 on the AOP processes is often unpredictable and inconsistent, varying from enhancement, inhibition or 'no effect'. In this context, as done in the case of MnO_2 and MnO_2-TiO_2, the effect of externally added H_2O_2 on the degradation of IC is tested under different conditions (Fig.4.63). Unlike in the case of MnO_2 or MnO_2-TiO_2 mediated degradation, where H_2O_2 functions as an inhibitor, the degradation increases mildly with increase in the concentration of H_2O_2 in the presence of Co_3O_4 (Fig.4.63d). In the absence of Co_3O_4 and UV the degradation increases upto ~10% in presence of 60 mg/L of H_2O_2

Microwave, Photo and Sono Activated Advanced Oxidation Processes and their Variations for the Decontamination of Water from Toxic Chemical Pollutants

319

(Fig.4.63a). Under UV irradiation, the degradation can be as high as ~35% in presence of 60 mg/L of H_2O_2 (Fig.4.63c).
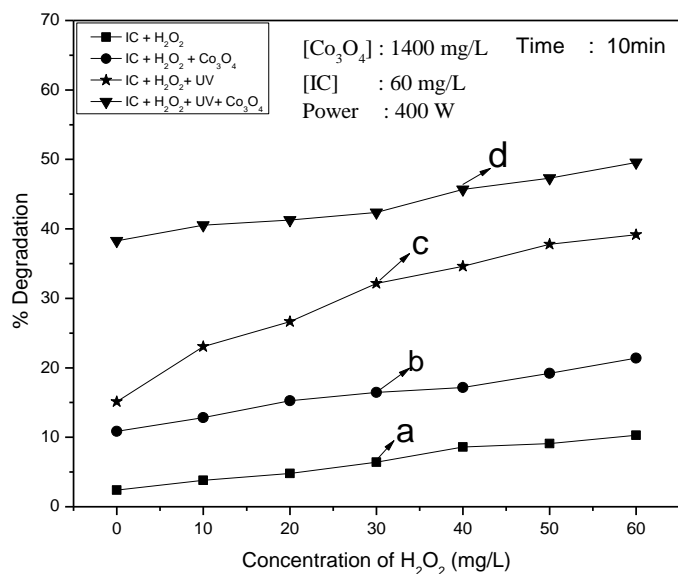
Fig. 4.63: Effect of added H_2O_2 on the UV/Co_3O_4 degradation of IC

The adsorption of IC on Co_3O_4 is not affected much by the presence of H_2O_2 irrespective of its concentration {Fig.4.63(b)}. The photocatalytic degradation of IC in presence of Co_3O_4 is not affected much by H_2O_2 upto 30mg/L (of H_2O_2). Thereafter, the degradation increases slowly with increase in the concentration of H_2O_2 {Fig.4.63(d)}. The increase can be attributed to the presence of more ˙OH radicals formed in the reaction system from added H_2O_2. It is possible that the enhancing effect of H_2O_2 increases only slowly because the concentration of the extra ˙OH radicals generated may not be adequate. Further, the ˙OH radicals may be participating in the recombination and other unproductive interactions

resulting in less efficient species. In order to verify this, higher quantity of H_2O_2 (100-200mg/L) is used in one experiment. The results are presented in Fig.4.64. It is seen that after the slow enhancement in degradation up to 60 mg/L of H_2O_2, when the concentration is increased to 100 and 200mg/L, the enhancement also is accelerated. Hence it is evident that the H_2O_2 in the system participates in multiple interactions and the increasing number of ·OH radicals generated in the process enhances the degradation of IC.
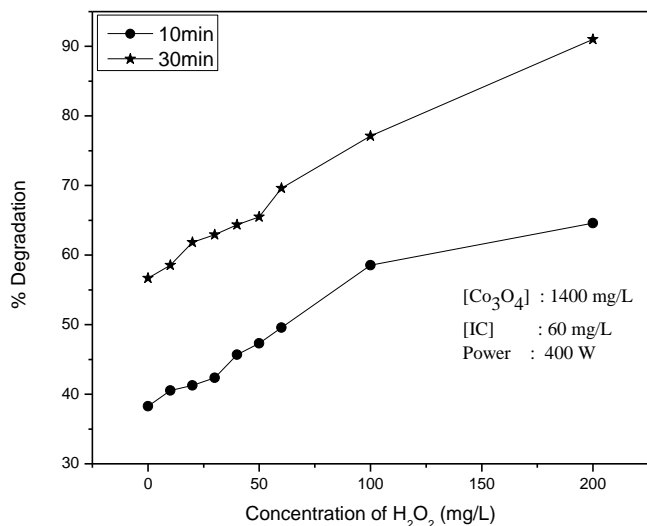
Fig. 4.64: Effect of higher concentration of H_2O_2 on the UV/Co₃O₄ degradation of IC

The effect of H_2O_2 is further confirmed by the addition of H_2O_2 in-between to the reaction Co₃O₄/IC/UV in progress. Results are shown in Fig. 4.65. Every extra addition of H_2O_2 (20 min and 40 min) increases the % degradation of IC.
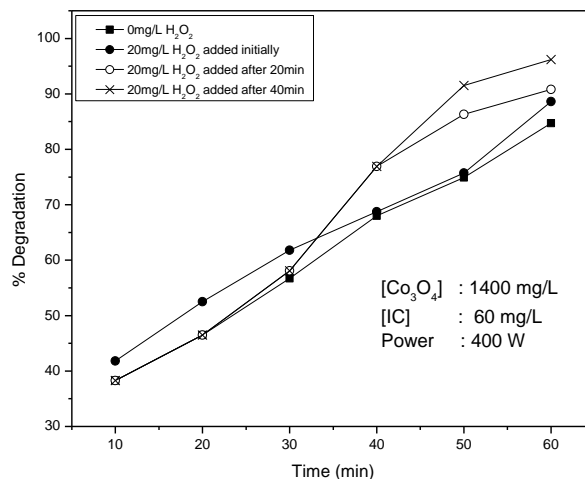
Fig. 4.65: Effect of in-between addition of H_2O_2 on the UV/Co_3O_4 degradation of IC.

It is interesting to note that H_2O_2 enhances the degradation of IC moderately in presence of Co_3O_4 which is contrary to the effect in presence of MnO_2 and MnO_2-TiO_2 catalyst. This is consistent with the results on the effect of H_2O_2 on the photocatalytic degradation of water pollutants, in presence of ZnO and TiO_2 catalysts as reported earlier [156]. In the case of MnO_2 which is very efficient for the decomposition of H_2O_2 even in the absence of any energy source, the added H_2O_2 is decomposed to H_2O and O_2. In presence of a source of activation such as MW or light, the insitu formed reactive free radicals such as ˙OH, HO₂˙ etc. will be deactivated by H_2O_2 by interacting with them. This results in net inhibition of the degradation of the target pollutants as explained in Section 3.3.9 Chapter 3. However in the case of Co_3O_4 the deactivation of H_2O_2 in to H_2O and O_2 is not as facile as in the case of MnO_2. Under UV irradiation H_2O_2 can generate more reactive free radicals ˙OH and HO₂˙ which can interact with IC and enhance the degradation. It is noteworthy that the enhancement by H_2O_2 is only mild and does not increase much

with increase in concentration of H_2O_2 (in the range 0-60mg/L). In this concentration range competing reactions involving H_2O_2 leading to the inactivation of the reactive free radicals also take place as explained in Section 4.3.6.1. When these interactions leading to the formation and consumption of reactive free radicals balance, the effect of H_2O_2 is stabilised. However at very high concentration of H_2O_2 (> 60mg/L) the rate of formation of reactive radicals such as ·OH will be more dominant compared to the consumption resulting in more frequent interaction with IC and increased enhancement of the degradation. Various free radical reactions occurring in presence of H_2O_2 are given in Section 4.3.6.1.

4.4.5.2 Effect of $K_2S_2O_8$

Persulfate is another oxidant investigated as a potential enhancer of the UV/Co_3O_4 degradation of IC. The effect of externally added $K_2S_2O_8$ on the degradation of IC is tested under different conditions and the results are presented in Fig.4.66.
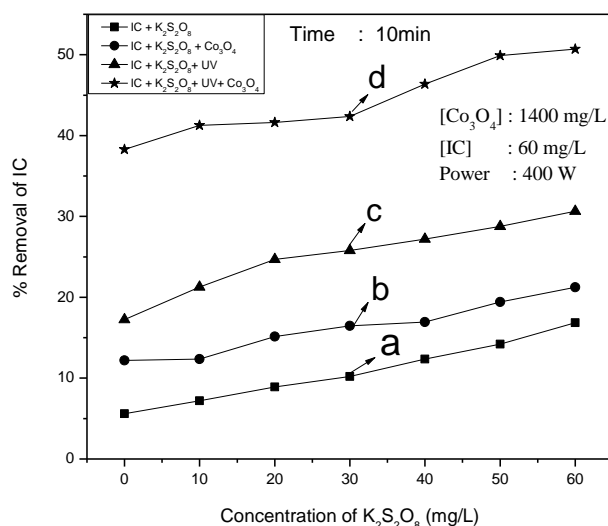
Fig. 4.66: Effect of added $K_2S_2O_8$ on the UV/Co_3O_4 degradation of IC

Even in the absence of catalyst and light PS assists the degradation of IC and the degradation increases mildly with increase in the concentration of PS {Fig.4.66(a)}. For the same system (without catalyst), the degradation of IC is more than doubled in presence of UV irradiation {Fig.4.66(c)}. The combination of Co_3O_4 and PS also leads to decrease in the concentration of IC, primarily due to adsorption {Fig.4.66 (b)}. Irradiation by UV enhances the degradation of IC in the IC/Co_3O_4/PS system significantly {Fig. 4.66(d)}.

The effect of PS at higher concentration, at different times of reaction is presented in Fig.4.67. The degradation increases steeply with increase in concentration and reaction time. This also confirms that PS does not have any negative effect on the degradation of IC even at very high concentration or after extended times of reaction. This is important in the commercial application of the process.
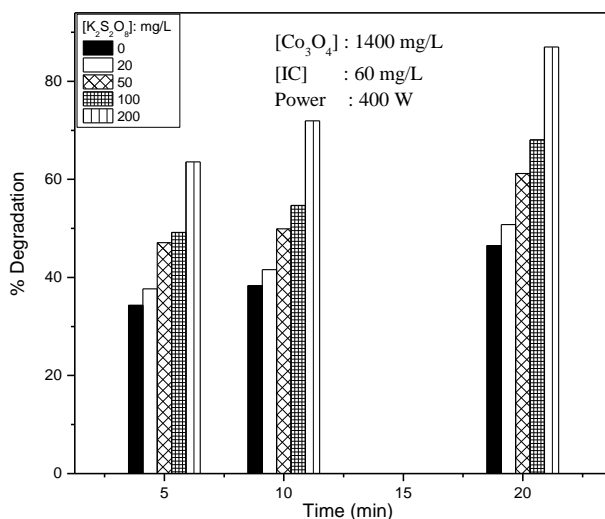
Fig. 4.67: Effect of higher concentration of $K_2S_2O_8$ on the UV/Co_3O_4 degradation of IC

The enhancing effect of $K_2S_2O_8$ is further confirmed by addition of $K_2S_2O_8$ in-between to a reaction in progress. Results are shown in Fig.4.68. Every extra addition of $K_2S_2O_8$ (20 min and 40 min) increases the % degradation of IC.
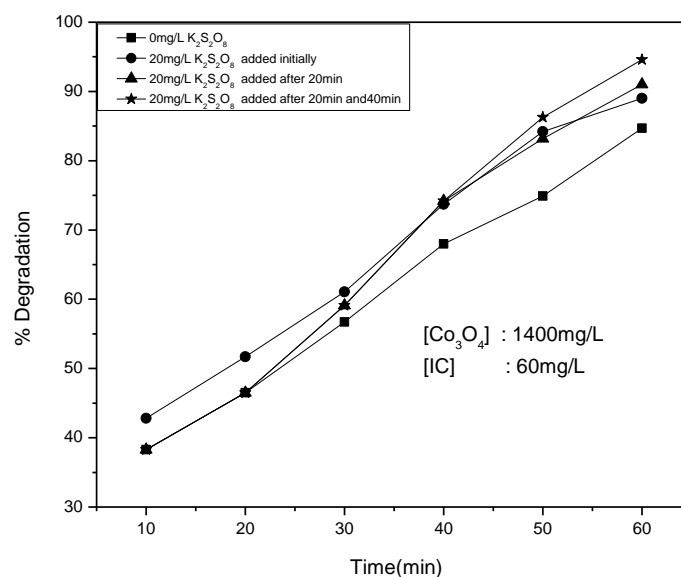
Fig. 4.68: Effect of in-between addition of $K_2S_2O_8$ on the UV/Co₃O₄ degradation of IC.

The enhancement of photocatalytic degradation of organics by PS is attributed to the formation of highly reactive $SO_4^{.-}$ as well as ˙OH radicals from various interactions (Details are given in Section 4.3.6.2). The advantage of using PS compared to H_2O_2 is that, excess of the oxidants does not have any negative effect and can be used in continuous type treatment systems.

The effect of combination of the two oxidants (H_2O_2 and PS) on the UV/Co₃O₄ degradation of IC is investigated and the results are plotted in Fig.4.69.
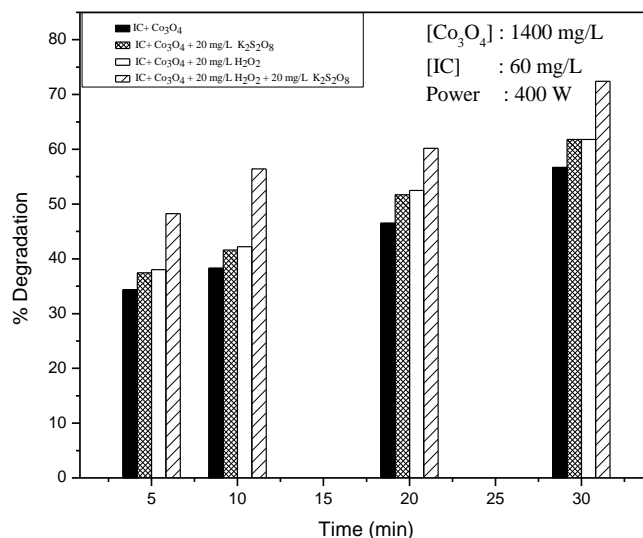
Fig. 4.69: Effect of combination of $K_2S_2O_8$ and H_2O_2 on the UV/Co_3O_4 degradation of IC

The combination enhances the degradation of IC and this enhancement is more than the sum of enhancement by the individual components H_2O_2 and PS. Hence the effect of the combination is synergistic. This is one of the rare cases of synergy in the oxidation efficiency of H_2O_2 and PS. In many cases, including the results reported earlier in this thesis also, the combination effect is at best additive and often less than additive. Hence this synergy can be attributed to the specific characteristics of Co_3O_4 as a photocatalyst. It is worth noting that H_2O_2 is an inhibitor of the degradation of IC in presence of MnO_2 while it is an enhancer in presence of Co_3O_4. The highly active MnO_2/ MnO_2-TiO_2 may be leading to multitude of formation and destruction reactions of free radicals ($^.OH$, $SO_4^{.-}$ etc.) which may be detrimental to any synergy. In this respect a more manageable moderately active Co_3O_4 may be another option.

The % synergy at different times of reaction is calculated as follows.

$$\% \text{ synergy} = [A - (B+C)] / (B+C)] \times 100 \quad \text{................................(108)}$$

where

A = % enhancement by (H_2O_2+PS)
B = % enhancement by H_2O_2
C = % enhancement by PS

The synergy increases with time reaches an optimum and then decreases steeply (Fig.4.70). Hence it is clear that the synergy is optimum when the concentration of the substrate is adequate to interact with highly reactive free radicals generated from H_2O_2 and PS and there are not many intermediates to compete for the ROS. At later stages of reaction when the system has too many competitors for interacting with the ROS, the degradation of the substrate slows down and so will the synergy. However, the inconsistency in the degradation of IC due to the simultaneous generation and consumption of ROS, is reflected in the synergy also as seen in the results after 20 and 30 minutes.
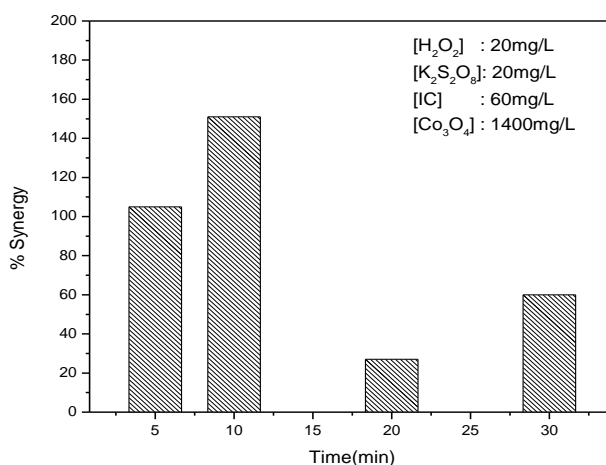
Fig. 4.70: % synergy of the oxidation efficiency of H_2O_2 and PS in their combined presence in UV/Co₃O₄ degradation of IC

4.4.6 Effect of Anions

The effect of added anions/salts on the photocatalytic degradation of IC has been investigated in presence of MnO_2 and MnO_2-TiO_2 as catalysts. Hence similar studies are undertaken in the case of Co_3O_4 as catalyst also.

The presence of ions /salts present in natural wastewater affects the efficiency of degradation. In most cases, these ions inhibit the degradation, by scavenging the reactive $^{\cdot}OH$ radicals by surface layer formation and blocking the active sites by preferential adsorption. The extent of inhibition depends on a number of factors such as nature of substrate, nature of salt and its concentration, pH etc. The effect of some of the commonly occurring anions in water, i.e. SO_4^{2-}, Cl^-, PO_4^{3-}, CO_3^{2-}, HCO_3^- and NO_3^- on the efficiency of UV/Co_3O_4 degradation of IC is tested at various concentrations and reaction times and the results are presented in (Figs. 4.71 A and B) respectively. The results showed that SO_4^{2-} and NO_3^- enhance the degradation moderately at all concentrations and reaction times. PO_4^{3-} and CO_3^{2-} inhibit the degradation. HCO_3^- and CH_3COO^-, Cl^- have practically no effect though at later stages of reaction HCO_3^- shows slight inhibition. The results show that the trend remains more or less the same at all concentrations and reaction times. The effect of concentration of anion on the degradation of IC is summarized in Tables 4.10.
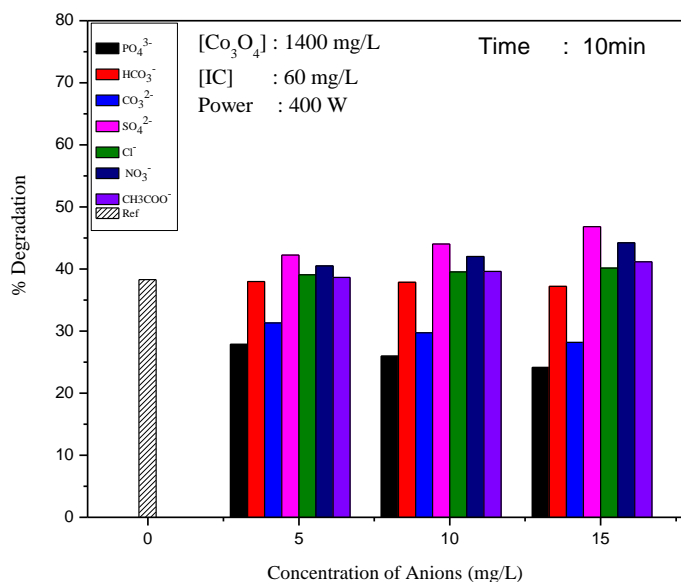
Fig. 4.71 A: Effect concentration of anions on the UV/Co_3O_4 degradation of IC.

Table 4.10: Effect of concentration of anions on the UV/Co_3O_4 degradation of IC   (Time: 10min)

Concentration of Anions(mg/L)	Inhibition	No Effect	Enhancement
5	$PO_4^{3-} > CO_3^{2-}$	HCO_3^-, Cl^-, CH_3COO^-	$SO_4^{2-} \geq NO_3^-$
10	$PO_4^{3-} > CO_3^{2-}$	HCO_3^-, Cl^-, CH_3COO^-	$SO_4^{2-} \geq NO_3^-$
15	$PO_4^{3-} > CO_3^{2-} > HCO_3^-$	Cl^-, CH_3COO^-	$SO_4^{2-} \geq NO_3^-$

The results show that the concentration of the anions does not change the nature of the effect on the degradation of IC much.
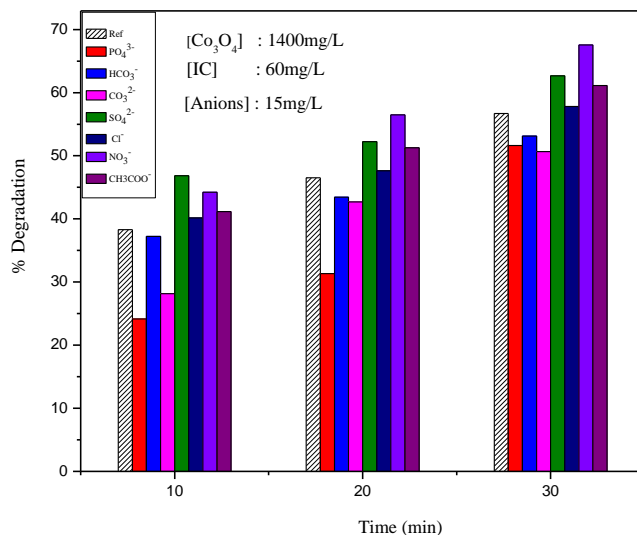
Fig. 4.71B: Effect of reaction time on the 'anion effect on the UV/Co$_3$O$_4$ degradation of IC'.

The effect of reaction time on the 'anion effect on the UV/Co$_3$O$_4$ degradation of IC' is given in Table 4.11.

Table 4.11: Effect of reaction time on the 'anion effect on the UV/Co$_3$O$_4$ degradation of IC'

Time (min)	Inhibition	No effect	Enhancement
10	PO$_4^{3-}$ > CO$_3^{2-}$ > HCO$_3^-$	Cl$^-$, CH$_3$COO$^-$	SO$_4^{2-}$ > NO$_3^-$
20	PO$_4^{3-}$ > CO$_3^{2-}$ ≈ HCO$_3^-$	Cl$^-$	NO$_3^-$ > SO$_4^{2-}$ ≈ CH$_3$COO$^-$
30	CO$_3^{2-}$ ≈ PO$_4^{3-}$ ≈ HCO$_3^{--}$	Cl$^-$	NO$_3^-$ > SO$_4^{2-}$ ≈ CH$_3$COO

The nature of the effect of anions on the degradation of IC does not change with time of the reaction except minor changes which may be treated as within the limits of experimental error as seen in Fig.4.71B and Table 4.11.

As done in earlier cases the effect of various anions on the photocatalytic degradation of IC is investigated in detail individually and the results are plotted in Fig. 4.72 to 4.78.

4.4.6.1 SO_4^{2-}

The effect of added SO_4^{2-} at different concentrations and reaction times on the degradation of IC is shown in Fig.4.72.
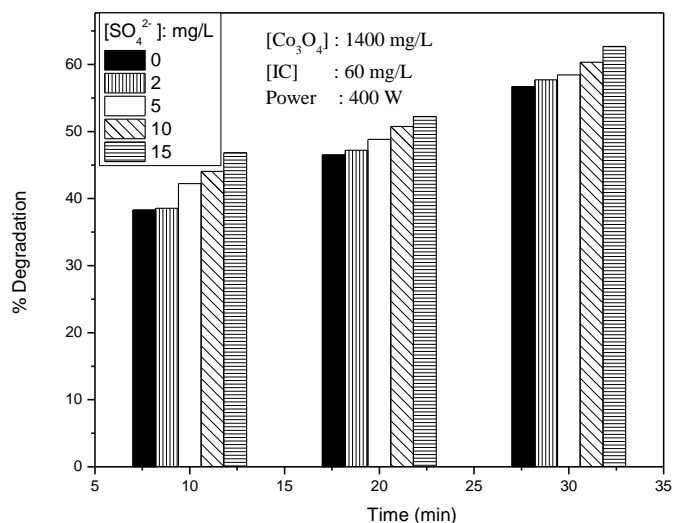
Fig. 4.72: Effect of SO_4^{2-} on the UV/Co₃O₄ degradation of IC in presence of Co₃O₄.

SO_4^{2-} enhances the photodegradation of IC moderately in presence of Co₃O₄. The enhancement increases with increase in concentration and reaction time. As concentration increases more reactive $SO_4^{-\cdot}$, $\cdot OH$ radicals etc are formed in the reaction system which enhance the degradation of IC.

4.4.6.2 PO_4^{3-}

PO_4^{3-} is a consistent inhibitor of photocatalytic degradation of IC (Fig.4.73).
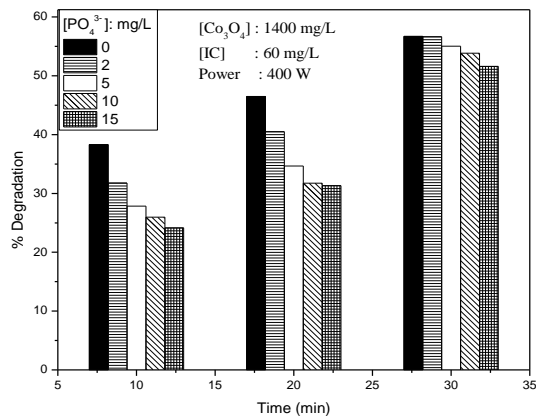
Fig. 4.73: Effect of PO_4^{3-} on the UV/Co_3O_4 degradation of IC

The inhibition is more with increasing concentration of the anion. However with time, the degree of inhibition weakens for all concentrations of PO_4^{3-}.

4.4.6.3 NO_3^-

The results presented in Fig.4.74 shows that added NO_3^- is an enhancer of the degradation at all concentrations and reaction times.
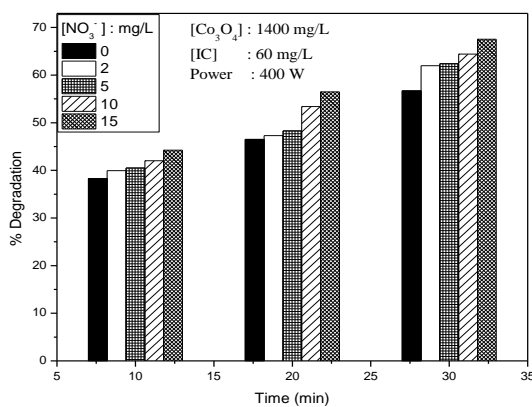
Fig. 4.74: Effect of NO_3^- on the degradation of IC in presence of Co_3O_4.

The degree of enhancement increases with increase in concentration of the anions and the reaction time.

4.4.6.4 Cl⁻

Added Cl⁻ has practically no effect on the degradation at all concentrations of the anion and reaction times studied here (Fig.4.75).
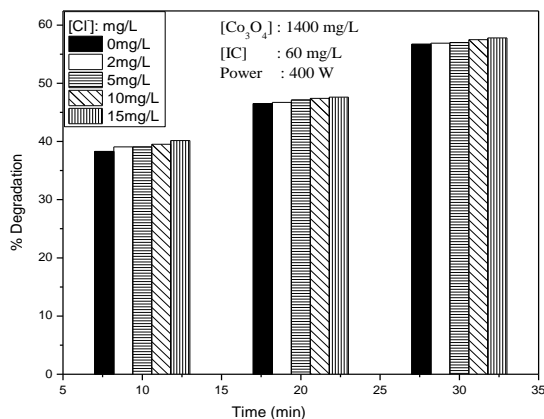
Fig. 4.75: Effect of Cl⁻ on the UV/Co₃O₄ degradation of IC

4.4.6.5 CO₃²⁻

CO_3^{2-} is a moderate inhibitor at all concentrations and reaction times.
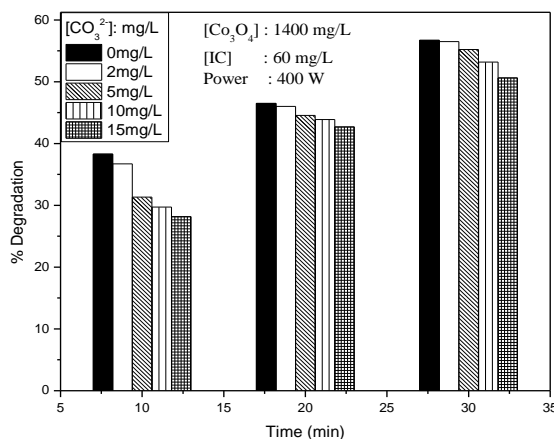
Fig. 4.76: Effect of CO_3^{2-} on the UV/Co₃O₄ degradation of IC

However, with time of reaction, the inhibition becomes weaker with practically no effect at lower concentrations of the anions.

Microwave, Photo and Sono Activated Advanced Oxidation Processes and their Variations for the Decontamination of Water from Toxic Chemical Pollutants

333

4.4.6.6 CH₃COO⁻

CH$_3$COO⁻ has no effect on the degradation at low concentration of anions (Fig.4.77).
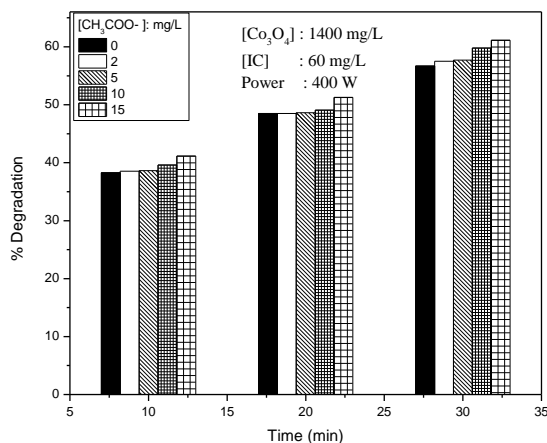
Fig. 4.77: Effect of CH$_3$COO⁻ on the UV/Co$_3$O$_4$ degradation of IC

However, with time of reaction, it becomes a mild enhancer especially at high concentration of the anion.

4.4.6.7 HCO₃⁻

HCO$_3$⁻ shows no effect in the initial stages of reaction (Fig.4.78).
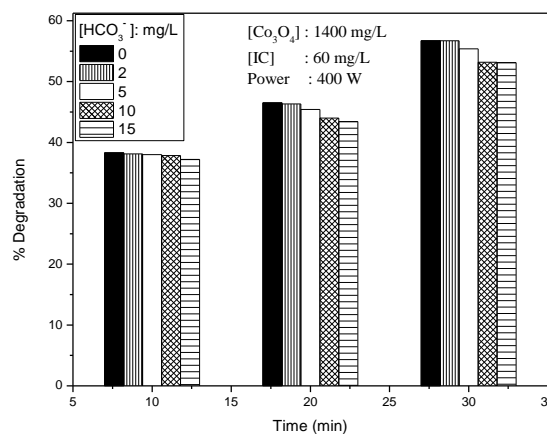
Fig. 4.78: Effect of HCO$_3$⁻ on the UV/Co$_3$O$_4$ degradation of IC

However, with reaction time, the 'no effect' changes to 'inhibition' at higher concentrations of the anion.

The results show that the anion effect remains generally the same for all salts in the case of MnO$_2$, MnO$_2$/TiO$_2$ and Co$_3$O$_4$ mediated photocatalysis with minor variations based on concentrations or reaction times. Hence the mechanism of action (inhibition, no effect, enhancement) also will be similar to that discussed in respective Sections 4.3.7 and 4.3.11.6 earlier.

4.4.7 Effect of oxygen

The role of dissolved O$_2$ in the degradation of IC is studied by deaerating the system using N$_2$. Deaeration has no influence on the degradation of IC and gives the same % degradation as the normal system (without deaeration). From the results presented in Fig.4.79, it is clear that dissolved O$_2$ in the system is not essential for the degradation of IC in presence of Co$_3$O$_4$. The same result was obtained in the case of MnO$_2$ and MnO$_2$-TiO$_2$ (as already explained in Sections 4.3.8 and 4.3.11.7). Hence in the case of Co$_3$O$_4$ also lattice O$_2$ from the catalyst plays an important role in the degradation of IC.

Fig. 4.79: Effect of deaeration with N$_2$ on the UV/Co$_3$O$_4$ degradation of IC

Microwave, Photo and Sono Activated Advanced Oxidation Processes and their Variations for the Decontamination of Water from Toxic Chemical Pollutants

335
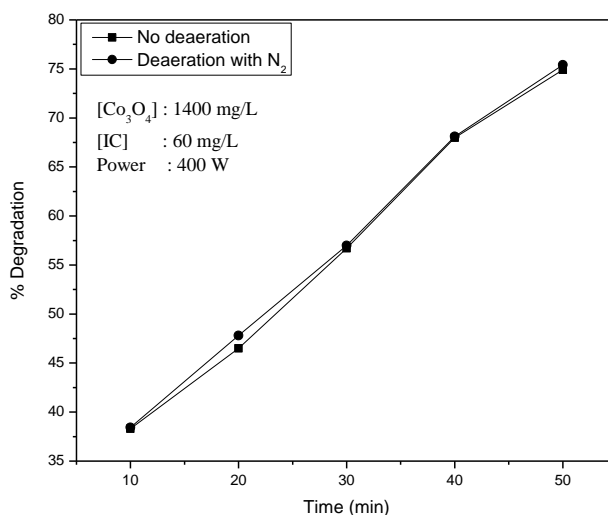
If the O_2 required for the degradation is extracted from the lattice and surface bound O_2 of the catalyst, the availability of O_2 will be less with decrease in catalyst dosage and this will lead to inhibition of the degradation in deaerated system. In order to verify this, experiments were done at two different lower Co_3O_4 dosages (50, 200 mg/L) (Fig.4.80).
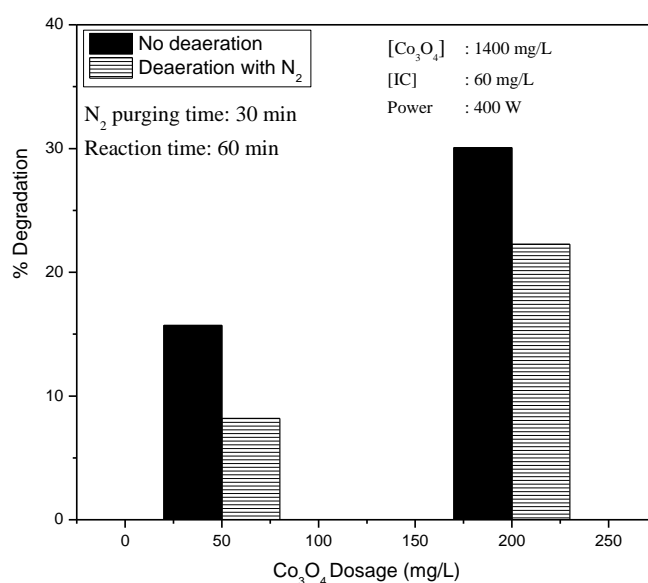
Fig. 4.80: Effect of deaeration with N_2 on the UV/Co_3O_4 degradation of IC at lower catalyst dosage

At very low concentration of Co_3O_4 (50 mg/L) its contribution of oxygen towards degradation of IC is less and hence deaeration by N_2 which drives the dissolved O_2 out inhibits the degradation. With increase in Co_3O_4 dosage, the availability of lattice and surface bound O_2 is more and hence the inhibition caused by the removal of dissolved O_2 (by deaeration) will be less. This is evident from the decreasing inhibition in deaerated system, when Co_3O_4 dosage is increased from 50 mg/L (inhibition ~ 50%) to 200 mg/L

(inhibition ~ 25%) and 1400 mg/L (inhibition ~ nil). The results suggest that dissolved O_2 is not the only source of O_2 in Co_3O_4 mediated photocatalysis. The required O_2 is also provided primarily by the surface (strongly bound) and the lattice of the catalyst which cannot be easily removed by flushing with N_2. This inference is further confirmed from the decreasing activity of Co_3O_4 with every recycling (Fig.4.81).

4.4.8 Recycling of Catalyst

The catalyst for recycling is prepared from the used catalyst as done in the case of Co_3O_4 used in MW catalysis. Experiments with fresh and used catalysts were conducted under identical conditions.
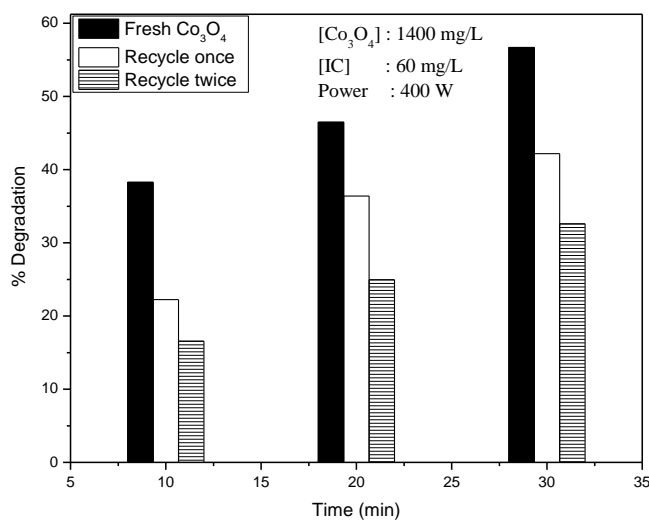
Fig. 4.81: Efficiency of recycled catalyst for the UV/Co₃O₄ degradation of IC

The degradation of IC (in 30 minutes) decreased from ~56 % in the presence of the fresh catalyst to ~ 42% in first recycling, ~32% in second recycling. i.e. catalytic activity decreases with every recycling. The reason

for the decreased activity such as partial deactivation of the catalytic site due to surface reactions, presence of the remnants of strongly bound substrate/ intermediate species on the surface, which prevent the efficient absorption of UV by Co_3O_4 and subsequent generation of reactive free radicals, depletion of adsorbed and lattice oxygen from Co_3O_4 etc. are already discussed in Section 4.3.9. The depletion of lattice O_2 from Co_3O_4, is also verified by comparing the EDX image of the used catalysts with the image of fresh catalyst, as under MW catalysis.

4.4.9 Verification of mineralisation by COD measurements

The complete mineralisation of IC under Co_3O_4/UV is verified by determining the chemical oxygen demand (COD at various intervals of irradiation. The system takes ~ 2 hr for complete decolourisation (Fig.4.82). During the period, COD decreases from 9.5 to 6 mg/L only. This indicates that degradation and subsequent mineralisation occurs through certain intermediates which are more difficult to be degraded compared to the parent compound. Hence the irradiation is continued even after decolourisation and COD is determined at regular intervals. Continued UV irradiation for another 2 hr brought down the COD to 4 mg/L. It needs another 7 hr UV irradiation to bring down the COD to nil, thereby suggesting the formation of even more stubborn intermediates towards the final stages of degradation. Eventually all the intermediates are also mineralised resulting in complete removal of COD.
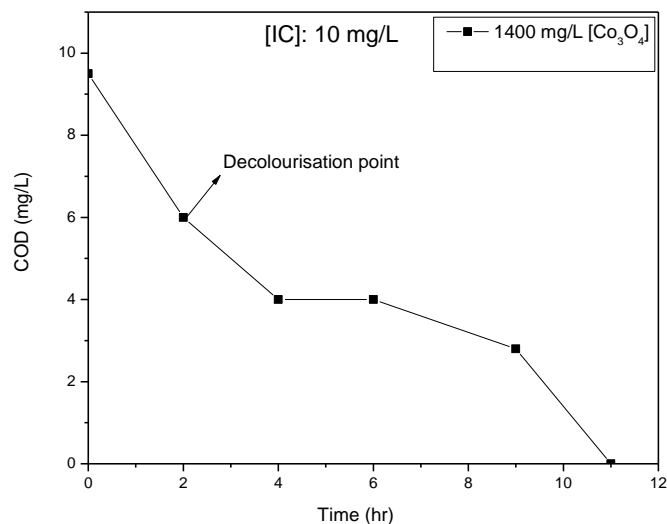
Fig. 4.82: COD of the UV/Co$_3$O$_4$ reaction system at different
times of irradiation

4.5 General mechanism

The mechanisms of various reactions/processes subjected to the study are discussed in respective Sections. The general mechanism of photocatalytic process can be explained as follows:

The primary step in the photocatalytic degradation of IC in presence of semiconductor oxides can be proposed as follows:

Catalyst + hν → Catalyst (e⁻, h⁺) (Formation of electrons and holes)   ....(109)

Catalyst (e⁻, h⁺) → Catalyst (Recombination of electrons and holes) ....(110)
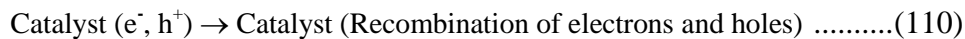
When the particles are small, as in the present case, the holes escape recombination in the bulk and reach the surface. The average transit time τ_D of the charge carriers, generated by the UV irradiation, to reach the surface is calculated by by Gratzel and Frank [164] as:

$$\tau_D \approx R^2 / \pi^2 D_c \dots\dots\dots\dots\dots\dots\dots\dots\dots\dots\dots(111)$$

where R is the radius of the particle and D_c is the diffusion coefficient of the charge carrier. The photogenerated hole, if it does not recombine with the electron, can react with the organic pollutant or even with water in the aqueous solution:

$$RH_2 + h^+ \rightarrow \dot{R}H + H^+ \, aq \dots\dots\dots\dots\dots\dots\dots\dots\dots(112)$$

$$H_2O + h^+ \rightarrow \dot{O}H + H^+ \, aq \dots\dots\dots\dots\dots\dots\dots\dots\dots(113)$$
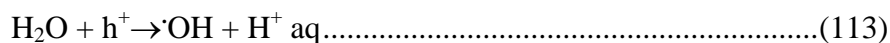
The hole can also react with the OH⁻ ions either present in the system under alkaline conditions or formed on the surface by the dissociative adsorption of water to H^+_{ads}. and OH^-_{ads}. [189]. The OH^-_{ads} can act as traps for the holes at the surface;

$$h^+ + OH^-_{ads} \rightarrow \dot{O}H_{ads} \dots\dots\dots\dots\dots\dots\dots\dots\dots (114)$$

Gerischer and Heller [190] proposed that reaction (114) is more likely than reaction (113) since the formation of ˙OH radicals by the reduction of H_2O_2 in photocatalytic systems can inject holes into the catalyst and $\dot{O}H_{ads}$ can exist as stable product at specific surface sites. The oxidation of organic pollutants can occur consecutive to reaction (114) as

$$RH_2 + .OH_{ads} \rightarrow \dot{R}H + H_2O \dots\dots\dots\dots\dots\dots\dots\dots (115)$$
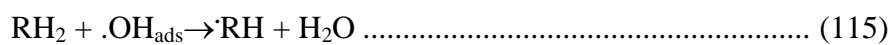
The direct reaction (112) between the organic pollutant (RH_2) and the hole can compete with reaction (115) if the concentration of RH_2 is high or the RH_2 molecules are strongly adsorbed on the surface.

If reaction (115) is the main path, the oxidation may be weaker in comparison to direct oxidation by holes as in reaction (112) since only

some of the holes are available for the formation of .OH$_{ads}$. This will lead to decrease in the oxidation rate and the quantum efficiency in the case of stable organic molecules.

When there is more H_2O_2 in the system, more $\cdot$OH radicals are formed. Hence reaction (115) becomes more prominent. However, it is less efficient than the hole-promoted reaction in the absence of added H_2O_2. The trapping of h^+ and quenching of $\cdot$OH also lead to decreased rate in presence of H_2O_2.

Oxygen plays an important role in photocatalytic degradation reactions in aqueous solutions by scavenging the electrons generated on the photocatalyst and thereby inhibiting the recombination of electrons and holes. Thus both electrons and holes will be available for the formation of free radicals and interaction with the pollutant. The electron is picked up by O_2 to generate superoxide radical anion and other reactive species. The effect of dissolved O_2 on the photocatalytic degradation IC, is tested by deaerating the system with N_2 and carrying out the experiments under otherwise identical conditions (Sections 4.3.8, 4.3.11.7 and 4.4.7).

The effect of deaeration of the suspension on the degradation is not significant in the case of MnO_2, MnO_2-TiO_2 and Co_3O_4. This suggests that the O_2 required for the reaction is not only from the dissolved form but also from the surface (adsorbed) and lattice of the above mentioned catalysts which cannot be easily removed by flushing with N_2.

Amorphous MnO_2 is known to release bulk oxygen more easily to the surface thereby making it a better catalyst in terms of facile activation

and regeneration [147]. MnO_2 with multiple oxidation states along with its electron donor-acceptor properties is an excellent oxidation – reduction catalyst. Photolysis of MnO_2 increases the oxygen species on the surface either by oxygen migration to the surface or by Mn migration to the bulk or both. Surface oxygen is consumed faster upon irradiation and oxygen from the bulk moves to the surface. Unless the oxygen is replenished periodically, the activity of the catalyst will be lost faster. This is verified by recycling the catalyst immediately after use by simple filtration followed by quick drying at 120^0C for 1 hour (Fig.4.28).

Similar results are obtained in the case of MnO_2-TiO_2 and Co_3O_4. Almost all results in terms of catalytic activity, kinetics, pH effect, effect of additives etc. are similar in the case of MnO_2, MnO_2-TiO_2 and Co_3O_4. Only the rates of reaction differ. Hence the general mechanism of the process is similar.

Various steps involved in photocatalysis in presence of O_2 can be summarized as follows:

$$O_2 \text{ (surface)} + e^- \rightarrow O_2^{\cdot-} \text{(surface)} \quad \dots (116)$$

$$H_2O \rightarrow OH^- + H^+ \quad \dots (117)$$

$$O_2^{\cdot-} + H^+ \rightarrow HO_2^{\cdot} \quad \dots (118)$$

$$2\ HO_2^{\cdot} \rightarrow H_2O_2 + O_2 \quad \dots (119)$$

$$HO_2^{\cdot} + e^- \rightarrow HO_2^{\cdot-} \quad \dots (120)$$

$$HO_2^{\cdot-} + H^+ \rightarrow H_2O_2 \quad \dots (121)$$

$$H_2O_2 + O_2^{\cdot-} \rightarrow\ ^{\cdot}OH + OH^- + O_2 \quad \dots (122)$$

$$H_2O_2 + e^- \rightarrow\ ^{\cdot}OH + OH^- \quad \dots (123)$$

$$H_2O_2 + 2\,h^+ \rightarrow O_2 + 2H^+ \quad\text{..(124)}$$

$$OH^- + h^+ \rightarrow\ ^\cdot OH \quad\text{...(125)}$$

$$H_2O + h^+ \rightarrow H^+ +\ ^\cdot OH \quad\text{..(126)}$$

$$IC +\ ^\cdot OH \rightarrow\ \text{Oxidation products} \rightarrow \text{Mineralisation} \quad\text{................(127)}$$

$$IC + h^+ \rightarrow \text{Oxidation products} \rightarrow \text{Mineralisation}\text{......................(128)}$$
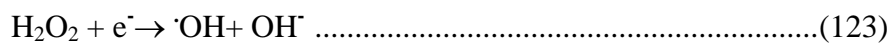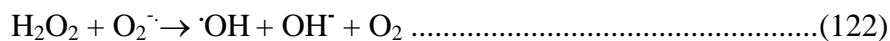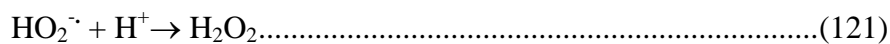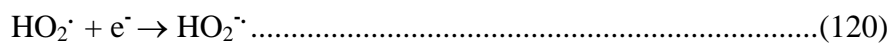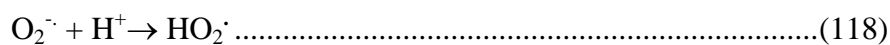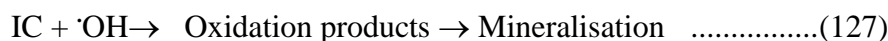
The mechanism can be schematically represented as
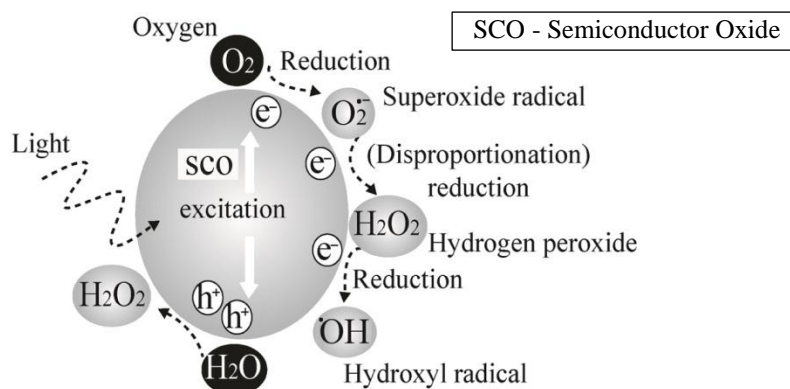
Fig. 4.83: Schematic presentation of the mechanism of photocatalytic process

The electrons are scavenged by the oxygen on the surface of the catalyst as in (116) above. The dye can also absorb visible light component from the light source and act as a sensitizer thereby transferring electrons from the excited dye molecule to the conduction band of MnO_2.

Schematic presentation of the dye sensitization is given in Fig.4.83.

$$\text{Dye}_{(ads)} \rightarrow \text{Dye}_{(ads)}^{*} \quad\text{..(129)}$$

$$\text{Dye}_{(ads)}^{*} + MnO_2 \rightarrow \text{Dye}_{(ads)}^{+\cdot} + MnO_2\,(e_{CB}^-) \quad\text{...........................(130)}$$

$$\text{Dye}_{(ads)}^{+\cdot} \rightarrow \text{Intermediates} \rightarrow \text{Oxidation/Degradation} \quad\text{.........(131)}$$

Microwave, Photo and Sono Activated Advanced Oxidation Processes and their Variations for the Decontamination of Water from Toxic Chemical Pollutants

343
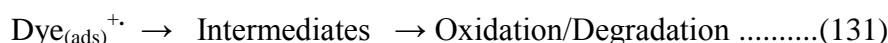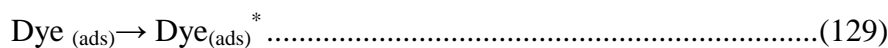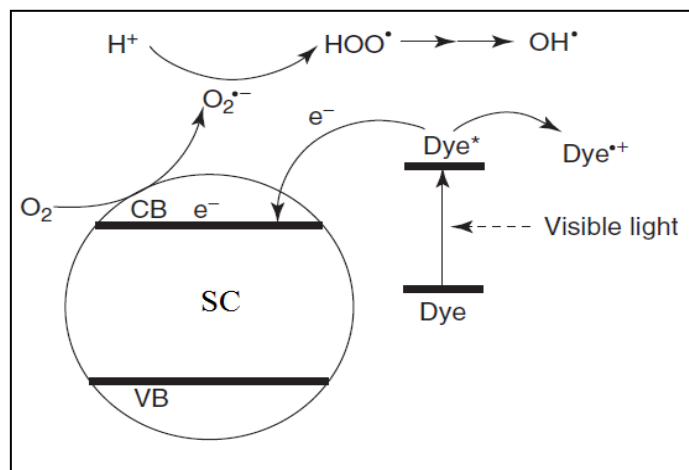
Fig. 4.84: Schematic presentation of the mechanism of dye sensitization process

Anandan et al. [191] also suggested a similar pathway for the degradation of dyes on Ag/TiO_2 catalysts. However, the contribution from the dye sensitization as above is highly concentration-dependent. There will be only monolayer coverage of the dye at lower concentration and the energy acquired by light absorption may not be adequate to be transferred to the semiconductor and activate it. At the same time, in the case of multilayer adsorption of the dye, the light absorption or photocatalytic efficiency of the catalyst may not increase significantly because the inner layers will tend to act as insulators with respect to outer layers.

The formation of H_2O_2 during the MnO_2/MnO_2-TiO_2/Co_3O_4 photocatalytic degradation of IC is verified and proven by analysing the reaction system immediately after decolorization and periodically thereafter under irradiation. The concentration of insitu formed H_2O_2 increases initially, reaches an optimum and decreases thereafter. This is

attributed to the oscillation in the concentration of insitu formed H_2O_2 as is the case with many semiconductor-mediated AOP systems. The concurrent formation and decomposition of H_2O_2 which leads to the phenomenon is explained in detail in Section 4.3.6.1.

In the case of MnO_2, the primary factors responsible for photocatalysis are the transfer of electrons as discussed above and the reducibility of MnO_2 as an efficient electron acceptor. On excitation by UV light, electrons are taken up from the reduced Mn species and this results in the formation of various ROS and their interactions with the substrate. This results in eventual degradation/mineralization of the pollutant. The bulk oxygen is recouped at least partially during the course of the interactions (see equations 119 and 122). One adsorbed oxygen molecule can fill two oxygen anion vacancies during photocatalysis. Thus the bulk of the catalyst returns to its original state thereby achieving effective regeneration.

According to Kung [187] evolution of oxygen from metal oxides occurs in three stages:

(i) Adsorbed molecular O_2 (ii) Adsorbed atomic oxygen and (iii) lattice oxygen. In the case of MnO_2, the loss of oxygen takes place at temperatures as low as 50^0C. The photo-initiated sequence of oxygen release from MnO_2 may be due to movement of O^{2-} (bulk) to the surface and subsequent weakening of MnO_2 bonds.

The re-oxidation of oxides occurs in a sequence of steps. Atmospheric oxygen and/or dissolved O_2 is taken up by the surface of the partially reduced MnO_2 as follows [147]:

Microwave, Photo and Sono Activated Advanced Oxidation Processes and their Variations for the Decontamination of Water from Toxic Chemical Pollutants

345

$$O_2 (g) \xrightarrow{-e^-} (O_2^-) \rightarrow 2(O^-) \xrightarrow{-e^-} O^{2-} (s) \quad \text{...(132)}$$
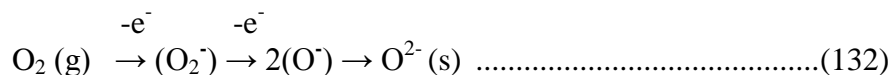
Most of the oxygen radicals are present in the bulk of the catalyst while some of them may remain on the surface for a short period. These highly active oxygen radicals can regenerate reduced manganese species. Under UV irradiation, the bonds in MnO_2 are weakened and O^{2-} is released from the bulk to the surface. Even though the lifetime of excited state oxygen species is short, they possess adequately high energy and electro negativity to facilitate the reduction or hydrogen abstraction from the substrate. Possible reaction pathways are:

$$O^{2-} (s) \xrightarrow[-e^-]{h\nu} (O^-) \xrightarrow[-e^-]{h\nu} O_2 (surface) \quad \text{...(133)}$$

$$O_2 (surface) + RH (IC) \rightarrow HO_2^{\cdot} (surface) + R^{\cdot} \quad \text{..........................(134)}$$

$$O_2 (surface) + R^{\cdot} \rightarrow Intermediates \rightarrow\rightarrow\rightarrow Mineralization (CO_2 + H_2O) \text{..(135)}$$

The H$^{\cdot}$ interacts with the hole and gets oxidized to form acid sites on the surface of MnO_2.

$$H^{\cdot} + h^+ \rightarrow H^+ \quad \text{...(136)}$$

The regeneration of MnO_2 may be represented as:

$$-Mn(^{3+} \text{ or } ^{2+}) \xrightarrow[-e^-]{h\nu} -Mn(^{4+} \text{ or } ^{3+}) \quad \text{(137)}$$

$$O_2 (g) \xrightarrow{e^-} (O_2^-) \rightarrow 2(O^-) \xrightarrow{e^-} O^{2-} (s) \text{..(138)}$$

$$(-Mn(^{4+} \text{ or } ^{3+})-) + O^{2-} \rightarrow MnO_2 (or\ Mn_3O_4) \quad \text{...............................(139)}$$

4.6. Summary of the comparative efficiency of MnO₂, MnO₂-TiO₂ and Co₃O₄ for the Photomineralisation of IC

Parameters	MnO_2	MnO_2-TiO_2(18:1)	Co_3O_4
Optimum Loading	1400 mg/L	1800 mg/L	1400 mg/L
Optimum Concentration of IC	40 mg/L	60 mg/L	60 mg/L
Kinetics	Variable kinetics. Pseudo first order at lower concentration (up to 40 mg/L) and zero order at higher (>50 mg/L) concentration	Variable kinetics. Pseudo first order at lower concentration (up to 60 mg/L) and zero order at higher (>60 mg/L) concentration	Variable kinetics. Pseudo first order at lower concentration (<60 mg/L) and zero order at higher (>60 mg/L) concentration
pH effect	Maximum degradation at pH 2 followed by gradual decrease up to 10 stabilizes >10.	Maximum degradation at pH 2 followed by decrease up to 4. Thereafter stable in the range 4-10. Slight increase in degradation at pH >10	Maximum degradation at pH 2 and 3 followed by decrease up to pH 6. Thereafter stable in the range 6-11
H_2O_2 effect	Inhibition, which increases with concentration up to 20 mg/L. Thereafter stable degradation with no further inhibition. However, the effect is not consistent.	Inhibition, which increases with concentration up to 20mg/L. Stabilizes thereafter	Moderate Enhancement which increases slowly with increase in concentration
Persulphate effect	Enhancement, increases with increase in concentration up to 60mg/L. Stabilisation thereafter.	Enhancement increases with increase in concentration up to 60mg/L. Then stabilisation.	Enhancement, increases with increase in concentration
Deaeration by N_2 bubbling	Effect dependent on MnO_2 dosage. No Effect at high dosages (1400mg/L) of MnO_2. Inhibition in the degradation of IC at lower dosages (~<200mg/L). Inhibition decreases with increase in dosage	Not Done. (Since the results are similar in the case of MnO_2 and MnO_2/TiO_2 in most cases)	Effect dependent on dosage. No Effect at high dosages (1400mg/L) Inhibition in the degradation of IC at lower dosages (~<200mg/L)

Microwave, Photo and Sono Activated Advanced Oxidation Processes and their Variations for the Decontamination of Water from Toxic Chemical Pollutants

347

Recycling	57% decrease in 1st recycling and 73% decrease in 2nd recycling and 85% decrease in 3rd recycling	Not Done. (Since the results are similar in the case of MnO_2 and MnO_2/TiO_2 in most cases)	40% decrease in 1st recycling and 54% decrease in 2nd recycling
COD decrease Under photolysis	1.1 mg/L/hr	2 mg/L/hr	0.9 mg/L/hr
Anions (2-15 mg/L)*			
i)PO_4^{3-}	Negligible effect at very low concentration<10mg/L. Thereafter inhibition which increases with increase in concentration and reaction time	Inhibition	Inhibition
ii)HCO_3^-	No effect at very low concentration (2mg/L). Thereafter inhibition.	Inhibition	Inhibition
iii)CO_3^{2-}	Inhibition	Inhibition	'Mild inhibition' initially. Becomes 'no effect' at later stages of reaction
iv)Cl^-	No effect	Mild Enhancement	No effect
v)CH_3COO^-	Mild inhibition	Inhibition	'No effect' to 'mild enhancement'
vi)SO_4^{2-}	'No effect'	'Inhibition' changes to 'no effect' and then to 'mild enhancement' with time.	Enhancement
vii)NO_3^-	Inhibition at low concentration changes to enhancement at higher concentration.	Enhancement	Enhancement

*·'Mild enhancement', 'Mild inhibition' and 'no effect' are often indistinguishable.

The decrease in activity of the recycled catalyst confirms the loss of oxygen from the lattice or the bulk of MnO_2. The lattice oxygen is oxidized to surface O_2 which remain adsorbed onto the surface and participate in the photocatalysis. Such migration of bulk oxygen to the less energetic surface sites has been proven experimentally and from ESR studies [192] and also from EDX data. Since the results are more or less similar in the case of MnO_2-TiO_2 as well as Co_3O_4, it is likely that the mechanism of their photocatalytic activity also will be similar. Various experimental and instrumental analysis data presented here also support this inference.

4.7 Conclusions

MnO_2, MnO_2-TiO_2 and Co_3O_4 mediated photocatalysis is a viable technique for the removal of trace amounts of chemical pollutants such as the dye IC from water. Various operating parameters such as catalyst loading, substrate concentration, pH, addition of oxidants, presence of anions, dissolved O_2, lattice and adsorbed O_2 etc. influence the degradation of IC. H_2O_2 which is a powerful oxidant for many photocatalytic reactions inhibits the degradation in the case of MnO_2 and MnO_2/TiO_2 which is attributed to the quenching of the photoproduced holes and reactive ˙OH radicals. Surprisingly H_2O_2 functions as a mild enhancer of the degradation in presence of Co_3O_4. The difference in the effect of H_2O_2 on the degradation of the substrate in presence of MnO_2 and Co_3O_4 is attributed to the higher reactivity of MnO_2 towards H_2O_2 decomposition thereby reducing the availability of reactive free radicals. Another oxidant persulphate enhances the degradation through the insitu

generation of reactive $SO_4^{\cdot-}$ radical anion and $^{\cdot}OH$. Lattice O_2 in the catalyst (MnO_2 and Co_3O_4) plays an important role in the degradation, unlike many other AOP catalysts, where the role of dissolved O_2 in the solution bulk is more prominent. The diminished activity of the recycled catalyst together with EDX data confirms the depletion of lattice oxygen. A reaction mechanism based on the observations is proposed and discussed.

.....ഇരു.....

Sonocatalysis mediated by MnO$_2$, MnO$_2$-TiO$_2$ and Co$_3$O$_4$ for the degradation of Indigo Carmine in water

5.1 Introduction

Ultrasound (US) irradiation (sonication) and US-initiated heterogeneous catalysis (sonocatalysis) have been investigated extensively in recent years as potential tertiary treatment processes for the removal of trace amounts of chemical and bacterial pollutants from water [193-198]. These advanced oxidation processes (AOPs) have been proven effective for the degradation and eventual mineralization of many types of recalcitrant organic pollutants such as pesticides, phenols, pharmaceuticals and dyes. Sonocatalysis mediated by zinc oxide has been demonstrated as highly efficient for the complete and irreversible destruction of bacterial pollutants such as *Escherichia coli, Bacillus subtilis, Vibrio harveyi* and *Pseudomonas aeruginosa* [195,196]. However, US based processes are

Microwave, Photo and Sono Activated Advanced Oxidation Processes and their Variations for the Decontamination of Water from Toxic Chemical Pollutants

351

generally less efficient for the removal of chemical contaminants compared to other similar AOPs such as photocatalysis or electrocatalysis under identical reaction conditions [97,196, 197]. Attempts to enhance the efficiency of sonocatalysis for wastewater treatment are mostly confined to their combination with additives such as H_2O_2, H_2O_2/Fe^{2+}, Fe^{3+}, cations, anions, dyes etc. and hybrid energy sources including light and microwave. Another approach is to modify the characteristics of the catalyst by doping, supporting and coating [199-203].

The primary effect of US in liquid is the phenomenon of cavitation which consists of nucleation, growth and collapse of bubbles. The bubble collapse results in localized supercritical conditions such as high temperature, pressure, electrical discharges and plasma effects [99, 193, 194, 204-205]. The gaseous contents of the collapsing cavity can reach temperatures of the order of $\sim$ 5500°C. Temperature of the liquid immediately surrounding the cavity can be as high as 2100°C. The localized pressure can reach as high as $\sim$500 atmospheres. These conditions result in the formation of transient supercritical water and the cavities can thus function as high energy microreactors. Dissolved oxygen and water molecules in the system can decompose under such extreme conditions to form reactive species such as H·, ·OH and O· radicals. These radicals can either get deactivated by combination with each other and/or interact with H_2O and O_2 during the rapid cooling phase giving HO_2· and H_2O_2. This highly reactive environment with multitude of reactive free radicals is congenial for the decomposition and eventual mineralization of organic pollutants. The effect of US such as increase in the surface area of

suspended particles due to fragmentation as well as deagglomeration, continuous cleaning of the surface by microstreaming etc. can be used beneficially in sonocatalysis. This will help in the sustained efficiency of the catalyst for repeated application.

Almost all reported sonocatalytic studies on water purification uses SiO$_2$, ZnO and TiO$_2$ as catalysts probably because of better availability, convenience, low cost and the possibility of exploiting the photocatalytic potential resulting from the sonoluminescence [99,195,112,206,207]. Nakajima et al. [207] reported that TiO$_2$ is more efficient than SiO$_2$ for the sonochemical destruction of 1,4-dioxane in aqueous systems. Dadjour et al. [208] reported that TiO$_2$ is more effective than Al$_2$O$_3$ for the disinfection of *E coli* while Anju et al. [195] and Vidya Lekshmi et al. [196] reported the high activity of ZnO for the sonocatalytic removal of a variety of gram positive and gram negative organisms. The relatively higher sonocatalytic activity of photosensitive semiconductor oxides such as ZnO and TiO$_2$ has been attributed to the combination of sonocatalysis and sonication-induced photocatalysis initiated by the intense UV light of single bubble sonoluminescence [112, 209]. Keck et al. [205] attributes the enhanced degradation in presence of even catalytically inactive particles to the change in the shape of US induced bubbles from spherical to asymmetric. The large surface area of these bubbles enable more insitu formed reactive radicals to escape into the bulk and interact with the substrate.

It has been demonstrated in previous Chapters that MnO$_2$, MnO$_2$-TiO$_2$ and Co$_3$O$_4$ mediated MW catalysis and photocatalysis are efficient AOPs for the removal of the dye pollutant IC from water. A similar study is

Microwave, Photo and Sono Activated Advanced Oxidation Processes and their Variations for the Decontamination of Water from Toxic Chemical Pollutants

353

extended in this Chapter with ultrasound (US) as the source of activation. All the three catalysts are investigated as potential sonocatalysts. To the best of our knowledge, this study is probably the first instance of the application of these materials (MnO_2, MnO_2-TiO_2 and Co_3O_4) as sonocatalysts.

5.2   Experimental details

5.2.1 Materials used

The materials used, relevant details and their characteristics are the same as provided in Section 2.2.1 of Chapter 2.

5.2.2 Analytical procedures

Sampling and analysis were performed as explained in Sections 2.4 and 3.2.3 of Chapters 2 and 3 respectively.

5.2.3 Sonocatalytic experimental set up

The sonocatalytic experiments were performed using aqueous solutions of IC of the desired concentration. Specified quantity of the catalyst was suspended in the dye solution taken in screw cap bottles of 250 mL capacity which are used as reactors. Experiments with and without mechanical mixing did not show significant difference in the sonocatalytic degradation of the dye thereby suggesting that sonication was sufficient to ensure adequate mixing of the suspension. However, mechanical mixing can influence the rate of degradation under sonication depending on the characteristics of the catalyst, substrate and sonication conditions [210]. In the current instance, the catalyst remains well suspended and is uniformly distributed in the reaction medium for longer time by sonication even without mechanical mixing.

An ultrasonic bath (Equitron, 53/42 KHz, 100 W) was used as the source of US. Water from the sonicator was continuously replaced by circulation from a thermostat maintained at the required temperature. The reaction temperature was maintained at 29 ± 1°C unless mentioned otherwise. The position of the reactor in the ultrasonic bath was always kept the same. Typical reaction assembly is shown in Fig. 5.1. The ultrasonic bath was operated at a frequency of 42 KHz and a power of 100 W unless indicated otherwise.
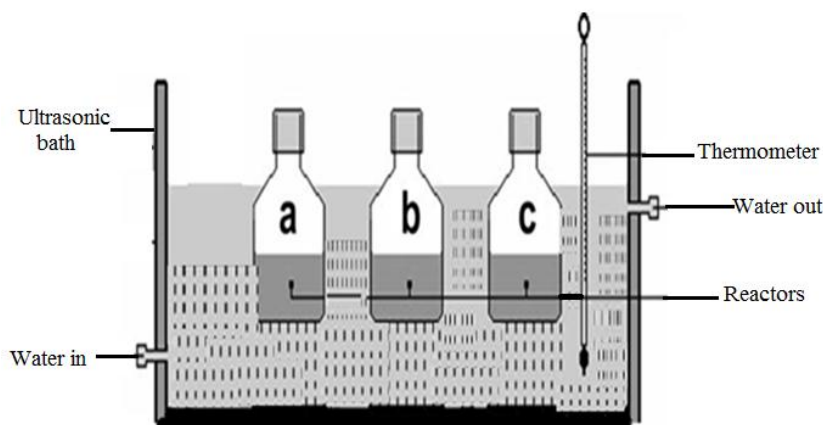
Fig. 5.1: Schematic diagram of the sonocatalytic experimental setup

Samples were drawn at periodic intervals of sonication, the suspended catalyst particles were removed by centrifugation and the concentration of IC left behind was analyzed by Spectrophotometry at 608 nm. Reaction system kept in the dark under exactly identical conditions (without US irradiation) served as the reference. H_2O_2 in the system is determined by standard iodometry. Mineralization of IC was tested by total organic carbon (TOC) and chemical oxygen demand (COD) measurements as explained in previous Chapters.

Microwave, Photo and Sono Activated Advanced Oxidation Processes and their Variations for the Decontamination of Water from Toxic Chemical Pollutants

355

5.3 Results and discussion

5.3.1 Preliminary results

Preliminary investigations on the decolorization/degradation of IC in the presence of MnO_2 and US individually and in combination under identical conditions showed that both the catalyst and US are essential for significant degradation. Very small quantity of IC degraded under US irradiation in the absence of the catalyst (Fig. 5.2).
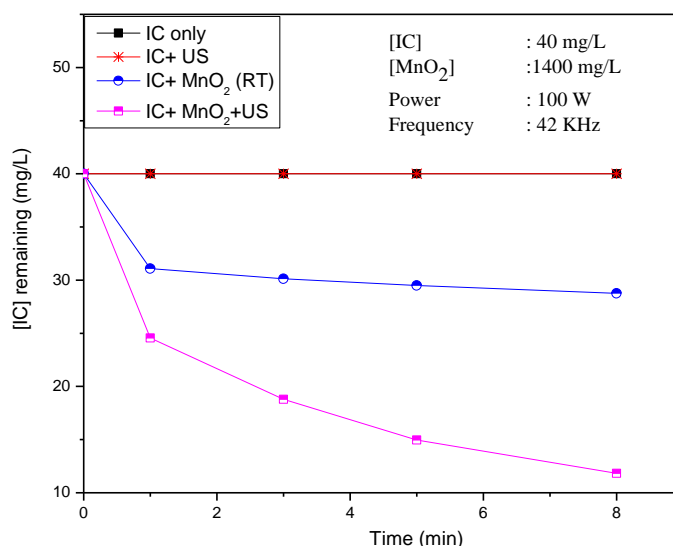
Fig. 5.2: Relative decrease in concentration of IC in presence of MnO_2 under various conditions

Water is known to dissociate under US irradiation into reactive free radicals H· and ·OH (reaction 140).

$$H_2O \quad \xrightarrow{\;>>>\;} \quad H· \;+\; ·OH \quad ....(140)$$
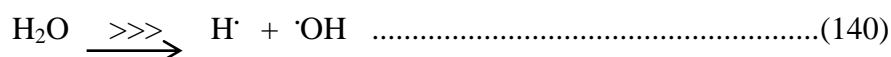
These radicals are capable of attacking the organic compounds in solution [211] resulting in their degradation and possible mineralization. In addition to the $\cdot OH$ radical-mediated degradation, pyrolytic degradation and oxidation by in situ formed H_2O_2 also take place, though only to limited extent [212]. The presence of suspended MnO_2 enhances the degradation significantly, at least by three times, in the present context. There is moderate reduction in the concentration of IC in presence of MnO_2 even without US irradiation. This is due to simple adsorption. MnO_2 is known to be a very good adsorbent for many organic pollutants in water. The adsorption of IC at different concentrations on MnO_2 is given in Fig.3.11 (Section 3.3.3 of Chapter 3). At constant weight of MnO_2 (1800 mg/L), the adsorption increases very slowly with increase in the concentration of the dye (10-70 mg/L) and reaches a steady adsorption of ~12 mg/L at an IC concentration of 60 mg/L.

The effect of various reaction parameters on the MnO_2 mediated sonocatalytic degradation of IC (US/MnO_2/IC) is investigated in detail as follows:

5.3.2 Effect of catalyst dosage

The effect of dosage of MnO_2 on the sonocatalytic degradation of IC under otherwise identical conditions is shown in Fig.5.3.

Microwave, Photo and Sono Activated Advanced Oxidation Processes and their Variations for the Decontamination of Water from Toxic Chemical Pollutants

357
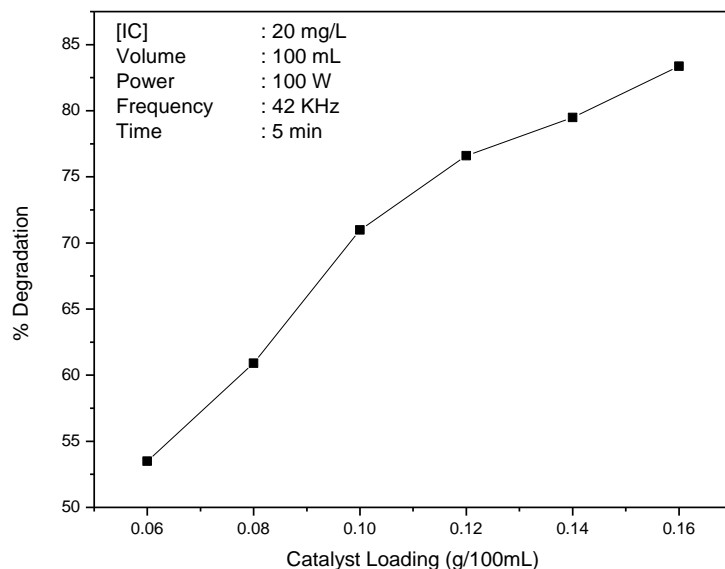
Fig. 5.3: Effect of loading on the US/MnO$_2$ degradation of IC

The degradation increases with increase in catalyst loading. Unlike in the case of many other AOPs, the degradation does not have a clear optimum with respect to catalyst loading and continues to increase with increase in the dosage. However, the rate of increase slows down around 0.12 - 0.14 g/100mL of MnO$_2$ when the degradation has reached ~ 75%. At this loading, which is taken as convenient optimum for further studies, the rate constant is about 1.6×10^{-1} min^{-1}. The degradation under identical conditions is practically negligible without MnO$_2$.

The increasing degradation efficiency with increase in loading is probably due to increased number of adsorption sites and more effective absorption of US which lead to enhanced cavitation and consequent effects. This leads to the formation of a higher number of reactive hydroxyl radicals and their interactions with the dye. The aggregation of

catalyst particles which causes a decrease in the number of available active surface sites and consequently decrease in the activity, observed in the case of other AOPs such as photocatalysis, sets in only at a much higher dosage in the case of sonocatalysis. This is because the US is deaggregating the agglomerated particles and thus increasing the surface area of the catalyst constantly. Hence the increase in sonocatalytic activity with catalyst dosage can be sustained even at higher loadings of MnO_2 compared to the 'dosage effect' in other AOPs. Presence of particles is also known to provide additional sites for the cavitation phenomena resulting in increased number of cavitation events and hence increased reaction [205-207]. With the reactants remaining adsorbed on MnO_2, the cavitation effect will be more efficiently transferred on to the molecules resulting in enhanced degradation. The IC gets adsorbed well on MnO_2 as demonstrated earlier. Hence adsorption of the substrate is an important factor that can contribute to the higher sonocatalytic efficiency of MnO_2. The activated molecules can degrade more efficiently and then get desorbed from the surface under US thereby making the surface continuously available for fresh molecules to get adsorbed. The sonocatalytic degradation is the net effect of simultaneous adsorption, desorption and actual degradation of the pollutant. This adsorption-desorption process is important though the degradation of the pollutant takes place mainly in the bulk. This is proven from the observation that even coal ash with relatively low catalytic activity enhances the sonocatalytic degradation of phenol [213]. Similar results are reported by Tuziuti et al. also [214]. Suspended particles can also help the break-up of the micro bubbles created by US into still smaller ones thereby increasing

Microwave, Photo and Sono Activated Advanced Oxidation Processes and their Variations for the Decontamination of Water from Toxic Chemical Pollutants

359

the number of regions of high temperature and pressure [211, 212]. This leads to an increase in the number of ˙OH radicals which can interact with the organic pollutant molecules present in water and oxidize them into various intermediates resulting in eventual mineralization. The surface of the suspended particles can also act as nucleation sites for cavitation bubbles [215]. Enhancement in the sono induced destruction of chemical and bacterial pollutants in the presence of suspended particles of Al_2O_3, TiO_2 and ZnO have been reported [195, 196, 216].

Another factor contributing to the higher optimum dosage of catalyst may be the US- induced increase of the mass transfer between the liquid phase and the catalyst surface [217], making the surface consistently and more readily available for fresh reactant molecules to get adsorbed and interact. The continued increase in degradation with increase in catalyst dosage and the absence of any optimum can also be explained based on the effects of microstreaming and increased mass transport induced by the interaction of US with solid matter. Microstreaming causes a jet of fluid directed onto the particle [213, 214-218] and this will clear the blockage of active adsorption sites of the catalyst partially or even fully. Consequently, the catalyst surface is getting constantly regenerated in situ which will help recycling of the catalyst.

The dynamic factors discussed above make the particle size variation of the catalyst within short to medium range less important in sonocatalysis [197]. In any case, the particles cannot be fully and effectively suspended beyond a particular loading in a particular reactor which leads to suboptimal penetration of US and reduced adsorption of

the substrate on the surface. Excess MnO_2 may also be deactivating at least a part of the originally activated catalyst by collision with ground state particles as explained under Section 3.3.3.1 of Chapter 3. At higher loading of the catalyst, the effective working volume of the suspension will be low [212] and this can affect the penetration of US through the dense medium. Consequently, the enhancement due to the deagglomeration of particles may be balanced or even negatively impacted. Hence any further enhancement in degradation beyond a particular catalyst loading will be slow unless the US power is increased significantly. In the current study also, enhancing the US power from 50 to 100 W at the selected optimum catalyst loading of 1.4 g/L, under otherwise identical conditions, increased the degradation of IC from 30.7 to 38.5% in one minute. Davydov et al. [219] also reported similar findings. The slowdown in the rate of degradation at higher catalyst dosages can also be due to the increased scattering of the incident sound waves thereby decreasing the available energy for cavity formation [220].

The optimum catalyst dosage under sonolysis is also dependent on the reactor geometry and operating conditions; in particular the power dissipation into the reactor. Hence, the optimization has to be made individually for each reactor configuration.

5.3.3 Effect of initial concentration of IC

The effect of initial concentration of IC in the range 10-60 mg/L on its sonocatalytic degradation in presence of MnO_2 is investigated. The % degradation decreases with increase in concentration of IC (Fig.5.4)
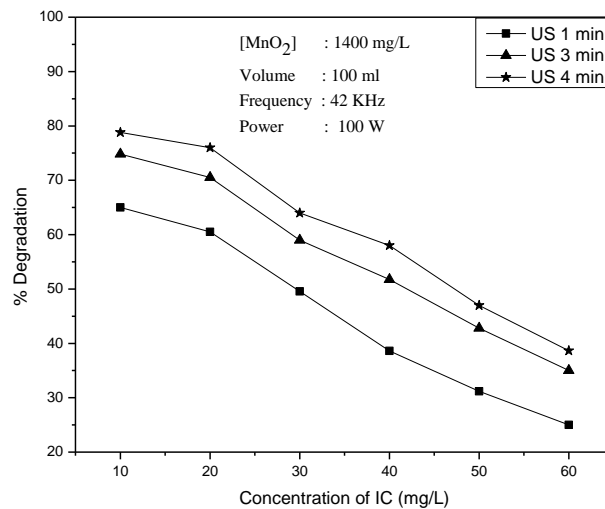
Fig. 5.4: Effect of concentration of IC on the US/MnO$_2$ degradation at different times of irradiation

However, it will be more appropriate to compare the rate of degradation to evaluate the concentration effect. The rate vs concentration plot is shown in Fig 5.5.
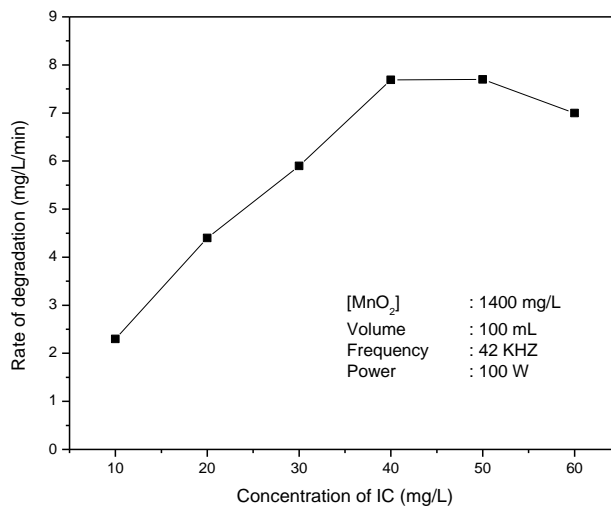
Fig. 5.5: Rate of US/MnO$_2$ degradation at various concentrations of IC

The degradation rate increases linearly with increase in concentration in the range 10-40 mg/L. At higher initial concentration (> 40 mg/L) the rate remains stable or even slows down slightly thereby demonstrating that the factors favoring degradation of IC under sonolysis are less effective at higher concentration. This also confirms the variable kinetics reported in the case of most AOP-initiated degradation of water pollutants [221]. The optimum rate of degradation under the current experimental conditions is 7.5 mg/L/min.

Sonocatalytic degradation reactions taking place at the solid-liquid interface generally follows pseudo first order kinetics and can be represented by the modified Langmuir-Hinshelwood (L-H) model [180, 181] as explained in Section 3.3.3.2 of Chapter 3. This is verified by the inverse plot of $1/r_0$ vs $1/C_0$. The inverse plot yields a straight line in the concentration range 10-40 mg/L which confirms first order kinetics and L-H mechanism (Fig.5.6)
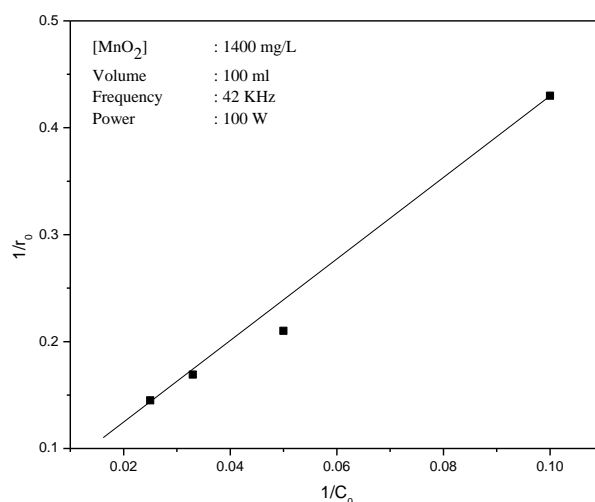
Fig. 5.6: Reciprocal plot of rate vs concentration for US/MnO₂/ IC degradation

The kinetics is further verified by the logarithmic plot of ln C_0/C vs t (discussed in detail in Section 3.3.3.2 of Chapter 3). The plot yields straight lines (Fig.5.7) for the concentration range 10-40 mg/L thereby reconfirming pseudo first order kinetics.
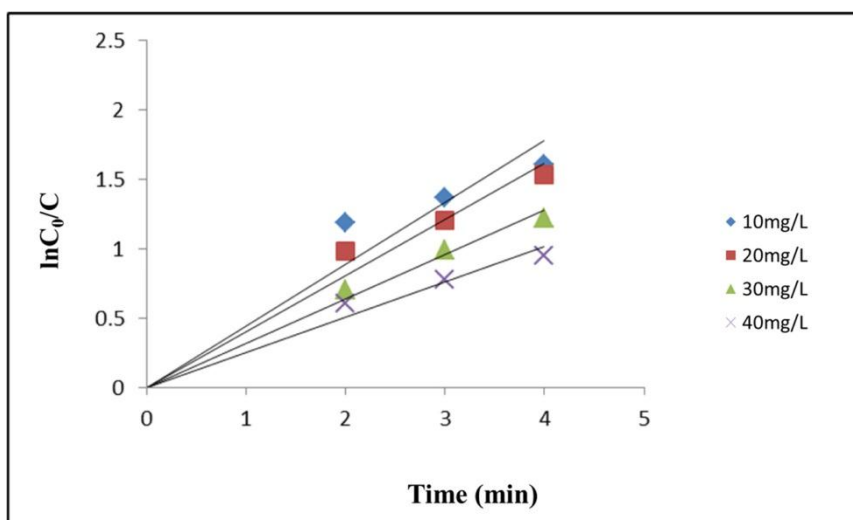
Fig. 5.7: Logarithmic plot for the MnO_2 mediated sonocatalytic degradation of IC.

The slope of each line gives the apparent rate constant of degradation k_{app} for the respective concentration of the substrate. The rate constants computed are given in Table 5.1.

Table 5.1: Pseudo first order rate constants for the US/MnO_2 degradation of IC

Sl. No.	[MnO_2] (g/L)	[IC] (mg/L)	k_{app} x 10^{-1}(min^{-1})
1	1.4	10	6.4
2	1.4	20	4.3
3	1.4	30	3.0
4	1.4	40	2.4

The rate constant decreases with increase in concentration of IC. The relative decrease is more in the lower concentration range (~33% in the range 10-20 mg/L, ~20% in the range 30-40 mg/L). Rationalization for this behavior is provided in Section 3.3.3.2 of Chapter 3 and may be summarized as follows: For specific reaction conditions, including fixed amount of catalyst, the number of surface-generated active species available for interaction also will be finite. Hence at higher concentrations, the number of substrate molecules is relatively excessive. Hence the relative % fraction of the substrate which can successfully interact with the ROS will be less resulting in decrease in the apparent rate constant. However, the absolute values of rate constants are relevant only under specific experimental conditions and cannot be generalized.

Decrease in the rate of degradation with increasing concentrations of the substrate beyond the optimum and consequent decrease in the order of the reaction has been reported earlier also in the case of sonocatalysis and sonophotocatalysis [180, 221].

The first order kinetics at lower concentrations of IC and higher % conversion ranges can also be explained from the effect of sonication on the catalytic role of MnO_2. With increase in the concentration of IC, more molecules get adsorbed on the catalyst site, get activated and interact with correspondingly more reactive oxygen species (ROS) including ·OH radicals (as explained under Section 3.3.3.2 of Chapter 3). This increase will continue until all the surface sites are occupied. Thereafter, the rate of degradation is stabilized or even decreases. Similar stabilization/decrease takes place in the bulk also where the

Microwave, Photo and Sono Activated Advanced Oxidation Processes and their Variations for the Decontamination of Water from Toxic Chemical Pollutants

365

Chapter 5

relative (to the substrate) concentration of OH radicals is smaller [182].
Higher concentration of the dye can utilize the limited $^{.}$OH radicals in
the bulk more effectively leading to increased degradation. This will
continue until the IC concentration is sufficiently high to interact with
optimum number of $^{.}$OH radicals. Thereafter the rate of degradation is
independent of the increase in IC concentration and the reaction is of
zero order. Also, at higher substrate concentration, it will absorb at least
part of the US radiation thereby decreasing the energy available for the
catalyst activation and the formation of ROS.

The above factors together can contribute to stabilization and
decrease in the rate of degradation. However, due to the US induced
deaggregation and consequent reduction in size and change of shape of
the catalyst particles, there will be in situ formation of newer surface
sites. Further, the reaction can also take place at the cavitation bubble
interface where the OH concentration can reach a higher limit [196].
Hence, the initial degradation rate of IC will be dependent on its
concentration on the surface, in the bulk and at the interface of the
cavitation bubble as well as the concentration of $^{.}$OH radicals.
Consequently, the catalyst dosage and substrate concentration for
optimum degradation will be higher compared to other AOPs. This
optimum may also depend on a number of other parameters such as
frequency and power of the US radiation, mass, type and physicochemical
characteristics of the sonocatalyst, type, size and geometry of the reactor
etc. Consequently any optimization will apply only to the particular
reaction conditions and it cannot be generalized.

When the concentration of the dye is small, many of the $^{\cdot}$OH radicals will get deactivated by interaction among themselves resulting in the formation of H_2O_2. At higher IC concentration, the probability of interaction of the dye with $^{\cdot}$OH is more and the rate of degradation increases until the optimum. Consequently, the concentration of H_2O_2 is often less at higher concentration of the substrate [112] though other factors also contribute to this as discussed below.

5.3.4 Formation and fate of H_2O_2

H_2O_2 is a byproduct of many AOPs, especially of those based on sono- and photo- catalysis.

The H_2O_2 undergoes simultaneous formation and decomposition and the net concentration at any point of time depends on relative rates of the two processes. More details on the possible reactions leading to the formation and decomposition of H_2O_2 and the resulting phenomenon of 'oscillation' are discussed in Section 4.3.6.1 Chapter 4. The effect of concentration of IC on the net amount of H_2O_2 present in the system is verified experimentally. The quantity of H_2O_2 present in the system immediately on decolourization is measured at different initial concentrations of IC and the results are shown in Table 5.2 (As explained in earlier Chapters, concentration of H_2O_2 was not measured, when the solution was still colored, due to constraints of the analytical procedure followed).

Microwave, Photo and Sono Activated Advanced Oxidation Processes and their Variations for the Decontamination of Water from Toxic Chemical Pollutants

367

Table 5.2: Effect of concentration of IC on the net amount of insitu formed H_2O_2 in the US/MnO$_2$/IC system (measured immediately after decolourization) [MnO$_2$]: 1.4 g/L

[IC] mg/L	Time for decolourization (min.)	[H$_2$O$_2$] mg/L
10	15	12.0
20	20	6.7
30	35	7.8
40	45	5.4
50	60	7.4
60	80	6.4
70	120	7.6

Obviously, the concentration of H_2O_2 does not increase consistently with increase in concentration of the dye or increasing rate of degradation. At the optimum concentration of the dye (in this case > 40 mg/L) its degradation rate is stabilized. However the concentration of concurrently formed H_2O_2 is not steady thereafter as expected and continues to increase and then fluctuate with the concentration (of IC).

When the relative concentration of the dye is less, the reactive $^{\cdot}$OH radicals will interact among themselves more frequently rather than with the dye resulting in higher concentration of H_2O_2 and lower degradation of IC. The $^{\cdot}$OH radicals will also interact with the H_2O_2 leading to the decomposition of the latter. The relative rates of the multiple competitive interactions in the system will depend on various reaction and system parameters and the dominating reaction at any point in time will determine the net concentration of H_2O_2 at that moment [112].

The concentration of H_2O_2 in the system with optimum concentration of IC (40 mg/L) at different times of irradiation (after the decolourization of the dye) is measured and the data is given in Fig.5.8.
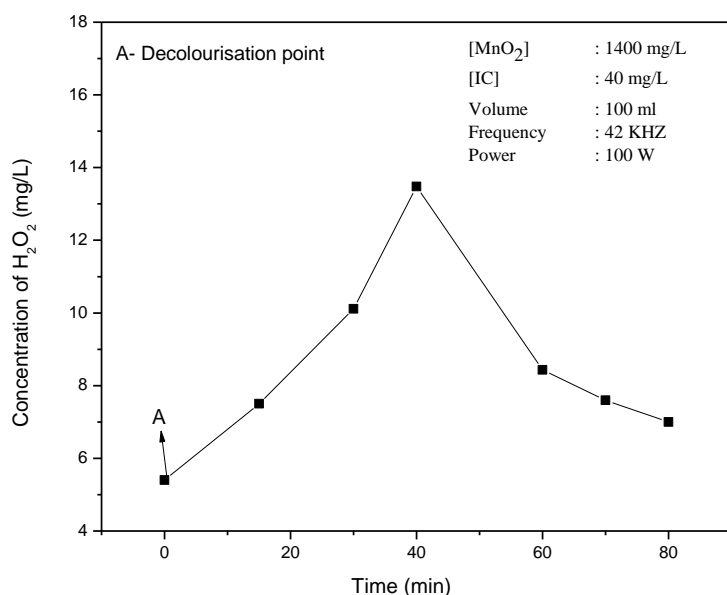
Fig. 5.8: Variation in the concentration of in situ formed H_2O_2 (measured after decolourization of IC with time irradiation).

Even after the decolorization of IC, the degradation of various insitu formed intermediates will continue (before they eventually get mineralized) and correspondingly, the concentration of H_2O_2 in the system must also be increasing and then stabilising. However, in this case, the increasing trend is observed only up to 45 minutes and thereafter the concentration of H_2O_2 decreases with time indicating concurrent competitive formation and decomposition reactions as reported earlier

[112]. The inconsistency and poor reproducibility in the concentration of H_2O_2 at any point of time during the US irradiation (though the fluctuating trend remains consistent) can be attributed to the phenomenon of 'oscillation' (in the concentration of H_2O_2) [112, 221]. Depending on the domination of the formation or decomposition process at any point in time, the net concentration of H_2O_2 will be increasing or decreasing.

Another factor which leads to the inconsistency in the concentration of H_2O_2 under sonocatalytic reaction conditions is its thermal decomposition (which may occur in the vicinity of cavitation bubble where extreme local conditions of temperature and pressure exist) to water and oxygen rather than to reactive radical species. Due to all these factors, there is no direct correlation between the degradation of IC and the net concentration of H_2O_2 in the system.

5.3.5 Effect of pH on the degradation of IC

The AOP-induced degradation of organic pollutants in water is often dependent on the pH of the solution. The effect of pH on sonocatalytic degradation of IC in presence of MnO_2 is investigated in the range 3-11. The pH of the suspension was adjusted initially and was not modified externally during the irradiation. The results are presented in Fig.5.9.
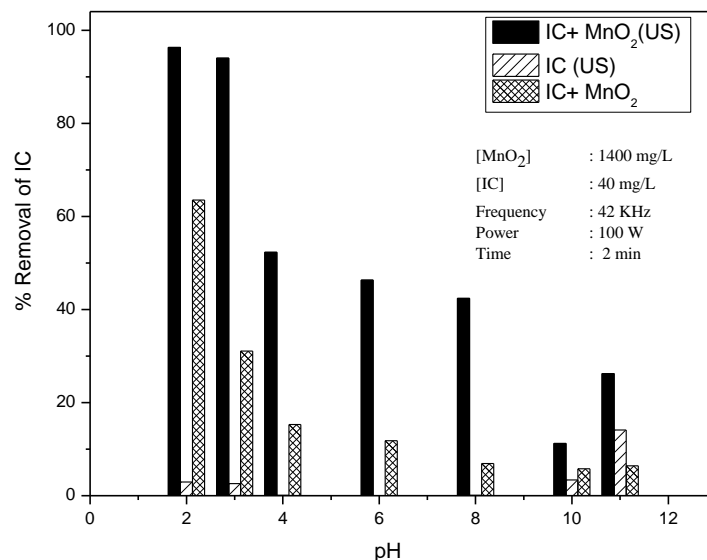
Fig. 5.9: Effect of pH on the removal of IC under various reaction conditions

The degradation is the highest at pH 2-3, decreases sharply from pH 3 to 4 and remains fairly steady or decreases slightly thereafter from pH 4 to 8. This is followed by another sharp decrease at pH 10 and slight increase at pH 11. Experiments with the dye solution under identical conditions, but without MnO_2 show practically 'no degradation' with or without US in the pH range of 2-10. However, in this case also there is sharp increase in degradation at pH 11. The pH effect in presence of MnO_2 without US irradiation is also shown in the figure. The degradation is more in presence of MnO_2 and US irradiation at all pH compared to the same system without US irradiaion. However, the trend of 'pH effect' remains qualitatively the same in the presence or absence of irradiation. This indicates that the effect of pH on the physicochemical and surface

characteristics of MnO_2 are primarily responsible for the 'pH effect' on the sonocatalytic degradation.

As explained in previous Sections 3.3.3.5 and 4.3.4 of Chapters 3 and 4 respectively the pH of the reaction medium influences the characteristics of the inorganic semiconductor oxide particles such as the surface charge, size of the aggregation and the band edge position. Hence pH can affect the adsorption – desorption properties of the catalyst-substrate combination. In addition to affecting the surface properties of the catalyst, pH also influences characteristics of the organic molecules and the reactive ˙OH radical formation [222]. Alkaline range is expected to favour the formation of more ˙OH radicals from the large quantity of OH ions present which could have enhanced the degradation significantly. However this is not fully reflected in the actual degradation rate possibly due to the poor adsorption of the dye as explained below.

The 'pH effect' on the sonocatalytic degradation of IC is more or less similar to that in the case of photocatalysis and MW catalysis. Hence the causes will also be similar to those explained in earlier Chapters. Those factors are discussed again here as relevant under sonolysis. In the context of sonocatalysis the effect of pH on the degradation of organic pollutants in presence of semiconductor oxides is often explained based on the point of zero charge (PZC) of the solid [197, 198]. The PZC of MnO_2 is ~ 4.7. Below this pH value the oxidizing ability of MnO_2 will be relatively higher. IC is a dianionic dye in aqueous solution and this configuration is maintained in the pH range 3-11 [151] even though the degree of ionization is less in the acidic

range. The electrostatic interaction between the positively charged MnO_2 surface and the dianions of IC irrespective of the degree of ionisation will be strong below the PZC leading to strong interaction/adsorption and subsequent reaction. The formation of a precursor complex between the surface bound Mn (IV) of MnO_2 and the organic contaminant [153] by the transfer of electrons from the latter to the former and its consequences are explained in Sections 3.3.3.5 and 4.3.4 of Chapters 3 and 4, respectively. This results in the oxidative degradation of the organic compound. The reductively formed Mn(II) is dissolved in the bulk solution. Thus MnO_2 plays the dual role of a catalyst as well as an oxidant. The O_2 dissolved in the system oxidises Mn(II) to Mn(IV) oxide again. Here dissolved O_2 is the oxidant and MnO_2 functions as a catalyst. The positively charged free Mn(II) ions in solution can get adsorbed on to the negatively charged MnO_2 surface only at pH > PZC. This will inhibit the generation of reactive species and consequently degradation of IC will be lower at higher pH. Since IC keeps its anionic configuration upto around pH 11 it cannot get adsorbed or even come closer to the catalyst above its PZC of 4.7. This may be the main reason for the relatively lower degradation of the dye at higher pH. However, the higher degradation of IC is not sustained at all pH below 4.7. The degradation falls steeply between pH 3 and 4 i.e, at pH < PZC of MnO_2. Hence the influence of pH on parameters other than the surface characteristics of MnO_2, especially the bulk processes, also is important. The lack of direct correlation between the PZC of MnO_2 and the 'pH effect' can also be attributed to the fact that the PZC itself is not rigid and depends on a number of factors including the size and nature of

Microwave, Photo and Sono Activated Advanced Oxidation Processes and their Variations for the Decontamination of Water from Toxic Chemical Pollutants

373

dispersion of the particles and the type of catalyst itself. It has also been reported that the zeta potential curve may remain positive over a wider range under sonication [223, 224]. The alleviation of pH dependence of MnO_2 mediated degradation of IC under microwave irradiation has also been reported [151].

The dramatic increase in the degradation of IC at low pH$\leq$ 3 has been reported in the case of the photocatalytic oxidation of the dye in presence of Mn supported TiO_2 [151]. This happens even without irradiation and can hence be at least partly due to pH induced interactions/transformations of the catalyst. However, US plays its own accelerating role, as in the case of many US initiated processes, once the reaction is initiated. In any case, the pH effect is very complex and depends on the interplay of many factors in the system which cannot be explained based on individual reaction parameters in isolation.

5.3.6 Volume effect

Chen and Smirniotis [212] and Anju et al. [154] reported that in the case of semiconductor oxide catalysts such as TiO_2 and ZnO, reducing the volume of the reaction suspension, without changing other parameters, results in dramatic increase in the synergistic effect of sonophotocatalysis over individual sono and photocatalysis. In this context, the effect of reaction volume on the MnO_2 catalyzed sonocatalytic degradation of IC is examined. The results are presented in Fig.5.10.
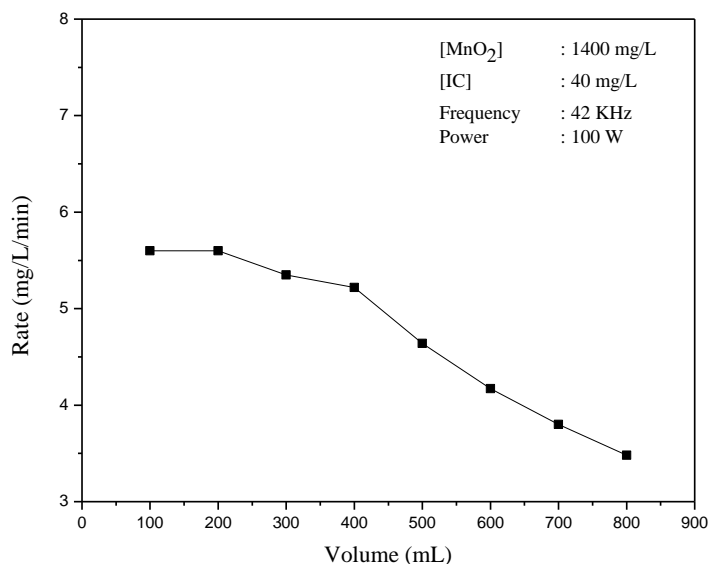
Fig. 5.10: Effect of reaction volume (at constant MnO_2 dosage) on the US/MnO_2 degradation of IC.

It is seen that under otherwise identical conditions, the degradation rate decreased slowly with increase in the reaction volume. This is partially due to the increase in the thickness of the irradiated region which in turn increases the attenuation of US intensity through the reaction medium. The negative effect of increasing volume can also be due to the relatively lower availability of catalyst particles (which is kept constant) per molecule of the dye for effective interaction. The possibility of compensating for this by keeping the catalyst-substrate ratio in the suspension constant by suitably varying the catalyst dosage is examined. The results are presented in Fig.5.11.
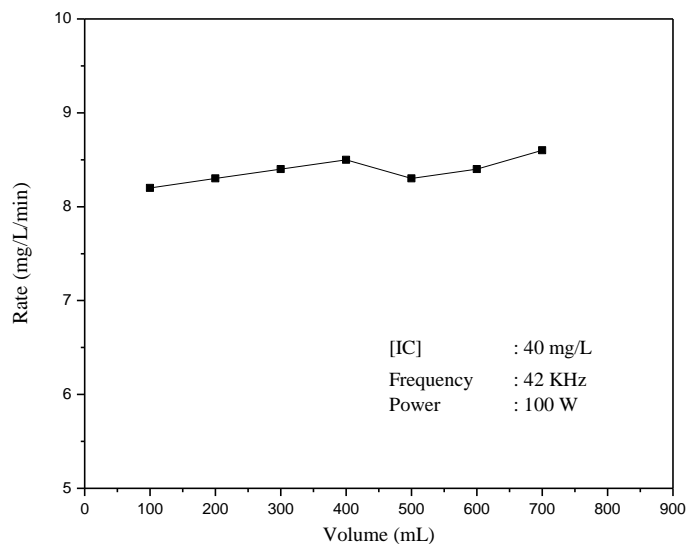
Fig. 5.11: Effect of volume (at constant volume/catalyst weight ratio) on the US/MnO$_2$ degradation of IC.

In this case the rate remains practically unaffected by changing volume indicating that the higher dosage of MnO$_2$ generates correspondingly more ·OH radicals to interact with the increasing number of IC molecules at higher volume. Absorption of ultrasonic energy by the surrounding apparatus, i.e. the reactor wall, cooling water and solvent/medium (in this case water), can also lead to decrease in rate at higher volume. In this case, experiments at all volumes were conducted in the same reactor assembly. As long as catalyst-substrate ratio is maintained at the optimum, the rate of degradation is unaffected. Hence it is inferred that as long as the power and frequency of US is adequate, the most important factor that determine the rate is the availability of sufficient catalyst to generate enough ROS to interact with the substrate molecules; i.e substrate-catalyst ratio is a critical parameter in sonocatalysis.

In the case of sonophotocatalysis, it has been reported that the decreasing reaction rate at higher volume can be reversed by applying correspondingly more power which results in increase in the number of active cavitation bubbles and consequent generation of more ˙OH radicals. [212, 154]. However, application of excessive power can disrupt the bubble dynamics resulting in abnormal bubble growth and poor cavitation. Hence proper correlation between frequency and power of US coupled with volume of the reaction medium and catalyst dosage is important in balancing the bubble growth and achieving optimum efficiency.

5.3.7 Effect of frequency

In addition to the role of power discussed above, another US parameter that can influence the sonication effect is the frequency. Preliminary study of the effect of frequency of US on the degradation of IC is verified at 42 and 53 KHz, keeping the power constant at 100W. The degradation decreases by 15% with increase in frequency from 42 to 53 KHz. Frequency of US influences the pressure cycle and causes high turbulence in the liquid [225-227]. This effect known as acoustic streaming dominates acoustic cavitation at high frequency and amplitude. Consequently the bubbles die prematurely resulting in poor cavitation and material growth. Increasing the frequency also reduces diffusion time which slows down the growth of cavitating bubble resulting in smaller bubbles and uniform distribution. Hence the rate and type of radical formation is dependent on frequency though there is no linear relation between the two. However the effect of frequency on the cavitation and subsequent processes cannot be generalized as it depends on the

characteristics of the reaction system. Detailed investigations on frequency and power effect are not made due to laboratory constraints. All investigations are hence made at 42 KHz.

5.3.8 Effect of dissolved oxygen

Presence of dissolved gases increases the cavitation threshold and hence adversely affects the sonocatalytic degradation efficiency. However, small amount of dissolved gases is necessary to effect efficient cavitation. The presence of dissolved O_2 during ultrasonic irradiation is known to play significant role in the formation of reactive $^\cdot OH$ radicals which are primarily responsible for the degradation of the pollutant. This role of O_2 is verified by measuring the sonocatalytic degradation of IC in MnO_2 systems deaerated with N_2. The degradation of IC is practically unaffected by deaeration thereby suggesting that the main source of O_2 for the reaction is not the dissolved form. This is similar to the observations made in the case of MW and UV activation of MnO_2 reported in previous Chapters.

As explained in earlier Chapters, MnO_2 is a rich reservoir of O_2. Hence significant amount of O_2 will be present in the MnO_2/IC suspension, even after long deaeration. It is already demonstrated that in the case of photocatalytic and microwave catalytic reactions, MnO_2 functions not only as a catalyst but also as a powerful oxidant. The required O_2 is provided primarily by the surface (adsorbed) and lattice of MnO_2 which cannot be easily removed by flushing with N_2. The participation of lattice oxygen which makes MnO_2 deficient in oxygen both atomically and by weight, is demonstrated by comparison of the Energy dispersive X-ray (EDX)

spectrum of the fresh and used catalysts (Figs. 5.12 and 5.13 respectively) and Table 5.3.
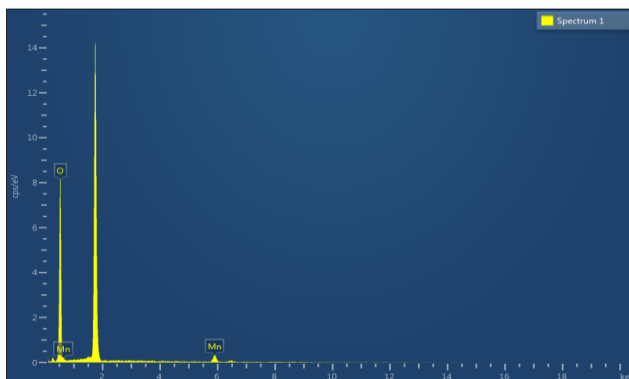
Fig. 5.12: EDX spectrum of Fresh MnO_2
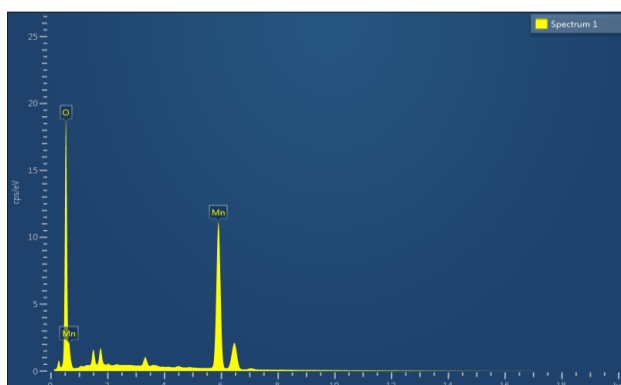
Fig. 5.13: EDX spectrum of used MnO_2

Table 5.3: Relative ratio of Mn and 'O' in MnO_2 before and after US/MnO_2/IC

[IC]	[MnO₂]	Wt% O		Wt% Mn		Atomic% O		Atomic% Mn	
		Before	After	Before	After	Before	After	Before	After
40 mg/L	1400 mg/L	85.8	35.24	14.2	64.76	95.4	65.14	4.6	34.86

If the effect of deoxygenation of the suspension by N_2 is compensated by the lattice and strongly bound O_2 in MnO_2 the effect will be dependent

Microwave, Photo and Sono Activated Advanced Oxidation Processes and their Variations for the Decontamination of Water from Toxic Chemical Pollutants

379

on the dosage of the catalyst, i.e. the less the amount of MnO_2, the more the effect of deaeration by N_2. This is verified by measuring the deaeration effect on the sonocatalytic degradation of IC at different dosages of MnO_2. The results are given in Table 5.4.

Table 5.4: Effect of MnO_2 dosage on the degradation of IC in systems deaerated with N_2
N_2 bubbling time: 60 min. [IC]: 60 mg/L

Sl. No.	MnO_2 dosage (mg/L)	Reaction time (min.)	% Degradation		Effect of N_2 bubbling on the degradation
			Standard	After N_2 bubbling	
1	1400	10*	74.5	76.2	+2.2%, i.e. ~ No change
2	1000	15*	62.8	64.3	+2.4%, i.e. ~ No change
2	200	30	12.4	11.3	- 8.8%, Inhibition
3	100	30	9.6	6.8	-29.2% Inhibition
4	50	30	5.6	2.6	-53.6% Inhibition

*Lower time is taken because the degradation was complete by 30 minutes

At lower MnO_2 dosage the deaeration by N_2 decreases the degradation of IC probably because the O_2 available from the MnO_2 is not adequate to compensate for the removed O_2. With increase in the quantity of MnO_2, more O_2 is available to compensate for the loss by deaeration and hence the effect is also less.

Under US irradiation, the O_2 present in the solution/suspension would be split into reactive $\cdot O$ radicals which interact with H_2O molecules (reaction 141) and form reactive $\cdot OH$. The 'hot spot effect' of US irradiation in water enhances the formation of $\cdot OH$ due to the pyrolysis of

water molecules as in reaction (140). This is followed by the generation of more free radicals as in reaction 142.

$$O + H_2O \quad \rightarrow \quad 2\ ^\cdot OH \dots\dots\dots\dots\dots\dots\dots\dots\dots\dots(141)$$

$$H^\cdot + O_2 \quad \rightarrow \quad O + ^\cdot OH \dots\dots\dots\dots\dots\dots\dots\dots\dots(142)$$

Additionally, the US induced 'sonoluminescence' [206, 207] generates light of wide wavelength range which can excite the semiconductor oxide and make it a potential photocatalyst capable of generating electron-hole pairs. This also leads to the production of reactive $^\cdot OH$ radicals as below:

$$MnO_2 + h\nu \quad \rightarrow \quad h^+ + e^- \dots\dots\dots\dots\dots\dots\dots\dots\dots\dots(143)$$

$$e^- + O_2 \quad \rightarrow \quad O_2^{\cdot -} \dots\dots\dots\dots\dots\dots\dots\dots\dots\dots\dots(144)$$

$$h^+ + H_2O \quad \rightarrow \quad ^\cdot OH + H^+ \dots\dots\dots\dots\dots\dots\dots\dots\dots(145)$$

Thus the unproductive recombination of the electrons and holes is also prevented in the presence of O_2. The presence of dissolved gases will also create deformities in the medium which eases the generation of cavitation events [228]. Hence it is reasonable to assume that the presence of O_2 is essential to initiate and enhance the degradation under US irradiation. During the process of sonication, when the cavitation induced bubbles break, temperature rises and some of the dissolved gases will be released. Hence an optimum amount of O_2 may be required for efficient generation of reactive free radicals and consequent sonocatalytic degradation. Irrespective of whether the US induced molecular activation is thermal and /or electrical, the molecules are brought into excited state and dissociate in the interior of the bubble cavities filled with gas (N_2/O_2/air) and/or vapour.

Microwave, Photo and Sono Activated Advanced Oxidation Processes and their Variations for the Decontamination of Water from Toxic Chemical Pollutants

381

Various steps leading to the formation of reactive $^\cdot$OH radicals in presence of O_2 under US irradiation were explained earlier. Further, even in deaerated system, the residual O_2 present in the gas bubble scavenges the $H^\cdot$ as:

$$H^\cdot + O_2 \rightarrow HO_2^\cdot \quad\text{..(146)}$$

$$2HO_2^\cdot \quad \rightarrow H_2O_2 + O_2 \quad\text{...(147)}$$

The detection of moderate amounts of H_2O_2 even in the deaerated system confirms the presence of this reaction.

In the presence of MnO_2, more interactions with H_2O_2 can occur;

$$MnO_2 + H_2O_2 + 2H^+ \rightarrow Mn^{2+} + 2H_2O + O_2 \quad\text{.............................. (148)}$$

Thus O_2 is regenerated in situ in the system in presence of MnO_2, even though part of it is consumed for the generation of ROS including H_2O_2. Hence the effect of deaeration by N_2 is not significant at higher dosage of MnO_2.

Amorphous MnO_2 is known to release bulk oxygen more easily to the surface which makes it a better catalyst in terms of facile activation and regeneration [147]. MnO_2 with multiple oxidation states together with its electron donor-acceptor properties is an excellent oxidation – reduction catalyst. Sonolysis of MnO_2 and resultant photoluminescence and consequent photolysis and sonophotolysis increase the number of oxygen species on the surface either by oxygen migration to the surface or by Mn migration to the bulk or both. Surface oxygen is consumed faster upon irradiation and oxygen from the bulk moves to the surface. In the case of MnO_2, the loss of oxygen takes place at temperatures as low as 50^0C. The

sono/photo-initiated oxygen release from MnO_2 may be due to movement of O^{2-} (bulk) to the surface and subsequent weakening of MnO_2 bonds [181]. In the re-oxidation of oxides, atmospheric oxygen and/or dissolved O_2 is taken up by the surface of the partially reduced MnO_2 as follows [147]:

$$O_2\,(g) + e^- \rightarrow (O_2^-) \quad\text{...} \quad (149) \quad \text{g-gas}$$

$$(O_2^-) + e^- \rightarrow 2(O^-) \rightarrow O^{2-}\,(s)\text{...} \quad (150) \text{ s-surface}$$

Most of the oxygen radicals are present in the bulk of the catalyst while some of them may remain on the surface for a short period. These highly active oxygen radicals can regenerate reduced manganese species. Under US irradiation, the bonds in MnO_2 are weakened and O^{2-} is released to the surface. Even though the lifetime of excited state oxygen species is short, they possess adequately high energy and electronegativity to facilitate the reduction or hydrogen abstraction from the substrate. Possible reaction pathways are:

$$O^{2-}\,(s) \underset{-\,e^-}{\overset{h\nu}{\longrightarrow}} (O^-) \underset{-\,e^-}{\overset{h\nu}{\longrightarrow}} O_2\,(s) \quad\text{...}(151)$$

$$O_2\,(s) + RH\ (i.e.,\ IC) \rightarrow HO_2^{\cdot}\,(s) + R^{\cdot}\text{...}(152)$$

$$O_2\,(s) + R^{\cdot} \rightarrow \text{Intermediates} \rightarrow\rightarrow\rightarrow \text{Mineralization}\ (CO_2 + H_2O)\text{..}(153)$$
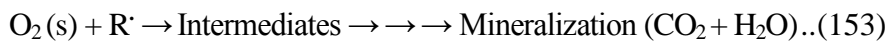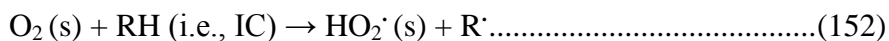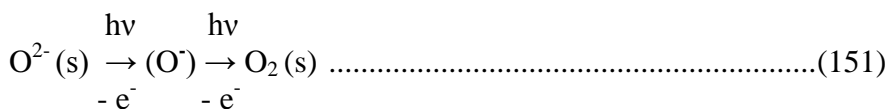
The abstracted $H^{\cdot}$ interacts with the hole and gets oxidized to form acid sites on the surface of MnO_2.

$$H^{\cdot} + h^+ \rightarrow H^+ \text{...}(154)$$

Microwave, Photo and Sono Activated Advanced Oxidation Processes and their Variations for the Decontamination of Water from Toxic Chemical Pollutants

383

The regeneration of MnO_2 may be represented as:

$$-Mn^{(3+ \text{ or } 2+)} \xrightarrow[- e^-]{h\nu} -Mn^{(4+ \text{ or } 3+)} \quad\dots\dots\dots\dots\dots\dots\dots\dots\dots\dots\dots\dots\dots(155)$$

$$n(-Mn^{(4+ \text{ or } 3+)}-) + O^{2-} \text{ (from reaction 150)} \rightarrow MnO_2 \text{ (or } Mn_3O_4) \dots(156)$$
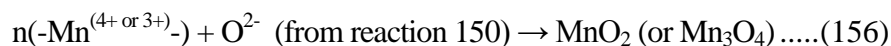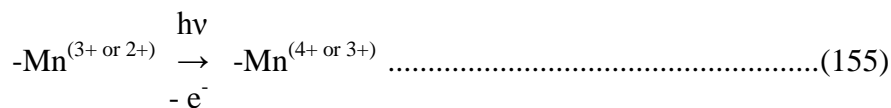
Unless the oxygen is replenished periodically, the activity of the catalyst will be lost faster. This is verified by recycling the catalyst immediately after use (Fig.5.14). The used catalyst is separated by simple filtration followed by quick drying at 120^0C for 1 hr. The degradation of IC (in 10 minutes) decreased steeply from ~70% in presence of fresh catalyst to ~ 62% in first recycling, ~ 42% in second recycling and ~ 23% in third recycling.
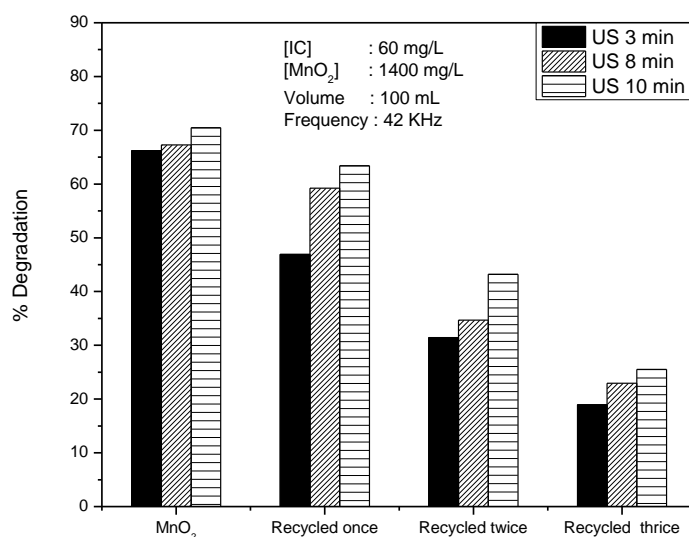
Fig. 5.14: Relative efficiency of recycled MnO_2 for the US/MnO_2 degradation of IC at different times of US irradiation

This confirms drastic change in the surface characteristics, loss of adsorption sites and loss of oxygen from the lattice, bulk and/or the surface of MnO_2 during the reaction which are not fully compensated by contact with atmospheric oxygen. The migration of bulk oxygen to the less energetic surface sites and its consumption by participation in catalytic reactions is evident from the experimental results as well as the EDX data discussed earlier. ESR evidence for the depletion of O_2 from the catalyst under AOP is also available [192].

The effect of replacement of air at least partially by N_2 or inert gases can be even more complex and unpredictable especially under sonolysis. When the dissolved air is replaced by degassing with N_2, the system will still contain moderate amounts of both N_2 and O_2. As explained earlier, O_2 is available from MnO_2 even in deaerated solution. The high temperature and pressure conditions of sonolysis will induce interaction between both these gases resulting in the formation of nitrogen oxides, nitrate, nitrites and even the unstable peroxy species peroxynitrous acid [229, 230]. These species will lead to a number of even more complex reactions under sonication, that too in presence of the highly active catalyst MnO_2. Substitution of air by N_2 can also modify the maximum temperature reached by the collapsing bubbles and the rate of heat dispersion. The facile ˙OH generation by sonolysis in presence of O_2 will also be slowed down.

The presence of gases in dissolved form or as individual bubbles is known to provide additional nuclei for the generation of cavitation leading to enhanced number of cavitational events. This will enhance the

pressure/temperature pulse generated in the system and the formation of reactive free radicals. However, too much of aeration (or of any gas) will result in decoupling effect leading to decreased energy input into the system [97]. Generation of large number of gaseous cavities is often not advantageous because the energy content of these cavities will be substantially lower compared to that of the vaporous cavities. The effect of the presence of gases can be further complicated because the physicochemical properties of the gas such as solubility, thermal conductivity, polytropic index etc. can affect the cavitation intensity. Hence in order to achieve maximum sono degradation of the pollutant, the aeration/gassing of the reaction systems has to be optimised with and/or without catalyst, especially so in the presence of a strong O_2 reservoir such as MnO_2.

5.3.9 Effect of oxidants

Oxidants such as H_2O_2, persulphate (PS), Chromate, permanganate, periodate etc. are known to enhance the AOP degradation of many organic pollutants in water. In this context, the effect of two typical oxidants, i.e. H_2O_2 and PS on the sonocatalytic degradation of IC in presence of MnO_2 is investigated and the results are as follows:

5.3.9.1 Effect of added H_2O_2

Effect of added H_2O_2 on the sonocatalytic degradation of IC is tested in presence of MnO_2. The results are shown in Fig.5.15.
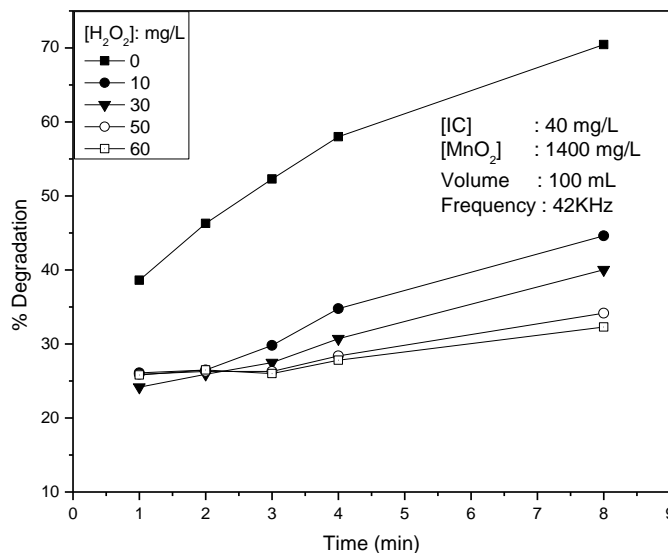
Fig. 5.15: Effect of H_2O_2 at different concentrations on the US/MnO$_2$/IC degradation

Contrary to expected enhancement, the degradation is inhibited by H_2O_2 at all concentrations. Initially the inhibition increases with increase in concentration of H_2O_2 upto 50 mg/L. Thereafter the degradation is stabilized with no further decrease, with increase in concentration of H_2O_2. This is consistent with the results on the contradicting effect of H_2O_2 reported in many earlier studies according to which H_2O_2 can be an enhancer or inhibitor depending on the reaction conditions. The inhibition effect is further verified by the in-between addition of H_2O_2 to the reaction system at different time intervals of irradiation. In this case, the inhibition of the degradation begins from the moment of addition of H_2O_2 (Fig.5.16).
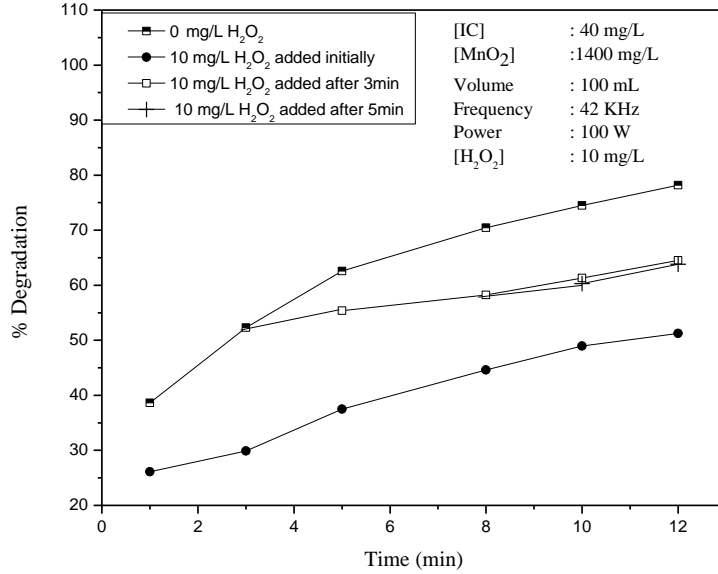
Fig. 5.16: Effect of initial and in-between addition of H_2O_2 on the US/MnO$_2$/IC degradation

Under US/MnO$_2$ conditions, added or insitu formed H_2O_2, which is an oxidant, undergoes decomposition. The reactive oxygen species, including the powerful ˙OH radicals, thus generated do not interact exclusively with the IC molecules, because, had it been so, the degradation of IC should have been enhanced. It is possible that under these conditions the following reactions may be taking place:

$$2H_2O_2 \quad \xrightarrow{US} \quad 2H_2O + O_2 \quad ....(157)$$

$$2H_2O_2 \quad \xrightarrow{US} \quad 2˙OH .... (158)$$
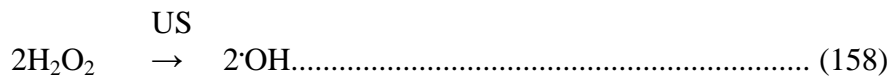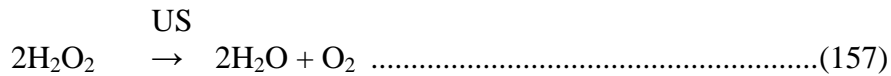
It is also possible that the H_2O_2 scavenges the insitu formed ˙OH radicals as follows:

$$H_2O_2 + {}^{\cdot}OH \rightarrow H_2O + HO_2^{\cdot} \dots\dots\dots(159)$$

$$HO_2^{\cdot} + HO_2^{\cdot} \rightarrow H_2O_2 + O_2 \dots\dots\dots(160)$$

$HO_2^{\cdot}$ is a poor oxidant (oxidation potential =1.7eV) compared to ${}^{\cdot}OH$ (oxidation potential = 2.8eV) or H_2O_2 (oxidation potential = 1.77eV). Higher concentration of H_2O_2 will scavenge the insitu formed ${}^{\cdot}OH$ (reaction 159). Part of the ${}^{\cdot}OH$ radicals formed in the system will be used for the degradation of IC and the other part will be interacting with H_2O_2 itself decomposing it. Thus the net quantum of ${}^{\cdot}OH$ radicals available for degrading the dye is reduced resulting in the inhibition. Absorption of US by H_2O_2 and consequent reactions naturally result in decrease in the US available for activation of the catalyst and the substrate which also leads to decrease in the degradation of IC. Similar results are reported in the case of sono, photo and sonophotocatalytic degradation of organic pollutants in water [162, 197].

It is possible that externally added or insitu formed H_2O_2 will utilize at least a few active sites on the surface of MnO_2 for adsorption and/or decomposition thereby reducing the number of sites available for IC. Measurement of the adsorption of IC (60 mg/L) on MnO_2 in presence of various concentrations of H_2O_2 (0-80 mg/L) under the sonocatalytic conditions used here, shows that the adsorption of IC is not affected significantly at lower dosages of the catalyst. However, at higher dosage of the catalyst, the adsorption of IC is inhibited. Hence competitive adsorption of H_2O_2 and consequent denial of surface sites for IC on MnO_2 is not the major cause of the inhibition at least at lower catalyst dosage used here. As demonstrated in Section 3.3.3.9 of Chapter 3 for every

Microwave, Photo and Sono Activated Advanced Oxidation Processes and their Variations for the Decontamination of Water from Toxic Chemical Pollutants

389

MnO_2-H_2O_2 combination there is an optimum for the adsorption of H_2O_2 beyond which there is only adsorption-desorption equilibrium (of H_2O_2). This explains the higher optimum adsorption of H_2O_2 at higher concentration even with same dosage of MnO_2. In the simultaneous presence of both IC and H_2O_2, there is competition between the two for surface sites, though the extent of competition depends on their relative concentration. Hence the inhibition in presence of H_2O_2 is partially due to competitive adsorption. There are other contributing factors also as discussed in Section 3.3.3.9 and 3.3.3.10.1 of Chapter 3 and Section 4.3.6.1 of Chapter 4. Other unidentified factors resulting from the multitude of free radical interactions also may lead to the contradicting effect ('inhibition', 'no effect' or 'enhancement') of H_2O_2 which needs to be investigated further in depth.

5.3.9.2 Effect of persulphate (PS)

In the context of inhibition of the sonocatalytic degradation by H_2O_2, another oxidant Persulphate ($S_2O_8^{2-}$) ($E^0 = 2.1$ V) is investigated as a potential enhancer. Persulphate (PS) has specific advantages such as high solubility and stability at ambient temperature as explained in earlier Chapters. Further, the SO_4^{2-} ions, which are the major products of PS reduction are relatively harmLess and considered environment-friendly. PS as such does not cause any degradation of IC. The effect of PS on the reactions is shown in Fig.5.17.
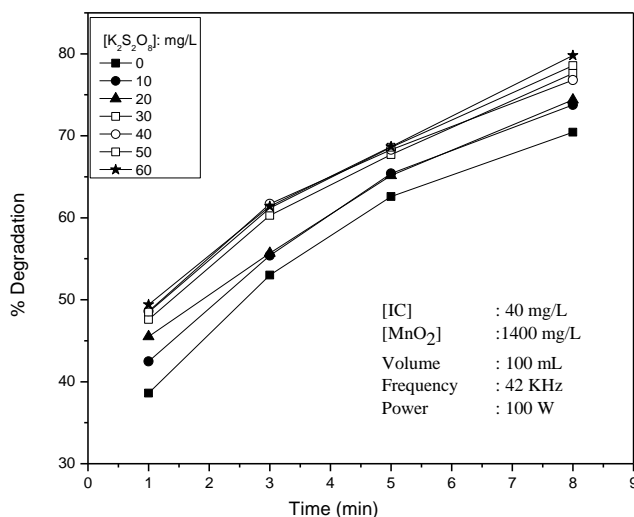
Fig. 5.17: Effect of $K_2S_2O_8$ on the US/MnO$_2$/IC degradation

The degradation is enhanced moderately in presence of PS in the range of 10-50 mg/L. Thereafter the degradation is stabilized with no enhancing effect by further increase of PS. The enhancement is further confirmed by in-between addition of PS to the reaction in progress (Fig.5.18) which shows marginal increase in degradation from the point of addition. Since there is no negative effect in the presence of excess of PS, any unused oxidant remaining in the system can be used for the treatment of fresh input of IC pollutant which is important from the angle of commercial application of the process.
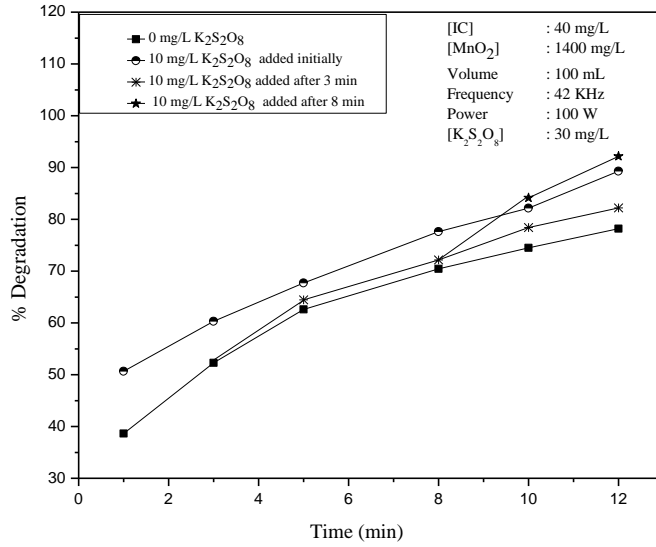
Fig. 5.18: Effect of initial and in between addition of K$_2$S$_2$O$_8$ on the US/MnO$_2$/IC degradation

Combination of the two oxidants H$_2$O$_2$ and PS showed that the effect on the degradation is the average of the effects of both (Fig.5.19).
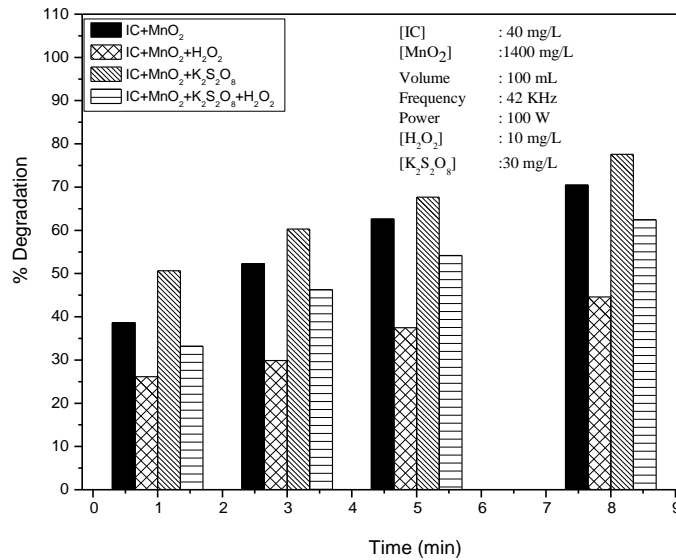
Fig. 5.19: Effect of combination of H$_2$O$_2$ and K$_2$S$_2$O$_8$ on the US/MnO$_2$/IC degradation

The enhancement of AOP degradation of organics by PS is explained based on the formation of highly reactive $SO_4^{\cdot-}$ radical anions insitu. Since the enhancement is only moderate, it may be inferred that the formation of $SO_4^{\cdot-}$ under US is not as significant as in the case of other radiations such as UV or microwave. The reactions leading to the formation of $SO_4^{\cdot-}$ radicals and the subsequent interactions with the substrate IC (already discussed in Chapter 4) are presented again (for convenience of reference) in equations 161-170 [185].

$$S_2O_8^{2-} \rightarrow 2SO_4^{\cdot-} \quad \text{..(161)}$$

$$SO_4^{\cdot-} + RH \rightarrow R^{\cdot} + HSO_4^{-} \quad \text{........................(162) where RH=IC}$$

$$SO_4^{\cdot-} + H_2O \rightarrow SO_4^{2-} + H^+ + {\cdot}OH \text{......................................(163)}$$

$$S_2O_8^{2-} + RH \rightarrow SO_4^{\cdot-} + HSO_4^{-} + R^{\cdot} \text{..................................(164)}$$

$${\cdot}OH + (RH, R^{\cdot}) \rightarrow \text{Intermediates} \rightarrow \text{products} \text{.....................(165)}$$

$$SO_4^{\cdot-} + (R^{\cdot}, {\cdot}OH) \rightarrow \text{Chain termination} \text{....................................(166)}$$

$$2SO_4^{\cdot-} \rightarrow S_2O_8^{2-} \text{ Chain termination} \text{.........................(167)}$$

$$2\ {\cdot}OH \rightarrow H_2O_2 \text{ Chain termination} \text{...........................(168)}$$

$$2R^{\cdot} \rightarrow \text{RR Chain termination/Further degradation (169)}$$

$$SO_4^{\cdot-} + S_2O_8^{2-} \rightarrow SO_4^{2-} + S_2O_8^{\cdot-} \text{...(170)}$$
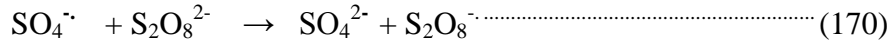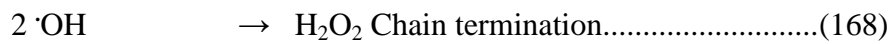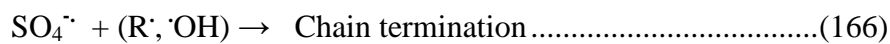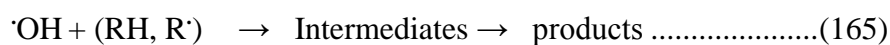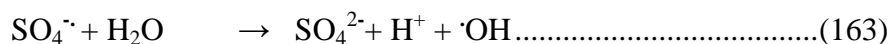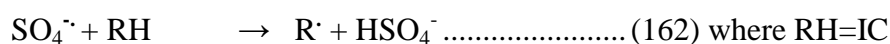
Various ROS such as H_2O_2, $HO_2^{\cdot}$, ${\cdot}OH$ etc. and $SO_4^{\cdot-}$ formed during the irradiation interact with IC on the surface of the catalyst as well as in the bulk, leading to its degradation into various intermediates and eventual mineralization. However, the degradation is not increasing with increase in concentration of PS, above 50mg/L. This shows that the reactive $SO_4^{\cdot-}$ radicals formed insitu at higher concentration of PS may be

getting deactivated as in reactions (167) and (170). This leads to stabilization in the rate of degradation at higher concentration of PS.

5.3.10 Effect of anions/salts on the degradation

As done in previous Chapters the effect of anions such as PO_4^{3-}, HCO_3^-, CO_3^{2-}, NO_3^-, SO_4^{2-}, CH_3COO^- and Cl^- on the degradation of IC is investigated under sonocatalysis also. The reaction parameters used are the same as those optimized already. The common cation in all cases was Na^+. The anions PO_4^{3-}, HCO_3^- and CO_3^{2-} inhibit sonocatalytic degradation of IC strongly; the inhibition increasing with increase in the concentration of the anions (Fig.5.20A).
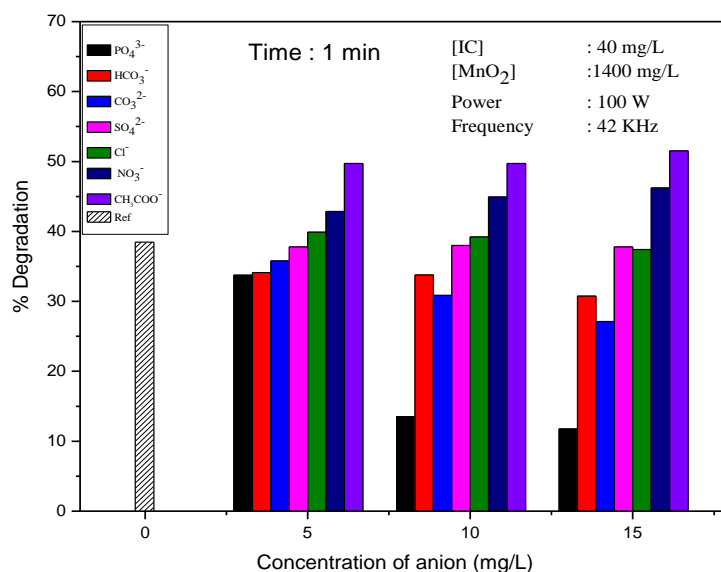
Fig. 5.20A: Effect of anions at various concentrations on the US/MnO$_2$/IC degradation

SO_4^{2-} and Cl^- have no effect while CH_3COO^- and NO_3^- enhance the degradation such that $CH_3COO^- > NO_3^-$. The inhibition by respective inhibitors increases with increase in their concentration. However, the

enhancement by CH_3COO^- and NO_3^- does not increase much with their concentration. Similarly with reaction time as the reaction proceeds and the net concentration of IC decreases, the degree of enhancement decreases, though the trend remains the same (Fig.5.20B). The relative inhibition by HCO_3^- also is less at later stages of reaction. However, the extent of inhibition by PO_4^{3-} and CO_3^{2-} remain practically unchanged even after extended reaction times.
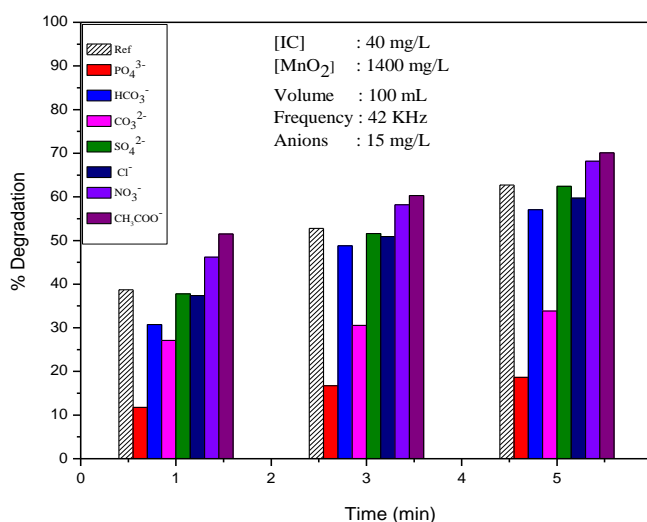
Fig. 5.20B: Effect of anions at varying reaction times on the US/MnO₂/IC degradation

The effect of concentration of the anions and the reaction times on the degradation of IC is summarized in Tables 5.5 and 5.6 respectively.

Table 5.5: Effect of concentration of anions on the US/MnO₂/IC degradation [MnO₂]: 1400 mg/L, [IC]: 40 mg/L, Time: 1min.

Concentration of Anions(mg/L)	Inhibition	No Effect	Enhancement
5	$PO_4^{3-} \approx CO_3^{2-} \approx HCO_3^-$	Cl^-, SO_4^{2-}	$CH_3COO^- > NO_3^-$
10	$PO_4^{3-} > CO_3^{2-} > HCO_3^-$	Cl^-, SO_4^{2-}	$CH_3COO^- > NO_3^-$
15	$PO_4^{3-} > CO_3^{2-} > HCO_3^-$	Cl^-, SO_4^{2-}	$CH_3COO^- > NO_3^-$

Table 5.6: Effect of reaction time on the 'anion effect on the US/MnO$_2$/IC degradation [MnO$_2$]: 1400 mg/L, [IC]: 40 mg/L, [Anion]:15 mg/L

Time	Inhibition	No Effect	Enhancement
1min	PO$_4^{3-}$ > CO$_3^{2-}$ > HCO$_3^-$	Cl$^-$, SO$_4^{2-}$	CH$_3$COO$^-$ > NO$_3^-$
3min	PO$_4^{3-}$ > CO$_3^{2-}$ > HCO$_3^-$	Cl$^-$, SO$_4^{2-}$	CH$_3$COO$^-$ > NO$_3^-$
5min	PO$_4^{3-}$ > CO$_3^{2-}$ > HCO$_3^-$	Cl$^-$, SO$_4^{2-}$	CH$_3$COO$^-$ > NO$_3^-$

The results show that reaction time has only modest effect on the nature of the influence of anions, thereby suggesting that reaction intermediates do not influence the anion effect significantly.

As done in the case of MW and photocatalysis, the effect of each anion on the sonocatalytic degradation of IC is investigated in detail and the results are plotted in Figs. 5.21 to 5.27.

5.3.10.1 Cl$^-$
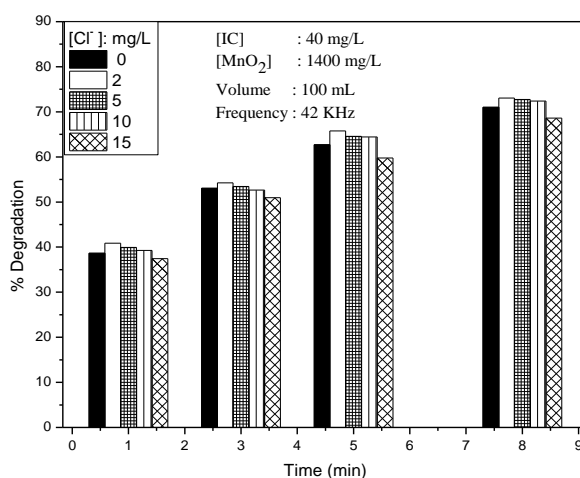
Fig. 5.21: Effect of Cl$^-$ on the US/MnO$_2$/IC degradation

Cl$^-$ ions in the concentration range of 2-10mg/L has practically no effect on the degradation of IC. At higher concentration of 15 mg/L there is mild inhibition. However, for all practical purpose this may be treated as 'no effect' within the limits of experimental error.

5.3.10.2 PO_4^{3-}
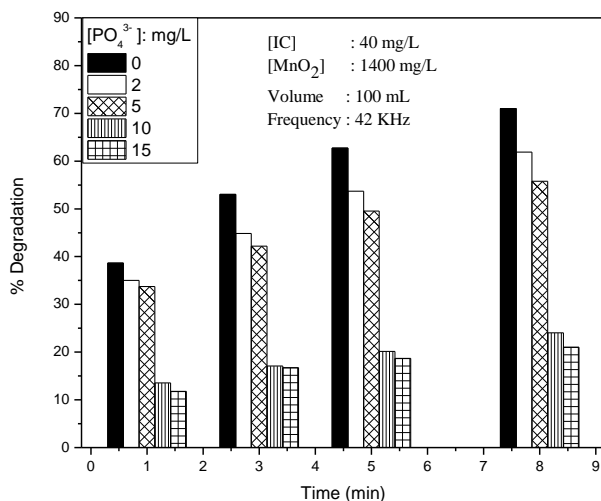
Fig. 5.22: Effect of PO_4^{3-} on the US/MnO₂/IC degradation

PO_4^{3-} remains as a strong inhibitor at all concentrations and reaction times.

5.3.10.3 SO_4^{2-}
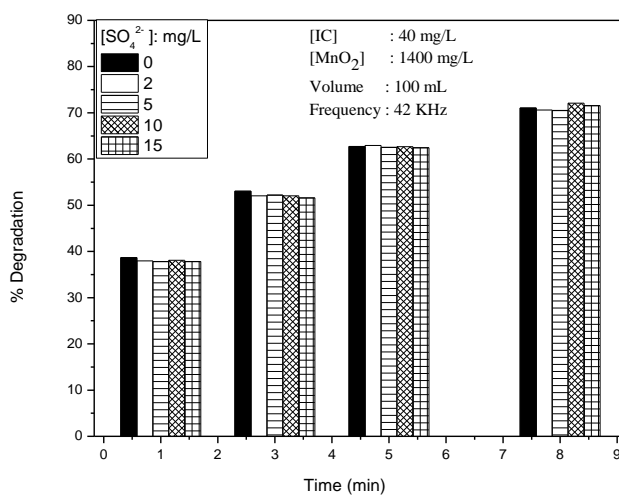
Fig. 5.23: Effect of SO_4^{2-} on the US/MnO₂/IC degradation

SO_4^{2-} has no effect at all concentrations and reaction times studied here.
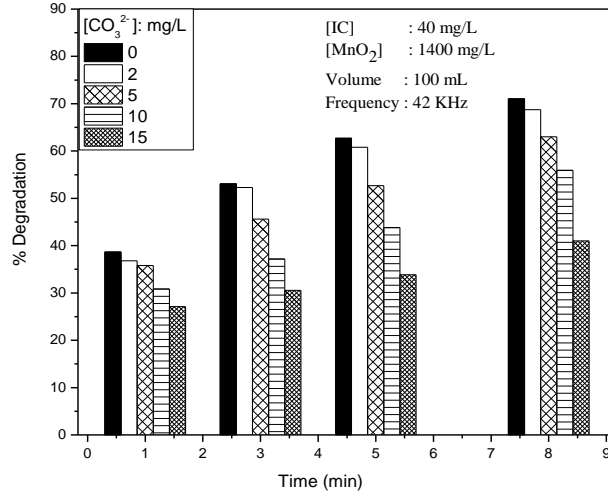
5.3.10.4 CO$_3$$^{2-}$

Fig. 5.24: Effect of CO$_3$$^{2-}$ on the US/MnO$_2$/IC degradation

CO$_3$$^{2-}$ ions remains a strong inhibitor throughout.

5.3.10.5 CH$_3$COO$^-$

Fig. 5.25: Effect of CH$_3$COO$^-$ on the US/MnO$_2$/IC degradation

CH$_3$COO- is a mild enhancer in the early stage of reaction. However at later stages of reaction, the mild enhancement become practically no effect.

5.3.10.6 HCO₃⁻

Fig. 5.26: Effect of HCO_3^- on the US/MnO₂/IC degradation

HCO_3^- is a moderate inhibitor at all concentrations of the anion and reaction times.

5.3.10.7 NO₃⁻

Fig. 5.27: Effect of NO_3^- on the US/MnO₂/IC degradation

Microwave, Photo and Sono Activated Advanced Oxidation Processes and their Variations for the Decontamination of Water from Toxic Chemical Pollutants

399

NO$_3^-$ is a mild enhancer in the early stages of reaction. The enhancement becomes weaker with time of reaction and eventually the effect becomes 'nil'.

The results illustrate that the effect of anions/salts on the sonocatalytic degradation of IC in presence of MnO$_2$ is complex and does not follow any consistent pattern with respect to concentration (of the anion) and/or the time of reaction. While inhibitors remain as inhibitors always, 'enhancement' becomes 'no effect' depending on the reaction conditions. Hence the effect of each anion has to be analyzed individually in the context of the reaction system, conditions and the composition. The effect, whether inhibition or enhancement, is only modest, except in the case of clear inhibitors (PO$_4^{3-}$ and CO$_3^{2-}$) probably because of the microstreaming effect of US on the catalyst particles which results in continuous cleaning of the surface.

The effect of anions on AOPs is often explained based on many factors which are often contradictory. The preferential adsorption of anions on the catalyst surface and consequent reduction in the availability of surface sites for the generation of ROS and the adsorption of the substrate is often cited as a reason for the inhibition. In this respect, the data on adsorption of IC on MnO$_2$ in presence of the anions reported in Table 4.4 Chapter 4 is relevant.

The adsorption of IC is inhibited in the order PO$_4^{3-}$ > CO$_3^{2-}$ > HCO$_3^-$. Other ions do not affect the adsorption significantly. Comparing the effect of anions on the degradation of IC, it may be inferred that the

inhibition can be at least partially attributed to the decrease in the adsorption of the dye. The enhancement in presence of CH_3COO^- and NO_3^- has to be explained based on other factors as done in previous Chapters.

Another possible reason for the inhibition of the degradation may be layer formation by the anions on the catalyst surface which is explained in detail under Section 3.3.3.12 of Chapter 3. Based on the solubility of salts the layer formation must be in the order.

$$HCO_3^- > PO_4^{3-} > Cl^- > CO_3^{2-} > SO_4^{2-} > CH_3COO^- > NO_3^- \quad ....(171)$$
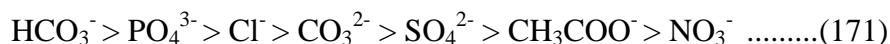
If layer formation is at least one of the causes for the inhibition the degradation also should be inhibited in the same order as in (171). This can partially explain the maximum inhibition in the case of PO_4^{3-}, HCO_3^- and CO_3^{2-} and the least (where it is even enhancement) in the case of NO_3^- and CH_3COO^-. This also confirms that the surface does play an important role in the sonocatalytic degradation of IC, even though the reactions taking place in the bulk are also significant.

Another major factor which can influence the effect of anions is their ability to function as ˙OH radical scavengers. The scavenging rate constants of ˙OH by some of the anions are summarized in Table 3.5, Chapter 3. The formation of various radical anions by the interaction of ˙OH with anion and the effect on the degradation of IC is also clearly demonstrated in Section 3.3.3.12 of Chapter 3. However the scavenging of ˙OH by anion cannot consistently explain the inhibition. Similarly the formation of reactive radical anion cannot fully explain the enhancement

Microwave, Photo and Sono Activated Advanced Oxidation Processes and their Variations for the Decontamination of Water from Toxic Chemical Pollutants

401

either. The radical anions, though less reactive than $^{\cdot}$OH, do not get deactivated as in the case of OH and will be available for longer time for interaction with the substrate. This will lead to no effect or enhancement eventually.

In any case, based on the observation, it may be inferred that the preferential adsorption of the anion and surface layer formation and consequent impact on the activation of the catalyst surface as well as generation of ROS are mainly responsible for the inhibition.

Since the degradation proceeds moderately well even in the presence of the inhibiting factors as above, there may be other factors which can compensate for them at least partially and assist the degradation. This is more evident in the enhancement of the degradation of IC, in the presence of the two anions CH_3COO^- and NO_3^-.

In the case of sonolysis/sonocatalysis the interaction between the $^{\cdot}$OH radicals and the anions forming the reactive radical anion takes place at the air-water interface of the cavitation bubbles where polarizable anions can get accumulated. These radical anions diffuse into the solution bulk and react with the substrate. The concentration of the $^{\cdot}$OH radicals in the bulk is less and hence their recombination is slower. Consequently, the $^{\cdot}$OH will interact with the more abundant substrate molecules and anions, both leading to enhanced degradation. Hence, indirectly, the anions are shielding the $^{\cdot}$OH radicals from unproductive recombination by transforming them into radical anions. Towards the later stages of reaction when the degradation of the

substrate has progressed substantially, its concentration in the system is less. Hence the radical anion $X^{-\cdot}$ which has only substrate as the sink, cannot sustain the enhanced degradation rate. From that point onwards, the anion-caused enhancement slows down gradually and they may even become inhibitors eventually. This can explain the slowdown or stabilization of the 'enhancement' or even its transition to 'inhibition' with concentration of the anion and time of reaction. In this instance, the 'enhancement' becomes 'stabilisation' and not 'inhibition', at least in the concentration and time range studied here, probably because MnO_2 is a highly efficient catalyst. Further details on radical anion formation by the anions and the impact on the degradation of IC are discussed in earlier Sections 3.3.3.12 and 4.3.7 of Chapters 3 and 4, respectively.

The possibility of the anions influencing pH of the reaction system and consequent variation in the reaction rate also can be ruled out based on the explanations provided in Section 3.3.3.12 of Chapter 3.   In this case also variation in pH is not the cause for the anion effect.

Even those anions which are getting competitively better adsorbed on the surface need not remain there for long under sonolytic conditions due to the phenomena of microstreaming and microbubbles eruption [207]. This type of surface cleaning can contribute to sustained long term activity of the catalyst. Since the inhibition is not significant, except in the presence of PO_4^{3-}, HCO_3^- and CO_3^{2-} which are proven to be strongly adsorbed, the surface cleaning may indeed be happening in sonocatalysis. This is further evident from the observation that the inhibition of the

Microwave, Photo and Sono Activated Advanced Oxidation Processes and their Variations for the Decontamination of Water from Toxic Chemical Pollutants

403

degradation of IC is not linearly increasing with increase in the concentration of the anion and the degree of inhibition is even decreasing at higher concentration (of the anion).

Accumulation of various reaction intermediates with reaction time which may get more strongly bound to the surface due to structural characteristics can challenge the efficiency of microstreaming. Diminishing concentration of the substrate, competition from the intermediates formed insitu and the anions for the reactive free radicals, relative concentration of the reactive radical anions, reduced penetration of US energy into the system at higher concentration of anions etc. will influence the degree of inhibition. Depending on the relative contributions of various factors, the net effect can be 'inhibition', 'no effect' or even 'enhancement'.

The effect of anions on the degradation of pollutants under sonolysis can also be examined based on the ionic strength of the medium. Anions increase the ionic strength of the solution leading to 'salting out' of the pollutant into the cavitation bubbles where gas phase pyrolysis could take place under sonolysis. This can assist the degradation in certain cases leading to enhancement. Presence of salts can also modify the partition coefficient and hence the distribution of aqueous and organic phases. Solid particles (such as MnO_2 in the present case) can facilitate better propagation of US in the reaction medium and create instabilities in the system. This will result in enhanced generation of more cavitation bubbles and better emission of light (sonoluminescence) through the reactor [218], thereby leading to photocatalysis and sonophotocatalysis

depending on the intensity of light. Suspended solid particles may also provide additional nucleation sites and facilitate surface cavitation due to surface roughness [182, 222]. Formation of crevices and the obstruction by the particles break up the spherical symmetry of the large sized cavitation bubble into many little ones. Increase in number of cavitation bubbles will increase the pyrolysis of water, generate more free radicals and enhance the degradation of IC. The adsorbed anions may also enhance the nucleation capability of the surface which reaches an optimum at certain concentrations. These factors also contribute to increase in the concentration of pollutant at the gas-liquid interface and the cavity implosion sites. This will result in more effective interaction of the substrate with the reactive free radicals leading to enhanced degradation rates. Presence of salt can also decrease the vapor pressure and increase the hydrophilicity as well as surface tension of the aqueous phase resulting in more violent collapse of the cavities and increased degradation. Surface tension can also affect the nucleation process and the cavitational threshold.

Thus it may be seen that multitude of complimenting and contradicting factors are operating in presence of anions under sonolysis making the 'anion effect' complex, inconsistent and unpredictable.

5.3.11 Determination of TOC, Identification of reaction intermediates

The mineralization of IC by MnO₂ mediated sonocatalysis is verified by total organic carbon (TOC) measurements. The TOC under

other reaction conditions (as described later in this Section) are also provided in the figure. The results are presented in Fig.5.28.
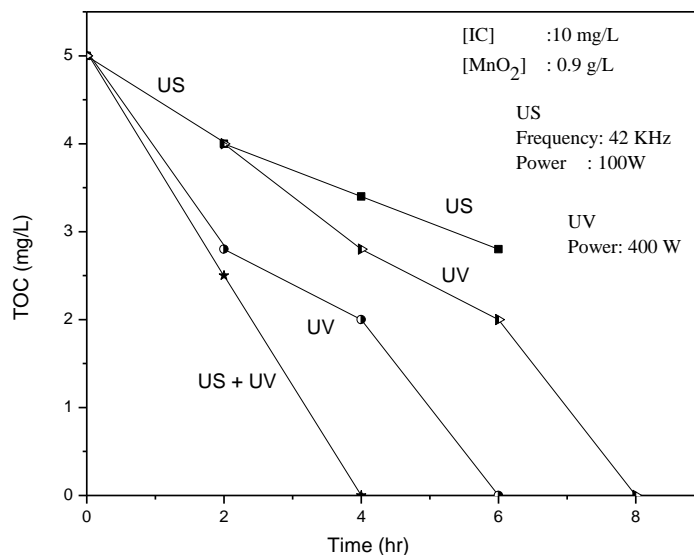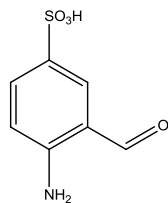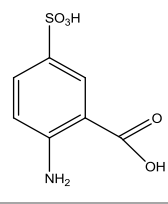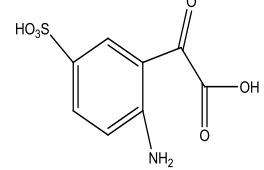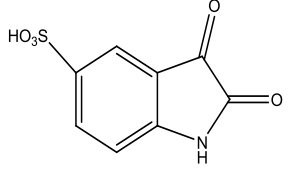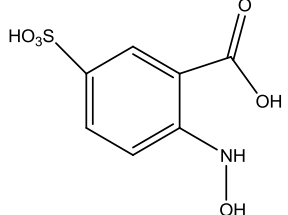
Fig. 5.28: COD of MnO_2/IC system under various conditions of activation.

The TOC of a representative reaction system (IC = 10 mg/L, MnO_2 = 0.9g/L) before US irradiation was 5 mg/L. After decolourization TOC becomes 3.5 mg/L. Further US irradiation reduces the TOC very slowly indicating that US irradiation alone is not powerful enough to effect rapid mineralization of the intermediate products. The reaction intermediates present in the system at this stage are identified by LC-MS and are listed in Table 5.7.

Table 5.7: Major Intermediates formed during the sonocatalytic degradation of IC

Sl No.	m/z	Proposed Structure
1	200	
2	217	
3	245	
4	227	
5	233	

The possibility of using photolysis/photocatalysis to drive the sonocatalytic degradation of IC upto complete mineralization is tested by subjecting the decolorized reaction suspension to UV irradiation and

Microwave, Photo and Sono Activated Advanced Oxidation Processes and their Variations for the Decontamination of Water from Toxic Chemical Pollutants

407

determining the TOC at different intervals. The results presented in Fig.5.28 show that sonocatalysis followed by photocatalysis leads to complete mineralization (TOC= 0) in 8 hr. Under simple UV photocatalysis the identical system is mineralized in 6 hr. However, simultaneous sono and photocatalysis (sonophotocatalysis) was the most efficient with the mineralization getting completed in 4 hr. This is consistent with the synergy reported in the case of sonophotocatalysis [212, 154]. Hence the efficiency of different AOPs for the mineralization of IC under otherwise identical conditions is:

sonophotocatalysis (simultaneous) > photocatalysis > (sonocatalysis + photocatalysis in sequence) > > sonocatalysis ....(172)

The superiority of photocatalysis and sonophotocatalysis suggests the possibility of using a combination catalyst which can harness the sonoenergy and photoenergy more efficiently at the same time. Hence as done in the case of MW catalysis and photocatalysis, in this case also MnO_2 is combined with TiO_2 and its sonocatalytic efficiency for the degradation of IC is evaluated. Depending on the sonocatalytic efficiency of MnO_2-TiO_2, the combination catalyst can be further tested in sonophotocatalysis. The superior adsorption, oxidation and sonocatalytic efficiency of MnO_2 together with the photocatalytic efficiency of TiO_2 is expected to be beneficial for the design of an appropriate sonophotocatalyst for the removal of organic chemical pollutants from water.

5.4 Sonocatalytic degradation of IC using MnO_2-TiO_2

5.4.1 Preliminary results

Studies reported in previous Chapters have shown that the optimum ratio of MnO_2-TiO_2 to take advantage of the combined catalyst is 1.8/0.1g/L. Hence the effect of addition of TiO_2 to MnO_2 is tested at two different concentrations i.e 0.1g/L and 0.2g/L (MnO_2 kept constant at 1.8g/L) for the degradation of IC. The results show that the effect of TiO_2 is only marginal irrespective of its concentration with less than 5% increase in degradation over that in presence of MnO_2 only (Fig.5.29). In any case, as done in the case of MW and photocatalysis, the degradation of IC is investigated in detail using MnO_2-TiO_2 in the ratio 18:1 and various parameters are optimized.
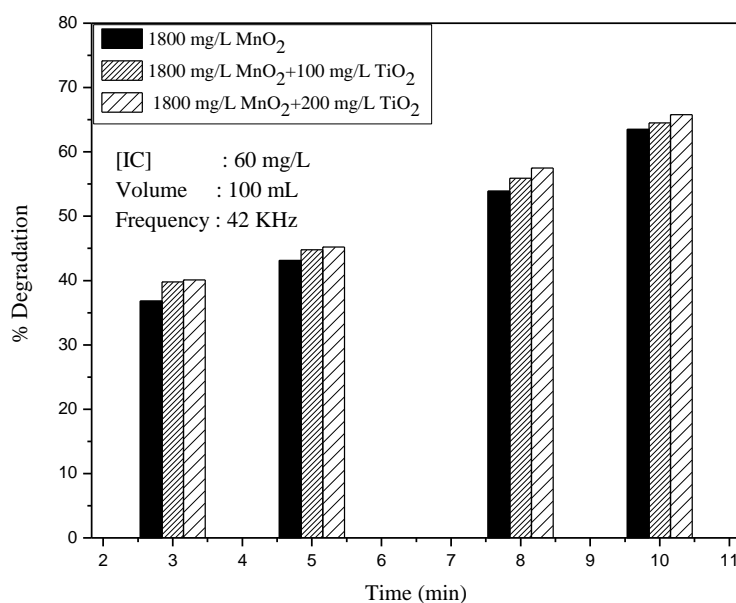
Fig. 5.29: Effect of TiO_2 on the sonoactivity of MnO_2 for the degradation of IC.

5.4.2 Effect of catalyst dosage

Effect of catalyst MnO_2-TiO_2 (18:1) dosage, on the sonocatalytic degradation of IC (keeping all parameters constant) is shown in Fig.5.30.
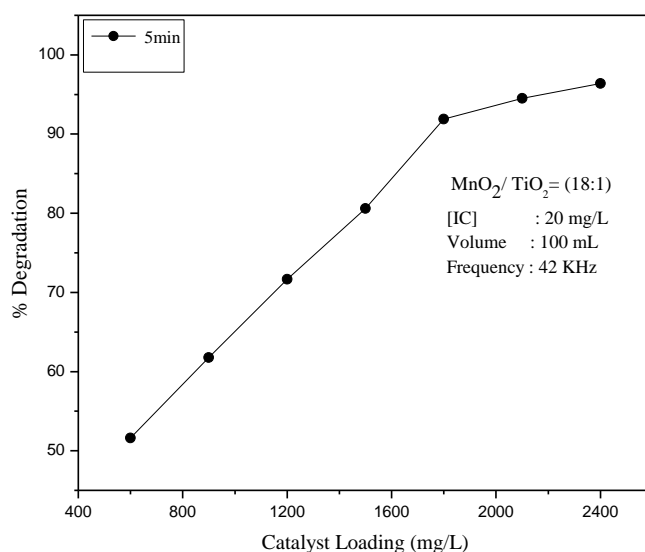
Fig. 5.30: Effect of dosage on the US/MnO_2 -TiO_2/IC degradation

The degradation goes on increasing with increase in catalyst dosage, and stabilizes at ~1800 mg/L. Hence this dosage (which is same as in the case of MnO_2) is selected as the optimum for further studies. Various factors responsible for optimum in the catalyst dosage in MW and photocatalysis are discussed in Chapters 3 and 4, Sections 3.3.3.1 and 4.3.2 respectively. Those factors are more or less applicable in this case as well.

5.4.3 Effect of concentration of IC

Effect of concentration of IC in the range 10-80 mg/L on its sonocatalytic degradation is tested and the results are presented in Fig.5.31. As in other AOPs in this case also, the % degradation decreases with increase in concentration of IC.
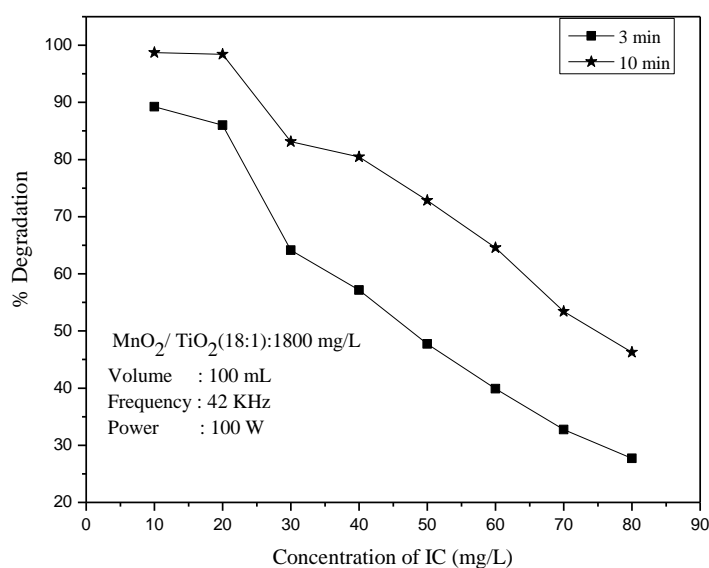
Fig.5.31: Effect of concentration on the US/MnO₂ -TiO₂/IC degradation

The rate of degradation at different concentrations is shown in Fig.5.32. It is seen that the rate of degradation of IC is optimum at 50-60 mg/L. This observation also is consistent with the results in the case of MW and photocatalysis. Hence all further studies were carried out at the IC concentration of 60 mg/L.

Microwave, Photo and Sono Activated Advanced Oxidation Processes and their Variations for the Decontamination of Water from Toxic Chemical Pollutants

411
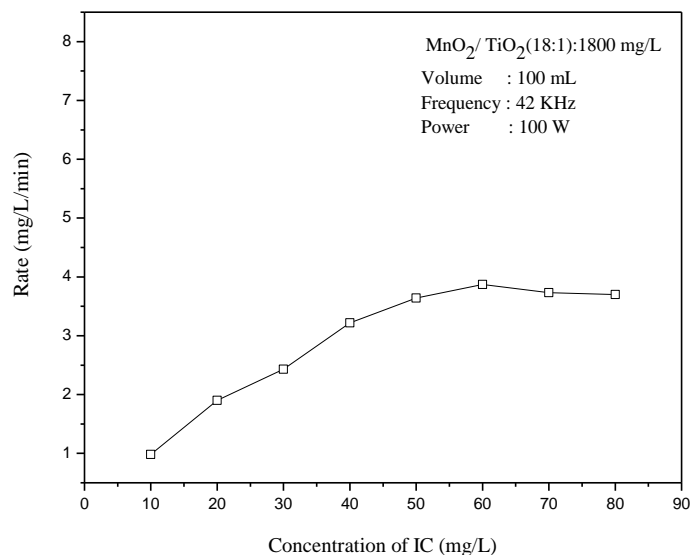
Fig. 5.32: Effect of concentration on the rate of US/MnO$_2$-TiO$_2$/IC degradation

The rate vs concentration plot shows variable kinetics for the degradation as observed in MW and photocatalysis. The kinetics of the degradation is further evaluated using the inverse plot $1/r_0$ vs $1/C_0$ (Fig.5.33) and the logarithmic plot (Fig.5.34), as explained in previous Chapters 3 and 4 and Sections 3.3.3.2 and 4.3.3 respectively. The data shows that the reaction follows pseudo first order kinetics and L-H mechanism thereby confirming that the presence of TiO$_2$ does not alter the kinetics of MnO$_2$ mediated sonocatalysis.
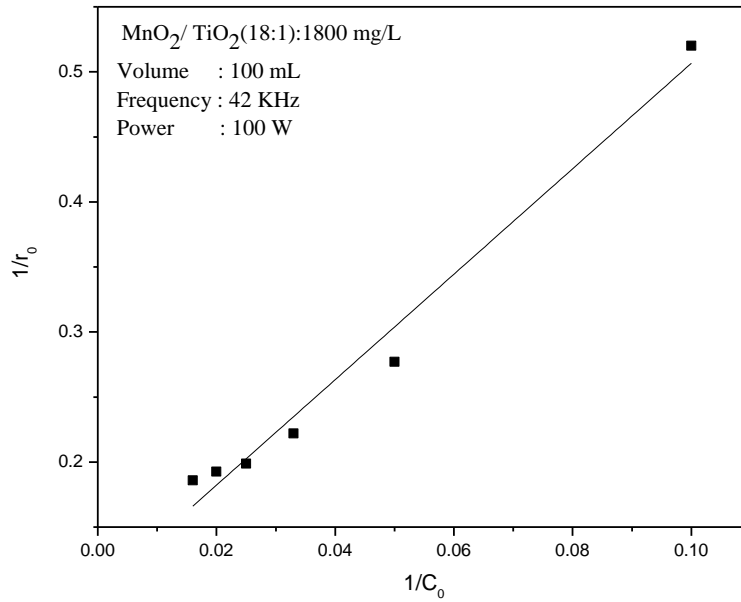
Fig. 5.33: Reciprocal plot of $1/r_0$ vs $1/C_0$ for various concentrations of IC
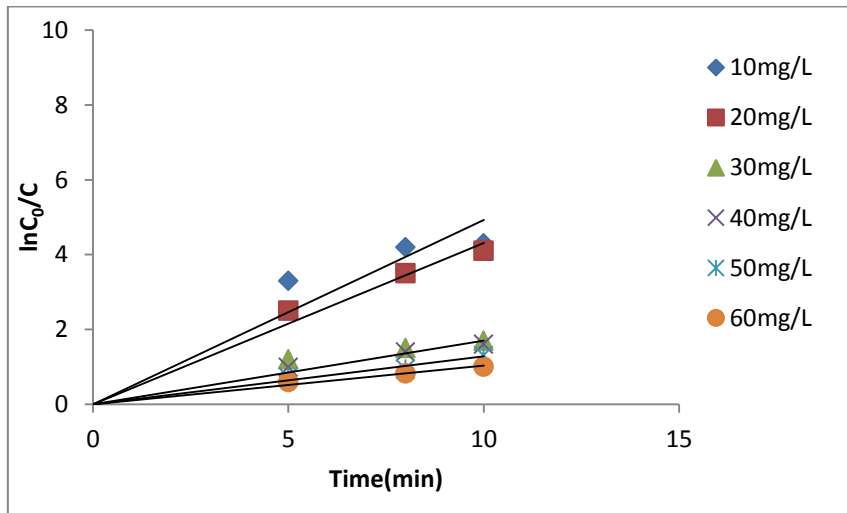
Fig. 5.34: Logarithmic plot for the US/MnO₂ -TiO₂/IC degradation

Microwave, Photo and Sono Activated Advanced Oxidation Processes and their Variations for the Decontamination of Water from Toxic Chemical Pollutants

413

5.4.4 Effect of pH

Effect of pH in the case of MnO_2-TiO_2 mediated degradation of IC is verified and the results are plotted in Fig.5.35. The effect is similar to that in the case of MnO_2 catalyst, with maximum degradation at pH 2-3, followed by steep decrease and then stabilization in the range 4-8. This is followed by another decrease at pH 8 and slight increase thereafter. Possible reasons for this kind of pH effect are already explained in Section 3.3.3.5. The complexicity and inconsistency of pH effect also are explained there in.
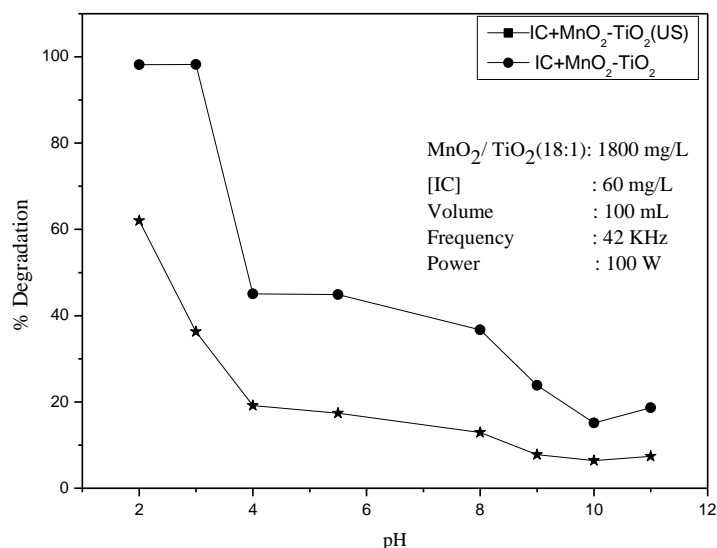
Fig. 5.35: Effect of pH on the US/MnO_2 -TiO_2/IC degradation

5.4.5 Effect of Oxidants

5.4.5.1 Effect of H_2O_2

The effect of addition of H_2O_2 on the MnO_2-TiO_2/US degradation of IC is tested at different concentrations of H_2O_2. The results are shown in Fig.5.36. As in the case of MnO_2, in this case also H_2O_2 inhibits the degradation at lower concentrations (upto 30 mg/L). Thereafter, the

degradation is stabilized with slight increase with increase in concentration of H_2O_2.
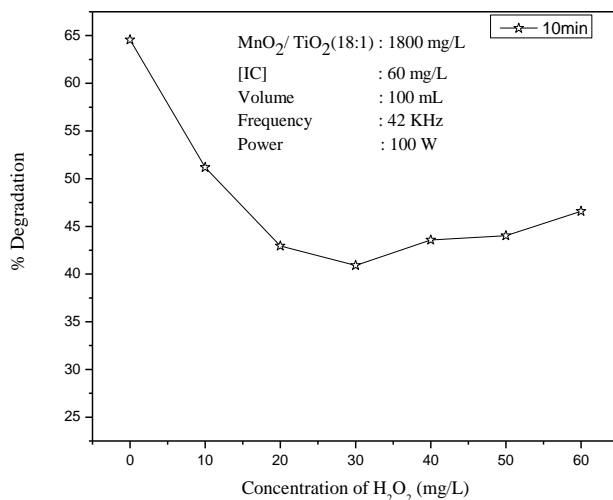
Fig. 5.36: Effect of H_2O_2 on the US/MnO$_2$ -TiO$_2$/IC degradation

The inhibition effect is further confirmed by the in-between addition of H_2O_2 after 5 min and 10 min of irradiation as shown in Fig.5.37.
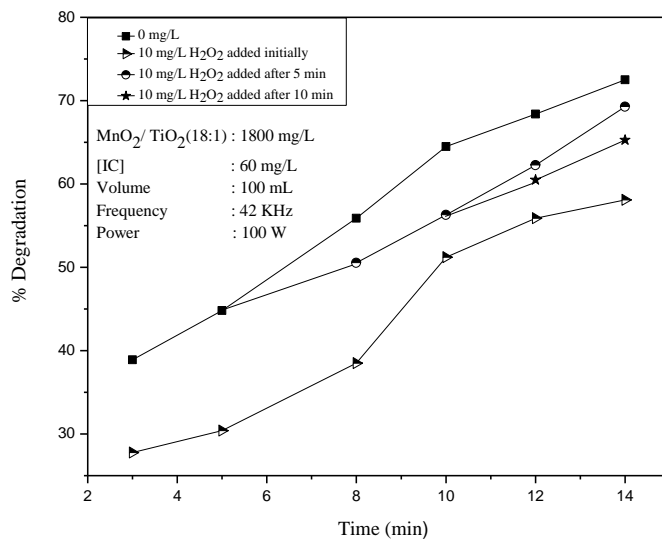
Fig. 5.37: Effect of initial & in between addition of H_2O_2
on the US/MnO$_2$ -TiO$_2$/IC degradation

Microwave, Photo and Sono Activated Advanced Oxidation Processes and their Variations for the Decontamination of Water from Toxic Chemical Pollutants

415

However the extent of inhibition is not sustained at higher concentration even though the net effect still remains as inhibition. The results are consistent with the unpredictable effect of H_2O_2, i.e, inhibition, stabilization or enhancement depending on concentration and other reaction parameters.

5.4.5.2 Effect of $K_2S_2O_8$

The effect of another oxidant $K_2S_2O_8$ on the degradation of IC is also tested at different concentrations and the results are shown in Fig.5.38.
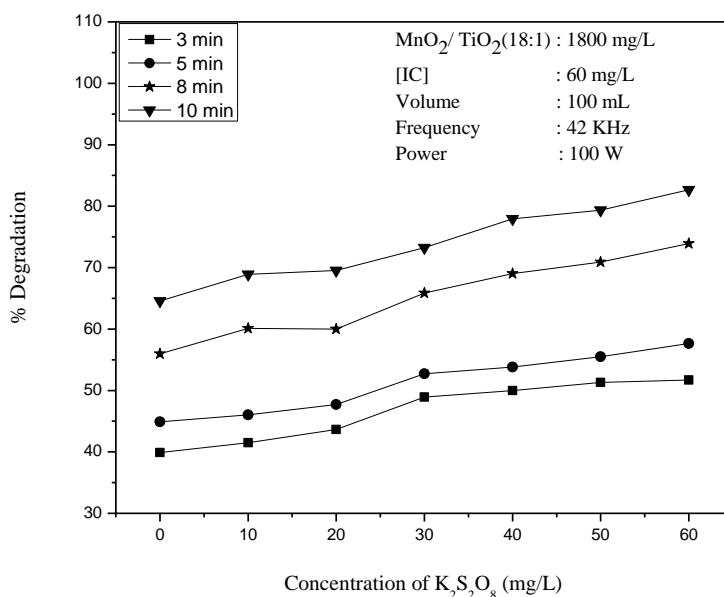
Fig. 5.38: Effect of $K_2S_2O_8$ on the US/MnO$_2$-TiO$_2$/IC degradation

As expected based on previous results with other catalysts $K_2S_2O_8$ is a moderate enhancer of the degradation at all concentrations, with ~15% enhancement achieved after 8 minutes with 40mg/L of PS. The

enhancement is further confirmed by the in-between addition of PS to the IC degradation in progress (Fig.5.39). The degradation increases with every in-between addition of PS.
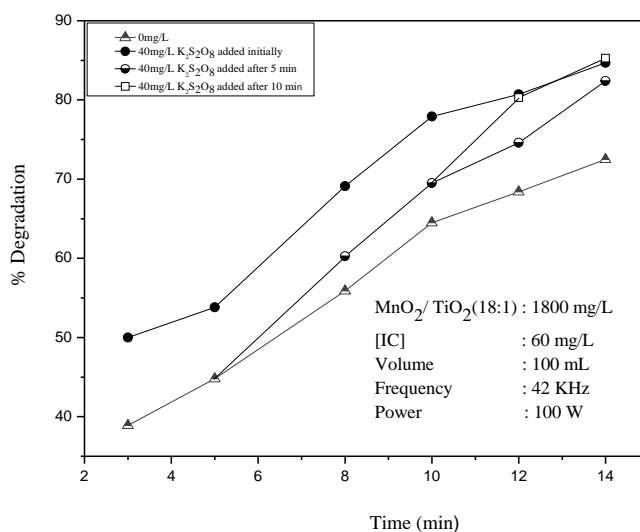
Fig. 5.39: Effect of initial & in between addition of $K_2S_2O_8$ on the US/MnO₂ -TiO₂/IC degradation

Since the results are similar in all respects in the case of MnO_2 and MnO_2-TiO₂, the mechanism of enhancement also will be identical as explained in Section 5.3.9.2.

The effect of combination of H_2O_2 and PS on the degradation is the average of their combined effect (Fig.5.40) as already seen in the case of photo and MW catalysis earlier.
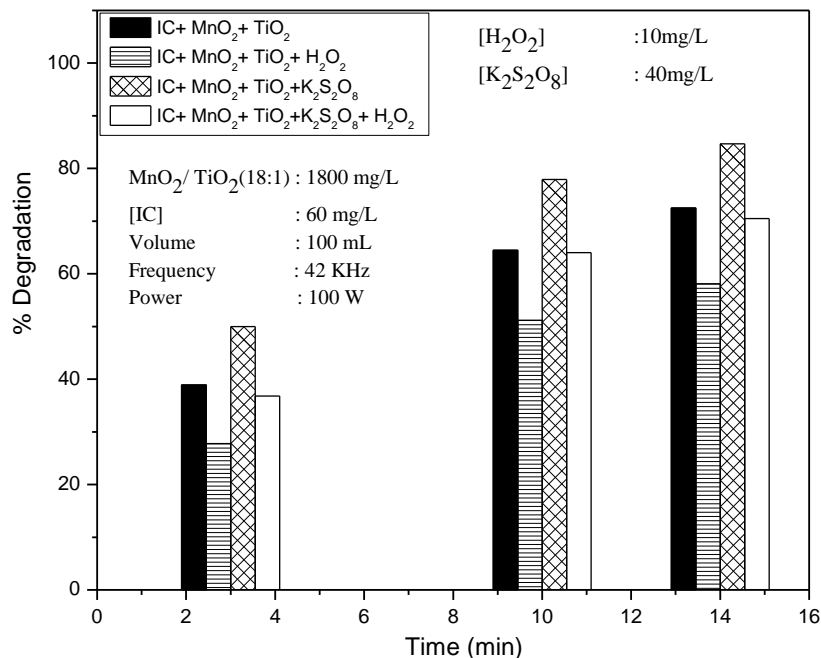
Fig. 5.40: Effect of combination of $K_2S_2O_8$ and H_2O_2 on the US/MnO_2 -TiO_2/IC degradation

5.4.6 Effect of Anions

As in the case of earlier studies the effect of various anions on the degradation of IC under US irradiation is investigated with different concentrations of the anions at various reaction times and the results are presented in Figs.5.41A and B. In this case also, PO_4^{3-} is a strong inhibitor while HCO_3^-, Cl^- and CH_3COO^- have practically no effect at lower concentrations. NO_3^- remains as a moderate to strong enhancer at all concentrations. However, the effects vary slightly with changing concentrations of the anion and reaction times as seen in the figures as well as in Tables 5.8 and 5.9.
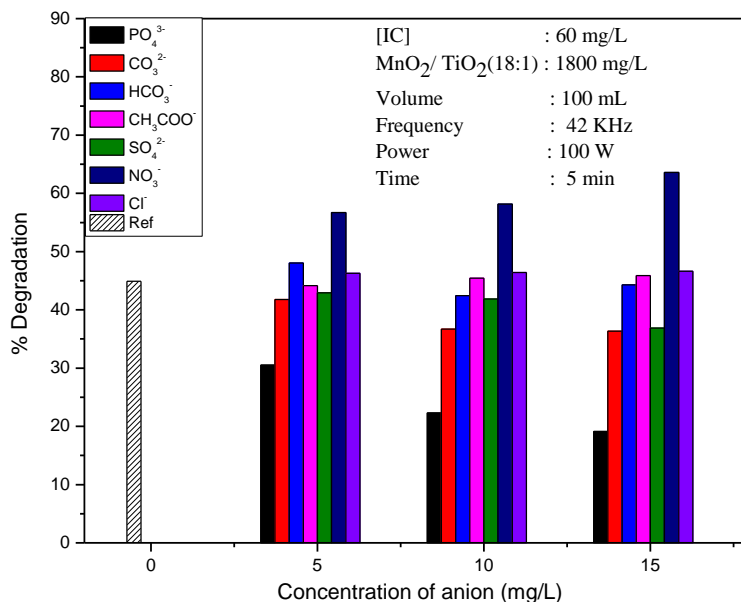
Fig. 5.41A: Effect concentration of anions on the US/MnO$_2$ - TiO$_2$/IC degradation

Table 5.8: Effect of concentration of anion on the US/MnO$_2$ -TiO$_2$/IC degradation
[IC]: 60mg/L, [MnO$_2$/ TiO$_2$(18:1) : 1800 mg/L, Time: 5 min

Concentration of Anions(mg/L)	Inhibition	No Effect	Enhancement
5	$PO_4^{3-} > CO_3^{2-} > SO_4^{2-}$	CH_3COO^-, Cl^-, HCO_3^-	NO_3^-
10	$PO_4^{3-} > CO_3^{2-} > SO_4^{2-} \approx HCO_3^-$	CH_3COO^-, Cl^-	NO_3^-
15	$PO_4^{3-} > CO_3^{2-} \approx SO_4^{2-}$	CH_3COO^-, Cl^-, HCO_3^-	NO_3^-

CO_3^{2-} and SO_4^{2-} are mild inhibitors or have 'no effect' at lower concentrations. At higher concentration, both these anions are clear inhibitors. NO_3^- remains as enhancer throughout. Other anions (CH_3COO^-, Cl^-, HCO_3^-) have no influence on the degradation of IC.

The effect of reaction time on the sonocatalytic degradation of IC is presented in Fig. 5.41B and the results are summarized in the Table 5.9.
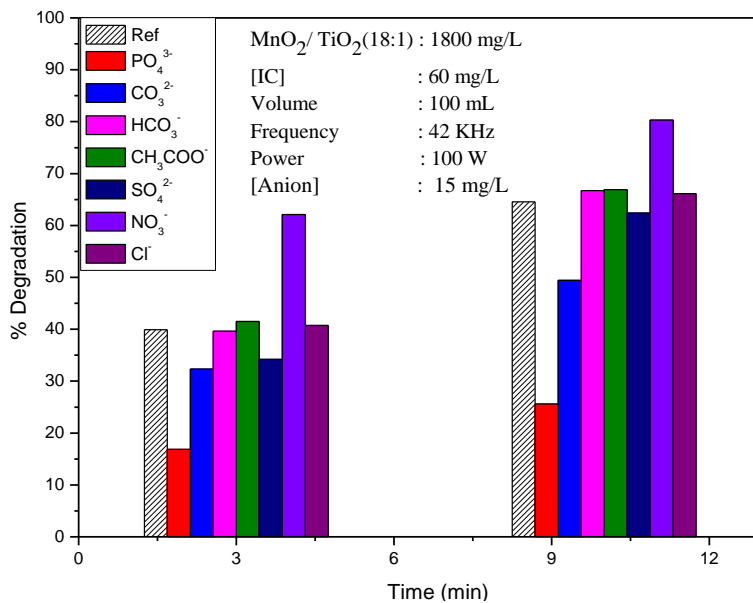
Fig. 5.41B: Effect of reaction time on the 'anion effect on the US/MnO$_2$ -TiO$_2$/IC degradation

Table 5.9: Effect of reaction time on the 'anion effect on the US/MnO$_2$ -TiO$_2$/IC degradation
[IC]: 60mg/L, [MnO$_2$/TiO$_2$]: 1800mg (18:1), [Anion]:15 mg/L

Time	Inhibition	No Effect	Enhancement
3min	PO$_4^{3-}$ > CO$_3^{2-}$ ≈ SO$_4^{2-}$	Cl$^-$, CH$_3$COO$^-$, HCO$_3^-$	NO$_3^-$
10min	PO$_4^{3-}$ > CO$_3^{2-}$ > SO$_4^{2-}$	Cl$^-$, CH$_3$COO$^-$, HCO$_3^-$	NO$_3^-$

As the reaction time proceeds, only NO$_3^-$ remains as an enhancer. Other anions show inhibition or no effect. Reaction time does not influence the 'anion effect' significantly.

The effect of each anion on the sonocatalytic degradation of IC is investigated in detail as done in earlier cases and the results are plotted in Figs. 5.42 to 5.48.

5.4.6.1 PO_4^{3-}
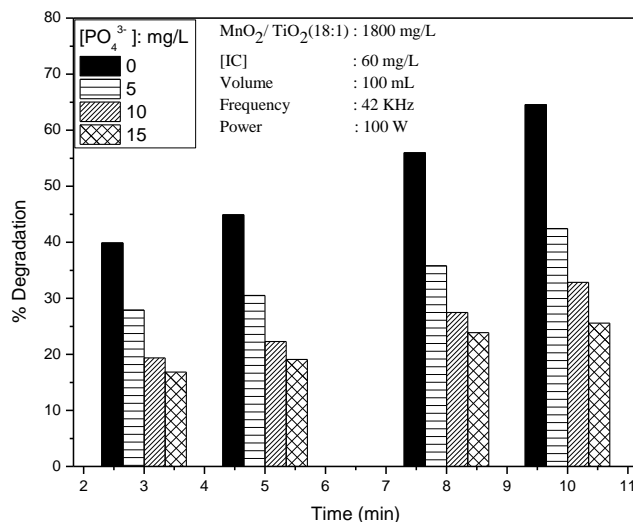
Fig. 5.42: Effect of PO_4^{3-} on the US/MnO$_2$ -TiO$_2$/IC degradation

PO_4^{3-} remains as a strong inhibitor throughout the reaction.

5.4.6.2 CO_3^{2-}
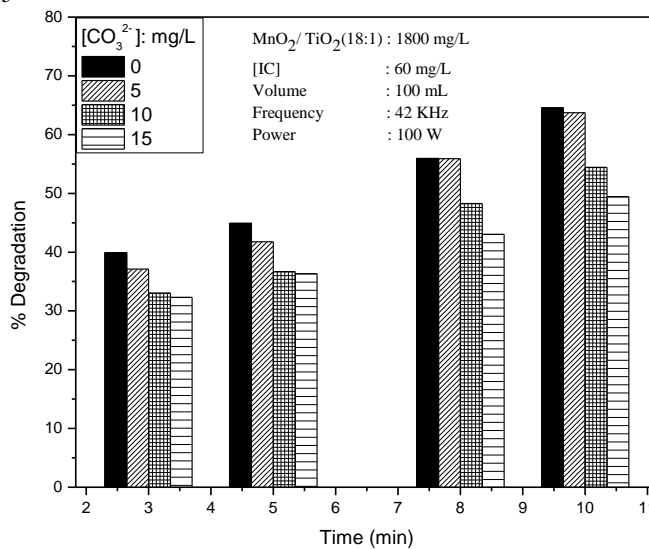
Fig. 5.43: Effect of Na$_2$CO$_3$ on the US/MnO$_2$ -TiO$_2$/IC degradation

CO_3^{2-} is a moderate inhibitor at all concentrations and reaction times tested.

5.4.6.3 HCO_3^-
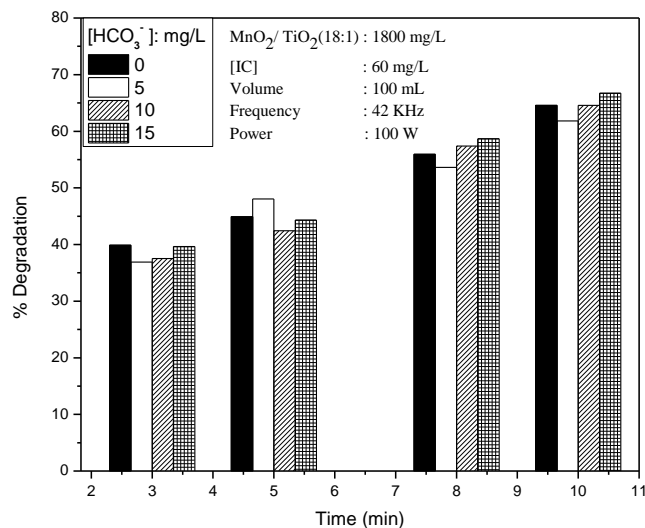
Fig. 5.44: Effect of HCO_3^- on the US/MnO_2 -TiO_2/IC degradation

HCO_3^- has practically no effect at all concentrations and reaction times.

5.4.6.4 CH_3COO^-
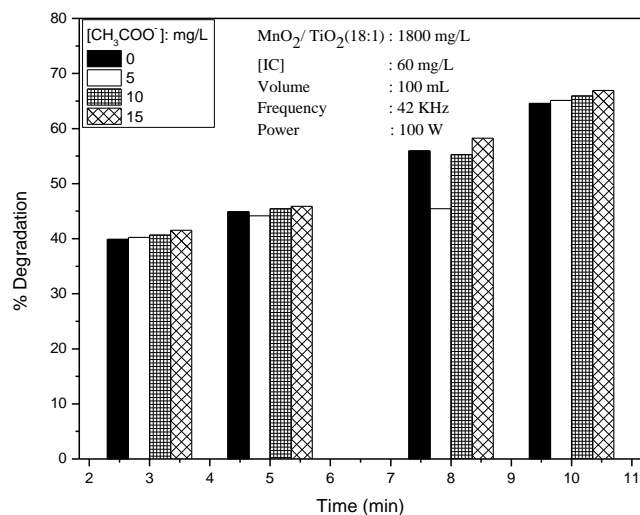
Fig. 5.45: Effect of CH_3COO^- on the US/MnO_2 -TiO_2/IC degradation

CH₃COO⁻ has no effect on the degradation of IC irrespective of its concentration and reaction times in the range tested.

5.4.6.5 SO_4^{2-}
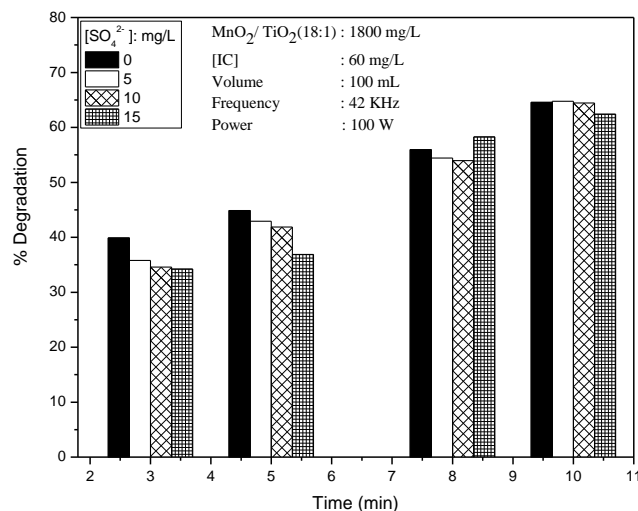
Fig. 5.46: Effect of SO_4^{2-} on the US/MnO₂ -TiO₂/IC degradation

SO_4^{2-} is a mild inhibitor in the initial stages of reaction. The extent of inhibition decreases with time of reaction and eventually the effect becomes 'no effect'.

5.4.6.6 NO_3^-
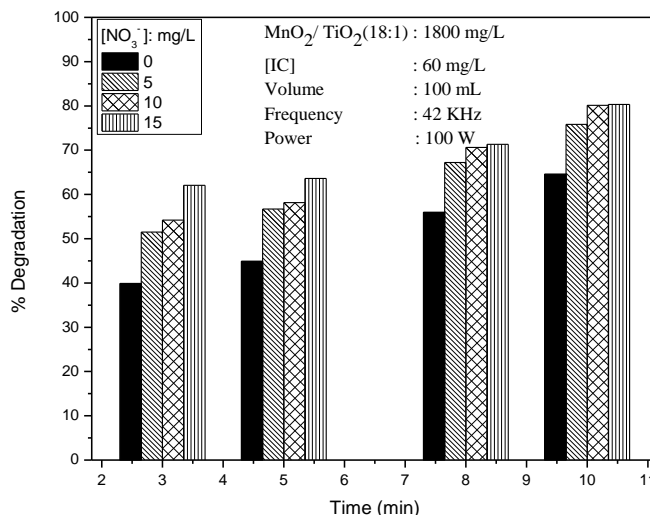
Fig. 5.47: Effect of NO_3^- on the US/MnO₂ -TiO₂/IC degradation

NO_3^- is a consistent enhancer at all concentration and reaction times.

5.4.6.7 Cl⁻
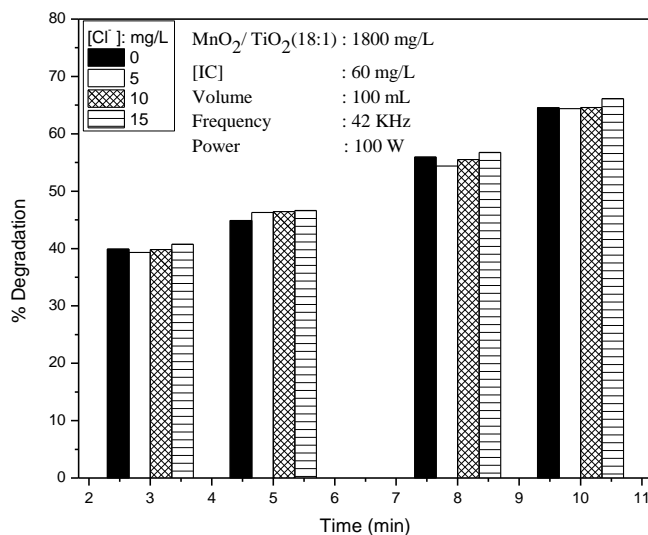
Fig. 5.48: Effect of Cl⁻ on the US/MnO$_2$-TiO$_2$/IC degradation

Cl⁻ has practically no effect on the degradation of IC.

Anion effect is generally the same as in the case of MnO$_2$ except minor variations ('mild enhancement'(MnO$_2$) to 'no effect'(MnO$_2$-TiO$_2$) in the case of CH$_3$COO⁻, 'no effect'(MnO$_2$) to 'mild inhibition' (MnO$_2$-TiO$_2$) in the case of SO$_4^{2-}$). However, as in other cases discussed earlier, 'mild inhibition', 'no effect' and 'mild enhancement' can be treated interchangeably, with the limits of experimental error.

Since the results are fairly similar to those in the case of MnO$_2$, the reasons for the anion effect explained in Section 5.3.10 will be applicable in the case of MnO$_2$-TiO$_2$ as well.

5.4.7 Mineralisation of IC under MnO$_2$-TiO$_2$/US

AOP based on MnO$_2$/US, MnO$_2$-TiO$_2$/US, though very efficient for the decolourisation of IC, is not efficient enough to mineralize the pollutants. However combination of US with UV light irradiation could achieve mineralization as demonstrated in Section 5.3.11 in the case of MnO$_2$.

This possibility and further enhancement of mineralization in presence of TiO$_2$ is examined in the case of MnO$_2$-TiO$_2$ catalyst also. Results are presented in Fig.5.49.
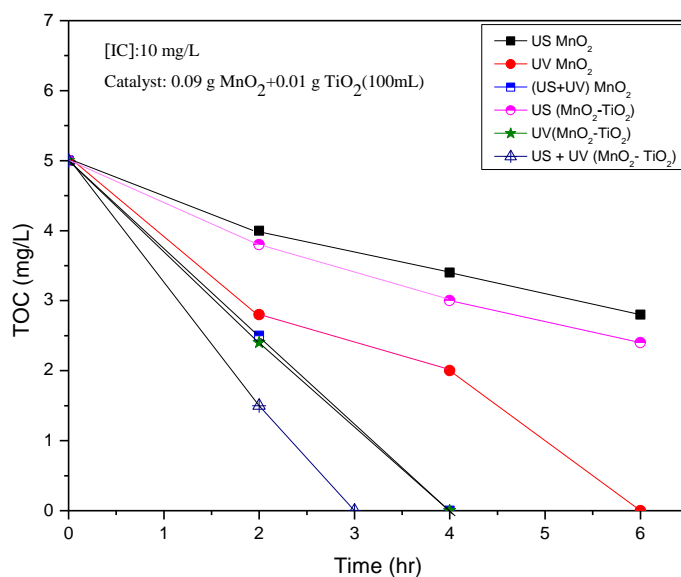
Fig. 5.49: TOC of MnO$_2$/IC and MnO$_2$-TiO$_2$/IC system under various conditions of activation.

The results clearly indicate that combination of MnO$_2$ and TiO$_2$ as the catalyst and 'US and UV' irradiation as the combined source of activation is a highly efficient technique for the decolourisation and

mineralization of traces of IC pollutants in H_2O. The mineralization efficiency of various catalysts-activation source combination is in the order

$$(US+UV)/MnO_2\text{-}TiO_2 > UV(MnO_2\text{-}TiO_2) \approx (US+UV)/MnO_2$$
$$> US/(MnO_2\text{-}TiO_2) > US/MnO_2 \quad ....(173)$$

Hence detailed investigation on the sonophotocatalytic (US+UV) degradation of IC with $MnO_2\text{-}TiO_2$ as the catalyst is undertaken and the results are reported in the following Chapter.

5.5 Sonocatalytic degradation of IC using Co_3O_4

Previous Chapters have demonstrated that Co_3O_4 also is a potentially effective catalyst for MW- and photo-activated AOPs. Hence the possibility of using Co_3O_4 as a sonocatalyst also is tested. Preliminary results are presented here. More detailed investigations are to be taken up at a later stage.

5.5.1 Effect of catalyst dosage

Effect of catalyst dosage on the sonocatalytic degradation of IC is shown in Fig.5.50. Degradation increases with increase in loading. However, there is no clear optimum at least in the range 0.06 to 0.2g/100mL studied here. Hence 0.16g/100mL of Co_3O_4 which is comparable to the dosage of MnO_2 and $MnO_2\text{-}TiO_2$ as explained in earlier studies is taken as a convenient dosage for further investigation.
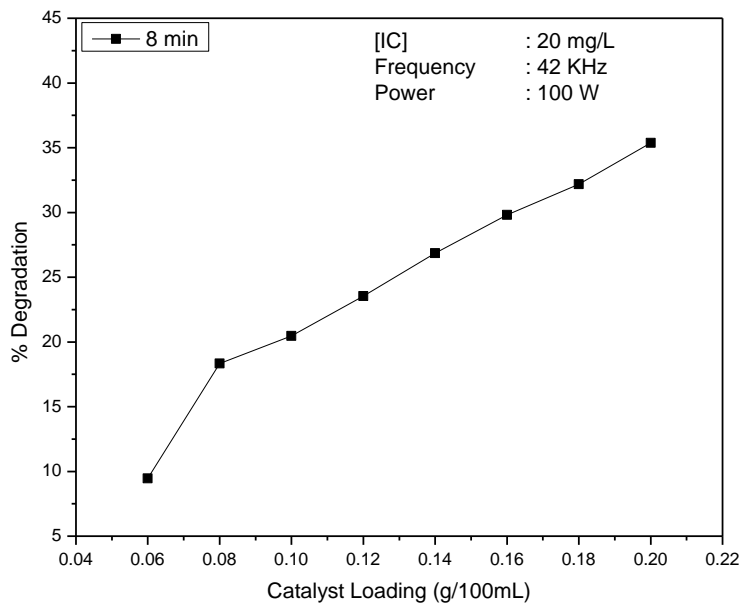
Fig. 5.50: Effect of catalyst loading on the sonocatalytic degradation of IC

The rationale for the 'catalyst dosage effect' and the optimum values are discussed in earlier Chapters.

5.5.2 Effect of concentration of IC

The effect of concentration of IC on its % degradation at different times of irradiation is tested and the results are shown in Fig.5.51. As expected the % degradation decreases with increase in concentration.
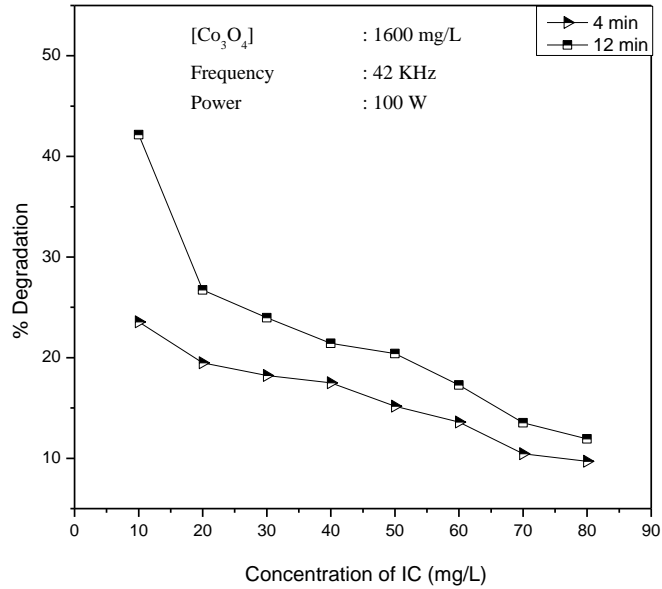
Fig. 5.51: Effect of concentration on the US/Co$_3$O$_4$/IC degradation

However, the realistic measure of the effect of concentration on the degradation in the rate, which is shown in Fig.5.52.
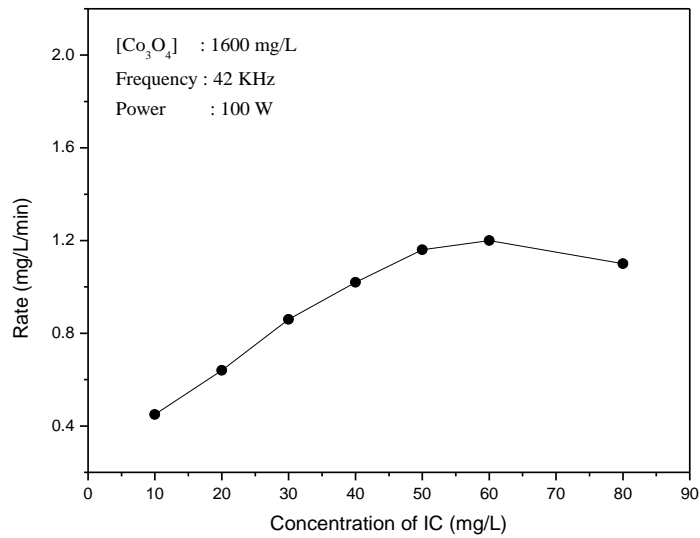
Fig. 5.52: Rate of degradation of IC at different concentrations.

Rate increases with increase in concentration and is almost stabilized at 60 mg/L. Hence all further studies are carried out at this concentration. The rate vs concentration plot (Fig.5.52) shows kinetics similar to that in the case of MnO_2 and MnO_2-TiO_2 for MW and photocatalysis.

The kinetics of the degradation is further evaluated from the inverse plot $1/r_0$ vs $1/C_0$ (Fig.5.53) and logarithmic plot (Fig.5.54) details of which are discussed in earlier Chapters. The characteristics of the two plots illustrate the pseudo first kinetics and L-H mechanism for the degradation in presence of Co_3O_4 also.
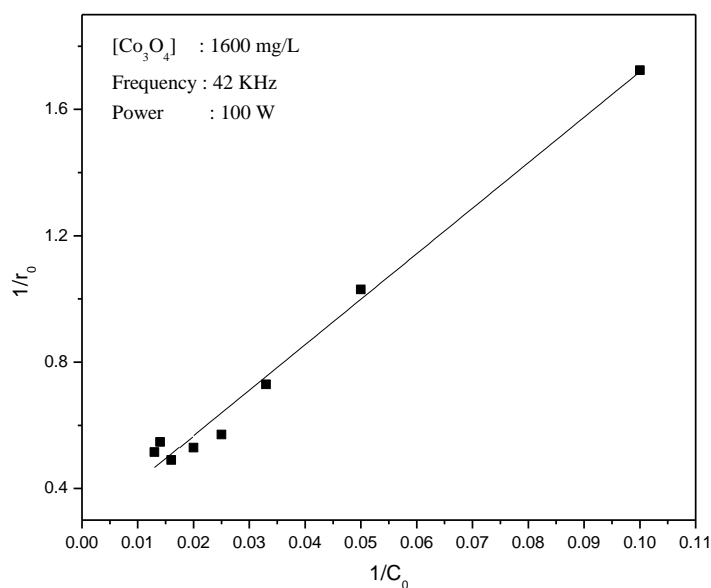
Fig. 5.53: Reciprocal plot of $1/r_0$ vs $1/C_0$ for US/Co_3O_4 at various concentrations of IC.

Microwave, Photo and Sono Activated Advanced Oxidation Processes and their Variations for the Decontamination of Water from Toxic Chemical Pollutants

429
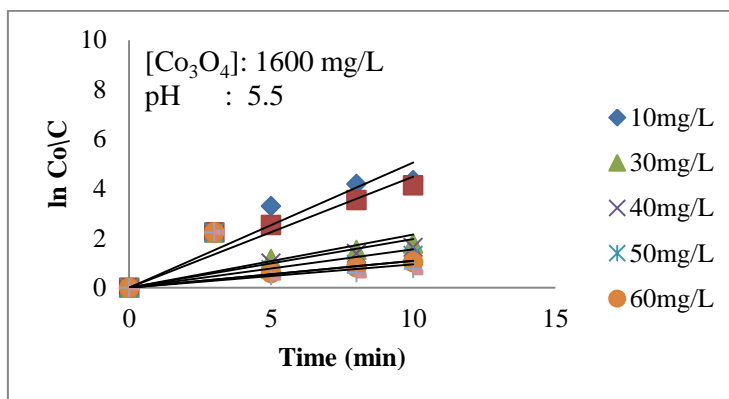
Fig. 5.54: Logarithmic plot for US/Co$_3$O$_4$/ IC degradation

Details of the pseudo first order kinetics and L-H mechanism are discussed in earlier Sections 3.3.3.2 and 4.3.3 of Chapters 3 and 4, respectively.

5.5.3 Effect of pH

The effect of pH on the degradation of IC is shown in Fig.5.55.
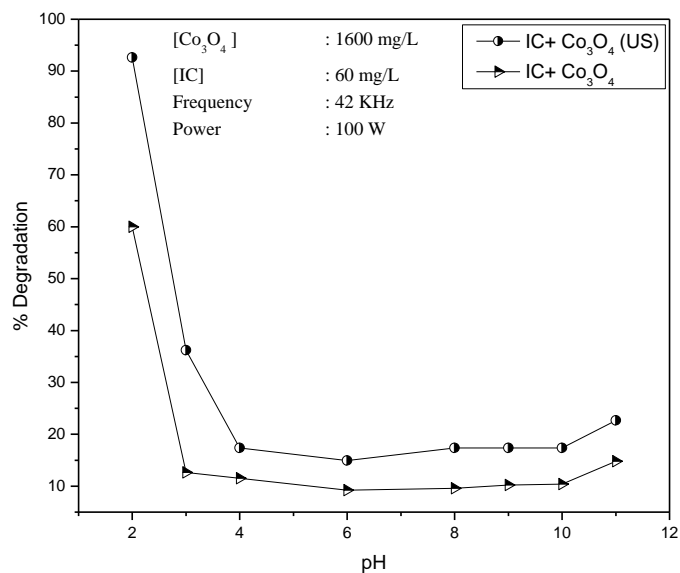
Fig. 5.55: Effect of pH on the US/Co$_3$O$_4$/ IC degradation

The decrease in concentration of IC is almost 100% at pH 2 under Co_3O_4/US. Under the same conditions in the absence of US irradiation the decrease in concentration of IC is ~60%. This shows that IC is getting strongly adsorbed on Co_3O_4 at pH~ 2 and together with the US- assisted degradation on the surface and in the bulk, the concentration of IC decreases by almost 100%. The effect is similar to that in the case of photo and MW catalysis in presence of Co_3O_4 which is explained partially based on the point of zero charge (PZC) of the catalyst. However there was no strict correlation of the pH effect and the PZC. This was attributed to the flexibility of PZC which itself depends on the type of irradiation. Together with the multitude of conflicting interactions, existing in the system the pH effect becomes extremely complex. More details are discussed in Section 3.3.3.5 of Chapter 3.

5.5.4 Effect of Oxidants

As done in the case of other AOPs and catalyst systems described in earlier Chapters, the effect of two common oxidants H_2O_2 and $K_2S_2O_8$ on the degradation of IC is investigated. Preliminary results are as follows.

5.5.4.1 Effect of H_2O_2

The effect of H_2O_2 on the degradation of IC is investigated in detail and is shown in Fig.5.56.

Microwave, Photo and Sono Activated Advanced Oxidation Processes and their Variations for the Decontamination of Water from Toxic Chemical Pollutants

431
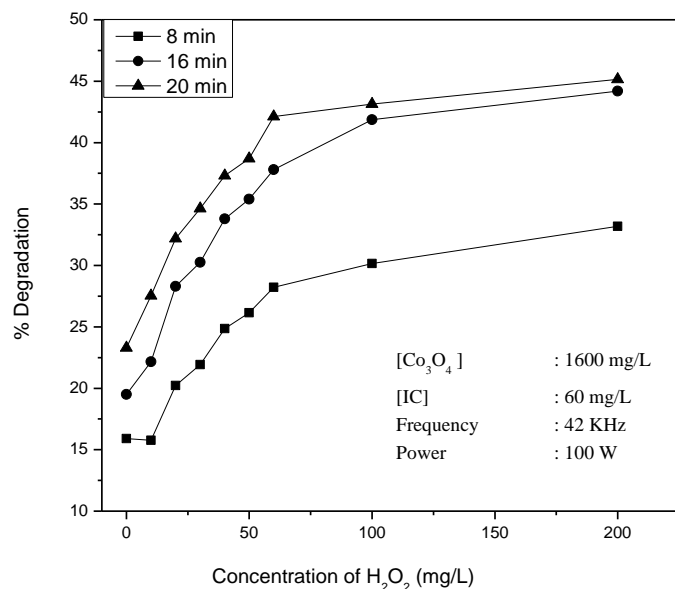
Fig. 5.56: Effect of H_2O_2 on the US/Co_3O_4/ IC degradation

H_2O_2 is a clear enhancer for the degradation of IC, in presence of Co_3O_4. Unlike in the case of MnO_2 or (MnO_2-TiO_2) the degradation increases sharply with increase in concentration of H_2O_2. However the enhancement is stabilized at an optimum H_2O_2 concentration of 60 mg/L beyond which the effect is practically negligible.

H_2O_2 is known to be an enhancer as well as inhibitor of the degradation of many organics which is explained based on its concurrent role in the production and destruction of ˙OH radicals. Another parameter relevant in this context is the oscillation in the concentration of H_2O_2 which is due to its simultaneous 'formation' and 'decomposition'. Details are given in Section 4.3.6.1 of Chapter 4. Depending on the domination of formation or decomposition of H_2O_2, the net concentration of ˙OH radicals in the system will vary. The more the ˙OH radicals present, the

more will be the degradation of IC. Consistent steady increase in the degradation of IC, in presence of H_2O_2, shows that the formation of ˙OH radicals is dominating upto at least 60mg/L of H_2O_2. Beyond this the formation and consumption of ˙OH radicals balance resulting in a stable concentration of ˙OH and consequently stabilized degradation.

The enhancement in the degradation of IC in presence of added H_2O_2, is further confirmed by the in-between addition of H_2O_2 to a reaction in progress (see Fig.5.57).
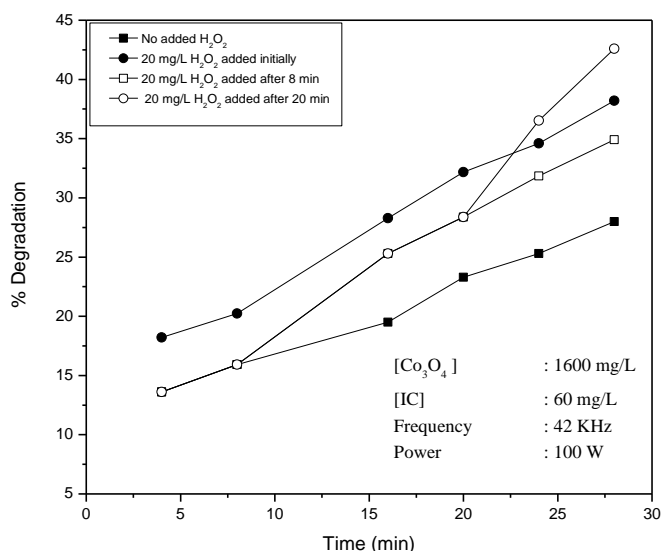
Fig. 5.57: Effect of initial and in-between addition of H_2O_2 on the US/Co₃O₄/ IC degradation

The degradation is clearly enhanced from the point of addition of H_2O_2. Incidentally, the results also prove that in the case of H_2O_2, periodic addition in small increments is more advantageous than bulk addition in one lot to achieve maximum enhancement.

5.5.4.2 Effect of $K_2S_2O_8$

The effect of another oxidant $K_2S_2O_8$ on the degradation of IC is shown in Fig.5.58.
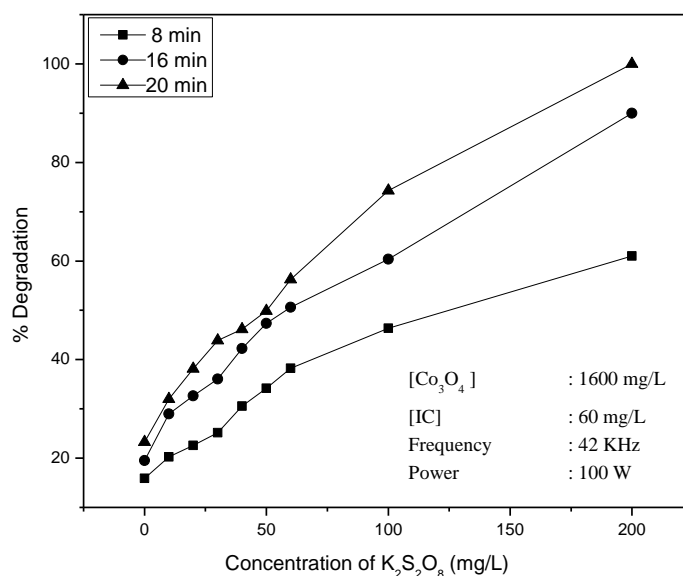
Fig. 5.58: Effect of $K_2S_2O_8$ on the US/Co_3O_4/ IC degradation

As in the case of other AOPs, $K_2S_2O_8$ enhances the degradation of IC, consistently with increase in concentration. The factors leading to the enhancement are discussed in detail in Section 5.3.9.2. The enhancing effect of $K_2S_2O_8$ is further confirmed by the in-between addition to a reaction in progress. The results presented in Fig.5.59 clearly show an increase in the degradation from the point of addition of $K_2S_2O_8$.
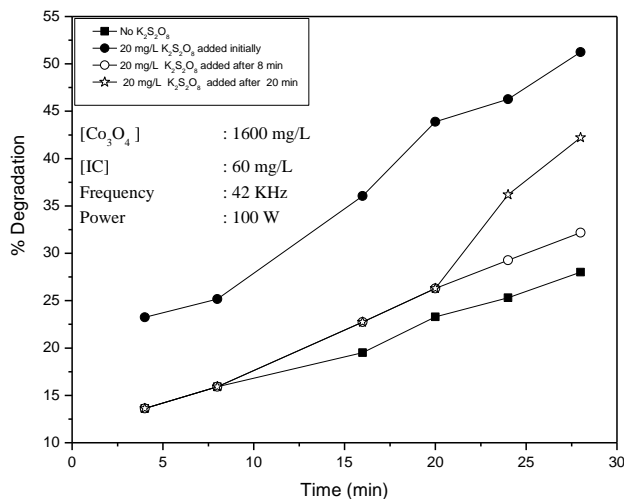
Fig. 5.59: Effect of initial and in-between addition of K$_2$S$_2$O$_8$ on the US/Co$_3$O$_4$/ IC degradation

The effect of combination of the oxidants H$_2$O$_2$ and K$_2$S$_2$O$_8$ on the degradation is shown in Fig.5.60. The effect is more or less additive thereby suggesting the potential of this combination for enhancing the sonocatalytic degradation of IC in presence of Co$_3$O$_4$.
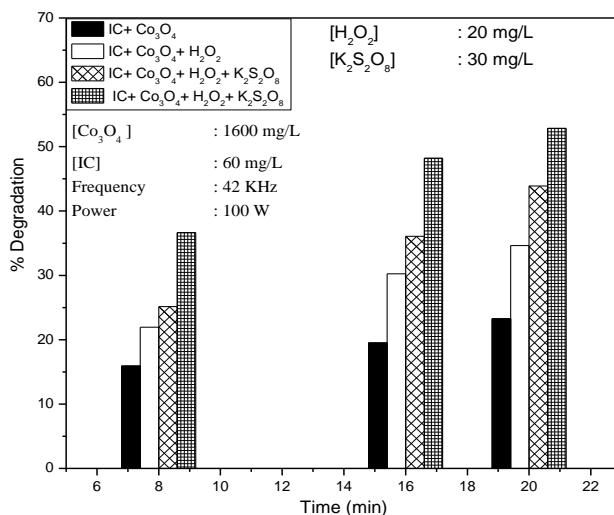
Fig. 5.60: Effect of Combination of K$_2$S$_2$O$_8$ and H$_2$O$_2$ on the US/Co$_3$O$_4$/ IC degradation

Microwave, Photo and Sono Activated Advanced Oxidation Processes and their Variations for the Decontamination of Water from Toxic Chemical Pollutants

435

5.5.5 Effect of Anions

The effect of some of the commonly occurring anions in water, i.e. SO_4^{2-}, Cl^-, PO_4^{3-}, CO_3^{2-}, HCO_3^- and NO_3^- on the efficiency of US/Co_3O_4 degradation of IC is tested at various concentrations and reaction times. The effect of concentration of anions on the degradation is presented in Fig.5.61A and is summarized in Table 5.10.
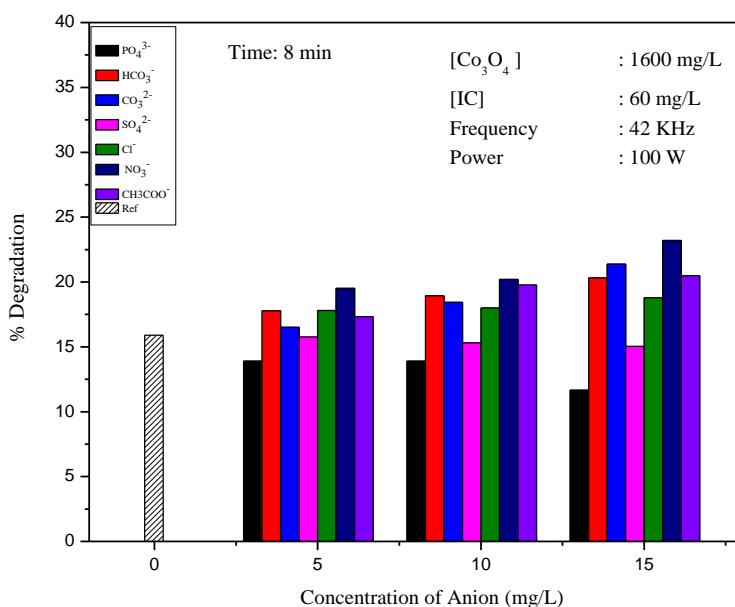
Fig. 5.61A. Effect concentration of anions on the US/Co_3O_4/ IC degradation

Table 5.10: Effect of concentration of anion on the US/Co_3O_4/ IC degradation [Co_3O_4]: 1600 mg/L, [IC]: 60 mg/L, Time: 8 min

Concentration of Anions(mg/L)	Inhibition	No Effect	Enhancement
5	PO_4^{3-}	SO_4^{2-}, CO_3^{2-}	$NO_3^- > HCO_3^- \approx Cl^- \approx CH_3COO^-$
10	$PO_4^{3-} > SO_4^{2-}$	-	$NO_3^- > CH_3COO^- > HCO_3^- \approx Cl^- \approx CO_3^{2-}$
15	PO_4^{3-}	SO_4^{2-}(no effect to mild enhancement)	$NO_3^- > CO_3^{2-} > CH_3COO^- \approx HCO_3^- > Cl^-$

PO_4^{3-} remains a strong inhibitor in this case also. The effect of SO_4^{2-} borders between 'inhibition' and 'no effect'. NO_3^- remain as a moderate to strong enhancer.

The effect of reaction time on the 'anion effect' is verified at three different times of irradiation i.e. 8, 16 and 20 min. The results are presented in Fig.5.61B and Table 5.11.
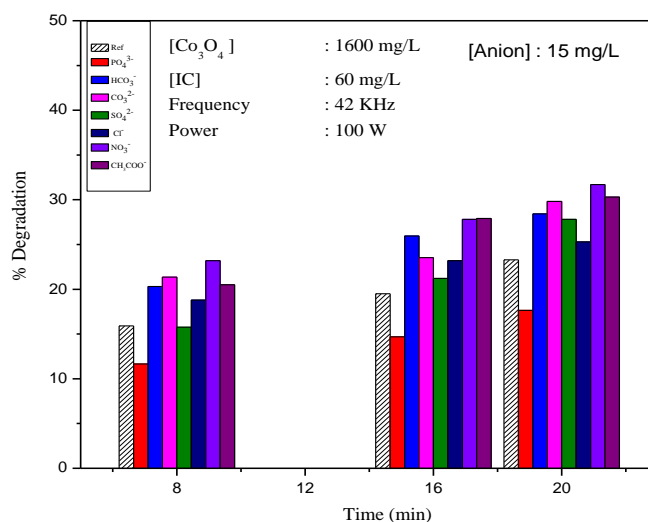
Fig. 5.61 B: Effect of reaction time on the US/Co₃O₄/ IC degradation

Table 5.11: Effect of reaction time on the US/Co₃O₄/ IC degradation
[Co₃O₄]: 1600 mg/L, [IC]: 60 mg/L, [Anion]:15 mg/L

Time (min)	Inhibition	No Effect	Enhancement
8	PO_4^{3-}	SO_4^{2-} (no effect to mild inhibition)	$NO_3^- > CO_3^{2-} > HCO_3^- \approx CH_3COO^- > Cl^-$
16	PO_4^{3-}	SO_4^{2-}(no effect to mild enhancement)	$NO_3^- \approx CH_3COO^- > HCO_3^- > CO_3^{2-} \approx Cl^- >$
20	PO_4^{3-}	-	$NO_3^- > CO_3^{2-} \approx CH_3COO^- > HCO_3^- > SO_4^{2-} > Cl^-$

Microwave, Photo and Sono Activated Advanced Oxidation Processes and their Variations for the Decontamination of Water from Toxic Chemical Pollutants

437

In this case, reaction time does not change the anion effect much. Many anions, which are either 'inhibitiors' or have 'no effect' in presence of MnO_2 and MnO_2-TiO_2 are enhancers in presence of Co_3O_4. Except PO_4^{3-}, all other anions are 'mild' to 'moderate enhancers'. In this respect Co_3O_4 may be a better sono catalyst useful for the treatment of a wide variety of water pollutants. As done in earlier cases, the effect of each anion on the degradation of IC under US/Co_3O_4 is verified at different concentrations of the anion and varying reaction times. The results are as follows.

5.5.5.1 HCO_3^-

The effect of HCO_3^- on the degradation of IC under US/Co_3O_4 is given in Fig.5.62.
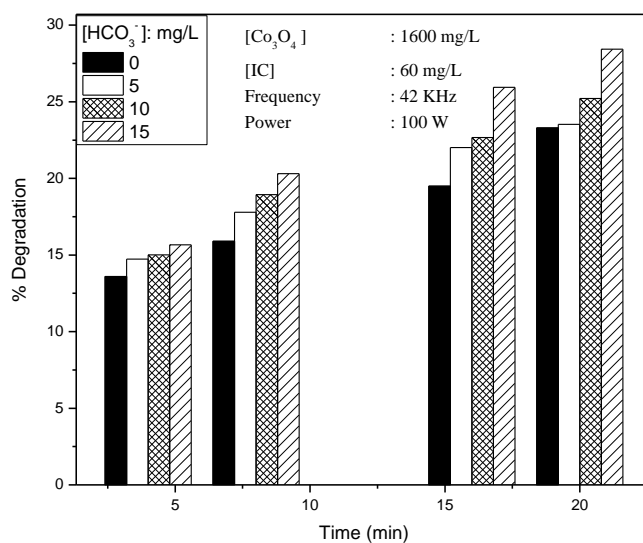
Fig. 5.62: Effect of HCO_3^- on the US/Co_3O_4/ IC degradation

HCO_3^- is a mild but consistent enhancer at all concentration and reaction times.

5.5.5.2 PO_4^{3-}

The effect of PO_4^{3-} on the degradation of IC is investigated and the results are given in Fig.5.63.
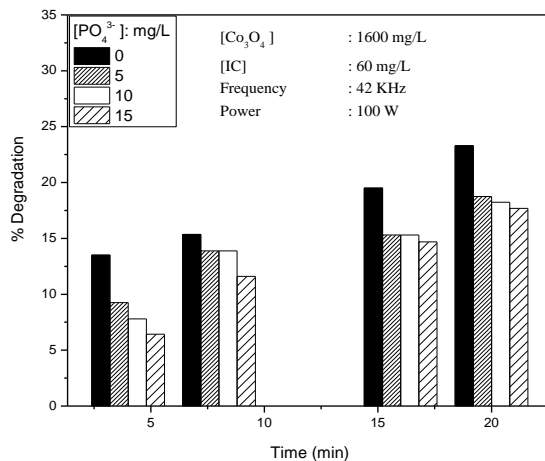
Fig. 5.63: Effect of PO_4^{3-} on the US/Co₃O₄/ IC degradation

PO_4^{3-} remains a strong inhibitor at all concentrations and reaction times.

5.5.5.3 CO_3^{2-}

The effect of CO_3^{2-} is plotted in Fig.5.64.
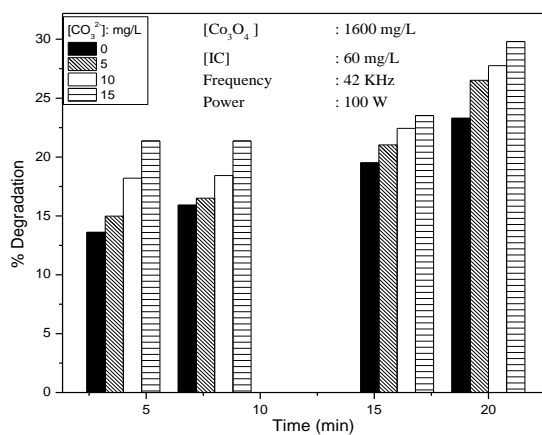
Fig. 5.64: Effect of CO_3^{2-} on the US/Co₃O₄/ IC degradation

CO_3^{2-} is an enhancer at all concentrations and reaction times.

5.5.5.4 SO_4^{2-}

Effect of SO_4^{2-} on the sonocatalytic degradation of IC in presence of Co_3O_4 is studied and the results are plotted in Fig.5.65.
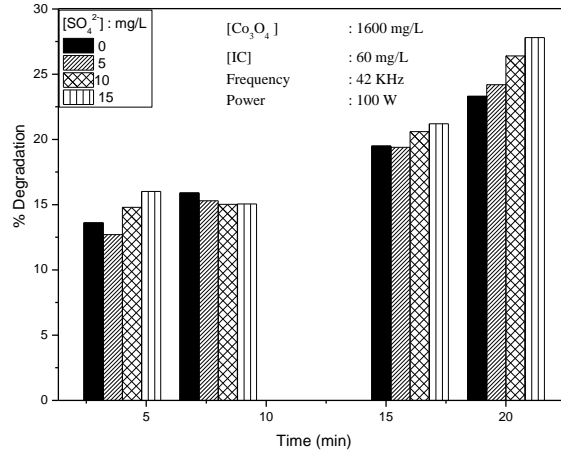
Fig. 5.65: Effect of SO_4^{2-} on the US/Co_3O_4/ IC degradation

At lower concentration and early reaction times SO_4^{2-} has no effect on the degradation. However at higher concentration of anions and later reaction times, it is a mild enhancer. This implies that the relative concentration of IC vs SO_4^{2-} has a role in the anion effect.

5.5.5.5 NO_3^-
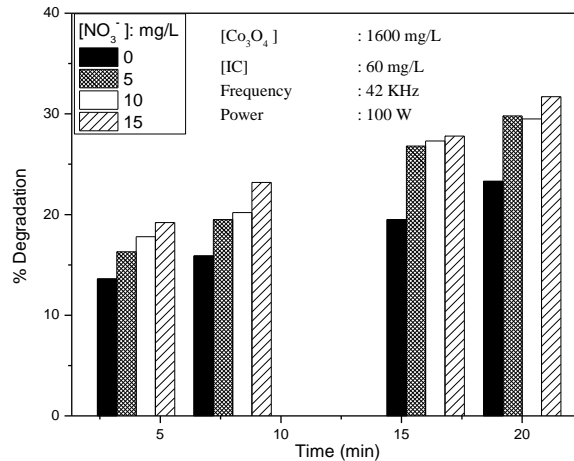
Fig. 5.66: Effect of NO_3^- on the US/Co_3O_4/ IC degradation

As always NO_3^- is a strong enhancer of the degradation in this case also, at all concentrations and reaction times (Fig.5.66)

5.5.5.6 CH_3COO^-
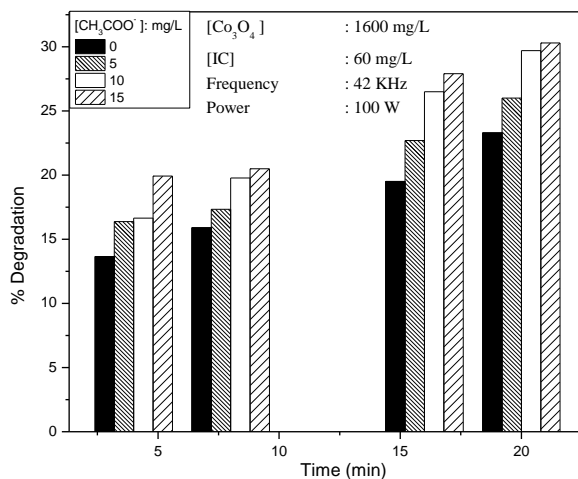
Fig. 5.67: Effect of CH_3COO^- on the US/Co₃O₄/ IC degradation

CH_3COO^- is a moderate enhancer of the degradation of IC under US/Co₃O₄ at all concentrations and reaction times (Fig.5.67).

5.5.5.7 Cl^-
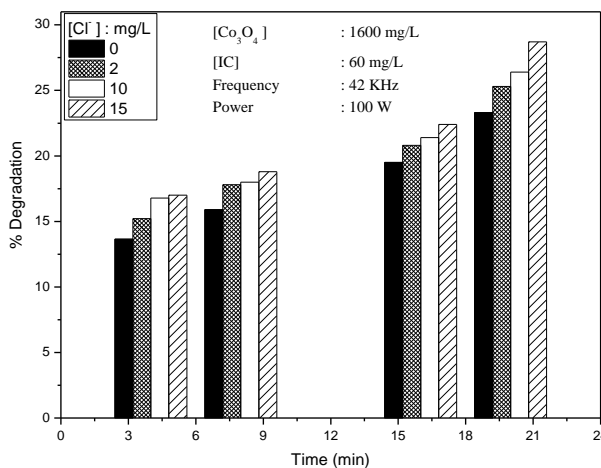
Fig. 5.68: Effect of Cl^- on the US/Co₃O₄/ IC degradation

Microwave, Photo and Sono Activated Advanced Oxidation Processes and their Variations for the Decontamination of Water from Toxic Chemical Pollutants

441

Cl^- is a moderate enhancer of the degradation at all concentrations and reaction times tested here (Fig.5.68).

The effect of anions on the sonocatalytic degradation of IC in presence of Co_3O_4 catalyst is somewhat different from the effect in presence of MnO_2 and MnO_2/TiO_2 catalysts. In this case all anions except PO_4^{3-} are moderate to strong enhancers of the degradation. Concentration of the anion and/or reaction time do not make any significant change in the effect.

Various factors which contribute to the effect of anions in AOPs are discussed in previous Chapters 3 and 4 (Sections 3.3.3.12 and 4.3.7 respectively). It has also been illustrated that the effect of anions depend on a multitude of complex interactions and will also depend on the nature of the anion, characteristics of the substrate, catalyst, energy source as well as the additives, if any, and the anion. Hence the effect cannot be generalized and has to be analysed on a case to case basis. The current results in the presence of Co_3O_4 also highlights these conclusions.

The effect of H_2O_2 on the degradation of IC is different in the case of Co_3O_4 catalyst. In depth investigation of the AOP activity of Co_3O_4 may lead to the development of an efficient catalyst for water purification under AOP without being inhibited by various other components present in water. Such a study is beyond the scope of this investigation which is primarily based on MnO_2 catalysts.

5.6 General Mechanism

Acoustic cavitation produces highly reactive primary radicals such as $^\cdot$OH and H$^\cdot$ as in reaction (140). Recombination and a number of other reactions occur on the surface as well as in the bulk as in reactions (174) to (181) following this primary radical generation. In the case of sonolysis and sonocatalysis the concentration of $^\cdot$OH radicals at the surface of the cavitation bubble is more compared to that in the solution bulk [218, 219]. The air-water interface of the cavitation bubble also will be rich in OH radicals. All these radicals will not be available exclusively to interact with and degrade IC because of the parallel multiple radical-radical reactions to give H_2O_2 and H_2O. This will also limit the diffusion of radical species to the solution bulk [220]. Various reactions of $^\cdot$OH at the bubble surface and in the bulk may be summarized as follows:

$$2^\cdot OH_{(s)} \quad \rightarrow \quad H_2O_{2(s)} \text{...} (174)$$

$$^\cdot OH_{(s)} + H^\cdot_{(s)} \rightarrow H_2O \text{...} (175)$$

$$H^\cdot_{(s)} + O_{2(s)} \quad \rightarrow \quad HO_2^\cdot_{(s)} \text{...} (176)$$

$$^\cdot OH_{(s)} \quad \rightarrow \quad ^\cdot OH_{(b)} \text{...} (177)$$

$$H^\cdot_{(s)} \quad \rightarrow \quad H^\cdot_{(b)} \text{...} (178)$$

$$H^\cdot_{(b)} + O_{2(b)} \quad \rightarrow \quad HO_2^\cdot_{(b)} \text{...} (179)$$

$$2^\cdot OH \quad \rightarrow \quad H_2O + O^\cdot \text{...} (180)$$
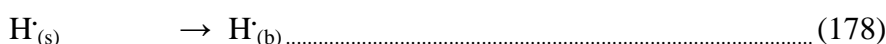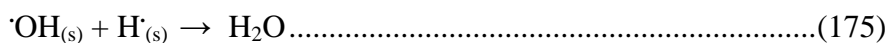
s: bubble surface, b: solution bulk

$$IC + ROS\ (H_2O_2,\ ^\cdot O_2^-,\ HO_2^\cdot,\ OH^\cdot,\ h^+ \text{ etc. formed under sonocatalysis)})\quad \rightarrow \quad Intermediates \rightarrow \rightarrow \rightarrow H_2O + CO_2 + salts \text{...} (181)$$
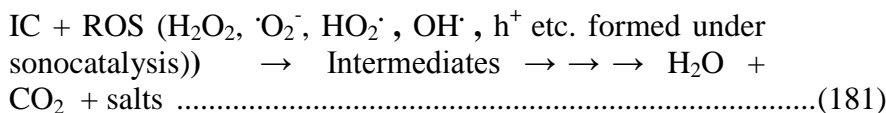
It is also possible that H_2O_2 decomposes under the same conditions as explained earlier.

$$H_2O_2 + US \rightarrow 2^\cdot OH \dots\dots\dots(182)$$
$$2H_2O_2 + US \rightarrow 2H_2O + O_2 \dots\dots\dots(183)$$

H_2O_2 also scavenges the insitu formed $^\cdot OH$ radicals as in reaction (159). However, part of H_2O_2 will be replenished by reaction (160).

Dissolved oxygen serves as a source of nucleus cavitation [225] which leads to the generation of more reactive species as in reactions 184-186.

$$O_2 \rightarrow 2O \dots\dots\dots(184)$$
$$O_2 + O \rightarrow O_3 \dots\dots\dots(185)$$
$$O + {^\cdot}O_2H \rightarrow {^\cdot}OH + O_2 \dots\dots\dots(186)$$

The ozone produced as in reaction 185 can decompose as in reaction 187 and the atomic oxygen can produce more ROS (reactions 188, 189).

$$O_3 + US \rightarrow O_2 + O \dots\dots\dots(187)$$
$$O + H_2O \rightarrow {^\cdot}OH + {^\cdot}OH \dots\dots\dots(188)$$
$$O + H_2O \rightarrow H_2O_2 \dots\dots\dots(189)$$

The $^\cdot OH$ radicals in the bulk are primarily those which escape recombination at the bubble surface [217]. The limited availability of $^\cdot OH$ radicals in the bulk will help their efficient utilization by the substrate molecules. The consumption/deactivation of $^\cdot OH$ radicals by anions and/or other processes take place mostly at the bubble surface.

The catalyst (MnO_2, MnO_2-TiO_2 and Co_3O_4) particles may get thermally excited and this can lead to the heat-induced catalytic degradation of the IC. The cavitation heat produces holes on the surface of the oxide which can interact with water and produce reactive ·OH radicals thereby enhancing the degradation. Similar results are reported in the case of TiO_2 sonocatalysis as well [229]. In the presence of suspended particles, an endothermic process exists in water upon US irradiation and this will result in the thermal excitation of the catalyst. However the excitation will occur only to a limited extent since it is difficult for the powder particles to be encapsulated within the cavities.

Since the catalysts used here have been shown to have good photocatalytic activity (Chapter 4), the sonoluminescence-induced photocatalysis also will be relevant here. US irradiation results in the formation of light of comparatively wider wavelength range of 200 -500 nm. Light of wavelength < 375 nm can excite the semiconductor catalyst leading to the formation of highly active ·OH radicals on the surface. MnO_2, TiO_2 and Co_3O_4 have been proven to be powerful photocatalysts for the mineralization of IC as demonstrated in earlier Chapters. Thus the basic mechanism of sonocatalysis can be partly of photocatalysis and possibly of sonophotocatalysis. Absorption of photons by the oxide catalyst leads to the formation of electron-hole pairs (reaction 143) which is the first step in photocatalysis. The efficiency of the process depends on the ability to prevent the electron-hole recombination which results in unproductive heat generation (reaction 190).

Microwave, Photo and Sono Activated Advanced Oxidation Processes and their Variations for the Decontamination of Water from Toxic Chemical Pollutants

445

$$h^+ + e^- \rightarrow \text{Heat} \quad ....(190)$$

The formation of reactive $^{\cdot}OH$ radicals from the electron and hole in presence of O_2 is shown in reactions (144) and (145). Another reactive free radical $HO_2^{\cdot}$ also is formed as in reactions (176), (179) and (191).

$$O_2^{\cdot\cdot} + H^+ \quad\quad\quad \rightarrow HO_2^{\cdot} \quad...(191)$$

These radicals lead to the formation of the oxidant H_2O_2 as follows:

$$O_2^{\cdot\cdot} + 2\,H^+ + e\text{-} \quad \rightarrow H_2O_2 ....(192)$$

$$2HO_2^{\cdot} \quad\quad\quad\quad \rightarrow H_2O_2 + O_2 ....(193)$$

$$HO_2^{\cdot} + O_2^{\cdot\cdot} + H_2O \rightarrow H_2O_2 + O_2 + {}^{\cdot}OH......................................(194)$$

$$h^+{}_{VB} + OH^- \quad\quad \rightarrow {}^{\cdot}OH...(195)$$

$${}^{\cdot}OH + {}^{\cdot}OH \quad\quad\quad \rightarrow H_2O_2...(196)$$
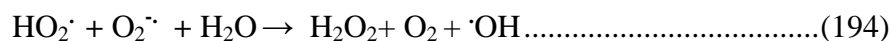
Once sufficient concentration of H_2O_2 is reached, its photodecomposition also sets in.

$$H_2O_2 + e^- \quad\quad\quad \rightarrow {}^{\cdot}OH + OH^- \quad ....(197)$$

$$H_2O_2 \quad\quad\quad\quad \overset{h\nu}{\rightarrow} 2\,{}^{\cdot}OH \quad ....(198)$$

$$H_2O_2 + {}^{\cdot}O_2^- \quad\quad \rightarrow 2\,{}^{\cdot}OH + O_2..(199)$$
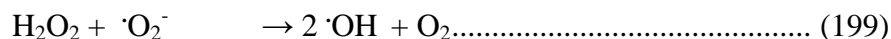
Thus photocatalysis and possibly mild sonophotocatalysis and consequent degradation of IC are also taking place in the sonocatalytic system.

The net concentration of $^{\cdot}OH$ radicals in the system at any point in time depends on the relative rates of their concurrent generation and

decomposition [112, 165]. The formation of ˙OH radicals under MnO_2 sonocatalysis is experimentally verified by the photoluminescence (PL) spectral studies (Section 2.5 of Chapter 2) and is shown in Fig.5.69. The concentration of the radicals increases with time of US irradiation. The oxidation of substrates by ˙OH radicals can take place both on the surface of the catalyst as well as in the solution bulk.
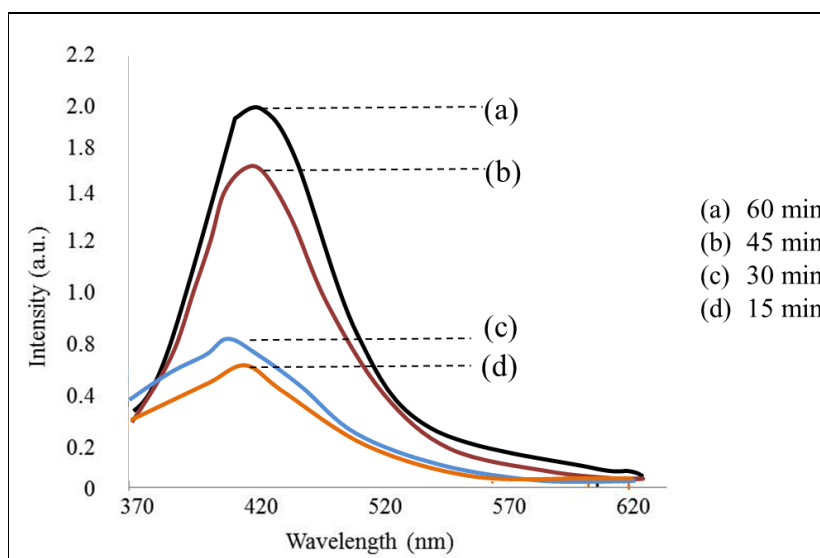
Fig. 5.69: PL Spectral changes observed during the US irradiation of MnO_2 with terephthalic acid, demonstrating the formation of ˙OH radicals and their increase with time of irradiation.

Microwave, Photo and Sono Activated Advanced Oxidation Processes and their Variations for the Decontamination of Water from Toxic Chemical Pollutants

447

5.7 Summary of the comparative efficiency of MnO_2, MnO_2-TiO_2 and Co_3O_4 for the sonomineralisation of IC

Parameters	MnO_2	MnO_2-TiO_2(18:1)	Co_3O_4
Optimum Loading	1400 mg/L	1800 mg/L	1600 mg/L
Optimum Concentration	40 mg/L	60 mg/L	60 mg/L
Kinetics	Variable kinetics. Pseudo first order at lower concentration (up to 40mg/L). Eventual zero order at higher concentrations.	Variable kinetics. Pseudo first order at lower concentration (up to 60mg/L). Eventual zero order at higher concentrations.	Variable kinetics. Pseudo first order at lower concentration (up to 60 mg/L). Eventual zero order at higher concentrations.
pH effect	Maximum degradation at pH 2 followed by gradual decrease up to pH 10 and a slight increase above pH10.	Maximum degradation at pH 2-3. Thereafter degradation decreases steeply at pH4. Then stabilizes in the range 4-10. Slight increase in degradation at pH >10	Maximum degradation at pH 2 followed by decrease up to pH 4. Thereafter stable in the range 4-11.
H_2O_2 effect	Inhibition, which increases with concentration up to 10 mg/L and then stabilises.	Inhibition, increases up to 30mg/L of H_2O_2. Degradation stabilizes thereafter.	Enhancement. Degradation increases with increase in concentration of H_2O_2.
Persulphate effect	Enhancement, increases with increase in concentration up to 40mg/L.	Enhancement increases with increase in concentration up to 40mg/L.	Enhancement, increases with increase in concentration up to 50 mg/L.
Deaeration by N_2 bubbling	Effect dependent on MnO_2 dosage. No Effect at high dosages (1400mg/L) of MnO_2 Inhibition in the degradation of IC at lower dosages ($\sim$<200mg/L)	Not Done. (Since the results are similar in the case of MnO_2 and MnO_2-TiO_2 in most cases)	Not done. Only preliminary investigation is made with Co_3O_4 as catalyst.

Recycling	29% decrease in degradation in 1st recycling and 52% in 2nd recycling and 71% in 3rd recycling	Not Done. (Since the results are similar in the case of MnO_2 and MnO_2/TiO_2 in most cases)	Not done
COD decrease US only	0.44 mg/L/hr. Stabilises after 40% decrease. Mineralisation completed in 4 hr when combined with UV irradiation in sequence.	0.55mg/L/hr. Stabilises after 40% decrease. Mineralisation completed in 3 hr when combined with UV irradiation in sequence.	Not done. Only preliminary investigation is made with Co_3O_4 catalyst
Anions (2-15 mg/L)			
i) PO_4^{3-}	Inhibition increases with increase in concentration and reaction time	Inhibition	Inhibition
ii) HCO_3^-	Inhibition except at 2mg/L	Mild inhibition to no effect	Enhancement
iii) CO_3^{2-}	Inhibition	Inhibition	Enhancement
iv) Cl^-	No effect	No effect	Enhancement
v) CH_3COO^-	Enhancement	No effect	Enhancement
vi) SO_4^{2-}	No effect	Inhibition	No effect to enhancement
vii) NO_3^-	Enhancement	Enhancement	Enhancement

Microwave, Photo and Sono Activated Advanced Oxidation Processes and their Variations for the Decontamination of Water from Toxic Chemical Pollutants

449

5.8 Conclusions

MnO_2, MnO_2-TiO_2 and Co_3O_4 have been identified as highly effective sonocatalysts for the decolourisation of the recalcitrant dye pollutant IC from water. Concentration of the substrate, catalyst loading, pH, reaction volume, US frequency, availability of O_2, presence of salts and other contaminants etc. are important parameters that determine the efficiency of the process. The degradation follows variable kinetics which depends on the concentration of the substrate. H_2O_2 inhibits the degradation in the case of MnO_2 and MnO_2-TiO_2 while it enhances the degradation in presence of Co_3O_4 catalyst. Persulphate which is a very powerful oxidant enhances the degradation in all cases. The effect of anions on the degradation varies from inhibition, 'no effect' or enhancement depending on the reaction conditions, characteristics of the components and the nature and intensity of interactions. The high affinity of MnO_2 for O_2 and its extremely efficient adsorption of H_2O_2 and the substrate play key role in the efficiency of the process. Even oxygen from the lattice participates in the reaction whenever there is a deficit of dissolved or adsorbed oxygen. Major transient intermediates formed during the process are identified by LC-MS. Combination of sonocatalysis with UV photolysis (sonophotocatalysis) in sequence enhances the efficiency of degradation and mineralization of IC. MnO_2-TiO_2 also behaves similarly while Co_3O_4 displays different characteristics especially in presence of oxidants and anions. These two catalysts (MnO_2-TiO_2 and Co_3O_4) need further in depth investigation to fully explore their AOP potential. The observations are discussed and a probable mechanism for the sonocatalytic degradation of IC is proposed.

…..ജാറ…..

Chapter **6**

Sonophotocatalysis mediated by MnO₂ and MnO₂-TiO₂ for the degradation of Indigo Carmine in water

6.1 Introduction

As discussed in Chapter1, Section 1.2.2.3, sonophotocatalysis (SPC) involves the use of a catalyst in presence of ultrasound and ultraviolet irradiation. This combination leads to the formation of a large number of free radicals which enhance the degradation of the pollutant. Synergic effect is reported in many cases i.e. the degradation under sonophotocatalysis is more than the sum of the degradation under individual sonocatalysis (SC) and photocatalysis (PC). Ultrasound enhances the mass transfer of organic pollutants between liquid phase and catalyst surface and also reduces the recombination of electrons and holes which in turn enhances the formation of ˙OH radicals. In sonocatalysis, catalyst particles act as additional nuclei

Microwave, Photo and Sono Activated Advanced Oxidation Processes and their Variations for the Decontamination of Water from Toxic Chemical Pollutants

451

for the formation of cavitational bubbles. Sonication alone in presence of MnO_2 and MnO_2-TiO_2 results in significant degradation of IC (Chapter 5). When combined with photocatalysis, the degradation as well as mineralisation of the pollutant is enhanced within a shorter period of time. In this context SPC has been investigated as a potential environment-friendly technology for the removal of traces of IC from water. To the best of our knowledge, this is the first instance of application of SPC with MnO_2 as the catalyst for the decolourisation and/or mineralisation of IC.

Relevant data from photo and sonocatalysis (from Chapters 4 and 5 respectively) are also provided side by side towards the end of the Chapter for convenience of comparison of the efficiency of the three processes. Since the degradation is relatively slower under PC, direct comparison of the PC data with SC and SPC data in the same Figure/Table may not be proper. Hence PC data is given in the inset of respective figures, unless indicated otherwise.

6.2 Experimental details

6.2.1 Materials used

Materials used for the studies in this Chapter are same as those described in Chapters 2, 3, 4 and 5.

6.2.2 Analytical procedures

Sampling and analysis were performed as explained in Chapter 3 of Section 3.2.3. The mercury vapour lamp for UV light, the ultrasonic bath for US as well as various other equipment used in the study are the same as those described earlier.

6.2.3 Sonophotocatalytic experimental setup

The experiments were performed using aqueous solutions of IC of desired concentration. Specified quantity of the catalyst is suspended in the solution. The reaction set up is a combination of those used in Chapters 4 and 5. The reactors are same as those used in photocatalysis. They are placed in an ultrasonic bath in which water from a thermostat at the required temperature was circulated. Unless otherwise mentioned, the reaction temperature was maintained at $35 \pm 1^{\circ}C$. The position of the reactor in the ultrasonic bath was always kept the same. A high intensity UV lamp (400 W medium pressure mercury vapour quartz lamp) mounted above is used as the UV irradiation source. The ultrasonic bath was operated at a frequency of 42 kHz and a power of 100 W unless indicated otherwise. Rest of the experimental procedure, sampling and analysis methods etc. are the same as those described in Chapters 4 and 5. Typical reactor set up is shown in Fig. 6.1.
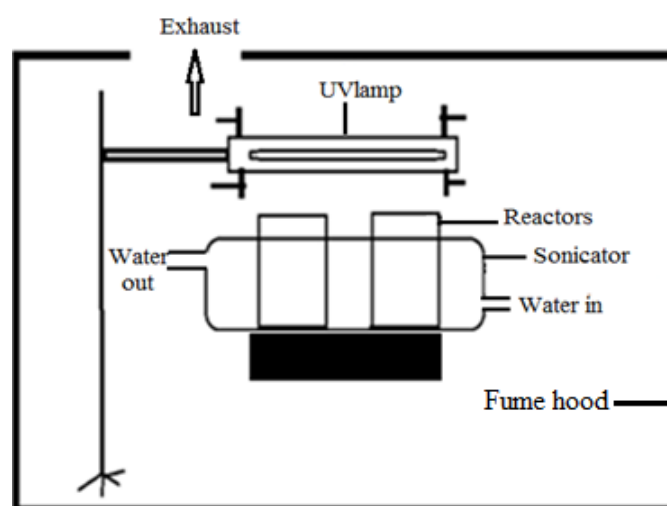
Fig. 6.1: Schematic diagram of the sonophotocatalytic experiment set up

Microwave, Photo and Sono Activated Advanced Oxidation Processes and their Variations for the Decontamination of Water from Toxic Chemical Pollutants

453

6.3 Results and discussion

6.3.1 Preliminary results

Preliminary results on the sonophotocatalytic degradation of IC are compared with those in sono and photocatalysis under identical reaction conditions. The results are shown in Fig.6.2.
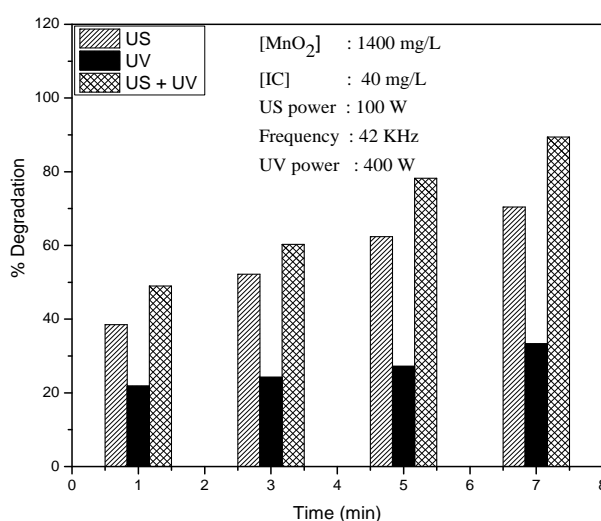
Fig. 6.2: Comparison of sono, photo and sonophotocatalytic degradation of IC in presence of MnO_2

The degradation is more facile in the presence of US irradiation compared to UV light. Ultrasound provides 70% degradation of IC within 7 minutes of irradiation in presence of MnO_2. But sonophotocatalysis provides 90% of degradation under the same conditions, i.e 20% increase in degradation is obtained in presence of sonophotocatalysis over the degradation in presence of sonocatalysis. However the effect is only partially additive of sono and photocatalysis and no synergy is observed. Various parameters relevant for the efficiency of sonophotocatalysis are identified and optimised as reported below.

6.3.2 Effect of catalyst dosage

The catalyst dosage for optimum sonophotocatalytic degradation of IC is experimentally determined and the result is shown in Fig.6.3. The catalyst dosage effects under comparable sono and photocatalytic (inset) conditions are also shown in the figure.
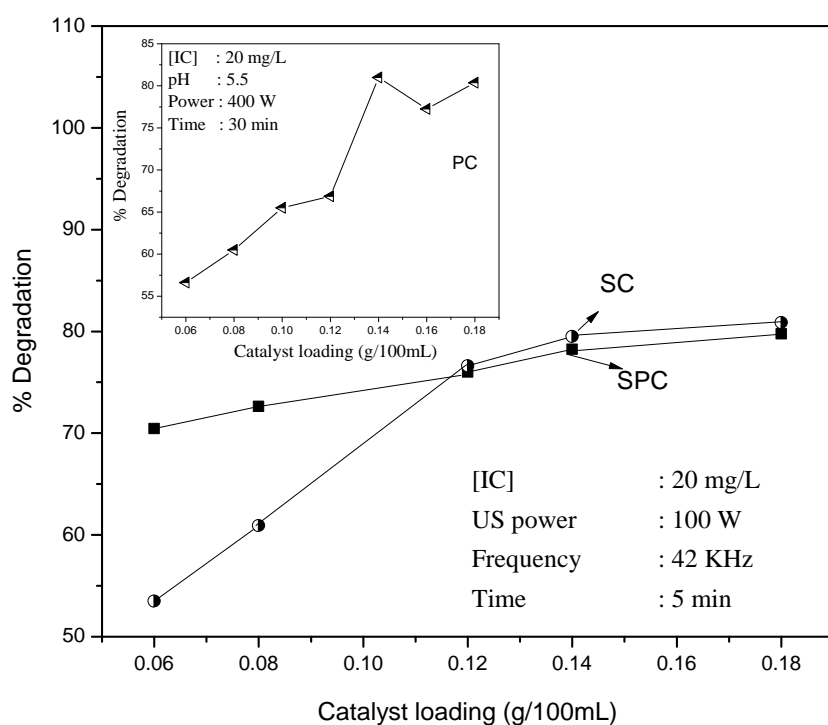
Fig. 6.3: Effect of catalyst dosage on the photocatalytic (PC) (Inset), sonocatalytic (SC) and sonophotocatalytic (SPC) removal of IC in presence of MnO_2

The degradation of IC under SPC increases slowly with increase in catalyst loading and reaches an optimum at ~ 0.14g/100mL. The stabilisation happens at the same range of catalyst dosage as in the case of sonocatalysis. The enhanced degradation efficiency with increase in catalyst dosage is

probably due to increased number of adsorption sites and more effective use of the UV and US radiation which lead to the generation of more reactive ·OH radicals and other ROS. In the case of photocatalysis also, as shown in the inset of the figure, the catalyst dosage is optimum at 0.14g/100mL. In the case of sonophotocatalysis, the degradation is around 70% in 5 minutes with catalyst dosage of 0.06g/100mL. In the case of sonocatalysis as well as photocatalysis, the same extent of degradation (70%) requires more than double this dosage (> 0.12 g/100 mL), thereby illustrating the far superior efficiency of sonophotocatalysis at much lower catalyst dosages. This can be attributed to the effect of sonication such as deaggregation of particles, in situ cleaning of surface sites by microstreaming, increased mass transfer of pollutants between liquid phase and catalyst surface etc and the more effective utilisation of photolysis made possible by these factors. Details of the effect of catalyst dosage on the efficiency of photo and sonocatalytic degradation of IC are discussed under Sections 4.3.2 and 5.3.2 of Chapters 4 and 5 respectively. The enhancement in sonophotocatalysis over sonocatalysis is not very distinct at higher dosages of MnO_2 (> 0.12g/100 mL). At this stage the degradation is already around 80% and the concentration of IC remaining in the system is very small. Consequently, the difference in the degradation under sono or sonophotocatalysis is not very distinct at higher dosages and at later stages of reaction. All further studies in sonophotocatalysis were made at the catalyst dosage of 1400 mg/L, which is the same dosage chosen for sono and photocatalysis.

6.3.3 Effect of concentration of IC

The % degradation decreases with increase in concentration of IC as shown in Fig.6.4.
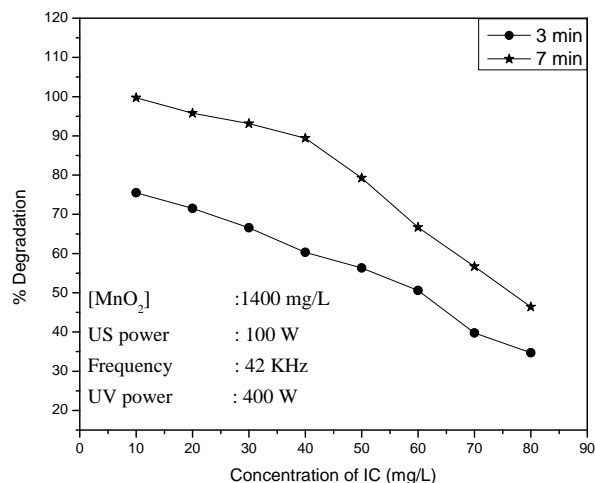
Fig.6.4: Effect of concentration of IC on its sonophotocatalytic degradation

The rate of degradation increases with increase in concentration up to 50 mg/L and is more or less stabilised thereafter (Fig.6.5).
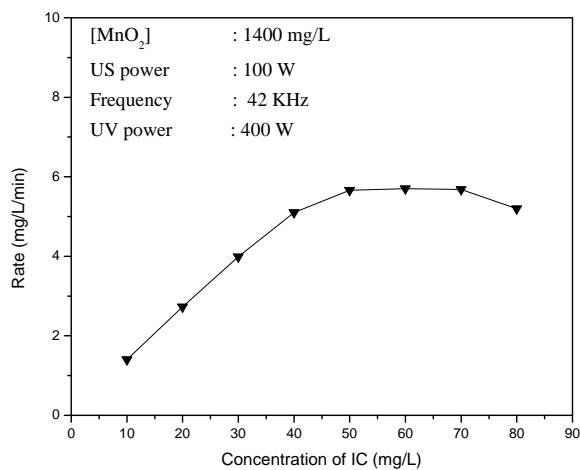
Fig.6.5: Rate of degradation of IC at its various concentrations

Microwave, Photo and Sono Activated Advanced Oxidation Processes and their Variations for the Decontamination of Water from Toxic Chemical Pollutants

457

Comparative rate of degradation under the 3 processes is presented in Fig.6.6, which shows that sonocatalysis is at least ~ 9 times more efficient than photocatalysis for the degradation of IC, whereas sonophotocatalysis is ~ 12 times more efficient. The degradation efficiency is in the order SPC > SC >> PC.
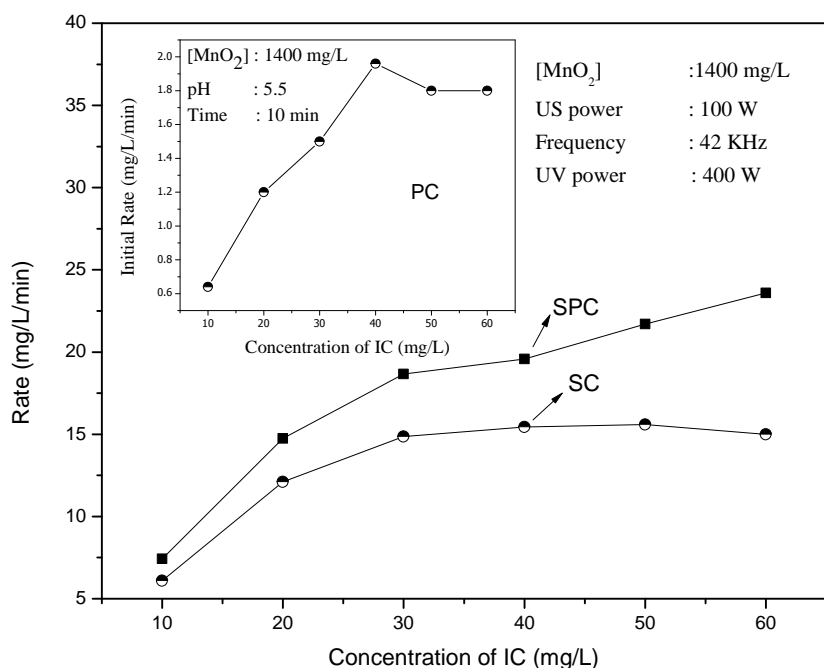
Fig. 6.6: Comparison of the rate of degradation of IC in presence of MnO$_2$ under SC, PC and SPC (PC results in 'inset')

The kinetics of the degradation under SPC is verified by the ($1/r_0$ vs $1/C_0$) plot (Fig.6.7) and the logarithmic plot of ln C_0/C vs time (Fig.6.8). Relevant details are explained in Chapter 3 Section 3.3.3.2.
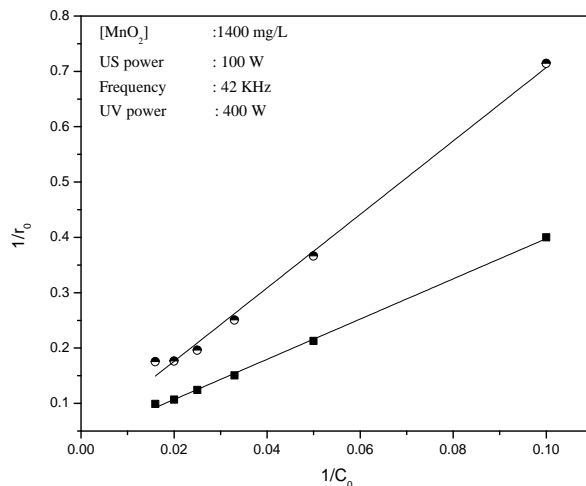
Fig. 6.7: Reciprocal plot of $1/r_0$ vs $1/C_0$ for various concentrations of IC under SPC

Plot of $1/r_0$ vs $1/C_0$ yields a straight line indicating first order kinetics and L-H mechanism as in the case of SC and PC. The logarithmic plot also follows trends similar to the case of SC and PC, and confirms the pseudo first order kinetics in the range 10-40 mg/L of IC. The kinetics is explained in Chapters 3, 4 and 5.
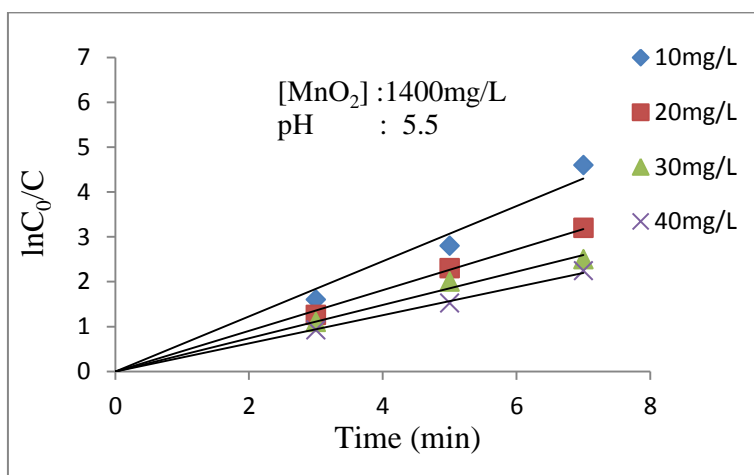
Fig. 6.8: Logarithmic plot for the MnO₂ mediated SPC degradation of IC

6.3.4 Effect of pH

pH has a significant effect on the sonophotocatalytic degradation of IC. pH affects surface charge, size of aggregation, band edge position and also the adsorption-desorption characteristics of the surface of catalyst. The effect of pH on the sonophotocatalytic degradation of IC is investigated in the range 2-11. The results showed that maximum degradation is in the acidic pH 2 and 3 (Fig.6.9). Thereafter, the degradation falls and is stabilised in the pH range 4-10. The trend is similar to that in the case of sono and photocatalysis individually, even though there is slight decrease in the degradation above pH 8 in the case of sonocatalysis (Fig.6.10). This may be due to the complexity and unpredictability of the effect of pH in sono and photocatalytic systems as discussed in Sections 4.3.4 and 5.3.5 of Chapters 4 and 5 respectively.
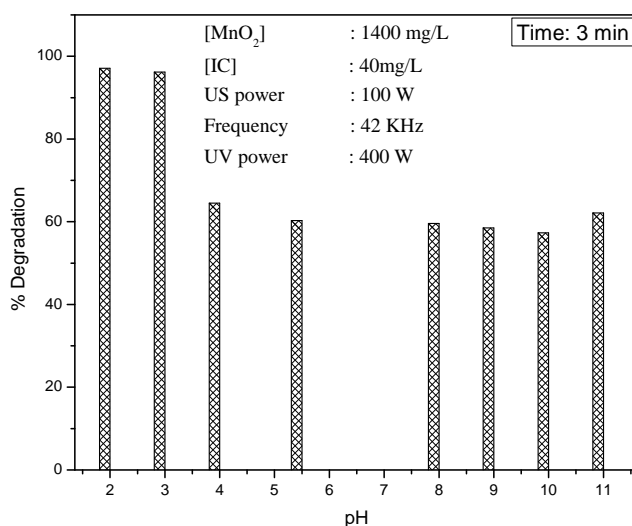
Fig. 6.9: Effect of pH on the SPC degradation of IC in presence of MnO_2.
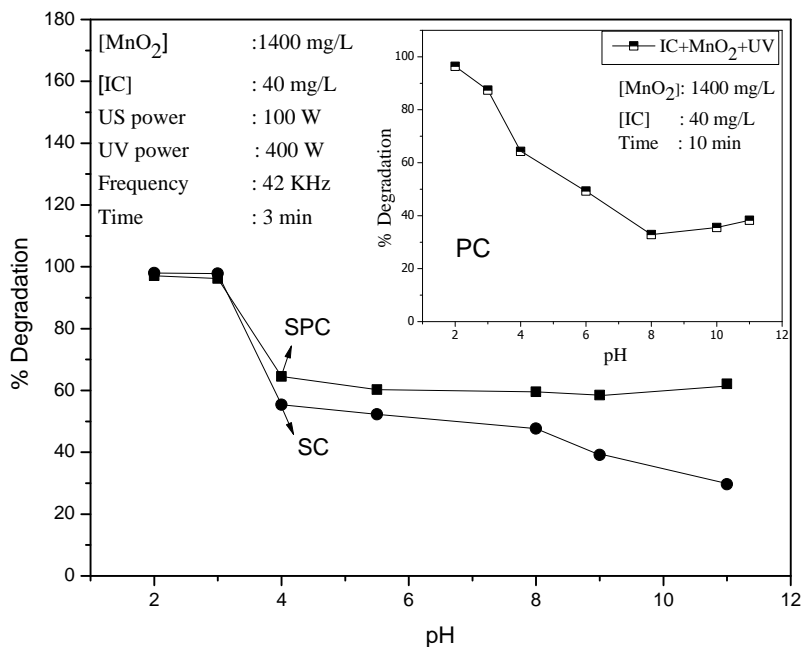
Fig. 6.10: Comparison of the effect of pH on the degradation of IC under SC, PC and SPC (PC results in the inset)

Various factors contributing to the pH effect as well as its complexity in heterogeneous AOP systems are explained in Chapters 3, 4 and 5.

6.3.5 Effect of Oxidants

Oxidants such as H_2O_2 and PS have been proven to influence the degradation of IC under sono and photocatalytic conditions. Hence the effect of these oxidants is tested under sonophotocatalysis as well.

6.3.5.1 Effect of added H_2O_2

The effect of externally added H_2O_2 at different concentrations on the sonophotocatalytic degradation of IC in presence of MnO_2 is tested. Addition of H_2O_2 inhibits the degradation of IC upto 20 mg/L. Thereafter it stabilises irrespective of concentration (See Fig. 6.11).
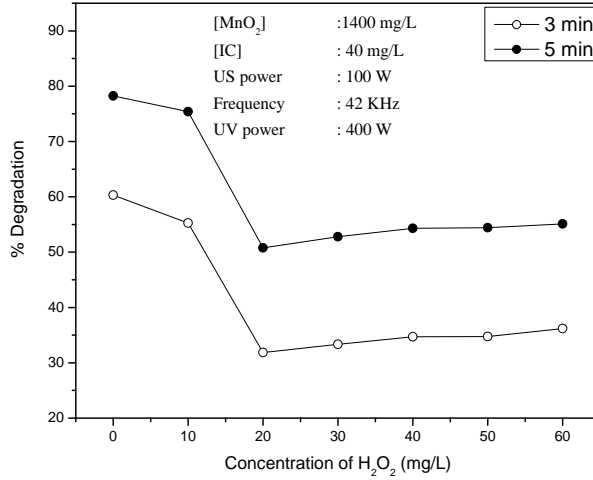
Fig. 6.11: Effect of H$_2$O$_2$ on the SPC degradation of IC in presence of MnO$_2$

The inhibition by H$_2$O$_2$ is further confirmed by the addition of H$_2$O$_2$ in-between to a reaction in progress. Results are shown in Fig. 6.12. Every extra addition of H$_2$O$_2$ (3 min and 7 min) decreases the % degradation of IC.
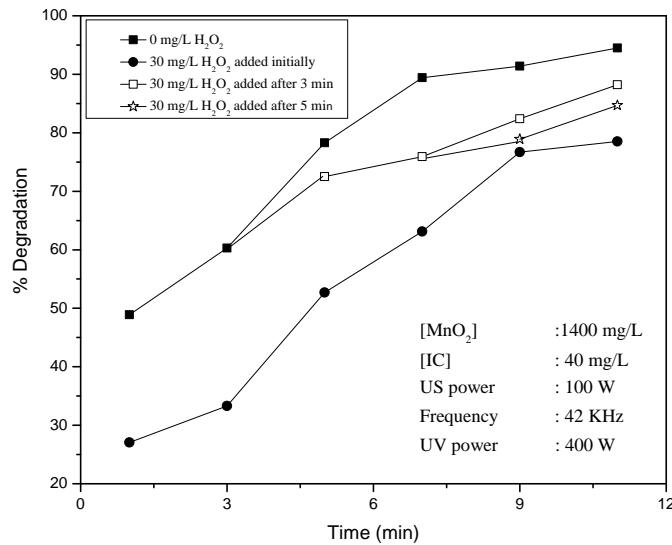
Fig. 6.12: Effect of initial and in-between addition of H$_2$O$_2$ on the SPC degradation of IC.

Comparison of the effect of externally added H_2O_2 on the degradation of IC under PC, SC and SPC is shown in Fig.6.13.
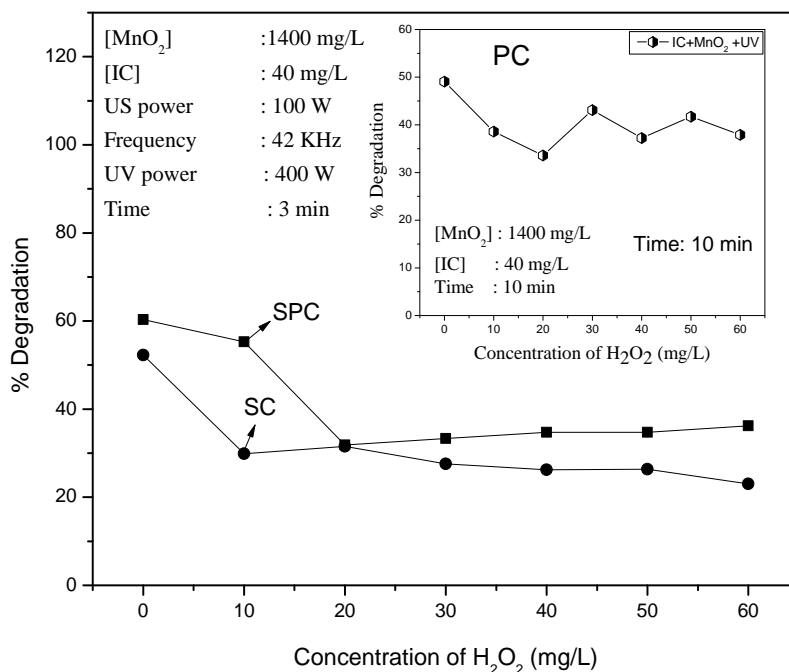
Fig. 6.13: Comparative effect of H_2O_2 on the degradation of IC under SC, PC and SPC conditions (PC results in the inset.)

The inhibitive effect of H_2O_2, is similar in the case of sono, photo and sonophotocatalysis with strong inhibition initially, followed by stabilisation at higher concentration of H_2O_2. In the case of PC the stabilised level of degradation at higher H_2O_2 concentration has slight oscillatory type behaviour. This may be partly due to the oscillation in the concentration of H_2O_2 itself as explained under Section 3.3.3.8 of Chapter 3. However, it may be concluded from the data that the general

Microwave, Photo and Sono Activated Advanced Oxidation Processes and their Variations for the Decontamination of Water from Toxic Chemical Pollutants

463

mechanism of the effect of H_2O_2 is the same, in all three cases, at least qualitatively.

6.3.5.2 Effect of added $K_2S_2O_8$ (PS)

The effect of externally added PS on the sonophotocatalytic degradation of IC is studied and the results are shown in Fig.6.14. The % degradation increases with increase in the concentration of PS and more than 97% degradation is obtained at a concentration of 100 mg/L within 5 min of irradiation time.
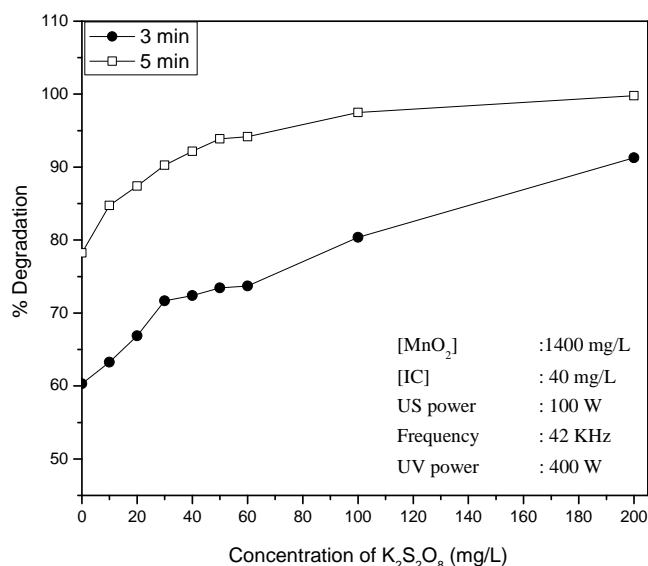
Fig. 6.14: Effect of PS on the SPC degradation of IC over MnO_2

The enhancing effect is also confirmed by the in-between addition (Fig 6.15) of PS to the reaction in progress after 3 and 7 minutes. The results show clear enhancement in the degradation of IC.
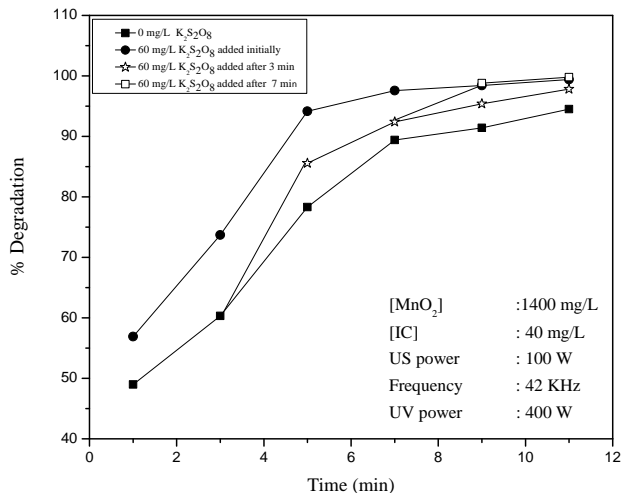
Fig. 6.15: Effect of initial and in-between addition of $K_2S_2O_8$
on the SPC degradation of IC.

The enhancement by $K_2S_2O_8$, follows a similar trend as in the case
of sono and photocatalysis (Fig.6.16). Hence the mechanism of
enhancement also will be identical, as explained in Sections 4.3.6.2 and
5.3.9.2 of Chapters 4 and 5 respectively.
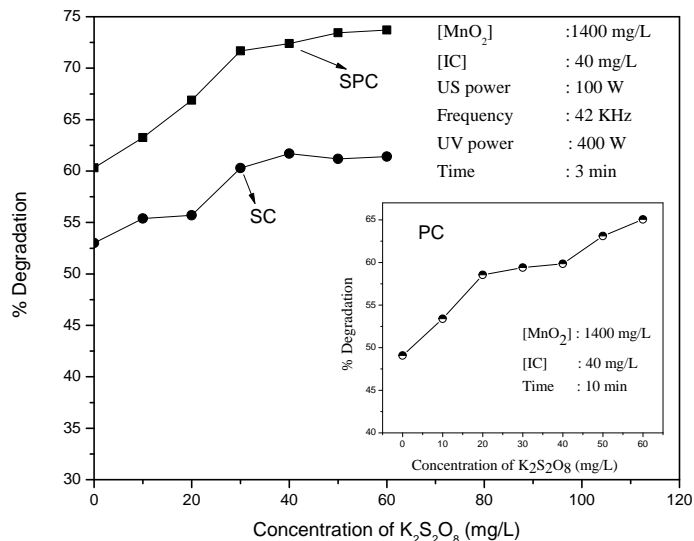
Fig. 6.16: Comparative effect of PS on the SC, PC and SPC
degradation of IC (PC results in the inset)

6.3.5.3 Effect of Combination of H_2O_2 and PS

The effect of combination of H_2O_2 and $K_2S_2O_8$ on the sonophotocatalytic degradation of IC is tested and the results are plotted in Fig.6.17. The effect of the combination is moderate enhancement. Had it been the average effect of the inhibition and enhancement by H_2O_2 and PS respectively, the net effect should have been moderate inhibition. Hence the mild enhancement indicates that PS can partially compensate for the inhibition by H_2O_2.
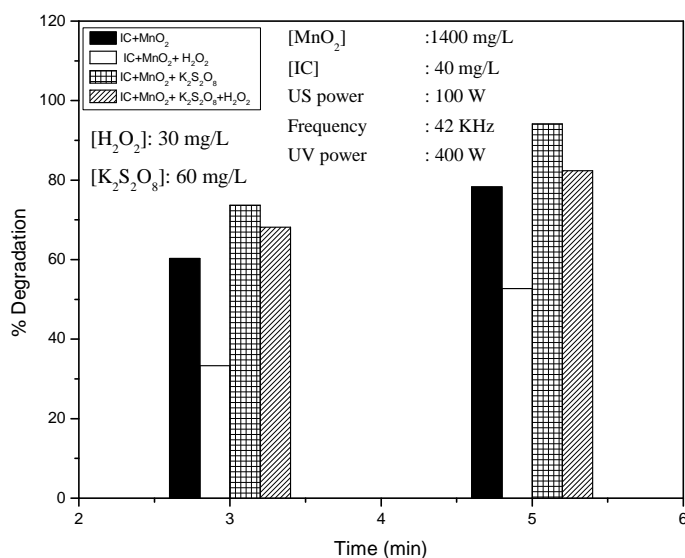
Fig. 6.17: Effect of combination of $K_2S_2O_8$ and H_2O_2 on the degradation of IC

The comparative effect of H_2O_2, PS and their combination on the sono, photo and sonophotocatalytic degradation of IC is given in Fig.6.18.
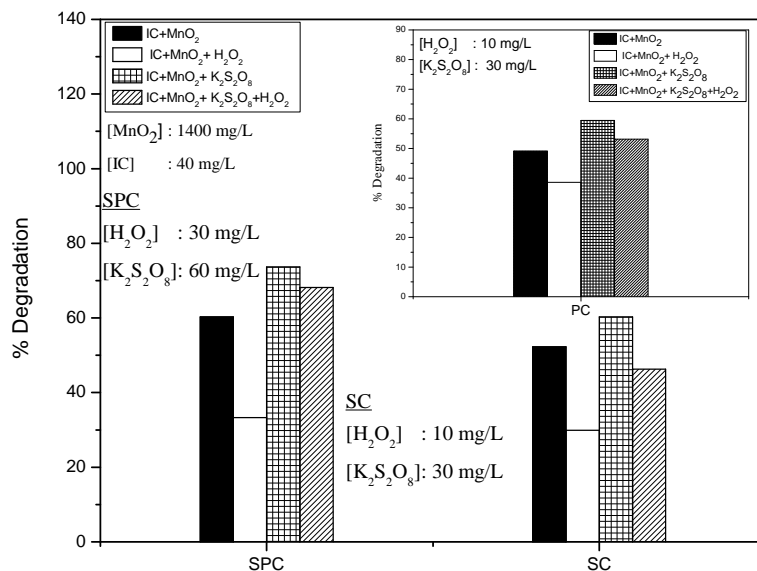
Fig. 6.18: Effect of combination of PS and H$_2$O$_2$ on the SC, PC and SPC degradation of IC (PC results in 'inset').

In the case of PC and SPC, PS compensates for the inhibition of H$_2$O$_2$. In the case of sonocatalysis, the combination effect is still inhibition. Hence it is clear that the potential of the oxidising efficiency of PS can be utilised more effectively in presence of UV light compared to US irradiation.

6.3.6 Effect of Anions

As done in the case of sono and photocatalysis, the degradation of IC in presence of anions was investigated under sonophotocatalysis as well. The effect of some of the commonly occurring anions in water, i.e. SO$_4^{2-}$, Cl$^-$, PO$_4^{3-}$, CO$_3^{2-}$, CH$_3$COO$^-$, HCO$_3^-$ and NO$_3^-$ on the efficiency of SPC/MnO$_2$ degradation of IC is tested at various concentrations (5, 10 and 15 mg/L) and reaction times (1, 3, and 5 min). The results are plotted

Microwave, Photo and Sono Activated Advanced Oxidation Processes and their Variations for the Decontamination of Water from Toxic Chemical Pollutants

467

in figures 6.19A and 6.19B respectively. The results showed that SO_4^{2-}, Cl^- and NO_3^- enhance the degradation mildly. PO_4^{3-}, HCO_3^- and CO_3^{2-} inhibit the degradation at all concentrations. CH_3COO^- has no effect.
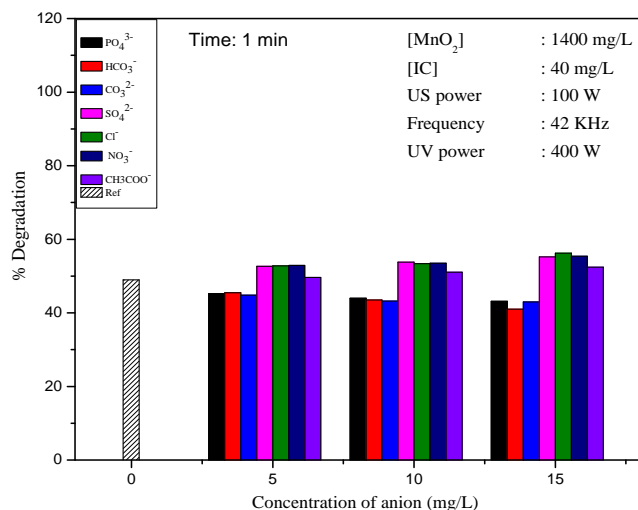
Fig. 6.19A: Effect concentration of anions on the sonophotocatalytic degradation of IC

The effect of different anions at different concentrations on the SPC degradation of IC after 1minute reaction time is summarised in Table 6.1.

Table 6.1: Effect of concentration of anions on the sonophotocatalytic degradation of IC   (Time: 1 min)

Concentration of anions (mg/L)	Inhibition	No Effect	Enhancement
5	$CO_3^{2-} \approx HCO_3^- \approx PO_4^{3-}$ (mild)	CH_3COO^-	$SO_4^{2-} \approx Cl^- \approx NO_3^-$ (mild)
10	$CO_3^{2-} \approx HCO_3^- \approx PO_4^{3-}$ (mild)	CH_3COO^-	$SO_4^{2-} \approx Cl^- \approx NO_3^-$ (mild)
15	$CO_3^{2-} \approx HCO_3^- \approx PO_4^{3-}$ (mild)	CH_3COO^-	$SO_4^{2-} \approx Cl^- \approx NO_3^-$ (mild)

Effect of reaction time on the sonophotocatalytic degradation of IC, in presence of various anions, is shown in Fig.6.19B and the data is summarised in Table 6.2.
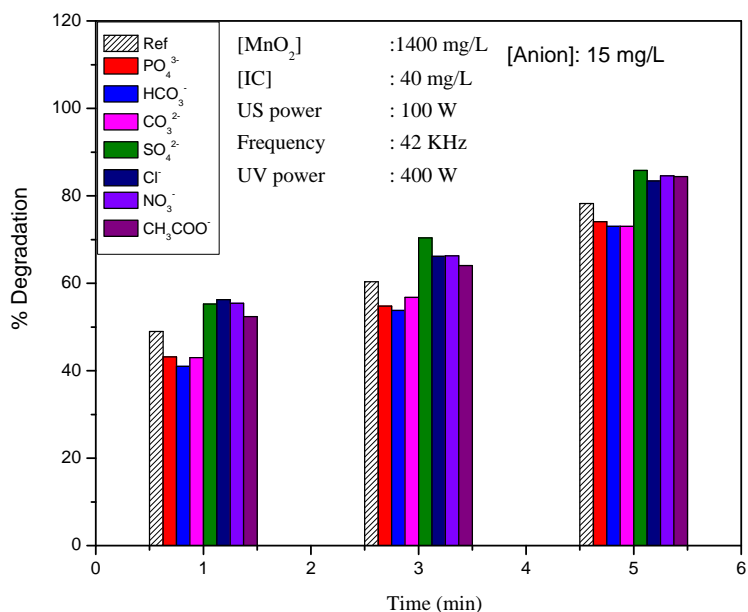
Fig. 6.19B. Effect of reaction time on the sonophotocatalytic degradation of IC on MnO_2, in presence of various anions.

Table 6.2: Effect of reaction time on the sonophotocatalytic degradation of IC, in presence of various anions. [Anion]: 15mg/L

Time (min)	Inhibition	No Effect	Enhancement
1	$CO_3^{2-} \approx HCO_3^- \approx PO_4^{3-}$	CH_3COO^-	$SO_4^{2-} \approx Cl^- \approx NO_3^-$
3	$CO_3^{2-} \approx HCO_3^- \approx PO_4^{3-}$	-	$SO_4^{2-} > Cl^- \approx NO_3^- \approx CH_3COO^-$
5	$CO_3^{2-} \approx HCO_3^- \approx PO_4^{3-}$	-	$SO_4^{2-} > Cl^- \approx NO_3^- \approx CH_3COO^-$

As the reaction time advances, the 'no effect' by CH_3COO^- gradually becomes mild enhancement. The mild enhancement by SO_4^{2-}, Cl^- and NO_3^- continues even after longer reaction time.

The nature of 'anion effect' does not vary with concentration (of the anion) or the reaction time as in the case of sono or photocatalysis. The inhibition caused by the anions, can be explained based on the reduced availability of surface sites for the substrate due to adsorption of anions on the catalyst surface. Scavenging of the Reactive Oxygen Species (ROS) by the anions which slows down the degradation of IC, surface layer formation by anions and various other reasons which contribute to the inhibition by respective anions are discussed in detail in Sections 3.3.3.12 and 4.3.7 of Chapter 3 and 4 respectively.

The enhancement by anions is explained based on the in situ formation of respective radical anions which are also oxidants. Other possible reasons for the enhancement of degradation by anions are explained in Chapter 4 (Section 4.3.7). Depending on the domination of inhibiting, balancing and/or enhancing factors, the effect will be 'inhibition', 'no effect' or 'enhancement'.

The effect of these anions at various concentrations, i.e, 5, 10, 15 mg/L and at various reaction times (1, 3, 5, 7 min) on the sonophotocatalytic degradation of IC is investigated and the results are shown in Figs. 6.20 to 6.26. The results in each case are compared with those under PC as well as SC. As done earlier, the anion effect under PC is shown in the 'inset' of respective figures.

6.3.7.1 PO₄³⁻
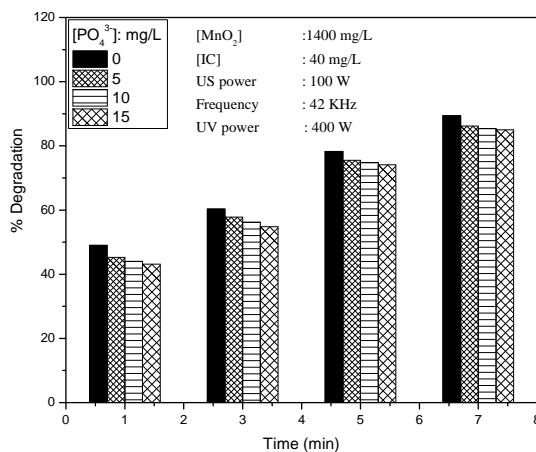
Fig. 6.20: Effect of PO₄³⁻ on the SPC degradation of IC in presence of MnO₂

PO₄³⁻ remains a mild inhibitor at all concentrations and reaction times. Comparative effect of PO₄³⁻ under SC, PC, and SPC is given in Fig. 6.20A which shows that PO₄³⁻ is a powerful inhibitor under SC and PC while the inhibition is mild or even practically negligible under SPC.
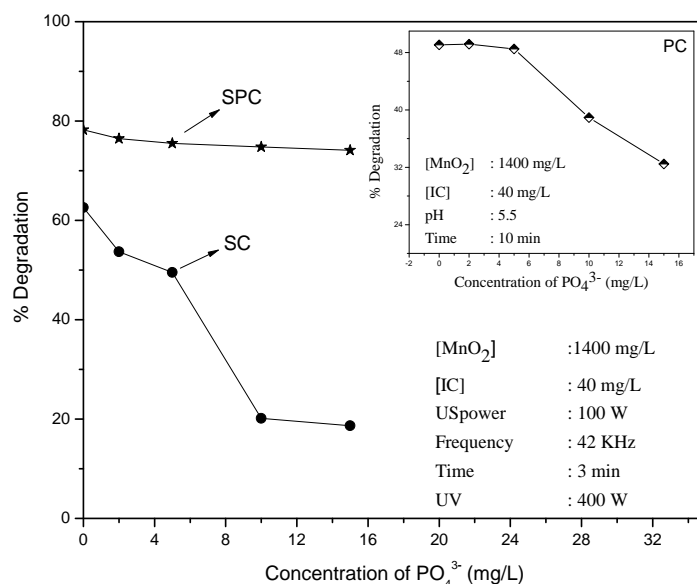
Fig. 6.20A: Comparison of the effect of PO₄³⁻ on the degradation of IC under SC, PC and SPC conditions (PC results in 'inset')

The synergy of the combination SPC is adequate enough to compensate for the strong inhibition of the degradation by PO_4^{3-} under PC and SC.

6.3.7.2 HCO_3^-

HCO_3^- remains a mild inhibitor under SPC at all concentrations and reaction times (Fig.6.21).
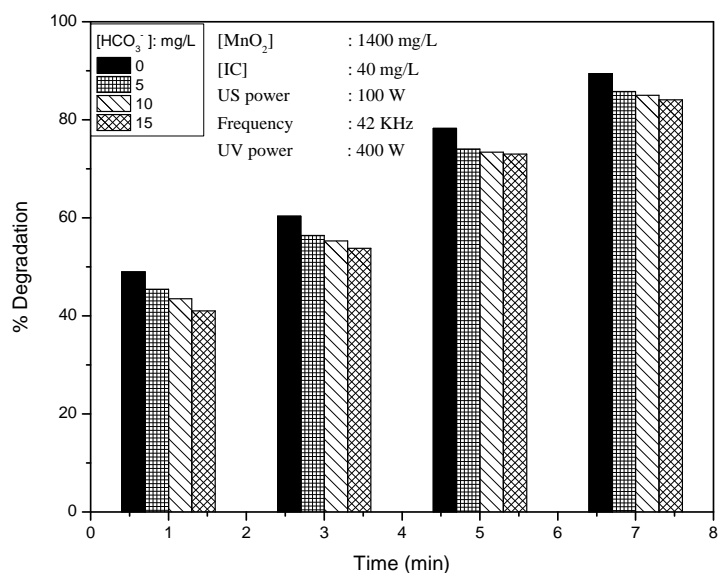
Fig. 6.21: Effect of HCO_3^- on the SPC degradation of IC in presence of MnO_2

Comparison of the effect of HCO_3^- under PC, SC and SPC is shown in (Fig.6.21A).
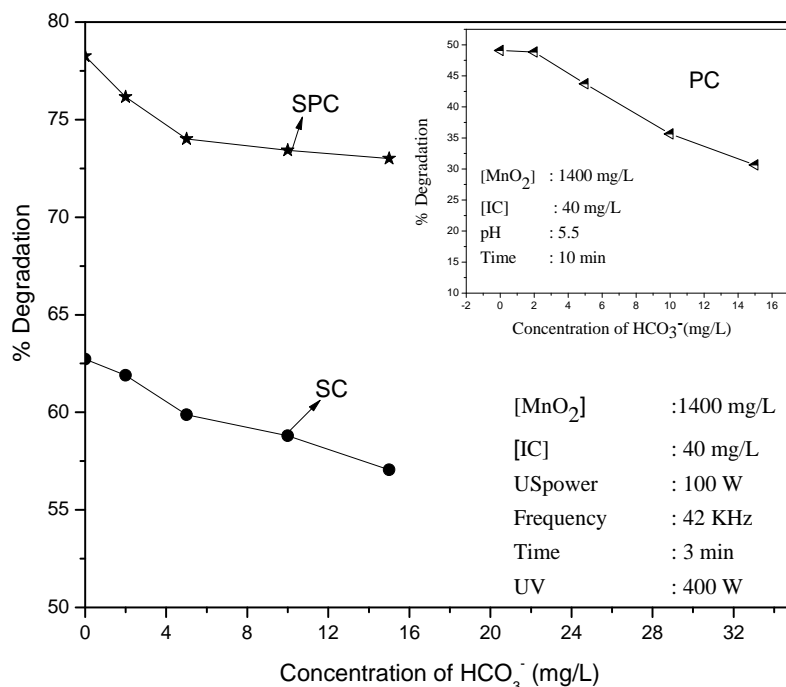
Fig.6.21A: Comparison of the effect of HCO_3^- on the degradation of IC under SC, PC and SPC (PC results in 'inset').

Comparison of the data shows that HCO_3^- is a powerful inhibitor under PC. The trend is same in the case of SC and SPC also, though the extent of inhibition is relatively less compared to PC.

6.3.7.3 CO_3^{2-}

CO_3^{2-} is a mild inhibitor at all concentrations and reaction times (Fig.6.22).

Microwave, Photo and Sono Activated Advanced Oxidation Processes and their Variations for the Decontamination of Water from Toxic Chemical Pollutants

473
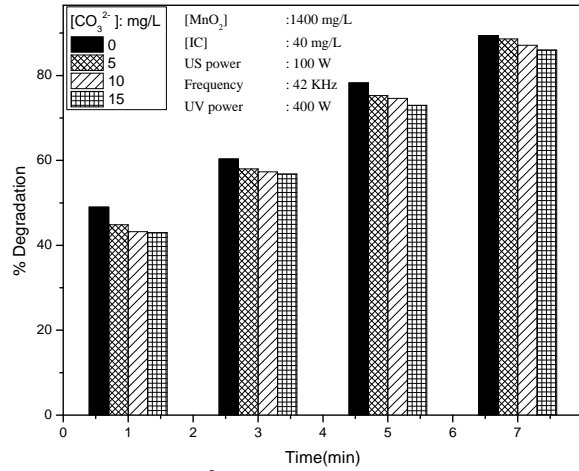
Fig. 6.22: Effect of CO_3^{2-} on the SPC degradation of IC in presence of MnO_2

Comparative effect of CO_3^{2-} under SC, PC and SPC is given in Fig.6.22A which shows that CO_3^{2-} is a powerful inhibitor under SC and PC, while the inhibition is mild under SPC.
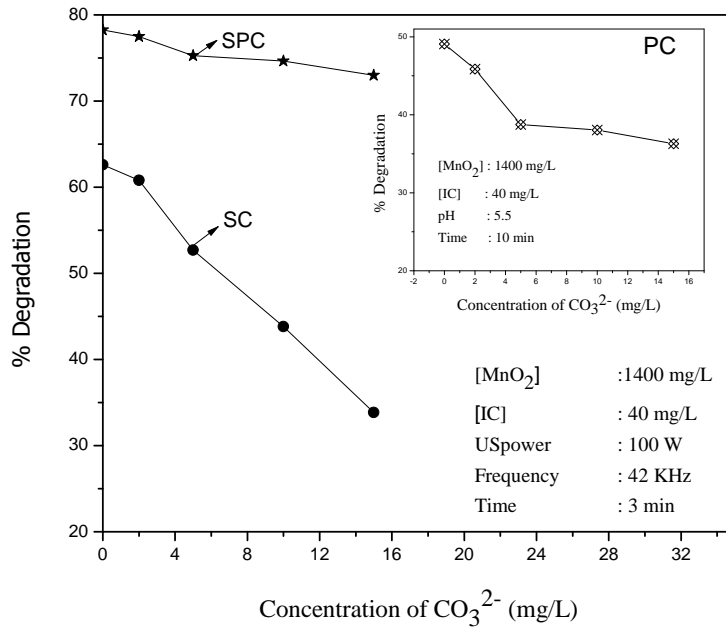
Fig. 6.22A: Comparison of the effect of CO_3^{2-} on the degradation of IC under SC, PC and SPC (PC results in 'inset').

This again reconfirms the potential of SPC as a powerful hybrid AOP which can eliminate or overcome the inhibiting effects by at least some of the natural water contaminants.

6.3.7.4 NO_3^-

NO_3^- remains as an enhancer of SPC degradation of IC at all concentrations and reaction times (Fig.6.23).
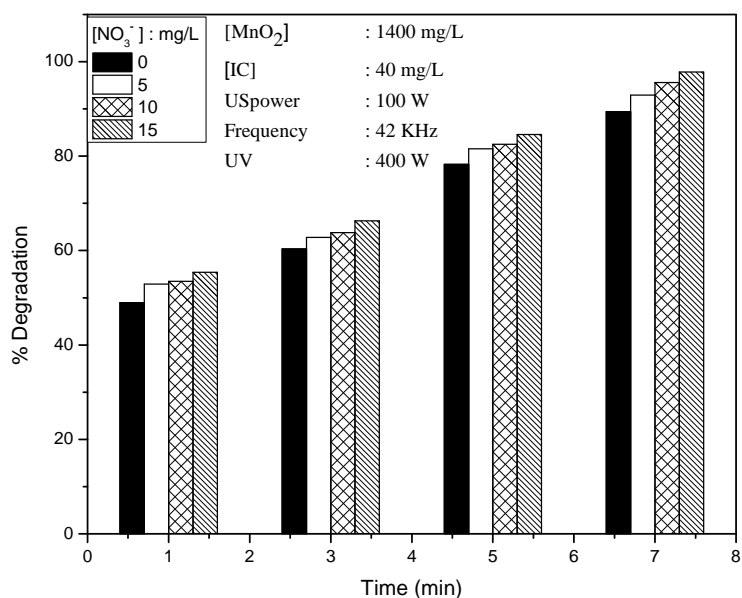
Fig. 6.23. Effect of NO_3^- on the SPC degradation of IC in presence of MnO₂

Comparative effect of NO_3^- under SC, PC and SPC is given in Fig.6.23A
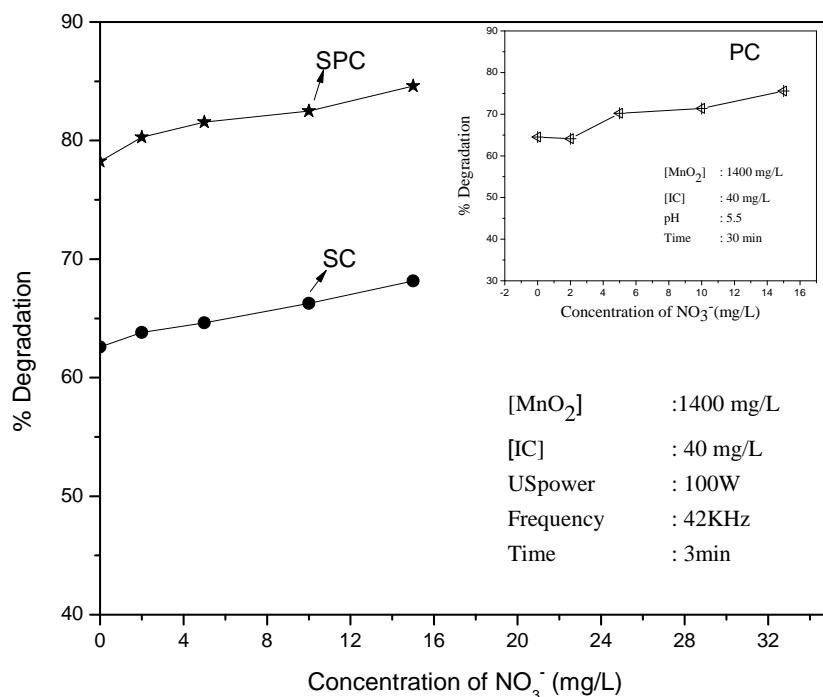
Fig. 6.23A: Comparison of the effect of NO_3^- on the degradation of IC under SC, PC and SPC (PC results in 'inset').

NO_3^- remains a moderate but consistent enhancer at all concentrations under SC, PC and SPC.

6.3.7.5 Cl⁻

Cl⁻ remains as a mild enhancer at all concentrations and reaction times (Fig.6.24).
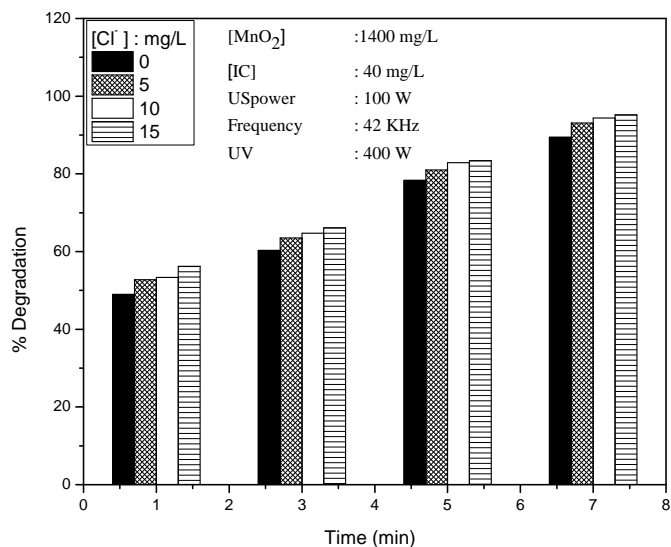
Fig.6.24: Effect of Cl⁻ on the SPC degradation of IC in presence of MnO₂

Comparison of the effect under SC, PC and SPC is shown in Fig.6.24A.
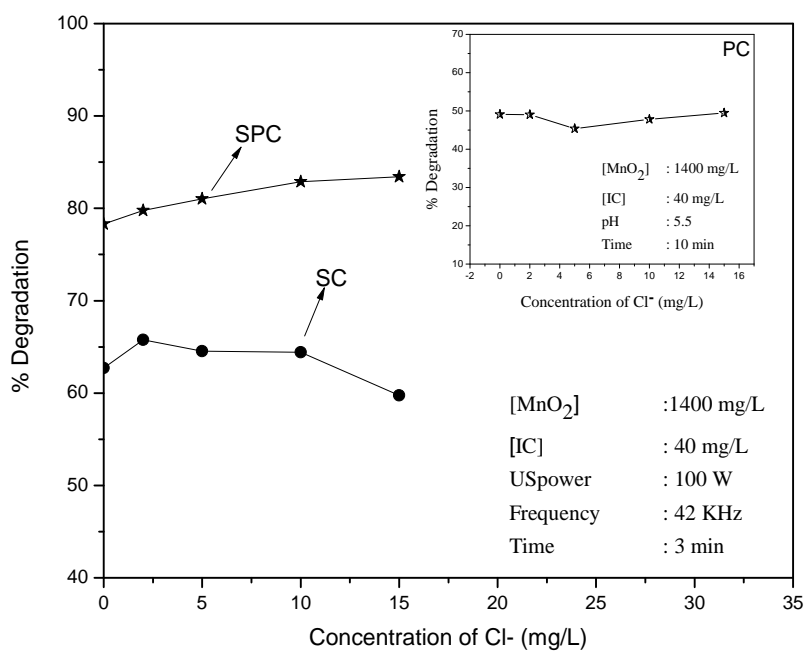
Fig. 6.24A: Comparison of the effect of Cl⁻ on the degradation of IC under SC, PC and SPC (PC results in 'inset').

Microwave, Photo and Sono Activated Advanced Oxidation Processes and their Variations for the Decontamination of Water from Toxic Chemical Pollutants

477

The inconsistency in the effect of Cl$^-$ with 'mild enhancement' in the case of SPC, 'mild inhibition' followed by 'no effect' in the case of PC and 'no effect' followed by 'inhibition' in the case of SC is evident from the figure 6.24A.

6.3.7.6 SO$_4^{2-}$

SO$_4^{2-}$ remains as a mild enhancer at all concentrations and reaction times (Fig.6.25).
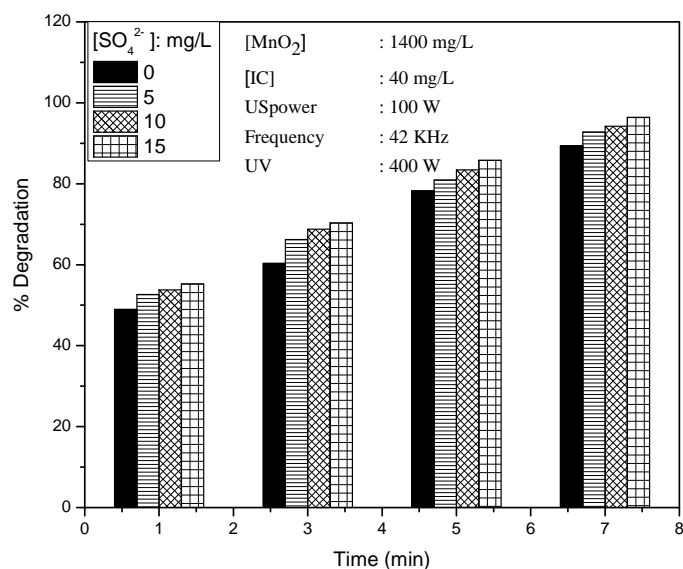
Fig. 6.25: Effect of SO$_4^{2-}$ on the SPC degradation of IC in presence of MnO$_2$

Comparative effect of SO$_4^{2-}$ under SC, PC and SPC is given in Fig. 6.25A. SO$_4^{2-}$ has practically 'no effect' under SC and PC at the concentration and reaction times studied here (see Fig.6.25A). However, under SPC, it is a mild enhancer.
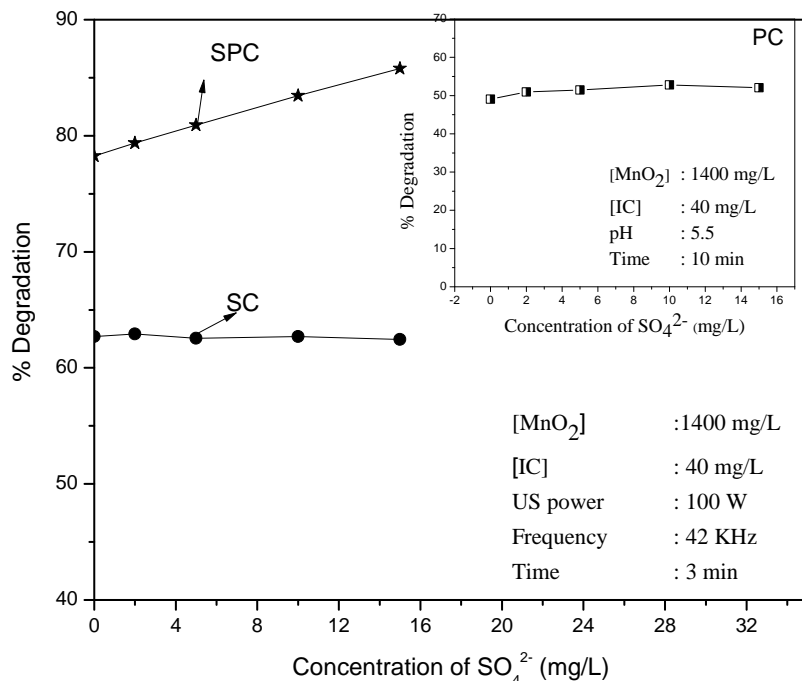
Fig. 6.25A: Comparison of the effect of SO_4^{2-} on the degradation
of IC under SC and SPC (PC results in 'inset')

Once again the superior efficiency of the combination AOP, i.e, SPC, even to compensate for the inhibiting effect by the individual AOPs (SC and PC), is demonstrated here.

6.3.7.7 CH₃COO⁻

CH_3COO^- has no effect on the SPC degradation in the early stages of reaction and at lower concentrations (Fig.6.26). It can be considered as a mild enhancer at later stages of reaction.

Microwave, Photo and Sono Activated Advanced Oxidation Processes and their
Variations for the Decontamination of Water from Toxic Chemical Pollutants

479
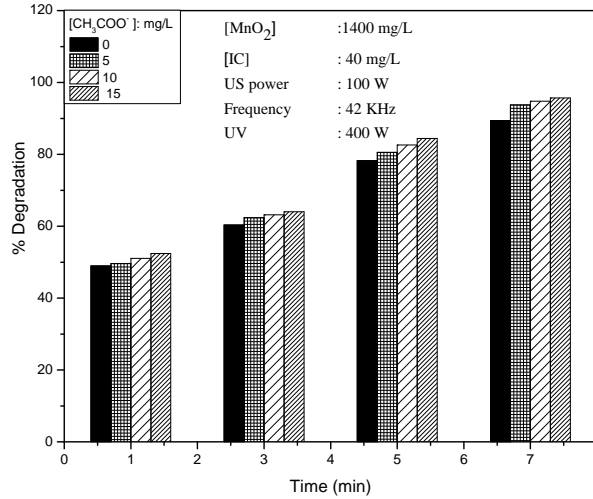
Fig.6.26: Effect of CH₃COO⁻ on the SPC degradation of IC in presence of MnO₂

Comparison of the effect of CH₃COO- under SC, PC and SPC is given in Fig.6.26A.
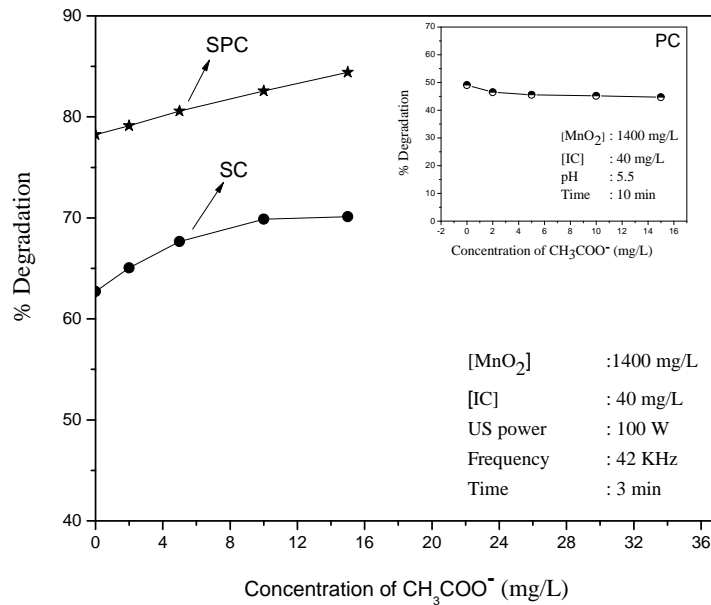
Fig. 6.26A: Comparison of the effect of CH₃COO⁻ on the degradation of IC under SC and SPC (PC results in 'inset').

The same trend is followed under SC and SPC, while the effect is practically 'nil' under photocatalysis.

6.3.7 Effect of SPC on the TOC of the reaction system

The efficiency of any AOP for the removal of toxic pollutants in water depends on its potential to bring down the TOC/COD to nil. Hence the TOC of the sonophotocatalytic system under optimised conditions is measured and compared with that of sono and photocatalysis. The results are shown in Fig.6.27.
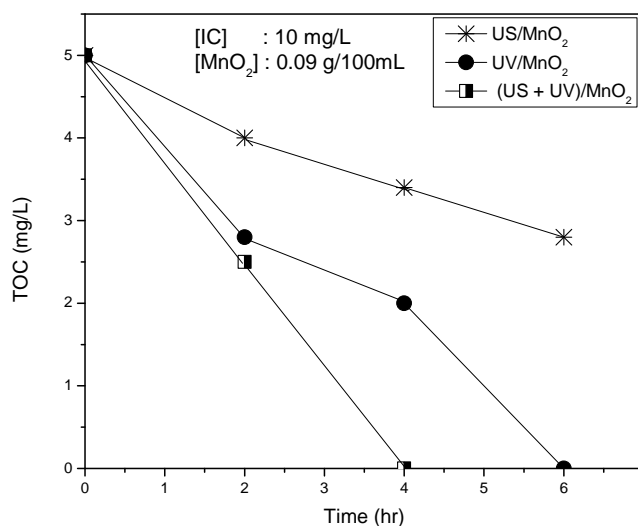
Fig. 6.27: TOC of the reaction system under SC, PC and SPC at various time intervals of irradiation

SPC accelerates the mineralisation and TOC value of 'zero' is reached in 4 hours in comparison to PC which takes 6 hours for the same. The TOC does not decrease below ~ 3 mg/L under SC even after continued US irradiation. In this respect also the combination of (US+UV) is more efficient than either of the individual processes based on UV or US.

Studies reported in previous Chapters have proven that combination of TiO_2 and MnO_2 can exploit the superior photocatalytic activity of TiO_2 and the microwave-, sono- activity as well as adsorption/oxidation capability of MnO_2. Hence this combination is tested for sonophotocatalytic degradation of IC also. The results are discussed in the following Sections.

6.4 Sonophotocatalytic degradation of IC in presence of MnO_2-TiO_2

6.4.1 Preliminary results

Preliminary results on the sonophotocatalytic degradation of IC in presence of MnO_2-TiO_2 and its comparison with sono and photocatalysis under identical conditions at different times (1,3,5,7 minutes) are presented in Fig.6.28.
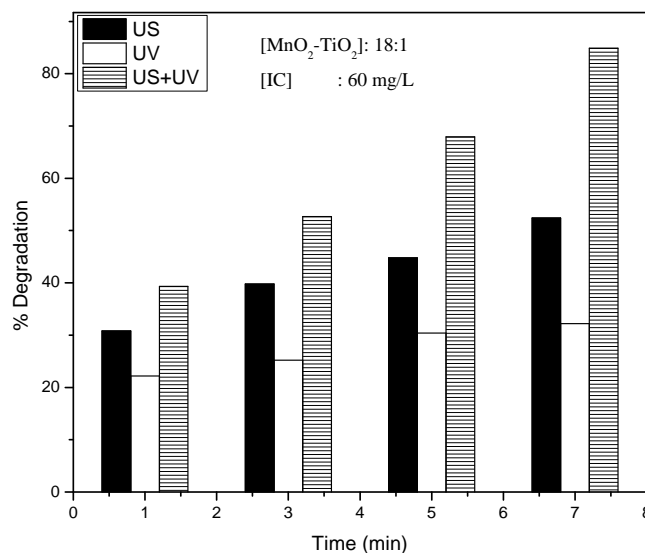
Fig. 6.28: Sono, photo and sonophotocatalytic degradation of IC in presence of MnO_2-TiO_2

The degradation under SPC is more than that in case of PC or SC individually. However, the degradation is less than the sum of the degradation under PC and SC. As the reaction advances, at later stages of reaction, SPC degradation is more or less the sum of the degradation under US and UV individually, as seen from the data after 5min and 7min. Hence the combination technique SPC using the combination catalyst (MnO$_2$-TiO$_2$) is a potential candidate to be evaluated in detail for the removal of toxic pollutants from water.

6.4.2 Effect of dosage

The effect of MnO$_2$-TiO$_2$ dosage at the optimised ratio of the components (18:1) on the degradation of IC is evaluated and the results are presented in Fig.6.29.
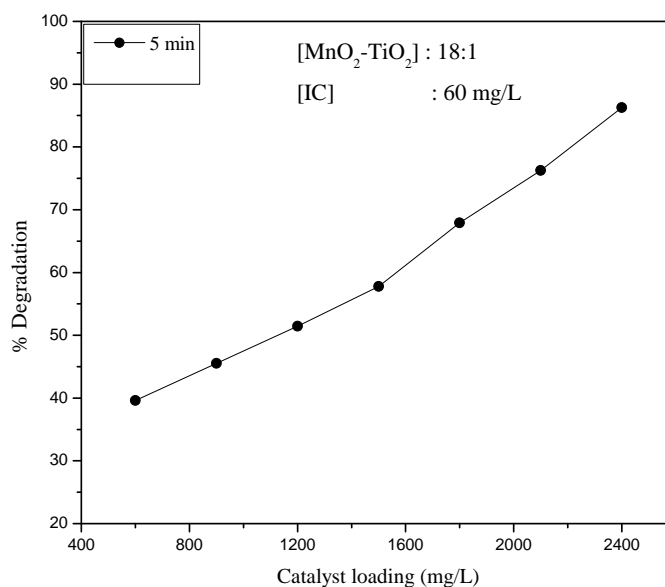
Fig. 6.29: Effect of MnO$_2$-TiO$_2$ dosage on the SPC degradation of IC

Microwave, Photo and Sono Activated Advanced Oxidation Processes and their Variations for the Decontamination of Water from Toxic Chemical Pollutants

483

The degradation increases with increase in catalyst loading as in the case of MnO_2. In this case also there is no clear optimum for the dosage. Hence 0.18g/100 mL of MnO_2-TiO_2: (18:1) is chosen for further studies.

6.4.3 Effect of concentration

As done in the case of sono- and photo- catalysis, the effect of change in concentration of the dye on the kinetics of degradation is examined in the case of sonophotocatalysis also. The results are presented in Fig.6.30.
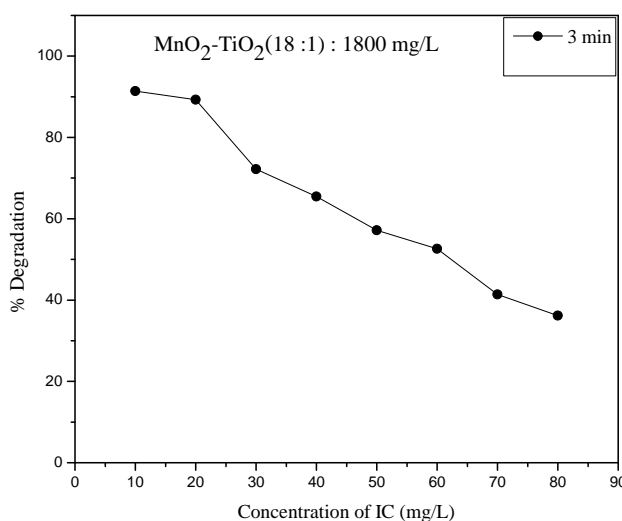
Fig. 6.30: Effect of concentration of IC on its SPC degradation

It is seen that the % degradation decreases with increase in concentration of IC (Fig.6.30). However, the rate of degradation increases with increase in concentration (Fig.6.31). There is no clear optimum in the concentration of IC for effective degradation. Hence for convenience and consistency with the studies reported in previous Chapters, 60 mg/L of IC is selected for further studies.
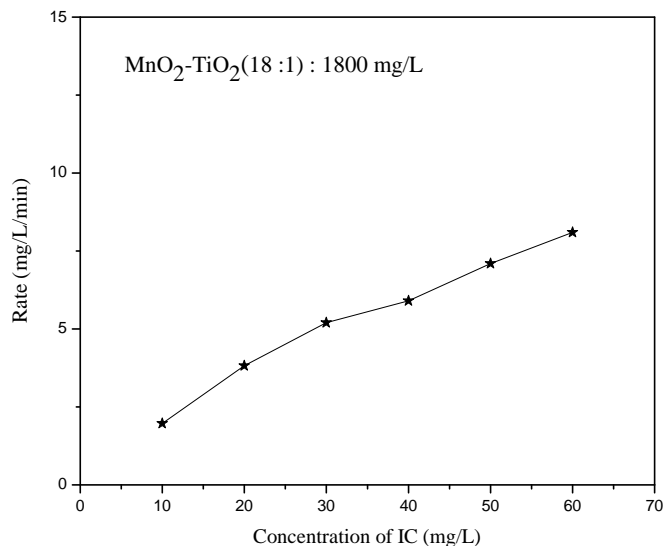
Fig. 6.31: Rate of degradation of IC at various concentrations

Comparison of the rate of degradation of IC in PC, SC and SPC under identical conditions shows that the rate is in the order SPC > SC > PC (see Fig.6.32).
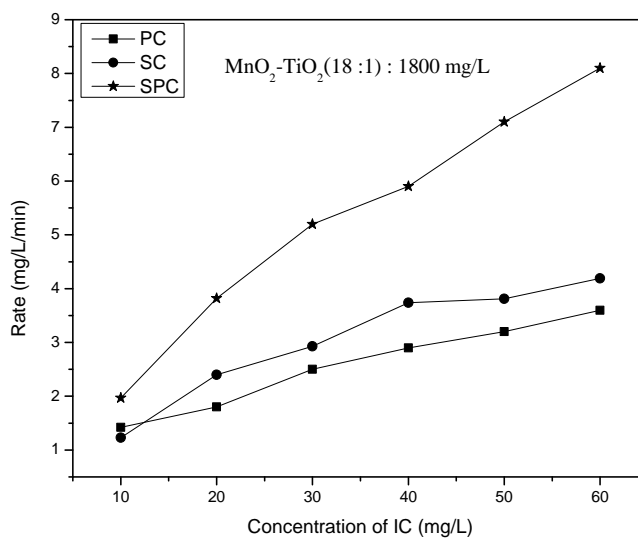
Fig. 6.32: Comparison of rate of degradation of IC in presence of MnO₂-TiO₂ under SC, PC and SPC.

It is seen that the SPC degradation is less than additive (SC+ PC) at lower concentration of IC. However, as the reaction proceeds the rate becomes additive and at higher concentration (> 50 mg/L), it becomes mildly synergistic. This synergy may be the reason for the absence of any clear optimum concentration, as was the case with sono- or photo-catalysis.

The kinetics of the degradation is analysed by the inverse plot of $1/r_0$ vs $1/C_0$ and the logarithmic plot of $\ln C_0/C$ vs t as shown in Fig.6.33 and 6.34 respectively. The analysis confirms pseudo first order kinetics and L-H mechanism. Details and relevant explanations are provided in Sections 4.3.11.2 and 5.4.3 of Chapters 4 and 5 respectively.
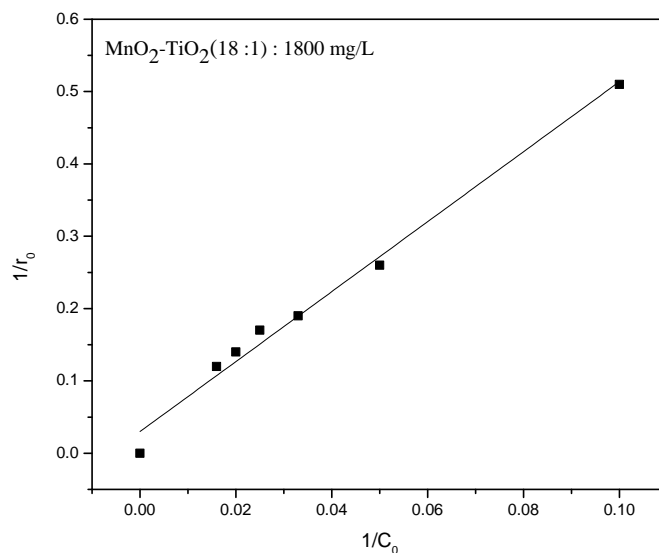
Fig. 6.33: Reciprocal plot of $1/r_0$ Vs $1/C_0$ for various concentrations of IC
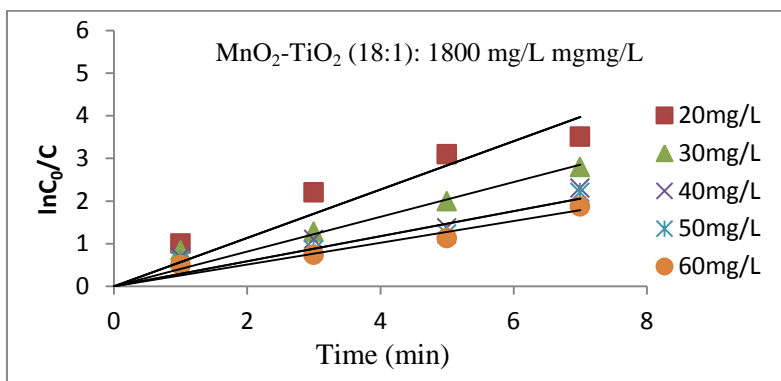
Fig. 6.34: Logarithmic plot of MnO_2-TiO_2 mediated SPC degradation of IC at different concentrations.

6.4.4 Effect of pH

As in the case of sono- and photo- catalysis, the degradation is very high under acidic pH of 2 and 3. Thereafter it decreases slowly with increase in pH up to pH ~ 10 (Fig.6.35).
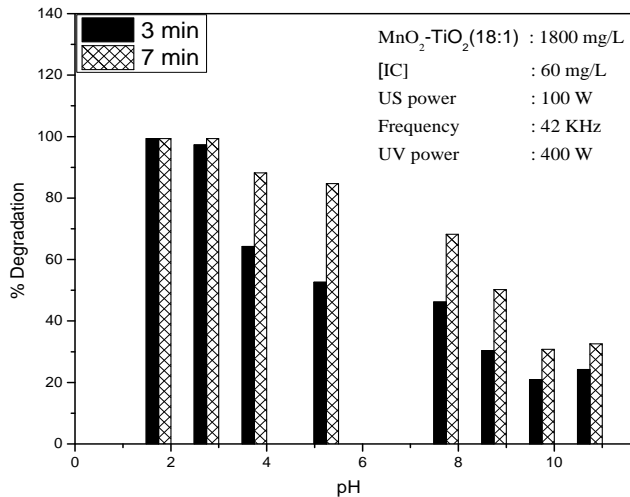
Fig. 6.35: Effect of pH on the SPC degradation of IC over MnO_2-TiO_2

This is followed by slight increase in degradation at pH 11. The comparative effect of pH in sono, photo and sonophotocatalysis is presented in Fig.6.36.

Fig. 6.36: Comparison of the effect of pH on the degradation of IC
under SC, PC and SPC (PC results in 'inset')

The trend of pH effect remains fairly the same and comparable in all three cases. This shows that the complexity and inconsistency of pH effect in AOPs is sustained in SC, PC and SPC. Hence possible explanations given for pH effect under PC and SC can be extrapolated to SPC also.

6.4.5 Effect of Oxidants

6.4.5.1 Effect of H_2O_2

The effect of H_2O_2 at different concentrations on the SPC degradation of IC in presence of MnO_2-TiO_2 is investigated. H_2O_2 inhibits the degradation at lower concentration (Fig.6.37). However with further increase in concentration the degradation is stabilised.
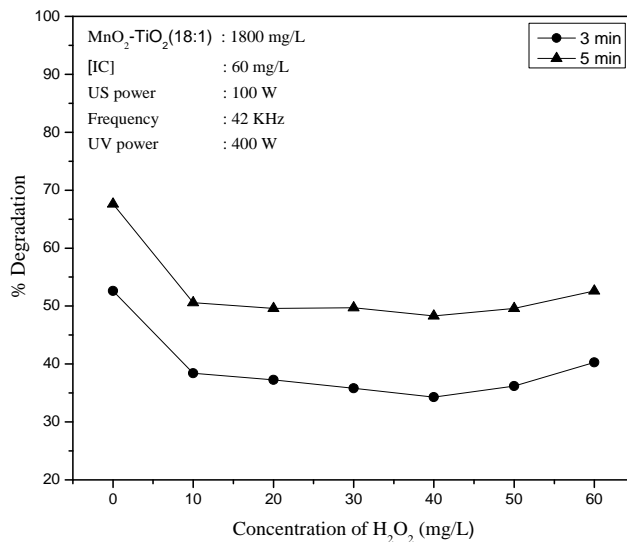
Fig. 6.37: Effect of H_2O_2 on the SPC degradation of IC over MnO$_2$-TiO$_2$

The inhibitive effect is further confirmed by the in-between addition of H_2O_2 to a reaction in progress (Fig.6.38).
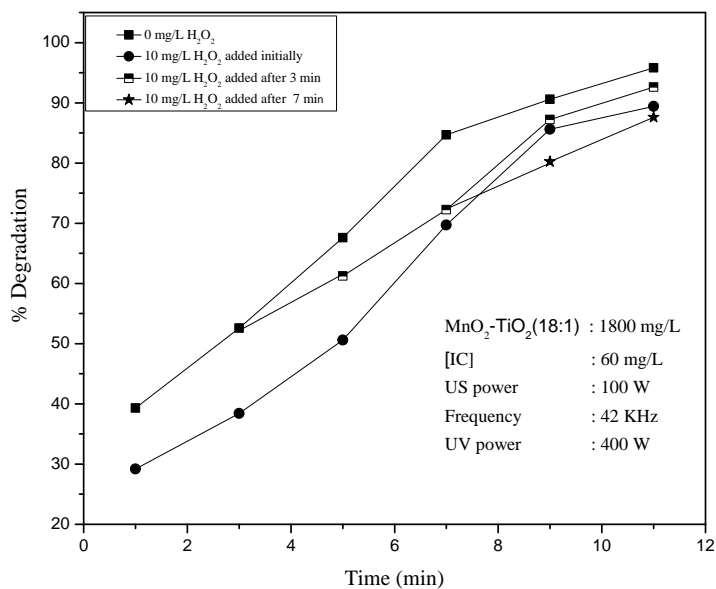
Fig. 6.38: Effect of initial and in-between addition of H_2O_2 on the SPC degradation of IC

The degradation is inhibited from the point of addition of H_2O_2 (3 min and 7 min).

Comparison of the effect of H_2O_2, on the degradation of IC in SPC, SC and PC is shown in Fig.6.39.
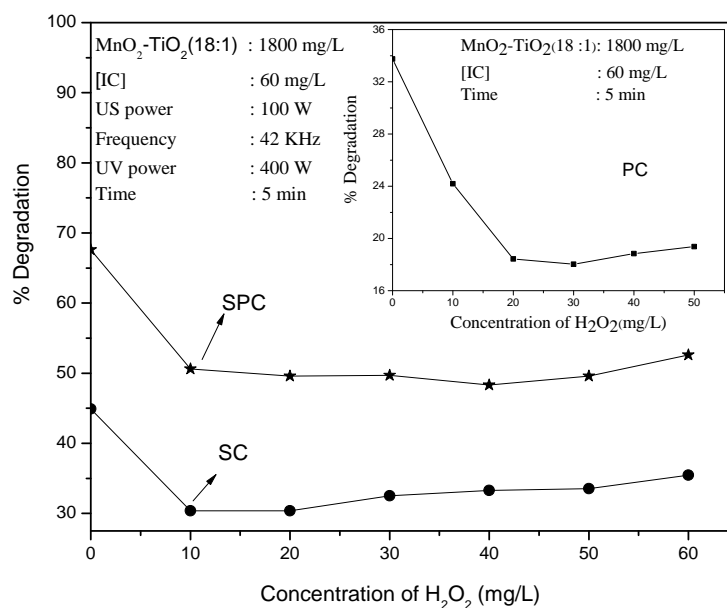
Fig. 6.39: Comparative effect of H_2O_2 on the degradation of IC under SC, PC and SPC (PC results in 'inset')

The effect is identical in all three cases, with inhibition in the initial stage followed by steady state at higher concentration. Thus, it is clear that the effect of H_2O_2 is qualitatively the same in the case of SC, PC and SPC, though the extent of degradation is quantitatively different.

6.4.5.2 Effect of $K_2S_2O_8$

Effect of another major oxidant $K_2S_2O_8$ on the sonophotocatalytic degradation of IC on MnO_2-TiO_2 is shown in Fig.6.40.
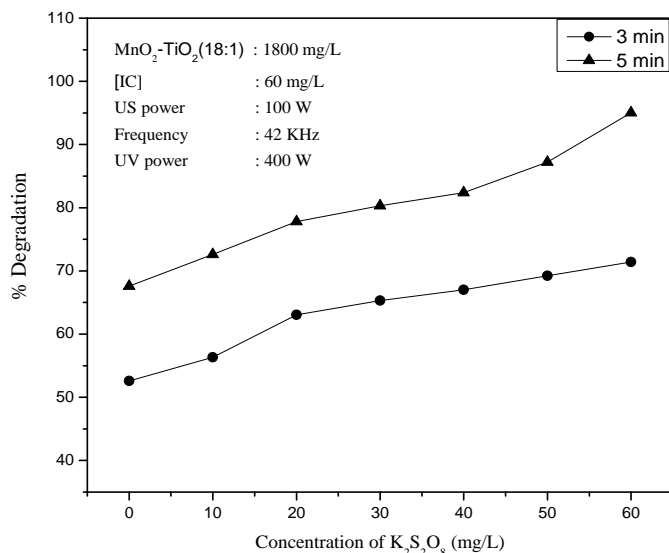
Fig. 6.40: Effect of K$_2$S$_2$O$_8$ on the SPC degradation of IC in presence MnO$_2$-TiO$_2$

As expected K$_2$S$_2$O$_8$ enhances the degradation at all concentrations, which is further verified by the in between addition of K$_2$S$_2$O$_8$ to a reaction in progress. The results are shown in Fig.6.41.
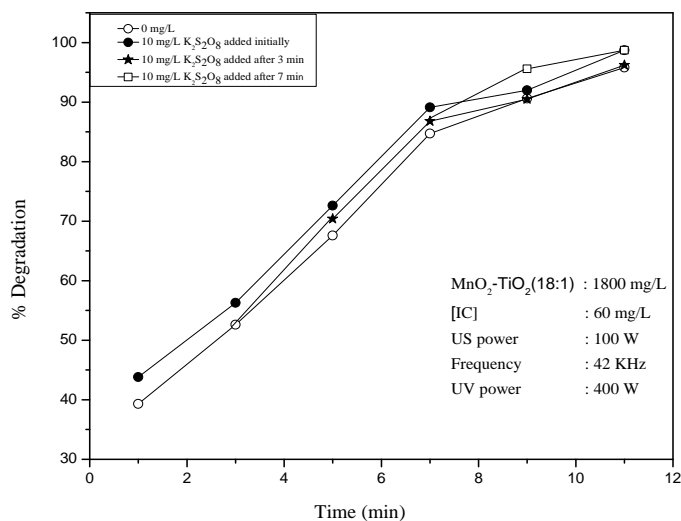
Fig. 6.41: Effect of initial and in-between addition of K$_2$S$_2$O$_8$ on the SPC degradation of IC.

The degradation is enhanced from the point of addition of $K_2S_2O_8$. These results confirm that the effect of PS on the SPC degradation of IC is similar to that in the case of MnO_2. Thus incorporation of small amounts of TiO_2 does not change the mechanism of the process.

The effect of PS on the degradation of IC under SC, PC and SPC is compared in Fig.6.42.
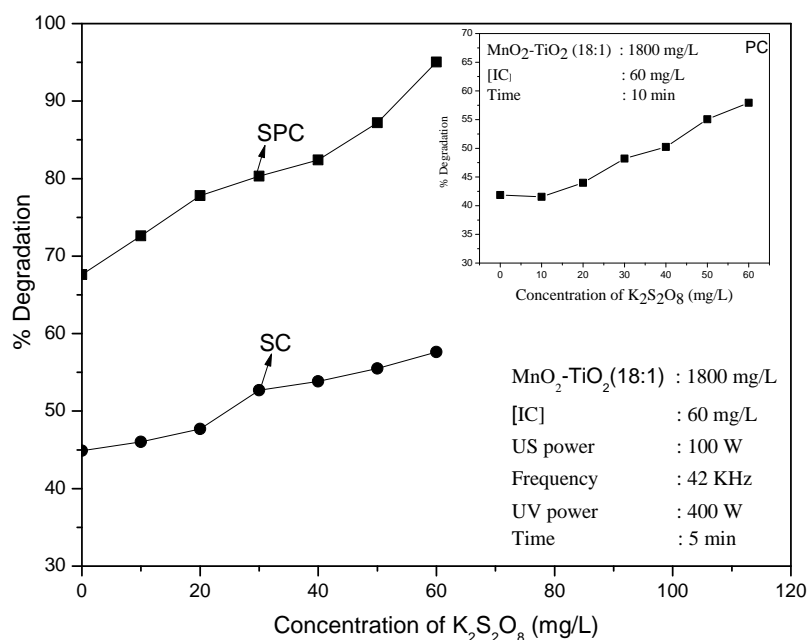
Fig. 6.42: Comparative effect of PS on the SC, PC and SPC degradation of IC (PC results in 'inset')

It is seen that the effect of PS is identical in all 3 cases with consistent increase in enhancement with increase in concentration of the oxidant. However, the enhancement is steeper under SPC thereby reconfirming the higher efficiency of SPC in comparison to PC or SC.

The effect of combination of K$_2$S$_2$O$_8$ and H$_2$O$_2$ on the degradation of IC on MnO$_2$-TiO$_2$ is shown in Fig.6.43.
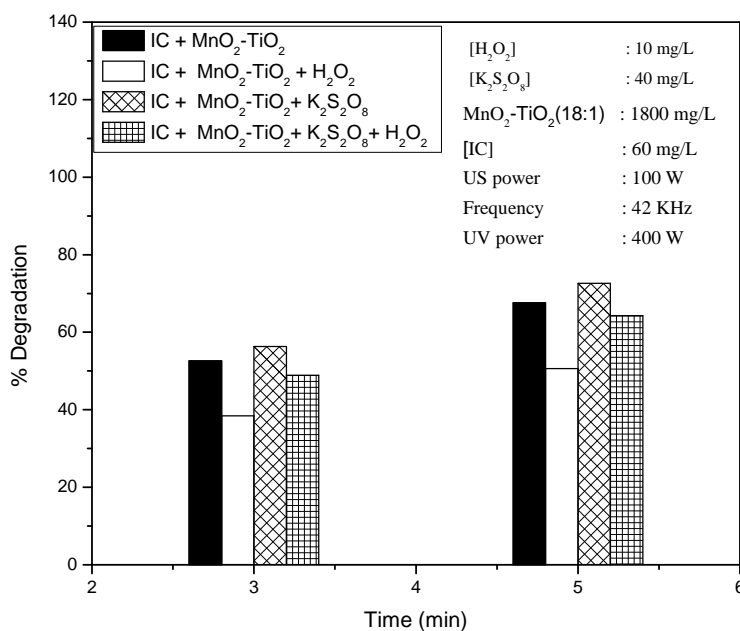
Fig. 6.43: Effect of combination of K$_2$S$_2$O$_8$ and H$_2$O$_2$ on the SPC degradation of IC

The effect of the combination on the degradation of IC is the average of the inhibition by H$_2$O$_2$ and the enhancement of PS; i.e practically no extra effect such as synergy by the combination.

6.4.6 Effect of anions

As in the case of earlier studies, the effect of anions which are likely to be present in water on the degradation of IC in SPC is investigated at different concentrations and reaction times. The results at different concentrations of anions are presented in Figure 6.44A.
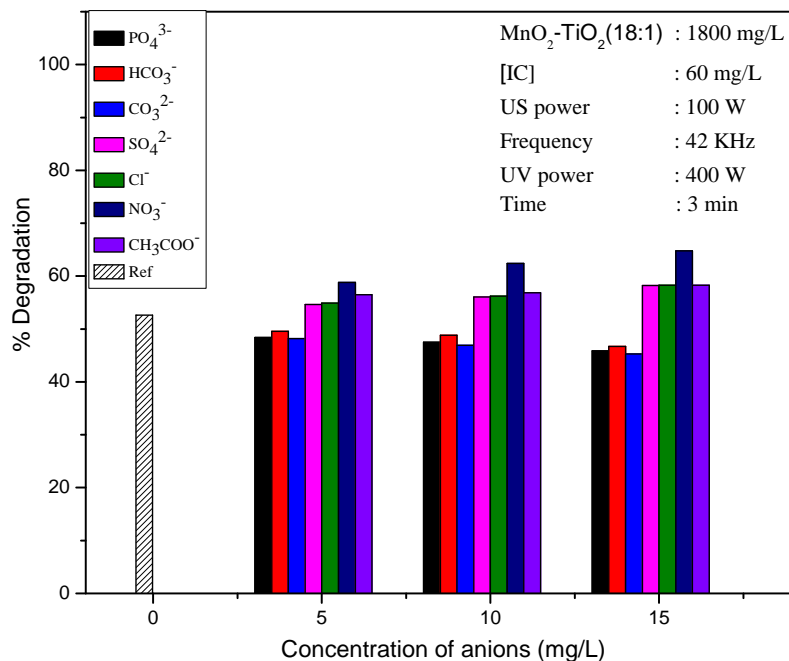
Fig. 6.44A: Effect of concentration of anions on the SPC degradation of IC

The effect is practically the same as that in presence of MnO_2 catalyst. CO_3^{2-}, PO_4^{3-} and HCO_3^- are inhibitors. NO_3^- is a moderate enhancer. CH_3COO^-, SO_4^{2-} and Cl^- are mild enhancers. The effect of anions at different concentrations is summarised in Table 6.3.

Table 6.3: Effect of concentration of anions on the sonophotocatalytic degradation of IC (Time: 3 min.)

Concentration of anion (mg/L)	Inhibition	No effect	Enhancement
5	$CO_3^{2-} \approx PO_4^{3-} \approx HCO_3^-$	-	$NO_3^- > CH_3COO^- > SO_4^{2-} \approx Cl$
10	$CO_3^{2-} \approx PO_4^{3-} \approx HCO_3^-$	-	$NO_3^- > SO_4^{2-} \approx Cl^- \approx CH_3COO^-$
15	$CO_3^{2-} \approx PO_4^{3-} \approx HCO_3^-$	-	$NO_3^- > SO_4^{2-} \approx Cl^- \approx CH_3COO^-$

The effect of anions at different times of irradiation is given in Fig. 6.44B.
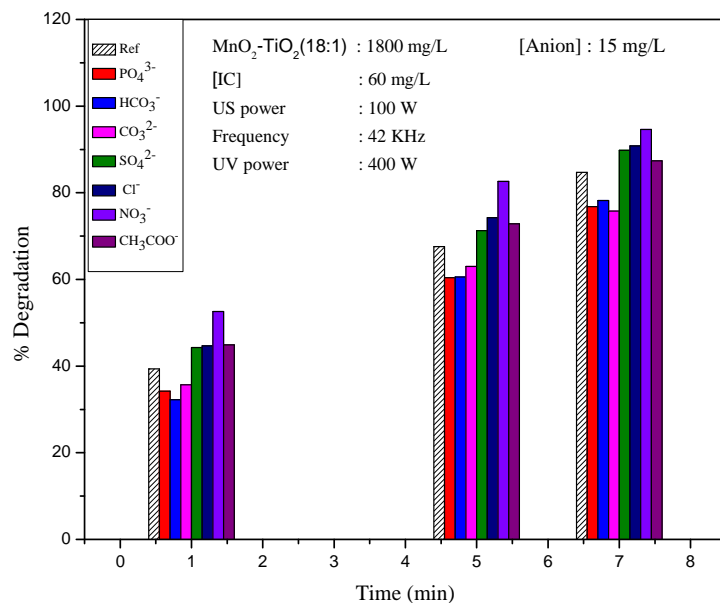
Fig. 6.44B: Effect of reaction time on the SPC degradation of IC, in the presence of various anions.

The results are summarised in Table 6.4.

The effect is same at all reaction times, i.e, the inhibitors remain as inhibitors and enhancers remain as enhancers at all reaction times. The effect of anions SO_4^{2-}, CH_3COO^- and Cl^- can be treated as 'no effect' or 'mild enhancement'.

Table 6.4: Effect of reaction time on the sonophotocatalytic degradation of IC, in presence of various anions [Anion]: 15 mg/L

Time (min)	Inhibition	No effect	Enhancement
1	$CO_3^{2-} \approx PO_4^{3-} \approx HCO_3^-$	-	$NO_3^- > SO_4^{2-} \approx Cl^- \approx CH_3COO^-$
5	$CO_3^{2-} \approx PO_4^{3-} \approx HCO_3^-$	-	$NO_3^- > SO_4^{2-} \approx Cl^- \approx CH_3COO^-$
7	$CO_3^{2-} \approx PO_4^{3-} \approx HCO_3^-$	-	$NO_3^- > SO_4^{2-} \approx Cl^- \approx CH_3COO^-$

The effect of individual anions is investigated further at more concentrations (5,10,15 mg/L) and reaction times (1, 3, 5,7 min) as done in the case of other catalysts. The results are as follows:

6.4.6.1 PO_4^{3-}

The effect of PO_4^{3-} at various concentrations and reaction times is given in Fig.6.45.
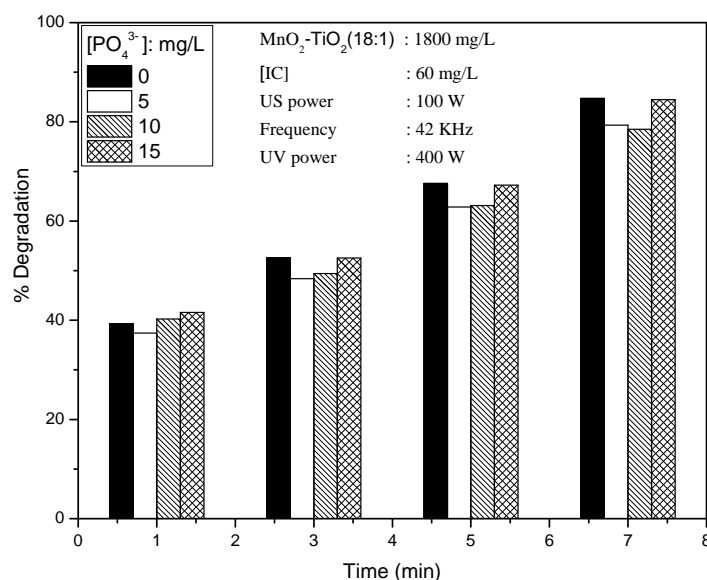
Fig. 6.45: Effect of PO_4^{3-} at different concentrations and reaction times on the SPC degradation of IC

PO_4^{3-} remains as a mild inhibitor at all concentrations and reaction times, except in the very early stage of reaction (1 min) where it has 'no effect'.

Comparison of the effect of added PO_4^{3-} in SC, PC and SPC is shown in Fig.6.45A.
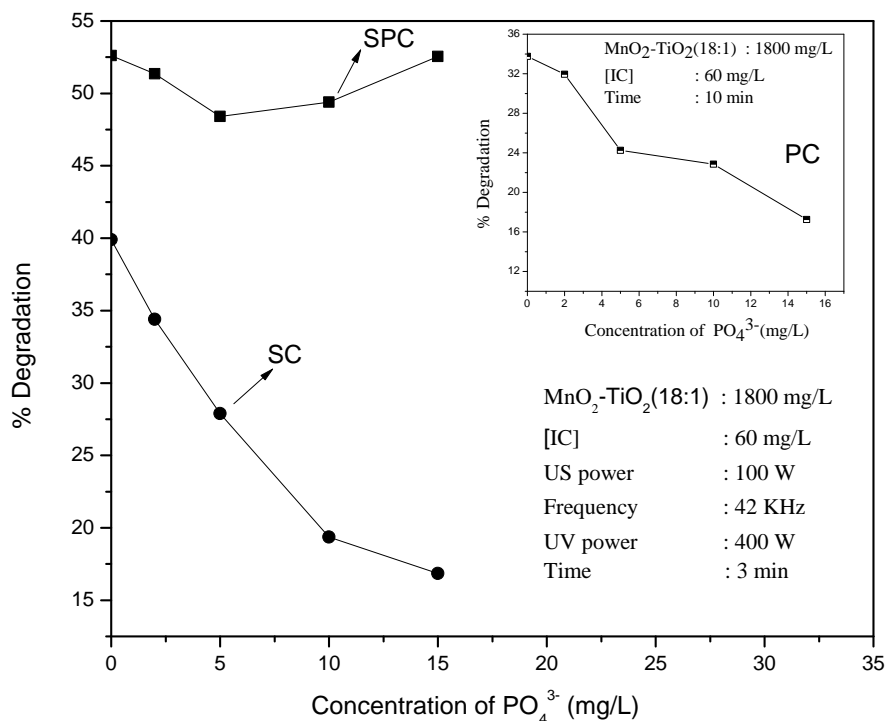
Fig. 6.45A: Comparison of the effect of PO_4^{3-} on the degradation of IC under SC, PC and SPC (PC results in 'inset').

PO_4^{3-} is a consistent inhibitor under PC, SC and SPC. However, the additive and synergestic effect of SPC may be compensating at least partially for the inhibition by PO_4^{3-}. Hence the strong inhibition in PC and SC becomes 'mild inhibition' to 'no effect' in SPC.

6.4.6.2 HCO_3^-

The effect of added HCO_3^- at different concentrations and reaction times is given in Fig. 6.46.

Microwave, Photo and Sono Activated Advanced Oxidation Processes and their Variations for the Decontamination of Water from Toxic Chemical Pollutants

497
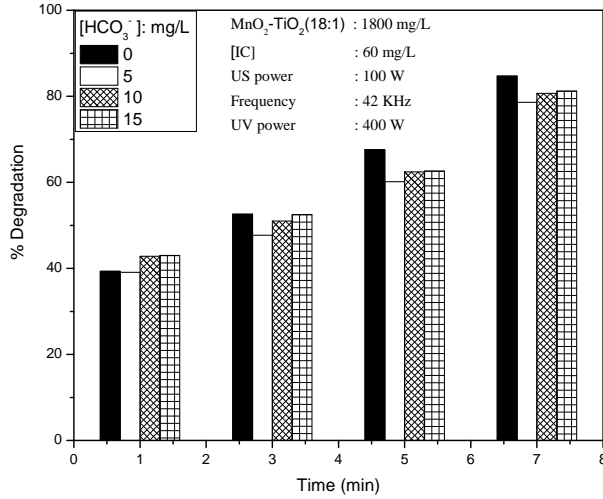
Fig.6.46. Effect of HCO$_3^-$ at different concentrations and reaction times on the SPC degradation of IC

HCO$_3^-$ also remains as a mild inhibitor throughout. Comparative effect of HCO$_3^-$ on the degradation of IC in SC, PC and SPC is given in Fig.6.46A.
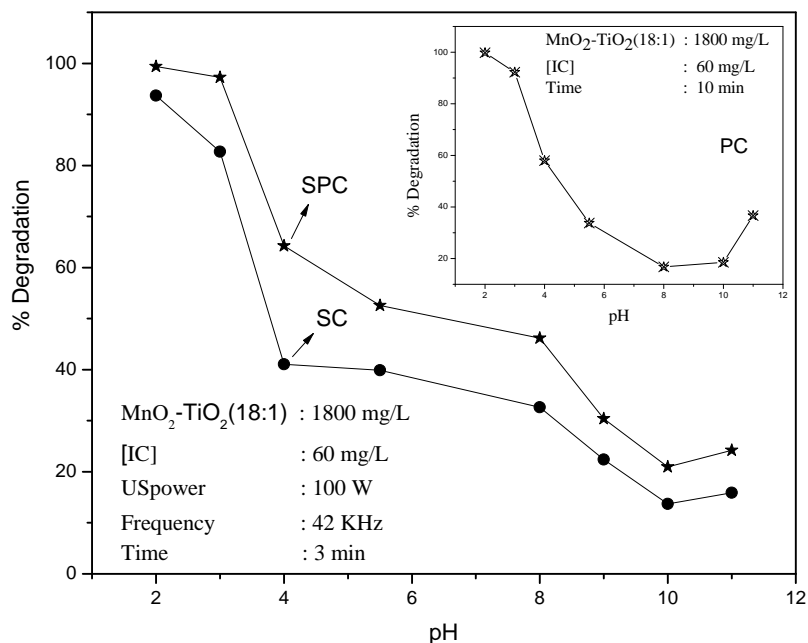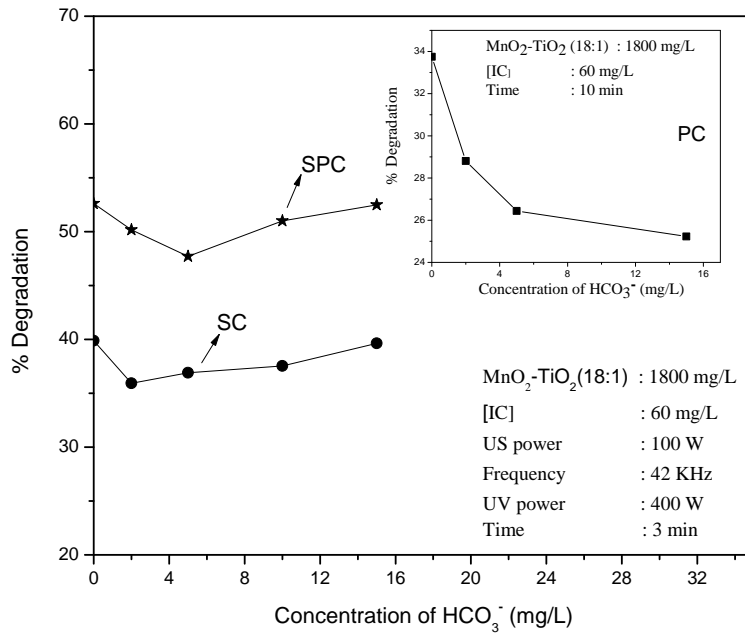

Fig. 6.46A: Comparison of the effect of HCO$_3^-$ on the degradation of IC under SC, PC and SPC (PC results in 'inset').

The effect follows same trend of mild inhibition at lower concentration of anions to 'no effect' at higher concentrations in sono as well as sonophotocatalysis. However, under PC, HCO_3^- is a strong inhibitor. Combination of PC with sonolysis helps to overcome the inhibitive effect thereby reconfirming the advantage of the hybrid process i.e sonophotocatalysis.

6.4.6.3. CO_3^{2-}

The effect of added CO_3^{2-} at different concentrations and reaction times on the degradation of IC is given in Fig.6.47.
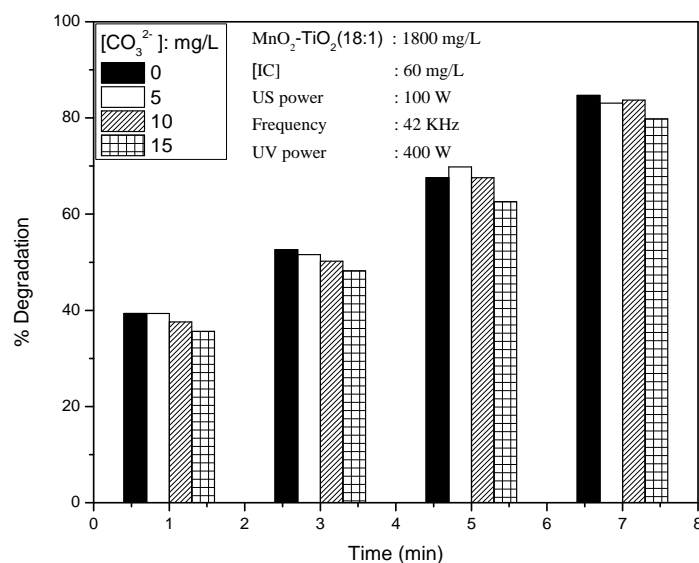
Fig.6.47: Effect of CO_3^{2-} on the SPC degradation of IC

CO_3^{2-} also a mild inhibitor at all concentrations and reaction times. Comparative effect of CO_3^{2-} in SC, PC and SPC on the degradation of IC is presented in Fig.6.47A.

Microwave, Photo and Sono Activated Advanced Oxidation Processes and their Variations for the Decontamination of Water from Toxic Chemical Pollutants

499
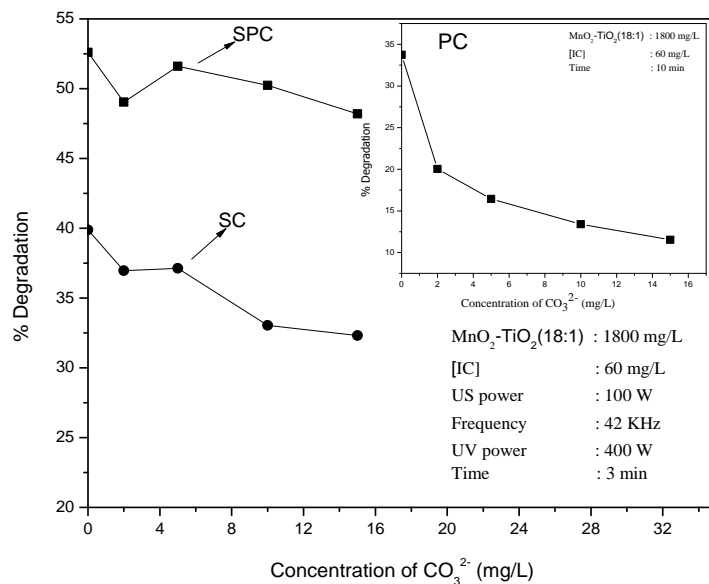
Fig. 6.47A: Comparison of the effect of CO_3^{2-} on the degradation
of IC under SC, PC and SPC (PC results in 'inset').

In this case also, the effect of CO_3^{2-} in SPC is more in line with its effect in SC. Thus the strong inhibition in PC is overcome by combining photocatalysis with sonolysis and the effect becomes 'mild inhibition' or 'no effect'.

6.4.6.4 Cl^-

Effect of Cl^- on the SPC degradation of IC is shown in Fig.6.48.
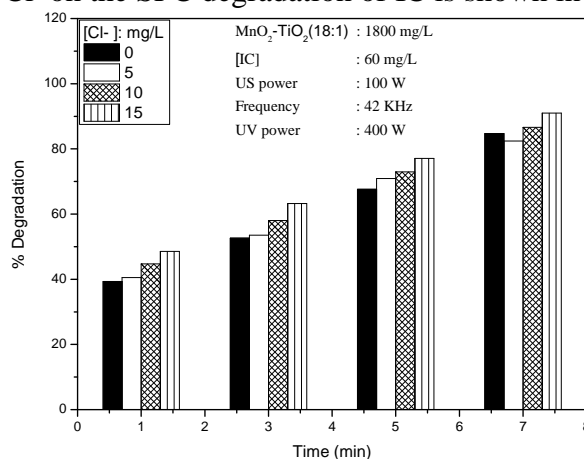
Fig. 6.48: Effect of Cl^- at different concentrations and reaction
times on the SPC degradation of IC

Cl⁻ remains as a mild enhancer at all concentrations and reaction times. The enhancement is more at the beginning of the reaction and the extent of enhancement decreases with time eventually becoming 'no effect' after 7 minutes.

Comparison of the effect of Cl⁻ on the degradation of IC in SC, PC and SPC is presented in Fig.6.48A.
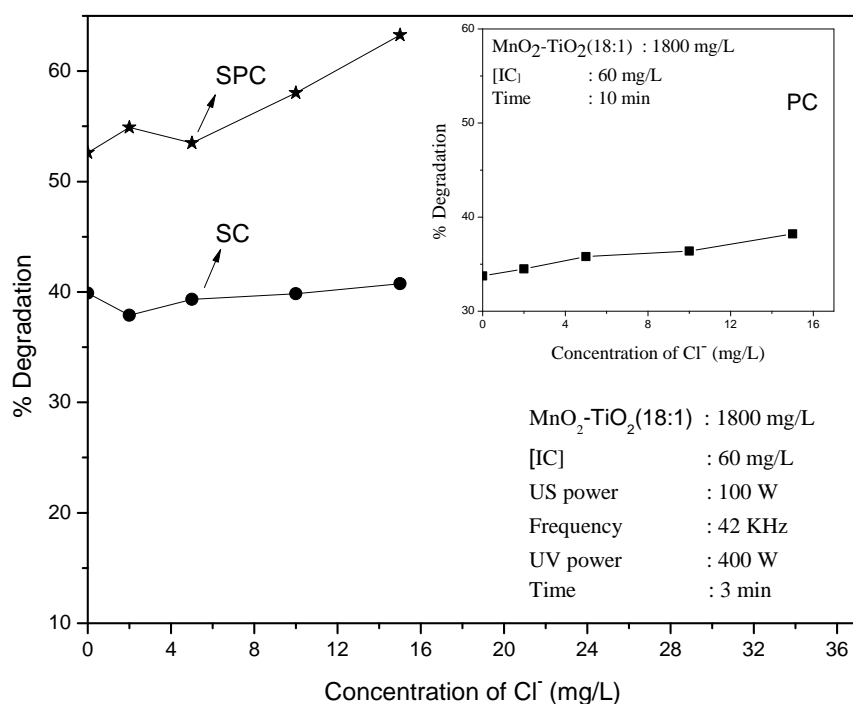
Fig. 6.48A: Comparison of the effect of Cl⁻ on the degradation of IC under SC, PC and SPC (PC results in 'inset').

In this case also the effect in SPC is moderate enhancement which is the net effect of the strong enhancement in PC and the 'no effect' in SC. The rate of enhancement is maximum in the case of SPC (3 mg/L/min)

Microwave, Photo and Sono Activated Advanced Oxidation Processes and their Variations for the Decontamination of Water from Toxic Chemical Pollutants

501

compared to 0.3mg/L/min in PC and 'no effect' by SC. In this case clear synergy is observed by combining sono and photocatalysis.

6.4.6.5 NO_3^-

The effect of added NO_3^- on the degradation of IC at various concentrations of the anions and different reaction times is given in Fig.6.49.
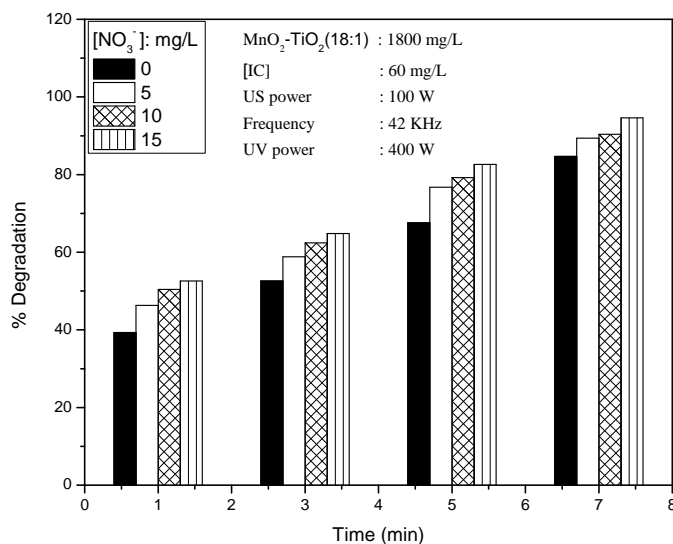
Fig. 6.49: Effect of NO_3^- at different concentrations and reaction times on the SPC degradation of IC

NO_3^- remains a consistent enhancer at all concentrations and reaction times. The enhancement increases with increase in concentration of NO_3^-. Comparison of the effect of NO_3^- in PC, SC and SPC is shown in Fig.6.49A.
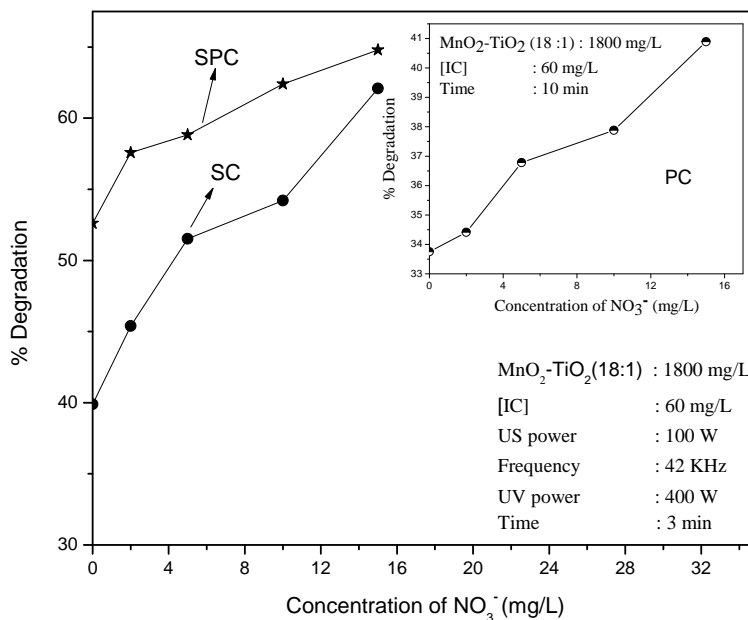
Fig. 6.49A: Comparison of the effect of NO_3^- on the degradation
of IC under SC, PC and SPC (PC results in 'inset').

The enhancement is steeper in all three cases of PC, SC and SPC. The results clearly prove that NO_3^- is a consistent enhancer of most AOPs. This is in agreement with many earlier reports on the effect of NO_3^- [165].

6.4.6.6 CH₃COO⁻

The effect of added CH_3COO^- can be considered as practically 'nil' at all concentrations and reaction times (Fig.6.50). Mild enhancement in the early stages and mild inhibition at later stages can be treated as practically 'no effect', within the limits of experimental error.

*Microwave, Photo and Sono Activated Advanced Oxidation Processes and their
Variations for the Decontamination of Water from Toxic Chemical Pollutants*

| 503
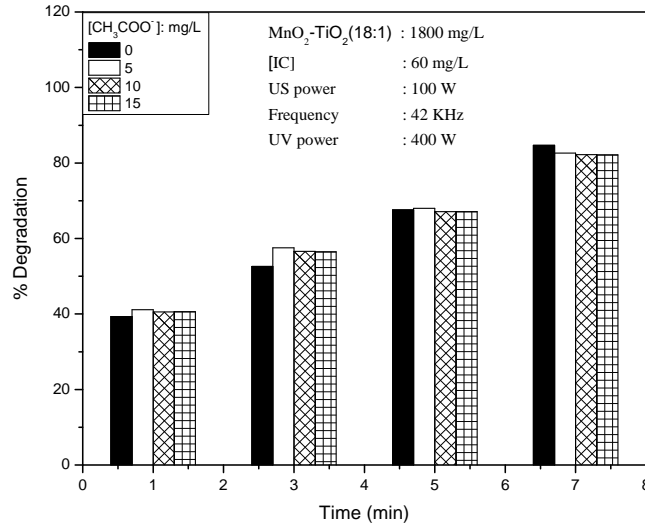
Fig. 6.50: Effect of CH₃COO⁻ on the degradation of IC

Comparative evaluation of the effect of CH₃COO⁻ on the SC, PC and SPC degradation of IC is shown in Fig.6.50 A.
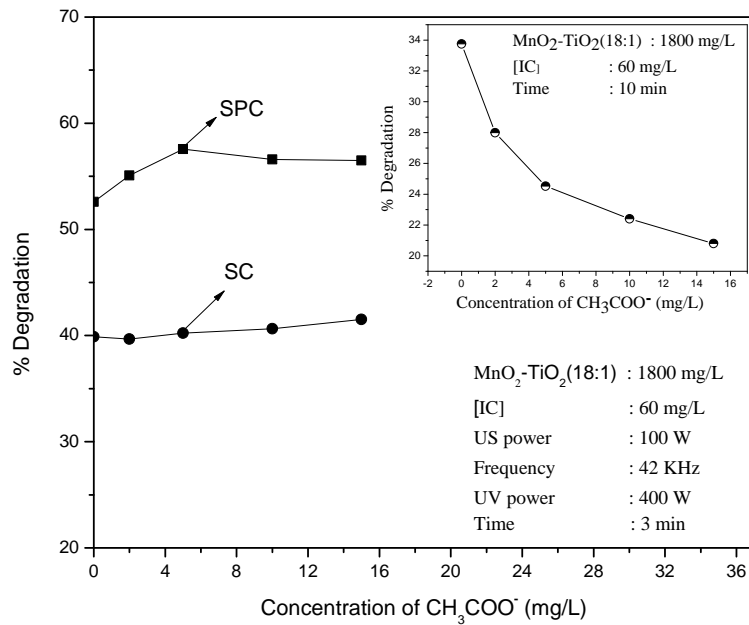
Fig. 6.50A: Comparison of the effect of CH₃COO⁻ on the degradation of IC under SC, PC and SPC (PC results in 'inset').

CH$_3$COO$^-$ is a mild enhancer in the case of SPC. In the case of SC, CH$_3$COO$^-$ has practically no effect on the degradation of IC. However in the case of PC, CH$_3$COO$^-$ is a an inhibitor. This shows that in this case also, SPC provides moderate synergy over the additive effect of SC and PC. The synergy was powerful enough to compensate for the net negative effect of the sum of PC and SC effect.

6.4.6.7 *SO$_4^{2-}$*

SO$_4^{2-}$ is a mild enhancer of the degradation at all concentrations and reaction times (Fig.6.51). However it can also be treated as 'no effect' since enhancement is very small except at the higher concentration of 15 mg/L.
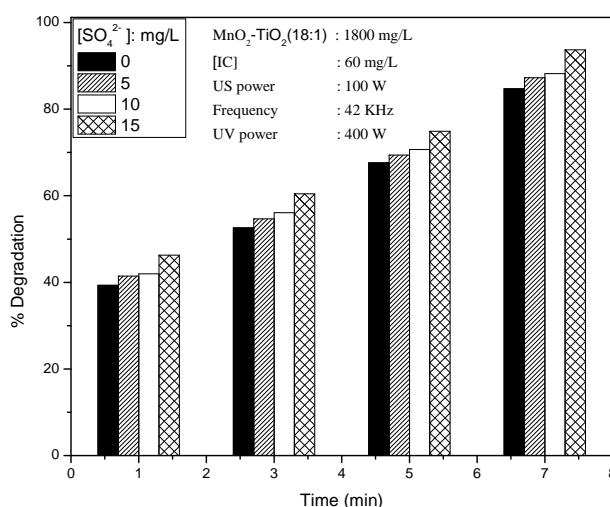
Fig. 6.51: Effect of SO$_4^{2-}$ on the SPC degradation of IC

Comparison of the effect of SO$_4^{2-}$ on the degradation of IC in SC, PC and SPC is given in Fig.6.51A.
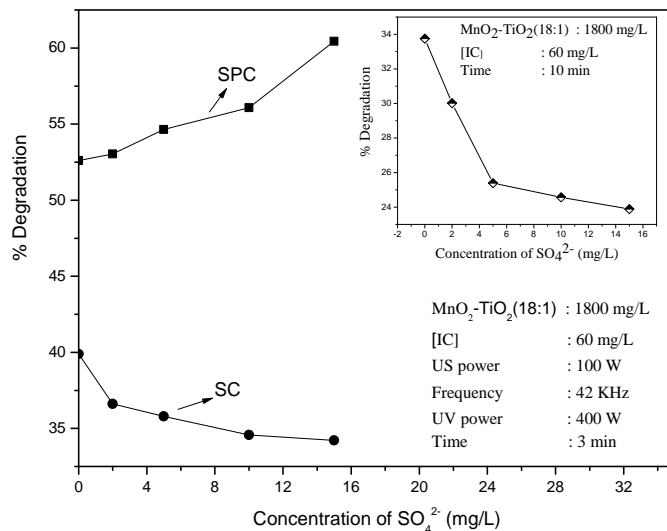
Fig. 6.51A: Comparison of the effect of SO_4^{2-} on the degradation of IC under SC, PC and SPC (PC results in 'inset').

It may be seen that the inhibition at lower concentration of the anion in sono and photocatalysis is more than compensated in sonophotocatalysis and inhibition becomes mild enhancement. This illustrates the insitu generation of highly active SO_4^- and $\cdot OH$ radicals in sonophotocatalysis which can instantly interact with the substrate and degrade it. Details are given in Section 4.3.11.6 of Chapter 4. This also points to the existence of mild synergy in SPC over (SC+PC) in presence of SO_4^{2-}.

6.4.7 TOC under (US+UV)/MnO$_2$-TiO$_2$

As discussed in Section 6.3.8 and Fig.6.27, combination of US and UV in sequence accelerates the degradation and mineralisation of IC. The mineralisation of IC is tested in presence of MnO_2-TiO_2 combination catalyst also in SPC. Comparison of the mineralisation of IC in presence of MnO_2-TiO_2 under different conditions of SC, PC and SPC is given in Fig.6.52.
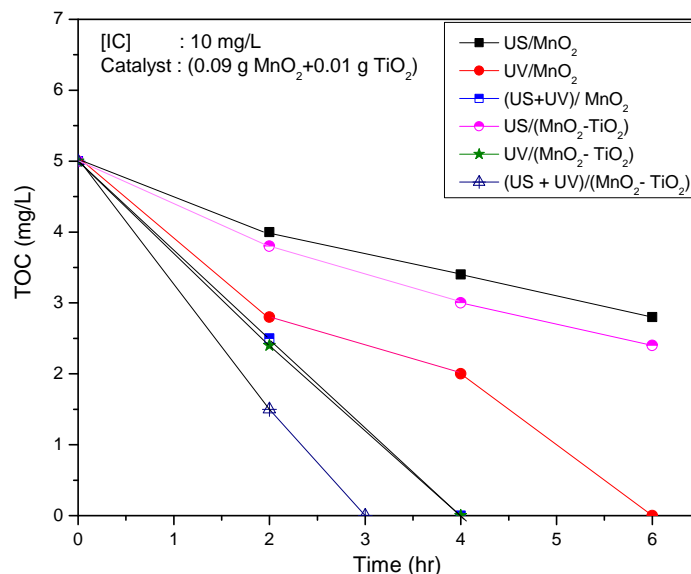
Fig. 6.52: TOC of the reaction system at various time intervals

SPC in presence of MnO_2 mineralises the dye in 4 hr. Under identical conditions when MnO_2 is replaced by MnO_2-TiO_2, the mineralisation is achieved in 3 hr time. Comparative efficiency of different systems tested here for the mineralisation of IC is:

MnO_2-TiO_2/(US+UV) > MnO_2-TiO_2/(UV) ≈ MnO_2/(US+UV) > MnO_2/UV > MnO_2-TiO_2/US > MnO_2/US ....(200)

The study thus proves conclusively that SPC in presence of the combination catalyst MnO_2-TiO_2 is a highly efficient AOP for the mineralisation of IC. In view of this, the potential of this combination for the possible mineralisation of few recalcitrant pollutants from different chemical categories is examined experimentally as discussed in the following Chapter.

Microwave, Photo and Sono Activated Advanced Oxidation Processes and their Variations for the Decontamination of Water from Toxic Chemical Pollutants

507

6.5 General Mechanism of SPC

The mechanism of sonophotocatalysis (SPC) is a combination of that of the individual processes, i.e sonocatalysis and photocatalysis. However, the synergy that has been reported in the case of sonophotocatalysis by Anju et al. [154] is not quite evident in the current study except in the presence of certain anions as discussed in the earlier Sections in this Chapter. In the current study, the effect is only additive or even slightly less than additive.

The mechanism of sonocatalysed degradation of IC in presence of semiconductor oxide catalysts has already been explained in Section 5.6 of Chapter 5. Sonolysis of water produces active $^{\cdot}$H and $^{\cdot}$OH radicals via cavitation which attack the substrate and degrade it through many intermediates. The presence of suspended catalyst particles in the system enhances the phenomenon as the microbubbles tend to break up into smaller ones. This will increase the number of regions of high temperature and pressure. The O_2 present in the system can serve as the nucleus for the cavitation. This results in enhanced formation of $^{\cdot}$OH radicals and consequently increased interaction with IC resulting in accelerated degradation.

In addition to the production of free radicals in presence of suspended particles, as explained above, sonolysis can also result in pyrolysis of the vaporised molecules and shear stress. Sonication of pure water also results in a series of chain reactions as follows.

$$H_2O \rightarrow {}^{\cdot}H + {}^{\cdot}OH \quad \text{...(201)}$$

$${}^{\cdot}H + {}^{\cdot}OH \rightarrow H_2O \quad \text{...(202)}$$

$${}^{\cdot}OH + {}^{\cdot}OH \rightarrow H_2O_2 \quad \text{..(203)}$$

$$2\,{}^{\cdot}OH \rightarrow H_2O + {}^{\cdot}O \quad \text{...(204)}$$

Other possible reactions in presence of O_2 are:

$$O_2 \quad\rightarrow\quad 2\,{}^{\cdot}O \dotfill (205)$$

$$O_2 + {}^{\cdot}O \quad\rightarrow\quad O_3 \dotfill (206)$$

$$O_2 + H \quad\rightarrow\quad HO_2{}^{\cdot} \text{ (or } O + {}^{\cdot}OH) \dotfill (207)$$

$$O + HO_2{}^{\cdot} \quad\rightarrow\quad {}^{\cdot}OH + O_2 \dotfill (208)$$

$${}^{\cdot}O + H_2O \quad\rightarrow\quad 2\,{}^{\cdot}OH \dotfill (209)$$

$$2\,HO_2{}^{\cdot} \quad\rightarrow\quad H_2O_2 + O_2 \dotfill (210)$$
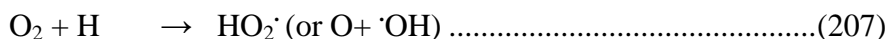
The reactive species generated as above will react with IC in the bulk solution or at the interphase between the bubbles and liquid phase. The O_3 generated as above also will promote the degradation as explained in Chapter 5.

Sonolysis of semiconductors also leads to sonoluminescence which can result in photocatalytic degradation of IC. Further, irradiation by UV will enhance this reaction as follows.

$$O_3 + h\nu \quad\rightarrow\quad O_2 + O \dotfill (211)$$

$$O + H_2O \quad\rightarrow\quad {}^{\cdot}OH + {}^{\cdot}OH \dotfill (212)$$

$$O + H_2O \quad\rightarrow\quad H_2O_2 \dotfill (213)$$

$$H_2O_2 + h\nu \quad\rightarrow\quad {}^{\cdot}OH + {}^{\cdot}OH \dotfill (214)$$

$$H_2O_2 + h\nu \quad\rightarrow\quad H_2O + {}^{\cdot}O \dotfill (215)$$

The reactions taking place in presence of UV irradiation are already explained in Chapter 4. Briefly they are reproduced below:

$$MnO_2 + h\nu \quad\rightarrow\quad e_{cb}{}^{-} + h_{vb}{}^{+} \dotfill (216)$$

$$h^{+} + OH^{-} \quad\rightarrow\quad {}^{\cdot}OH \dotfill (217)$$

$$h^{+} + H_2O \quad\rightarrow\quad {}^{\cdot}OH + H^{+} \dotfill (218)$$

Microwave, Photo and Sono Activated Advanced Oxidation Processes and their Variations for the Decontamination of Water from Toxic Chemical Pollutants

509

Scavenging of conduction band electrons by O_2

$$O_2 + e_{cb}^- \quad \rightarrow \quad O_2^{\cdot-} \dots\dots\dots\dots\dots\dots\dots\dots\dots\dots\dots\dots(219)$$

$$H^+ + O_2^{\cdot-} \quad \rightarrow \quad HO_2^{\cdot} \dots\dots\dots\dots\dots\dots\dots\dots\dots\dots\dots\dots(220)$$

$$HO_2^{\cdot} + e- + H^+ \rightarrow H_2O_2 \dots\dots\dots\dots\dots\dots\dots\dots\dots\dots\dots(221)$$
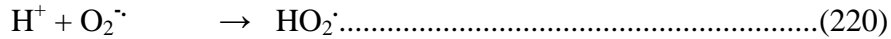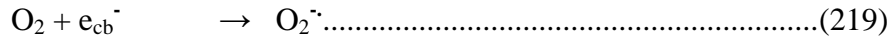
The ROS ($^{\cdot}OH$, $HO_2^{\cdot}$, H_2O_2, $O_2^{\cdot-}$) will interact with the substrate, degrade it and eventually mineralize through the formation of intermediates

$$ROS + IC \rightarrow Intermediates \rightarrow CO_2 + H_2O \dots\dots\dots\dots\dots\dots(222)$$
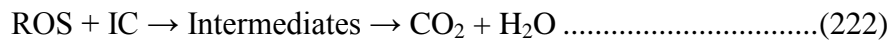
The sonophotocatalytic process can be schematically presented as Fig.6.53 [231].
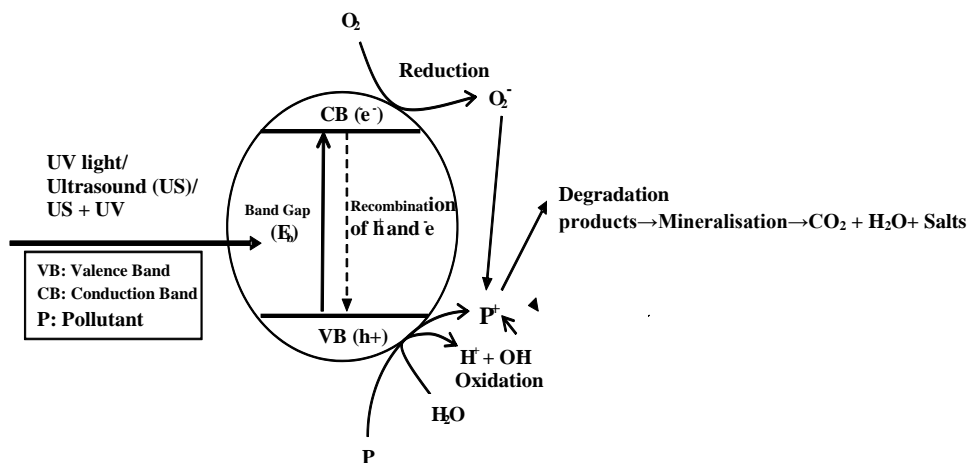
Fig. 6.53: Sonophotocatalytic activation of semiconductor oxides and the formation of ROS

In the case of photocatalysis, the catalyst particles will get agglomerated during the course of the reaction. This will reduce the efficiency of absorption of light, decrease the number of catalytically active sites and consequently decrease the generation of reactive free radicals. However, in the presence of US the agglomerated particles will be getting deaggregated constantly thereby exposing the surface sites to

the US and UV. The effect is thus equivalent to having fresh highly active catalyst surface throughout and this leads to longer and higher activity. Thus sonophotocatalysis is more efficient than either sono or photocatalysis individually and may even exceed the additive effect resulting in synergy.

6.6. Summary of the comparative efficiency of MnO_2 and MnO_2-TiO_2 for the sonophotocatalytic (US+UV) mineralisation of IC

Parameters	MnO_2	MnO_2-TiO_2(18:1)
Optimum Loading of catalyst	1400 mg/L	1800 mg/L
Optimum Concentration of IC	40 mg/L	60 mg/L
Kinetics	Variable kinetics. Pseudo first order at lower concentration up to 40mg/L.	Variable kinetics. Pseudo first order at lower concentration up to 40 g/L.
pH effect	Maximum degradation at pH 2-3 followed by steep decrease at pH 4. Stabilizes thereafter at higher pH.	Maximum degradation at pH 2-3. Then it decreases slowly up to pH 10. Then a slight increase above pH 10.
H_2O_2 effect	Inhibition, up to 20 mg/L. Stabilizes thereafter.	Inhibition, up to 10mg/L. Stabilizes thereafter.
Persulphate effect	Enhancement, increases with increase in concentration upto 300 mg/L. Stabilises thereafter	Mild enhancement, which increases slowly with increase in concentration.
COD decrease	1.25 mg/L/hr	1.7 mg/L/hr
Anion effect (2-15 mg/L)		
i)PO_4^{3-}	Inhibition	Inhibition
ii)HCO_3^-	Inhibition	Inhibition
iii)CO_3^{2-}	Inhibition	Inhibition
iv)Cl^-	Enhancement	'No effect' to 'mild enhancement'
v)CH_3COO^-	'No effect' to 'mild enhancement'	Enhancement
vi)SO_4^{2-}	Enhancement	Enhancement
vii)NO_3^-	Enhancement	Enhancement

6.7 Conclusions

Sonophotocatalysis mediated by the combination catalyst MnO_2-TiO_2 is a highly efficient AOP for the degradation and mineralisation of IC. The technique takes advantages of the oxidation capacity, adsorption efficiency and sonoactivity of MnO_2 and the photocatalytic activity of TiO_2 in the same reaction. The degradation of IC follows variable kinetics with pseudo first order kinetics at lower concentrations and zero order at higher concentration. The pH effect on the degradation remains complex as in the case of many other heterogeneous catalyst-mediated AOPs eluding any consistent generally applicable explanations. H_2O_2 inhibits the degradation while PS is a moderate enhancer of the degradation. The inhibition effect of anions on the sono- or photo- catalytic degradation of IC is reduced by combining sono- and photo- catalysis simultaneously. Thus even a strong inhibitor like PO_4^{3-} under individual sono or photocatalysis, has only 'mild effect' or 'no effect' under sonophotocatalysis. The synergy of sonophotocatalysis in the degradation of IC is able to compensate for the negative effect of many reaction parameters and inhibiting components thereby making it a potential process for commercial water purification. The study thus demonstrates that appropriately selected and optimised combination catalysts and hybrid AOPs can additively or synergistically contribute their catalytic and activation effects to the mineralisation of pollutants and the decontamination of water.

.....ജ്ഞാ.....

Chapter **7**

Sonophotocatalysis mediated by MnO₂-TiO₂ as a versatile AOP for the mineralisation of different category of pollutants

Contents

7.1 *Dyes*
7.2 *Petrochemicals*
7.3 *Pharmaceuticals*
7.4 *Pesticides*
7.5 *Conclusions*

The present study has revealed that sonophotocatalysis mediated by MnO_2-TiO_2 is a highly efficient AOP for the mineralisation of the dye pollutant IC in water. The application of this hybrid AOP (US+UV) using a combination catalyst (MnO_2-TiO_2) which can maximise the utilisation of US energy (by MnO_2) and UV energy (by TiO_2) for the decontamination of water from different types of pollutants is tested by selecting 4 typical families of chemical pollutants: Dyes, Petrochemicals, Pesticides and Pharmaceuticals. Only the qualitative application of the AOP is tested here to establish the suitability of the process. Specific parameters need to be optimised for specific applications, which is not within the scope of the current study.

Microwave, Photo and Sono Activated Advanced Oxidation Processes and their Variations for the Decontamination of Water from Toxic Chemical Pollutants

513

7.1 Dyes

The application of Sonophotocatalysis (SPC) for the mineralisation of Indigo Carmine (IC), a recalcitrant dye with a wide spectrum of application has already been investigated in detail and reported in Chapter 6. The potential of this technique is further tested for the mineralisation of another recalcitrant pollutant dye, Rhodamine B (RhB).

7.1.1 Sonophotocatalytic degradation of RhB

RhB (structure given below) is a basic dye widely used for industrial purposes such as printing and dyeing in textiles, paper, paints etc.
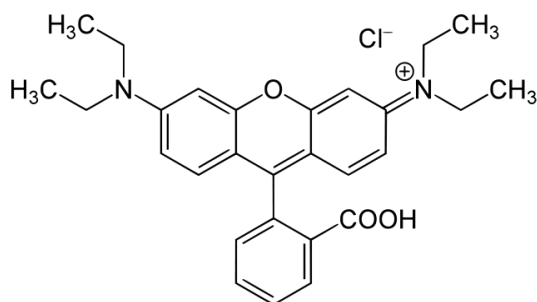
The SPC degradation of RhB in presence of MnO_2-TiO_2 is tested at two different concentrations, i.e. 10 and 20 mg/L using the conditions already optimised with respect to IC. The degradation is followed by UV- Visible spectroscopy at $\lambda_{max} = 554$ nm. The degradation is completed in about 120 to 180 minutes, for 10mg/L (Fig.7.1).
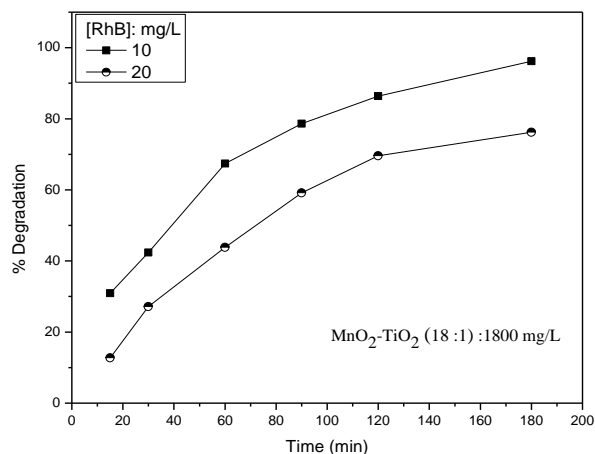
Fig. 7.1: Sonophotocatalytic degradation of RhB in presence of MnO_2-TiO_2

The possibility of mineralisation is tested by determining the COD at different times during the reaction. The COD decreases by only about ~ 40% when the solution is fully decolourised (Fig.7.2). Hence the irradiation is continued and the COD is measured after 9 hr.(arbitrarily chosen time period, to confirm the mineralisation). In this case complete COD removal is achieved.
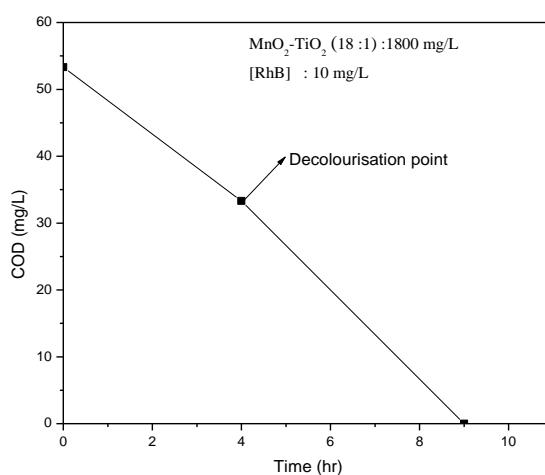
Fig. 7.2: COD of the reaction system MnO_2-TiO_2/(US+UV)/RhB at various time intervals of irradiation

The study thus shows that two dyes (Indigo Carmine and Rhodamine B) which are structurally very different can be mineralised by SPC mediated by MnO_2-TiO_2.

7.2   Petrochemicals

In this category, two widely used petrochemicals; Acetophenone (ACP) and Phenol are used as test pollutants to verify the efficiency of (US+UV)/ MnO_2-TiO_2

7.2.1 Sonophotocatalytic degradation of Acetophenone (ACP)

Acetophenone (structure given below) is a by-product in phenol-acetone synthesis and finds application in many industries such as polymers, catalysts, food flavours, fragrance, dyes etc.
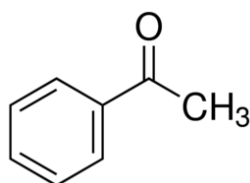
ACP is analysed by Gas Chromatography using Flame Ionisation Detector, Elite 1301 column and hydrogen as the carrier gas.

The sonophotocatalytic degradation/mineralisation of ACP is tested under the standardised conditions, using MnO_2-TiO_2, as the catalyst. Almost 60% of ACP (10mg/L) is degraded in 180 minutes. The results are presented in Fig.7.3.
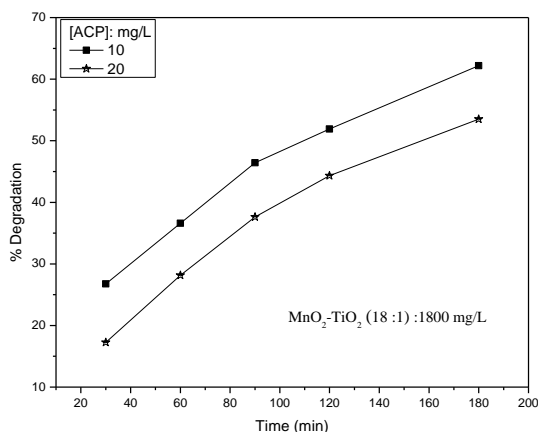
Fig. 7.3: Sonophotocatalytic degradation of ACP in presence
of MnO$_2$-TiO$_2$

ACP is a highly recalcitrant petrochemical which takes much longer time for degradation in presence of ZnO or TiO$_2$ [138]. The mineralisation of ACP also is followed in parallel by COD measurements. Analysis of the reaction solution after 8hr. (arbitrarily chosen time just to confirm mineralisation) irradiation shows that the ACP is completely mineralised (Fig.7.4).
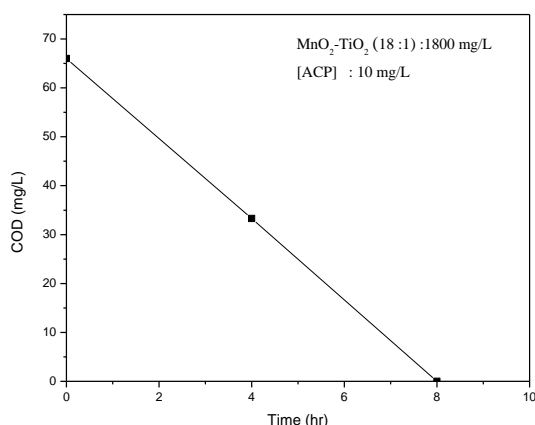
Fig. 7.4: COD of the reaction system MnO$_2$-TiO$_2$/(US+UV)/ACP
at various time intervals of irradiation

Thus it is seen that SPC is efficient for the mineralisation of ACP.

Microwave, Photo and Sono Activated Advanced Oxidation Processes and their
Variations for the Decontamination of Water from Toxic Chemical Pollutants

517

7.2.2 Sonophotocatalytic degradation of Phenol

Another petrochemical subjected to the study is phenol (structure given below). Phenol is produced and used widely in industries such as detergents, polymers, pharmaceuticals, disinfectants and bulk chemicals.
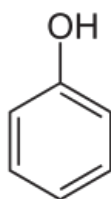
Phenol is analysed by Gas Chromatography using Flame Ionisation Detector, Elite 1301 column and hydrogen as the carrier gas. The sonophotocatalytic degradation of phenol under SPC is shown in Fig.7.5.
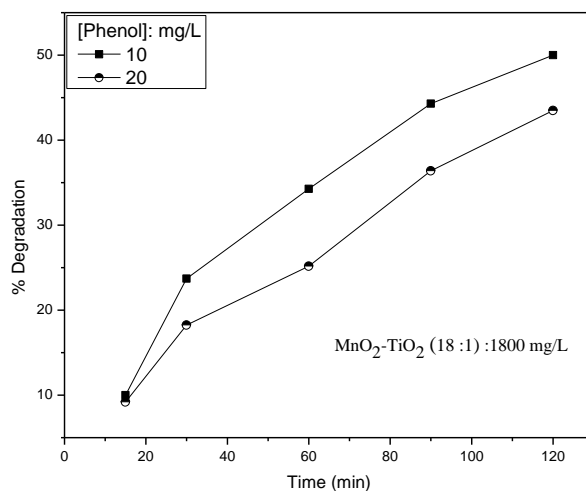
Fig. 7.5: Sonophotocatalytic degradation of Phenol in presence of MnO_2-TiO_2

More than 50% degradation (of 10mg/L) is completed within 120min. Continued irradiation results in mineralisation. Analysis of reaction products after 6hr. (arbitrarily chosen time just to verify

mineralisation) of irradiation shows the absence of any COD thereby confirming complete mineralisation (Fig.7.6).
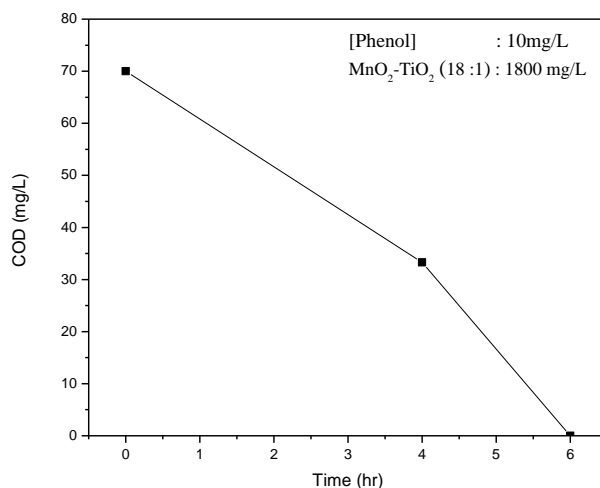
Fig. 7.6: COD of the reaction system MnO₂-TiO₂/(US+UV)/Phenol at various time intervals of irradiation

Thus it is seen that sonophotocatalysis mediated by MnO_2-TiO_2 is an efficient AOP for the mineralisation of two typical petrochemicals i.e, acetophenone and phenol.

7.3 Pharmaceuticals

Two pharmaceutical molecules of widespread use i.e acetaminophen (common name paracetamol) and diclofenac are selected as the test pollutants in this category.

7.3.1 Sonophotocatalytic degradation of paracetamol

Paracetamol (structure given below) is a synthetic drug used to relieve and reduce fever. It is often found in effluent water from related industries and also in water and wastewater from hospitals. The

concentration of paracetamol in water is analysed by UV-VIS spectroscopy at λ_{max} 243 nm.
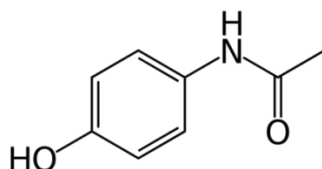
The SPC degradation of paracetamol is investigated at two different concentrations 10 and 20 mg/L. Almost 50% degradation is achieved in 120 minutes irradiation time (Fig.7.7).
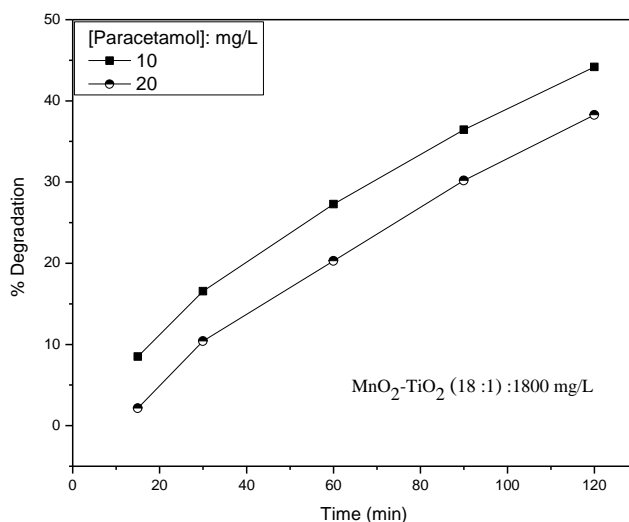
Fig. 7.7: Sonophotocatalytic degradation of Paracetamol at various time intervals

Analysis of COD after 8 hr. (arbitrarily chosen time to confirm mineralisation) of irradiation shows complete mineralisation (Fig.7.8)
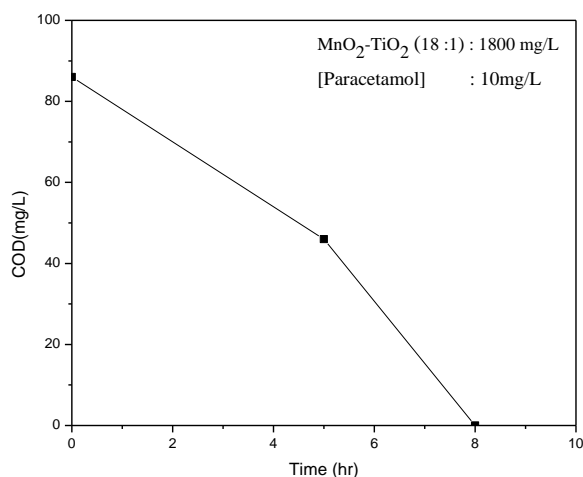
Fig. 7.8: COD of the reaction system MnO₂-TiO₂/(US+UV)/ Paracetamol at various time intervals of irradiation

7.3.2 Sonophotocatalytic degradation of Diclofenac Sodium

Diclofenac (structure given below) is available in various forms such as ointment, tablets, capsules etc. and is one of the most widely used analgesics in the world. Hence the probability of water contamination from manufacturing and formulation sites, hospitals, individual households etc. is very high. It is analysed by UV-VIS spectroscopy at λ_{max} 340 nm.
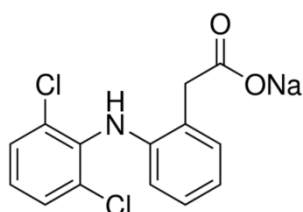
The possibility of using SPC for degradation and eventual mineralisation of diclofenac is investigated. Preliminary results on sonophotocatalytic degradation of diclofenac at two different concentrations 10 and 20mg/L are shown in Fig.7.9.

Microwave, Photo and Sono Activated Advanced Oxidation Processes and their Variations for the Decontamination of Water from Toxic Chemical Pollutants

521
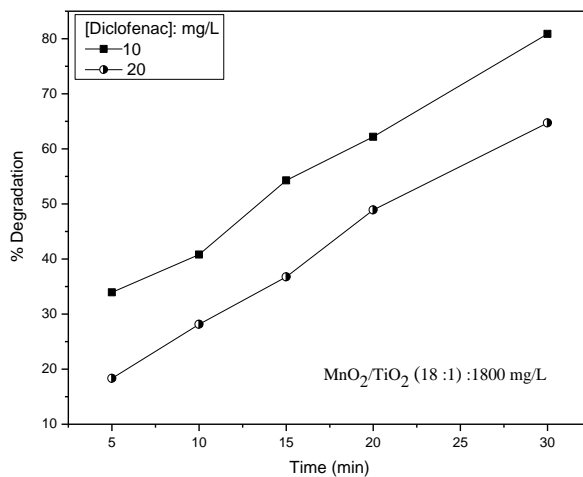
Fig. 7.9: Sonophotocatalytic degradation of Diclofenac at various time intervals

More than 80% of diclofenac (10mg/L) is degraded within 30 minutes of irradiation time. Complete mineralisation is verified by COD measurements. The results are presented in Fig.7.10.
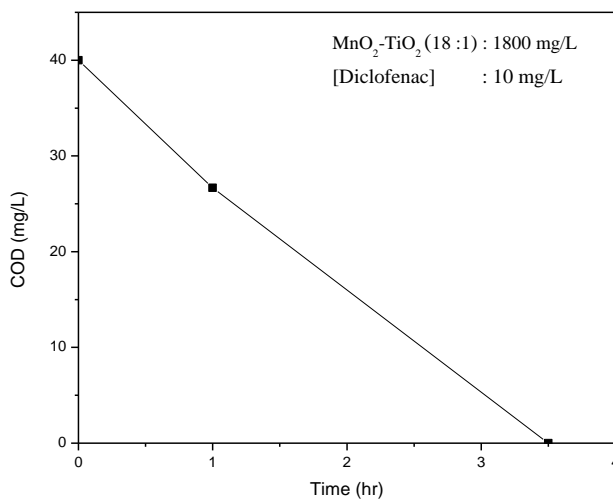
Fig.7.10: COD of the reaction system MnO_2-TiO_2/(US+UV)/ Diclofenac at various time intervals of irradiation

The mineralisation is faster compared to the other molecules discussed earlier and is completed in less than 3 ½ hours (This time is chosen arbitrarily to confirm mineralisation efficiency of the process. Optimisation of parameters may yield a lower time period for the mineralisation).

Once again the ability of SPC mediated by MnO_2-TiO_2 as a highly efficient AOP for the mineralisation of recalcitrant pharmaceutical pollutants is established here.

7.4   Pesticides

Two widely used pesticides Diquat (herbicide) and Carbendazim (fungicide) are selected in this category for the study.

7.4.1 Sonophotocatalytic degradation of Diquat

Diquat (structure given below) is one of the widely used herbicides in agriculture and is hence a major contaminant of water. The concentration of diquat in water is estimated by UV-VIS spectroscopy at its λ_{max} 310 nm.
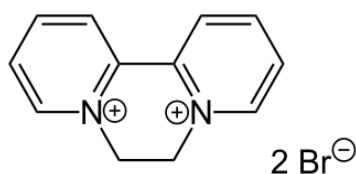
The potential of SPC for the degradation and mineralisation of diquat is investigated. The results are presented in Figs.7.11 and 7.12.

Fig.7.11 shows the degradation of diquat at two concentrations, i.e, 10 and 20 mg/L. More than 60% of the herbicide (10mg/L) is degraded in 45 minutes.
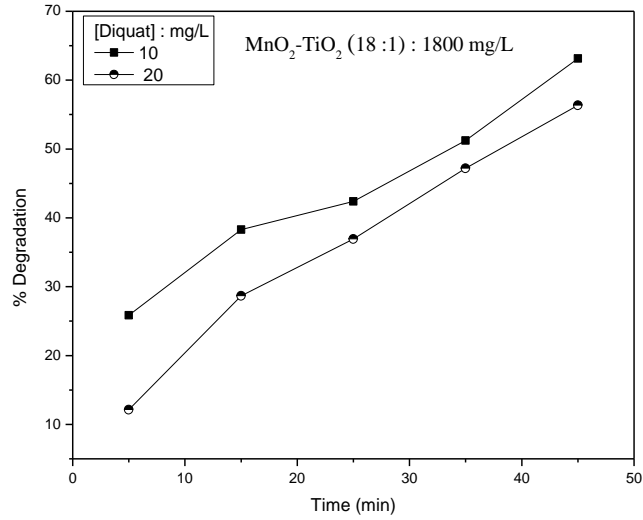
Fig. 7.11: Sonophotocatalytic degradation of Diquat various time intervals

The COD measurements of the reaction system after 5 hr. of irradiation (arbitrarily chosen time to confirm mineralisation) confirmed complete mineralisation (Fig.7.12).
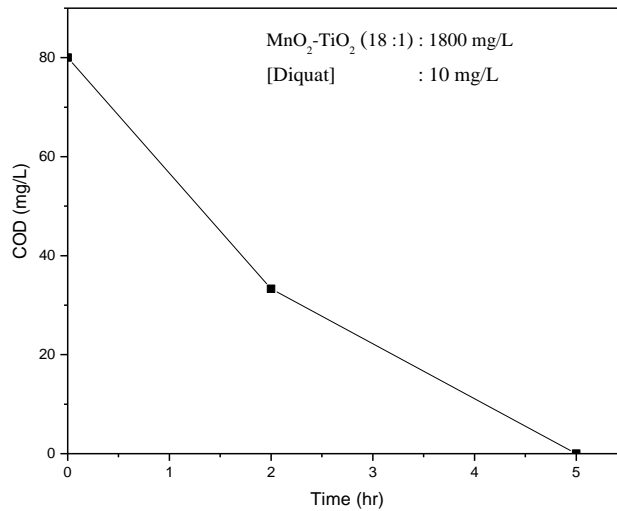
Fig. 7.12: COD of the reaction system MnO_2-TiO_2/(US+UV)/Diquat at various time intervals of irradiation

7.4.2 Sonophotocatalytic degradation of Carbendazim

Carbendazim (structure given below) is a wide-spectrum fungicide. It is also used as a worm control agent in amenity turf situations such as golf green. Because of such wide- spread use in a variety of applications, probability of its presence in water is very high. The concentration of carbendazim is analysed by UV-VIS spectroscopy at its λ_{max} 284 nm.
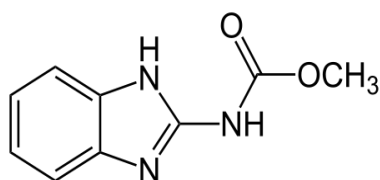
The SPC degradation of carbendazim in presence of MnO_2-TiO_2 catalyst is investigated and the results show that 70% (of 10mg/L) is degraded in 3 hr. (Fig.7.13).
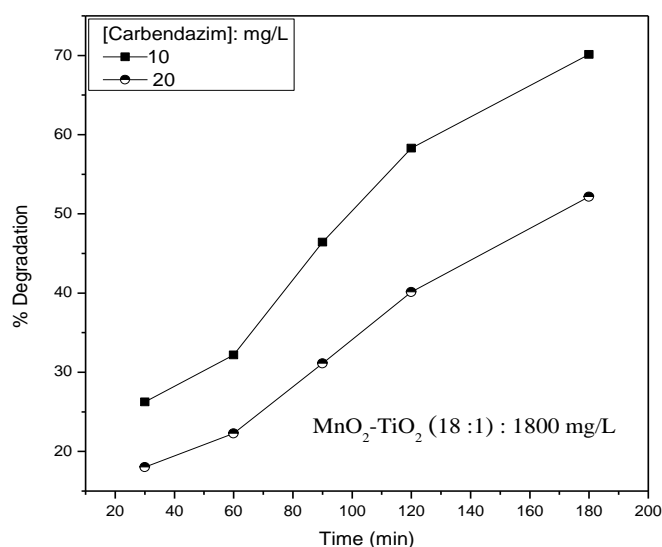
Fig. 7.13: Sonophotocatalytic degradation of Carbendazim at various time intervals

COD measurements after 6 hr. (time chosen arbitrarily to verify mineralisation) shows that complete mineralisation is achieved (Fig.7.14).
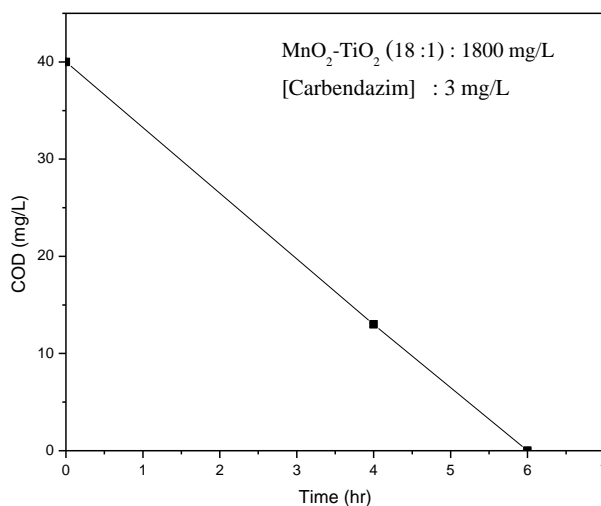
Fig. 7.14: COD of the reaction system MnO$_2$-TiO$_2$/ (US+UV)/Carbendazim at various time intervals of irradiation

Thus it is seen that sonophotocatalysis mediated by MnO$_2$-TiO$_2$ catalyst (in the optimised ratio) is highly efficient AOP for the mineralisation of recalcitrant pesticide molecules as well.

7.5 Conclusions

The results in this Chapter illustrate that SPC mediated by MnO$_2$-TiO$_2$ is a highly efficient AOP for the degradation/mineralisation of a wide spectrum of chemical pollutants. The study is only preliminary and qualitative in nature with the limited objective of testing the versatility of MnO$_2$-TiO$_2$/ (US+UV) for the decontamination of water from toxic chemical pollutants. The results conclusively establish that the catalyst MnO$_2$-TiO$_2$, identified by the current investigation as a highly efficient

sonophotocatalyst possesses huge potential for commercial application in the purification of chemical contaminated wastewater. Relevant parameters, identified as important, from the investigation reported in earlier Chapters need to be further optimised and scaled up for commercial application. The study conclusively established the versatility of SPC for the purification of water from a wide variety of toxic chemical pollutants irrespective of their diverse physicochemical characteristics.

.....෫൫.....

Microwave, Photo and Sono Activated Advanced Oxidation Processes and their Variations for the Decontamination of Water from Toxic Chemical Pollutants

527

Chapter **8**

Summary and Conclusions

This Chapter summarises the findings of the current study and highlights the major conclusions. The application of five important Advanced Oxidation Processes i.e. Microwave catalysis, Photocatalysis, Sonocatalysis, Microwave-photocatalysis (in sequence) and Sonophotocatalysis (concurrent) is investigated in detail for the irreversible removal of toxic dye pollutant Indigo Carmine (IC) from water. Novel AOP catalyst systems based on the least tested MnO_2, Co_3O_4 and the combination MnO_2-TiO_2 are investigated in detail under MW, US and UV activation for their degradation and mineralisation efficiency under different conditions. The influence of various reaction parameters such as catalyst dosage, concentration of the dye, pH of the medium, temperature, presence of natural salt contaminants in water, dissolved O_2, oxidants such as H_2O_2 and $K_2S_2O_8$ etc. on the degradation efficiency of the substrate is investigated in detail and the relevance of each of these parameters is identified and optimised.

The catalysts used in the study were characterized before and after use by various techniques including surface area measurement, particle size and pore size distribution analysis, XRD, FTIR, SEM, TEM and UV-DRS. The degradation and decolourisation of the dye does not

automatically result in mineralisation which requires extended irradiation and more vigorous reaction conditions. This indicates that the degradation is proceeding through a number of intermediates which are more stable and recalcitrant compared to the parent molecule. Such intermediates were identified by LC-MS techniques.

An important component of the current study is the practical illustration of the application of the best identified AOP, i.e, 'Sonophotocatalysis mediated by MnO_2-TiO_2' for the complete mineralisation of diverse chemical pollutants such as dyes, petrochemicals, pharmaceuticals and pesticides.

Other salient findings of the study and the conclusions are summarised as follows:

1) MnO_2 is a highly efficient and effective MW catalyst for the degradation of Indigo Carmine dye. However, the degradation does not lead to complete mineralisation as seen from COD/TOC measurements. This is the first instance of the application of MW energy and MnO_2 catalyst in an AOP for the decontamination of water. Another MW catalyst emerged from the study is Co_3O_4 though it is relatively less efficient compared to MnO_2.

2)   The importance of non-thermal component of microwave energy for the activation of catalysts and consequent degradation of pollutants is established in the study. Major contribution of the 'non-thermal effect' of MW is 'reduction in the activation energy' of degradation of the pollutant. This is demonstrated in the case of both MnO_2 and Co_3O_4 as catalysts.

3) MnO_2 is also identified as an efficient catalyst for water purification under sono-, photo- as well as sonophoto-catalytic conditions.

4)   The current study has identified MnO_2 as one of the most efficient sonocatalysts, reported so far, for the removal of IC from water, with an efficiency of over 56% achieved in ~ 5 minutes.

5)   Another major outcome of the study is the observation that combination of MW and UV irradiation in sequence can accelerate the decolourisation and mineralisation of IC.

6)   Demonstrated the potential of combining the MW activity of MnO_2 and the photoactivity of TiO_2 at a critical ratio of the two components for the mineralisation of toxic pollutants using the hybrid technique of Sonophotocatalysis. Multiple experiments confirmed the superior capability of this combination.

7)   An interesting observation of the study is that H_2O_2 which is generally an enhancer of AOP degradation of organics functions as an inhibitor in presence of MnO_2 and MnO_2-TiO_2. However, in presence of Co_3O_4, it functions as an enhancer. Possible causes for this contradicting behaviour are analysed and discussed.

8)   Another oxidant $K_2S_2O_8$ is a consistent enhancer of the degradation of IC in presence of MnO_2, MnO_2-TiO_2 and Co_3O_4. Combination of H_2O_2 and $K_2S_2O_8$ results in synergy in the enhancement in the case of Co_3O_4/UV while it is only additive in the case of other systems.

9)   The kinetics of the degradation is concentration dependent. The degradation follows variable kinetics ranging from first order to zero

order (higher order at lower concentrations) and L-H mechanism under MW, sono, photo and sonophotocatalytic processes.

10) Many of the anions/salts naturally present in water, do not influence the AOP degradation of pollutants significantly at the concentration, in which they are normally present. However PO_4^{3-}, CO_3^{2-} and HCO_3^- function as inhibitors except in the case of Co_3O_4 as catalyst. NO_3^- is a consistent enhancer of the degradation in presence of all catalysts studied here.

11) Advanced Oxidation Processes are promoted by insitu formed reactive O_2 species such as $^.OH$, $HO_2^.$, H_2O_2 etc., the source of O_2 being the dissolved O_2. Surprisingly in presence of MnO_2 and Co_3O_4 the degradation of IC proceeds unaffected even in systems deoxygenated by N_2. With the help of suitably designed experiments (as explained in the respective Chapters) and EDX spectra, it was discovered that O_2 from the lattice of the catalyst is participating in the degradation reaction. The depleted O_2 from the lattice can be replenished by dissolved O_2 thereby making the recycling of the catalyst possible.

12) Combination of sono and photocatalysis (sonophotocatalysis) with MnO_2 as catalyst could achieve almost 75% degradation of the dye in 7 minutes, thereby illustrating the versatility of MnO_2 as a highly efficient AOP catalyst under different activation conditions.

13) Another significant outcome of the study is the identification of the hybrid AOP, i.e 'Sonophotocatalysis mediated by the combination

catalyst MnO_2-TiO_2' as a highly efficient AOP, for the decontamination of water from dye pollutants. In this case 90% of the dye is degraded within 5 minutes. Comparative efficiency of different AOPs tested here for the mineralisation of IC is:

MnO_2-TiO_2/(US+UV) > MnO_2-TiO_2/(UV) > MnO_2/(US+UV) > MnO_2/UV > MnO_2-TiO_2/US > MnO_2/US

14) The potential of sonophotocatalysis as a versatile AOP for the mineralisation of a wide spectrum of structurally different chemical pollutants in water is established with:

Dyes (Indigo Carmine, Rhodamine B), Petrochemicals (Acetophenone, Phenol), Pharmaceuticals (Paracetamol, Diclofenac) and Pesticides (Diquat, Carbendazim) as pollutants.

.....ஜஒஜ.....

References

[1]   P. Koch, Principles and practices of water supply operations, Publishers: Amer. Water Works Assn., Second edition (1995)

[2]   T.H.Y. Tebbutt, Principles of water quality control, Publishers: Butterworth-Heinemann, Fifth edition (1997)

[3]   S.J. Arceivala, S.R. Asolekar, Wastewater treatment for pollution control and reuse, Publishers: Tata Mc Graw- Hill Education, Third edition (2006)

[4]   J. Dhote, S. Ingole, A. Chavhana, Review on wastewater treatment technologies, Int. J. Eng. Res. Technol., 1 (2012) 1-10

[5]   J.O. Tijani, O.O. Fatoba, G. Madzivire, A review of combined advanced oxidation technologies for the removal of organic pollutants from water, Water Air Soil Polln., (2014) 225:2102

[6]   J. R. Jasmann, T. Borch, T. C. Sale, J. Blotevoge, Advanced electrochemical oxidation of 1, 4-dioxane via dark catalysis by novel TiO_2 pellets, Environ. Sci. Technol., 50 (2016) 8817−8826

[7]   C. K. Remucal, D. Manley, Emerging investigators series: The efficacy of chlorine photolysis as an advanced oxidation process for drinking water treatment, Environ. Sci. Water Res. Technol., 2 (2016) 565-579

[8]   N. Banic, B. Abramvic, F. Sibul, D. Orcic, M. Watson, M. Vranes, S.Gadzuric, Advanced oxidation processes for the removal of third generation ionic liquids: Effect of water matrices and intermediates identification, RSC Adv., 6 (2016) 52826-52837

[9]   B.P. Chaplin, Critical review of advanced oxidation processes for water treatment applications, Environ. Sci. Processes Impacts., 16 (2014) 1182 −1203

[10]   L.G. Covinich, D.I. Bengoechea, R.J. Fenoglio, M.C. Area, Advanced oxidation processes for wastewater treatment in the pulp and paper industry: A review, Am. J. Env. Eng., 4 (2014) 56-70

[11]   J.P. Guin, D.B. Naik, Y.K. Bhardwaj, L. Varshney, An insight into the effective advanced oxidation process for treatment of simulated textile dye waste water, RSC Adv., 4 (2014) 39941-39947

[12]   M. Swaminathan, M. Muruganandham, M. Sillanpaa, Advanced oxidation processes for wastewater treatment, Int. J. Photoenergy, 2013 (2013), Article id. 683682, 1-3

[13]   O.S. Keen, K.G. Linden, Degradation of antibiotic activity during UV/H_2O_2 advanced oxidation and photolysis in wastewater effluent, Environ. Sci. Technol., 47 (2013) 13020−13030

[14]   O.S. Keen, S. Baik, K.G. Linden, D.S. Aga, N.G. Love, Enhanced biodegradation of carbamazepine after UV/H_2O_2 advanced oxidation, Environ. Sci. Technol., 46 (2012) 6222−6227

[15]   A.D. Bokare, W. Choi, Advanced oxidation process based on the Cr (III)/Cr (VI) redox cycle, Environ. Sci. Technol., 45 (2011) 9332–9338

[16]   N.O. Landsman, K. Swancutt, C. Bradford, C. Cox, J.J. Kiddle, S. Mezyk, Free radical chemistry of advanced oxidation process removal of nitrosamines in water, Environ. Sci. Technol., 41(2007) 5818-5823

[17]   J.L. Capelo, C. Maduro, A.M. Mota, Advanced oxidation processes for degradation of organomercurials: Determination of inorganic and total mercury in urine by FI-CV-AAS, J. Anal. At. Spectrom., 19 (2004) 414 – 416

[18]   M.M. Huber, S. Canonica, G.Y. Park, U.V. Gunten, Oxidation of pharmaceuticals during ozonation and advanced oxidation processes, Environ. Sci. Technol., 37 (2003) 1016-1024

[19]   B. Boye, M.M. Dieng, E. Brillas, Degradation of herbicide 4-Chlorophenoxyacetic acid by advanced electrochemical oxidation methods, Environ. Sci. Technol., 36 (2002) 3030–3035

[20]   Z. Wu, M. Zhou, Partial degradation of phenol by advanced electrochemical oxidation process, Environ. Sci. Technol., 35 (2001) 2698-2703

[21]   I. Hua and M. R. Hoffmann, Optimization of ultrasonic irradiation as an advanced oxidation technology, Environ. Sci. Technol., 31 (1997) 2237–2243

[22] S.E. Braslavsky, Glossary of terms used in photochemistry, Third edition, Pure Appl. Chem., 79 (2007) 293-465

[23] K. Demeesstere, J. Dewulf, H.V. Langenhove, Heterogeneous photocatalysis as an advanced oxidation process for the abatement of chlorinated, monocyclic aromatic and sulfurous volatile organic compounds in air: state of the art, Crit. Rev. Environ. Sci. and Technol., 37 (2007) 489–538

[24] K. Mondal, A. Sharma, Photocatalytic oxidation of pollutant dyes in wastewater by TiO_2 and ZnO nano-materials – A Mini-review, in Nanoscience & Technology for Mankind, Ed. A. Misra, J. R. Bellare, Publishers: The National Academy of Sciences India (NASI), (2014) pp.36-72

[25] G.R.L. Samanamud, C.C.A. Loures, A.L. Souza, R.F.S. Salazar, I.S. Oliveira, M.B. Silva, H.J.I. Filho, Heterogeneous photocatalytic degradation of dairy wastewater using immobilized ZnO. ISRN Chem. Eng., 2012 (2012) Article id. 275371, 8 pages

[26] K. Elahee, Heat recovery in the textile dyeing and finishing industry: Lessons from developing economies, J. Energy in Southern Africa., 21 (2010) 9-15

[27] M.R. Kumar, K. Saravanan, Advanced treatment of textiles yarn dying waste water towards reuse using reverse osmosis membrane, Int. J. Appl. Bioeng., 4 (2010) 25-33

[28] F.H. Hussen, T.A. Abass, Photocatalytic treatment of textile industrial wastewater, Int. J. Chem. Sci., 8 (2010) 1353-64

[29] P.A. Pekakis, N.P. Xekoukoulotakis, D. Mantzavinos, Treatment of textile dye house wastewater by TiO_2 photocatalysis, Water Research, 40 (2006) 1276–1286

[30] M.A.H. Devadi, M. Krishna, H.N.N. Murthy, B.S. Sathyanarayana, Statistical optimisation for photocatalytic degradation of Methylene Blue by Ag-TiO_2 nano particles, Proc. Mater. Sci., 5(2014) 612-621

[31] A. Giwa, P. O. Nkeonye, K. A. Bello, K. A. Kolawole, Photocatalytic decolourization and degradation of C. I. Basic Blue 41 using TiO_2 nanoparticles, J. Environ. Protection, 3 (2012) 1063-1069

Microwave, Photo and Sono Activated Advanced Oxidation Processes and their Variations for the Decontamination of Water from Toxic Chemical Pollutants

537

[32] N.P. Mohabansi, V.B. Patil, N. Yenkie, A comparative study on photo degradation of Methylene Blue dye effluent by advanced oxidation process by using TiO_2/ZnO photo catalyst, RASAYAN J. Chem., 4 (2011) 814-819

[33] H. S. Wahab, A. A. Hussain, Photocatalytic oxidation of phenol red onto nanocrystalline TiO_2 particles, J. Nanostruct. Chem., 6 (2016) 261–67

[34] R. Mehta1, M. Surana, Photodegradation of dye Acid Orange 67 by titanium dioxide in the presence of visible light and UV light, Research and Reviews: Journal of Chemistry, 2 (2013) 12-16.

[35] M.A. Rauf, S.S. Ashraf, Fundamental principles and application of heterogeneous photocatalytic degradation of dyes in solution, Chem. Eng. J., 151 (2009) 10-18

[36] E.S. Elmolla, M. Chaudhuri, The feasibility of using combined TiO_2 photocatalysis - SBR process for antibiotic wastewater treatment, Desalination, 272 (2011) 218–224

[37] D.R Stapleton, I.K. Konstantinou, D. Mantzavinos, D. Hela, M. Papadaki, On the kinetics and mechanisms of photolytic/TiO_2-photocatalytic degradation of substituted pyridines in aqueous solutions, Appl. Catal. B: Environ., 95 (2010) 100-109

[38] W. Sun, H. Chu, B. Dong, D. Cao, S. Zheng, The degradation of Naproxen and Diclofenac by a nano- TiO_2/diatomite photocatalytic reactor, Int. J. Electrochem. Sci., 9 (2014) 4566 – 4573

[39] J. Akach, M.S. Onyango, A. Ochieng, Adsorption and solar photocatalytic degradation of Diclofenac in wastewater, Proc. Intl' Conf. on Chemical, Integrated Waste Management & Environmental Engineering (ICCIWEE'2014) April 15-16 (2014) Johannesburg.

[40] B. Czech, K. Rubinowska, TiO2-assisted photocatalytic degradation of Diclofenac, Metoprolol, Estrone and Chloramphenicol as endocrine disruptors in water, Adsorption, 19 (2013) 619–630

[41] M.H. Florencio, E. Pires, A.L. Castro, M.R. Nunes, C. Borges, F.M. Costa, Photodegradation of Diquat and Paraquat in aqueous solutions by titanium dioxide: Evolution of degradation reactions and characterisation of intermediates, Chemosphere, 55 (2004) 345-355

[42] M. Cruz, C. Gomez, C.J. Duran-Valle, L.M. Pastrana-Martinez, J. L. Faria, A. M. T. Silva, M. Faraldos, A. Bahamonde, Bare TiO_2 and graphene TiO_2 photocatalysis on the degradation of selected pesticides and influence of water matrix, Appl. Surf. Sci., 416 (2017) 1013-1021

[43] J. Saien, S. Khezrianjoo, Degradation of the fungicide carbendazim in aqueous solutions with UV/TiO2 process: Optimization, kinetics and toxicity studies, J. Hazard. Mater., 157 (2008) 269–276

[44] L. Lhomme, S. Brosillon, D. Wolbert, Photocatalytic degradation of a triazole pesticide, Cyproconazole, in water, J. Photochem. Photobiol. A: Chemistry, 188 (2007) 34–42

[45] P. Liwsirisaeng, C. Kalambaheti, D.P. Kashima, S. Jiemsirilers, S. Jinawath, Photocatalytic degradation of phenolic compounds by TiO_2 powder, Proc. 18th Intl. Conference on composite materials, August (2011) Jeju Island, Korea

[46] M.R. Hoffmann, S.T. Martin, W. Choi, D.W. Bahnemannt, Environmental applications of semiconductor photocatalysis, Chem. Rev., 95 (1995) 69-96

[47] Z. Meng, Z. Juan, Wastewater treatment by photocatalytic oxidation of nano-ZnO, Global Environmental Policy Japan, 12 (2008) 1-9

[48] B.M. Reddy, G.K. Reddy, K.N. Rao, I. Ganesh, J.M.F. Ferreira, Characterization and photocatalytic activity of TiO_2–MxOy (MxOy = SiO_2, Al_2O_3, and ZrO_2) mixed oxides synthesized by microwave- induced solution combustion technique, J. Mater. Sci., 44 (2009) 4874-82

[49] F.K.M. Alosfur, M.H.H. Jumali, S. Radiman, N.J. Ridha, M.A. Yarmo, A.A. Umar, Modified microwave method for the synthesis of visible light-responsive TiO_2/MWCNTs nanocatalysts, Nanoscale Res. Lett., 8 (2013) 1-6

[50] P. Zhang, C. Shao, Z. Zhang, M. Zhang, J. Mu, Z. Guo, Core/shell nanofibers of TiO_2@carbon embedded by Ag nanoparticles with enhanced visible photocatalytic activity, J. Mater. Chem., 21(2011)17746-53

[51] R. Tang, H. Su, Y. Sun, X. Zhang, L. Li, C. Liu, B. Wang, S. Zeng, D. Sun, Facile fabrication of Bi_2WO_6/Ag_2S heterostructure with enhanced visible- light-driven photocatalytic performances, Nanoscale. Res. Lett., 11 (2016)1-12

[52] M.V. Savoskin, A.P. Yaroshenko, N.I. Lazareva, V.N. Mochalin, R. D. Mysyk, Using graphite intercalation compounds for producing exfoliated graphite–amorphous carbon–TiO_2 composites, J. Phys. Chem. Solids, 67 (2006) 1205–7

[53] R.S. Devan, R.A. Patil, J.H. Lin, Y.R. Ma, One-dimensional metal-oxide nanostructures: Recent developments in synthesis, characterization, and applications., Adv. Funct. Mater., 22 (2012) 3326–70

[54] E.R. Carraway, A.J. Hoffman, M.R. Hoffmann, Photocatalytic oxidation of organic acids on quantum-sized semiconductor colloids, Environ. Sci. Technol., 28 (1994) 786–93

[55] O.M. Shibin, B. Rajeev, V. Veena, E.P. Yesodharan, S. Yesodharan, ZnO photocatalysis using solar energy for the removal of trace amounts of Alfa-methylstyrene, Diquat and Indigo Carmine from water, J. Adv. Oxid. Technol., 17 (2014) 297-304

[56] P.D. Phonsy, S. Yesodharan, E.P. Yesodharan, Enhancement of semiconductor mediated photocatalytic removal of polyethylene plastic wastes from the environment by oxidizers, Res. J. Rec. Sci., 4 (2015) 105-112

[57] G. Alhakimi, L.H. Studnicki, M. Al-Ghazali, Photocatalytic destruction of potassium hydrogen phthalate using TiO_2 and sunlight: application for the treatment of industrial wastewater. J. Photochem. Photobiol. A: Chem., 154 (2003) 219–28

[58] W. Choi, A. Termin, M.R. Hoffmann, The role of metal ion dopants in quantum-sized TiO_2: Correlation between photoreactivity and charge carrier recombination dynamics, J. Phys. Chem., 98 (1994) 13669–79

[59] B. Zielińska, J. Grzechulska, R.J. Kaleńczuk, A.W. Morawski, The pH influence on photocatalytic decomposition of organic dyes over A11 and P25 titanium dioxide. Appl. Catal.B: Environ., 45 (2003) 293–300

[60] K. Naeem, O. Feng, Parameters effect on heterogeneous photocatalysed degradation of phenol in aqueous dispersion of TiO_2, J. Environ. Sci., 21 (2009) 527–33

[61] K. Wantala, A. Tosuwan, N. Grisdanurak, Manganese loaded on titania surface by impregnation method for photocatalytic degradation of Reactive Red-3 dye , Materials Science Forum, 734 (2013) 295- 305

[62]   N. Mittal, A. Shah, P.B. Punjabi, V.K. Sharma, Photodegradation of Rose Bengal using manganese dioxide, RASAYAN. J. Chem., 2 (2009), 516-520

[63]   P.P. Hankare, A.V. Jadhav, R.P. Patil, K.M. Garadkar, I.S. Mulla, R. Sasikala, Photocatalytic degradation of Rose Bengal in visible light with Cr substituted $MnFe_2O_4$ ferrospinel, Archives of Physics Research, 3 (2012) 269-276

[64]   S.I. Mogal, M. Mishra, V.G. Gandhi, R.J. Tayade, Metal doped titanium dioxide: synthesis and effect of metal ions on physico- chemical and photocatalytic properties, Materials Science Forum., 734 (2013) 364- 378

[65]   J. Schneider, M. Matsuoka, M. Takeuchi, J. Zhang, Y. Horiuchi, M. Anpo, D.W. Bahnemann, Understanding TiO_2 photocatalysis: Mechanism and materials, Chem. Rev., 114 (2014) 9919-9986

[66]   W.Z. Tang, Z. Zhang, H. An, M.O. Quintana, D.F. Torres, TiO_2/UV photodegradation of azo dyes in aqueous solutions, Environ. Technol., 18 (1997) 1-12

[67]   K. Bubacz, J. Choina, D. Dolat, A.W.M. Polish, Methylene Blue and Phenol photocatalytic degradation on nanoparticles of anatase TiO_2, Pol. J. Environ. Stud. 19 (2010) 685-691

[68]   M. Kaise, H. Nagai, K. Tokuhashi, S. Kondo, S. Nimura, O. Kikuchi, Electron spin resonance studies of photocatalytic interface reactions of suspended M/TiO_2 (M = Pt, Pd, Ir, Rh, Os, or Ru) with alcohol and acetic acid in aqueous media, Langmuir, 10 (1994) 1345–47.

[69]   F. Kiriakidou, D.I. Kondarides, X.E. Verykios, The effect of operational parameters and TiO_2-doping on the photocatalytic degradation of azo-dyes, Catal. Today, 54 (1999) 119–30

[70]   T.W. Kim, M.J. Lee, Effect of pH and temperature for photocatalytic degradation of organic compound on carbon-coated TiO_2, J. Adv. Eng. Technol., 3 (2010) 193-98.

[71]   M. Lindner, J. Theurich, D. W. Bahnemann, Photocatalytic degradation of organic compounds: accelerating the process efficiency. Water Sci. Technol., 35 (1997) 79–86

[72]   P.R. Gogate, S. Mujumdar, A.B. Pandit, Large-scale sonochemical reactors for process intensification: Design and experimental validation, J. Chem. Technol. Biotechnol., 78 (2003) 685–693

[73]   S. Vajnhandl, A. Majcen L. Marechal, Ultrasound in textile dyeing and the decolouration/mineralization of textile dyes, Dyes Pigm., 65 (2005) 89–101

[74]   M.A. Behnajady, N. Modirshahla, M. Shokri, B. Vahid, Investigation of the effect of ultrasonic waves on the enhancement of efficiency of direct photolysis and photooxidation processes on the removal of a model contaminant from textile industry, Global Nest Journal, 10 (2008) 8-15

[75]   A.S. Ozen, V. Aviyente, G.T. Guyer, N.H. Ince, Experimental and modeling approach to decolourization of azo dyes by ultrasound: degradation of the hydrazone tautomer, J. Phys. Chem. A, 109 (2005) 3506-3516

[76]   N.H. Ince, G.T Guyer, Impacts of pH and molecular structure on ultrasonic degradation of azo dyes Ultrasonics, 42 (2004) 591-596

[77]   M. Goel, H.Q. Hu, A.S. Mujumdar, M.B. Ray, Sonochemical decomposition of volatile and non-volatile organic compounds – a comparative study, Water Research, 38 (2004) 4247-4261

[78]   C. Minero, P. Pellizzari, V. Maurino, E. Pelizzetti, D. Vione, Enhancement of dye sonochemical degradation by some inorganic anions present in natural waters, Appl. Catal. B -Environ., 77 (2008) 308-316

[79]   X. Chen, R. Jiang, J. Wang, K. Li, Y. Li, B. Wang, J. Gao, P. Kang, [Sonocatalytic degradation of organic dyes and influence of Al2O3, Y2O3 and Fe2O3 on catalytic activity of TiO2 under ultrasonic irradiation, Water Sci. Technol., 63 (2011) 1513-1518

[80]   R. Jothiramalingam, T.M. Tsao, and M.K. Wang, High-power ultrasonic-assisted phenol and dye degradation on porous manganese oxide doped titanium dioxide catalysts, Kinetics and Catalysis, 50 (2009) 741-747

[81]   H. Destaillats, A.J. Colussi, J.M. Joseph, M.R. Hoffmann, Synergistic effects of sonolysis combined with ozonolysis for the oxidation of azobenzene and methyl orange, J. Phys. Chem. A., 104 (2000) 8930-8935

[82]   J.J Yao, N.Y. Gao, C. Li, L. Li, B. Xu, Mechanism and kinetics of parathion degradation under ultrasonic irradiation, J. Hazard. Mater., 175 (2010) 138-145

[83]   J. Hartmann, P. Bartels, U. Mau, M. Witter, W.V. Tumpling, J. Hofmann, E. Nietzschmann, Degradation of the drug Diclofenac in water by sonolysis in presence of catalysts, Chemosphere, 70 (2008) 453–461

[84]   M. Hoseini, G.H. Safari, H. Kamani, J. Jaafari, M. Ghanbarain, A.H. Mahvi, Sonocatalytic degradation of tetracycline antibiotic in aqueous solution by sonocatalysis, Toxicol. Environ. Chem., 95 (2013) 1680–1689

[85]   K. Okitsu, B. Nanzai, K. Thankavadevel, Sonochemical degradation of aromatic compounds, surfactants, and dyes in aqueous solutions, in Handbook of Ultrason. Sonochem., (2015) pp.1-28.

[86]   A. Khataee, S. Saadi, M. Safarpour, S. W Joo, Sonocatalytic performance of Er-doped ZnO for the degradation of textile dye, Ultrason. Sonochem., 27 (2015) 379-388

[87]   Y.L. Pang, A.Z. Abdullah, S. Bhatia, Review on sonochemical methods in the presence of catalysts and chemical additives for treatment of organic pollutants in water, Desalination, 277 (2011) 1-14

[88]   J. Wang, Y. Lv, L. Zhang, B. Liu, R. Jiang, G. Han, R. Xu, X. Zhang, Sonocatalytic degradation of organic dyes and comparison of catalytic activities of CeO_2/TiO_2, SnO_2/TiO_2 and ZrO_2/TiO_2 composites under ultrasonic irradiation, Ultrason. Sonochem., 17 (2010) 642-648

[89]   P.N.V. Lakshmi, P. Saritha, N. Rambabu, V. Himabindu, Sonochemical degradation of 2-Chloro-5-methyl phenol assisted by TiO2 and H2O2, J. Hazard. Mater., 174 (2010) 151-155

[90]   M.A. Behnajady, N. Modirshahla, M. Shokri, B. Vahid, Effect of operational parameters on degradation of Malachite Green by ultrasonic irradiation, Ultrason. Sonochem., 15 (2008) 1009–1014

[91]   Z. Xiong, X. Cheng, D. Sun, Pretreatment of heterocyclic pesticide wastewater using ultrasonic/ozone combined process, J. Environ. Sciences, 23 (2011) 725-730

[92]   H. Zhao, G. Zhang, Q. Zhang MnO_2/CeO_2 for catalytic ultrasonic degradation of methyl orange Ultrason. Sonochem., 21 (2014) 991-996

[93]   Z. Eren, Ultrasound as a basic and auxiliary process for dye remediation: A review, J. Env. Management., 104 (2012) 127-141

[94]   C. Little, M.J. Hepher, M. E. Sharif, The sono-degradation of Phenanthrene in an aqueous environment, Ultrasonics, 40 (2002) 667-74

[95] S.G. Anju, K.P. Jyothi, S. Joseph, Y. Suguna, E.P. Yesodharan, Ultrasound assisted semiconductor mediated catalytic degradation of organic pollutants in water: Comparative efficacy of ZnO, TiO_2 and ZnO-TiO_2, Res. J. Rec. Sci., 1 (2012) 191-201

[96] Y. Li -Song, J-T. Li , H. Chen, Degradation of C.I. Acid Red 88 aqueous solution by combination of Fenton's reagent and ultrasound irradiation, J. Chem. Technol. Biotechnol.,84 (2009) 578-583

[97] P.R. Gogate, A.B. Pandit, Sonophotocatalytic reactors for wastewater treatment: A critical review AIChE Journal, 50 (2004) 1051–1079

[98] S.K. Kavitha, P.N. Palanisamy, Photocatalytic and sonophotocatalytic degradation of Reactive Red 120 using dye sensitized TiO_2 under visible light, Int. J. Civil Environ. Eng., 3(2011) 1-6

[99] C.G. Joseph, G. Li Pumab, A. Bono, D. Krishnaiah, sonophotocatalysis in advanced oxidation process a short review, Ultrason. Sonochem., 16 (2009) 583-589

[100] X. Hua, Q. Zhua, Z. Gua, N. Zhanga, N. Liua, M.S. Stanislausa, D. Lia, Y. Yang, Wastewater treatment by sonophotocatalysis using PEG modified TiO_2 film in a circular Photocatalytic -Ultrasonic system, Ultrason. Sonochem., 36 (2017) 301–308

[101] V. Ragaini, E. Selli, C.L. Bianchi, C. Pirola, Sono-photocatalytic degradation of 2-Chlorophenol in water: kinetic and energetic comparison with other techniques, Ultrason. Sonochem., 8 (2001) 251–258

[102] M. Mrowetz, C.Pirola, E. Selli, Degradation of organic water pollutants through sonophotocatalysis in the presence of TiO_2, Ultrason. Sonochem., 10 (2003) 247–254

[103] E. Selli, C.L. Bianchi, C. Pirola, M. Bertelli, Degradation of Methyl tert-butyl ether in water :Effects of the combined use of sonolysis and photocatalysis, Ultrason. Sonochem., 12 (2005) 395-400

[104] N. Hayashi, S. Koike, R. Yasutomi, E. Kasai, Weight and volume reduction of organic sludges and enhanced recovery of biomass resources using sonophotocatalysis, Songklanakarin J. Sci. Technol., 31 (2009) 635-639

[105] E. Selli, C.L. Bianchi, C. Pirola, G. Cappeltelli, V. Ragaini, Efficiency of 1,4-dichlorobenzene degradation in water under photolysis, photocatalysis on TiO_2 and sonolysis, J. Hazard. Mater., 153 (2008) 1136-41

[106] J. Theerthagiri, R.A. Senthil, D. Thirumalai, J. Madhava, Sonophotocatalytic degradation of organic pollutants using nanomaterials, in Handbook of Ultrasonics and Sonochemistry, (2015) pp. 553-586

[107] A.V. Volkova1, S. Nemeth, E.V. Skorb, D.V. Andreeva, Highly efficient photodegradation of organic pollutants assisted by sonoluminescence, Photochem. Photobiol., 91 (2015) 59–67

[108] E. Selli, Synergistic effects of sonolysis combined with photocatalysis in the degradation of an azo dye, Phys. Chem. Chem. Phys., 4 (2002) 6123–6128

[109] S. Mosleha, M.R. Rahimi, M. Ghaedi, K. Dashtian, Sonophotocatalytic degradation of Trypan blue and Vesuvine dyes in the presence of blue light active photocatalyst of Ag_3PO4/Bi_2S_3-HKUST-1-MOF: Central composite optimization and synergistic effect study, Ultrason. Sonochem., 32 (2016) 387-397

[110] A. Jelic, I. Michael, A. Achilleos, E. Hapeshi, D. Lambropoulou, S. Perez, M. Petrovic, D. Fatta-Kassinos, D. Barcelo, Transformation products and reaction pathways of carbamazepine during photocatalytic and sonophotocatalytic treatment, J. Hazard. Mater., 15 (2013) 177-186

[111] D. panda, S. Manickan, Recent advancements in the sonophotocatalysis (SPC) and doped sonophotocatalysis (DSPC) for the recalcitrant hazardous organic water pollutants, Ultrason. Sonochem., 36 (2017) 481–496

[112] K.P. Jyothi, S. Yesodharan, E.P. Yesodharan, Ultrasound (US), Ultraviolet light (UV) and combination (US+UV) assisted semiconductor catalysed degradation of organic pollutants in water: Oscillation in the concentration of hydrogen peroxide formed in situ, Ultrason. Sonochem., 21 (2014) 1787–1796

[113] D. Xu, F. Cheng, Y. Zhang, Z. Song, Degradation of Methyl Orange in aqueous solution by microwave irradiation in the presence of granular-activated carbon, Water Air Soil Pollut., 225 (2014) 1983

[114] D.Y. Xu, X. Lai, W. Guo, P. Dai, Microwave assisted catalytic degradation of Methyl Orange in aqueous solution by ferrihydrate/maghemite nanoparticles, J. Water Proc. Eng., 16 (2017) 270-276

Microwave, Photo and Sono Activated Advanced Oxidation Processes and their Variations for the Decontamination of Water from Toxic Chemical Pollutants

545

[115] S.H. Park, S-J. Kim, S-G Seo, S-C Jung, Assessment of Microwave/ UV/O$_3$ in the photo-catalytic degradation of Bromothymol Blue in aqueous nano TiO$_2$ particles dispersions, Nanoscale. Res. Lett., 5 (2010) 1627–1632

[116] J. Yin, J. Cai, C. Yin, L. Gao, J. Zhou, Degradation performance of Crystal Violet over CuO@AC and CeO$_2$-CuO@AC catalysts using microwave catalytic oxidation degradation method, J. Environ. Chem. Eng., 4 (2016) 958-964

[117] C. Yin, J. Cai, L. Gao, J. Yin, J. Zhou, Highly efficient degradation of 4-nitrophenol over the catalyst of Mn$_2$O$_3$/AC by microwave catalytic oxidation degradation method, J. Hazard Mater., 305 (2016) 15- 20

[118] J. Chen, S. Xue, Y. Song, M. Shen, Z. Zhang, T. Yuan, F. Tian, Dion, Microwave-induced carbon nanotubes catalytic degradation of organic pollutants in aqueous solution, J. Hazard Mater., 310 (2016) 226-234

[119] S-T. Liu, A-B. Zhang, K-K. Yan, Y. Ye, X- G Chen, Microwave-enhanced catalytic degradation of Methylene Blue by porous MFe$_2$O$_4$ (M = Mn, Co) nanocomposites: Pathways and mechanisms, Sep. and Purif. Technol. 135 (2014) 35-41

[120] Z. Zhang, X. Shan, Investigation on the rapid degradation of Congo Red catalysed by activated carbon powder under microwave irradiation, J. Hazard. Mater., 147 (2007) 325–33

[121] X. Zhang, Y. Wang, G. Li, J. Qu, Oxidative decomposition of azo dye C.I. Acid Orange 7 (AO7) under microwave electrodeless lamp irradiation in the presence of H$_2$O$_2$, J. Hazard. Mater., (2006) 183-189

[122] P.V. Gayathri, K.P. Vidyalekshmi, S. Yesodharan, E.P. Yesodharan, Microwave assisted catalytic degradation of traces of Rhodamine B in water in presence of H$_2$O$_2$, IOSR J. Appl. Chem., 1 (2015) 1-11

[123] X. Zhang, G. Li, Y. Wang, J. Qu, Microwave electrodeless lamp photolytic degradation of Acid Orange- 7, J. Photochem. Photobiol. A: Chem., 184 (2006) 26–33

[124] E. Hu, Y. Hu, H. Cheng, Performance of a novel microwave-based treatment technology for atrazine removal and destruction: sorbent reusability and chemical stability, and effect of water matrices, J. Hazard. Mater., 299 (2015) 444- 452

[125] X. Wang, L. Mei, X. Xinga, L. Liaoa, G. Lva, Z. Li, L. Wua, Mechanism and process of Methylene Blue degradation by manganese oxides under microwave irradiation, Appl. Catal B: Environ., 160-161 (2014) 211-216.

[126] T- L. Lai, C- C. Lec, K- S. Wu, Y-Y. Shu, C-B. Wang, Microwave-enhanced catalytic degradation of Phenol over nickel oxide, Appl. Catal. B: Environ., 68 (2006) 147–153

[127] X. liu, S. An, Wenshi, Q-Yang, L. Zhang, Microwave-induced catalytic oxidation of malachite green under magnetic Cu-ferrites: New insight into the degradation mechanism and pathway, J. Mol. Catalysis A: Chemical, 395 (2014) 243-250

[128] M. Ravera, A. Buico, F. Gosetti, C. Cassino, D. Musso, D. Osella, Oxidative degradation of 1,5-naphthalenedisulfonic acid in aqueous solutions by microwave irradiation in the presence of H_2O_2 Chemosphere, 74 (2009) 1309-1314.

[129] G. Cheng, J. Lin, J. Lu, X. Zhao, Z. Cai, J. Fu, Advanced treatment of pesticide-containing wastewater using Fenton reagent enhanced by microwave electrodeless ultraviolet, Biomed. Res. Int., 2015 (2015), Article id.205903, 8 pages

[130] C. Pitteloud, R. Kanno, The structure of manganese dioxide and position of proton studied by neutron diffraction with isotopic substitution, J. Solid State Chem.,181 (2008) 467-472

[131] I.D. Brown, D. Altermatt, Bond-valence parameters obtained from a systematic analysis of the inorganic crystal structure data base, Acte. Cryst., 41B (1985) 244-247

[132] A.A. Gribb, J. F. Banfield, Particle size effects on transformation kinetics and phase stability in nanocrystalline TiO2, American Mineralogist, 82 (1997) 717–728

[133] A.G. Agrios, P. Pichat, State of the art and perspectives on materials and applications of photocatalysis over TiO2: Reviews, Appl. Electrochem., 58 (2005) 655–63

[134] K. Demeestere, J. Dewulf, V.H. Langenhove, Heterogeneous photocatalysis as an adavanced oxidation process for the abatement of chlorinated, monocyclic aromatic and sulfurous volatile organic compounds in air: state of the art. Crit. rev. Environ. Sci.Technol., 37 (2007) 489–538

Microwave, Photo and Sono Activated Advanced Oxidation Processes and their Variations for the Decontamination of Water from Toxic Chemical Pollutants

547

[135] A. Mohamed, R.E-Sayed, T.A. Osman, M.S. Toprak, M. Muhammed, A. Uheida, Composite nanofibers for highly efficient photocatalytic degradation of organic dyes from contaminated water, Env. Research, 145(2016) 18-25

[136] Material Safety Data Sheet from Fischer Scientific.

[137] D.J. Dire, J.A. Wilkinson, Acute exposure to Rh B, J. Toxicol: Clinical Toxicology, 25 (1987) 603-607

[138] B. Rajeev, S. Yesodharan, E. P. Yesodharan, Sunlight activated ZnO mediated photocatalytic degradation of Acetophenone in water'', IOSR J. Appl. Chem., 2 (2016) 55-70

[139] Medical Management Guidelines for Phenol, Publisher: Agency for Toxic Substances and Disease Registry, U.S.A.

[140] E.M. Boyd, S.E. Hogan, The chronic oral toxicity of paracetamol at the range of the LD50 (100days) in albino rats, Can. J. Physiol. Pharmacol., 46 (1968) 239-45.

[141] R. Menasse, P.R. Hedwall, J. Kraetz, C. Pericin, L. Riesterer, A. Sallmann, R. Ziel, R. Jaques, Pharmacological properties of Diclofenac sodium and its metabolites, Scand. J. Rheumatol., 7 (1978) 5-16

[142] Pesticide Dictionary, Publishers: Farm Chemicals Handbook, Ed. F.R. Hall, E.L. Knake, R.M. McCarty, J.J. Mortvedt, D.L. Jerry (1990)

[143] Standard methods for the examination of water and waste water, [APHA] sixteenth edition (1985) 445-446.

[144] S. Horikoshi, N. Serpone, Photochemistry with microwaves: Catalysis and environmental applications, J. Photochem. Photobiol. C. Photochem Rev., 10 (2009) 96-110

[145] D.A.C. Stuerga, P. Gaillard, Microwave athermal effects in chemistry: a myth's autopsy. Part 1: historical background and fundamentals of wave-matter interaction, J. Microwave power and Electromagnetic Energy, 31(1996) 87-100

[146] E.T. Thostenson, T.W. Chou, Microwave processing: Fundamentals and applications, Composites Part A. 30 (1999) 1055-1071

[147] H. Cao, L. Suib, Highly efficient heterogeneous photooxidation of 2-propanol to acetone with amorphous MnO_2 catalysts, J. Am. Chem. Soc., 116 (1994) 5334-5342

[148] S. Horikoshi, H. Hidaka, N. Serpone, Environmental remediation by an integrated microwave/UV illumination method. 1. Microwave assisted degradation of Rhodamine B dye in aqueous TiO_2 dispersions, Environ. Sci. Technol., 36 (2002) 1357-1366

[149] M. Vautier, C. Guillard, J.M. Hermann, Photocatalytic degradation of dyes in water: Case study of Indigo and Indigo carmine, J. Catal. 201(2001) 46-51

[150] I. Dalmazio, A.P.F.M. de Urzedo, T.M.A. Alves, R.R. Catharino, M.N. Eberlin, C.C Nascentes, R. Augusti, Electrospray ionization mass spectrometry monitoring of indigo carmine by advanced oxidation process, J. Mass Spectrometry., 42 (2007) 1273-1278

[151] I. Othman, R.M. Mohamed, F.M. Ibrahem, Study of photocatalytic oxidation of Indigo Carmine dye on Mn-supported TiO_2, J. Photochem. Photobiol A: Chem., 189 (2007) 80-85

[152] W.H Kuan, C. Y. Chen, C .Y. Hu, Removal of Methylene Blue from water by γ-MnO_2, Water Science and Technology, 64 (2011) 899-903

[153] H. Zhang, W.R. Chen, C.H. Huang, Kinetic modelling of oxidation of antibacterial agents by MnO_2, Environ. Sci. Technol., 42 (2008) 5548-5554

[154] S.G. Anju, S. Yesodharan, E.P. Yesodharan, Zinc oxide mediated sonophotocatalytic degradation of phenol in water, Chem. Eng. J., 189-190 (2012) 84-93

[155] L. Zhang, X. Zhou, X. Guo, X. Song, X. Liu, Investigations on the degradation of Acid Fuchsin induced oxidation by $MgFe_2O_4$ under MW irradiation, J. Mol. Catal. A., 335 (2011) 31-37

[156] B. Rajeev, S. Yesodharan, E.P. Yesodharan, Application of solar energy in wastewater treatment: Photocatalytic degradation of α –Methyl styrene in water in presence of ZnO, J. Water Proc. Eng., 8 (2015) 108-118

[157] C. Guillard, E. Puzenat, H. Lachheb, A. Houas, J-M. Herrmann, Why inorganic salts decrease the TiO_2 photocatalytic efficiency, Int. J. photoenerg., 07 (2005) 1-9

[158] A. Tauber, G. Mark, H-P. Schuchmann, C. von Sonntag, Sonolysis of tert-butyl alcohol in aqueous solution, J. Chem. Soc., Perkin Trans., 2 (1999) 1129-1135

[159] C. Minero, V. Maurino, E. Pelizzetti, D. Vione, An empirical, quantitative approach to predict the reactivity of some substituted aromatic compounds towards reactive radical species ($Cl_2^{-\bullet}$, $Br_2^{-\bullet}$, $^\bullet NO_2$, $SO_3^{-\bullet}$, $SO_4^{-\bullet}$) in aqueous solution, Environ. Sci. Pollut. Res., 13 (2006) 212-214

[160] A-G Rincon, C. Pulgarin, Effect of pH, inorganic ions, organic matter and H_2O_2 on E.coli K12 photocatalytic inactivation by TiO_2. Implications in solar water disinfection, Appl,Catal. B: Environ., 51 (2004) 283-302

[161] L. Amalric, C. Guillard, E. Blanc-Brude, P. Pichat, Correlation between the photocatalytic degradability over TiO_2 in water of meta and para substituted Methoxybenzenes and their electron density, hydrophobicity and polarizability properties, Wat. Res., 30 (1996)1137-1142

[162] C. Galindo, P. Jacques, A. Kalt, Photochemical and photocatalytic degradation of an Indigo dye: A case study of acid blue 74 (AB 74), J. Photochem. Photobiol A: Chem., 141 (2001) 47-53

[163] J. Kiwi, A. Lopez, V. Nadtochenko, Mechanism and kinetics of .OH radical intervention during Fenton oxidation in the presence of significant amount of radical scavenger, Environ. Sci. Technol., 34 (2000) 2162-216

[164] M. Gratzel, A J Frank, Interfacial electron transfer reactions in colloidal semiconductor dispersions. Kinetic analysis, J. Phys. Chem., 86 (1982) 2964-2967

[165] K.P. Jyothi, S. Yesodharan, E. P. Yesodharan, Contaminant salts as enhancers of sonocatalytic degradation of organic water pollutants: Effect of concentration, reaction time and adsorption on the efficiency of enhancement and the fate of concurrently formed H_2O_2, J. Env. Chem. Eng., 6 (2018) 3574-3589

[166] W-K. Kuan, C-Y. Chen, C-Y. Hu, Y-M. Tzou, Kinetic modelling for Microwave enhanced degradation of Methylenve Blue using MnO_2, Int. J. Photoenergy,2013 (2013) Article id. 916849, 9 pages

[167] R.V. Narayan, V. Kanniah, A. Dhathathreyan, Synthesis, characterization and photocatalytic study of cobalt oxide/ Zeolite-NaX, J. Chem. Soc., 118 (2006) 179-184

[168] W-Y. Li, L-N. Xu, J. Chen, Co_3O_4 nonmaterial in Lithium –ion batteries and gas sensors, Adv. Funct. Mater., 15 (2005) 851-857

[169] K. Agilandeswari, A. R. Kumar, Characterisation, optical and magnetic properties of Co_3O_4 nanoparticles by quick precipitation, J. Synth. React. Inorg. Metal-org. and Nano Metal Chem., 46 (2016) 1-18.

[170] K.P. Jyothi, S. Yesodharan, E.P. Yesodharan, Sono, photo and sonophotocatalytic decontamination of organic pollutants in water: Studies on the lack of correlation between pollutant degradation and concurrently formed H_2O_2, Current Science, 109 (2015) 189-194

[171] E. Evgenidou, K. Fytianos, I. Poulios, Semiconductor sensitised photodegradation of Dichlorvos in water using TiO_2 and ZnO as catalysts, Appl. Catal B:Environ., 59 (2005) 81-89

[172] W.H. Kuan, Y.C. Chan, pH dependent mechanisms of Methylene Blue reacting with tunnelled manganese oxide pyrolusite, J. Hazard Mater., 239-240 (2012) 152-159

[173] C. Marun, L.D. Conde, M. L. S. Suib, Catalytic oligomerization of methane via microwave heating, J Phys Chem. A., 103 (1999) 4332-4340

[174] C. Doornkamp, V. Ponec, The universal character of the Mars and Van Krevelen mechanism, J. Mol. Catal. A., 162 (2000) 19-32

[175] S. Horikoshi, A. Matsubara, S. Takayama, M. Sato, F. Sakai, M. Kajitani, M. Abe, N. Serpone, Characterization of microwave effects on metal-oxide materials: Zinc oxide and titanium dioxide, Appl. cat. B., 91 (2009) 362-367

[176] S. Horikoshi, A. Osawa, M. Abe, N. Serpone, On the generation of hot-spots by microwave electric and magnetic fields and their impact on a microwave assisted heterogeneous reaction in the presence of metallic Pd nano particles on an activated carbon support, J. Phys. Chem., 115 (2011) 23030-35

[177] B. Neppolean, H.C. Choi, S. Sakthivel, B. Aurobindo, B. Murugesan, Solar/UV induced photocatalytic degradation of three commercial textile dyes, J. Hazard. Mater., 89 (2002) 303-317

[178] Y. F. Shen, R.P. Zorger, S.L. Suib, L. McCarty, D.l. Potter, C. L. O' Young, J Chem. Soc. Chem. Commun., 17 (1992)1213-1214

[179] H.C. Yatmaz, A. Akyol, M. Bayramoglu, Kinetics of photocatalytic degradation of an Azo reactive dye in aqueous ZnO suspension, Ind. Eng. Chem Res., 43 (2004) 6035-6039

Microwave, Photo and Sono Activated Advanced Oxidation Processes and their Variations for the Decontamination of Water from Toxic Chemical Pollutants

551

[180] K.E. O'Shea, I. Garcia, M Aguilar, Titanium dioxide photocatalytic degradation of Dimethyl and Diethyl methylphosphonate: Effect of catalyst and environmental factors, Res. Chem. Intermed., 23 (1997) 325-339

[181] S. Zhou, A.K. Ray, Kinetic studies for photocatalytic degradation of Eosin B on a thin film of Titanium dioxide, Ind. Eng. Chem. Res., 42 (2003) 6020-6033

[182] J. Saien, A.R. Soleymani, Degradation and mineralization of Direct blue 71 in a circulating up-flow reactor by UV/TiO$_2$ process and employing a new method in kinetic study, J Hazard. Mater., 14 (2007) 507-512

[183] J. Cunningham, G. Al-Sayyed, Factors influencing efficiencies of TiO$_2$-sensitised photodegradation, J. Chem Soc. Faraday Trans., 86 (1990) 3935-3941

[184] N. Barka, A. Assabane, A. Nounah, I. A. Ichou, Photocatalytic degradation of Indigo Carmine in aqueous solution by TiO$_2$ – coated non-woven fibres, J. Hazard. Mater., 152 (2008) 1054-1059

[185] A. A. Berlin, Kinetics of radical chain decomposition of persulphate in aqueous solution of organic compounds, Kinetics. Catal., 27 (1986) 34-39

[186] R. G. Zepp, J. Hiogne, H. Bader, Nitrate induced photo oxidation of organic chemicals in water, Environ. Sci. Technol., 21 (1987) 443-450

[187] H. Kung, 'Transition metal oxides: Surface chemistry and catalysis; Elsevier: Amsterdam, (1989) pp100-120

[188] M.W. Peterson, J.A. Turner, A.J. Nozik, Mechanistic studies of the photocatalytic behaviour of TiO$_2$ particles in a photoelectrochemical slurry cell and the relevance to photodetoxification reactions, J. Phys. Chem., 95 (1991) 221-225

[189] P. Salvador, Influence of pH on the potential dependence of the efficiency of water photo-oxidation at n-TiO$_2$ electrodes, J. Electrochem. Soc., 128 (1981) 1895-1900

[190] H. Gerischer, A. Heller, The role of O$_2$ in photooxidation of organic molecules on semiconductor surfaces, J Phys Chem., 95 (1991) 5261-5267

[191] S. Anandan, P. Sathish kumar, N. Pugazhenthiran, J. Madhavan, P. Maruthamuthu, Effect of loaded silver nanoparticles on TiO$_2$ for photocatalytic degradation of Acid Red 88, Solar Energy Mater. and Solar Cells, 92 (2008) 929-937

[192] J.C. Kuriacose, V. Ramakrishnan, E.P. Yesodharan, Surface changes on a ZnO catalyst during dehydrogenation of alcohols, Ind. J. Chem., 13 (1975) 1350-1352

[193] K.S. Suslick, D.A. Hammerton, R.E. Cline Jr., The sonochemical hot spot, J. Am. Chem. Soc. 108 (1986) 5641-5642

[194] V.A. Shutilov, Fundamentals of Physics of ultrasound, Publishers: Gordon and Breach Science (1988) New York,

[195] S.G. Anju, I.S. Bright Singh, E.P. Yesodharan, S. Yesodharan, Investigations on semiconductor sonocatalysis for the removal of pathological micro-organisms in water, Desalination and Water Treatment, 54 (2014) 3161-3168

[196] K.P. Vidyalekshmi, P.V. Gayathri, K.P. Jyothi, S.G Anju, S. Yesodharan, E.P. Yesodharan, Application of ultrasound under different conditions for the purification of water contaminated with chemical and bacterial pollutants, Gurukulam Int. J. Innovations Sci. and Tech. 1 (2016) 35-52

[197] S. Merouani, O. Hamdaoui, F. Saoudi, M. Chiha, Sonochemical degradation of Rhodamine B in aqueous phase; Effect of additives, Chem. Eng. J., 158 (2010) 550-557

[198] L. Song, C. Chen, S. Zhang, Sonocatalytic performance of Tb_7O_{12}/TiO_2 under ultrasonic irradiation, Ultrason. Sonochem., 18 (2011) 713-717

[199] Y. Chen, D.D. Dionysiou, A comparative study of physicochemical properties and photocatalytic behaviour of macroporous TiO_2 –P25 composite films and macroporous TiO_2 films coated on stainless steel substrates, Appl. Catal. A: General, 317 (2007) 129-137

[200] R.A. Torres-Palma, E. Combet, C. Petrier, C. Pulgarin, An innovative ultrasound, Fe^{2+} and TiO_2 photoassisted process for bisphenol A mineralization, Water Res., 44 (2010) 2245-2252

[201] P.R.Gogate, Treatment of wastewater streams containing phenolic compounds using hybrid techniques based on cavitation: a review of the current status and the way forward, Ultrason. Sonochem.,15 (2008) 1-15

[202] M.G. Antonio, P.A. Nicolaou, J.A. Shoemaker, A.A. de la Cruz, D.D. Dionysiou, Detoxification of water contaminated with cyanotoxin Microcystin-LR by utilizing thin TiO_2 photocatalyst films, Applied Catal. B: Environmental, 91 (2009) 165-173

[203] L. Andronic, A. Enesca, C.Vladuta, A. Duta, Photocatalytic activity of cadmium doped TiO_2 films for photocatalytic degradation of dyes, Chem. Eng. J., 152 (2009) 64-71

[204] E.A. Nepiras, Acoustic cavitation: An introduction, Ultrasonics, 22 (1984) 25-40

[205] A. Keck, E. Gilbert, R. Koster, Influence of particles on sonochemical reactions in aqueous solutions, Ultrasonics, 40 (2002) 661-665

[206] H. Sekiguchi, Y Saita, Effect of alumina particles on sonolysis degradation of chlorobenzene in aqueous solution, J Chem. Eng. Jpn., 34 (2001) 1045-1048

[207] A. Nakajima, H. Sasaki, Y. Kameshima, K. Okada, H. Harada, Effect of TiO_2 powder addition on sonochemical destruction of 1,4 dioxane in aqueous systems, Ultrason. Sonochem., 14 (2007) 197-200

[208] M. F. Dadjour, C Ogino, S. Matsumura, N Shimizu, Enhancement of sonocatalytic cell lysis of *Escherichia coli* in the presence of TiO_2, Biochem. Eng. J. 25 (2005) 243-248

[209] H. Ogi, M. Hirao, M. Shimoyama, Activation of TiO_2 photocatalyst by single bubble sonoluminescence for water treatment, Ultrasonics, 40, 2002, 649.

[210] K. Kang, M. Jang, M. Cui, P. Qiu, S. Na, Y. Son, J. Khiom, Enhanced sonocatalytic treatment of Ibuprofen by mechanical mixing and reusable magnetic core titanium dioxide, Chem. Eng. J., 264 (2015) 522-530

[211] K.S. Suslick, L.A. Crum, in M.J. Crocker (Ed.), Encyclopaedia of Acoustics, Vol.1, Wiley Interscience, New York, (1997), pp 271-282

[212] Y.C. Chen, P. Smirniotis, Enhancement of photocatalytic degradation of Phenol and Chlorophenols by ultrasound, Ind. Eng. Chem. Res., 41 (2002) 5958- 5965

[213] H. Nakui, K. Okitsu, Y. Maeda, R. Nishimura, Effect of coal ash on sonochemical degradation of phenol in water, Ultrason. Sonochem., 14 (2007) 191-196

[214] T. Tuziuti, K. Yasui, M. Sivakumar, Y. Iida, N. Miyoshi, Correlation between acoustic cavitation noise and yield enhancement of sonochemical reactions by particle addition, J Phys. Chem. A., 109 (2005) 4869-4875

[215] L.A. Crum, Tensile strength of water, Nature, 278 (1979) 148-149

[216] M. Kubo, R. Onodera, N. Shibasaki-kitakawa, K. Tsumoto, T. Yonemoto, Kinetics of ultrasonic disinfection of *E coli* in the presence of TiO_2 particles, Biotech. Prog., 21(2005) 897-901

[217] N. H. Ince, G. Tezcanli-Guyer, R. K. Belen, I. G. Apikyan, Ultrasound as a catalyzer of aqueous reaction systems: the state of the art and environmental applications, Appl. Catal B: Environmental, 29 (2001) 167-176

[218] Y.G. Adewuyi, Sonochemistry: Environmental science and engineering applications, Ind. Eng. Chem. Res., 40 (2001) 4681-4715

[219] L. Davydov, E.P. Reddy, P. France, P.P. Smirniotis, Sonophotocatalytic destruction of organic contaminants in aqueous systems on TiO_2 powders, Appl. Catal.B: Environmental, 32 (2001) 95-105

[220] K.P. Mishra, P.R Gogate, Intensification of degradation of aqueous solutions of Rhodamine B using sonochemical reactors at operating capacity of 7 L, J. Env. Management, 92 (2011) 1972-1977

[221] S. Rabindranathan, S. Devipriya, S. Yesodharan, Photocatalytic degradation of Phosphamidon on semiconductor oxides, J. Hazard. Mater. 102 (2003) 217-229

[222] I. M. Khokhawala, P.R. Gogate, Degradation of Phenol using a combination of ultrasonic and UV irradiations at pilot scale operation. Ultrason. Sonochem., 17 (2010) 833-838

[223] W.H. Kuan, C.Y. Chen, C.Y. Hu, Removal of Methylene Blue from water by γ - MnO_2, Water Sci.Technol., 664, 2011, 899-903

[224] C. Petrier, M.F. Lamy, A. Francony, A. Benahceene, B. David, V. Renaudin, N. Gondreson, Sonochemical degradation of phenol in dilute aqueous solutions: comparison of the reaction rates at 20 and 487 kHz, J Phys. Chem., 98 (1994) 10514-10520

[225] N. Pokhrel, P. K. Vabhina, N. Pala, Sonochemistry: Science and Engineering, Ultrason Sonochem., 29 (2016) 104-128

[226] S. Merouani, O. Hamdoui, Y. Rezgui, M. Guemini, Effects of ultrasound frequency and acoustic amplitude on the size of sonocatalytically active bubbles-theoretical study, Ultrasonic. Sonochem., 20 (2013) 815-819

Microwave, Photo and Sono Activated Advanced Oxidation Processes and their Variations for the Decontamination of Water from Toxic Chemical Pollutants

555

[227] A. H-Roshan, S M Kazemzadeh, M R Vaezi, A Shokuhfar, The effect of sonication power on the sonochemical synthesis of titania nano particles, J.Ceram. Process Res., 12 (2011) 299-30

[228] A.K. Shriwas, P.R. Gogate, Intensification of degradation of 2,4,6-trichlorophenol using sonochemical reactors: Understanding mechanism and scale up aspects, Ind. Eng. Chem. Res., 50 (2011) 9601-9608

[229] G. Mark, S.P. Schuchumann, C von Sontag, Formation of peroxynitrite by sonication of aerated water, J. Am. Chem. Soc., 122 (2000) 3781-3782

[230] C. Minero, P. Pellizzari, V. Maurino, E. Pelizzetti, D. Vione, Enhancement of dye sonochemical degradation by some inorganic anions present in natural waters, Appl. Catal B: Environ., 77 (2008) 308-316

[231] K.P. Jyothi, S. Joseph, S. Yesodharan, E.P. Yesodharan, Periodic change in the concentration of hydrogen peroxide formed during the semiconductor mediated sonocatalytic treatment of wastewater: Investigations on pH effect and other operational variables, Res. J. Rec. Sci., 2 (2013) 136-149

.....ℰℭ.....

ANNEXURES

Annexure 1

||||| List of Abbreviations and Symbols |||||

AOP	Advanced Oxidation Process
AOT	Advanced Oxidation Technology
AC	Activated Carbon
ACP	Acetophenone
BET	Brunauer-Emmett Teller
BOD	Biological Oxygen Demand
CB	Conduction Band
CNTs	Carbon Nano Tubes
COD	Chemical Oxygen Demand
CWAO	Catalytic Wet Air Oxidation
EDX	Energy Dispersive X-ray Spectroscopy
eV	Electron Volt
FTIR	Fourier Transform Infra Red
GAC	Granulated Activated Carbon
h	Plank's Constant
HPLC	High Performance Liquid Chromatography
HTPA	2-hydroxy terephthalic acid
IC	Indigo Carmine
KHz	Kilo Hertz
LH	Langmuir- Hinshelwood
M	Molar
MB	Methylene Blue
MG	Malachite Green
MHz	Mega Hertz
mM	Milli Molar
MMT	Montmorillonite K10

Microwave, Photo and Sono Activated Advanced Oxidation Processes and their
Variations for the Decontamination of Water from Toxic Chemical Pollutants

557

MW	Microwave
nm	Nano Meter
PC	Photocatalysis
PL	Photoluminescence
ppb	Parts per billion
ppm	Parts per million
PZC	Point of Zero Charge
RhB	Rhodamine B
ROS	Reactive Oxygen Species
rpm	Rotations per minute
SC	Sonocatalysis
SCO	Semiconductor Oxide
SEM	Scanning Electron Microscopy
SPC	Sonophotocatalysis
TEM	Transmission Electron Microscopy
TOC	Total Organic Carbon
TPA	Terephthalic acid
TSS	Total Suspended Solids
US	Ultrasound
UV	Ultraviolet
V	Volt
VB	Valence Band
XRD	X-ray diffractogram
μm	Micro meter
μmol/L	Micro mols/Liter

.....&CR.....

Annexure 2

||||| List of Publications |||||

A. Published in peer reviewed journals: 5

1) K.P. Vidya Lekshmi, P.V. Gayathri, Suguna Yesodharan, E.P. Yesodharan, 'MnO$_2$ Catalysed Microwave Mediated Removal of Trace Amount of Indigo Carmine Dye from Water', *IOSR-J Applied Chem.*, Vol.1 (2014) 29-40.

2) P.V. Gayathri, K.P. Vidya Lekshmi, Suguna Yesodharan, E.P. Yesodharan, 'Microwave Assisted Catalytic Degradation of Traces of Rhodamine B in Water in Presence of H$_2$O$_2$', *IOSR-J Applied Chem.*,Vol.1 (2014) 1-11

3) K.P. Vidya Lekshmi, Suguna Yesodharan, E.P. Yesodharan, 'Co$_3$O$_4$ mediated microwave catalysis: A new innovative Advanced Oxidation Process (AOP) for the removal of dye pollutants from water' *IOSR-J Applied Chem.*, Vol.1 (2016) 25-46

4) K.P. Vidya Lekshmi, P.V. Gayathri, S.G Anju, K.P. Jyothi, Suguna Yesodharan, E.P. Yesodharan, 'Application of ultrasound under different conditions for the purification of water contaminated with chemical and bacterial pollutants' *Gurukulam International Journal of Innovations in Science and Engineering*, Vol.1 (2016) 35-52.

5) K.P. Vidya Lekshmi, Suguna Yesodharan, E.P. Yesodharan, 'MnO$_2$ and MnO$_2$ mediated persulphate enhanced photocatalysis for the removal of Indigo Carmine dye pollutant from water' European Chemical Bulletin, Vol.6 (2017) 177-191.

B. Presented in Conferences: 5

i) International

1) 'Microwave assisted Advanced oxidation Process for the degradation of Indigo Carmine in water using MnO_2'; Presented at the International Conferences on Advanced Oxidation Process, Munnar, India (2014).

2) 'MnO_2 catalysed microwave mediated removal of trace amount of Indigo Carmine dye from water'; Presented at the International Conference on Emerging Trends in Engineering and Management (ICETEM'15) at Sree Narayana Gurukulam College of Engineering, Ernakulam, India (2014)

3) 'Co_3O_4 mediated microwave catalysis: A new innovative advanced oxidation process (AOP) for the removal of dye pollutants from water'; Presented at the International Conference on Emerging Trends in Engineering and Management (ICETEM 16) at Sree Narayana Gurukulam College of Engineering, Ernakulam, India (2016)

4) 'MnO_2 and MnO_2/TiO_2 as efficient photocatalysts for the removal of last traces of indigo carmine dye from water'; Presented at the International Conferences on Advanced Oxidation Process, at Goa, India (2016)

ii) National

5) 'Novel unusual application for microwave radiation: removal of last traces of toxic chemical pollutants from industrial wastewater'; Presented as a competition paper at the 28th Kerala Science Congress held at Calicut, India (2016).

.....ജ്ഞ.....

Annexure 3

▐▐▐▐ Reprints of Papers Published ▐▐▐▐

1) MnO_2 catalysed microwave mediated removal of trace amount of Indigo Carmine dye from water

2) Microwave Assisted Catalytic Degradation of Traces of Rhodamine B in Water in Presence of H_2O_2

3) Co_3O_4 mediated microwave catalysis: A new innovative Advanced Oxidation Process (AOP) for the removal of dye pollutants from water

4) Application of ultrasound under different conditions for the purification of water contaminated with chemical and bacterial pollutants'

5) 'MnO_2 and MnO_2/TiO_2 as efficient photocatalysts for the removal of last traces of indigo carmine dye from water

Microwave, Photo and Sono Activated Advanced Oxidation Processes and their Variations for the Decontamination of Water from Toxic Chemical Pollutants

561